We are in the position of a little child entering a huge library filled with books in many different languages. The child knows someone must have written those books. It does not know how. It does not understand the languages in which they are written. The child dimly suspects a mysterious order in the arrangement of the books but doesn't know what it is. That seems to me, is the attitude of even the most intelligent being toward God. We see a universe marvellously arranged and obeying certain laws, but only dimly understand those laws. Our limited minds cannot grasp the mysterious force that moves the constellations.

-Albert Einstein-

UNIVERSITA' DEGLI STUDI DI UDINE

CORSO DI DOTTORATO DI RICERCA IN SCIENZE BIOMEDICHE E BIOTECNOLOGICHE

CICLO XXVI

ROLE OF POST-TRANSLATIONAL MODIFICATIONS IN MODULATING APE1 FUNCTIONS IN TUMOUR CELLS

Candidate: LISA LIRUSSI

Supervisor: Prof. GIANLUCA TELL

ACADEMIC YEAR 2013/2014

TABLE OF CONTENTS

ABBREVIATIONS

8-oxoG, 8-oxoguanine
AD, Alzheimer disease
ADP, adenosine diphosphate
ALS, amyotrophic lateral sclerosis
AML, acute myeloid leukemia
AP, abasic site
AP-1, activating protein-1
APE1, apurinic/apyrimidinic endonuclease-1
APE1-SCR1, APE1 scramble
APE1-WT, APE1 wild-type
APE1-NΔ33, N-terminal APE1 deletion mutant
BER, base excision repair
BLM, bleomycin
CK I and II, casein kinase I and II
DAPI, 4',6-diamidino-2-phenylindole
DDR, DNA damage response
DNA Pol β, DNA polymerase β
DR, direct repair
DSB, double-strand breaks
E3330, 2E-3-[5-(2, 3 dimethoxy-6- methyl-1, 4-benzoquinolyl)]-2-nonyl-2- propenoic acid
Egr-1, early growth response protein-1
FC, fibrillar center
FEN1, flap endonuclease 1
GC, granular component
GG-NER, global genome NER
GO, gene ontology
GSK III, glycogen synthase kinase III
GzmA and K, granzyme A and K
HAT, histone acetyltransferase
HDAC, histone deacetylase
hnRNP-L, Heterogeneous nuclear ribonucleoprotein L
hOGG1, human OGG1
HR, homologous recombination
IDP, intrinsically disordered regions
LC-ESI-MS, liquid chromatography-electrospray ionization-mass spectrometry
LP-BER, long-patch base excision repair
MDM2, murine double minute 2
MEF, mouse embryonic fibroblasts
MMR, mismatch repair
MMS, Methylmethanesulfonate
mtBER, mitochondrial BER
nCaRE, Negative calcium responsive element
NES, nuclear export signal
NER, nucleotide-excision repair
NF-κB, nuclear factor-kappaB

NHEJ, non-homologous end joining
NLS, nuclear localization signal
NPM1, nucleophosmin 1
NPM1wt, NPM1 wild-type
NPM1c+, cytoplasmic nucleophosmin 1
NO, nitric oxide
NoLS, nucleolar localization signal
OGG1, 8-oxoguanine DNA glycosylase
PARP1, Poly(ADP-ribose) polymerase 1
PCNA, proliferating cell nuclear antigen
PD, Parkinson disease
PKC, protein kinase C
PTMs, post-translational modifications
PTH, parathyroid hormone
Rac1, ras-related C3 botulinum toxin substrate 1
RF-C, replication factor C
RNA pol I/II, RNA polymerase I and II
ROS, reactive oxygen species
Sir2, silent information regulator 2
SIRT1, sirtuin 1
SNPs, single-nucleotide polymorphisms
SP-BER, short-patch base excision repair
SSB, single-strand break
TC-NER, transcription-coupled NER (TC-NER)
TSH, thyrotropin
TO-PRO3, Quinolinium, 4-[3-(3-methyl-2(3H)-benzothiazolylidene)-1-propenyl]-1-[3-(trimethylammonio)propyl], diiodide
Trx, thioredoxin
XRCC1, X-ray cross-species complementing 1

ABSTRACT

Apurinic/apyrimidinic endonuclease 1 (APE1) is the main mammalian endonuclease involved in the repair of DNA lesions caused predominantly by oxidative and alkylating stresses through its participation in base excision repair (BER) pathway. Although APE1 was discovered for its ability to cleave and remove AP-sites and to enhance the DNA binding properties of several cancer-related transcription factors, through redox-dependent mechanisms (involving its so-called Ref-1 activity), in the latest years investigators have described new and broader functions for this DNA repair enzyme. In fact, it has been demonstrated a direct role for APE1 in the regulation of gene transcription and an unexpected role in the RNA metabolism being able to cleave damaged or site-specific RNAs. Despite different works regarding the transcriptional and post-translational mechanisms that cells used to control and to redirect APE1 to its several functions, it is still a matter of debate the role of the first 33 amino acids, a unique evolutionary N-terminus specific for the mammalian protein, that impacts, through macromolecules interaction and post-translational modifications, on controlling APE1 activities. In this work of Thesis, new acetylated lysine residues were identified *in vivo* and the role of acetylation sites at N-terminus (Lys 27-35) in regulating APE1 functions and subcellular localization were studied. Moreover, seventeen new interacting partners were identified. Among these, the attention was focused on APE1 and Nucleophosmin 1 (NPM1) interaction within nucleoli and nucleoplasm. NPM1 is a nucleolar protein, mainly involved in ribosome biogenesis, stress responses and genome maintenance. Growing body of evidences emphasizes a role for NPM1 in DNA repair field, but its exact role(s) has not been identified yet. Interestedly, patients with acute myeloid leukemias (AMLs), characterized by the expression of a mutated form of NPM1 (NPM1c+), causative for its aberrant cytoplasmic localization, represent better responders to chemotherapy and for favorable overall survival. At present, the molecular reasons underneath the role for NPM1 in tumorigenesis of solid tumors and in AMLs are still lacking. In this framework, a clear contribution of NPM1 in DNA repair control, through the functional regulation of the APE1 endonuclease activity in BER pathway, its subcellular localization and stability has been demonstrated *in vivo*. In this light, the positive clinical impact of NPM1c+ in chemotherapeutic response might be related to the potential interference with the functions of NPM1 interacting partners, once delocalized in the cytoplasm. An intriguing mechanism for explaining also the biological effects of APE1 genetic variants, considered in this work of Thesis, supported by the observation that the majority of the polymorphisms presents an altered complex network of interactions, protein stability and stress response, affecting the APE1 functional status.
Our findings provide a glimpse into the role of the nucleolus and NPM1 in controlling APE1 functions, suggesting a critical role for the intricate network of APE1 interacting partners, especially NPM1, and post-translational modifications in BER *in vivo* that might be important for explaining the APE1 dysregulation seen in different types of tumors.

1. INTRODUCTION

1.1 THE "WATSON AND CRICK" DOMINO EFFECT

Sixty years have passed since Watson and Crick unveiled the structure of the DNA double helix and tentatively explained some genetical implications deriving from the proposed structure[1]. Since then, several investigators concentrate their attention on understanding the properties and rules that govern our genetic material. Indeed, as correctly supposed by Watson "*Biology has at least 50 more interesting years*". Maybe much more.

Shortly after this breakthrough, it became quite clear that DNA, for its intrinsic nature, is susceptible to numerous DNA damages, being exogenous or endogenous, that could ultimately lead to alterations of the coding information of the genome, potentially driving to mutagenesis phenomena and activation of cell death programs. The next paragraphs will be dedicated to a brief overview of the different types of DNA damages and the enzymatic processes evolutionary arise for specifically recognizing the DNA alteration, ensuring the accuracy of the genetic material. A particular attention will be given to the Base Excision Repair (BER) pathway and to the main mammalian endonuclease, APE1.

1.2 THE MOLECULAR STRUCTURE OF DNA AND ITS INTRINSIC VULNERABILITY

Within the complex machinery of each cells, all biomolecules, inclusive of proteins, lipids and nucleic acids, run into an inescapable series of damages caused both by spontaneous reactions, such as hydrolysis, and by numerous endogenous and exogenous reactive agents. Of note, DNA damage could have more severe consequences than the other damaged molecules, due to its intrinsic nature and function. The other macromolecules are all renewable and when they lose their function or stability they could be easily replaced; this is not true for nuclear DNA, that accounts for all cellular RNA and proteins, being irreplaceable. Acquiring mutations in a permanent way might lead to irreversible outcomes, as malignancies predisposition, neurological abnormalities and ageing[2-4].

For these reasons, to combat threats posed by DNA damage, eukaryotic cells have developed and evolutionary acquired a complex range of DNA damage repair systems, tolerance pathways and checkpoint steps, collectively named DNA damage response (DDR), to detect DNA lesions, signal their presence and promote their repair, restoring the DNA integrity and guaranteeing the genome maintenance during lifespan of an organism. Although this intricate apparatus, in case of too severe DNA damages, nature has also provided cells with effector machineries for triggering senescence or cell death to avoid the transmission of altered genomes. In fact, more complicated and larger the genome is, more sensitive to several DNA damages it appears. The chemical events that lead to DNA damage, besides exogenous sources as UV and ionizing radiation, are

usually triggered by endogenous metabolic processes, i.e. exposure to reactive oxygen species (ROS), including superoxide anions, hydrogen peroxide and hydroxyl radicals and other reactive metabolites[5]. Generation of ROS originates other subsequent altered products: endogenous alkylating agents, spontaneous hydrolysis and deamination products. As estimated by Lindahl and colleagues, an impressive number of lesions (roughly thousands of single-strand breaks and spontaneous base losses) occur spontaneously per mammalian genome every day. Moreover, with the existence of other types of spontaneous damages, this significant number may arise to about ten thousands per cell per day[6].

The consequences of DNA injury are determined by several factors:

- The type of DNA damage. Some lesions are mainly mutagenic (i.e. 8-oxo-G, induced by oxidative damage), promoting the development of malignancies; others are cytotoxic and lead to senescence and ageing. Bulky lesions, such as double-strand breaks or inter-strand cross-links, generally provoke cellular senescence or cell death;
- The frequency and the severity of the DNA damage;
- The location of DNA injuries in the genome;
- Efficiency and accuracy of the repair systems involved in removing the DNA lesions may depend to cell type or cell cycle stage when damage occurs.

The wide variety of DNA lesions and their effects have given a boost to the development of an intricate system of DNA repair pathways, each selective for a specific subset of DNA lesions (Figure 1). Often described as a series of distinct pathways, DNA repair is more likely to be a complex and integrated network that coordinates the canonical pathways described in literature[7]. While some lesions are easily repair through a direct protein-mediated reversal (direct repair, DR), the majority of injuries requires a complex sequence of enzymatic steps mediated by multiple proteins, that belong to the same pathway[8]. In base excision repair (BER), a damaged base is recognized by DNA glycosylase, that removes it generating an abasic (AP) sites, before endonuclease (APE1), polymerase and ligase proteins complete the repair[9]. In mismatch repair (MMR), detection and removing of biosynthetic errors (insertion/deletion) from newly synthesized DNA triggers a single-strand incision, followed by the action of nuclease, polymerase and ligase enzymes, improving the fidelity of DNA replication[10]. The nucleotide excision repair (NER) system senses helix-distorting base lesions and operates using two different sub-pathways that differ in the mechanism of lesion recognition: transcription-coupled NER (TC-NER) that copes with replication blocking lesions, and global genome NER (GG-NER). Then they converge for the incision/excision steps and subsequent gap filling and ligation steps[11]. Notably, some lesions are not repair but are by-passed during DNA replication by error-prone polymerases. For double-strand break (DSB) repair, nature has evolved two different mechanisms: non-homologous end joining (NHEJ) and homologous recombination (HR)[8]. In NHEJ, Ku proteins, after recognition of the break,

binds the DNA termini and activates the protein kinase DNA-PKcs, with the subsequent recruitment and activation of end-processing enzymes (Polμ and Ligase IV). Although error-prone, NHEJ can occur throughout the cell cycle[12]. By contrast, HR is restricted to late S or G2 cell cycle stages, because it uses the sister-chromatid sequences as template to repair the damage[13]. The MRN (MRE11-RAD50-NBS1) complex triggers the initial single-strand (ssDNA) generation and, in a BRCA1/2-RAD51 mechanism, the ssDNA invades the undamaged template followed by action of polymerases, ligase for substrate resolution. Assisted by the Fanconi anaemia complex, HR is generally used for restarting stalled replication forks and to repair inter-strand DNA cross-links[8]. This integrated system is engaged in a continuous effort to maintain and preserve genome integrity; its impairment or lack of coordination within the same pathway may give arise to mutagenesis, chromosome instability and gene expression defects; this entire set of events lead to cellular dysfunction and pathologies usually associated with DNA repair defects[8].

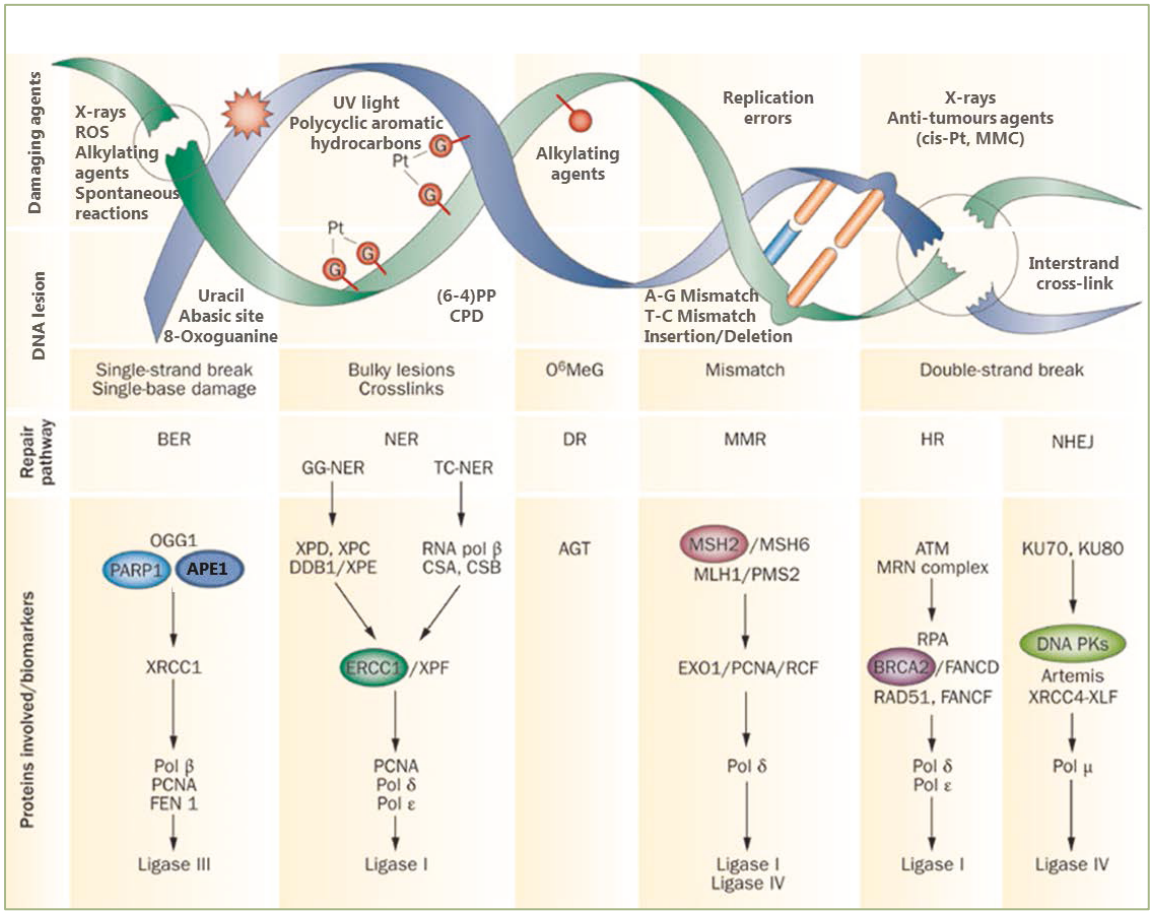

Figure 1: Schematic representation of some common damaging agents, the main DNA lesions induced by these agents and the corresponding DNA repair pathways responsible for the removal of the lesions. The wide range of DNA lesions requires a network of specific DNA repair pathways, selective for each subgroup of damages. For example, DNA damages that do not distort the DNA helix structure, such as abasic sites, oxidative bases and single strand breaks, are usually repaired by BER pathway; DNA lesions, instead, that cause a perturbation in the DNA helix structure, are repaired by NER. The direct removal of a single chemical modified base is operated, in a suicide reaction, by the direct repair enzymes, as AGT. MMR copes with errors introduced during the replication process and HR and NHEJ both deal with double-strand break lesions. While HR is "error-free" Abbreviations: (6-4)PP, 6-4 photoproduct; AGT, O^6-

alkylguanine-DNA alkyltransferase; ATM, ataxia telangiectasia mutated; BER, base excision repair; *cis*-Pt, cisplatin; CPD, cyclobutane pyrimidine dimer; DR, direct repair; GG-NER, global genome NER; HR, homologous recombination; O^6MeG, O^6-methylguanine; MMC, mitomycin C; MMR, mismatch repair; NER, nucleotide excision repair; NHEJ, non-homologous end joining; TC-NER, transcription-coupled NER. (Adapted image from Postel-Vinay S. *et al.*, *Nat Rev Clin Oncol*, 2012)

1.3 APURINIC/APYRIMIDINIC ENDONUCLEASE FACTOR 1 (APE1)

The major mammalian Apurinic/apyrimidinic Endonuclease 1/Redox effector factor 1 (APE1/Ref-1, and from here on referred to as APE1), the mammalian ortholog of *Escherichia coli* Xth (Exo III), is a multifunctional and essential protein protecting cells from oxidative and alkylative insults[14], maintaining genome stability through its DNA repair, redox signalling and gene regulation activities (Figure 2). It is expressed ubiquitously and at high levels in human cells (around 10^4-10^5 copies/cell[15]), although its intracellular localization pattern may appear heterogeneous among different tissues[16]. As suggested by its acronym, it exerts two main functions, the AP endonuclease activity in the BER pathway, that copes with DNA damages induced by oxidative and alkylating agents, through its C-terminus[17] and the redox-dependent transcriptional regulatory activity in modulating the DNA binding activity of different cancer-related transcription factors (i.e. AP-1, NF-kB, p53, Egr-1 and Pax family), function related to its N-terminal domain[16]. The protein C-terminus is highly conserved during phylogenesis, while the N-terminal domain (~ first 40 residues) is not. In contrast with the DNA repair-dedicated domain, conservation of APE1 N-terminus, high in mammals, present wider variability in other organisms, suggesting a potential recent evolutionary acquisition. In the last years, over the past two decades, several efforts were made for understanding the biological functions, mechanisms of action and regulation of APE1. Beside its two principal functions, recent findings have demonstrated an unexpected and novel role for APE1 in the RNA metabolism. With its N-terminal domain, APE1 contacts and interacts with different proteins involved in ribosome biogenesis and pre-mRNA maturation/splicing[18] and it acts as endonuclease towards abasic RNA both *in vitro*[19], as described for the mRNA of c-Myc[20], and *in vivo*[18], thus indicating a possible role in the RNA quality control process[21]. Another poorly characterized APE1 function is the transcriptional regulation of genes by binding in their promoter regions particular negative calcium responsive elements, called nCaRE sequences, present for example in the PTH and in APE1 promoter itself[22]. Being involved in several cellular processes, not only limited to the DNA repair field, a fine tuning of its functions appear necessary. Regardless of transcriptional control, modulation of its interactome network under different conditions and post-translational modifications on some specific residues may modify the chemical characteristic and structural conformation of the protein, redirecting APE1 toward a specific function. Lately, the first 35 amino acids acquired more and more value in the eyes of investigators; until few years ago this disordered extreme N-terminus was considered useful for a proper subcellular localization but dispensable for protein functions. Nowadays, instead, it is emerging a key role of this domain in mediating

protein-protein interactions, with the majority of APE1 binding partners[18], in controlling the catalytic activity on abasic DNA[23] and as acceptor of different post-translational modifications, such as acetylation[23] and ubiquitination[24]. While the functional role has been described for some post-translational modifications, as acetylation at Lys6/7[25], ubiquitination at Lys24/25/27[24] and phosphorylation at Thr232[26], the APE1 interacting partners which could modulate its functions are still under investigations. Notably, dysregulation of APE1, consisting in both its subcellular localization and its overexpression, has been associated to tumor differentiation and aggressiveness[16,27], and the onset of radio- and chemo-resistance[28,29]. Actually, APE1 is considered as a promising therapeutic target for both preventative and curative treatment paradigms. Nevertheless, since its pleiotropic involvement in several cellular processes, the effects of its attenuation by small molecule compounds have to be carefully defined. In this scenario, understanding the molecular mechanism underlying APE1 regulation and biological functions represents an important step towards enhancing the efficacy of cancer treatments.

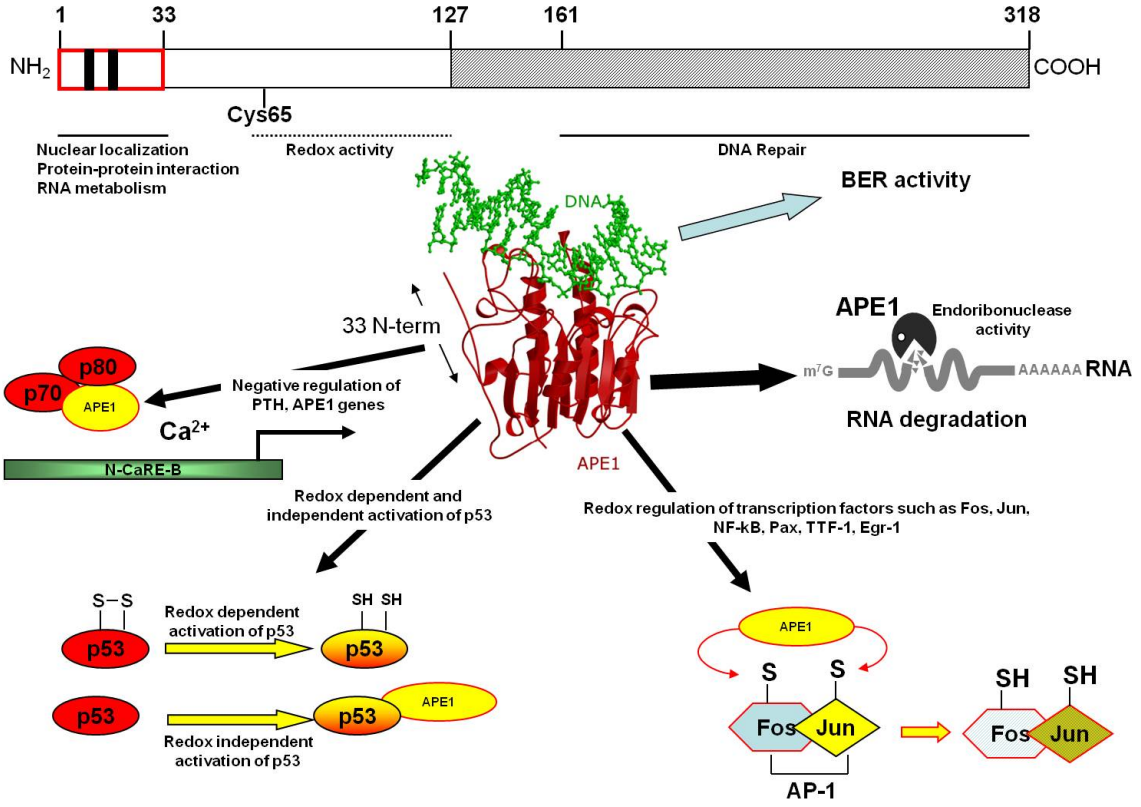

Figure 2: Schematic representation of APE1 structure and its main functions. As highlighted within, key elements in the human APE1 protein are marked: the nuclease domain of APE1 encompasses DNA repair activity while the N-terminus is involved in the transcriptional regulatory functions. The first 33 amino acids are responsible for the nuclear localization, protein-protein interaction and RNA metabolism. APE1 structure (α/β-sandwich) has shown as ribbon representation. The main functions in which APE1 is engaged are depicted; from the top, clockwise, (i) endonuclease activity in BER pathway; (ii) RNA quality control; (iii-iv) redox-dependent and independent transcriptional regulation of several cancer-related factors; and (v) negative transcriptional regulation by binding nCaRE sequences. (Image from Tell G. *et al.*, *Cell Mol Life Sci*, 2010)

1.3.1 APE1 GENE

The human APE1 gene (HAP1 or APEX), located on chromosome 14q11.2-12[30], spans roughly 2.5 to 3 kb of DNA and consists in four introns and five exons, the first of which is not coding. The main mRNA transcript is approximately 1.5 kb in length and is ubiquitously expresses in all tissue and cell types. Lacking a consensus TATA box, it harbors multiple transcription start sites with a CCAAT-like sequence and several putative CpG regulatory elements[31]. The functional basal promoter (approximately 300 bp) and putative recognition sites for several transcription factors within exon 1 (Sp1, USF, AP-1, CREB and ATF) both map in a CpG island. Roughly 3 kb upstream the transcription start site, three negative regulatory elements (one nCaRE-A type and two nCaRE-B type sequences) have been found (Figure 3). Reporter assays performed on deletion mutant suggest that the nCaRE-A sequence might be dispensable for negative regulation; conversely, the nCaRE-B2, able to form complexes with APE1, appears strongly involved in APE1 transcriptional activity, suggesting the existence of an auto regulatory loop in which APE1 binds to its own promoter and ultimately inhibits its transcription[32].

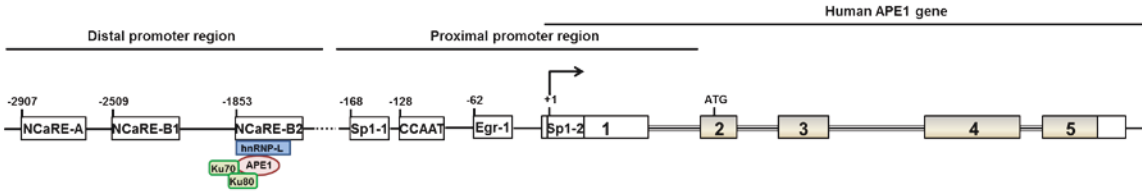

Figure 3: Human APE1 gene structure on chromosome 14q11.2-12. APE1 gene contains four introns and five exons for a total length of 2.7 kb. The coding exons are shaded with the transcription start site marked. The promoter is located in a CpG island; three nCaRE elements map roughly 3 kb upstream the transcription start site. The CCAAT sequence, two Sp1 element and one Egr-1 recognition site are highlighted. Distal promoter region (between -3000 and -1000 from the transcription start site) and proximal promoter region (between -500 and +200 from the transcription start site). (Adapted image from Evans A. R. *et al.*, *Mutat Res*, 2000)

1.3.2 APE1 STRUCTURE AND DOMAIN ORGANIZATION

The APE1 gene encodes a monomeric protein of 318 amino acids with a theoretical molecular weight of 35.5 kDa[17]. As shown by bioinformatic sequence analysis, APE1 is a part of a divalent cation-dependent phosphoesterase superfamily of proteins (EEP family), including for example DNase I and RNase H, by which it shares a similar topology and structure similarity (a conserved four-layered α/β-sandwich structural core)[33]. These proteins maintain a generally conserved catalytic mechanism, but possess specific loop regions and active site elements that account for substrate specificity[31,34]. APE1 is a globular α/β protein, comprising two domains partly overlapping, the N-terminal domain core, packed onto the core of the molecule through a number of hydrogen bond and salt bridge interactions (residues 44-136 and 295-318) and the C-terminus (approximately from residue 60 to residue 260) with overall dimensions of

40x45x40 Å[32,34]. Each domain is composed by six-stranded β-sheet surrounded by α-helices, which pack together to form a four layered α/β sandwich (Figure 4)[34].

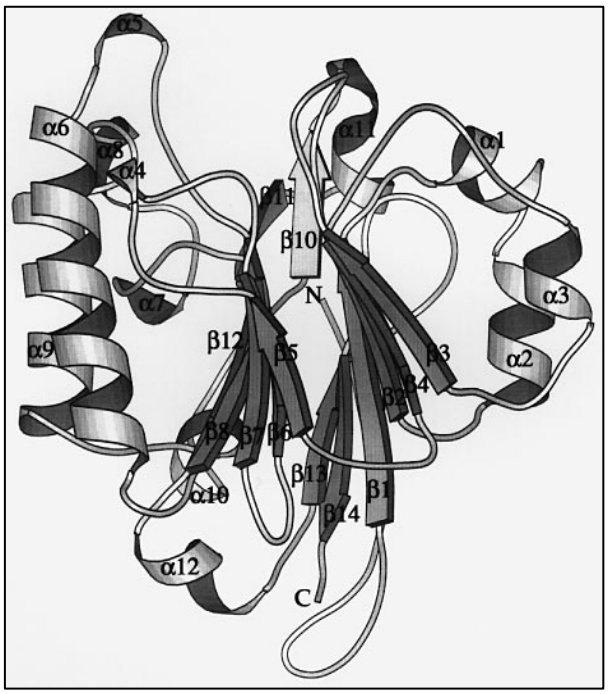

Figure 4: Human APE1 ribbon structure. The conserved four-layered α/β-sandwich structural core consists of two six-stranded β-sheets surrounded by α-helices, packed together. The strand order is β3-β4-β2-β1-β1-β13 for domain 1 and β5-β6-β7-β8-β12-β9 for domain 2. The α-helices and β-strands are numbered sequentially from the N-terminus. (Image from Gorman M. A. *et al.*, *EMBO J*, 1997)

Considering the APE1 biological functions, three functionally independent domains could be recognized:

i. The first 35 N-terminal residues, formed by an unstructured sequence, contains the bipartite nuclear localization signal (NLS) and is required for protein-protein interactions, for RNA binding activities and for coordinating the protein catalytic activity of abasic DNA[18,23];
ii. The classical N-terminus, evolutionary acquired in mammals, that spans roughly from residue 35 to residue 127, is dedicated to the redox activity of APE1;
iii. The C-terminal domain (approximately residue 60 to the end of the protein) encompasses the nuclease activity and is highly conserved from bacteria to humans.

The C-terminal and the N-terminal domain, although independent, present a partial overlapping (residues 61-80 are involved in the DNA repair activity of the protein)[35]. The next paragraphs will be dedicated to the functional division of APE in domains.

1.3.2.1 THE FIRST 33 RESIDUES: A NEW UNSTRUCTURED APE1 N-TERMINAL DOMAIN

Recent evidences pointed to the first 35 amino acids as a new independent APE1 functional and structural subdomain. Crystallographic structure demonstrated that the first 42 residues of APE1 consist of a highly disordered domain[36]. Long disordered segments, called intrinsically disordered regions (IDP), have been observed for a large number of proteins under physiological conditions. These regions are characterized by structural plasticity, feature as multitasking devices, domains whose functions has to be fluid, dynamic and diverse, as common interface for protein binding and acceptor sites for covalent modifications, providing an opportunity for alternative splicing. These peculiarity may provide important functional advantages. Notably, the nonconserved disordered terminal peptide in mammals result essential for several biological functions including damage sensing, repair regulation through post-translational modifications, macromolecule associations and intracellular localization (bipartite NLS)[37]. Their flexibility, in fact, allows them to interact simultaneously with numerous different targets with high affinity and specificity through small common interface, forming dynamic complexes. As shown in literature for several hub proteins as NEIL1[37], this extreme N-terminal domain of APE1 is involved in protein-protein interactions[18], being implicated as a common interaction surface. The positively charged residues located in these N-terminal disordered tails confer the capability to APE1 and other DNA-binding protein to scan the DNA through nonspecific and transient DNA binding, followed by a DNA recognition by the active site[37]. Recently, Yu and colleagues also demonstrated that concomitant with the DNA binding and catalysis, the APE1 structure may encounter local conformational changes of the nucleoprotein complexes, suggesting for the first time that this domain acts as a switch to govern redox and nuclease activity on AP-DNA[38].

1.3.2.2 THE CLASSICAL N-TERMINAL DOMAIN

As discussed in the previous paragraph, the N-terminal domain can be subdivided in two subdomains, the first 35 amino acids, formed by a disordered region and residues comprised between 43 and 65, required for the APE1 redox transcriptional co-activation function, respectively. This section will be dedicated to the latter.

The usage of reduction-oxidation (redox) mechanism to control the DNA binding capability of transcription factors was first suggested for the avian homolog of Jun, a mutant in a conserved cysteine, with acquired oncogenic potential, that demonstrated an increased DNA binding and resistance to oxidizing agents[32]. It is known that the oxidation of the cysteine residue abolishes DNA binding, whereas reduction to a sulphydryl state promotes it. Interestingly, in 1992, Xanthoudakis and Curran identified APE1 as a crucial activator of the DNA binding of transcription factors Fos and Jun, subunits of activator protein 1 (AP-1)[39]. Since this initial identification, APE1 has been documented as redox co-activator for several transcription factors, like p53[35], c-Jun[40], HIF-alpha[41], NF-κB[42], and AP-1[39], facilitating their DNA binding via the reduction of a

critical cysteine residue. This region, that forms an extended loop which lies across the β-strands β13 and β14, contact the globular core of the molecule via numerous hydrogen bond and salt bridge interactions. The crucial residues implicated in the redox activity are Cys65, Cys93 and Cys99, as recently confirmed by Georgiadis and colleagues[40,43]. Cys65 is located on β1 with the side chain pointing into a hydrophobic pocket. Cristallographic analysis and solvent accessibility studies suggested that both the residues are inaccessible to solvent and would be unable to contact directly the cysteine residue target[34,43,44]. Georgiadis and colleagues proposed a model that involves the exposure of Cys65 where APE1 may undergo to conformational change, ceating in this way a binding site that will accommodate the different transcription factors[44]. Further studies are required to understand which factors are capable of stimulating this conformational rearrangement. A recent cascade model have been recently proposed for the formation of disulfide bonds[43].

Besides the redox mechanisms, an alternative redox-independent mode has been described for APE1 activation of transcription factors such as p53[45] and AP-1[35].

1.3.2.3 THE C-TERMINAL DOMAIN

The C-terminal domain is dedicated to the AP-endonuclease activity of the protein. Mutagenesis studies aimed at characterizing the contributions of residues in nuclease activity and sequence alignment analyses comparing *E. coli* ExoIII and human APE1 identified potential conserved residues that could represent the APE1's active site[34,46]. Later, X-ray crystallography analysis by Tainer and colleagues that solved the co-crystal structure of human APE1 protein (a fully active N-terminal truncated protein lacking its first 40 N-terminal amino acids) bound to its natural substrate, an abasic DNA (AP-DNA) and by Rupp and coworkers, that gained more informations about the coordination of the metal ions required and kinetic data, detailed all the residues involved and that contribute to the formation of the active site[36,47]. The active site, located in a pocket at the top of the α/β sandwich and surrounded by loop regions, is composed by different residues (His309, Glu96; Asp283, Thr265, Tyr171, Asn68, Asp210, Asp70 and Asn212), involved in hydrogen bonds. A recent APE1 structure reveals a single Mg^{2+} ion in the active site coordinated by two carboxylate groups (Asp70 and Glu96) and four water molecules, one of which binds to the imidazole of His309, typically referred to as the "A site"; however Drohat and colleagues didn't found any evidence for a second Mg^{2+} ion at the "B site", coordinated through side chains of Asp210, Asn212 and His309, as observed previously[48]. Interestingly, in the enzyme-product (EP) complex, recently determined by Tainer and colleagues, the Mg^{2+} ion is coordinated directly by the carboxylate group of Glu96, the 3'-OH (leaving group), a nonbridging O atom of the nascent 5'-phosphate and by three water molecules, one of which is bound to Asp70[49] (Figure 5). The observations derived from the alignment structure of the EP complex and the DNA-free bound APE1 structure determined by Tainer and coworkers and Drohat and colleagues, respectively, suggest that Mg^{2+} might perform its catalytically essential function(s), including positioning of the target phosphate, polarization of the P-O bond and stabilization of the negative charge developed at 3'-oxygen in the transition state, close to its location in the

free enzyme (Figure 5, *panel A*)[48,49]. Moreover, a water molecule coordinated by Asp210 and Asn212 and activated by Asp210 (in contrast with previous works proposing His309 as a general base for activating the water nucleophile[34,50-52]) in the DNA-free structure by Drohat and coworkers, although not observed by Tainer and collegues[47], seems to be in the right position to serve as nucleophile for hydrolysis of the phosphodiester bond (Figure 5, *panel B*)[48], as suggested by recent molecular-dynamics studies[49]. Nonetheless, the observation that the Asp210-bound and His309-bound waters are not seen in all three active sites proposes that the water molecules found in the active sites are dynamic and that the position of these water molecules in the DNA-free enzyme might change upon formation of the enzyme-substrate (ES) complex[48].

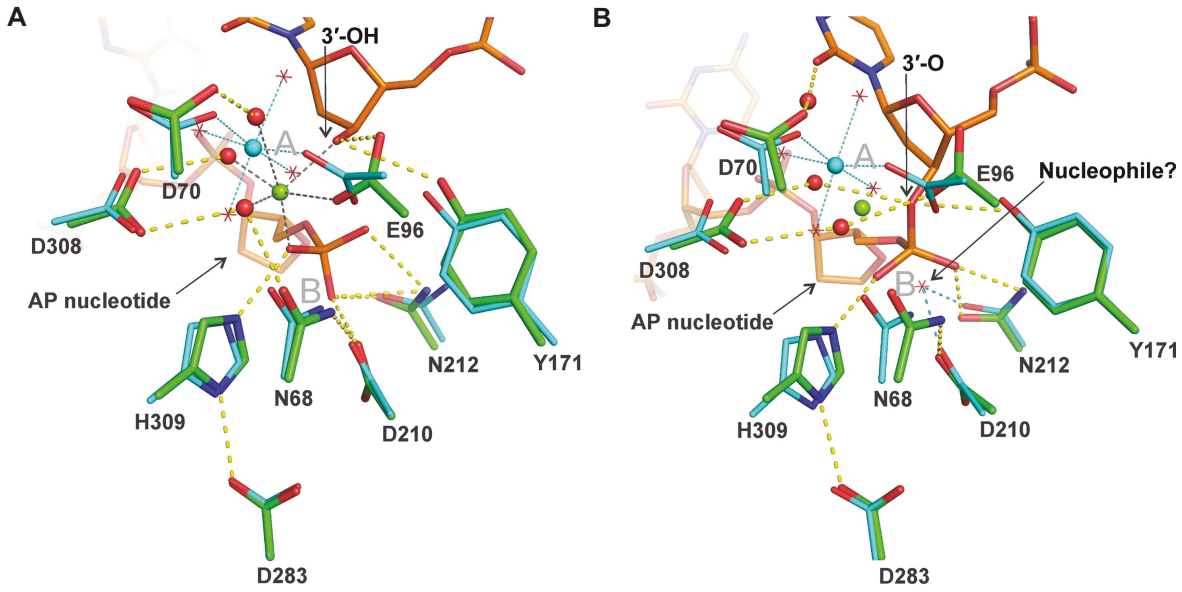

Figure 5: Alignment of $Mg2^{+}$-bound APE1 structure with DNA-bound structures. A | APE1 enzyme-product (EP) complex, recently determined by Tainer and colleagues (green, PDB entry 4iem)[49], aligned with the structure of Mg^{2+}-bound APE1 structure (cyan), identified by Drohat and coworkers[48]. DNA from the EP complex (orange) contains a 3'-OH and a 5'-deoxyribose phosphate (dRP). The conserved catalytic residues are positioned nearly identically in the aligned structures, except for Glu96. **B** | APE1 enzyme-substrate (ES) structure, determined by Tainer and colleagues in 2000 (green, PDB entry 1dew)[47], aligned with the structure of $Mg2^{+}$-bound APE1 structure (cyan), identified by Drohat and coworkers[48]. The DNA in the ES complex (orange) contains an intact abasic site and Mg^{2+} was omitted from the ES complex to halt P-O bond cleavage. The potential nucleophilic water from DNA-free structure by Drohat and coworkers is shown as a red star, with cyan dashes indicating hydrogen bonds to Asp210 and Asn212. This water molecule was also observed in previous structures of APE1 with Sm^{3+} or a single Pb^{2+} ion. The Mg^{2+} ion from the EP complex is colored green and its coordination is indicated by black dotted lines. The Mg^{2+} ion from the new DNA-free structure is colored cyan and its coordination is indicated by cyan dotted lines, with coordinating water molecules shown as red stars. Hydrogen-bond interactions (yellow dashes) are shown for the EP complex (A) and ES (B) structure only. The approximate locations of the A and B sites are noted (gray symbols). (Image from Manvilla B. A. *et al.*, *Acta Crystallogr D Biol Crystallogr*, 2013)

It has proposed that APE1 orients a rigid pre-formed DNA binding surface, positively charged, and penetrates the DNA helix inserting loops in both the major and minor grooves, stabilizing an extra-helical conformation for the target abasic deoxyribose and excluding any normal DNA nucleotide. Although APE1 contacts the DNA from both the grooves, it interacts preferentially with the abasic site-containing DNA strand, binding the abasic site phospates at 5' and at 3'. The resulting APE1-bound DNA is bended

approximately of 35°. Across from the flipped-out abasic site with a unique mechanisms reflecting specific APE1 functions, Met270 and Arg177 insert through the minor and the major groove, respectively, to pack against the orphan base of the abasic site and to provide a hydrogen bond to the AP site 3' phosphate, locking APE1 onto abasic DNA[47]. This model, called "passing the baton", while supported by biochemical and structural data, lacks biological evidence[31]. In spite of these recent evidences illustrating the APE1 active site and giving light on the stoichiometry and the role of Mg^{2+} in APE1-catalyzed reactions[48,49] and our understanding of how APE1 specifically recognizes AP sites, the catalytic mechanism used by APE1 to cleave the phosphodiester backbone remains controversial. Further studies are needed to delineate the precise APE1 catalytic process.

1.3.3 APE1 BIOLOGICAL ACTIVITIES

As already hinted at first, APE1 exerts a crucial role in maintaining genome stability as major apurinic/apyrimidinic endonuclease in mammals. Its functions in redox signaling and in regulation of gene transcription make APE1 considered as a multifunctional protein with unique properties that are beyond the classical DNA repair enzyme. In the next paragraph, the major APE1 canonical (DNA repair and redox chaperone functions) and non-canonical activities (RNA cleavage and trans-acting modulation) will be concisely described.

1.3.3.1 DNA REPAIR THROUGH PARTICIPATION IN BER PATHWAY

A common type of DNA lesion is arranged by abasic sites, that threaten cellular viability and genomic integrity, blocking DNA replication and being cytotoxic and mutagenic[32]. They arise as a consequence of spontaneous hydrolysis of the N-glycosylic bond connecting the deoxyribose sugar moiety and the DNA base, as result from the activity of DNA glycosylases and they are generated by exogenous or/and endogenous DNA damaging agents. Therefore cells have evolved an intricate mechanism to preserve the fidelity of the genetic material and remove baseless lesions. The base excision repair (BER) pathway is committed to the removal of small, non-helix distorting base lesion, restoring the chemical DNA integrity. Different base lesions are sensed by BER, that converts them into a common intermediate, the AP sites, which then are recognized and processed by APE1. Subsequent steps follow either of two distinct BER subpathways, the short (SP-BER) or long patch repair (LP-BER), that replaces one or 2-13 nucleotides, respectively[53,54].

The BER pathway can be described as a process of five sequential steps (Figure 6):

i. recognition and excision of the inappropriate base moiety (e.g. 8-oxo-dG),
ii. incision of the DNA backbone adjacent to the resulting abasic site,
iii. clean-up of the DNA termini to generate a 3′-hydroxyl group (3′-OH) and a 5′-phosphate moiety (5′-P),

iv. repair synthesis to replace the missing nucleotide(s), and

v. DNA ligation to seal the remaining nick.

As just mentioned, the initial step of BER involves the catalytic activity of DNA glycosylases, which hydrolyze the N-glycosylic bond connecting the targeted base with the deoxyribose sugar moiety. The product of this reaction is an abasic site. Currently, there are two major classes of glycosylases; the monofunctional ones excise the damaged base, exhibiting only the glycosylase activity, whereas the bifunctionals, which are glycosylases/β-lyases, cleave via β- or βδ-elimination the damaged base from the deoxyribose moiety and nick the phosphodiester backbone, leaving a 3′-phospho-α,β-unsaturated aldehyde (3′-PUA) or a 3'-phosphate (3'-P), respectively[55,56]. Afterwards, in mammalian cells, APE1 recognizes the AP sites and nicks, via a Mg^{2+}-dependent mechanism, the phosphodiester backbone 5' to the AP sites, leaving a 3'-hydroxyl group (3'-OH) and a 5'-deoxyribose phosphate (dRP) termini flanking the nucleotide gap. Before the repair synthesis step, the elimination of the obstructive 3'- and 5'-termini to generate the 3'-OH and 5'-P termini, which are the normal substrate for DNA polymerases, is required. These termini, in fact, prevent primer extension by DNA polymerases and nick ligation by DNA ligases[31]. APE1 is responsible for removing the 3'-phospho-α,β-unsaturated aldehyde by β-elimination via its 3'-phosphodiesterase activity, while DNA polymerase β (DNA Pol β) removes the 5'-dRP moiety through its 5'-dRP lyase activity. Since the 3'-phosphate is a poor substrate for APE1, these blocking groups are processed *in vivo* by the phosphatase activity of PNKP[56].

At this point, repair can proceed along with one of the two BER subpathways (SP- or LP-BER), which rely on a different set of repair proteins and depend on the AP state. Normal AP sites are repaired via SP-BER whereas several sites or modified ones are corrected by LP-BER[32]. In the SP-BER, DNA Pol β excises the 5'-dRP moiety and inserts a single nucleotide. Then, the complex formed by DNA ligase III and XRCC1 completes the repair by sealing the resulting nick. The LP-BER, instead, covers the strand displacement of two or more nucleotides surrounding the AP sites. In this case, the repair synthesis might be accomplished by polymerase β, δ or ε in a process that requires additional factors, sometimes not even acting directly on DNA, such as proliferating cell nuclear antigen (PCNA), replication factor C (RF-C) and Poly(ADP-ribose) polymerase (PARP1), able to bind immediately to an incised AP sites for recruiting other BER factors[57,58]. Following the replacement of the missing nucleotides, flap endonuclease 1 (FEN1) removes the 5'-dRP terminus containing displaced strand. The repair is complete only when DNA ligase I restores the phosphodiester backbone[32].

Although BER is composed by five distinct steps, in which the DNA molecule is passed from one enzyme to the next one in a "passing the baton" scheme, model corroborated by macromolecule associations, that avoids the exposure of the DNA to the cellular environment, recent evidences of a "irrational" binding priority irrespective of the "passing the baton" model propose the existence of a multi-protein repair complexes, that require a tight coordination[59]. Even if how these steps are orchestrated is still under

investigation, a clear APE1 function in coordinating BER pathway, interacting directly or not with other BER factors, such as glycosylases, DNA Pol β and XRCC1, has emerged[60-63]. The molecular basis of the specificity, the exact role and the biological significance of these interactions remains to be determined.

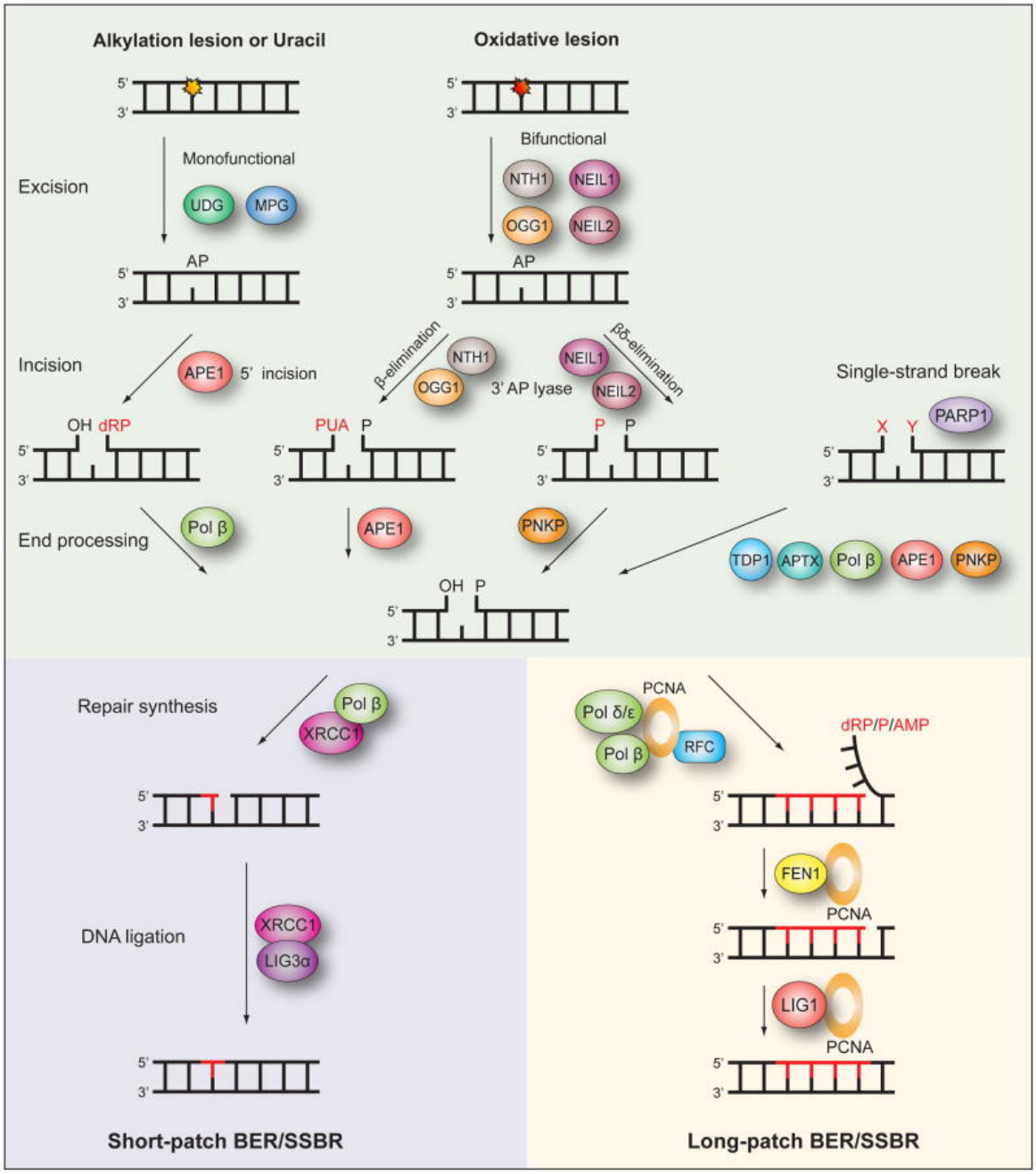

Figure 6: Base excision repair pathway. Base excision repair (BER) is initiated by removal of the modified base by either a monofunctional or bifunctional DNA glycosylase to leave an abasic site (AP). Excision by either one of the monofunctional DNA glycosylases (UDG or MPG) is followed by incision of the DNA backbone 5′ to the AP site by APE1. Excision by one of the bifunctional DNA glycosylases NTH1, OGG1, NEIL1 or NEIL2 is followed by incision 3′ to the AP site via β- or βδ-elimination facilitated by the intrinsic 3′ AP lyase activity of these enzymes. The resulting single-strand break will contain either a 3′ or 5′ obstructive termini. End processing is then performed by Pol β, APE1 or PNKP depending on the specific nature of the terminus. PARP1 recognizes single strand breaks and the end processing may utilize the additional factors tyrosyl phosphodiesterase 1(TDP1) and aprataxin (APTX). When end processing has produced the necessary 3′-OH and 5′-P termini the following BER and single-strand break repair (SSBR)

steps diverge into two subpathways, short-patch and long-patch. In short-patch BER/SSBR repair synthesis of the single nucleotide gap is by Pol β aided by the XRCC1 scaffold, and subsequent ligation by LIG3α finishes the repair. In long-patch BER/SSBR repair synthesis of the 2–13 nucleotide gap is by Pol β, and/or Pol δ/ε aided by PCNA and RFC. A resulting 5′ flap is removed by FEN1 and the the final ligation step is by LIG1. (Image from Jeppesen D. K. *et al.*, *Prog Neurobiol*, 2011)

1.3.3.2 REDOX REGULATION

Oxidative stress threatens all living aerobic organisms, resulting in macromolecular damage to lipids, carbohydrates, proteins and nucleic acids with deleterious consequences (i.e. loss of function or DNA mutation)[64] and is associated with different diseases such as cancer, neurodegeneration and aging[65]. It refers to the imbalance due to excess of reactive oxygen species (ROS) over the capability of the cell through enzymatic and non-enzymatic systems to sense the oxidants and to mount an effective antioxidant response[66]. Reactive oxygen species are generated mainly during mitochondrial oxidative metabolism; any enzyme able to process oxygen may give arise to ROS. Paradoxically, beside the toxic effects, ROS play a critical role as signaling molecules, altering the cellular and extracellular redox state, in a broad variety of cellular processes as cellular proliferation and survival, DNA damage response and gene regulation. A large body of research demonstrates a general effect of oxidative stress on gene expression via direct modulation of transcription factors activity, regulation mediated by the redox state of thiol groups exposed by critic cysteine residues, located within the DNA binding domain of the transcription factors. At first, independent studies have identified APE1 as factor able to stimulate the binding activity of several transcription factors through a redox-dependent mechanism[39]. Since this first report, several transcription factors, both ubiquitous (e.g. NF-κB, Egr-1, p53, CREB, HIF-1α) and tissue-specific (e.g. TTF-1 and Pax proteins), with opposite effects on cell fate, have been reported to be modulate by APE1[67]. Interestingly, it is likely that APE1 could select, in response to specific stimuli, which transcription factors regulate, binding them with different efficiencies. It has been proposed that APE1 might regulate the binding activity of transcription factors via regulation of the cysteine state, located in the DNA binding domain or domains critical for their activity, maintaining them in a reduced state by direct interaction (Figure 7)[63,68,69]. Three possible mechanisms, not mutually esclusive, may explain the APE1 redox chaperone activity. In the so called recruitment model, APE1 may facilitate the reduction of the transcription factors by bridging them to the reducing molecule (GSH or Trx). Second, in the conformational change model, APE1 may induce a conformational change in the target factor, rendering accessible the cysteine residues otherwise buried in the structure. Third, in the oxidation barrier model, APE1 may stabilize the reduced state, preventing the oxidation, via formation of hydrogen bond with thiol groups[69]. The detailed molecular steps for the activation of the transcription factors by APE1 remain to be largely investigated. Up to now, however, none of APE1 cysteine has been found in a C-X-X-C motif, common to most redox regulatory factors, such as thioredoxin (Trx), which is implicated in the redox APE1 cascade restoring APE1 in a reduced form[31,70]. Several evidences propose Cys65 as the redox-active site for APE1[40,44]; however, 3-dimensional structure demonstrates that none of the APE1 cysteine residues are located in

a right position and distance for forming a disulfide bond with Cys65, a prerequisite for resolving activity of redox factors. Moreover, both Cys65 and Cys93, residues identified as responsible the redox regulation, are buried within the APE1 structure, being surface inaccesible, whose activities may be influenced by partial APE1 unfolding[43]. Recently, Georgiadis and coworkers have proposed a new model based on current knowledge, suggesting that APE1 is a unique redox factor with properties distinct from those of other redox factors. In this model, (i) Cys65 acts as nucleophile for the reduction of the disulfide bond in the target factor, (ii) Cys93 operates as resolving residue and (iii) APE1 undergoes a significant partial unfolding to expose a third cysteine residue, probably Cys99, to facilitate the redox reaction[43]. Further works are needed to delineate the precise molecular mechanism of the reaction.

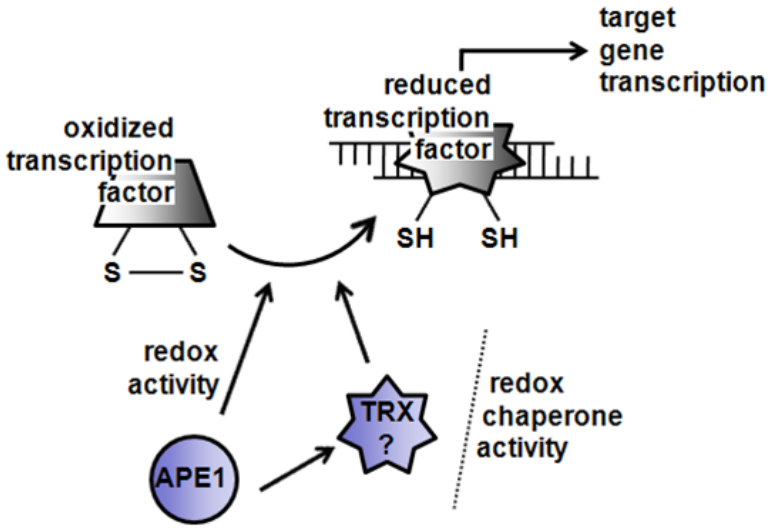

Figure 7: APE1 redox chaperone activity. Schematic representation of APE1 redox chaperone activity. Cysteine residues, located within the DNA binding domain or regulatory domain of transcription factors, are maintained in a reduced state by APE1, involved in a redox cycle with reducing molecules as Trx. The detailed mechanism by which APE1 control via redox the activity of the transcription factors needs further experiments. (Image from Tell G. *et al.*, *Cell Mol Life Sci*, 2010)

1.3.3.3 RNA CLEAVAGE

As its bacterial counterpart, human APE1 possesses, even if at a lesser extent (~400 fold lower activity), RNase H activity[71]. Although Hickson and colleagues showed any general nuclease activity towards single- or double-stranded RNA, they found that with low affinity APE1 could bind, through Asp219, to intact single- and double-stranded nuclei acid substrates and that the presence of an abasic site did not modify the strength of these interactions[71]. Although RNA is oxidized to a greater extent than cellular DNA due to its intrinsic nature and to its relatively higher amount[72], up to now how cells cope with damaged RNA is still uncertain. What is clear is that such damaged RNA can impair protein synthesis, affecting cell function and viability. The existence of surveillance mechanism for RNA has been put forward from the identification of the biochemical activities of the mammalian homolog of AlkB (hABH3) against alkylated RNA[72], but a possible mechanism for oxidized RNA has not been found yet. The recent and

independent findings of Vascotto *et al.*, Barnes *et al.* and Berquist *et al.* have indicated a direct role for APE1 in RNA metabolic pathways[18-20]. Recent work has found that APE1 can cleave abasic single-stranded RNA molecules, depending on their molecule conformation, possibly participating in a RNA quality control mechanism[18,19]. Notably, beside the direct binding between APE1 and RNA molecules, a growing body of evidences demonstrates that APE1 is able to interact with a variety of protein involved in RNA metabolism, as YB1[73] and hnRNP-L[74], suggesting a role for APE1 in RNA metabolism. The ability to cleave AP site-containing RNA indicates that APE1 could remove damaged RNA from the endogenous pool, being a perfect candidate for a novel RNA cleansing mechanism[19]. Notably, APE1 knock-down leads to an impaired 8-hydroxyguanine containing rRNA removal, affecting cell growth and gene expression by directly acting on RNA quality control mechanisms[18]. Another way by which APE1 affects gene expression has been recently described by Lee and colleagues; they identified APE1 as endonuclease involved in the cleavage of the coding region determinant (CRD) of the c-myc mRNA, resulting in a impaired transcript turnover through mRNA decay[20]. Further analysis based on structure-function comparison reveals that APE1 reuses most of the active sites residues (i.e. Glu96 and His309), excluding Asp283, used for its AP-DNA cleavage to promote RNA incision, requiring a 2'-hydroxyl group on sugar moiety for the catalysis and generating a 3'-phosphate terminus[75].

Altogether, all these data support a direct APE1 involvement, previously unknown, in RNA metabolism; additional studies are needed to test the biological role for its RNA cleavage function *in vivo* and to determine its contribute to mRNA turnover, analyzing the enzyme specificity for particular mRNA or if its RNA substrates might be other types of RNA, affecting a broad variety of cellular functions.

1.3.3.4 TRANS-ACTING MODULATION

In addition to its function as redox regulator of several transcription factors, APE1 has been identified as a component of a trans-acting complex that bind to negative Ca^{2+} response element (nCaREs, type A and B), modulating gene expression. These elements were first identified in the promoter region of the human parathyroid (PTH) gene and only later in the APE1 promoter itself[22,76]. In particular, the mobilization of Ca^{2+} from the storage tissues leads to an increased APE1 protein level with a consequent augmented assembly in trans-activating complex to nCaREs of the PTH gene, promoting a gene suppression and activating a negative feedback mechanism[22]. The presence of nCaREs in APE1 promoter indicates that APE1 could suppress its own gene transcription in a negative feedback loop, representing the first example of such self-regulatory mechanism for a DNA repair enzyme[74]. Evidences that APE1 is not able to directly bind to nCaREs suggest the requirement of additional factors for a cooperative binding, later identified in the two subunits of the Ku antigen, p70 and p80[77], and hnRNP-L protein[74]. Moreover, the complex formation of APE1 with the promoter elements is controlled by the acetylation status of two lysine residues (Lys6 and Lys7): an increase of extracellular calcium concentration induces p300-dependent APE1 acetylation, resulting in increased APE1

binding to nCaREs[25]. Specific post-translational modifications as acetylation may act as a switch to redirect the protein towards a specific function and interaction. Recent bioinformatic analyses, looking for other human genes regulated by APE1 through nCaREs binding, identified 57 new gene, broadening the spectrum of genes APE1 could control. Among these, the sirtuin-1 deacetylase (SIRT1), involved in cell stress responses and in the deacetylation of APE1 after genotoxic stress[78], has been studied; in particular APE1 stably binds through its N-terminus the two nCaREs located within the SIRT1 promoter in a complex including hOGG1, Ku70 and RNA Polymerase II recruited during early oxidative stress response, providing new insights into the role of nCaRE and APE1 in the transcriptional regulation[79]. Further work are needed to better determine if APE1 has a broader role in controlling gene expression via nCaREs or other promoter sequences.

1.3.4 MODULATION OF APE1 SEVERAL FUNCTIONS

As multifunctional protein, APE1 could play a critical role in determing the cell fate participating in several cellular mechanisms. For this reason, a fine-tuning of its functions is needed. There are several ways by which cells modulate the activity of a protein, redirecting it towards a specific biological function. Generally regulation can be accomplished at five possible levels, resulting summarizied in:

i. Transcriptional regulation of a gene;
ii. Post-transcriptional modulation refers to all the mechanism of maturation, trafficking and degradation controlling the fate of mRNA. For APE1, no examples of editing or alternative splicing have been reported;
iii. Post-translational modifications such as phosphorylation, acetylation and proteolysis, a rapid and reversible covalent chemical modification for regulating protein functions directly on the final protein product, switching on or off specific protein's activities;
iv. Changes in macromolecule associations establishing a different interactome network may address a protein towards another specific function. These protein assemblies contain highly coordinated moving parts, and within each protein assembly, all reactions are carried out one after the other in a very precise and coordinated way, so that reactions can usually proceed only in one direction[80];
v. Intra cellular trafficking in compartments other than the nucleus (i.e. cytoplasm and mitochondria), enhancing or reducing some protein activity, masking its natural substrate due to compartimental sequestration.

In the next paragraphs, the main APE1 regulatory mechanisms will be briefly described.

1.3.4.1 TRANSCRIPTIONAL REGULATION OF APE1 GENE

As already mentioned in "APE1 gene" paragraph, several potential recognition sites for different factors (Sp-1, USF, CREB, ATF and AP-1) have been revealed by *in silico* analyses[16], even if two independent works demonstrate any effect for AP-1 binding site

on gene transcription[81,82]. Later on, Demple and colleagues demonstrated a strong correlation between APE1 transcription and cell cycle progression; in particular, the APE1 mRNA levels rise after the G_1-S transition with a pick (~ 4 fold) in early to mid-S phase due to Sp1-2 dependent transcriptional activation in response to cell growth and not increased mRNA stability[83]. Afterwards, although no putative p53 binding sites have been retrivied by *in silico* analyses, a p53 binding element has been located upstream the transcription start site, close to the CCAAT box, since a p53-dependent downregulation of APE1 mRNA level has been suggested by Bhakat and coworkers[84]. The authors hypothesized that p53 might be indirectly recruited to APE1 promoter through a physical interaction with Sp1 bound to Sp1-1 element, inhibiting the basal APE1 gene transcription[84]. These data suggest a stimulating hypothesis about an inversal relationship between nuclear p53, as pro-apoptotic factor, and APE1 level, as pro-survival protein. Notably, in tumors p53 downregulation, due to gene mutations, corresponds to augmented APE1 expression, mechanism that could be at the basis of tumor chemotherapy resistence[84].

Besides the regulation of APE1 gene transcription under basal conditions, several reports are available in literature concerning mechanisms of inducible activation of APE1 gene, such as following stimulation with hormones (i.e. TSH)[85] and subtoxic doses of ROS[86-88]. Although the molecular mechanisms of ROS-induced transcriptional activation are not still detailed, some authors successfully associate CREB[89] and Egr-1[90] factors, already implicated in activation of ROS-responsive genes, in APE1 activation, with a recognition site for both the factors upstream the APE1 transcription start site. Future studies will better determine the range of this type of regulation.

Finally, APE1 gene contains also negative regulatory sequence upstream the transcription start site, the nCaREs sequences, one of type A and two of type B. As already hinted at first, deletion of nCaRE-A sequence does not suppress the expression of a reporter gene, suggesting that this element appears dispensable for APE1 regulation. Conversely, the deletion of nCaRE-B2 sequence strongly influnces the negative regulation of a reporter gene[76]. Moreover, APE1 stably binds nCaRE-B2 sequences forming complexes. Overall, these data indicate the existence of a possible negative loop by which APE1, bound to this element, could inhibit its own expression.

1.3.4.2 POST-TRANSCRIPTIONAL MODIFICATIONS

Post-translational modifications are covalent chemical modifications occurring on proteins and represent a rapid and reversible mechanism to modulate their activities within the cellular environment. Regarding APE1, the knowledge of post-translational modifications affecting and coordinating its functions has exponentially grown in the last years. Up to now, six different types of post-translational modifications (acetylation, phosphorylation, ubiquitination, S-nitrosation, proteolysis and redox regulation) occurring *in vivo* have been described and might explain the mechanisms and the stimuli involved in switching on and off specific activities of the protein.

In Figure 8, several of the post-translational modifications occurring on APE1 *in vivo* are depicted. Major details for APE1 PTMs will be discussed throughout.

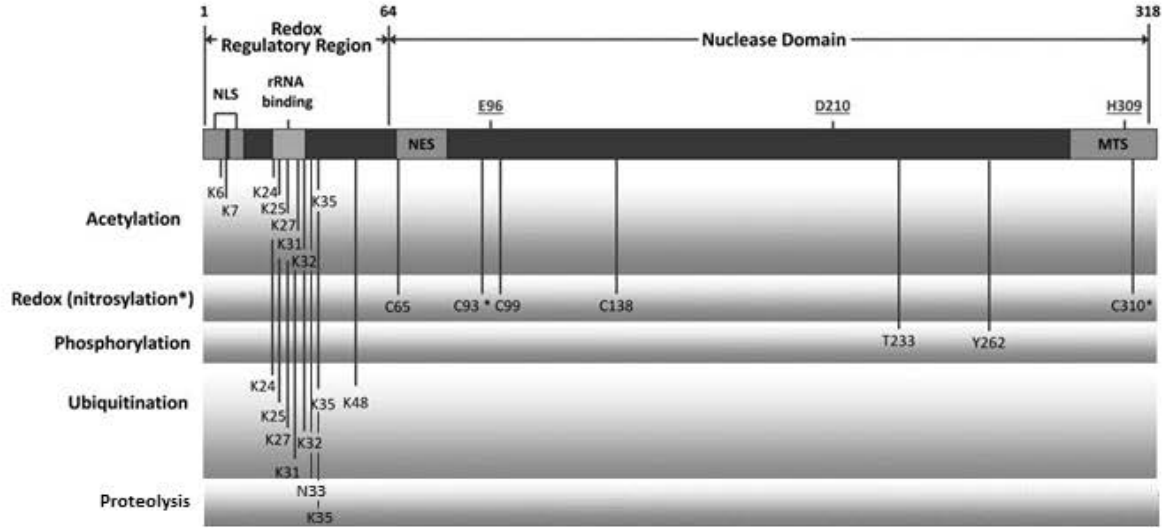

Figure 8: APE1 post-translational modifications. Schematic linear representation of the key post-translational modification acceptor sites on human APE1. The sites of acetylation, S-nitrosylation, phosphorylation, ubiquitination and proteolysis have been precisely mapped on APE1 sequence. The nuclease domain spans roughly from residues 64 to 318, with some over-lap with the N-terminus, dedicated to the redox regulatory function. Key active site residues for the nuclease activities of APE1 (Glu96, Asp210 and His309) are highlighted. NLS, nuclear localization signal; NES, nuclear export signal; MTS, mitochondrial targeting sequence. (Adapted image from Li M. and Wilson, D. M. 3rd, *Antioxid Redox Signal*, 2013)

1.3.4.2.1 ACETYLATION

To date, APE1 acetylation is the most studied post-translational modification for this multifunctional protein. Despite the elevated number of lysine residues, twenty-nine along all its sequence, only lysines 6 and 7 have been identified as target of acetylation by the histone acetyl transferase p300 both *in vitro* and *in vivo*[25]. The authors demonstrate that acetylation at these residues enhance binding of APE1-histone deacetylases (HDAC) complex to the nCaRE sequences within the parathyroid hormone (PTH) promoter, suggesting an important role for APE1 transcriptional regulatory function[25]. Recent data from our group and from Irani and colleagues show that other stimuli, as oxidative or genotoxic stresses, different from extracellular calcium level that was demonstrated to stimulate p300[25], are capable to induce APE1 acetylation at early times[78,91]. Notably, few years later, Tell and coworkers demonstrate that four lysine residues (Lys27, 31, 32 and 35), located within the N-terminus of the protein, crucial for APE1 interaction with rRNA and NPM1 and for controlling its catalytic activity on abasic DNA, are acetylated *in vivo*[23]. Moreover, as discussed in the Results paragraph of this work of Thesis, we show that APE1 acetylation at Lys27-35 is induced by genotoxic stress and influences the APE1 subnuclear distribution[92].

In spite of the identification of p300 as the main histone acetyl transferase responsible for APE1 acetylation *in vivo*, scanty information regarding the deacetylation process are available. In the paper of Mitra and coworkers, the authors suggest the involvement of a

class I HDAC enzyme[25]. More recently, Irani *et al.* show that Sirtuin 1 (SIRT1), the closest mammalian ortholog of yeast Silent Information Regulator 2 (Sir2) and component of a class III HDAC, may deacetylate APE1 at Lys6 and 7 both *in vitro* and *in vivo*, shutting down, in a feedback mechanism, the cellular response mediated by APE1 acetylation[78]. In fact, in concomitance with APE1 acetylation at Lys6 and 7 induced by genotoxic stress, SIRT1 expression level increases. Activation of SIRT1 promotes an augmented APE1-XRCC1 complex formation suggesting that SIRT1 plays an important role in maintaining genome stability[78]. Taken together, different groups raise the hypothesis that after genotoxic stress, p300 activity prevails over SIRT1, leading to increased APE1 acetylation. Later, probably when the lesions are completely removed, SIRT1 activity, prevailing over p300 one, restore the basal APE1 acetylation levels. Intriguingly, SIRT1 promoter contains two nCaRE sequences, stably bound by APE1 through its N-terminus. APE1 forms a complex with the glycosylase OGG1, Ku70 and RNA polymerase II is recruited on SIRT1 promoter for promoting gene transcription under genotoxic stresses, suggesting for the first time a positive role for APE1 transcriptional regulatory activity[79]. However further evidences are required to confirm this feedback loop mechanism; moreover, the identification of the acetyl transferase involved in APE1 acetylation at Lys27-35 has still to be addressed.

1.3.4.2.2 NITROSYLATION

Nitric oxide (NO) is a highly reactive free radical, that plays a crucial role in different signaling pathways, both cGMP-dependent and independent, the latter involving S-nitrosation[93,94]. S-nitrosation is a ubiquitous redox-related modification of cysteine thiols by nitric oxide and has been implicated in multiple cellular activities as regulation of gene transcription[95], protein nuclear translocation[96] and enzyme activity[97]. APE1 contains three redox-sensitive cysteine residues; two of these sites (Cys93 and Cys310) may undergo S-nitrosation after nitric oxide stimulus and are responsible for APE1 reversible shuttling from nucleus to cytoplasm in a non canonical CRM1-independent manner[98]. In addition, the authors show that under nitric oxide condition, importin-mediated nuclear import systems were repressed, mechanism which may prevent cytosolic APE1 from re-entering into the nucleus[98]. The effect of APE1 nuclear export may negatively reflect on its endonuclease and redox regulatory activities, connecting APE1 to nitric oxide physiological and pathological processes, as recently demonstrated for non-small cell lung cancer (NSCLC)[99,100]. It remains to elucidate which stimuli and signaling pathways could be associated with nitric oxide production within cells and APE1 cytoplasmic relocalization.

1.3.4.2.3 PHOSPHORYLATION

Several putative phosphorylation sites, located in both the nuclease and the redox regulatory APE1 domains, have been identified *in vitro* for a broad range of kinases, as Casein Kinase 1 and 2 (CK-I and CK-II), Glycogen Synthase Kinase 3 (GSK-III) and Protein Kinase C (PKC). Phosphorylation may occur on serine/threonine residues[86] and

might be responsible in controlling macromolecule (protein-protein and protein-DNA) associations involved in redox regulation and in DNA repair[101]. Early works demonstrate that although *in vitro* phosphorylation by CK-I and PKC has no effect on APE1 endonuclease activity, CK-II dependent phosphorylation at residues Thr19, Ser123, or Thr233 strongly abolished the DNA repair activity[102]. An *in vivo* phosphorylation CK-II mediated has been also suggested even if never experimentally demonstrated[103]. In addition, the usage of specific CK-II inhibitors *in vivo* did not confirm *in vitro* results. Despite its ineffectiveness on nuclease activity, PKC-dependent phosphorylation might be involved in an augmented APE1 redox activity, hypothesis supported by *in vitro* and *in vivo* studies, since it has been found to increase *in vitro* binding of c-Fos and c-Jun to AP-1 binding elements. Moreover, according with these data, following oxidative stress, a stimulus known to induce PKC, *in vivo* studies have shown that APE1 phosphorylation level increased, stimulating its redox activity, though the phosphorylation target site has not been identified yet[101]. Up to date, the biological relevance of these findings has not been established.

More recently, in agreement with a previous study[102], Park and colleagues found that APE1 was phosphorylated at Thr233 *in vivo* by threonine kinase CDK5, a paralog of CDK2/4, resulting in reduced endonuclease capability. CDK5 is expressed in neurons and is speculated to be involved in cell death triggered by uncontrolled DNA damage replication. High levels of APE1 phosphorylated at Thr233 was observed in post-mortem brain samples from Alzheimer's and Parkinson's patients. The APE1 inactivation due to CDK5 mediated phosphorylation and consequent accumulation of DNA damage contributes to neuronal death, profoundly affecting the severity of the diseases[104]. Up to now, it is not clear if the phenotype observed might be associated with the solely endonuclease activity or if other functions might be responsible for it. Further works are needed to understand the molecular mechanism of APE1 funtions in neuronal death and its role in neurodegenerative diseases.

1.3.4.2.4 UBIQUITINATION

The conjugation of ubiquitin, an evolutionary conserved small protein of seventy-six residues, to other cellular proteins regulates a broad range of eukaryotic cell functions. An E3 enzyme catalyzes the formation of an isopeptide bond between the substrate (or ubiquitin) and ubiquitin, tagging and targeting it to the proteasome when poly-ubiquitinated[105]. The destruction of proteins is as important as their synthesis for cellular homeostasis. Other functions, not involving the proteasomal system, have been discovered. Mono-ubiquitination, in fact, could act at different level altering protein function or localization[106]. For the first time in 2009, Izumi and colleagues show that both *in vitro* and *in vivo* the E3 ligase MDM2 (murine double minute 2), a negative regulator of p53, ubiquitinate APE1 at one of these Lys residues (24, 25 or 27)[24]. Moreover, oxidative conditions can induce MDM2-mediated ubiquitination of APE1. For the authors, the mono-ubiquitination of APE1 may induce a cytoplasmic translocation[24], data in contrast with several papers in literacture affirming a role for oxidative stress to induce

a net APE1 movement toward the nuclear compartment. Two years later, the same group gave further insights in the APE1 ubiquitination process, reporting an interesting cross-talk between ubiquitination and phosphorylation of APE1 at Thr233[26]. In particular, phosphorylation of APE1 may induce MDM2 activity, leading to augmented ubiquitination of APE1. The mono-ubiquitinated form, in contrast with the previous work, localized in the nucleus[26]. Moreover, a recent paper of Dianov's group identified, through *in vitro* ubiquitination studies, UBR3 as the main enzyme that poly-ubiquitinated APE1 at multiple targets within the N-terminal domain, proposing an important role for UBR3 in the control of the steady state levels of APE1[107]. Up to now, no information are available about the kinetic of APE1 ubiquitination upon oxidative stress; further work has to be done to better clarify the occurrence of ubiquitination *in vivo*.

1.3.4.2.5 PROTEOLYTIC CLEAVAGE

A truncated form of APE1 lacking its first N-terminal 33 or 35 amino acids, lately named APE1 NΔ33, was first identified by Pommier *et al.*, who isolated a 34 kDa, Mg^{2+}-dependent endonuclease from apoptotic human promyelocytic leukemia HL-60 cell line, characterized for its ability to incise DNA generating single strand breaks[108]. Only few years later, the same authors demonstrated that this enzyme was a truncated form of APE1, resulting from a cleavage at its N-terminus by an unidentified trypsin-like enzyme, activated during caspase-3 apoptotic process[109]. An independent study conducted by Lieberman's group involved APE1 in granzyme-induced caspase-independent cell death, characterizing APE1 as a component of the SET complex, an endoplasmic reticulum (ER)-associated DNA repair complex recruited to the nucleus in response to oxidative stress. Within the SET complex, APE1 is targeted by a highly homologous serine protease, contained in cytotoxic granules of innate and adaptive immune killer cells[110], the granzyme A (GzmA). GzmA cleaves APE1 at Lys31 during cell-mediated death and this cleavage blocks APE1 binding to DNA and suppresses APE1 redox regulatory and its AP endonuclease activities[111]. Cells overexpressing a noncleavable form of APE1 result more resistant to GzmA-mediated cell death, supporting their hypothesis. The authors conjectured that cleaving the N-terminus of APE1, GzmA may block cellular repair, favouring the apoptotic process[111]. Few years later, another component of the granzyme family, granzyme K (GzmK), has been associated as responsible for APE1 cleavage at the N-terminus. GzmK is able to induce the formation of reactive oxygen species, accumulation that triggers a cell death program. In this light, since APE1 can antagonize reactive oxygen species, suppressing the cell death, APE1 cleavage by GzmK facilitates intracellular reactive oxygen species accumulation, enhancing the GzmK-induced cell death[112]. Notably, all the groups identified a role for the APE1 truncated form (APE1 NΔ33) in two different cell death pathways (caspase-dependent and GzmA/K-induced) as factor responsable for accumulation of single strand breaks on nuclear DNA. Nevertheless, previous evidences on APE1 deletion mutants show that the APE1 NΔ33 maintains both the AP endonuclease and redox functions and did not display any additional nuclease activity[40]. To date, further studies are needed to elucidated the mechanisms responsible for the APE1 NΔ33 nuclear translocation, since the truncation

leads to the loss of the nuclear localization signal. Recently, APE1 NΔ33 has been proved to localize in the cytoplasm of some cell types, within the mitochondria, where it may act as a specific AP endonuclease involved in mitochondrial BER pathway[113]. A mitochondrial targeting sequence has been recently discovered at the C-terminus of APE1 (residues 289-318), which is normally masked by the intact N-terminal structure[114]. Although interesting, more recent observations contested the accumulation of the truncated form within mitochondria, showing that the prevalent form within mitochondria is the full length and suggesting a central role of Cys65 in redox-assisted folding of APE1 and internalization *in vivo*[115].

In conclusion, the truncation of the N-terminal of APE1 has been associated with different cell death programs, being extremely interesting. This irreversible post-translational modification may represent a regulatory switch for controlling APE1 functions. Up to now, many unresolved question remain to be answered, regarding the identification of the proteases, the stimuli responsible for the generation of the truncated form and the effects of such modification on APE1 cellular translocation.

1.3.4.3 APE1 INTERACTOME NETWORK

Biological processes encompass a concerted action of multi-protein molecular machineries rather then subsequent isolated enzymatic steps. Understanding the network in which a protein operates may better elucidate its role and the process involved. However, so far information about interactome of APE1 was very limited, especially because sensitivity of available techniques was still quite poor. Our group, by using a inducible cell model based on HeLa cells, in which endogenous APE1 is replaced by an ectopic FLAG-tagged form, has recently identify the APE1 interactome network under basal condition and characterized the role of the first 33 N-terminal residues in stabilization of this interacting network[18]. Unexpectedly, most of the new APE1 interacting partners are involved in ribosome biogenesis and RNA processing as NPM1, PRP19 and YB1. During this analysis, what emerged was that the APE1 33 N-terminus is required for a stable interaction with the majority of APE1 binding partners, including NPM1 and RNA. NPM1 stimulates APE1 endonuclease activity on abasic double-stranded DNA, decreasing its activity on abasic single-stranded RNA by masking the N-terminus, required for a stable association with the nucleic acid. Moreover, APE1 silencing does not alter pre-rRNA synthesis and rRNA processing, but affects the total capability of the cell to deal with RNA oxidation; thus suggesting that genotoxic stress may reduce NPM1 affinity for APE1, allowing it to act as a cleansing factor on abasic RNA. In Table 1 all the APE1 interacting partners retrived in literature are listed. It is possible clusterized APE1 binding partners in different groups concerning their main fuction or pathway in which they are involved.

- Group 1. Enzymes involved in DNA repair pathways, in particular base excision repair (e.g. XRCC1, PCNA, FEN1 and Polβ) and double-strand break repair (Ku70 and PRP19) pathways;

- Group 2. Proteins responsible for recognizing damaged nucleic acids (both DNA and RNA molecules), such as OGG1, hS3 and YB1;
- Group 3. Proteins involved in redox or redox-chaperone activities of APE1 (i.e. Trx, PRDX6);
- Group 4. Proteins target of APE1-mediated redox regulation, comprising several transcription factors that physically bind APE1 as p53 and ERα;
- Group 5. Enzymes that account for APE1 post-translational modifications like MDM2, CDK5, SIRT1 and p300;
- Group 6. Proteins involved in RNA metabolism as YB1 and hS3, that are included also in other groups. Within the same group we could find factors involved in rRNA metabolism or in ribosome biogenesis (NPM1 and RLA0), in pre-mRNA maturation or splicing (hnRNP-L and PRP19) and enzymes operating in general ribonucleotides metabolism and synthesis pathways (PRPS1 and PRPS2);
- Group 7. Proteins involved in signal transduction and cytoskeleton remodeling, like K2C8, TWF2 and CAPSN1;
- Group 8. Proteins responsible for cell cycle progression and control as TCEB1, POLR3D and TERF1/2.

All these interacting networks that encompass diversified cellular pathways, among which the newly discovered RNA metabolism, suggest an important role for APE1 as central hub within cells.

Table 1: APE1 binding partners

Protein	Function	References
Ku Antigen (p70 and p80)	Double-strand breaks repair of DNA	[77]
Pol β	Polymerase in base excision repair of DNA	[62]
p53	Tumor suppressor protein that responds to diverse cellular stresses to regulate expression of target genes, inducing cell cycle arrest, apoptosis, senescence, DNA repair, or changes in metabolism	[116]
Thioredoxin (Trx)	Cytoplasmic redox-sensitive signaling factor, that facilitates protein–nucleic acid interactions	[117]
FEN1	Base excision repair of DNA	[118]
PCNA	Base excision repair of DNA	[118]
hMYH	Glycosylase in base excision repair of DNA	[119]
XRCC1	Base excision repair of DNA	[61]
hnRNP-L	pre-mRNA splicing, involved in regulating chromatin modification	[74]
HDACs	Histone deacetylases, involved in transcriptional gene repression	[25]
SET	Associated with the endoplasmic reticulum (ER), involved in the nuclear single-stranded DNA nicking in GzmA induced apoptosis	[111]
MDM2	E3 ubiquitin ligase for p53	[24]
GzmA	Released by T- and NK- cells; induces a caspase-independent cell death pathway with	[111]

Protein	Function	References
	morphological features of apoptosis	
HMG2	Involved in facilitating cooperative interactions between cis-acting proteins by promoting DNA flexibility and in DNA end-joining processes of DNA double-strand breaks repair and V(D)J recombination	[111]
NM23-H1	Involved in cell proliferation, differentiation and development, signal transduction, G protein-coupled receptor endocytosis, and gene expression	[111]
GzmK	Protects the host by lysing cells bearing on their surface 'nonself' antigens, usually peptides or proteins resulting from infection by intracellular pathogens	[112]
MPG	Methylpurine glycosylase, involved in base excision DNA repair	[120]
hS3	Binds to 8-oxoG residues on DNA	[121]
OGG1	DNA glycosylase involved in base excision DNA repair	[60]
Rad9/Rad1/Hus1	DNA damage sensing and signaling pathways; the complex plays also a direct role in various DNA repair processes	[122]
YB1	It may bind Y-box elements on DNA; it is involved in DNA repair pathways; it may bind ssDNA, and RNA molecules as well; it protects mRNA against degradation; it binds to 8-oxo-G containing RNAs	[73]
SIRT1	Class III histone deacetylase; it is a stress response and chromatin-silencing factor, involved in various nuclear events such as transcription, DNA replication, and DNA repair	[78]
ERα	Transcription factor; hormonal ligand, 17β-estradiol facilitates the interaction of the receptor with estrogen-response elements (EREs) on DNA	[123,124]
NPM1	Hub protein within nucleolus: it may organize and interact with many other nucleolar proteins; involved in ribosomal protein assembly and transport; involved in control of centrosome duplication, and in the regulation of the tumor suppressor ARF	[18]
TCP1-alpha	Molecular chaperone that is a member of the chaperonin containing TCP1 complex (CCT)	[18]
KRT8	Keratin, type II; part of the cytoskeleton	[18]
PRP19	DNA double-strand break (DSB) repair and premRNA splicing	[18]
RSSA	Belongs to the ribosomal protein S2P family	[18]
MEP50	Component of the 20S PRMT5-containing methyltransferase complex, which modifies specific arginines to dimethylarginines in several spliceosomal Sm proteins	[18]
RLA0	Acidic ribosomal protein, rich in hydrophobic amino acid residues	[18]
PRPS1 and PRPS2	Phosphoribosylpyrophosphate synthetase 1 and 2	[18]

Protein	Function	References
PRDX6	Redox regulation of several biological processes and in protection under oxidative injuries	[18]
TDG	Thymine-DNA glycosylase in base excision DNA repair	[125]
DNA Lig I	Function in DNA replication, recombination, and the base excision repair process	[126]
TCEB1	Activates elongation by RNA polymerase II by suppressing transient pausing of the polymerase at many sites within transcription units	[127]
TXNRD1	Reduces thioredoxins and plays a role in selenium metabolism and protection against oxidative stress.	[127]
TWF2	Actin-binding protein involved in motile and morphological processes	[127]
AID	The ability of activation-induced cytidine deaminase (AID) to efficiently mediate class-switch recombination (CSR)	[128]
ANP32A and ANP32C	Tumor suppressor pp32 that can inhibit several types of cancers	[111]
RNF4	Inhibit the activity of TRPS1, a transcription suppressor of GATA-mediated transcription	[129]
TRAF2	Required for TNF-alpha-mediated activation of MAPK8/JNK and NF-kappaB and functions as a mediator of the anti-apoptotic signals	[130]
STAT3	Mediates the expression of a variety of genes in response to cell stimuli, and plays a key role in many cellular processes such as cell growth and apoptosis. The small GTPase Rac1 has been shown to bind and regulate the activity of this protein	[131]
p300	Histone acetyltransferase that regulates transcription via chromatin remodeling	[25,132]
ARIH2	E3 ubiquitin-protein ligase mediating 'Lys-48'-and 'Lys-63'-linked polyubiquitination and subsequent proteasomal degradation of modified proteins	[127]
CCDC124	Required for proper progression of late cytokinetic stages	[127]
hnRNP-K	Associated with pre-mRNAs in the nucleus and appear to influence pre-mRNA processing and other aspects of mRNA metabolism and transport. It binds tenaciously to poly(C). This protein is also thought to have a role during cell cycle progession	[127]
PABP1	Binds to the 3' poly(A) tail of eukaryotic messenger RNAs via RNA-recognition motifs, promoting ribosome recruitment and translation initiation; it is also required for poly(A) shortening which is the first step in mRNA decay	[127]
GAL1	Beta-galactoside-binding proteins implicated in modulating cell-cell and cell-matrix interactions	[127]
CAPNS1	Calcium-dependent, cysteine proteases. It has been implicated in neurodegenerative processes, as their activation can be triggered by calcium influx and oxidative stress	[127]
NAE1	Binds to the beta-amyloid precursor protein and	[127]

Protein	Function	References
	plays a role in the pathogenesis of Alzheimer's disease. In addition, it can activate NEDD8, a ubiquitin-like protein. This protein is required for cell cycle progression through the S/M checkpoint	
RIC8A	Involved in regulation of microtubule pulling forces during mitotic movement of chromosomes	[127]
hnRNP-UL1	Binds specifically to adenovirus E1B-55kDa oncoprotein. It may play an important role in nucleocytoplasmic RNA transport	[127]
SK2	Bifunctional enzyme with both ATP sulfurylase and APS kinase activity, which mediates two steps in the sulfate activation pathway	[127]
PSMG1	Chaperone protein which promotes assembly of the 20S proteasome as part of a heterodimer with PSMG2	[127]
XPOT	Mediates export of tRNA from the nucleus to the cytoplasm	[127]
Cdk5	Proline-directed serine/threonine-protein kinase essential for neuronal cell cycle arrest and differentiation	[104]
SUMO1 and SUMO2	Binds to target proteins as a post-translational modification system and is involved in a variety of cellular processes, such as nuclear transport, transcriptional regulation, apoptosis, and protein stability	[133,134]
Ubiquitin C	It has been associated with protein degradation, DNA repair, cell cycle regulation, kinase modification, endocytosis, and regulation of other cell signaling pathways	[135]
HIF-1 alpha	Master regulator of cellular and systemic homeostatic response to hypoxia by activating transcription of many genes	[136]
NUDT3	Nudix proteins act as homeostatic checkpoints at important stages in nucleoside phosphate metabolic pathways, guarding against elevated levels of potentially dangerous intermediates, like 8-oxo-dGTP, which promotes AT-to-CG transversions	[137]
Ubc9	Ubiquitin-conjugating enzyme; involved in the protein degradation of Ref-1	[138]
APP	Bind to the acetyltransferase complex APBB1/TIP60 to promote transcriptional activation	[139]
ASCL2	Member of the basic helix-loop-helix (BHLH) family of transcription factors. It activates transcription by binding to the E box. Involved in the determination of the neuronal precursors in the peripheral nervous system and the central nervous system	[132]
HOX3	Important role in morphogenesis in all multicellular organism	[140]
POLR3D	It leads to a block in progression through the G1 phase of the cell cycle at nonpermissive temperatures	[140]

Protein	Function	References
TCF21	Transcription factor of the basic helix-loop-helix family. The TCF21 product is mesoderm specific	[140]
TRF1 and TRF2	Function as inhibitors of telomerase, acting in cis to limit the elongation of individual chromosome ends	[141]
TERF21P	Complex involved in telomere length regulation	[141]
SMD1	Act as a charged protein scaffold to promote SNRNP	[142]
SFPQ	DNA- and RNA binding protein, involved in several nuclear processes and in regulation of signal-induced alternative splicing	[142]
Rev	Involved in the late phase of virus replication	[143]
AP-4	Activates both viral and cellular genes by binding to the symmetrical DNA sequence CAGCTG	[144]
HHV8GK18_gp81	Maintenance of episomal genome	[145]
CKII	Casein kinase II is a serine/threonine protein kinase that phosphorylates acidic proteins	[103]
p21	Regulator of cell cycle progression at G1; regulatory role in S phase DNA replication and DNA damage repair	[146]
Hsp70-1	Stabilizes existing proteins against aggregation and mediates the folding of newly translated proteins in the cytosol and in organelles. It is also involved in the ubiquitin-proteasome pathway	[147,148]
HMGA-1	Non-histone protein involved in many cellular processes, including regulation of inducible gene transcription	[149]
HMGA-2	Architectural factors and essential component of the enhancesome. It may act as a transcriptional regulating factor.	[149]
SRPK1 and SRPK2	Protein kinase that plays a role in regulation of both constitutive and alternative splicing by regulating intracellular localization of splicing factors	[150]

1.3.4.4 INTRA-CELLULAR TRAFFICKING AND SUBCELLULAR LOCALIZATION

Alteration of subcellular localization of a protein may represent an important way to control its functions. For a multifunctional protein that exerts both nuclear and extranuclear function, it could be important to elucidate the molecular mechanisms involved in APE1 translocation within the different cellular districts. As main AP endonuclease enzyme and regulatory protein acting on several cancer-related transcription factors, APE1 has long been recognized as nuclear protein. In the 2005, Izumi and colleagues identified the nuclear localization signal harbored within the APE1 N-terminus: it consists in a bipartite signal within the first twenty amino acids (residues 2-7, with a classic NLS, and residues 8-13, where two critical acidic amino acids, Glu12 and Asp13, fall)[151]. Despite the nuclear targeting sequence, a large number of studies indicated that in some cell types, with elevated metabolic and proliferative rates, APE1 may localized within mitochondria and endoplasmic reticulum[16,152]. Except for the

mitochondrial APE1, which biological significance is emerging, the role of the protein in the other districts and its clinical significance are not fully understood yet.

Stimuli as oxidative stress and other signaling molecules such as TSH or calcium have been shown to trigger APE1 nuclear translocation[86,87]. Moreover, as already mentioned in the previous paragragh, APE1 is targeted by different proteases forming a truncated form, named APE1 NΔ33, that lacks both NLS sequences. Despite the deletion of the NLS sequences, APE1 NΔ33 results not completely excluded from nuclei[18], suggesting that additional mechanisms, not yet fully elucidated, may compensate for the absence of a classic NLS and regulate the subcellular distribution of APE1. Recently, beside the nuclear localization, Tell and coworkers show a strong nucleolar pattern for APE1, maybe through protein-protein and protein-nucleic acids interaction[18]. Intriguingly, other BER enzymes such as XRCC1 and FLAP1 endonuclease have been found to accumulate in this subnuclear district[153], raising the question whether nucleolus acts as a storage site for DNA repair proteins or whether they carry out an active repair function within nucleoli, maintaining a proper ribosome biogenesis (Poletto *et al.*, submitted to MBoC).

APE1 cytoplasmic distribution has been demonstrated, raising the hypothesis that in some circumstances APE1 need to be sequestered from nuclei; but, the exact mechanism responsable for redirecting APE1 in this subcellular compartment remains to be clearly elucidated. Up to now, a classic nuclear export sequence (NES) has not been found yet. However, two recent papers identify a possible mechanisms for explaining the cytoplasmic translocation. Firstly, S-nitrosation at Cys93 and Cys310 has been demonstrated to redirect APE1 in the cytoplasm in a CRM1-dependent manner[98]; secondly, a mitochondrial targeting sequence has been retrived in the APE1 C-terminal domain (residues 289-318)[114]. Besides its extranulear role in controlling intracellular ROS production through modulation of Rac1-regulated NADPH oxidase[154], APE1 localizes within mitochondria. Mitochondria are the main cellular source of ROS, resulting from the mitochondrial respiratory chain and oxidative phosphorylation. Given its proximity to the respiratory chain and its vulnerable status, contrarily from the nuclear genome, mitochondrial DNA (mtDNA) is continuously exposed to high levels of ROS. Thus, it has not been surprising the observation of different groups regarding the existence of a DNA base excision repair (mtBER) within mitochondria[155-157]. Along with the mtBER apparatus, also APE1 has been found in mitochondria. Although a first study hypothesized that the truncation of the N-terminal domain of the protein allows the protein to be imported in mitochondria[113], a more recent paper shows that in different cell types APE1 full length is imported within mitochondria, possibly through a mechanism that involved a distinct machinery composed by Mia40 and Erv1 via an oxidation-driven process[115,158].

All togheter these data suggest that the subcellular APE1 distribution is very dynamic (Figure 9). However further studies are needed to elucidate the molecular mechanisms responsible for APE1 intracellular trafficking.

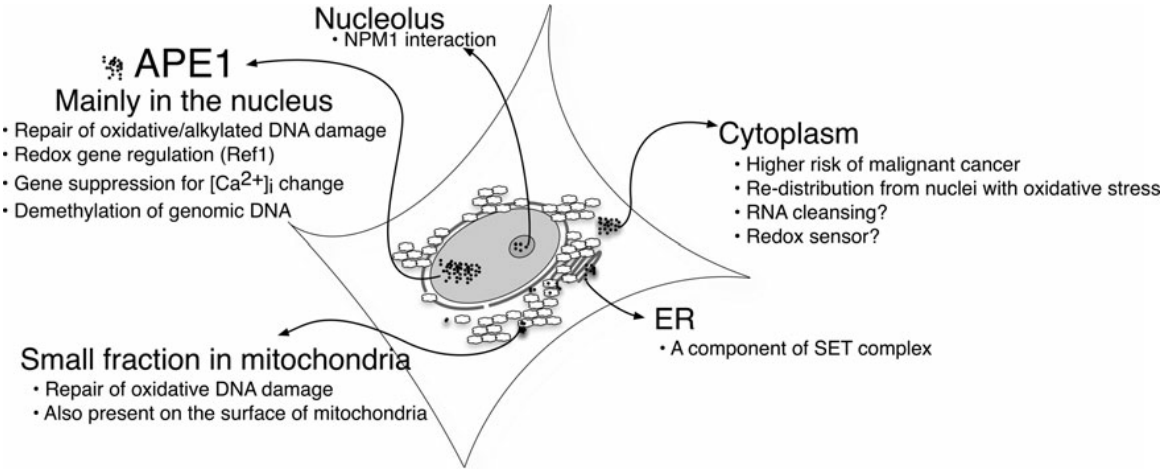

Figure 9: APE1 intracellular trafficking. APE1 subcellular distribution appears very dynamic. The main subcellular compartments where APE1 have been identified and its influence on cell physiology are highlighted. (Image from Scott T. L. *et al.*, *Antioxid Redox Signal*, 2013)

1.3.5 APE1 IN DISEASE

As already mentioned, APE1 is a fundamental protein: deletion of both the alleles of Apex1, similarly to that of other core enzymes in BER pathway, leads to embryonic lethality in mice[159] and triggers apoptosis in differentiated cells[160], thus suggesting its biological and clinical relevance in normal and tumoral cells. Defects in its activities, although the exact contribution of each function to the deficiencies observed has not been discerned yet, has been linked to human pathologies, ranging from cancer to neurodegenerative diseases. Accumulation of oxidative stress and inefficient base excision DNA repair have been described as clinical feature of several degenerative disorders, including neurophatologies as Alzheimer disease (AD), Parkinson disease (PD) or amyotrophic lateral sclerosis (ALS)[161,162]. Several observations suggest a relationship between APE1 and cancer etiology. APE1 deficiences leads to augmented mutagenesis and carcinogen susceptibility; moreover, overexpression or dysregulation in terms of atypical subcellular localization, usually within cytoplasm, have been found in many cancers types, including prostate, pancreatic, ovarian, cervical and colon type[31,163]. What are the causes of the increased APE1 levels or of the subcellular distribution pattern observed in several cancer types are largely unknown; what is becoming clear and clearer are the consequences. In these tumors, an elevated nuclear level of APE1 correlates with aggressive proliferation, reduced sensitivity to chemotherapeutic agents and poor prognosis[28]. Additionally, in some tumors, APE1 is predominantly cytoplasmic. Since cancer cells present an high metabolic rate, producing elevated amounts of reactive oxygen species as result of the mitochondrial oxidative phosphorylation, an intriguing hypothesis concerning a possible role for APE1 in response to ROS for maintaining the mtDNA integrity has been put forward[154]. Elucidating the molecular mechanisms of an altered APE1 expression signifies a crucial step for a better treatment for specific cancer types. Nowadays, APE1 represents a predictive marker for sensitivity of the tumor toward radio- or chemotherapy and a promising target for pharmacological treatment. Even though efforts to determine the effects of inhibiting either the DNA repair or redox

regulatory functions are still ongoing and the extra-nuclear activities are not fully elucidated, several studies suggest that a consequence of the increase AP activity accompanying tumorigenesis might account for therapy resistance. Besides the genetic variants that have been correlated with repair capacity (see "Genetic variants" section), thus, APE1 inhibitors could be used alone or in combination with other chemotherapeutic agent such as bleomycin, temozolomide or gemcitabine to enhance the cytotoxic effects[164]. Few compounds were already reported as APE1 redox (soy isoflavones, resveratrol and E3330) and DNA repair (CRT0044876, lucanthone, methoxyamine, compound 3 and 52) inhibitors (for an exhaustive review of APE1 inhibitors, the reader is redirect to Abbotts R. and Madhusudan S., *Cancer Treat Rev*, 2010)[163,165]. Though for some of these, in particular for methoxyamine, an indirect APE1 inhibitor, the preclinical and clinical evidence is promising, for Abbotts and Madhusudan a direct targeting of APE1 may represent a better strategy[163]. Further studies are needed to identified new potent APE1 small molecule inhibitors, specific for one function of the protein, and to evaluate the side effects of combination therapies with APE1 inhibitors. In conclusion, APE1 biological relevance is reflected by its involvement in human pathologies and therapeutic approaches aimed to block a specific APE1 activity are very promising.

1.3.5.1 GENETIC VARIANTS

DNA repair capability differs among individuals. Estimates suggest that between 10-30% of the normal population may be "sensitive" to DNA injuries. This is a fact. But, which is the cause of this disparity? The answer to this question is still a matter of debate. Case-control studies have drawn attention to the correlation between the risks of bladder, kidney, esophageal and lung cancer, and who exhibit higher levels of oxidative DNA damage[166]. For sure, with the improvement of sequencing techniques, investigators went one step further in the understanding the phenotypes observed within the population. The presence of single-nucleotide polymorphisms (SNPs) in regulatory regions of DNA repair genes might be responsible for impacting on phenotype, usually resulting in reduced DNA repair capacity[167]. In humans, defects in BER have been linked to cancer risk, immunological dysfunction and neurodegenerative disease[166,168]. Nonetheless, APE1 deficiencies have not been clearly associated to disease initiation and progression[31]. Lack of core BER components as APE1, Polβ and XRCC1 leads to embryonic or post-natal lethality in mice[169], probably correlated with elevated DNA damage accumulation resulting in aborted development[170]. Therefore, since complete homozygous knock-out of BER enzymes is incompatible with life, mild reduction in BER capability might be associated with disease risk and susceptibility. In the latest year, thanks to many re-sequencing efforts, several genetic variants of APE1 (Figure 10) and other DNA repair genes, that potentially represent reduced-function alleles, have been identified within the normal and disease population[31,166,167]. Analysis of the current sequence associated with computational studies evidences that (i) rare mutations, with a frequency lower than 3%, account for more than 75% of the total and (ii) about one third of the genetic variants identified are predicted to be adversely impacting on structure and function[166]. In some instances, the SNP or the mutation identified alters coding sequence of the gene, resulting

in a modification of an amino acid. The synonymous variations and the nucleotide differences observed in the untranslated regions or promoter regulatory elements will not be a matter of this paragraph.

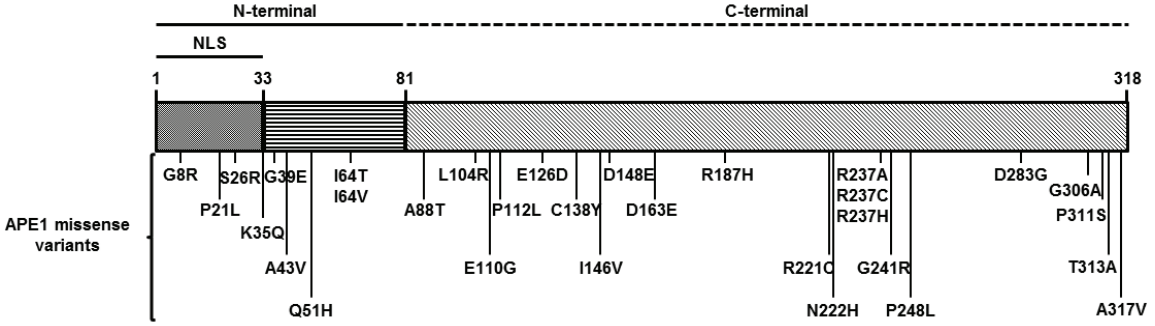

Figure 10: APE1 missense variants identified so far. Schematic APE1 representation; within the linear structure, the genetic APE1 variants and their reciprocal position are highlighted. NLS, nuclear localization signal.

Nowadays, it still unclear the effect of the sequence variation on the AP-endonuclease activity and the DNA repair capability; however, it has been hypothesized that these genetic variants might lead to changes in mRNA stability, translation efficiency or protein structure/function, indicating a role for APE1 polymorphisms in disease progression or initiation, leading to an increased disease susceptibility within the population. In fact, as its vital role in development, APE1 genetic variants, with impaired APE1 functions, might be involved in cancer etiology[31].

To identify and examine the consequences of these missense variants in the APE1 gene, several studies began. One of the best known sequence variants is an amino acid change from aspartic acid to glutamic acid (D148E) in exon 5, currently associated with cancer risk[31,166,167]. Other reports described APE1 missense mutations (L104R, E126D, D148E, D283G and G306A)[171] in cases of sporadic amyotrophic lateral sclerosis (ALS), but it was then contradict by later screenings[166]. A clear picture of the existence of association between APE1 polymorphisms and cancer disease has not been found yet. Table 2 summaries all the data retrieved by literature about potential associations to date.

Table 2: APE1 missense variations and their correlation with the pathogenesis.

APE1 missense variation	Pathology	Association/Frequency	References
D148E	Breast cancer	Increased hypersensitivity to ionizing radiation may contribute to breast carcinogenesis. Larger studies have not supported this association	[172-177]
L104R, E126D, D148E, D283G and G306A	Amyotrophic lateral sclerosis (ALS)	8/11 patients displays APE1 variants. Mutated APE1 might be implicated in the pathogenesis of ALS	[171]

APE1 missense variation	Pathology	Association/Frequency	References
D148E	Amyotrophic lateral sclerosis (ALS)	D148E may contribute to ALS etiology	[178]
D148E	Amyotrophic lateral sclerosis (ALS)	No association observed	[179]
D148E	Parkinson's disease (PD)	Positive correlation with PD risk	[180]
D148E	Alzheimer's disease (AD)	No association with AD	[181]
P112L and R237C	Endometrial tumor	3/20 patients exhibit APE1 polymorphisms. Role for these mutation for cancer developmental	[182]
Q51H and D148E	Ovarian and endometrial cancer	Authors found a frequency of 4.8% for Q51H and of 56.2% for D148E	[182]
Q51H and D148E	Prostate cancer	In association with XRCC1 variant, increased cancer risk in white men population. No association for black men	[183]
D148E	Lung cancer	Synergistic effect with tobacco carcinogen-induced lung cancer risk (gene-environment interaction)	[184]
D148E	Cutaneous melanoma (CM)	No association. significantly Observed a decreased risk of CM in D148E samples	[185]
D148E	Squamous cell carcinoma of the head and neck (SCCHN)	No altered risk for D148E patients	[186]
D148E	Spina bifida and oral clefts	Decreased risk for spina bifida; no association for oral clefts	[187]
I64V and D148E	Non-small cell lung cancer (NSCLC)	The variant I64V has a protective effect towards NSCLC; no association for D148E	[188]
D148E	Bladder cancer	No overall association. In stratified analyses a positive association with risk was observed with an increasing number of D148E alleles among never smokers, but not among smokers.	[189]
D148E	Vitiligo	Increased risk with D148E in Chinese population	[190]
D148E	Lung cancer and lung adenocarcinoma	Increased lung cancer risk in Asians and smokers; association with decreased lung adenocarcinoma risk	[191]
D148E	Cancer	No evident association	[192]
D148E	Lung cancer	Significant association observed; increased risk of lung	[193]

APE1 missense variation	Pathology	Association/Frequency	References
		cancer in Caucasians	
D148E	Colorectal cancer	Significant association observed; increased risk of colorectal cancer in Turkish population	[194]
D148E	Colorectal cancer	D148E is associated with the susceptibility, but not with the prognosis in Chinese population	[195]
D148E	Bladder cancer	Not associated with bladder cancer risk among Asians nor non-Asians.	[196]
D148E	Non-small cell lung cancer	D148E displayed a decreased risk of p53 mutation in non-small cell lung cancer.	[197]
D148E	Lung cancer	Not associated with lung cancer risk among Asians or Caucasians. D148E shows an increased risk factor for developing lung cancer among smokers	[198]
D148E	Gastric cancer	Marker for the development of gastric cancer in Chinese population	[199]
D148E	Cancer	D148E polymorphism does not contribute to the development of cancer.	[200]
D148E	Lung cancer	D148E may not be directly associated with lung cancer risk, nor enhance the effects of smoking habit on lung cancer development in Taiwan population	[201]
D148E	Nasopharyngeal carcinoma (NPC)	The combined effects of polymorphisms within BER genes of XRCC1 and APE1 may contribute to a high risk of NPC	[202]
D148E	Breast cancer	Associated with an increased risk of breast cancer. Combined effect of different SNPs within BER genes may be useful in predicting breast cancer risk in Korean population	[203]
D148E	Breast cancer	Two-way SNP-SNP interactions (APE1 D148E and RPAP1-rs2297381) conferred elevated risks for breast cancer	[204]
D148E	Coronary artery disease (CAD)	No association for D148E as risk factor	[205]
D148E	Endometrial carcinoma	D148E may be associated with endometrial carcinoma in Turkish population	[206]

APE1 missense variation	Pathology	Association/Frequency	References
D148E	Cutaneous melanoma	Not associated with cutaneous melanoma risk	[207]
D148E	Acute myeloid leukemia (AML)	No association with AML risk	[208]
D148E	Non-small cell lung cancer	An association with treatment response was suggested for D148E	[209]
D148E	Childhood acute lymphoblastic leukemia	No significant association observed	[210]
D148E	Chronic atrophic gastritis	No significant association observed	[211]
D148E	Lung cancer	Small but non significant increased risk of lung cancer in Chinese population	[212]
D148E	Malignant melanoma	No significant association observed	[213]
D148E	Prostate cancer	Any association was found. D148E may be indicated as a potential marker for prostate cancer risk.	[214]
D148E	Gastric cancer	Increased association for gastric cancer	[215]
D148E	Bladder cancer	Increased risk. D148E may contribute to susceptibility	[216]
D148E	Pre-eclampsia	Any significant association	[217]
D148E	Bladder cancer	Any significant association	[218]
D148E	Glioblastoma	Any significant association	[219]
D148E	Breast cancer	D148E was identified as risk factor for breast cancer susceptibility in Asian population	[220]
D148E	Primary open angle glaucoma (POAG)	D148E may decrease the risk of POAG progression in Polish population	[221]
D148E	Biliary tract cancer and biliary stones	D148E may alter susceptibility to biliary tract cancer and stone. Further studies required to confirm the data	[222]
D148E	Lung cancer	D148E was significantly associated with a poorer overall survival	[223]
D148E	Pancreatic ductal adenocarcinoma	Significant increase risk for carriers of D148E in Caucasians	[224]
D148E	Differentiated thyroid carcinoma	Any significant association	[225]
D148E	Breast cancer	D148E might be involved in contributing towards breast cancer susceptibility in North Indian women	[226]
Q51H	Colorectal adenoma	Identified a borderline	[227]

APE1 missense variation	Pathology	Association/Frequency	References
		significant decreased risk of colorectal adenoma	
D148E	Pancreatic cancer	Observed a weak but significant effect on overall survival	[228]
D148E	Bladder cancer	D148E showed an ability to predict bladder cancer risk	[229]
Q51H	Upper aerodigestive tract carcinoma (UADT)	Protective effect for UADT	[230]
D148E	Non-Hodgkin lymphoma (NHL)	Any significant association with NHL	[231]
D148E	Pancreatic cancer	XRCC1 R194W polymorphism had a significant interaction with the APE1 D148E in modifying the risk of pancreatic cancer	[232]
D148E	Breast cancer	D148E allele may be protective against the development of acute side effects after radiotherapy in patients with normal weight	[233]
D148E	Esophageal Squamous Cell Carcinoma (ESCC)	Any significant association was found	[234]
D148E	Lung cancer	D148E may alter the risk of lung cancer in a special population in China	[235]
D148E	Ionizing radiation (IR) sensitivity	D148E may contribute to IR hypersensitivity	[236]

In spite of several attempts to identify a potential correlation of APE1 genetic variants and cancer risk or neuropathology diseases, a restrict number of studies concerns the biochemical characterization of a subgroup of APE1 polymorphisms[170,237]. In these papers, the authors demonstrated that D148E, G241R, P112L and G306A variations did not alter the AP site incision activity *in vitro*, whereas L104R, E126D, R237A/C and D283G polymorphisms exhibited strong reduction (40-90%) in their endonuclease capabilities.

1.4 THE NUCLEOLUS: STRUCTURE AND CLASSICAL FUNCTION OF THE RIBOSOME FACTORY

The nucleolus is considered as a ribosome factory of the cells[238,239], in which processes of synthesis, maturation and processing of ribosomal RNA and assembly with ribosomal proteins take place[238]. It is considered as a dynamic structure[240,241], where protein complexes are in continuously exchange with the nucleoplasm[242]. Its classical tripartite organization could be distinguished by their morphology using electron microscopy and results from the ribosomal activity[242], reflecting the different steps of ribosomal biogenesis: fibrillar center, where the Polymerase I transcription starts (or in the boundary between FC and DFC), dense fibrillar component where the initial stages of processing pre-rRNA occurs and granular component (GC) for the late processing[238] (Figure 11). Transcription of rDNA repeats generates 47S pre-rRNAs that are cleaved and processed into 28S, 18S, and 5.8S rRNAs, concomitantly assembled into large and small ribosomal subunits together with the 5S rRNA[239,243]. These complex series of events is controlled, in yeast, by 150 small nucleolar RNAs (snoRNAs) and two large RNP complexes, named small subunit (SSU) processome for the 40S ribosomal subunit and the large subunit (LSU) processome for the 60S ribosomal subunit[242]. Two types of modified nucleotides (2'-O-methylation and pseudouridylation) are added during the maturation steps from snoRNAs, belonging to the box C/D snoRNAs or the box H/ACA snoRNAs families, and mediate endonucleolytic cleavages of pre-RNAs[242,243]. Moreover, ribosomal gene transcription is regulated by modulation of the transcriptional apparatus and by epigenetic silencing[244]. Mature ribosome particles (large and small) are independently exported in the cytoplasm through a CRM1 and Ran-GTP-dependent mechanism: export of 60S subunit requires the exchange of complexes Noc1-Noc2 by Noc3-Noc2[245] and the association with the adaptor shuttling protein NDM3[246], whereas the 40S needs the heterodimer Noc4p/Nop14p[247]. Few years later, Hinsby and collegues applied a machine learning-based predictor of NES to analyze the late stage pre-40S complex suggesting a role also for the human homolog of yeast DIM2p in targeting and translocation of late 40S in the cytoplasm[248].

The organization, the number and the size of these nuclear sub-structures is directly dependent of the nucleolar activity (RNA Pol I transcription), which in turn depends on cell growth and metabolism[249]: generally in highly proliferating cells, these present many small nucleoli[238,242]. Ribosomal biosynthesis is a high cellular energy and resources consuming process[250], tightly regulated by changes in cell proliferation, growth rates and metabolic activities. Nucleoli constantly receive and respond to different signaling events, maintaining the ribosomal subunit pool necessary to support protein synthesis during cell growth and division[239].

Biosynthesis of ribosomes is very efficient process, since could be estimated that 14,000 new ribosomal subunits can be synthesized every minute in an exponentially growing cell[251]. The process has to be fine-tuned and several evidences indicate that ubiquitin and UBL-based regulatory circuits control different stages of ribosome formation[252]. Lam and

collegues[253] demonstrated that the levels of unassembled ribosomal protein within the nucleoli exceeds the required RP:rRNA ratio and identified an ubiquitin-mediated proteasome mechanism on the ribosome biosynthesis pathway to monitor and degrade this exceed[254]. Ribosomal structural protein are imported from the cytoplasm in supra stoichiometric levels and exported in the form of assembled ribosomal subunits: the excess of protein not required for the process undergoes ubiquitinylation and degradation in the nucleoplasm by the proteasome system[252,255], indicating that mammalian cells produce large amount of these protein and degrade those that are not assembled with rRNA.

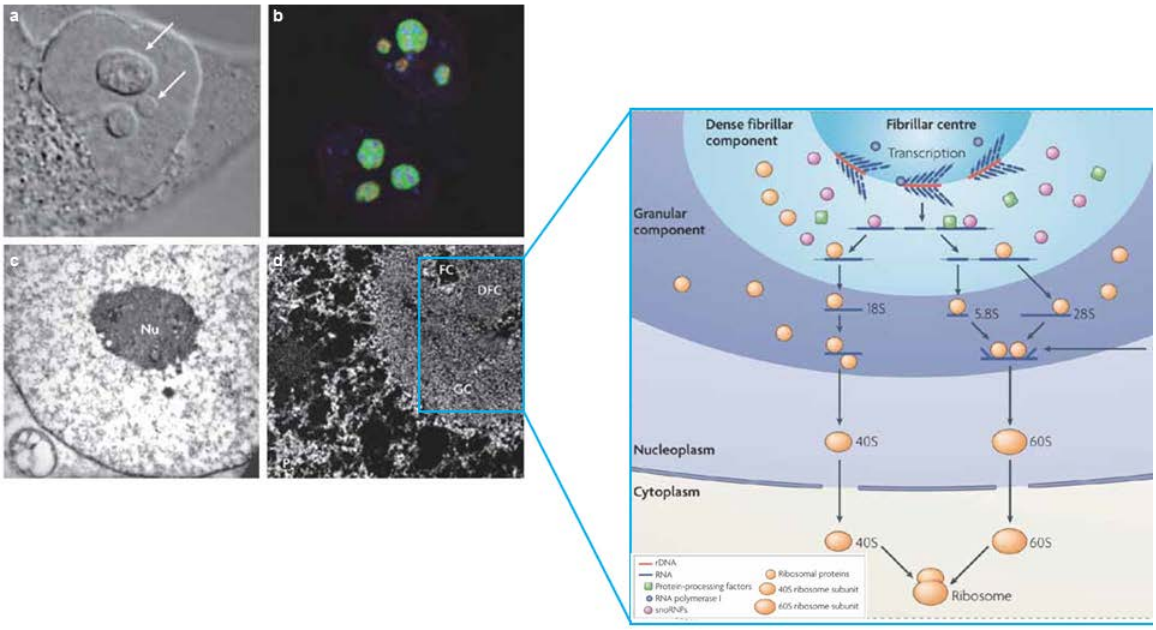

Figure 11: Visualization, organization of the nucleolus and the ribosome biogenesis model. HeLa cells were subjected to different imaging techniques, used to identify distinct aspects of nucleolar morphology and composition (*left panel*). **a** | Hela cell with prominent nucleoli (indicated by white arrows) visualized as differential interference contrast (DIC). **b** | Nucleolar subcompartments identified with the marker proteins enriched for each compartment NPM1 (GC – shown in green), fibrillarin (DFC – shown in red) and RNA polymerase I subunit RPA39 (FC – shown in blue) by immunofluorescence labelling. **c** | Nucleus with nucleolus (Nu) imaged by transmission EM following uranyl-acetate-staining. **d** | Nuclear region analyzed by electron spectroscopic imaging for the nucleic acids containing. *Right panel.* Representation of the different steps of the ribosome biogenesis within the three nucleolar subregions. (Adapted image from Boisvert F. M. *et al.*, *Nat Rev Mol Cell Biol*, 2007).

1.4.1 DYNAMIC TRAFFICKING, KEYWORDS FOR NUCLEOLAR PHYSIOLOGY

Nucleolus appears as a very dynamic organelle and different types of movement could be ascribed to this complex: first, the ribosome assembly is a vectorial process, where the ribosomal particles move away from their biogenesis sites; second kind of motion, the constant flux of proteins from nucleoli to the nucleoplasm; and third, nucleolar components present scheduled movements every cell cycle during steps of assembling/disassembling for the redistribution on nucleolar components between the two daughter cells[256]. Infact, nucleoli are subjected to cyclic assembling/disassembling

processes during the cell cycle: they assemble at the end of the mitosis and until the start of the next mitosis they are functionally active[238,240]. The nucleolar disassembling during mitosis could be linked to rDNA repression caused by CDK1-cyclin B-directed phosphorylation of components of the rDNA transcription machinery[242]. Conversely, the formation of functional nucleoli at the exit from mitosis, instead, is not governed solely by the resumption of rDNA transcription but by a two-steps process regulated by CDK(s) that connect the resumption of rDNA transcription and restoration of rRNA processing[242].During late telophase, nucleoli form around the nucleolar organization regions (NORs), chromosomal region where rDNA, formed by a transcribed sequence and an external non-transcribed spacer[242] and clustered in head-to-tail arrays[238,241]. This sub-compartment allows the cells to locally concentrate all the factors required for the ribosomal biogenesis[239,249]. In human mitotic cells, rDNA clusters are localized on the short arm of the five pairs of chromosomes 13, 14, 15, 21 and 22[242].

1.4.1.1 THE WAY TO MOVE: VISITORS *VS* RESIDENTS NUCLEOLAR PROTEINS

Different from NLS, nucleolar targeting sequences (NoLSs) are not well characterized and any consensus sequence has been described[242,254]. At the moment all the NoLSs described presents richness in basic residues as Arg and Lys[257], but also Trp residues were described as functional for the nucleolar localization of NPM1 (B23)[258]. The capability of different proteins to localize in the nucleolus has been correlated with interaction with already anchored resident protein as NPM1, acting as a transporter into the nucleolar compartment or as retention block in the nucleoli, supporting the idea that the residence time of nucleolar proteins is strongly related to their specific interactions[242,254,257]. In theory, all the molecules resident in the nucleoplasm could entry in the nucleoli, but only those with an affinity for nucleolar resident proteins would be retained for longer times[256]. Some authors, in fact, suggest the term “retention signal” instead of targeting signal for the nucleoli[259]. Since the residence time is very brief and most of the nucleolar protein shuttles from nucleoli to nucleoplasm and *vice versa*, these nucleolar proteins-anchored proteins interactions appear reversible[254,256]. Current models show that proteins and RNAs are continually in a state of flux and freely diffuse through the nuclear space[244]: the mean residence time of most nucleolar proteins in nucleoli can be calculated to be only a few tens of seconds. The nucleolus appears as a steady state structure with its component in dynamic equilibrium with the surrounding nucleoplasm[259]. Since the mass per unit volume of nucleoli is only twice higher than that of nucleoplasm, all diffusing macromolecules could enter in nucleoli: for this reason the residence time of nucleolar proteins depends from their relative affinities for the pre-anchored complexes present within the nucleolus[254,255]. However, in spite of this continual exchange of molecules between these two compartments (nucleolus and nucleoplasm), nucleolar domains are maintained because the number of proteins within a domain is higher to the number of proteins that are released from the same domain[243]. These proteins, able to connect and bind multiple protein partners, are considered as hub proteins and might be responsible for the nucleolar localization of the majority of visitor

protein in absence of RNA-protein binding. Each hub protein may have different recognition requirements, fact that may explain the occurrence of several NoLSs. Two great examples of hub proteins are considered Nucleolin and NPM1, which contain disordered regions, involved in nucleolar protein-RNA interactions[257].

Recently, a protein retention method based on GTP-driven cycle has been identified for Nucleostemin[259], but the exchange of GTP-GDP is not the only characterized intracellular signal able to move nucleolar proteins: stimulus as hydrogen ion was described by Mekhail *et al.*[260], that demonstrated how the nucleolar sequestration of von Hippel-Lindau (VHL) protein after an increase of pH promotes the stabilization of hypoxia-inducible factor (HIF), giving arise to a general cell response to hypoxic conditions[254].

1.4.1.2 NEW CONCEPTS FOR THE NUCLEOLUS: BEYOND THE RIBOSOME FACTORY

In the 1960s, through the identification and localization of ribosomal genes (rDNAs)[242], the main function of the nucleolus had been already described from several groups and it was nicely summarized in "an organelle formed by the act of building a ribosome''[248]. In the last decades, thanks to the evolution of techniques as isolation of large amount of nucleoli and the improvement of high-throughput mass-spectometry-based proteomic approaches, several proteomic analysis were undertaken partially unveiling the nucleolome[239,240,243,251,261]. Over 4500 proteins were described to localize in the nucleoli and bibliographic and bioinformatic analyses allowed the classification into 9 major functional groups (ribosomal proteins, ribosome biogenesis, chromatin structure, mRNA metabolism, translation, chaperones, fibrous proteins, others, and unpredictable function)[239,243,249,262,263]. A further idea of complexity has been added to the characterization of nucleolar proteome under different stress conditions (e.g. Actinomycin D), suggesting how dynamic the nucleolome could be[261].

The protein composition includes protein related to cell cycle regulation, DNA damage and pre-mRNA processing[241], suggesting that this organelle acts as a multifunctional domain and it is more than a "simple" ribosome factory, highlighting its plurifunctionality[238,239,241,248,251]. This variety could possibly be related to the different nucleolar proteins that act as multifunctional proteins, i.e. Nucleolin and Nopp140[264].

Nucleoli carry out many non-ribosomal activities[238] such as cell cycle and cell proliferation control sequestrating key factors normally active in the nucleoplasm[238,242,248], stress sensing[239,262,265-269] and tumor surveillance pathways, DNA damage repair[239,241,270], regulation of protein stability and apoptosis, telomere metabolism[239], maturation of small RNAs, including tRNA and snRNA of the spliceosome and the signal recognition particle (SRP), a complex of an RNA with several proteins that targets translation of certain protein in the endoplasmic reticulum[248,254,259], viral life-cycle[238,271], acting in several ways as a sequestration core facility[248,257,267] (Figure 12). The nucleolar proteins unrelated to ribosome assembly mostly contain an

RNA-binding motif or have a chaperone function and shuttle between the nucleolus and the nucleoplasm[264].

Seven most abundant motifs found in nucleolar proteins include RNA recognition motif, DEAD/DEAH box helicase, helicase conserved C-terminal domain, WD domain, intermediate filaments proteins, myosin tail and elongation factor Tu GTP-binding domain[264].

The assumption that a protein acts and executes its functions where it is more abundant does not work for some nucleolar component: a quantitative signal might not correspond to a protein's concentration in a cellular compartment[255]. A great example is represented by the many DNA repair proteins that resides in the nucleoli (see more in "The nucleolus as stress responsive organelle" paragraph), where nucleoli act as a storage site. Following nucleolar stress or DNA damage, these proteins can freely re-localize in the nucleoplasm. The nucleolar stress might carry out a physiological aim and could be considered as a control surveillance mechanism that monitors the synthesis and the correct assembly of ribosomal units: it may halt the cell cycle progression until enough functional ribosomes are built or it may induce p53-mediated apoptosis or senescence[250].

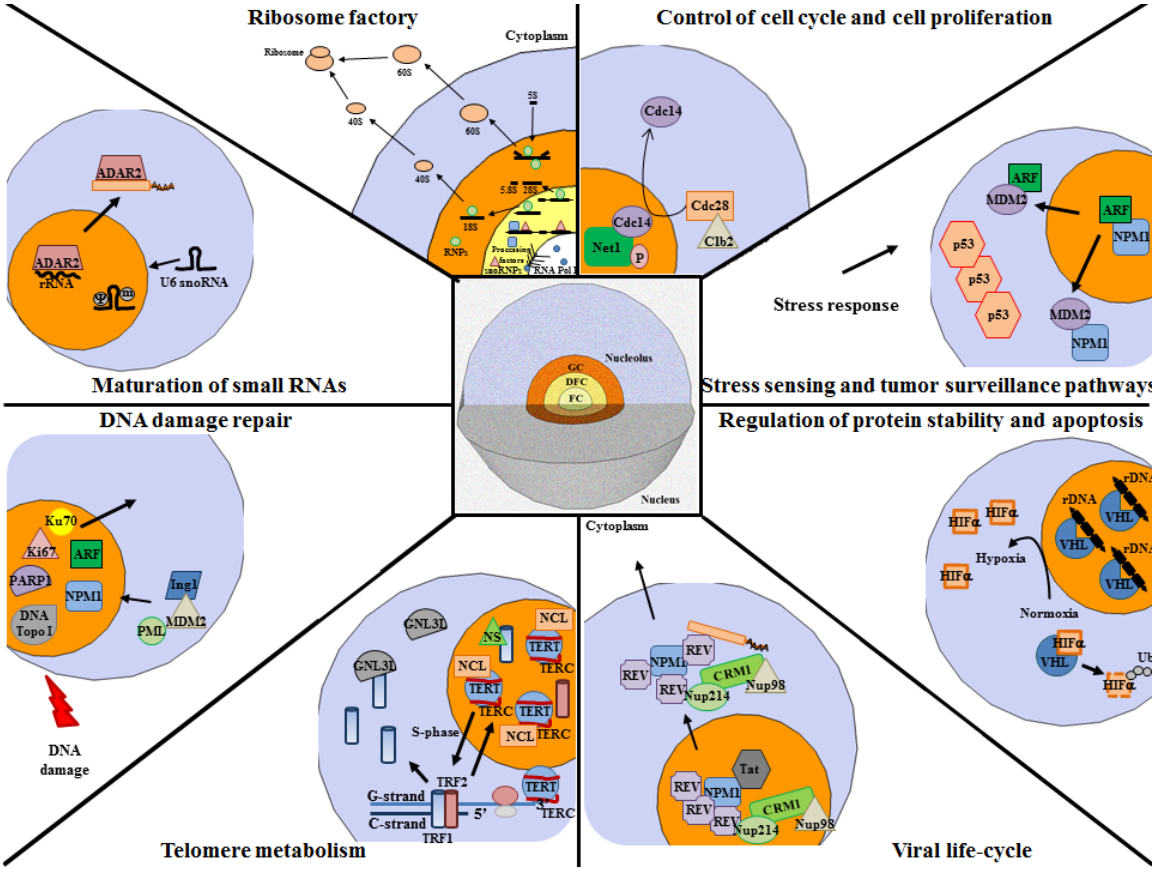

Figure 12: The nucleolus, a multifunctional domain. Unveiling of the "nucleolome" allows the understanding of the complexity of the nucleolus, first described only as a ribosome factory. The multifunctionality of the nucleolus includes different noncanonical functions as the control of cell proliferation and cell growth, regulation of protein stability, stress and DNA damage response, telomere metabolism, maturation of small RNAs and control of viral life-cycle. An illustrative mechanism for each function is summarized. **CRM1**, Exportin 1; **snoRNA**, small nucleolar RNA; **NPM1**, Nucleophosmin 1;

NCL, Nucleolin; **MDM2**, Mouse double minute 2 homolog; **ARF**, p14 alternative reading frame; **p53**, tumor protein p53; **ADAR2**, Double-stranded RNA-specific adenosine deaminase 2; **NS**, Nucleostemin; **VHL**, von Hippel-Lindau; **HIF**, hypoxia-inducible factor; **Ing1**, inhibitor of growth family, member 1; **Ki67**, antigen KI-67; **Cdc28**, cyclin-dependent kinase 28; **Cdc14**, Tyrosine-protein phosphatase; **Clb2**, G2/mitotic-specific cyclin; **Net1**, nucleolar protein; **PML**, promyelocytic leukemia protein; **DNA Topo I**, DNA Topoisomerase I; **Ku70**, ATP-dependent DNA helicase 2 subunit KU70; **TERC**, telomerase RNA component; **TERT**, telomerase reverse transcriptase; **GNL3L**, guanine nucleotide binding protein-like 3 (nucleolar)-like; **TRF1**, telomeric repeat-binding factor 1; **TRF2**, telomeric repeat-binding factor 2; **REV**, Regulator of Expression of Virion Protein; **Tat**, Trans-Activator of Transcription; **Nup98**, nucleoporin 98kDa; **Nup214**, nucleoporin 214kDa; **Ub**, ubiquitin. (Image from Antoniali G. *et al.*, *Antiox Redox Signal*, 2013)

1.4.1.3 THE NUCLEOLUS AS A STRESS RESPONSE ORGANELLE

The main function of the nucleolus is a rapid and efficient production of ribosomes, process strictly regulated for a correct cell proliferation and growth[249]. Under stress, cells, in an attempt to compensate and to maintain cellular energy homeostasis[272], halt and inhibit several cellular processes as replication, transcription and ribosome biogenesis, a highly energy-consuming process, altering their metabolism to allow a quick cell response through the activation of specific stress response pathways (e.g. DNA repair). The response of the stress could lead to different cellular results ranging from cell-cycle arrest to apoptosis, depending on the severity of the insult and to the capability of the cell to recover from the damage[72,249]. In this scenario, the nucleolus reacts to several form of cellular stress (e.g. DNA damage, cytotoxic drugs and agents that inhibits transcription by RNA polymerase I-complex) which disturb the normal nucleolar functions and appears a central hub in stress response, where tumor suppressor p53 and its negative regulator MDM2 represent the key players of the nucleolar stress response[72,249,266,267,273]. Commonly, the perturbation of nucleolar activity is accompanied by dramatic changes in its architectural organization and composition[261,274-276], in well-described phenomenon called nucleolar segregation, caused by DNA damage (UV irradiation, etoposide) and /or RNA Pol I inhibition (Actinomycin D) and characterized by the condensation of FC and GC with the concomitant formation on "nucleolar caps"[249]. Nucleolar stress signaling pathways rely on translocation from nucleoli to the nucleoplasm or targeting to the nucleoli in a dynamic way proteins involved in stress response[249]. Several players of this nucleolar sensing have been described, such the Cdc14B-Cdh1-Plk1 axis in yeast, with the translocation of cdc14B upon DNA damage to the nucleoplasm activating the G2 checkpoint[277], the opposite axis RelA-COMMD1, that leads to apoptosis following the nucleolar stress-dependent targeting of RelA[278] and the well-described NPM1-p14ARF-p53 pathway[266]. This pathway leads to the stabilization and activation of p53 via interaction of p14ARF with MDM2, a negative controller of p53[254,266]. In the nucleoplasm, p53 up regulates the transcription of RNA Polymerase II-transcribed genes and inhibits RNA Pol I transcription, whereas in the cytoplasm it triggers apoptosis via mitochondria[279]. Under physiological conditions, p53 levels are kept low through its interactions with MDM2 (called Hdm2 in human), an E3 ubiquitin ligase, that targets p53 to the proteasomal degradation. To keep the cellular homeostasis, p14ARF, a negative regulator of MDM2, is kept within nucleoli by the interaction with NPM1. Upon stress, the p53 stability is increased via protein-protein interaction involving the up regulation of

p14ARF. This up regulation prevents the proliferation of cells with damaged DNA preventing the duplication of injured cells: p14ARF binds MDM2, blocking its interaction with p53 and in turn leading to the stabilization of it. NPM1 itself and other ribosomal proteins, as L5, L11, L23 and S7, translocate from the nucleoli to the nucleoplasm following stress, binding directly MDM2 and preventing the degradation of p53[249].

1.5 NUCLEOPHOSMIN 1 (NPM1)

Nucleophosmin 1, also known as B23, NO38 and numatrin[280] and hereafter indicated with the acronym NPM1, was first identified as a nucleolar phosphoprotein[281], ubiquitously expressed in the granular region of the nucleolus[282], belonging to the nuclear Nucleoplasmin/Nucleophosmin chaperone family[283]. NPM presents a high degree of homology within the vertebrates and is widely distributed among different species; alternative splicing events generated three protein isoforms (NPM1, NPM2 and NPM3)[280].

To date, several distinct cellular functions for NPM1, related to both proliferative and growth suppressive roles, have been described[280,281]. Even though it resides predominantly within nucleoli, carrying out important nucleolar activities, as factor in ribosome biogenesis, transporting pre-ribosomal particles[284] and as retention block for non-resident nucleolar protein[257], by shuttling between cellular compartments, from nucleoli to the cytoplasm, NPM1 could take part in various cellular processes. They include the nucleolar stress response and the control of stability of p53 and p14ARF (see "The nucleolus as stress response organelle" paragraph), the maintenance of genome stability, controlling the ploidy of cells during centrosome duplication[280], the regulation of the chromatin condensation status and the involvement in different DNA repair pathways[281]. The acquisition of a deeper comprehension of the intricate network of all the biological roles played by NPM1 contributes to the emerging of a more complex scenario that had been expected. Much of the interest for this multifunction protein has been sustained by its implications in human tumorigenesis. It is frequently overexpressed in solid tumors of different histological origin (gastric, colon, prostate and ovarian carcinomas)[285] and the NPM1 locus is involved in chromosomal translocations/mutations/deletions in several haematological malignancies, as acute myeloid leukemia (AML), where in high percent of cases (35%), NPM1 has been found to be mutated and to be aberrantly localized in the cytoplasm of blasts[286], and solid tumours[281].

1.5.1 STRUCTURE OF THE GENE AND THE PROTEIN ENCODED

The NPM1 gene maps to the chromosome 5q35 in humans and contains 12 exons. NPM1 is translated from exons 1 to 9 and 11 to 12[287]. It encodes for 3 alternatively spliced isoforms, but NPM1 is the prevalent one.

NPM1 is a 294 amino acids protein of about 37kDa and presents functional modular organization in mainly independent, but slightly overlapping, domains (Figure 13).

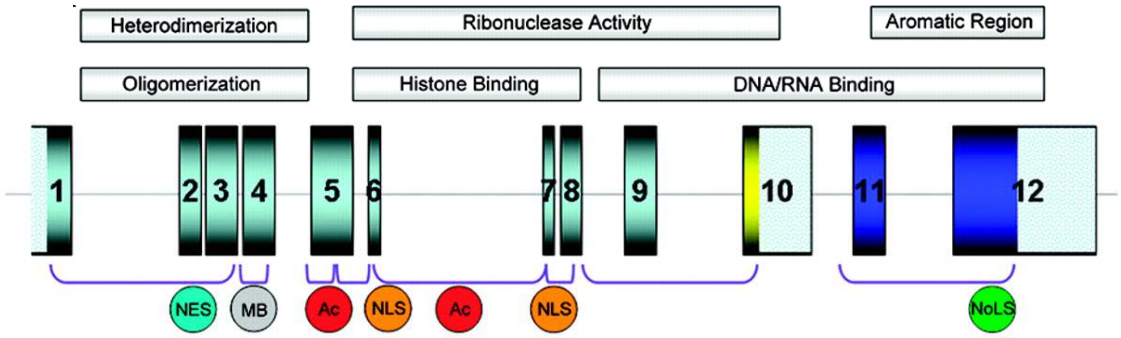

Figure 13: Structural organization of NPM1 gene and modular structure of the encoded protein. The NPM1 gene contains 12 exons. Three different regions could be defined within the protein structure: the N-terminus, a nonpolar domain required for oligomerization and heterodimerization, with a functional nuclear export signal (NES) and a metal-binding (MB) domain; a central portion characterized by two acidic stretches (Ac), responsable for histone binding, and a bipartite nuclear localization signal (NLS). This region confers ribonuclease activity. The C-terminus presents ribonuclease activity and basic regions involved in nucleic-acid binding. Two tryptophan residues (Trp288 and 290) form an aromatic region, constituting the nucleolar localization signal of the protein (NoLS). (Image from Falini B. *et al.*, *Blood*, 2006)

The N-terminus region, that contains a hydrophobic portion, controls the oligomerization status of the protein: in resting and proliferative cells, in fact, more than 95% of cellular content of NPM1 consists of pentamers, in which five wedge-shaped monomers are linked by apolar interactions[287,288]. The oligomerization by apolar contacts confers higher thermostable properties to NPM1, critical for its molecular chaperone activity avoiding protein aggregation at high temperatures[288]. This domain is also responsable for the chaperone activity of NPM1 towards protein, nucleic acids and histones[281,287,288] and for the regulation of acetylation-dependent transcription[289]. The central portion, responsible for the histone binding and nucleosome assembly, presents two acidic stretches whereas the fragment in between and part of the C-terminus domain are devoted to ribonuclease activity. The C-terminus region, characterized by basic regions for the nucleic acid binding, presents the nucleolar localization signal (NoLS), an aromatic section composed by tryptophan 288 and 290, required for its binding to nucleoli and responsible for its prevailing cellular localization[281,290]. The C-terminal domain is composed by three right-handed helix bundle that confers to the domain a well-defined tertiary structure[290]. The three helices are interconnected with each other and the overall structure is stabilized by a hydrophobic core, formed by aromatic residues (Phe268, Phe276, Trp288 and Trp290)[291]. Sequence alignments indicate that the folding of this domain and the aromatic core is strictly conserved along the evolutionary tree, with any insertions and/or deletion to perturb the helix bundle (Figure 14)[290,291].

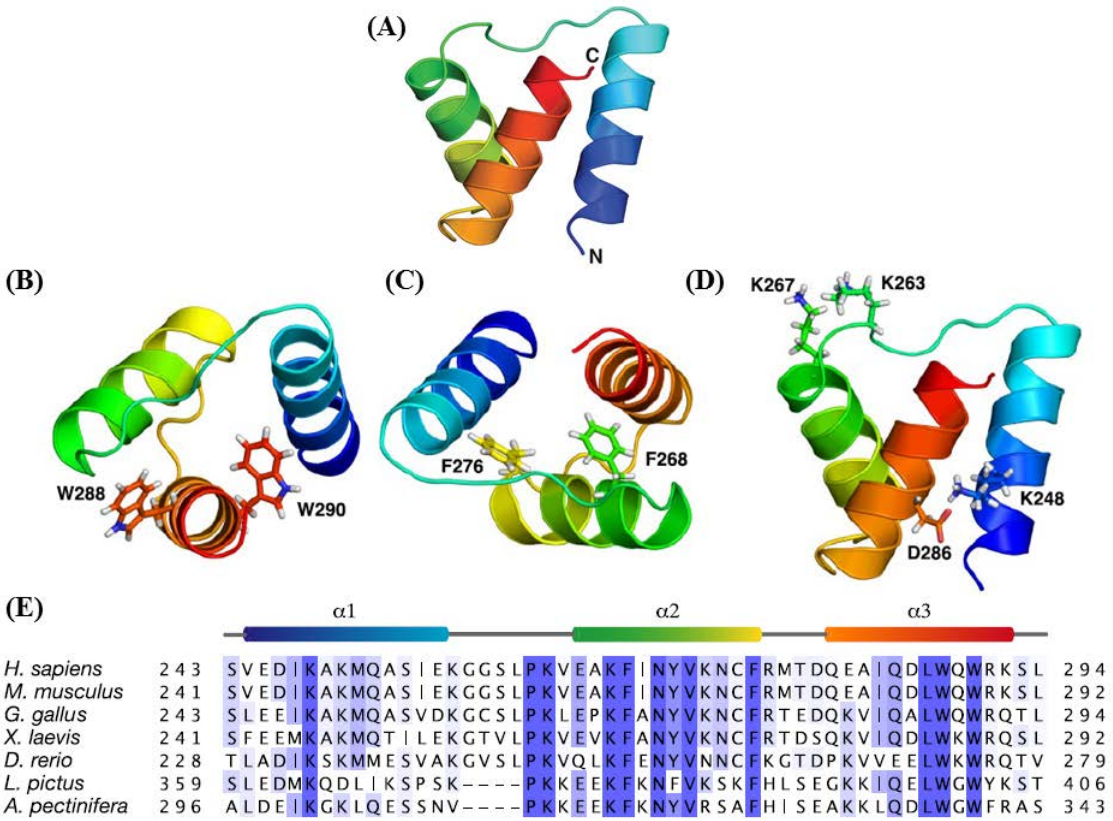

Figure 14: Schematic representation of the C-terminus region of NPM1 and sequence alignment of structurally and functionally important aromatic residues conserved within species. A | Lowest energy structure representation of the NPM1 C-terminus as prepared by PyMOL. The NPM1 C-terminal domain is formed by three right-handed helices. Helices H1 and H3 are coaxial but divergent, whereas the connecting helix H2 is tilted by 45° with respect the other two. **B-D |** C-terminal domain of NPM1 with functionally important residues that formed the hydrophobic core (B and C) and conserved lysines (D) represented as sticks. The two tryptophan residues represents a unique NoLS for NPM1. **E |** Sequence alignments, using ClustalW and Jalview programs, of NPM1 C-terminus and related proteins. In shades of blue are marked the conserved amino acids throughout the evolutionary tree. The helices are colored blue to red from the N- to the C-terminus domain. (Adapted image from Grummit C.G. *et al.*, *J Biol Chem*, 2008)

Within this domain, several lysine and arginine residues are found distributed throughout all the C-terminus length[291]; in particular three lysine residues (Lys248, 263 and 267) appear highly conserved and surface-exposed, indicating a hypothetical functional role for these residues[290]. Lys-to-Ala mutations demonstrated an important structural role for Lys248 in maintenance of the tertiary structure, since it forms a salt bridge with Asp286, whereas Lys263 and Lys267, freely orientate on the surface, with Cys275, play a role in the nucleolar localization of NPM1, probably through the binding with protein or nucleic acids abundant in the nucleoli, although they are not critical to the structural integrity of this domain (Figure 15)[290].

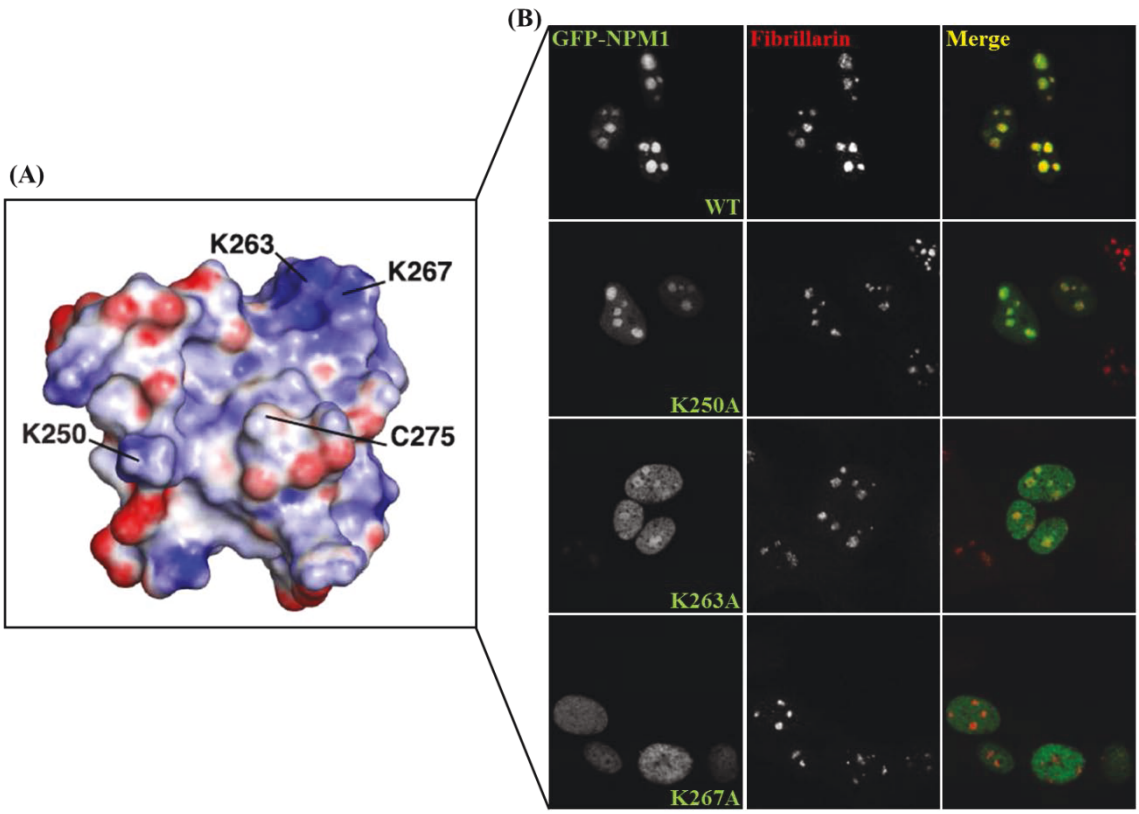

Figure 15: The NPM1 C-terminal domain is required for the nucleolar localization of the protein. A | Eletrostatic representation of NPM1 marked with the position of functionally important surface-exposed residues. The electrostatic surface potential was obtained used the APBS program, colored using a ramp from red (-20.0 kiloteslas) to blue (+20.0 kiloteslas). **B |** Lys-to-Ala mutants demonstrated the role for Lys263 and Lys267 in controlling NPM1 cellular localization in NIH-3T3 cells. Single mutants K263A and K267A, as the double one (not shown) are displayed throughout the nucleoplasm; K263A retains some nucleolar staining. Fibrillarin staining was used as nucleolar marker. Lys250 was used as control as surface-exposed residue but not involved in the regulation of NPM1 localization. (Adapted image from Grummit C.G. *et al.*, *J Biol Chem*, 2008).

To exert all its functions NPM1 ought to move freely between the cellular compartments; for this reason, in addition to the NoLS in the C-terminus, for shuttling from nucleoli to the cytoplasm and *vice versa*, NPM1 is equipped with a bipartite nuclear localization signal (NLS) in the central portion and with a leucine-rich nuclear export signal (NES) motifs at the N-terminus domain for Exportin CRM-1[292]. The usage of the NES motifs may be subjected to the association with particular binding partners and/or post-translational modifications. Phosphorylation sites, widespread throughout all its structure, define and regulate its association with centrosome and subnuclear compartments[288].

1.5.2 PRINCIPLE MECHANISMS FOR NPM1 REGULATION

NPM1, as multifaceted nucleolar protein involved in several cellular processes, is strictly subjected to different regulation mechanisms controlling its physiological functions, ensuring a correct expression level and localization for the protein. The regulatory mechanisms that govern NPM1 could be outlined as follow:

- NPM1 undergoes to a variety of posttranslational modifications such as phosphorylation[288,293], acetylation[289,294], SUMOylation[295-297], poly(-ADP-ribosyl)ation[298] and ubiquitination[284,299] that controls the NPM1 subcellular localization dissecting within its numerous function;
- By shuttling within the different compartments, NPM1 exerts its functions: sequestering in one compartment or entering/exiting mechanisms;
- In growing cells, NPM1 forms oligomers. The dynamic equilibrium existing between the different forms of NPM1 (monomer vs pentamer/decamer) could regulate the half-life of the protein. For instance, p14ARF, binding the NPM1 N-terminus, destabilizes the oligomer status of the protein redirecting the monomers towards the proteasome degradation[288];
- NPM1 shares the N-terminus, domain responsible for its oligomerization, with the other two components of the family, NPM2 and 3. The capability of these forms to heterooligomerize with NPM1 could negatively regulate the C-terminus activities of NPM1. The balance of the different components within the pentamer seems critical for NPM1 function[288].

A particular mention has to be done for the numerous post-translational modifications occurring on NPM1, which represent a key mechanism responsible for its regulation (Figure 16).

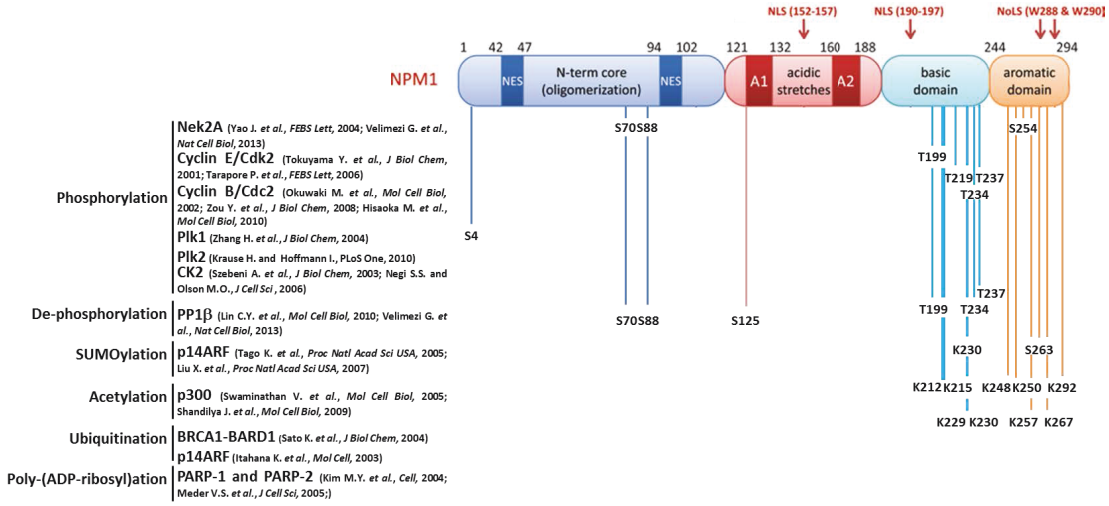

Figure 16: Schematic representation of the posttranslational modification acceptor sites for NPM1. Even if the association of NPM1 with PARP-1 and PARP-2 has been demonstrated, as the p14ARF and BRCA1-BARD1 induced ubiquitination, the exact sites are still unknown. On the contrary, the real acceptor sites for several phosphorylations, SUMOylation and acetylation have been precisely mapped on NPM1 (Adapted image from Yip S.P., Springer Ed., 2011)

NPM1 was first discovered in 1973 as phosphoprotein and several residues have been identified so far as phosphorylation sites *in vivo*. Several kinases have been identified. NPM1 phopshorylation by cyclin E/Cdk2[300,301] and Plk2[302] has been demonstrated during the G1 phase in relation to the centrosome duplication by dissociating NPM1 from the centriole. The activity of cyclin B/Cdc2 on NPM1 (Thr199) is associated with a diminished RNA binding activity during mitosis, reinforcing the idea of disassembling

nucleoli by disrupting RNA-protein binding interaction of NPM1[303,304] and inhibits the GCN5-mediated histone acetylation[305]. During mitosis, NPM1 has been also found phosphorylated by Plk1 which might have a critical role in mediating mitosis[306]. De-phosphorylation events take place on three threonine residues (Thr199, 234 and 237) by the serine/threonine phosphatase called PP1β in response to DNA damage (UV irradiation), facilitating the DNA repair process[307,308]. Interestingly, a role for Nek2A has been recently demonstrated for the phosphorylation of NPM1 at Ser70 and Ser88: such modification, antagonized by PP1β when it is activated by ATM, seems to be fundamental in controlling the ARF stability in an ATM-dependent pathway, elucidating the role of the ATM-ARF-NPM1 axis in the DNA damage response[308]. Acetylation p300-mediated, described especially at the C-terminus domain of NPM1, increases its binding affinity to histones[289,294]. Association of factors involved in poly-(ADP-rybosil)ation such as PARP-1 and PARP-2 has been documented for NPM1, event which might correlate with the functional transcription within nucleoli[309]. Two different ubiquitination processes (BRCA1-BARD1[299]- and p14ARF[284]-mediated) have been recognized for NPM1, although only the p14ARF one redirects the protein to the proteasome-dependent protein degradation. Last, SUMOylation is another mechanism by which cells control NPM1 functions. NPM1 has been described to be SUMOylated by p14ARF, modulating its stability and leading to a re-localization of NPM1[295,297].However, the complete profile of post-translational modifications remains to be fully elucidated.

1.5.3 NPM1 AS A MULTIFUNCTION PROTEIN

Elucidating the various physiological functions of NPM1 has become a new research issue, especially for cancer research. NPM1 has been described as a critical protein involved in a wide range of biological processes. It has been associated with different human pathologies (the reader is redirected to the paragraph "Alteration of NPM1 in human cancers" for more details), so a deep comprehension of the complicate network of molecular mechanisms controlling NPM1 and of the scenarios in which it operates might improve the therapeutic approaches. In Table 3, all the physiological functions are listed; each of those will be briefly introduced to the reader in the following paragraphs.

Table 3: List of all the known NPM1 physiological functions.

NPM1: summary of physiological functions and posttranslational modifications involved in its regulation	
▪ **Molecular chaperone**	(304,310-318)
▪ **Involvement in ribosome biogenesis**	(284,313,319-322)
▪ **Regulation of transcription**	(289,294,304,305,323-334)
▪ **Inhibition of apoptosis**	(293,335-341)
▪ **Modulation of tumour suppressors**	(281,284,326,329,341-350)
▪ **Maintenance of genomic stability**	(337,342)
▪ **Regulation of cell cycle**	(239,281,314)
▪ **DNA repair**	(18,280,281,285,322,337,342,351,352)

1.5.3.1 NPM1 AS A MOLECULAR CHAPERONE

The ability of NPM1, through its N-terminal domain, to bind denatured proteins, preventing their aggregation, misfolding and denaturation, and nucleic acids, controlling chromatin assembly and disassembly, define NPM1 as molecular chaperone[311,312,353]. Initially, NPM1 was described as ribosome chaperone or assembly factor, since it associates with pre-ribosomal particles and exerts different activities on rRNA transcripts and ribosome biogenesis[313,314]. Recent works, on the contrary, ignited particular interest in the function of NPM1 as histone chaperone[304,315-317] suggesting a dual role for NPM1 as nucleolar histone and ribosome chaperone and reinforcing the multi-functionality of this protein.

1.5.3.2 A ROLE FOR NPM1 IN THE RIBOSOME BIOGENESIS MACHINERY

NPM1 plays a key role in ribosome synthesis since it presents all the necessary features for the processing and assembly of ribosomes, as the abundant nucleolar localization, its capability to shuttle between nucleus and cytoplasm and its role as ribosome chaperone in transporting ribosomal particles[319]. NPM1 has been found to have ribonuclease activity towards pre-ribosomal RNA, processing the internal transcribed sequence (ITS2)[284,320,321], activity facilitated by the chaperone ability of NPM1, avoiding nucleolar protein aggregates during the ribosome biogenesis. Knocking-down of NPM1 leads to an inhibition of the processing of pre-ribosomal RNA and to changes in the ribosomal profiles[284,322], supporting the significance of NPM1 in this process. Moreover, acting as histone chaperone, NPM1 controls the transcription of genes involved in the ribosome synthesis, promoting the maintenance of an open chromatin conformation accessible for the synthetic machinery of the ribosome. Indirect observations of a close association of NPM1 with this machinery have been collected; in fact NPM1 regulates the export and transport of numerous ribosomal components such as L5 (rpL5) and its cargo 5S rRNA in a CRM-1-dependent mechanism[313]. Inhibition of NPM1 shuttling or knock-down of the protein causes a block of rpL5 export and leads to cell-cycle arrest[313], providing new evidences for the important role of NPM1 as ribosome chaperone.

1.5.3.3 REGULATION OF GENE TRANSCRIPTION BY NPM1

NPM1 contributes to the regulation of gene transcription and ultimately to the cell growth control; its correlation with gene transcription has been related to several mechanisms. Of particular interest, several lines of evidences point toward an important role for NPM1 in both RNA Pol I and Pol II transcription. First, NPM1 interacts with different transcription factors, including p53[323], NF-κB[324], YY1[325], ARF[326], ATF5[327] and IRF1[328], controlling their stability and activity and acts as co-repressor or co-activator. Second, through the direct binding to c-Myc, NPM1 facilitates the RNA Pol II recruitment at the promoter of the c-Myc target genes[330] and controls its subcellular localization[331]. NPM1, regulating the c-Myc turnover through the control of Fbw7γ[329], may have an important role on cell

growth and tumor development. Third, recently has been demonstrated an association *in vitro* and *in vivo* of NPM1 with HEXIM1, an inhibitor of positive transcription elongation factor b (P-TEFb), a key regulator of RNA Pol II machinery[332]. The binding of NPM1 with HEXIM1 leads to a negative regulation for the inhibitor, enhancing the P-TEFb-driven transcription. Fourth, a key role for acetylation has been found for NPM1 transcriptional activity. Swaminathan *et al.* demonstrated that NPM1 could enhance transcription in an acetylation-dependent manner and may have an impact on chromatin remodelling: the combination of acetylation of the core histones, which NPM1 interacts with (H3, H2B and H4), and NPM1 itself generates an open chromatin conformation by disrupting the nucleosomal structure, resulting in the transcriptional activation[289]. Moreover, the p300-acetylated form of NPM1 interacts in the nucleoplasm with the transcriptionally active RNA Pol II: either inhibition of p300 or mutation of acetylatable lysine residues of NPM1 results in a reduced occupancy of NPM1 on target gene promoters[294]. On the other hand, during mitosis NPM1 negatively regulates the acetyltransferase GCN5, inhibiting its activity towards both free and mononucleosomal histones[305]. Fifth, NPM1 is also involved in the regulation of RNA Pol I transcription within the nucleolus: as a nucleolar histone chaperone, NPM1 associates with rRNA gene chromatin, facilitating its transcription and the cell growth rate[318], and induces, during G2/M, the rDNA transcription factor $TAF_{(I)}48$[333], required for the recruitment of the Upstream Binding Factor (UBF) to rDNA. All these factors are responsible for initiating the transcription of ribosomal RNA by RNA Pol I in the nucleolus. Interestingly, the RNA binding activity of NPM1, inhibited during mitosis by Cdc2 kinase-mediated phosphorylation, and the recruitment of UBF are essential features for NPM1 binding to the chromatin[304]. Furthermore, NPM1 controls the subnuclear localization of TTF-1, the RNA Pol I transcription terminator factor, and might promote its nucleolar import, in contrast to the action of ARF, facilitating its role in rRNA synthesis[334].

1.5.3.4 INHIBITION OF APOPTOSIS

Accumulating evidences support the concept that an overexpression on NPM1, as found in actively proliferating and cancer cells, could promote cell survival by inhibition of cellular apoptosis elicited by various stimuli[336]. On the contrary, loss of NPM1 induces cell death. Different studies aimed to deciphering the anti-apoptotic function of NPM1 have been conducted. First evidences demonstrated a nuclear association between NPM1 and the phosphatidylinositol 3,4,5-triphosphate [$PI(3,4,5)P_3$], interaction that mediates the anti-apoptotic effect of nerve growth factor (NGF) by inhibiting DNA fragmentation activity of caspase-activated DNase (CAD) in PC12 cells[335]. Frequently, the anti-apoptotic effect of NPM1 hinges on its prompt up-regulation following different stimuli, such as UV irradiation[337], hypoxia[338], ionizing radiation (IR)[339] and extra- and intra-cellular cues that activates the interferon-inducible, double-stranded RNA-dependent protein kinase (PKR)[340], resulting in an increased resistance to apoptosis and enhanced protein synthesis. Additionally, the cellular protection from apoptosis exerted by NPM1 has been related to a mechanism involving p53[293,338,339]. NPM1 might inhibit the activating phosphorylation of p53 (Ser15), suppressing in this way the p21-driven

response. Lastly, NPM1 interacts with the pro-apoptotic factor GADD45α, an important player in cell cycle arrest during G2/M in response to genotoxic stress that lacks a functional NLS and for this reason it needs the aid of a nuclear chaperone. Gao *et al.* identified NPM1 as chaperone involved in controlling GADD45α; it mediates the nuclear import of GADD45α, localization required to induce the cell cycle arrest[341].

1.5.3.5 MODULATION OF TUMOUR SUPPRESSORS

NPM1 is engaged in the regulation of activity and stability of some key tumor suppressors as Miz1[347], Fbwγ, required for c-Myc degradation[329], p53 and ARF[281]. The association between NPM1 and ARF influences the stability of the latter: NPM1 retards the turnover of ARF[296,348], resulting in a maintenance of its biological function within cells. Inhibition of the proteasome, in cell expressing ARF mutants unable to interact with NPM1, only partially restores the stability of ARF proteins, indicating that the protective role exerted by NPM1 on ARF turnover involves both proteasome-dependent and – independent degradation[348]. ARF prevents cell proliferation through p53-dependent and – independent mechanisms[284,349]: it blocks the cell cycle progression via MDM2-p53 axis[326] and concomitantly inhibits the ribosomal biogenesis through the retardation of rRNA production involving a p53-independent pathway[343,350]. On the contrary, deficiencies in NPM1 expression/functions are correlated with accelerated transformation, probably attributed to ARF destabilization[344] and mislocalization[342]. To sum up, NPM1 has a key role in the cellular response to oncogenic stimulus, modulating ARF functions. Cells lacking NPM1 gene shows decreased stability of ARF protein and susceptibility to tumorigenesis, supporting the concept of NPM1 as tumor suppressor, in which expression level and localization are features of major interest.

The tumor suppressor p53 protein, crucial for preventing proliferation or survival of cells with irreparable damage and genomic instability[345], has been found to be another tumor suppressor gene regulated by NPM1. Tumor protein p53 expression levels are controlled by MDM2, a p53-specific ubiquitin ligase that constantly mediates its degradation, but is inhibited during cellular stresses. The nucleolar integrity plays has an important role in p53 stability in proliferating cells[266]. During stresses able to disrupt nucleoli, NPM1 redistributes in the nucleoplasm[269]; such redistribution might lead to a stabilization of p53 through the inhibition of MDM2 activity[346]. The cross-talk NPM1-p53 also involves proteins downstream of p53, as GADD45α[341] (for more details, the reader is redirected to the previous paragraph). In conclusion, NPM1 might facilitate DNA repair followed oncogenic and genotoxic stresses, reinforcing the p53 pathways, acting again as a tumor suppressor molecule.

1.5.3.6 THE MAINTENANCE OF GENOMIC STABILITY

NPM1 has been implicated in the maintenance of genomic stability through the control of chromosomal ploidy and DNA repair. Interestingly, UV-irradiation leads to a rapidly up-regulation of NPM1; elevated NPM1 expression levels have been associated with

improved DNA repair processes[337] and, on the contrary, loss of NPM1 causes accumulation of γ-H2Ax, a downstream target of the DNA repair kinases ataxia telangiectasia mutated (ATM) and ataxia telangiectasia and RAD3-related (ATR), with increased number of ATM positive foci[342]. NPM1's role in maintenance of genomic stability has been associated with its studied and physiological function in cell cycle regulation.

1.5.3.7 REGULATION OF CELL CYCLE BY NPM1

During mitosis, within eukaryotic cells profound changes in their structure and architecture take place. Nucleoli, as dynamic structure, undergo reversible disassembling when cells enter in the mitosis and transcription shut down[239]. Many nucleolar proteins, including NPM1, re-localize in the cytoplasm where NPM1, from the chromosome periphery, migrates at the poles of the mitotic spindles together with NUMA, a nuclear mitotic apparatus protein associated with the mitotic spindle. The presence of NPM1 at the mitotic spindle seems to protect cell to centrosome hyper-amplification, allowing the cells to proceed in the G2/M phase. It has been demonstrated that NPM1 associates with the unduplicated centrosome and following a CDK2-cyclin E-dependent phosphorylation at Thr199 it dissociates from the centrosome, enabling the initiation of duplication[281]. *Npm1*$^{-/-}$ cells show increased genomic instability with consequent augmented oncogenic transformation[281]. Moreover, NPM1 also associates with a centromere protein A (CENPA), complex necessary for a correct segregation during mitosis, suggesting a novel role for NPM1 in centromere control, possibly mediated by its histone chaperone function[314]. In summary, NPM1 plays a key role in maintenance of genomic stability through a proper regulation of centrosome duplication and its loss causes aneuploidy and the activation of proliferation checkpoints during the cell cycle.

1.5.3.8 PARTICIPATION OF NPM1 IN DNA REPAIR

DNA strand breaks, resulting in global and local chromatin structural modifications, trigger activation of cellular pathways resulting in DNA damage response and DNA repair with the recruitment of several repair proteins and signaling factors at the damage sites. Growing body of evidences emphasize a role for NPM1 in the so called DNA damage response (DDR), response that encompasses DNA repair mechanisms, cell cycle control pathways, replication bypass mechanisms and, when damage is excessive, cell death pathways[280,285,342]. Several groups have demonstrated that NPM1 knock-out leads to embryonic lethality, highlighting the essentiality of the protein for the development; loss of a functional allele of NPM1 gene and the formation of oncogenic fusion proteins or mutated ones contribute to the onset on genomic instability and to uncontrolled cell proliferation, facilitating the process of tumorigenesis[281,285,322]. Interestingly, NPM1 has been implicated in DNA repair, although its exact role(s) has not been identified yet. An early response to damage involves a rapid transcriptional up-regulation of NPM1 and its augmented expression has been linked to an improve DNA repair process[337] whereas the absence has been correlated with downstream target of ATM/ATR kinases (γH2Ax foci).

Upon sensing DNA damage, NPM1 translocates from the nucleolus to the nucleoplasm in IR-induced DNA damage foci[351] and acts as chromatin-binding factor after DNA double–strand breaks[281,342,352]. Our group recently has demonstrated a physical association between APE1 and NPM1 within nucleoli and in nucleoplasm of tumor cells[18]. It is reasonable that NPM1 may act as a histone chaperone under or following DNA repair.

1.5.4 ALTERATION OF NPM1 IN HUMAN CANCERS

NPM1 has been widely implicated in cancer pathogenesis for both its growth promoting and tumor suppressive functions. In general, overexpression of NPM1 enhances cell growth and cell proliferation, probably through promoting ribosome biogenesis, stimulating rDNA transcription and ribosome export, DNA replication during S-phase and inhibiting cellular apoptosis[281]. It has been suggested a proto-oncogenic activity for NPM1: as Ras, it was found that its overexpression leads to cellular senescence in human fibroblasts[323]. The level of NPM1 is generally more elevated in tumor cells compared to normal cells and it is overexpressed in many solid tumors of different origins, but not limited to, including tumors of the gastric, colon, liver, breast, ovarian, prostate, bladder, thyroid, brain and multiple myeloma[281,314]. The ability of NPM1 to inhibit apoptosis and to promote and stimulate the DNA repair might be a significant aspect for its pro-survival role during tumor development. In addition to its overexpression, genetic alteration of NPM1 were found in common solid cancer, as lung and hepatocellular carcinoma, but particularly in human hematopoietic malignancies (leukemias and lymphomas)[314,354]. Disruption of the NPM1 gene by frame-shift mutations, translocations and deletions has been found in acute promyelocytic leukemia (APL), anaplastic large cell lymphoma (ALCL) and in premalignant myelodysplastic syndromes (MDS)[314,354]. Translocations occur usually at the N-terminal domain of NPM1 that fuses with the C-terminus of the other gene involved in the translocation. The results usually produce an oncogenic fusion protein; the remaining functional allele encodes a reduced amount of NPM1 wild-type protein. The major genes involved in this fusion are anaplastic lymphoma kinase (ALK), retinoic receptor α (RARα) or myeloid leukemia factor 1 (MLF1) in ALCL, APL and MDS, respectively[354]. In all these cases, NPM1 activates the oncogenic potential of the fused genes, contributing to cancer development. The fused protein localized in the cytoplasm but was unexpectedly found also in the nucleoplasm, since it keeps its ability to oligomerize with the wild-type form, protein that retains the nuclear localization signal[354]. A breakthrough in this field was the finding that one-third of adult acute myeloid leukemia (AML) cases display aberrant cytoplasmic localization of NPM1, due to a frame-shift mutation in exon 12 in patients with AML carrying a normal karyotype, implying for the first time a direct involvement of NPM1 as cancer gene[286]. In the next section, a dedicate review of AML with abnormal cytoplasmic NPM1 (NPM1c+) will be covered.

1.5.4.1 ACUTE MYELOID LEUKEMIA CARRYING CYTOPLASMIC NPM1 (NPM1C+ AML)

NPMc+ AML accounts for one-third of all cases of adult AML, up to two-third of patients with normal karyotype but presents a less frequency in children (~7%)[282,286]. A recent report documents 55 somatic NPM1 mutations, including insertions, insertions and deletions, base substitutions in exon 12 that result in similar alterations at the C-terminus of the protein (a complete destabilization of the domain without any regular tertiary structure[290]), producing NPM1c+[282]. All these mutations generate a shift in the reading frame of the transcripts from the point of insertion/deletion. Even though the numerousness of the found alterations, the most common mutation, accounting for 70-80% of adult NPM1c+ AML, is a duplication of a 4-base sequence (TCTG) at position 956-959 of the sequence[286]. This duplication leads to two crucial events at the C-terminus of the protein for the aberrant cytoplasmic localization[292]. First, this insertion leads to the loss of both Trp288 and Trp290 or just Trp290, residues that constitute the nucleolar localization signal for NPM1[258], disrupting the C-terminus and reducing NPM1 nucleolar storage[290]. Second, the duplication produces a new leucine-rich NES motif in the C-terminus, in addition to the NES signals already present in the NPM1 sequence (Figure 17)[292]. Interestingly, the C-domain as a whole plays a role in regulating the NPM1 localization: AML-independent mutations (F268A and F276A) within the C-terminus predicted to disrupt the tertiary structure of the domain while retaining the two tryptophans lead to a nucleoplasmic localization of NPM1 without any strong accumulation in the nucleoli, demonstrating the importance on this domain[290]. Moreover, depending of the exact position of the insertion, leading to the loss of both tryptophans or not, the new NES motif presents different efficiency in delocalize NPM1 in the cytoplasm: the balancing between the NES and tryptophans'forces determines the subcellular localization of NPM1[355]. Usually Trp288-remaining mutants are always associated with a strong new NES motif; a weak NES sequence together with the retention of Trp288 has never been detected in AML, suggesting a selective pressure towards the nuclear export of NPM1 in favor of a cytoplasmic localization and pointing out to this re-localization as a crucial event in leukomogenesis[355].

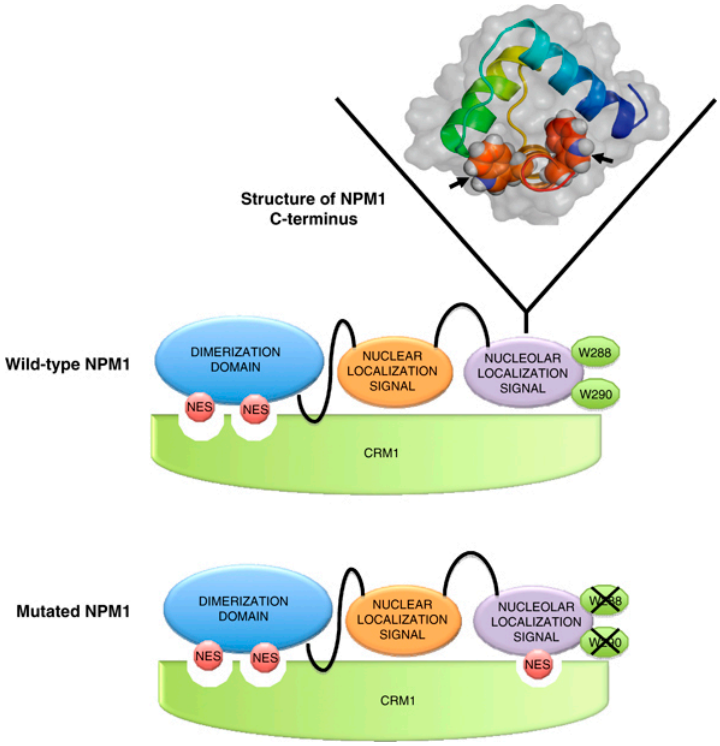

Figure 17: NPM1c+ loses its nucleolar localization signal and acquire a new NES motif. Schematic view of all the signals that govern NPM1 trafficking within cells. The mutated form of protein, found in AML, differs from the wild-type form for the insertion at the C-terminus that disrupts the reading frame of the transcript. The mutation leads to the loss of the two tryptophan residues, or just tryptophan 290, and to the formation, in concomitance, of a new NES motif, bound by Crm1. On the top, the 3-helix structure of the C-terminus with the two tryptophans highlighted by arrows within the hydrophobic core (Image from Falini B. *et al.*, *Leukemia*, 2009)

Recently, another additional mechanism to explain the aberrant cytoplasmic localization of NPM1c+ has been demonstrated. The existence of a direct correlation between NPM1 C-terminal folding, G-quadruplex binding and proper nucleolar localization has been shown[291,356]: through the C-terminus NPM1 binds G-quadruplex structures found in ribosomal DNA both *in vivo* and *in vitro*[357], whereas the leukemic variant completely loses this capability due to a G-quadruplex binding domain destabilization[356]. The disruption of the binding of G-quadruplex in rDNA and NPM1 wild-type using a specific ligand for the G-quadruplex leads to a loss in nucleolar NPM1 accumulation, suggesting a novel role for these structure in assuring the proper localization for NPM1[356]. In NPM1c+ AML, since the leukemic blast is heterozygous retaining one wild-type allele[354], a nucleolar/nucleoplasmic localization could be found for the wild-type protein while the mutated form is limited to the cytoplasm[292,358]. However, the mutated form acts as a negative dominant, due to the fact that it maintains the ability to form oligomers: hence, NPM1c+ could generate a heterodimer with the wild-type protein, delocalizing the latter in the cytoplasm (Figure 18).

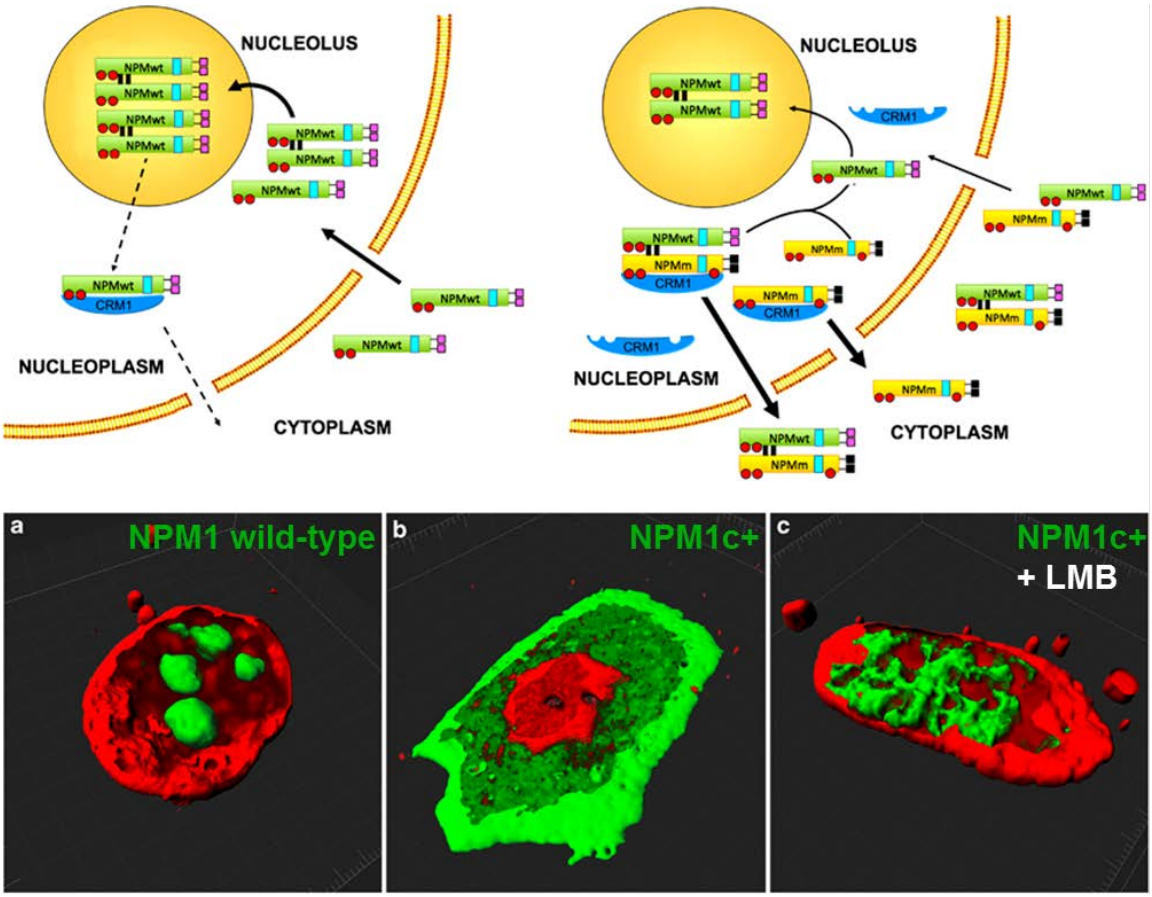

Figure 18: Mechanism of the NPM1 shuttling from the nucleoli to the cytoplasm in normal cells (top, left) and in NPM1c+ AML cells (top, right). In normal cells, NPM1 wild-type localizes mainly in the nucleoli, since the nuclear import prevails over the Crm1-mediated export. On the contrary, in AML cells, both of the coexisting NPM1 forms (wild-type and mutated) delocalizes in the cytoplasm due to the prevalence of the export to the nuclear import. Purple squares indicate tryptophans 288 and 290; black squares the mutated tryptophans; light blue rectangle indicates the NLS sequence and the red circles indicate the NES motifs. To notice that NPM1c+ presents three NES motifs while the wild-type counterpart two sugnals. (Bottom panel) Confocal 3D-reconstruction of NIH-3T3 cells expressing NPM1 wild-type GFP tagged protein (a); NPM1c+ GFP tagged mutant (b) and NPM1c+ GFP tagged mutant after incubation with the Crm1 inhibitor Leptomycin B (LMB) (c). The nucleus is counterstained in red with the propidium iodide. In contrast to the wild-type protein that localizes mainly in the nucleoli, the NPM1c+ mutant shows a prevalent localization in the cytoplasm. The treatment with LMB blocks the NPM1c+ export and the mutant present a strong accumulation within nucleoli. The nucleus was cut electronically to analyse the localization of NPM1 within the subcellular compartment (Image from Falini B. *et al.*, *Leukemia*, 2009)

This aberrant cytoplasmic localization of NPM1c+ may play a crucial role in leukemogenesis, and besides the founder genetic lesion, secondary cooperating mutations participate in the process; however, the causative link between this gene mutation and the occurrence of NPM1c+ AML remains elusive. Two main aspects should be pointed out: the remaining NPM1 wild-type allele produces a reduced amount of wild-type protein in comparison to a condition of homozygosis, and often the protein results dislocated in the nucleoplasm and in the cytoplasm due to the formation of heterodimers with NPM1c+. In addition, the mutated allele produces NPM1c+ protein, localized in the cytoplasm: this mutated form may recruit and bind several natural NPM1 partners, dislocating them from the normal subcellular compartment and abrogating their physiological function, as already demonstrated for ARF[358-360], HEXIM1[332], Fbw7γ[329] and Miz1[347], and may also

interact with new different protein partners in the cytoplasm, where it acquires new functions (i.e. inhibition of apoptosis through the binding to the cleaved forms of Caspase 6 and 8)[361]. The attenuation of the physiological functions of these protein partners may lead in some cases, such as for Fbw7γ and Miz1, to the stabilization of c-Myc and to the deactivation of cell barriers (ARF[358-360] and Miz1-controlled cell cycle inhibitors as p21, p15Ink4b[347]), conditions that could affect the oncogenic potential of NPM1c+, contributing to the transformation and to uncontrolled cell proliferation[329,347]. All these phenomena perturb ultimately multiple cellular pathways in which the protein takes part, establishing a condition of "loss of function", as result of the NPM1 partners delocalization in the cytoplasm, and/or "gain of function", as a consequence of the increased nuclear export of NPM1[362]. Mutant mice with only one functional NPM1 allele leads to genomic instability, promoting cancer susceptibility both *in vivo* and *in vitro* and developing of hematological malignancies[362]. Interestingly, the NPM1c+ AML defines a subgroup of AML with distinctive features such as a determined gene expression profile, including up-regulation of HOX genes and other genes involved in the stem cell maintenance and down-regulation of CD-34, and a specific microRNA signature, with the up-regulation of miR-10a and miR-10b[362]. Patients with NPM1c+ AML demonstrate a good-response to therapy and the prognosis is positive in absence of FTL3-ITD mutations[362].

2. AIMS OF THE PROJECT

As discussed previously, APE1 is an essential gene and exerts a key role in the maintenance of genome stability and redox signaling through its two main functions, the DNA repair and the redox regulation of different cancer-related transcription factors. These two functions are exerted by two independent domains. Through its C-terminus (residues 61-318), it acts as an essential endonuclease in the base excision repair (BER) pathway of DNA damages caused by endogenous and exogenous oxidative and alkylating agents. On the other hand, its N-terminal domain (residues 1-127) is devoted to redox regulation of different transcription factors, maintaining them in an active reduced state. Even if these two activities are quite well characterized and studied, the mechanisms that regulate cellular APE1 functions are still poorly understood. Intriguingly, in the latest years, a novel role for the first 35 amino acids of the protein has been revealed, although until few years ago, this extreme disordered N-terminal domain was considered dispensable for protein functions. This unique functional feature endowed by disorder within the first 35 amino acids contributes to and influences the mechanisms of action of APE1. It has been described that this lack of an ordered structure leads to several benefits, as an increased ability to bind to several proteins, allowing an extremely important plasticity in cellular response through a process of adaptation in recognizing the different partners, both proteins and nucleic acids[18,61,363,364], a controlled catalytic activity on abasic DNA through the regulation of product binding, as recently demonstrated by our group[23] and an effective regulation by degradation after a proteolytic event[111,112]. Moreover, as a multifunction protein, after gene transcription APE1, and its N-terminus, can be edited by different post-translational modifications *in vivo*, as reported previously for acetylation at Lys residues 6 and 7[25] and for ubiquitylation at Lys24, 25 and 27[24], acting as a novel and rapid mechanism for APE1 to modulate its different protein functions and dynamically coordinate its signaling networks. In addition, the complex protein networks in which APE1 takes place is a further mechanism able to redirect APE1 toward a specific function, by controlling its trafficking within the cells and its expression. However, a clear picture of the multiple ways by which cells regulates APE1 is still missing; for these reasons my PhD project aimed to fill this gap. In particular, I focus on the role of acetylation at APE1 N-terminus (Lys27, 31, 32 and 35) in controlling APE1/NPM1 interaction, its activity and its trafficking; interestingly, NPM1 itself, a new APE1 interacting partner, controls APE1 expression and AP endonuclease activity within cells. Finally, the effect of APE1 genetic variants in a cellular context was studied, with particular attention to the APE1 interaction with its binding partners. Accumulating evidences, in fact, indicate a firm linkage between the APE1 genetic variants and cancer etiology, but the molecular basis is still unknown. Elucidating the mechanisms and the consequences of an altered APE1/NPM1 interaction, possibly associated to the different APE1 polymorphic variants, and their role in tumorigenesis represent a critical step towards better patient treatments or therapeutic strategies for specific cancer types.

3. RESULTS

Data reported in this chapter have been partly published in Oncogene (2013): Vascotto, Lirussi *et al.*, *Functional regulation of the apurinic/apyrimidinic endonuclease 1 by nucleophosmin: impact on tumor biology.*

3.1 THE APE1 PROTEIN INTERACTOME AND THE ROLE OF ACETYLATION IN CONTROLLING ITS FUNCTIONS

3.1.1 IDENTIFICATION OF NEW APE1 ACETYLATION SITES *IN VIVO*

Previous reports have shown that post-translational modifications, such as proteolysis, ubiquitylation and acetylation, strongly impact on regulation of APE1 localization and its activities[23-25,111,112]. In particular, recent data from our lab demonstrated that acetylation occurring on APE1 N-terminal domain (Lys27-35) plays an import role in modulating the APE1 association with rRNA and NPM1[23], a novel APE1 interactor[18]. Given the importance of this post-translational modification, I proceeded with a systematic identification of lysine acetylation sites in HeLa cell lines expressing a FLAG-tagged form of the protein[18]. APE1-WT was immunopurified, taking advantage of the FLAG-tag, separated in SDS-PAGE, digested with trypsin and Lys-C and subjected to mass spectrometry. Fourteen lysine acetylation sites *in vivo* were identified, including twelve novel sites (Lys27, 31, 32, 35, 125, 141, 194, 197, 203, 224, 227, 228) in addition to two previously described sites (Lys 6 and 7)[25] (Figure 19). Notably, the majority of the acetylated sites fall into the first 35 amino acids of the protein, suggesting an important role of this domain in APE1 regulation. Interestingly, the acetylated sites found are localized close to the identified proteolytic site (Lys31 and 32)[111,112], indicating a possible role in regulating the protein cleavage.

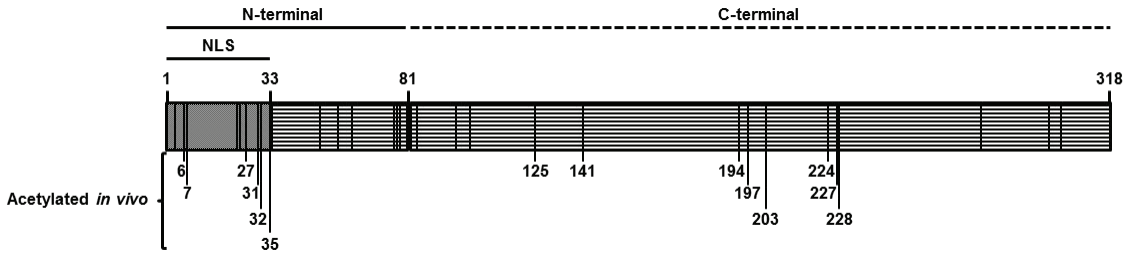

Figure 19: Schematic representation of APE1 structure. Within the structure, all the lysine residues are highlighted (vertical black lines); in black the acetylated lysine residues *in vivo* identified by MS are marked.

3.1.2 CHARACTERIZATION OF APE1 INTERACTOME MAP AND THE ROLE OF APE1 ACETYLATION IN CONTROLLING APE1 COMPLEX WITH ITS PROTEIN PARTNERS

Our group previously characterized the APE1 interacting partners under basal conditions through a functional proteomic approach based on 2-DE resolution of APE1 immunopurified complexes from HeLa cells[18]. This approach has the limitation of a poor efficiency for the analysis of proteins having a high molecular mass, a poor solubility and a basic pI value. Since post-translational modifications, including acetylation, can affect APE1 interaction with its associated proteins, we decided to extend APE1 interactome analysis, in order to evaluate the role of acetylation and of its N-terminus in controlling APE1 equilibrium with its partners. Therefore, to prevent any methodological bias, we now separated immunopurified complexes through SDS-PAGE and applied nLC-ESI-IT-MS/MS analysis directly to gel slice digests from protein having an apparent mass of 50-300 kDa (Figure 20). To evaluate the effect of the loss of the APE1 N-terminal domain on protein interactome, we first compared immunopurified APE1 complexes obtained from HeLa cell lines stably expressing a FLAG-tagged APE1-WT with that of the APE1-NΔ33 deletion mutant (Figure 20, *left*); experiments were performed under basal conditions as previously described[18]. Then, we analyzed the impact of HDACs-inhibitor trichostatin A (TSA), which is known to induce APE1 hyperacetylation on lysine residues 6 and 7[25,91], by comparatively evaluating the APE1 interactome under basal conditions and after treatment of cells with TSA (Figure 20, *right*). As a control, we used immunoprecipitated material from HeLa cells stably transfected with the empty vector and expressing a scrambled siRNA sequence (APE1-SCR-1). In both comparative interactome analyses, identified components were subtracted from protein entries occurring in gel portions associated with control (APE-SCR1).

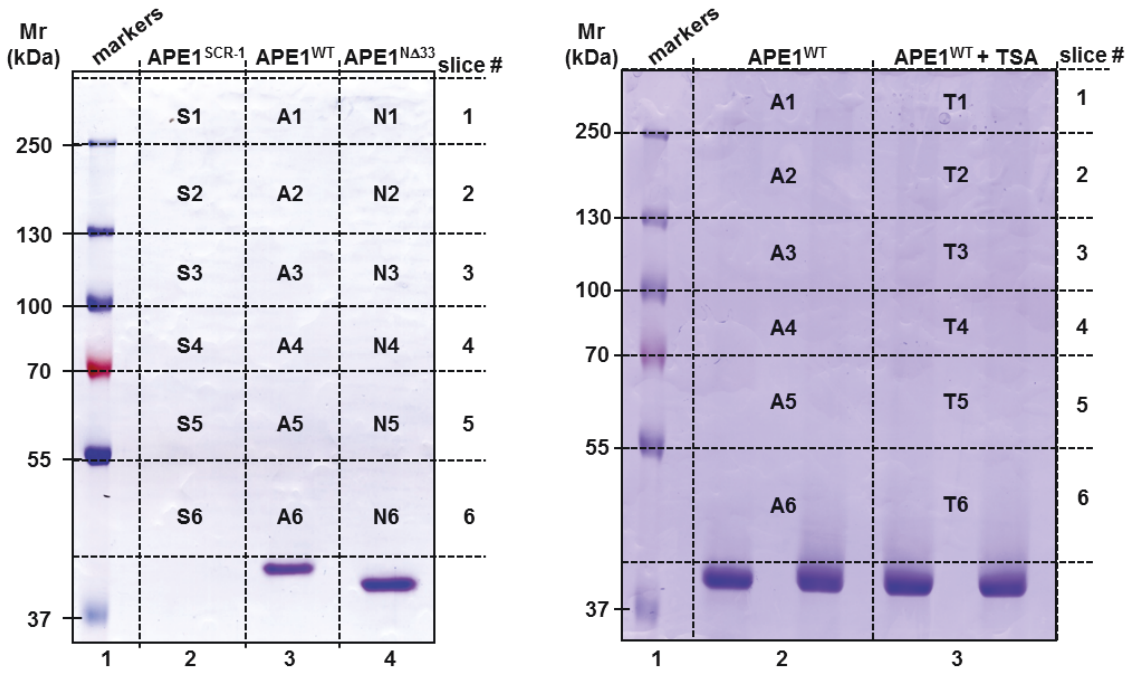

Figure 20: Coomassie Brilliant Blue staining and mass spectrometry identification of APE1 immunopurified complexes under native conditions, expressing different forms of APE1 (*left*) and upon Trichostatin A (300nM for 4hr) treatment (*right*). Vertical and horizontal axes indicate apparent molecular mass (kDa) and clones/treatment considered for each lane, respectively. Control represents HeLa cells stably transfected with a scrambled shRNA sequence (APE1-SCR-1), APE1-WT represents cells expressing only the ectopic APE1 protein in spite of the endogenous one while APE1-NΔ33 cells expressing the ectopic APE1 deletion mutant.

Duration of TSA treatment (4 hr) was chosen on the basis of kinetics experiments (Figure 21, *panel A*), where the extent of Lys6 and 7 acetylation status was maximal, as deduced by Western blotting using a specific antibody raised for this APE1 acetylated form[25] (Figure 21, *panel B*).

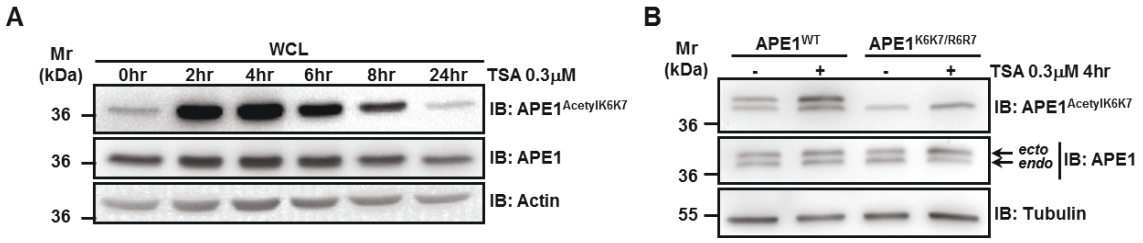

Figure 21: TSA treatment increases APE1 acetylation at Lys6 and 7. A | HeLa cells were left untreated or incubated with TSA (0.3μM) for the indicated times. A fraction of total cell extracts were separated onto SDS-PAGE and Western blotting analysis was performed to evaluate the time of treatment inducing maximal APE1 acetylation at Lys6 and 7, as revealed by a specific antibody for acetylated APE1 at K6/K7. Actin was used as loading control. **B |** Western blotting analysis of total extracts of cells expressing APE1-WT and a non acetylatable mutant of the protein in Lys6 and 7 (APE1-K6K7/R6R7) after TSA treatment to evaluate the specificity of the antibody used for the detection of acetylation at Lys6 and 7. HeLa cells were transiently transfected with APE1-WT and APE1-K6K7/R6R7 constructs. After transfection, cells were left untreated or incubated with TSA (0.3μM for 4hr), as indicated. As evident, APE1K6K7/R6R7 was not recognized by the antibody used. β-tubulin was used as loading control. Arrows indicated the two forms of APE1, the endogenous (endo) and the ectopic ones (ecto).

Besides confirming a number of APE1 interacting partners[18], highlighted in italics in Table 4, 17 novel protein species were identified. Again, the majority of these proteins classified within RNA metabolism (RL14, RL3, RL4, hnRNP-H, hnRNP-U, NCL, PABP1 and YB1), cytoskeleton dynamics (ACTN-1, KIF11, MOES, MYH9, MYO1C), secretion (SPTB2), transcriptional regulatory processes (BASP1 and THRAP3) and RNA metabolism, transcriptional activation and non-homologous end joining repair of DNA double strand breaks (SFPQ).

Taken together with results obtained in our previous work[18], a list of 26 specific APE1 interacting partners was obtained (Table 4). Interestingly, most of them required the APE1 N-terminal domain for stable interaction and were modulated by acetylation. Notably, our approach did not identified known DNA-repair enzymes involved in BER, such as Polβ or XRCC1, which are already known binding to APE1 and that were found by subsequent Western blot analyses in this work of Thesis[61]. This may be essentially due to the low sensitivity of the method we used, able to efficiently recognize only highly abundant proteins, and to the low representation of DNA repair enzymes in mammalian cells[365].

As confirmatory data, validation experiments with some of the identified protein species (Figure 20 and Table 4) and evaluation of the effect of the N-terminus truncation and acetylation after TSA treatment on the other interacting partners identified were performed by Western blot analysis on an independent set of immunoprecipitated material (Figure 22).

Table 4: List of APE1 interacting partners as revealed by combined SDS-PAGE/nLC-ESI-IT-MS/MS analysis and previous combined 2-DE/MALDI-TOF peptide mass fingerprint analysis. Protein name, accession number (SwissProt entry), molecular mass (kDa), sequence coverage, number of identified peptides and known protein functions are listed. Interacting protein ability to bind APE1-NΔ33 and modulation of protein interacting partners after TSA treatment are also indicated. Down-arrows indicate a decrease interaction with respect to APE1-WT.

Protein identity	Swiss Prot entry	Mr (kDa)	Sequence coverage %	Peptide number	Function	Interaction with APE1-NΔ33	TSA treatment	Slice nr
40S ribosomal protein SA (RSSA)	*P08865*	*33*	*4,41*	*2*	*Required for the assembly and/or stability of the 40S ribosomal subunit. Processes the 20S rRNA-precursor to mature 18S rRNA*	↓		
60S acidic ribosomal protein P0 (RLA0)	*P05388*	*34*	*13*	*7*	*Functional equivalent of E.coli protein L10*	*No*		
60S ribosomal protein L14 (RL14)	P50914	23	9,39	3	Component of the large subunit of cytoplasmic ribosomes		+	T1
60S ribosomal protein L3 (RL3)	P39023	46	5,21	3	Component of the large subunit of cytoplasmic ribosomes		-	A6
60S ribosomal protein L4 (RL4)	P36578	48	2,58	4	Component of the large subunit of cytoplasmic ribosomes	No		A3, A4, A5, T5, T6
Alpha-actinin-1 (ACTN1)	P12814	103	2,47	4	F-actin cross-linking protein		-	A3
Aminopeptidase N (hAPN)	P15144	109	3,41; 1,45	11, 4	Broad specificity aminopeptidase. Used as a marker for acute myeloid leukemia and played a role in tumor invasion			A2, T2
Brain acid soluble protein 1 (BASP1)	P80723	23	48,46	20	Trascriptional corepressor and promoter binding protein	Yes		A3, A4, A5, N4, N5
Heterogeneous nuclear ribonucleoprotein F (hnRNP-F)	P52597	46	8,21	4	Component of the heterogeneous nuclear ribonucleoprotein (hnRNP) complexes			A6, T6
Heterogeneous nuclear ribonucleoprotein H (hnRNP-H)	P31943	49	7,57	4	Component of the heterogeneous nuclear ribonucleoprotein (hnRNP) complexes		+	T5
Heterogeneous nuclear ribonucleoprotein U (hnRNP-U)	Q00839	90	5,22	2	Binds to pre-mRNA and to to double- and single-stranded DNA and RNA		+	T2
Keratin, type II cytoskeletal 8 (K2C8)	*P05787*	*50*	*12*	*9*	*Helps to link contractile apparatus to dystrophin at costameres of striated muscle. Belongs to ribosomal protein S2P family*	*No*		
Kinesin-like protein (KIF11)	P52732	119	3,6	10	Motor protein	No		A1, A2, T1, T2
Moesin (MOES)	P26038	68	1,73	2	Connects major cytoskeletal structures to the plasma membrane	No		A4

Myosin-9 (MYH9)	P35579	227	2,14	6	Role in cytokinesis, cell shape, and specialized functions		+	T1
Myosin-Ic (Myosin I beta) (MYO1C)	O00159	118	2,82	3	Unconventional myosins involved in intracellular movements ans Involved in glucose transporter recycling in response to insulin		+	T2
Nucleolin (Protein C23) (NCL)	P19338	77	2,97	6	Role in pre-rRNA transcription and ribosome assembly. Chromatin decondensation inducing protein	No		A2, A3, A4, A5, T2, T3
Nucleophosmin (NPM1)	*P06748*	*35*	*19*	*9*	*Associated with nucleolar ribonucleoprotein structures and binding to single-stranded nucleic acids; assembly and transport of ribosome*	*No*		
Peroxiredoxin 6 (PRDX6)	*P30041*	*25*	*37*	*7*	*Involved in redox regulation of cell and protection against oxidative injury (lipid peroxidation)*	↓		
Polyadenylate-binding protein 1-A (PABP 1)	P11940	71	7,9	4	Binds the poly(A) tail of mRNA		-	A4
Pre-mRNA-processing factor (PRP19)	*Q9UMS4*	*53*	*22*	*6*	*DNA double strand break repair and pre-mRNA splicing reaction*	*No*		
Ribose-phosphate pyrophosphokinase 1 (PRPS1)	*P60891*	*31*	*29*	*8*	*Ribose metabolism*	*Yes*		
Ribose-phosphate pyrophosphokinase 2 (PRPS2)	*P11908*	*31*	*19*	*6*	*Ribose metabolism*	*Yes*		
Spectrin beta chain, brain 1 (SPTB2)	Q01082	275	0,89	3	Involved in secretion, interacts with calmodulin in a calcium-dependent manner		+	T1
Splicing factor, proline- and glutamine-rich (SFPQ)	P23246	76	2,15	4	DNA and RNA binding protein; pre-mRNA splicing factor. Involved in NHEJ and required for double strand break. Trascriptional regulator	No		A3
T-complex protein 1 subunit alpha (TCPA)	*P17987*	*57*	*20*	*10*	*Molecular chaperone*	*No*		
Thyroid hormone receptor-associated protein 3 (THRAP3)	Q9Y2W1	109	0,95	4	Role in transcriptional coactivation	No		A2
Y-box-binding protein (YB1)	P67809	36	20,19	8	Mediates pre-mRNA alternative splicing regulation. Binds and stabilizes cytoplasmic mRNA	No		A6, T6

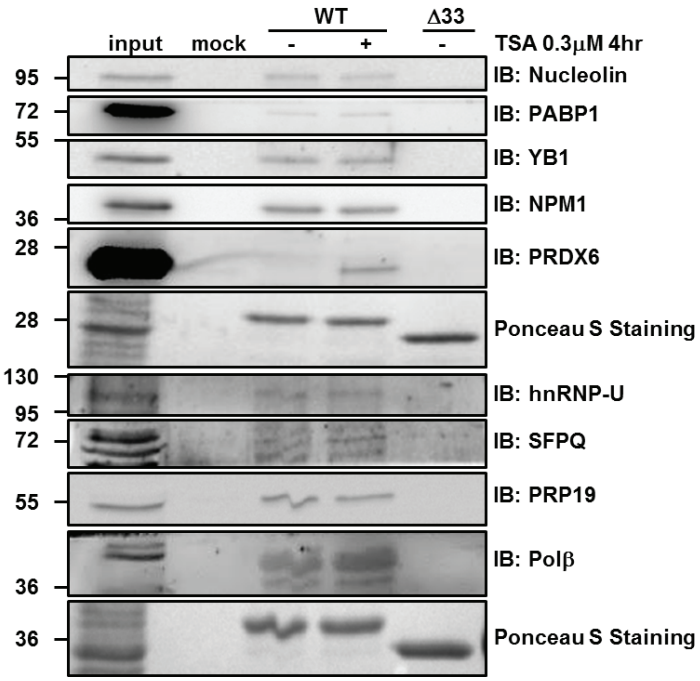

Figure 22: Validation of new APE1 interacting partners identified by combined SDS-PAGE/nLC-ESI-IT-MS/MS analysis. Co-immunopurified material from APE1-WT and APE1-NΔ33 cell lines left untreated or incubated with TSA (0.3μM for 4hr) was separated onto SDS-PAGE and Western blotting analysis was performed to validate the APE1 interacting partners identified by mass spectrometry through independent experimentes. Ponceau S staining was used as loading control.

Functional enrichment analysis indicated that within the 26 APE1 interacting partners, identified in our previous paper[18] and in the present work, the majority was enriched in RNA binding and metabolism (Figure 23 and Supplementary Table 1).

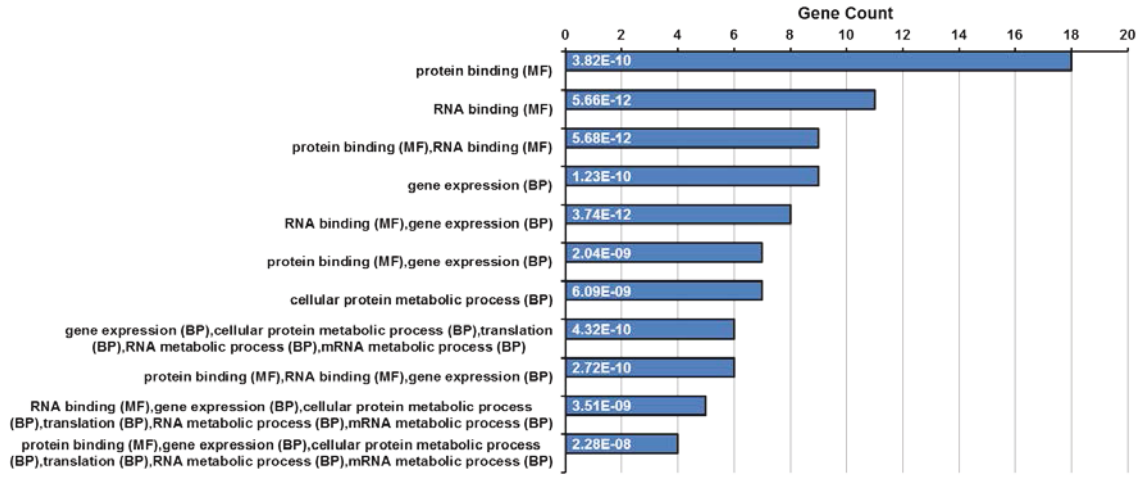

Figure 23: Functional enrichment analysis of the interacting protein species identified by mass spectrometry analysis according to molecular function. GeneCodis analysis of 26 unique identified interacting proteins. For simplicity only the most representative functional categories are represented. The number of genes for each category is provided on horizontal axis and list only the first five co-occurrence terms. Statistical significance belonging to each category is shown within each bar.

Then, prompt by these data, I decided to expand my analysis to all the seventy-three APE1 interacting partners known in literature (Supplementary Table 2). As shown in

Figure 24 (Figure 24), the analysis shows an enrichment of GO terms related to protein and nucleic acids binding, but also to DNA repair and gene expression, demonstrating its association with different protein complexes within cells and reinforcing the idea of APE1 as multifunctional protein further highlighting the new role of APE1 in the RNA metabolism.

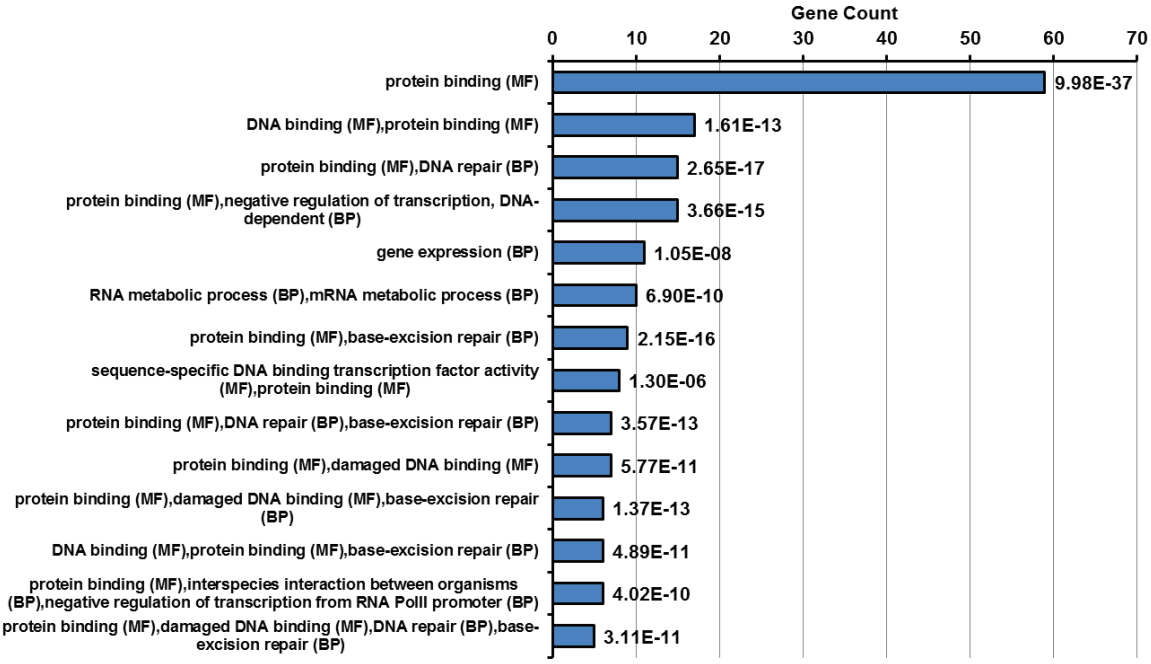

Figure 24: Functional enrichment analysis of all the 73 APE1 interacting partners retrieved in literature according to molecular function. GeneCodis analysis of all the 73 APE1 identified interacting proteins in literature. The number of genes for each category is provided into the specific sector. Statistical significance belonging to each category is shown for each bar.

3.1.3 IN SOME CASES NUCLEIC ACIDS MEDIATE THE APE1 INTERACTION WITH ITS PROTEIN PARTNERS

Several evidences support the concept that nucleic acids, in particular RNA molecules, are important mediators of the interaction of DNA repair proteins with their interacting partners[18,366,367]. Our group, in fact, has recently demonstrated that the strong interaction between APE1 and NPM1 may involve RNA molecules through electrostatics[18]. Therefore, to check whether the APE1 interaction with proteins involved in RNA binding, as YB-1, and in DNA repair, as Polβ and XRCC1, may also be mediated by RNA and/or DNA molecules, cell lysates were digested with nuclease/RNase before coimmunoprecipitation. APE1 association with its interacting partners was not mediated by DNA, as demonstrated by DNase I treatment (the interaction rather increases upon the treatment, possibly as a consequence of the change in the equilibrium of the APE1 binding to nucleic acids, from DNA to RNA), while treatment with DNase-free chromatographically purified RNase A mostly reduced it (Figure 25).

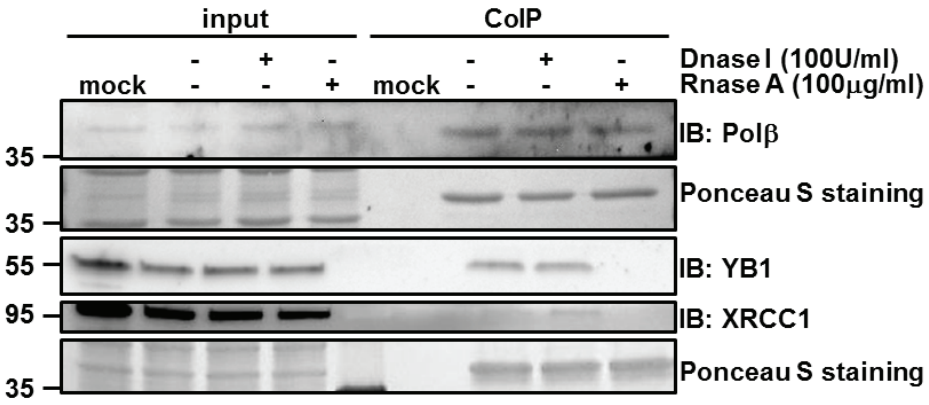

Figure 25: APE1 interaction with its protein partners is mediated by RNA. The interaction between APE1 and some of its interacting partners is mediated by RNA. HeLa cells were transiently transfected with FLAG-tagged APE1-WT constructs. Coimmunoprecipitation (Co-IP) was performed using anti-FLAG monoclonal antibody-conjugated resin with identical aliquots of cell lysates. Cell lysates were pretreated with 100 U/ml DNase I and 100 μg/ml DNase-free RNase A for 30 min at 30°C before coimmunoprecipitation. Coimmunoprecipitates were separated onto SDS-PAGE gel and analyzed by western blotting with the specific anti-Polβ, anti-XRCC1, anti-YB-1. Ponceau S staining was used as loading control. The analysis was repeated in two independent experimental sets. The variability between the two data sets is less than 20 percent.

These data suggest that the strong interaction between APE1 and some of its interacting partners may involve RNA molecules, as previously described for the interaction between APE1 and NPM1[18].

3.1.4 DYNAMIC OF APE1 INTERACTOME DURING GENOTOXIC DAMAGE: A SWITCH FROM RIBONUCLEO- TO DEOXYRIBONUCLEO- PROTEIN COMPLEXES

The data described so far may drive the hypothesis that genotoxic damage modulates the dynamic equilibrium of APE1 interactome network to guarantee the maintenance of genome stability, as already demonstrated for Ku70[366]. Since the DNA-repair function of APE1 is essential in the initial steps of BER, for recognition of the abasic lesions and generation of the cleavage products further accessible to Pol β re-synthetic activity, I evaluated the dynamic of APE1 interactome under genotoxic treatment conditions, i.e. after treatment with MMS, treatment that increases APE1 acetylation at K27-35[92]. Taking advantage of the interacting partners recently identified by proteomic analysis[18], I analyzed the interaction dynamics of proteins associated with RNA metabolism (NCL, NPM1, YB-1 and PRP19) in comparison with that involved in BER (Pol β and XRCC1). This analysis demonstrated that APE1 interaction with DNA-repair enzymes upon MMS treatment resulted increased in a time-dependent manner in a biphasic fashion, while that with proteins involved in RNA metabolism was reduced (Figure 26). After 4 hr of MMS treatment, interaction with Pol-β and XRCC1 was maximal, whereas an apparent decrease of association with proteins involved in RNA metabolism was apparent. Thus, genotoxic treatment switches APE1 interactome network from binding to protein partners involved in RNA metabolism to those involved in DNA repair and directly to DNA as a substrate.

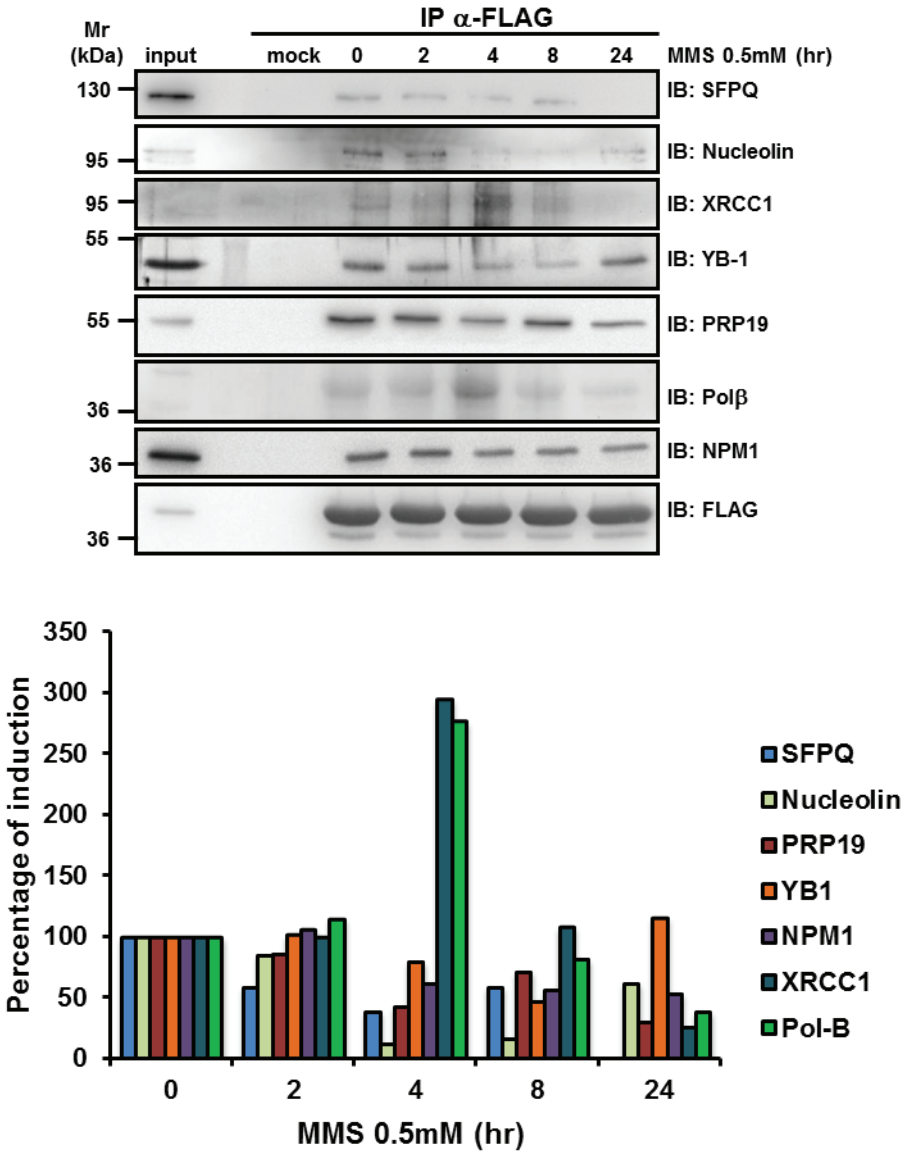

Figure 26: MMS-treatment causes increased APE1 interaction with proteins involved in DNA repair and decreased that with those involved in RNA metabolism. (*Top*) Western blotting analysis of the co-immunoprecipitated material from HeLa cells transfected with an empty vector (*mock*) and APE1-WT and treated for different times (0, 2, 4, 8 and 24 hr) with 0.5mM MMS. After normalisation for immunoprecipitated APE1-WT protein, the levels of different APE1 interacting partners were evaluated by using specific antibodies. In line 1 (*input*), total cell extract was used as a positive control. Absence of signal in the mock line confirmed the specificity of interaction. (*Bottom*) Quantification of APE1-WT interacting partners levels after MMS treatment. Normalized volume values of band intensities obtained after densitometric analysis of the ratio between the specific interacting partner and the APE1-WT form were reported as histograms. Data shown are the mean of two independent experimental sets. The variability between the two data sets is less than 20 percent.

Overall, these data clearly show that, during cell response to genotoxic damage, the equilibrium of APE1 interactions shifts from binding to NPM1 (thus from nucleolar storage) to DNA-repair proteins and that acetylation occurring at Lys27, 31, 32 and 35 is an important molecular player in controlling this equilibrium mechanism.

Genotoxic treatment therefore may switch APE1 interactome network from binding to protein partners involved in RNA metabolism to those involved in DNA repair and directly to DNA as a substrate.

Since genotoxic damage, such as MMS, is able to induce APE1 acetylation at Lys27-35[92] and modulates its interacting network, switching APE1 binding towards DNA repair partners, we decided to better characterize the functional role of acetylation at Lys27-35 during genotoxic damage and its relevance *in vivo*[92]. In our recent paper, we demonstrated that in cells expressing a specific K-to-A mutant (APE1-K4pleA), mimicking a constitutive acetylated form of the protein, APE1 presents a nuclear localization, showing nucleolar deficiency, and an increased AP activity. Cells expressing this mutant are more resistant to genotoxic treatment than those expressing the wild-type, although its nucleolar absence negatively influences the cellular proliferation. Notably, the acetylation status of Lys27-35 is strongly connected with that observed at Lys6/Lys7, involved in the coordination of BER activity, through a mechanism regulated by sirtuin 1 deacetylase (SIRT1)[78]. Of interest, structural studies show that acetylation at Lys27-K35 may account for local conformational changes on APE1 protein structure. All these results highlight the emerging role of acetylation of critical Lys residues in regulating APE1 functions. They also suggest the existence of cross-talk between different Lys residues of APE1 occurring upon genotoxic damage, which may modulate APE1 subnuclear distribution and enzymatic activity *in vivo*[92].

These evidences allowed to draw a model (Figure 27) that describes how, during DNA damage stress response, acetylated APE1 dissociates from NPM1 within nucleoli and accumulates into the nucleoplasm, where it can exert its endonuclease activity on damaged DNA. Notably, genotoxic treatment significantly alters the APE1 interactome network redirecting the enzyme from protein complexes associated with RNA metabolism toward those involved in DNA repair.

Through multiple interactions with various protein partners and coordinated occurrence of different post-transcriptional modifications, such as acetylation and ubiquitylation[24], subcellular distribution of APE1 and its enzymatic activity seem to be finely tuned, on demand, in a time-dependent manner. Nucleolar role of APE1 storage and regulation may have profound biological consequences during cell response to stressor signals, also in light of recent evidences pointing to nucleolus as a central hub in DNA damage.

As importantly, data obtained in this work show that nucleoli may not only act as a storage site for securing a proper amount of APE1 readily available for maintenance of genome stability, but also emphasize that nucleolar APE1 may control cell proliferation, possibly through its rRNA cleansing function or through an hypothetical role on ribogenesis. Accordingly, APE1-K4pleA expressing cells, under basal conditions, showed impairment in proliferation rate with respect to APE-WT expressing ones. Therefore, it may be speculated that nucleolar APE1 is responsible for functional activity of the nucleolus in ribosome biogenesis. APE1 release from nucleoli upon genotoxic treatment may constitute a signal for blocking active protein synthesis and allowing activation of

proper DNA-repair mechanisms. This hypothesis is in accordance with the most recent evidences considering the nucleolus as a DNA damaging stress sensor[262].

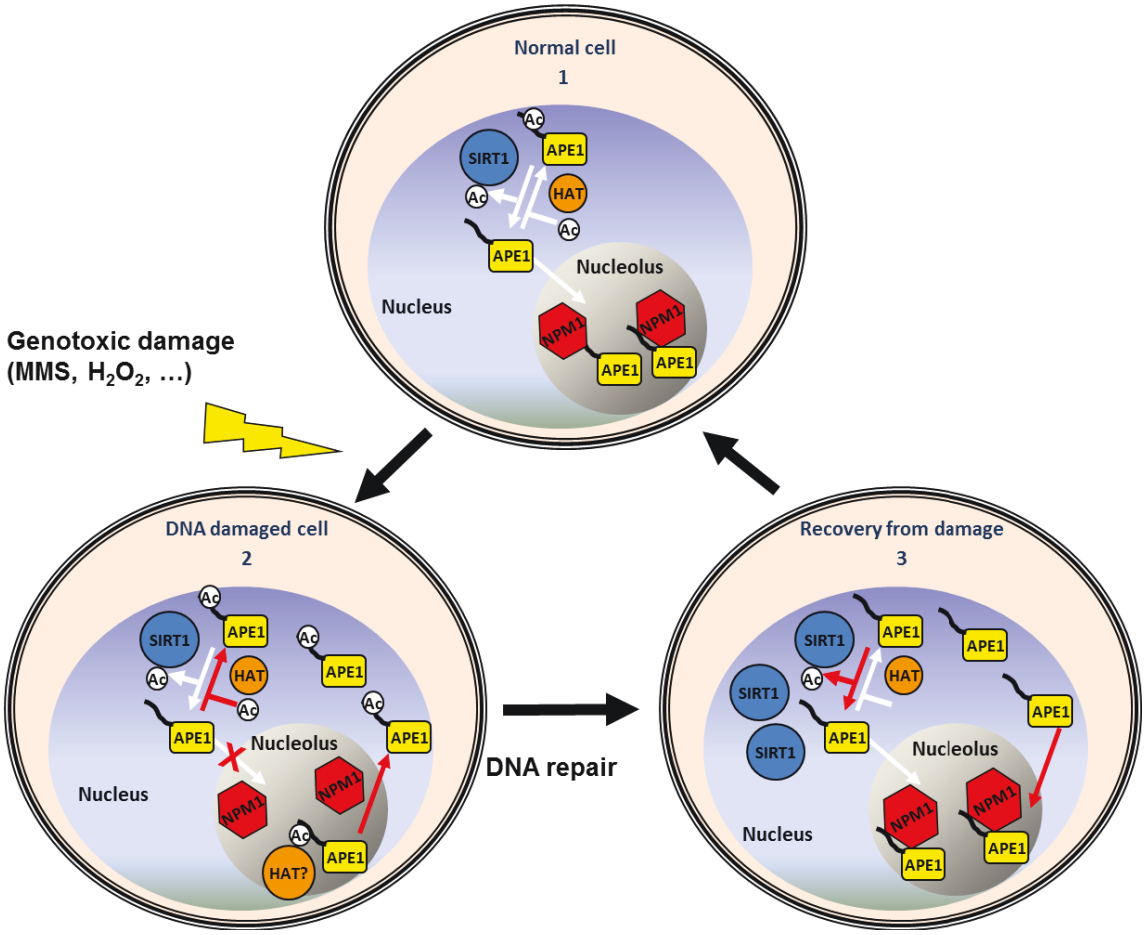

Figure 27: Nucleolus acts as a hub in regulating different APE1 functions. Within mammalian cells, acetylated APE1 (Ac-APE1) is present with different degree of modification at K27-K35 and it localizes mainly in the nucleoplasm; conversely, the non-acetylated form (APE1) is prevalently nucleolar, where it become stored once bound to interacting partners, such as NPM1. During genotoxic stress conditions, as those determined by alkylating or oxidative agents, which generates abasic sites that are removed by APE1 endonuclease activity, the equilibrium between Ac-APE1 and APE1 forms changes toward the former, thus stimulating protein participation in BER response. In nucleolar compartment, a yet unidentified histone acetyl transferase (HAT(s)) may acetylate APE1 at K27-K35; this post-translational modification may control subcellular compartmentalization of APE1 within specific structures and its functions. In fact, APE1 acetylation inhibits APE1/NPM1 interaction, allowing APE1 movement from nucleoli to nucleoplasm. SIRT1, which is essentially located in the nucleoplasm and excluded from nucleoli, may control the acetylation status of $K^{27}/K^{31}/K^{32}/K^{35}$, in addition to that of K^{6}/K^{7}, thus modulating the further steps of BER pathway, by coordinating APE1/XRCC1 interaction[368], and controlling re-accumulation of APE1 into nucleoli.

What comes out from this model is the importance of NPM1 interaction in regulating APE1 subcellular localization and functions. We, therefore, focused our attention on the role of NPM1 in functional regulation of APE1 activities. The next paragraphs will be dedicated to it.

3.2 FUNCTIONAL REGULATION OF APE1 BY NPM1

3.2.1 NPM1$^{-/-}$ CELLS ARE MORE SENSITIVE THAN CONTROL CELLS TO DNA DAMAGES REPAIRED THROUGH THE BER PATHWAY

Our group has previously demonstrated that NPM1 has a positive role in regulating APE1 endonuclease activity *in vitro* through protein-protein interaction, interaction that increases ten fold the APE1 catalytic activity, hastening the product release step[18,23].

Since no studies relative to the role of NPM1 in regulation APE1 *in vivo* have been performed yet, I evaluated the effect of the absence of NPM1 on APE1 participation in BER process upon different stresses, known to be repaired by BER, in a mouse embryonic fibroblast (MEF) cell line model NPM1 knock-out (hereafter called NPM1$^{-/-}$). These cells have a p53$^{-/-}$ background for immortalization, in order to prevent triggering of apoptosis[342]. As a control, an isogenic control cell line p53 knock-out (NPM1$^{+/+}$) was used[342].

First, I tested whether the absence of NPM1 might have an influence on APE1 expression level. Western blot analyses carried out on nuclear cell extracts obtained from NPM1$^{-/-}$ and NPM1$^{+/+}$ MEFs revealed an up-regulation of APE1 protein level of about 40% in comparison to the control cell lines (Figure 28).

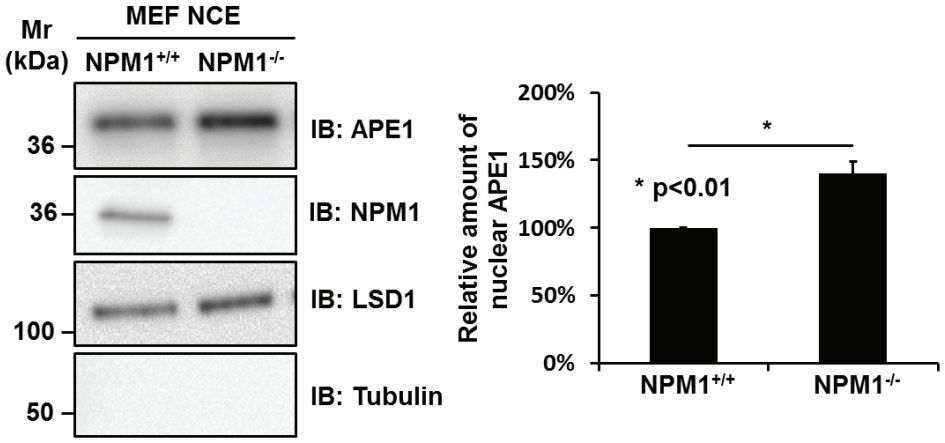

Figure 28: Absence of NPM1 positively regulates APE1 protein level in MEFs. (*Left*) Representative Western blotting analysis on NPM1$^{+/+}$ and NPM1$^{-/-}$ nuclear cell extracts (5μg) showing an increase APE1 expression level of about 40% in the absence of NPM1 expression. Lysine demethylase 1 (LSD1) was used as nuclear marker and loading control; tubulin was used as cytoplasmic marker to evaluate possible cytoplasmic contaminations. Antibodies used are indicated on the right-hand side. (*Right*) Histogram reporting the densitometric quantification of Western blotting chemiluminescent signals from at least three independent experiments. Relative nuclear APE1 content is expressed as mean±SD of the signal, considering NPM1$^{+/+}$ as reference sample.

To gain further insights into the molecular mechanisms by which NPM1 exerts its effect on APE1 expression, I compared the mRNA levels of APE1 in NPM1$^{+/+}$ and NPM1$^{-/-}$ MEFs. As measured by Q-PCR analyses, APE1 exhibited a marginal variation (less than

20%) at the transcript level (Figure 29), suggesting that the NPM1 effect on APE1 could be mediated mainly via post-transcriptional mechanisms.

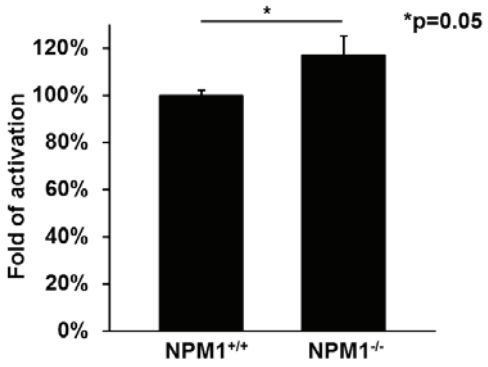

Figure 29: APE1 mRNA level is only marginally increased in NPM1$^{-/-}$ cells. Q-PCR analysis of APE1 mRNA level in NPM1$^{+/+}$ and NPM1$^{-/-}$ MEF cells. ΔΔCt method was used to compare the APE1 mRNA expression in the two cell lines. Actin β was used as housekeeping gene to normalize the samples.

Interestingly, challenging NPM1$^{-/-}$ MEFs with different genotoxic stresses inducing DNA lesions repaired by BER pathway[369], in an effort to evaluate the functional relevance of NPM1 in BER, demonstrated a higher sensitivity of NPM1$^{-/-}$ MEFs, despite an increased APE1 content (Figure 30). A wide range of stresses that elicit a BER response was used as methyl methansulfonate (MMS)[370], a mono-functional methylating agent, oxidizing agents as hydrogen peroxide (H_2O_2) and potassium bromate ($KBrO_3$)[371] causing oxidation of bases (e.g. 8-oxoG), and the radiomimetic bleomycin (BLM)[372].

Cell viability assay experiments showed that in the absence of NPM1, cells were significantly more sensitive than the isogenic control cell line to MMS (Figure 30, *panel A*) and to acute doses of H_2O_2 in combination with methoxyamine (MX)[373], an inhibitor of APE1-dependent repair (Figure 30, *panel B*). As confirmation, I used an alternative oxidizing agent, as $KBrO_3$, known to produce 8-oxoG lesions on DNA after a metabolic activation of bromate by glutathione[371]; as shown in Figure 30 (*panel C*), at all the release time, the treatment with KBrO3 renders NPM1$^{-/-}$ MEFs less viable.

Finally, the response to BLM was tested. BLM targets single stranded- and double stranded-DNA, as well as RNA molecules, inducing the formation of 4-oxidized AP-sites or 3'phosphoglycolate products[372]. Cell viability, as measured by cell counting, on MEFs cells after 1h-treatment with increasing doses of BLM, followed by 48 hr of recovery, is in accordance with the experiments performed using alternative genotoxins, reporting an increased sensitivity to BLM in absence on NPM1 (Figure 30, *panel D*).

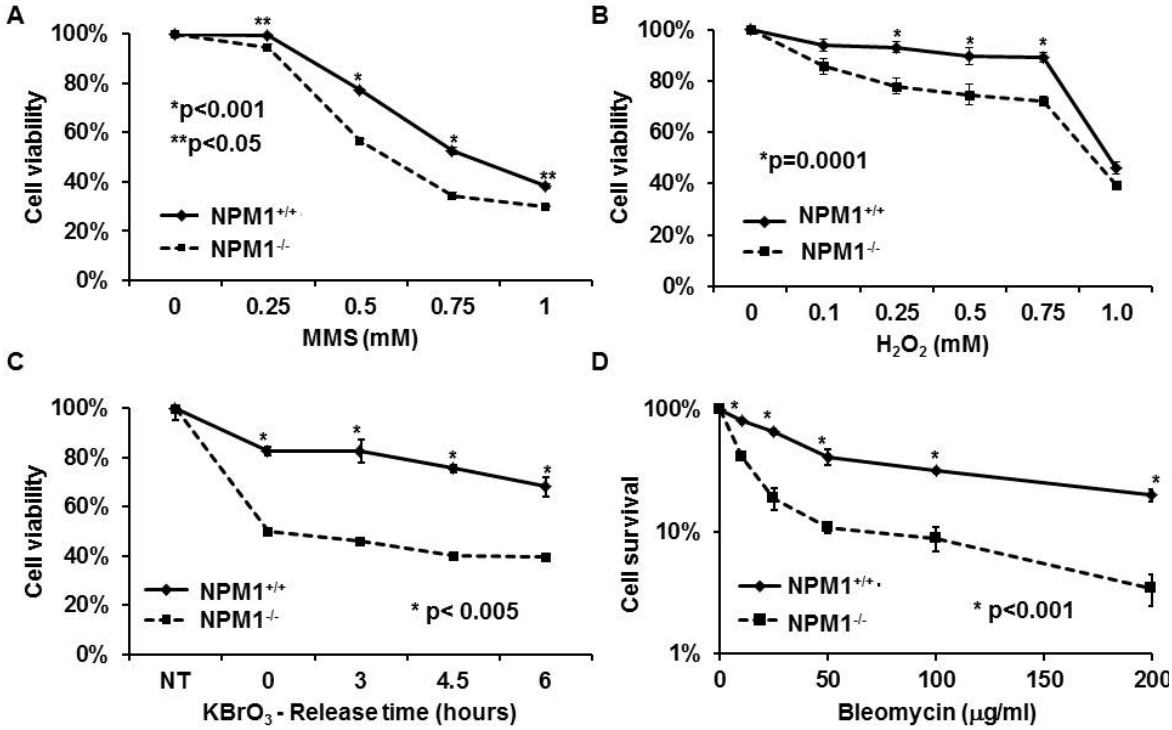

Figure 30: NPM1$^{-/-}$ MEFs displays increased sensitivity to a wide range of DNA damaging agents. A | MTS assay was used to evaluate cell viability of MEF cells after treatment with increasing amounts of MMS for 8 hr. **B |** Cell viability were tested using MTS assay on MEFs. After 24 hr-pretreatment with MX, cells were incubated with increasing doses of H_2O_2 for 1 hr. **C |** Evaluation of cell survival of MEFs after $KBrO_3$ treatment (40 mM for 30 min) using MTS assay. After removing the compound, cells were allowed to recover for the indicated periods of time. **D |** Trypan blue cell counting was used to measure cytotoxicity of BLM in MEF cells. Mean±SD values are the result of three independent experiments.

Remarkably, DNA lesions induced by PJ34, a PARP-inhibitor[374], and UVC, that require a NER participation for recovery, did not lead to any significant differential sensitivity between the two cell lines, supporting a specific impairment of BER pathway, involving APE1, in NPM1$^{-/-}$ cells (Figure 31).

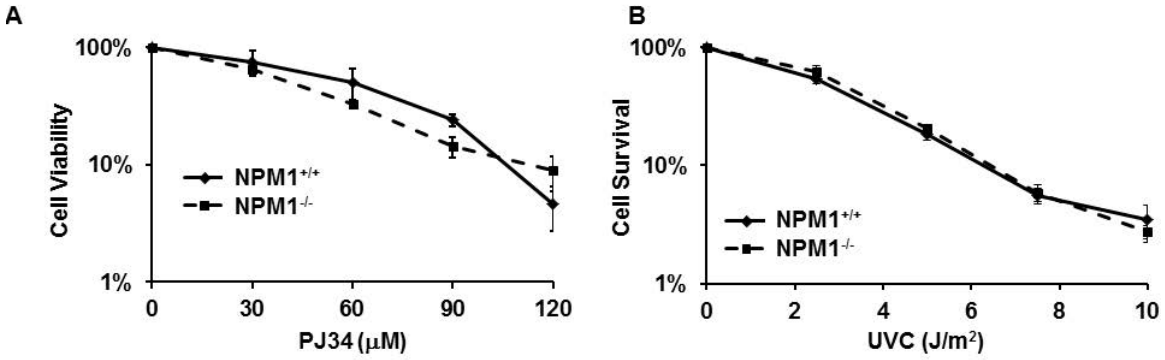

Figure 31: NPM1$^{-/-}$ MEFs did not display any differential sensitivity to DNA lesions repaired by NER. A |PARP inhibitor PJ34 was used as damaging agents that elicit a NER response to evaluate the cell viability by using WST-1 cell proliferation assay. Cells were incubated with increasing amounts of PJ34 for 48 hr. **B** | Cell survival was evaluated after UVC light on MEFs cells by cell counting. Cells were exposed to the indicated amounts of UVC light followed by a recover of 48 hr.

Then, the persistence of AP sites induced by MMS was tested on MEFs to evaluate the efficiency of the two cell lines to remove them. As displayed in Figure 32, NPM1$^{-/-}$ cells retained a significantly higher amount of AP sites upon MMS treatment than the isogenic control cell line. Notably, the two cell lines present a statistical significant difference under basal conditions, pointing to impairment at the AP-sites incision step in BER pathway in the absence of NPM1.

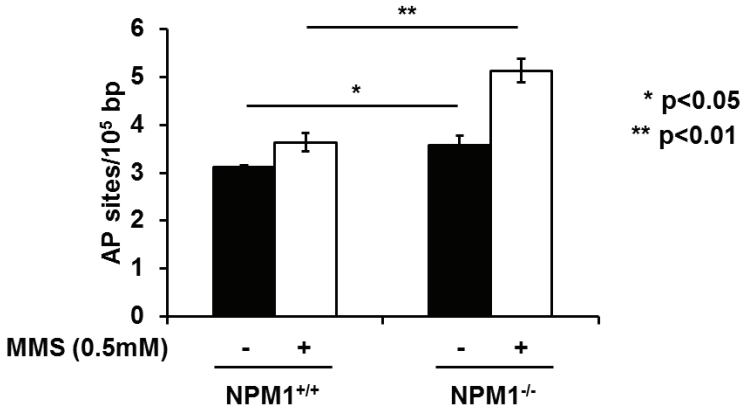

Figure 32: In absence of NPM1, cell retains a higher amount of AP sites. The amount of abasic (AP) sites was measured in MEFs after incubation with 0.5 mM of MMS for 4 hr. NPM1$^{-/-}$ cells display a significantly higher amount of AP sites if compared with control cells. Treatment with an alkylating agent leads to the accumulation of AP sites in NPM1$^{-/-}$ cells (5.14±0.25/10^5 bp) if compared with NPM1$^{+/+}$ cells (3.58±0.20/10^5 bp). Mean±SD values are the result of three independent experiments.

Collectively, all these data support a protective role exerted by NPM1 towards different DNA-damaging agents through stimulation of the BER response.

3.2.2 THE LOWER APE1 BER ACTIVITY OBSERVED IN NPM1$^{-/-}$ CELLS IS RESCUED BY NPM1 RECONSTITUTION

To determine whether the AP-site incision activity of APE1 was affected by NPM1 depletion, the APE1 enzymatic activity was measured in nuclear cell extracts of MEFs. Endonuclease assay showed that the AP-endonuclease activity of APE1 did not present any significant difference between the two cell lines, in spite of an increased APE1 expression level in the NPM1 knock-out MEFs (Figure 33, *panel A*). To better investigate the role played by NPM1 in controlling the APE1 endonuclease activity *in vivo*, the same experiment after the normalization of nuclear APE1 content was repeated. As already shown by our group using recombinant protein[18], NPM1 exerts a positive regulatory effect on APE1: NPM1$^{-/-}$ MEFs displayed a significant lower AP-activity in comparison to the isogenic control cell line (Figure 33, *panel B*). Hence, in absence on NPM1, in an attempt to maintain a steady state level of the BER activity, a compensatory mechanism based on an increased APE1 nuclear content might be induced, although this higher amount is still not sufficient to efficiently remove DNA lesions under genotoxic environment.

To assess whether the effect presented so far were directly linked to NPM1 loss and not to some other unspecific effect due to the knock-down of the gene, NPM1$^{-/-}$ MEFs were transfected with a vector encoding for NPM1, restoring NPM1 expression in this cell line.

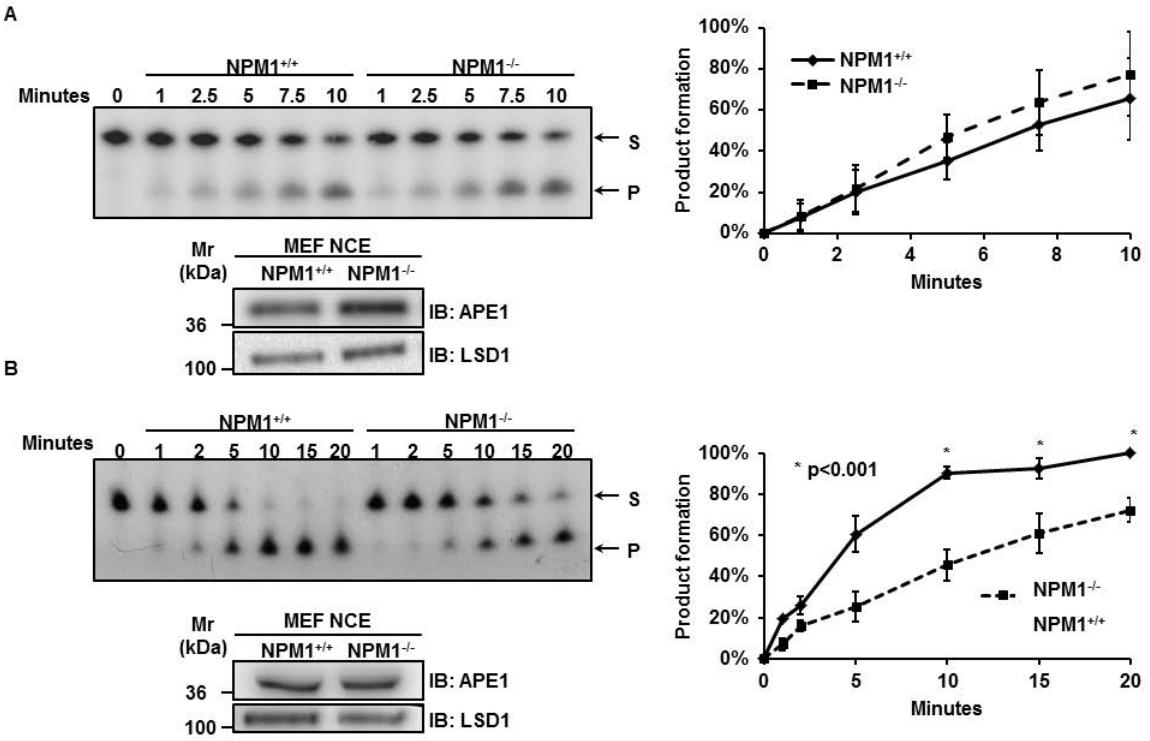

Figure 33: Absence of NPM1 impaired the APE1 AP-incision activity. A | Endonuclease assay comparing equal amounts of nuclear cell extracts (600ng) from NPM1$^{+/+}$ and NPM1$^{-/-}$ MEFs. A representative image shows the conversion of the substrate (S) in the product (P) operated by APE1 at the indicated periods of time. In the diagram on the right, the densitometric quantification of the product formation of three independent experiments is shown. Western blotting indicating the amount of cell extract used during the analysis is reported. LSD1 is used as nuclear marker. **B |** *In vitro* endonuclease assay performed using comparable amount of nuclear APE1, as shown by Western blotting analysis after normalization of the two nuclear cell extracts. A representative image shows the conversion of the substrate (S) in the product (P) during time, as indicated. The diagram on the right displays the product formation as obtained by densitometric quantification of three independent experiments.

On this background, the APE1 AP-incision activity was re-tested by endonuclease assay using nuclear cell extracts (Figure 34)

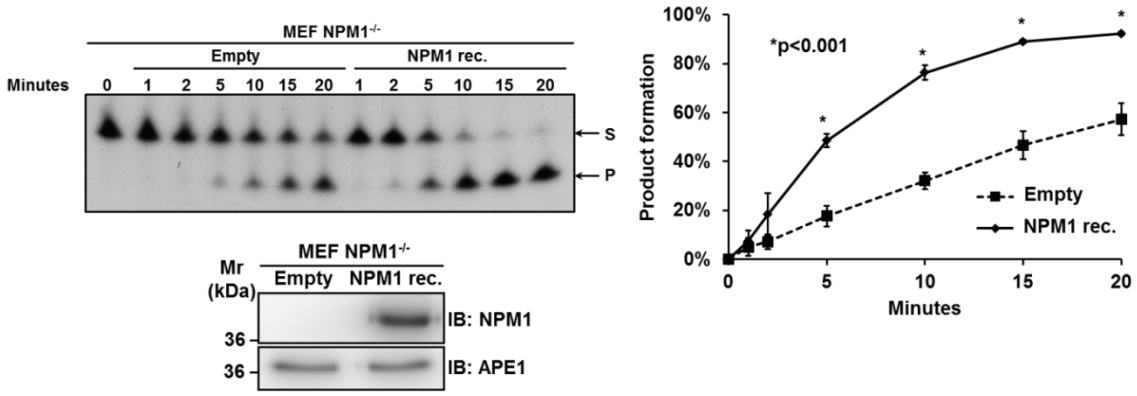

Figure 34: NPM1 positively regulates APE1 AP-incision activity. Endonuclease assay performed on NPM1$^{-/-}$ MEFs reconstituted (rec.) or not (Empty) by ectopic expression of NPM1, as shown by Western blotting analysis. A representative image displays the conversion of the substrate (S) in the product (P) in the indicated periods of time. The diagram on the right reports the mean±SD of densitometric quantification of the product formation of three independent experiments.

Data reported demonstrated that the re-expression of NPM1 in NPM1$^{-/-}$ MEFs restores the APE1 AP-incision activity when compared to NPM1$^{-/-}$ cells, transfected with an empty vector as control.

To assess the biological role of NPM1 reconstitution and to test whether the presence of NPM1 was able to ameliorate the DNA damage repair towards genotoxins elicited by BER, stable cell lines re-expressing NPM1 wild-type on the NPM1$^{-/-}$ background were obtained. As shown in Figure 35, the re-expression increases the cellular resistance to MMS, making reconstituted cells less sensitive to DNA damage and confirming the biochemical data obtained with endonuclease assays.

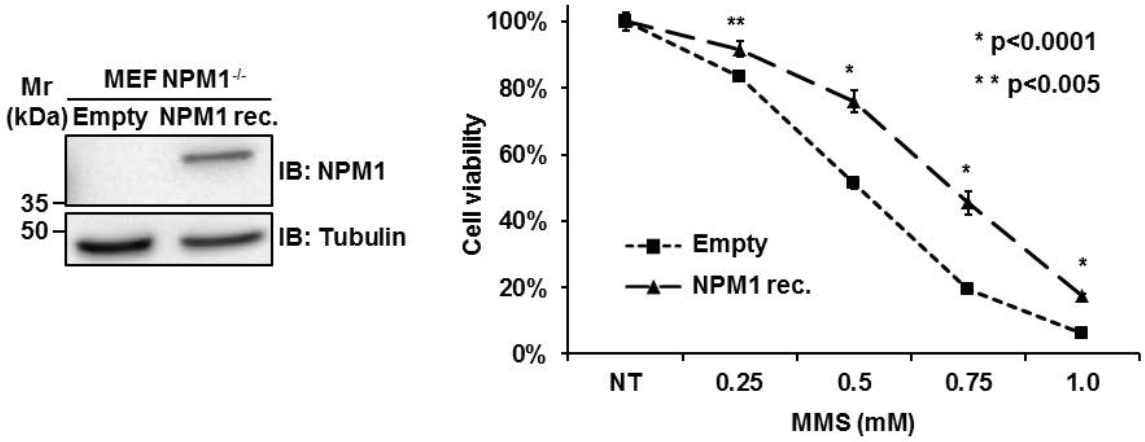

Figure 35: NPM1 expression reduces MEFs sensitivity toward MMS. (*Left*) NPM1$^{-/-}$ MEFs stably re-expressing NPM1 were obtained, as shown by Western blotting analysis. (*Right*) Cell viability assay using MTS assay were performed. Cells were incubated with the indicated increased doses of MMS for 8hr. Mean±SD values are the result of three independent experiments.

Together, all the data illustrated so far point to a novel role for NPM1 as an indirect effector of BER by regulating APE1 activity *in vivo*.

3.2.3 NPM1 CONTROLS APE1 SUB-CELLULAR LOCALIZATION

NPM1 is responsible for the nucleolar retention for several proteins, mediating their nucleolar localization[257]. Given the impairment of APE1 AP-incision activity and increased sensitivity of NPM1$^{-/-}$ cells to DNA damages elicited by BER, I investigated whether the absence of NPM1 might influence the APE1 subcellular localization in a NPM1$^{-/-}$ background. Immunofluorescence analyses were carried out on NPM1$^{+/+}$ and NPM1$^{-/-}$ MEFs.

As already described for some tumour cells[18], in NPM1$^{+/+}$ cells, APE1 showed a nuclear localization with strong accumulation within nucleoli (Figure 36; yellow arrows). On the contrary, in absence of NPM1 APE1 did not accumulate within nucleolar structures (Figure 36), while the nucleolar structures remained intact in these cells[342].

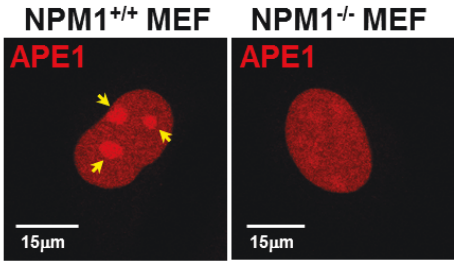

Figure 36: NPM1 controls APE1 subcellular localization. A representative immunofluorescence images of APE1 localization in NPM1$^{+/+}$ and NPM1$^{-/-}$ MEFs. APE1 presents nucleolar accumulation (yellow arrows) only in the presence of NPM1. A diffuse nuclear staining could be observed in NPM1$^{-/-}$ cells. Bars correspond to 15 μm.

NPM1 reconstituted cell clones were also tested to assess whether the re-expression of NPM1 could restore the APE1 nucleolar accumulation. As displayed in Figure 37, the presence of NPM1 promotes again APE1 nucleolar localization, pointing to an important role for APE1/NPM1 interaction in controlling APE1 distribution.

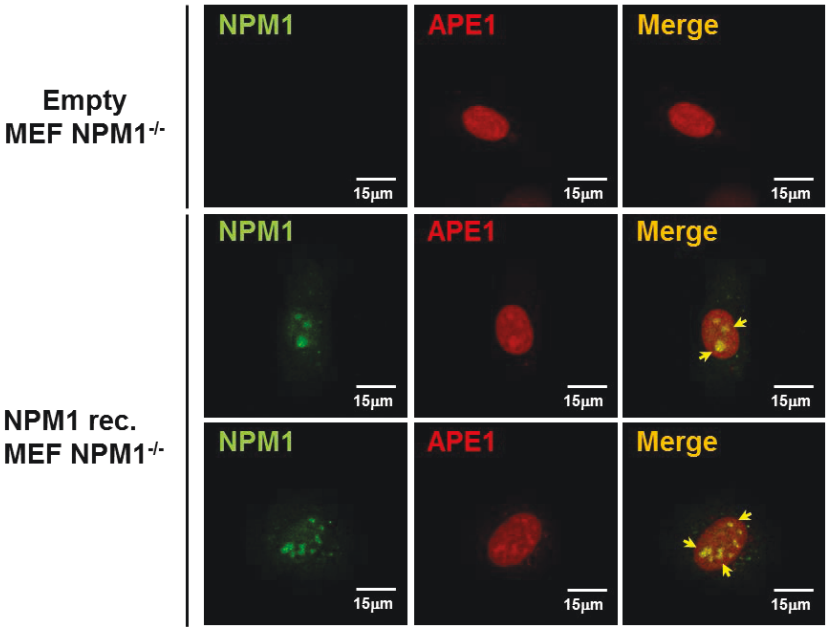

Figure 37: NPM1 controls APE1 subcellular distribution. A representative immunofluorescence images showing a nuclear APE1 localization in NPM1$^{-/-}$ MEFs and a nucleolar accumulation of it when NPM1 is re-express in NPM1$^{-/-}$ cells (NPM1 rec.). Yellow arrows indicated APE1 strong nucleolar localization in NPM1 reconstituted cells. Bars correspond to 15 µm.

As a confirmation, an APE1 mutant, unable to bind to NPM1, shows a diffuse nuclear staining[92], reinforcing the essential role played by NPM1 through protein-protein interaction in controlling APE1 physical redistribution within cells.

Given the role of NPM1 in mediating APE1 localization, I focused my attention to the effects of a mutated form of NPM1, i.e. NPM1c+, found in one third of acute myeloid leukemia (AML), on APE1 distribution and on APE1/NPM1 interaction.

First, ectopic expression of NPM1c+ was tested in a heterologous cell system, i.e. HeLa cells, to verify the NPM1 accumulation in the cytoplasmic compartment, whereas the wild-type counterpart, used as control, shows the classical nucleolar staining (Figure 38, *panel A*). Then, a Proximity Ligation Assay (PLA) was performed to assess the effects of NPM1c+ in modulating the APE1/NPM1 interaction taking advantage of a FLAG-tagged APE1 protein (Figure 38, *panel B, left*): in cells expressing NPM1 wild-type, the interaction primarily occurs in the nuclear compartment, while in cells expressing the mutated form of NPM1, the majority of the PLA signal was detected in the cytoplasm, as shown by PLA dots quantification (Figure 38, *panel B, right*). Notably, in accordance with the predominance of APE1/NPM1 interaction in the cytoplasmic compartment, APE1 itself was found re-distributed from a solely nuclear to a cytoplasmic/nuclear staining in cells carrying NPM1c+ (Figure 38, *panel B, left*).

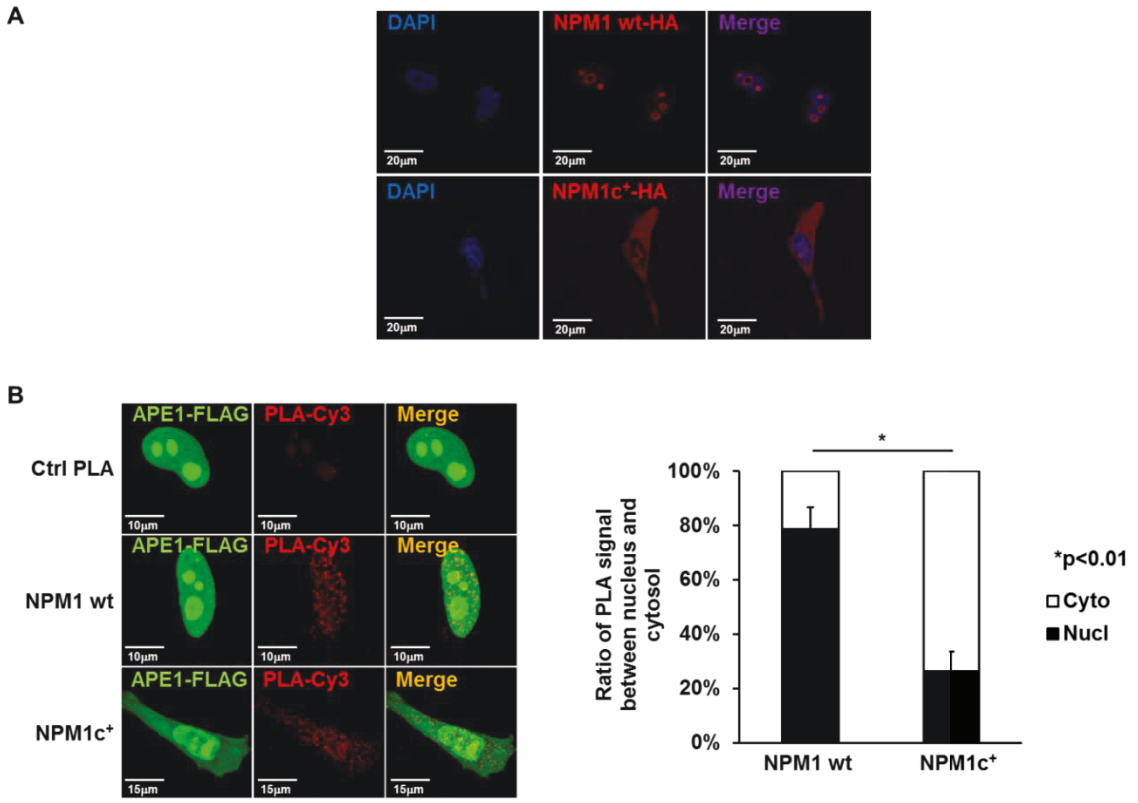

Figure 38: NPM1c+ expression causes APE1 redistribution in the cytoplasmic compartment in HeLa cells. A | A representative immunofluorescence images showing the NPM1 localization pattern in HeLa cells transiently transfected with constructs encoding for NPM1 wild-type and for NPM1c+ mutated form HA-tagged. In control cells, as expected, NPM1 mainly localizes in the granular region of nucleoli; by contrast, in NPM1c+ transfected cells, NPM1 presents a strong accumulation in the cytoplasm. **B** | PLA technology indicating the occurrence of APE1/NPM1 interaction in HeLa cells expressing NPM1 wild-type or NPM1c+ in the nuclear and in the cytoplasmic compartment, respectively. (*Left*) A representative immunofluorescence images for PLA assay; in green, the staining for APE1and in red the PLA dots. The expression of NPM1c+ leads to an increased cytoplasmic APE1/NPM1 association and to APE1 distribution in the cytosolic compartment. PLA control was performed omitting the primary antibody for NPM1. (*Right*) Dot quantification with relative nuclear/cytoplasmic distribution of PLA signals, using Blob Finder software. Reported data are the mean of 30 cells analyzed per condition.

Interestingly, given that uniquely the expression of NPM1c+ leads to a cytoplasmic redistribution of APE1, re-localization already described for other NPM1 interacting partners[362], a direct correlation between this mutated form of NPM1 and APE1 occurrence in the cytoplasm could be envisioned, stressing the importance of NPM1 as a novel APE1 regulator.

3.2.4 BLASTS FROM AML PATIENTS, EXPRESSING THE NPM1C+ MUTANT PROTEIN, HAVE INCREASED CYTOPLASMIC APE1-NPM1 INTERACTION AND SHOW IMPAIRED BER ACTIVITY

Since NPM1 results mutated in its cytoplasmic form in one third of acute myeloid leukemia and its ectopic expression in HeLa cells carries to an altered cytoplasmic APE1/NPM1 interaction and to an aberrant accumulation of APE1 in this compartment (Figure 38), it could be hypothesized that the same occurs in blasts from AML patients,

constitutively bearing NPM1c+. To verify this hypothesis, immunofluorescence and PLA assay were performed on AML blasts, as shown in Figure 39 (Figure 39).

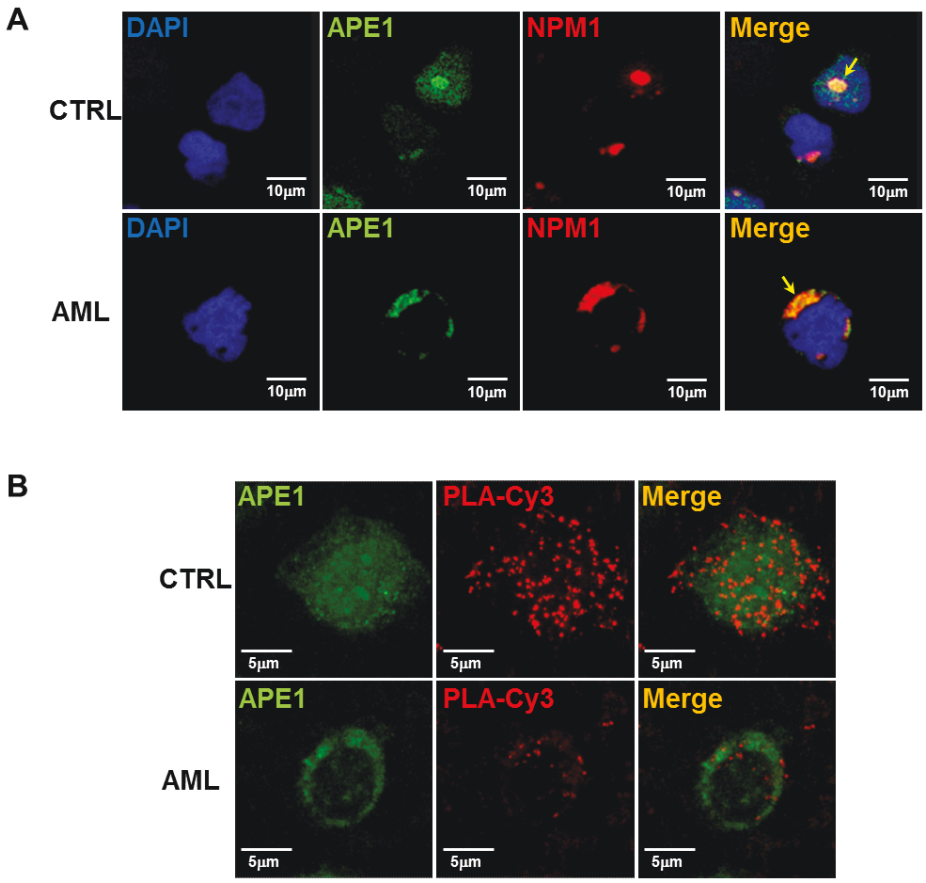

Figure 39: NPM1c+ alters APE1 localization in AML blasts. A | A representative immunofluorescence image showing the APE1 cytoplasmic re-localization in blasts from patients with AML bearing NPM1c+ mutation. In control cells from healthy donors (CTRL), expressing NPM1 wt, as expected, APE1 mainly localizes in the nuclear region with strong accumulation within nucleoli; by contrast, in AML cells, harboring NPM1c+, APE1 presents a robust increase in the cytoplasm. **B |** PLA technology evaluating the occurrence of APE1/NPM1 interaction in blasts from healthy donors (CTRL) and from patients with AML bearing NPM1c+ mutation (AML). As expected, since APE1 mainly excluded from the nuclear region in AML cells, the interaction APE1/NPM1 was also delocalizes from nucleus to the cytoplasm.

In accordance to what previously observed in a heterologous cell system, the expression in blasts from patients with AML carrying NPM1c+ leads to an aberrant APE1 localization in the cytoplasmic compartment, coupled with a nuclear reduction in APE1/NPM1 interaction towards an increased association in the cytoplasm.

To assess the biological relevance of this phenotype, the sensitivity of blasts from healthy donors and both patients with AML bearing NPM1wt and NPM1c+ protein expression were tested toward DNA alkylation damage by MMS. Cell viability assay demonstrates that blasts harboring the NPM1 mutation at the C-terminus were significantly more sensitive to MMS than healthy controls and AML blasts with NPM1wt (Figure 40).

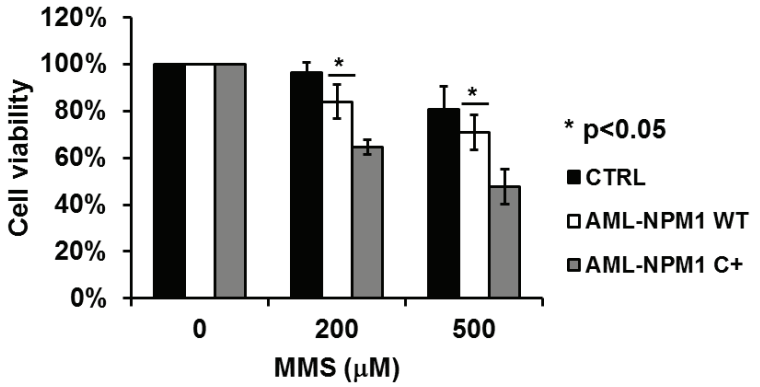

Figure 40: AML blasts bearing NPM1c+ are more sensitive to DNA damage than healthy donors. MTS assay showing the differential sensitivity of blast from healthy donors (n=3), AML with NPM1wt (n=3) and AML carrying NPM1c+ (n=4) to increased doses of MMS for 4 hr.

All these data suggest that NPM1c+ expression causes an alteration of APE1 distribution, having a strong impact on the BER activity *in vivo*, and shows a functional relevance in AML pathogenesis.

3.2.5 NPM1c+ EXPRESSION IS ASSOCIATED WITH ALTERED APE1 PROTEIN STABILITY IN BOTH AML CELL LINES AND BLASTS FROM AML PATIENTS

To better assess the biological role of APE1 cytoplasmic re-localization due to NPM1c+ expression, a myeloid cell line (OCI/AML3), which constitutively expresses the mutated form of NPM1, was studied. Immunofluorescence analyses demonstrated that the APE1 cytoplasmic accumulation was clearly linked to the expression of NPM1c+ in OCI/AML3, whereas in the control cell line (OCI/AML2), bearing NPM1wt, APE1 appears mainly nuclear (Figure 41, *panel A*).

In parallel, to support the immunofluorescence data, a biochemical sub-fractionation analysis was performed. Whole, cytoplasmic and nuclear extracts were tested for the APE1 content through Western blotting analyses. Although the cellular APE1 content was comparable between the two cell lines, the OCI/AML3 cells present a lower nuclear APE1 level (Figure 41, *panel B*). Moreover, as shown in Figure 41 (*panel B*), in the presence of NPM1c+ protein, a truncated form of APE1 in the whole and cytoplasmic cell extracts could be detected (Figure 41, *panel B*). Interestingly, a truncated APE1 form was also detectable in blasts from patients with AML harboring NPM1c+ (data not shown)[375]. Nevertheless further analyses confirmed that this truncated form corresponds to the APE1NΔ33 protein, already described in literature as result of Granzyme A and K cleavage[111,112], in OCI/AML3 cells the specific proteolysis process is Granzyme-independent, since these myeloid cell lines do not express the enzyme (data not shown).

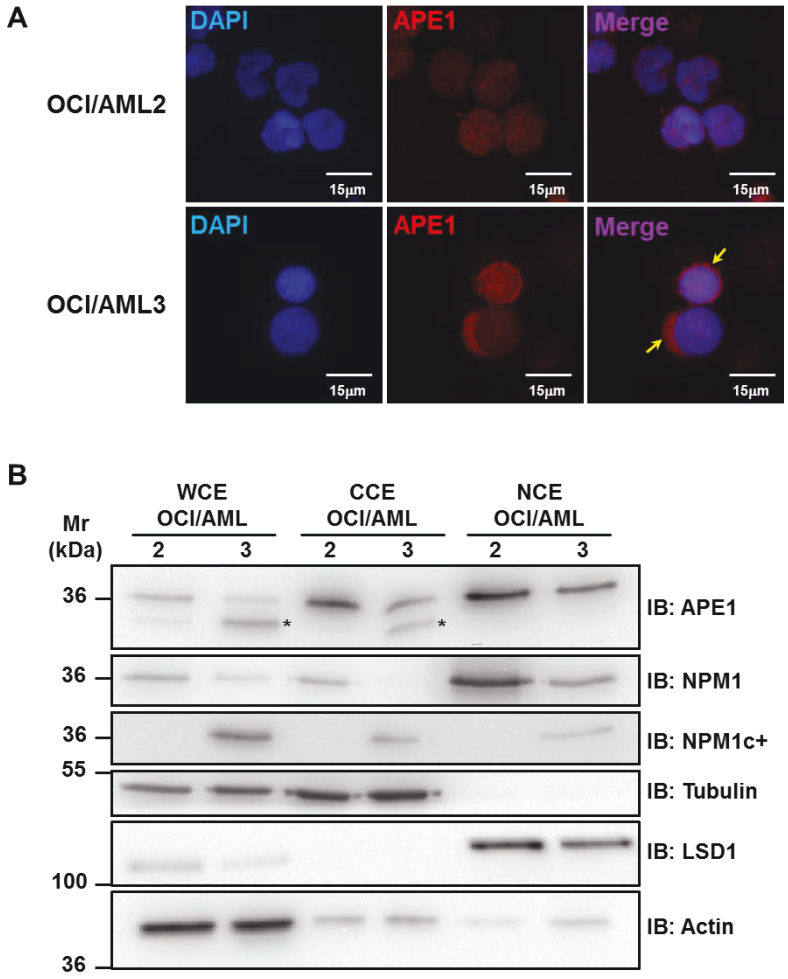

Figure 41: NPM1c+ alters the APE1 localization and stability in OCI/AML3 cell line. A |A representative immunofluorescence image showing the APE1 cytoplasmic accumulation in myeloid cell lines bearing NPM1wt (OCI/AML2) or NPM1c+ mutation (OCI/AML3). In control cells, as expected, APE1 mainly localizes in the nuclear region; by contrast, in OCI/AML3 cells, harboring NPM1c+, APE1 presents a strong accumulation in the cytoplasm. **B** | Representative Western blotting analysis on OCI/AML2 and 3 whole (WCE), cytoplasmic (CCE) and nuclear (NCE) cell extracts (10 µg for WCE and CCE, 5 µg for NCE) showing a cytoplasmic truncated APE1 form, indicated by *, only in cells harboring NPM1c+. Lysine demethylase 1 (LSD1) was used as nuclear marker and loading control; tubulin was used as cytoplasmic marker to evaluate possible cytoplasmic contaminations. Antibodies used are indicated on the right-hand side.

Previously, our group showed that the expression of a non-cleavable form of APE1 results in an increased cellular resistance to genotoxic stresses[115], suggesting a functional impairment *in vivo* due to the loss of the first 33 residues at the N-terminus. To evaluate the impact of APE1 truncation in OCI/AML3 cells and to test the hypothesis of a APE1 deficiency in its total endonuclease capability due to the loss of the N-terminus, AP endonuclease assays with the two nuclear extracts were performed, confirming the significant reduction of APE1 incision activity in OCI/AML3 cells in comparison to the control cell line (Figure 42).

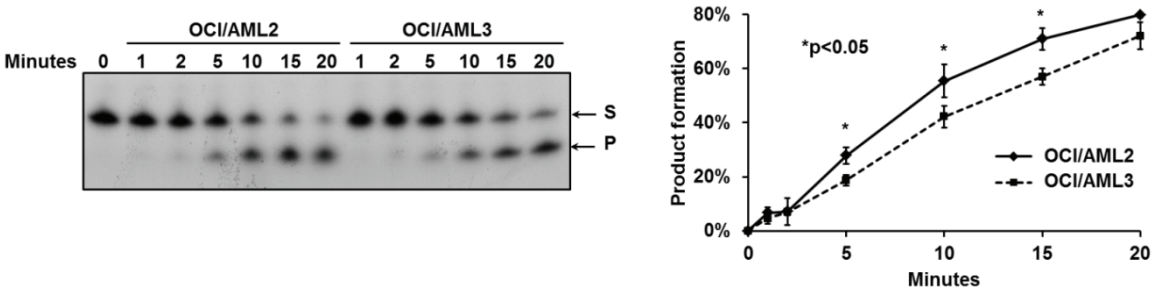

Figure 42: NPM1c+ mutation negatively affects APE1 endonuclease activity. Endonuclease assay performed on OCI/AML 2 and 3 nuclear extracts (50ng). A representative image displays the conversion of the substrate (S) in the product (P) in the indicated periods of time. The diagram on the right reports the mean±SD of densitometric quantification of the product formation of three independent experiments.

Then, we investigated the ability of APE1 to efficiently remove AP-sites induced by genotoxic stress from OCI/AML 2 and 3 genomic DNA. As shown in Figure 43, OCI/AML3 cells retained a significant higher amount of AP-sites if compared to OCI/AML2 cell line under basal condition and following MMS treatment, confirming an APE1 functional impairment in the presence of NPM1c+ (Figure 43).

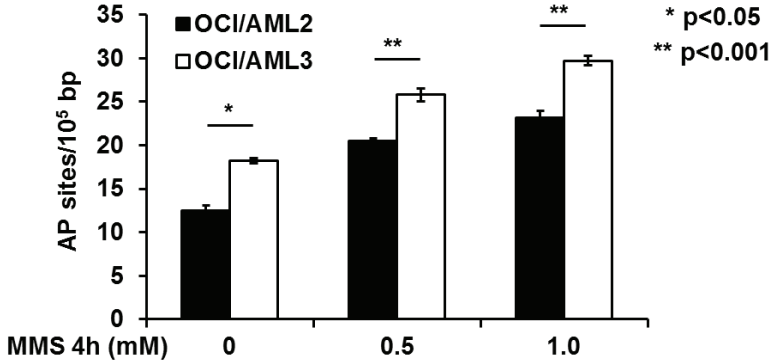

Figure 43: NPM1c+ mutation reduces the APE1 capability to efficiently remove AP sites. OCI/AML3 cells show an increased extent of AP sites both at basal condition and after MMS treatment when compared to OCI/AML2 control cell line. In histogram, the amount of abasic sites measured in OCI/AML2 and 3 cells, treated with the indicated doses of MMS (mM) for 4 hr. Mean±SD values are the results of three independent experiments.

Cell viability assays confirms these observations, demonstrating that OCI/AML3 cells were significantly more sensitive to MMS treatment than OCI/AML2 control cell line (Figure 44).

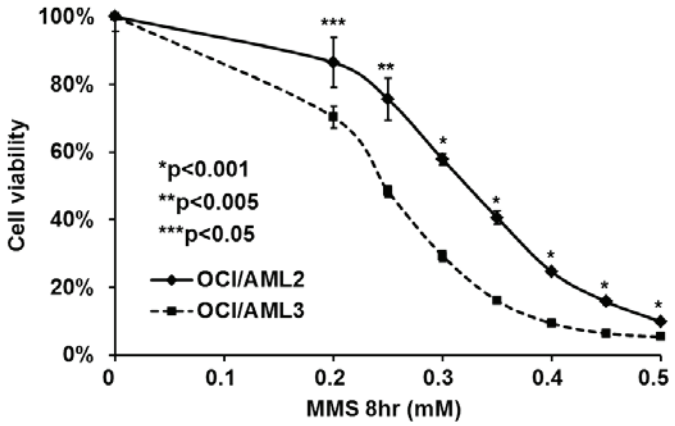

Figure 44: NPM1c+ reduces cellular resistance to MMS-induced DNA damage. OCI/AML3 cells show a higher sensitivity to MMS when compared to OCI/AML2 cell line. Cell viability was evaluated after MMS treatment on OCI/AML 2 and 3 cells by CellTiter-Glo Luminescent assay. Cells were incubated with the indicated doses of MMS (mM) for 8 hr. Mean±SD values are the results of three independent experiments.

In conclusion, all these data demonstrate that in cells harboring NPM1c+, the APE1 functional impairment due to its cytoplasmic re-localization, caused by the mutated form of NPM1, is critical in mediating cellular response to DNA damage through an altered BER activity.

3.3 FUNCTIONAL REGULATION OF TUMOUR ASSOCIATED-APE1 GENETIC VARIANTS

Although abnormal APE1 expression and localization patterns have been demonstrated for different types of solid and liquid tumours[63] and have been associated with several tumorigenic processes[16], the investigators have never looked into the molecular mechanisms that drive the overexpression and/or a cytoplasmic accumulation of APE1 seen in pathology. As proposed in this work of Thesis, a molecular explanation involving a critical role of its complicated network of interacting partners in regulating APE1 functions has been provided, with particular attention to NPM1. Altered levels of its partners or abnormal expression of them in nucleus/cytoplasm, as for example NPM1c+, may impact on APE1 subcellular distribution rather than a mutation in APE1 itself. Interestingly, in the latest years few APE1 amino acids genetic polymorphic variants have been identified throughout normal and disease population[166], but none of these occurs on residues responsible for neither the DNA repair activity, nor the redox functions of the protein and is possibly explained by the strong selective pressure on these vital functions of the protein. However, in most cases, it is still unclear the possible effect of the sequence variation on the AP-endonuclease activity and the DNA repair capability *in vivo*; notably, it has been hypothesized that these genetic variants might lead to changes in mRNA stability, translation efficiency or protein structure/function, rather than causing a severe effect on its AP-endonuclease activity. These observations suggest a role for APE1 polymorphisms in disease progression or initiation, which may lead to increased disease susceptibility within the population. Some of these polymorphisms occur at the N-terminal domain of the protein, suggesting that they might influence APE1 macromolecule associations, since the N-terminus has been described as fundamental for establishing protein-protein interactions[18]. At present, little information is available regarding the biological roles of these variants *in vivo*. The last part of this work of Thesis, which is still in progress, is aimed to fill in this gap.

3.3.1 COMPUTATIONAL EVALUATION OF APE1 VARIANT STRUCTURE AND FUNCTION

As initial analysis, four different computational on-line approaches were used to evaluate the possible impact of the tumour associated-polymorphisms studied in this work of Thesis (Figure 45) on APE1 structure/functions, as recently did by Illuzzi and co-workers for others APE1 variants[170].

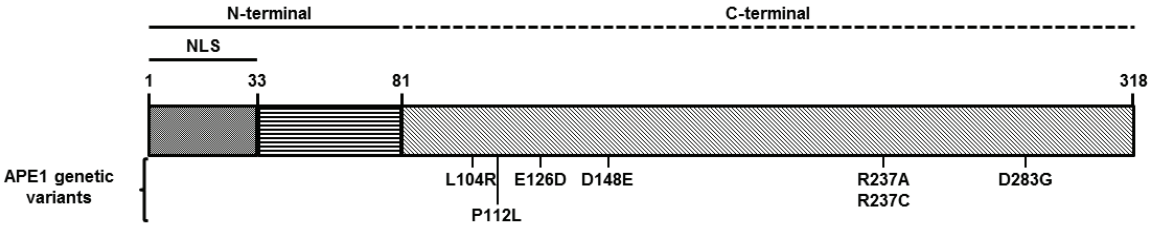

Figure 45: APE1 genetic variants considered in this study. Schematic APE1 representation; within the linear structure, the genetic APE1 variants analyzed in this Thesis and their reciprocal position are highlighted. NLS, nuclear localization signal.

The software tools used were:

- the PROVEAN (Protein Variation Effect Analyzer) score calculates whether an amino acids substitution may have an impact on the biological function of a protein[376];
- the SIFT (Sorting Intolerant From Tolerant) approach predicts if an amino acids substitution affects protein function on the base of the amino acids conservation in sequence alignments from closely related sequences[377];
- the PolyPhen-2 (Polymorphism Phenotyping v2) software collects predictions of the impact of amino acids changes on the structure and function using physical and comparative features[378];
- the CUPSAT (Cologne University Protein Stability Analysis Tool) tool computes the effect of the point mutations on protein stability, using amino acids-atom potentials and torsion angle distribution to evaluate the amino acid environment of the mutation site[379].

All the modeling program used were mainly in accordance, predicting that five out of seven variants (L104R, P112L, R237A/C and D283G) would affect the protein function, with an overall destabilizing effect, being possibly or probably damaging; the other two polymorphisms (E126D and D148E) instead, although destabilized, are considered tolerant and benign (Table 5). In support of these data, Illuzzi *et al.*[170] demonstrated that the population variants, such as the D148E one, did not show any altered AP-activity *in vitro*, consistent with the hypothesis that strong functional impairment in the APE1 activity would be negatively selected within the healthy population. Notably, in this study, only the R237C change reflects a diminished APE1 *in vitro* activity, being deficient in 3' to 5' exonuclease and 3'-damage excision activities[170]. Interestingly, none of these residues have been described as site for post-translational modification, remarking the importance of such modifications in controlling APE1 functions.

Table 5: APE1 genetic variants considered and impact of amino acids substitution on APE function/structure as predicted by four online modeling methods. For the PROVEAN software (http://provean.jcvi.org/index.php), a cut-off of -2.5 was used. Scores ≤-2.5 are considered as deleterious, while values greater than the cut-off are predicted as neutral. The SIFT modeling (http://sift.jcvi.org/) considered scores ≤0.05 as deleterious whereas >0.05 as tolerated. As template, the APE1 sequence (NP_001632.2) was used. For the PolyPhen-2 tool (http://genetics.bwh.harvard.edu/pph2/) and PROVEAN model, APE1 UniProtKB sequence (P27695) was used as query. CUPSAT predictions (http://cupsat.tu-bs.de/) were obtained using a thermal experimental method and the PDB APE1 protein structure (1DE8) was employed. N/A = not available. Once = observed a single time.

APE1 genetic variants	Source	Percentage of frequency	Functional consequences	PROVEAN		SIFT		CUPSAT		PolyPhen-2	
				Score	Prediction	Score	Prediction	Overall stability	Torsion	Score	Prediction
L104R	ALS	once	Reduced AP endonuclease activity (~40%)[237]	-4.925	Deleterious	0.00	Affected protein function	Stabilizing	Unfavorable	0.987	Probably damaging
P112L	Tumor	once	Normal 3' to 5' exonuclease and 3'-damage excision activities and AP-DNA complex stability[170]	-5.106	Deleterious	0.05	Affected protein function	Destabilizing	Favorable	0.632	Possibly damaging
E126D	ALS	once	Reduced AP endonuclease activity (~40%)[237]	-1.000	Neutral	0.44	Tolerated	Destabilizing	Unfavorable	0.004	Benign
D148E	NCBI rs1130408	48.5	Normal AP endonuclease activity[170,237]	-0.204	Neutral	1.00	Tolerated	Destabilizing	Favorable	0.000	Benign
R237A	NCBI	N/A	Reduced AP endonuclease activity (~65%)[237]	-5.907	Deleterious	0.00	Affected protein function	Stabilizing	Favorable	1.000	Probably damaging
R237C	Tumor (NCBI	once	Reduced 3' to 5' exonuclease	-7.884	Deleterious	0.00	Affected protein	Stabilizing	Unfavorable	1.000	Probably damaging

	rs375526265)		and 3'-damage excision activities; slightly reduced AP-DNA complex stability[170]				function				
D283G	ALS	once	Reduced AP endonuclease activity (~90%)[237]	-6.910	Deleterious	0.00	Affected protein function	Destabilizing	Unfavorable	1.000	Probably damaging

3.3.2 THE APE1 GENETIC VARIANTS CONSIDERED ACCUMULATE IN THE NUCLEAR COMPARTMENT

Preliminary experiments were aimed at characterizing the APE1 genetic variants considered in terms of protein expression level and subcellular. Overexpression analysis on transiently transfected HeLa cells were performed using a battery of mutagenized plasmids encoding for FLAG-tagged APE1 polymorphisms (see Material and Methods section for details). As shown in Figure 46, while the majority of the polymorphisms analyzed is expressed at a similar protein level to APE1wt and to the endogenous form of the protein, the D148E and R237C variants are up-regulated almost 2 fold (Figure 46).

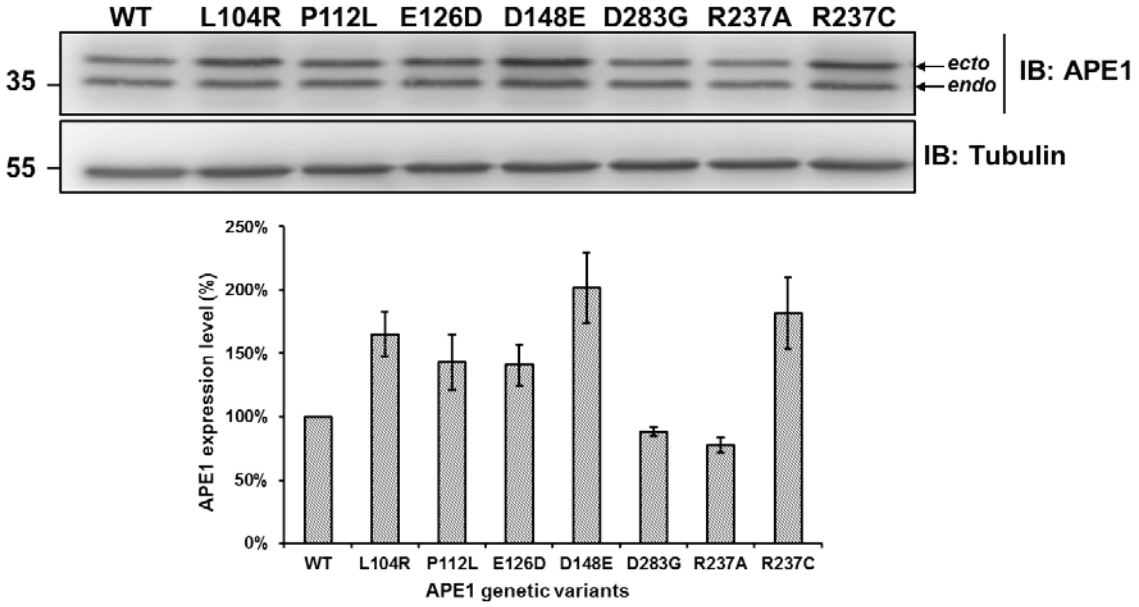

Figure 46: APE1 genetic variants expression level. (*Top*) Representative Western blotting analysis on whole cell extracts (20 μg) of HeLa cells transiently transfected with plasmids encoding FLAG-tagged APE1 genetic variants considered in this work of Thesis. Antibodies used are indicated on the right-hand side. Tubulin was used as loading control. (*Bottom*) Histogram reporting the densitometric quantification of Western blotting signals from at least two independent experiments. Protein amounts are expressed as mean±SD of the signal, considering APE1wt as reference.

Then, to test a potential biological impact of these amino acid substitutions in the intracellular localization, immunofluorescence analyses were employed taking advantage of the tagged form of the APE1 variants with a C-terminal 3x-FLAG, in order to discriminate the ectopic form from the endogenous one. After transfection of the different plasmid constructs into HeLa cells, the subcellular distribution was monitored. All the variants displayed a distribution comparable to APE1wt, with a predominant nucleoplasmic localization associated with strong nucleolar accumulation (Figure 47).

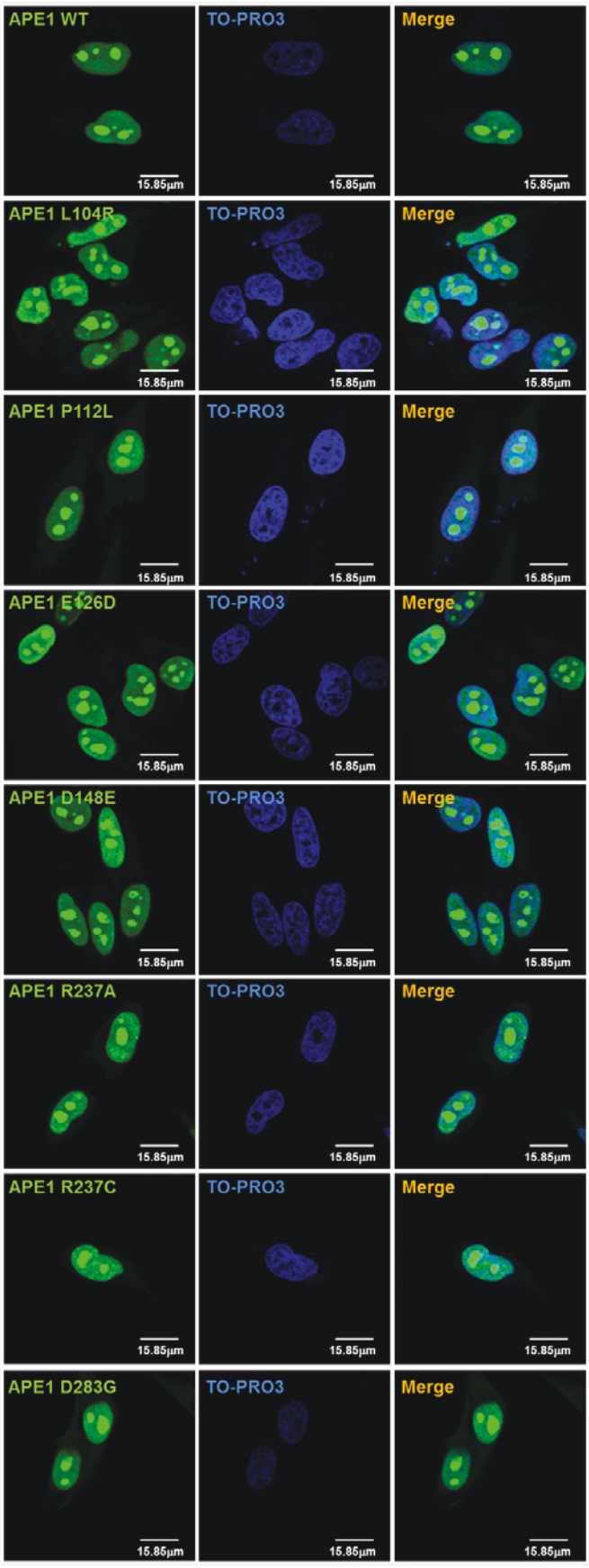

Figure 47: APE1 genetics variants localizes in the nucleoplasm with strong accumulation in the nucleoli, similarly to APE1wt protein. Representative immunofluorescence panels showing the

subcellular localization of the different APE1 genetic variants. Ectopic APE1 staining (α-FLAG, green) was used to localize HeLa cells positively transfected with the FLAG-tagged APE1 genetic variants constructs. TO-PRO3 counter-staining was used to mark nuclei; bars correspond to 15.85 μM.

In conclusion, APE1 genetic variants displayed a similar distribution pattern to the wild-type protein, as already suggested by Illuzzi and coworkers[170] for the other APE1 polymorphisms examined (Q51H, I64V, G241R, P311S, A317V).

3.3.3 APE1 POLYMORPHISMS AFFECT THE COMPLEX NETWORK OF MACROMOLECULE ASSOCIATIONS

We decided to focus our attention on three polymorphisms (L104R, D148E and R237C) whereof two of them (L104R and R237C) were predicted to impact on APE1 functions, being probably damaging, whereas the D148E was calculated not to influence APE1 activities and appears benign by our computational analyses (Table 5).

To assess the possible effect of this subgroup of APE1 variants (L104R, R237C and D148E) in establishing protein-protein interactions, co-immunoprecipitation analyses were carried out on HeLa cells after transient transfection with FLAG-tagged APE1 plasmid constructs. The binding with six known APE1 interacting partners were tested (Figure 48): four are involved in RNA metabolism functions, as NPM1, PRP-19, PABP-1 and YB-1, while the other two (XRCC1 and DNA Polβ) participate with APE1 in DNA repair through BER pathway. In general, APE1 D148E, predicted as tolerated with all the four analyses tools used, presents an association pattern with both RNA metabolism and DNA repair proteins comparable with the wild-type protein. Only a slight decrease was detected for the interaction with YB-1 protein, reduction that was analogous to that observed for the other APE1 genetic variants. On the contrary, a completely different scenario appeared for L104R and R237C variants. Notably, the expression of the two impacting polymorphisms (L104R and R237C) leads to an overall diminished association with all the interacting partners analysed; this strong effect was observed and was similar for all the proteins except for NPM1. Interestingly, for NPM1 the behaviour of the two forms completely differs, showing an opposite effect: the L104R presents an increased association with NPM1 (~ 2 fold) while the R237C halves its interaction in comparison to the wild-type one. The same results were also obtained for the D283G change, even if the NPM1 reduction observed was less pronounced than the R237C one (data not shown).

In conclusion, all these data demonstrate that although the overall intracellular localization for the entire APE1 genetic variants array was similar to that of the APE1wt with a nuclear and nucleolar distribution, the amino acid substitutions considered (L104R, R237C and D283G), all predicted to affect the protein structure/function lead to a marked reduction in its interacting network. This suggest a possible explanation about one of the mechanisms through which APE1 polymorphisms, though not directly affecting neither the DNA repair nor the redox functions, can ultimately affect DNA repair or transcriptional regulation, thus leading to disease susceptibility. Further studies are underway for better characterizing the effects of APE1 polymorphisms on its endonuclease and transcriptional activities *in vivo*.

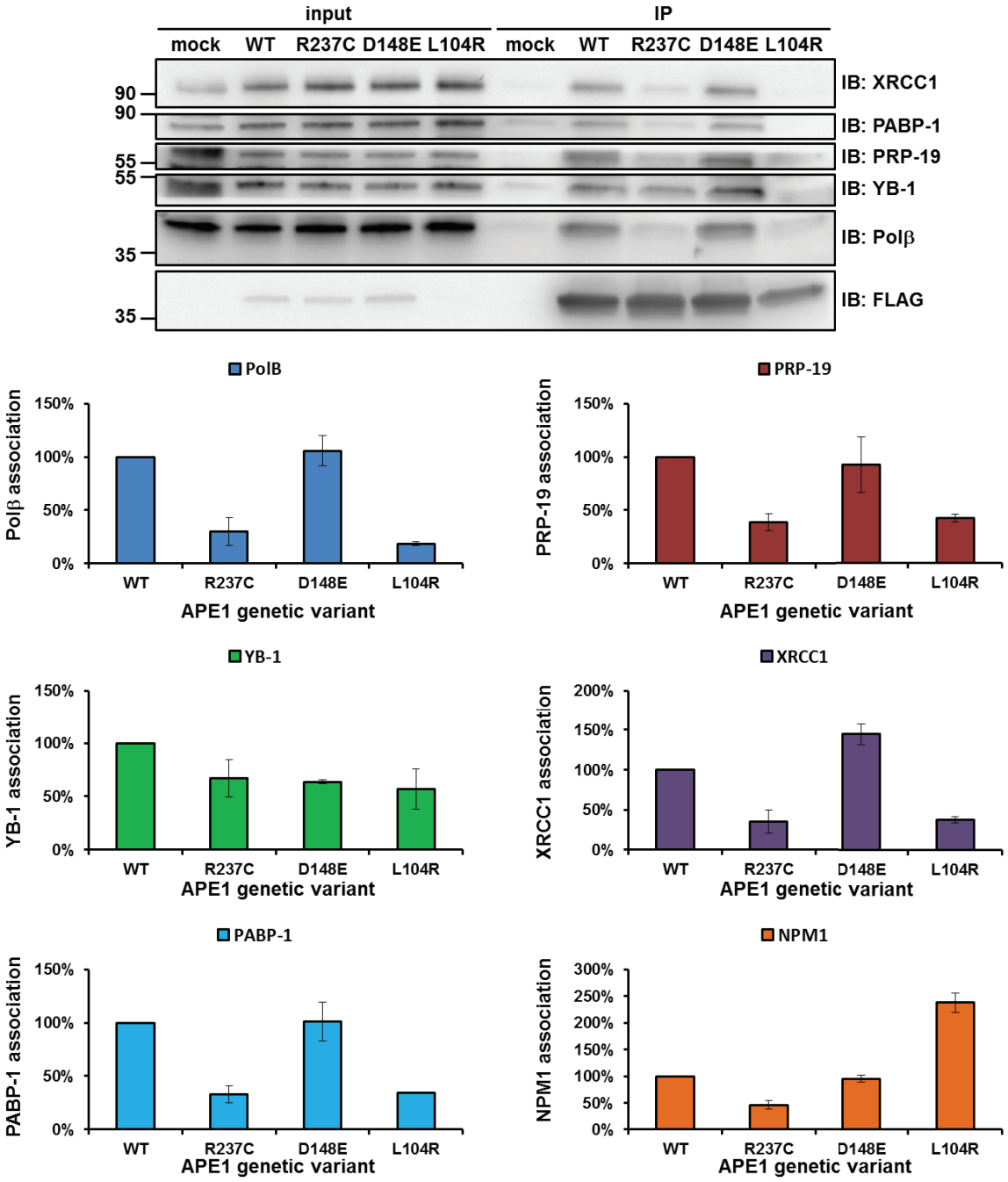

Figure 48: Expression of R237C and L104R negatively affect APE1 protein-protein interaction. (*Top*) A representative Western blotting analysis on input and co-immunoprecipitated material obtained from HeLa cells transiently transfected with APE1 polymorphisms FLAG-tagged constructs. Immunoprecipitation was performed using an anti-FLAG M2 affinity gel. Antibodies used are indicated on the right-hand side. FLAG was used as loading control. (*Bottom*) Histograms reporting the normalized values for the association of the different APE1 genetic variants (horizontal axis) with six interacting partners (DNA Polβ, *blue*; PRP19, *maroon*; YB-1, *green*; XRCC1, *violet*; PABP1, *light blue* and NPM1, *orange*), considering APE1wt as 100% of interaction. Mean±SD values are the results of three independent experimental sets.

Then, since the critical role played by NPM1 in controlling APE1 functions, to better assess and confirm the strong reduction observed for R237C in its binding to NPM1, an *in vitro* binding assay was performed using recombinant proteins. The wild-type and R237C variant proteins were purified from *E. coli*, displaying similar expression levels, solubility

and column elution profile during FPLC purification (data not shown), indicating any marked structural change or protein instability due to the amino acid substitution as already noticed by Illuzzi and coworkers[170]. Following precise quantification of the purified recombinant proteins, using Bradford assay and Coomassie staining, a Glutathione S-transferase (GST) pull-down approach was employed to evaluate *in vitro* the direct interaction between APE1 and NPM1. As shown in Figure 49, the expression of R237C causes a striking decrease in APE1/NPM1 interaction, confirming the results obtained *in vivo*.

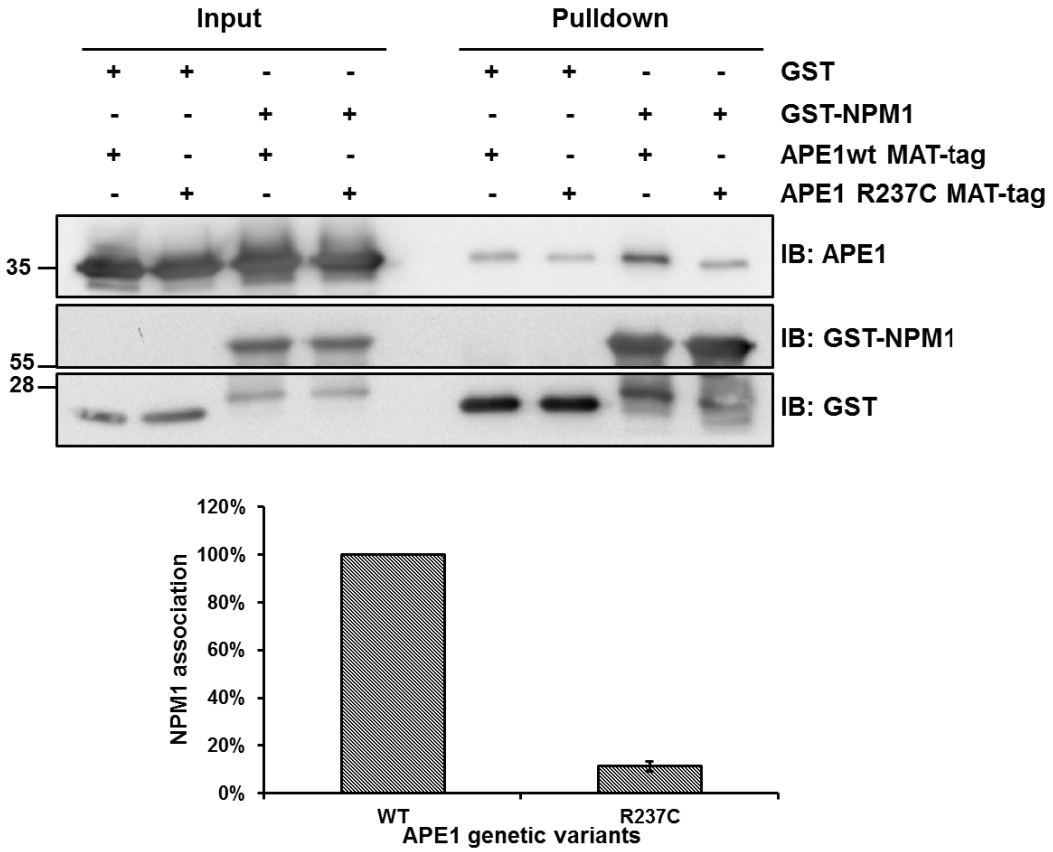

Figure 49: APE1 R237C loses its NPM1 interaction. (*Top*) A representative Western blotting analysis on input (20% of the reaction, 5µl) and GST pull-down fractions (30% of the reaction, 10µl). GST-NPM1 was used as bait, while APE1wt and R237C MAT-tagged proteins were used as preys. GST alone represent a negative control for the specificity of the APE1/NPM1 association. GST and GST-NPM1 were used as loading controls. Antibodies used are indicated on the right-hand side. Input fractions demonstrate the comparable amount of recombinant proteins used for the assay. The image also shows that the two APE1 proteins exhibit similar migration properties. (*Bottom*) Histogram reporting the densitometric quantification of Western blotting signals, considering APE1wt as reference. Protein amounts are expressed as mean±SD of the signal from at least three independent experiments.

All these data confirm that R237C variant has a strong influence in controlling APE1 interacting network with NPM1 through a direct effect on protein-protein interaction.

3.3.4 APE1 GENETIC VARIANTS ARE ASSOCIATED WITH PROTECTIVE OR SENSITIZING EFFECTS, IN CELLS, IN RESPONSE TO GENOTOXIC DAMAGE

Recent analyses regarding the APE1 polymorphisms concentrate their attention in evaluating the possible APE1 functional impairment in its DNA repair and redox functions due to the amino acid substitutions performing *in vitro* studies[170,237].

To gain insights into a potential biological role of a subgroup of APE1 genetic variants (L104R, R237C and D283G), all impacting on APE1 structure/function, but with different behaviour in term of NPM1 interaction, a reconstitution strategy based on RNAi technology for the silencing of the endogenous protein and expression of the mutated sh-RNA resistant ectopic protein form was chosen (Figure 50). Knock-in clones on inducible APE1 silenced clone were generated. On the inducible APE1 silenced clone background, already described in Vascotto and co-workers[380], I generated triple stable cell clones expressing shRNA-resistant ectopic Flagged forms of APE1 genetic variants.

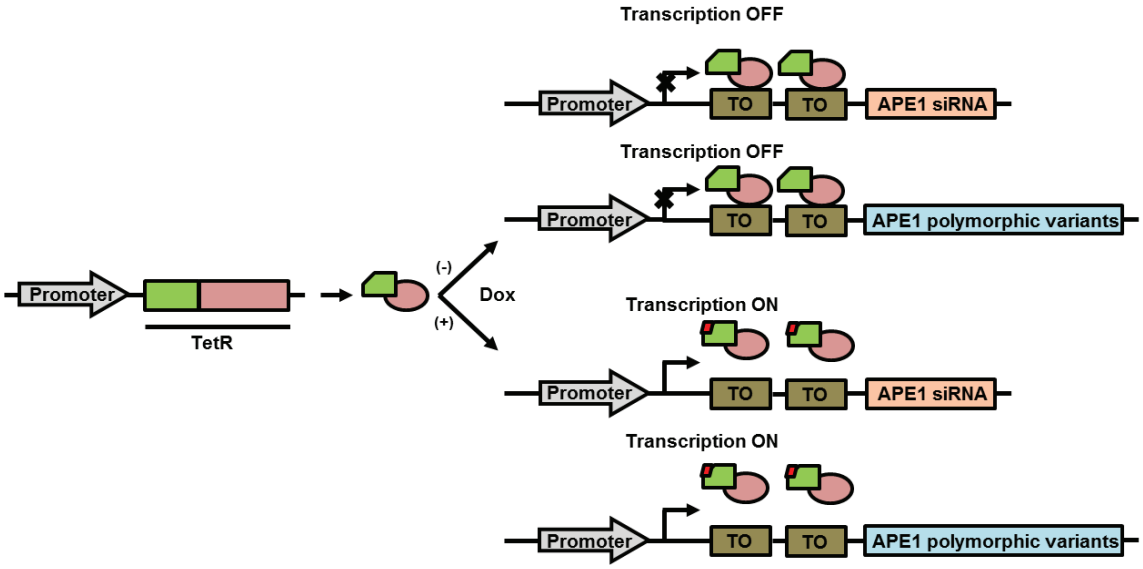

Figure 50: Knock-in strategy for generation of APE1 genetic variants stable cell clone. HeLa cells were used as general cellular model. Briefly, HeLa cells were subject to reiterative transfection cycle for the stable acquisition in series of: a) a Tet repressor constitutively expressed; b) a specific APE1 shRNA under the control of a doxycycline-responsive promoter; and c) shRNA-resistant FLAG-tagged APE1 genetic variants under the control of a doxycycline-responsive promoter. Adding doxycycline in the culture medium allows the expression of the APE1 shRNA, with the subsequent silencing of endogenous form of the protein, and the concomitant expression of the ectopic protein.

Following a screening for the expression of the ectopic APE1 proteins, two clones for each APE1 variants were chosen and treated with doxycycline for seven days to induce the expression of the specific shRNA. Western blotting analysis was performed to check the silencing and the expression level of the ectopic form (Figure 51). As shown in Figure 51, the treatment with doxycycline leads to the endogenous APE1 silencing to a level of about 25% and the expression of the ectopic APE1 FLAG-tagged forms, being shRNA

resistant. To notice, the presence of 3x-FLAG used permits to differentiate between the two APE1 forms.

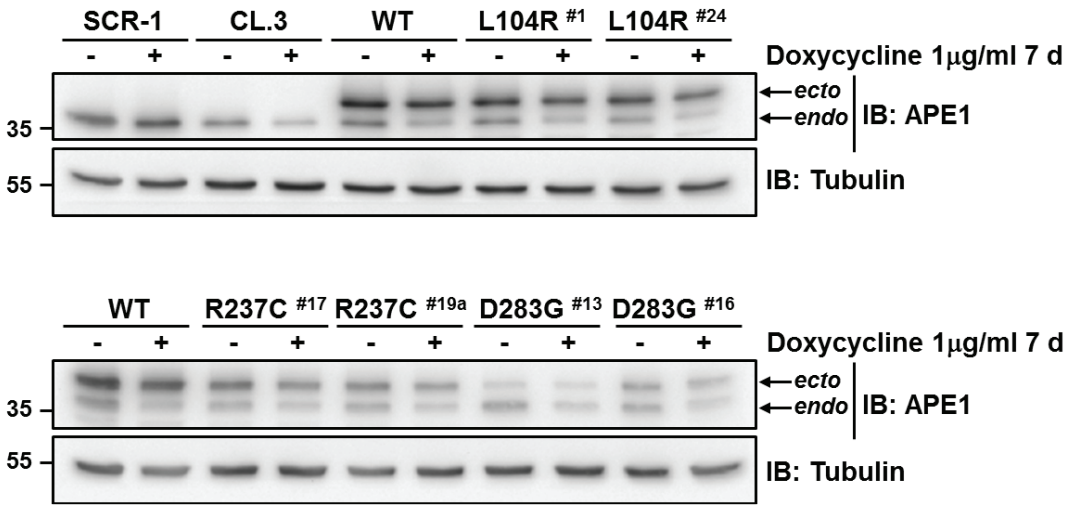

Figure 51: Suppression of endogenous APE1 and expression of APE1 genetic variants in HeLa cells. A representative Western blotting image on whole cell extracts (20μg) showing the reconstitution of APE1 silenced clone (CL.3) with the ectopic FLAG-tagged form of APE1 L104R, R237C and D283G proteins after seven days of doxycycline. A control clone (SCR-1), transfected with a scramble shRNA is shown. Two clones for each polymorphism were assayed. Tubulin was used as loading control. Antibodies used are indicated on the right-hand side. Ecto, ectopic; endo, endogenous.

Flow cytometry analysis (FACS) were performed on cell clones expressing the different APE1 polymorphic variants to evaluate a possible role of these variants in impacting cell cycle stages, but any variation in respect to the wild-type protein could be identified so far (data not shown).

Then, to investigate the possible biological impact of the APE1 genetic variants on the DNA repair function, the cell response to different genotoxic damages, such as MMS and cisplatin, was evaluated. Both the treatment may evoke a BER response: MMS, as alkylating agents, provokes DNA damages that elicit BER pathway for repair[370]; cisplatin, instead, promotes the accumulation of oxidative stress and markers of DNA single-strand breaks[381]. Notably, it has been recently proposed a link between BER and repair of cisplatin-induced DNA damages[382-384]. Our group has also demonstrated that cisplatin induces a re-distribution on NPM1 and BER proteins, included APE1, from nucleoli to the nucleoplasm. The re-localization observed for APE1 seems to protect cells from cisplatin-induced damage, enhancing cellular resistance (Poletto *et al.*, submitted to MBoC).

Cell viability assays were carried out upon 8 days of doxycycline silencing, when the endogenous APE1 protein levels were minimal (about 15%). Figure 52 shows that all the APE1 genetic variants analyzed exhibit a protective role towards DNA-damaging agents. In particular and somehow unexpectedly, both the L104R and D283G present a higher resistance to MMS and cisplatin if compared to wild-type and R237C proteins.

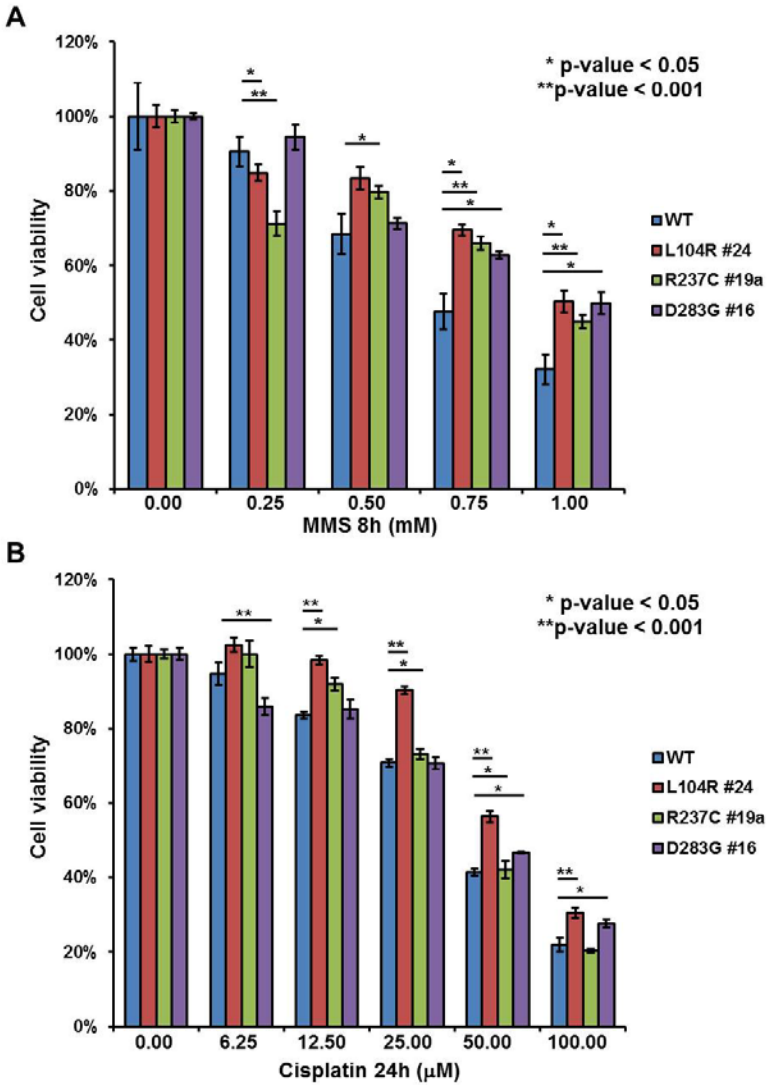

Figure 52: APE1 genetic variants exhibit a protective role towards genotoxic damage. A | MTS assay was used to evaluate cell viability of APE1 genetic variant clones after treatment with increasing amounts of MMS for 8hr. **B |** Cell viability were tested using MTS assay on APE1 polymorphisms clones. Cells were incubated for 24hr with increasing doses of cisplatin, as indicated. Mean±SD values are the result of three independent experiments.

4 DISCUSSION

Abasic sites are a common form of DNA damage, generating by spontaneous reactions or damage-induced hydrolysis. APE1 possesses a stong AP endonuclease activity, acting as the main mammalian endonuclease in base excision repair (BER) pathway. In addition to its role in DNA repair, several biochemical and cell-based observations support the relevance of its redox regulatory function and gene regulation in modulating different cellular contexts, including proliferation and growth, apoptosis, stress responses and metabolism, to name a few, supporting the notion of a multifunctional protein, with features that go beyond the classical DNA repair enzyme activities. How these various functions of APE1 are regulated is still poorly understood; however, in the latest years, a novel role for the first 35 amino acids of the protein has been revealed. Several evidences suggest a possible role of protein-protein interactions and post-translational modifications in controlling the different APE1 cellular activities. Though considered for many years dispensable for APE1 activities, the APE1 N-terminus could be targeted by numerous post-translational modifications, such as phosphorylation, ubiquitination, proteolysis and acetylation. Moreover, this disordered domain seems to account for protein-protein interactions with APE1 binding partners. Nowadays, although several studies show that APE1 deficit strongly impairs cell survival and sensitivity to DNA-damaging agents with a consequent enhanced risk of disease development, a firm linkage between an APE1 defect and human disease has not been established yet, probably due to the fact that a severe APE1 deficiency would be incompatible with life. APE1 appears as a promising candidate for therapeutic approaches and few compunds, that inhibit the DNA repair or the redox activities, have been used alone or in combination therapy with the classic chemotherapeutic agents for specific cancer types in pre-clinical and clinical studies. Thus, understanding the molecular mechanisms involved in modulating APE1 functions may be helpful for designing better therapeutic treatment to enhance cytotoxicity only in tumoral cells. Although this increasing interest in post-translational control of APE1, a clear picture of the multiple ways by which APE1 different functions are regulated is still missing. For these reasons, during my PhD I focused my attention on the biological roles and relevance of the post-translational modifications occurring on a specific portion of APE1 N-terminus, the first 35 amino acids, with particular attention to the role of APE1 acetylation occurring at lysine residues 27-35 in controlling APE1/NPM1 interaction, its activity and its trafficking. Here, prompted by previous work of our lab indicating that acetylation occurring at N-terminal domain of APE1 may modulate its association with rRNA and NPM1[18,23], through a systematic analysis I identified fourteen lysine residues acetylated *in vivo*, including twelve novel sites (Lys27, 31, 32, 35, 125, 141, 194, 197, 203, 224, 227, 228) in addition to the two previously described (Lys6 and 7)[25]. Interestingly, the majority of the acetylated sites found, fell within the N-terminus and localized close to the identified proteolytic site (Lys31 and 32), indicating a possible role in regulating the protein cleavage. Then, in order to evaluate the role of acetylation and of its N-terminus in controlling APE1 equilibrium with its protein partners, by using an unbiased approach, I extended the APE1 interacting map, identifying new nineteen

interacting proteins, involved in RNA metabolism, cytoskeleton dynamics, secretion and transcriptional regulatory processes. Most of them required the APE1 N-terminal domain for a stable interaction and were modulated by acetylation. These data reinforced the idea of APE1 as multifunctional protein, further highlighting the new role of APE1 in the RNA metabolism. Intriguingly, genotoxic stresses may switch APE1 interactome network from binding to protein partners involved in RNA metabolism to those involved in DNA repair and directly to DNA as a substrate. In addition, increased acetylation at Lys27-35 was observed during cell response to genotoxic damage[92]. We hypothesized that under physiological conditions, non acetylated APE1 may be stored in the nucleoli through its binding to NPM1 and rRNA (Figure 27). In our recent paper, we investigated the role of acetylation at Lys27-35 *in vivo* in controlling APE1 subcellular distribution and DNA damage response[92]. A K-to-A mutation at residues Lys27-35, mimicking a constitutive acetylated APE1 form, poorly binds NPM1 and rRNA *in vivo*, with a consequent inability to accumulate within nucleolar structures. Genotoxic damage experiments, performed on reconstituted HeLa cells with this mutant upon treatment with alkylating agents (MMS) show a protective phenotype through increased DNA-repair activity, although its nucleolar absence negatively influences the cellular proliferation, probably through its RNA cleansing activity. Furthermore, we demonstrated a cross-talk between acetylation occurring at Lys6 and 7 with Lys27-35 residues, involving the deacetyl-transferase SIRT1. All these observations, prompted us to draw a model (Figure 27), in which, under physiological conditions APE1 mainly localized in the nucleoli, where it is required for the maintenance of a proper ribosome biogenesis (Poletto *et al.*, submitted to MBoC), acting as a putative storage site and central hub in DNA damage[262]. Following genotoxic stress, a still unknown acetyltransferase, present within nucleoli, may acetylate APE1 at the N-terminus, shifting the equilibrium from the nonacetylated toward the acetylated APE1 form and favouring the release of the interaction from NPM1 and rRNA for a proper activation of DNA-repair mechanisms. The acetylated form accumulates in the nucleoplasm where it could act on abasic DNA as AP endonuclease in BER pathway. When the DNA damage is repaired, SIRT1 deacetylates APE1 in the nucleoplasm, redirecting APE1 within the nucleoli and restoring a pre-damaged condition. From this model, what emerged is the relevance of the unstructured N-terminal domain of APE1 with its post-traslational modifications (i.e. acetylation) for association with both proteins and nucleic acids, supporting an evolutionary "gain-of-function" hypothesis, but also a crucial role for NPM1 in controlling APE1 subcellular redistribution upon stress conditions. Therefore, subcellular distribution of APE1 and its enzymatic activity may be finely tuned through macromolecular associations and coordinated occurrence of different post-translational modifications. Prompted by these observations, I focused my attention to NPM1 and its possible role as APE1 regulator. Here, for the first time, I demonstrated that NPM1 plays an indirect but significant role in base excision repair through a functional regulation of APE1 andonuclease activity, thus indicating a novel role for NPM1 in DNA repair. NPM1 knock-down cell showed a differential sensitivity to different genotoxicants, as alkylating agents, oxidative stressors and chemotherapeutic agents, thus implying an impaired ability of these cells to repair DNA-strand breaks. Nevertheless, treatment with PARP1 inhibitor (PJ-34) or UV-treatment excluded a

possible involvement of dysregulated strand-break repair systems, within the two isogenic cell lines, supporting a BER impairment as the main process affected by the loss of NPM1 expression. Notably, the effect of NPM1c+, a NPM1 mutation found in one third of acute myeloid leukemia (AML), on APE1 subcellular distribution and APE1/NPM1 interaction may explain the response to chemotherapy observed for patients with AML expressing NPM1c+ mutation. As already described for other NPM1 interacting partners, some biological effect observed in AML with NPM1c+ may be caused by impaired function of NPM1 binding proteins, due to an abnormal cytoplasmic dislocation[285,359]. In cells expressing NPM1 c+ (ectopically as in transient transfected HeLa cells or constitutively as in OCI/AML3 cells and blasts from AML patients), APE1 showed an increased cytoplasmic localization, associated with an impaired DNA repair activity and a general higher sensitivity to DNA-damaging agents. In many types of cancers, APE1 presents a different localization pattern, being cytoplasmic or nuclear/cytoplasmic and its increased expression is associated with higher tumor aggressiveness and chemoresistance[16,63]. Beside its nuclear activities, extranuclear APE1 functions within mitochondria were demonstrated to play a role in repairing mitochondrial DNA damages and in controlling the intracellular reactive oxygen species production through inhibition of Rac1 have been described[154]. However, the molecular mechanisms that drive the APE1 cytoplasmic translocation and its association with tumors are not fully characterized. The data presented in this work of Thesis may explain at least one mechanism for APE1 delocalization in the cytoplasm of AML cells with NPM1c+. Moreover, in OCI/AML3 cells, as well in AML blasts with NPM1c+, APE1 is destabilized in a granzyme A-indpendent manner. It can be inferred that, in accordance to the case of p19Arf, NPM1 may act as a chaperone for APE1, ensuring a proper subcellular localization and protecting it from degradation. All these data are in accordance with the model shown in Figure 53, that extends a previous one[285] and explains the relative contribution (both direct and indirect) of NPM1 expression to cellular transformation. This model takes into account the evidence that hematopoietic malignancies, as AML, are associated with NPM1 wild-type deficit (*panel A*) whereas solid tumors show increased expression of NPM1 wild-type protein (*panel B*). In the first case (*panel A*), the NPM1 mutation is causally linked to the transformation process. Reduced nuclear NPM1 levels may lead to genomic instability due to BER impairment, with a consequent accumulation of DNA damage. Thus, the impaired DNA-damage response may inefficiently block cell proliferation: as a consequence some cells would escape DNA damage checkpoints, establishing an immortalized clone prone to further oncogenic transformation. In case of solid tumors (*panel B*), elevated NPM1 wt expression levels would contribute to the generation of a permissive status for oncogenic transformation. High levels of NPM1 wt may limit DNA damage, promoting DNA-damage response, due to an increased BER activity, and therefore it may support cell survival and eventually transformation. Our evidences suggest that interfering with the APE1/NPM1 interaction, that could be associated with the genomic instability, may sensitize tumor cells to chemotherapy and radiotherapy.

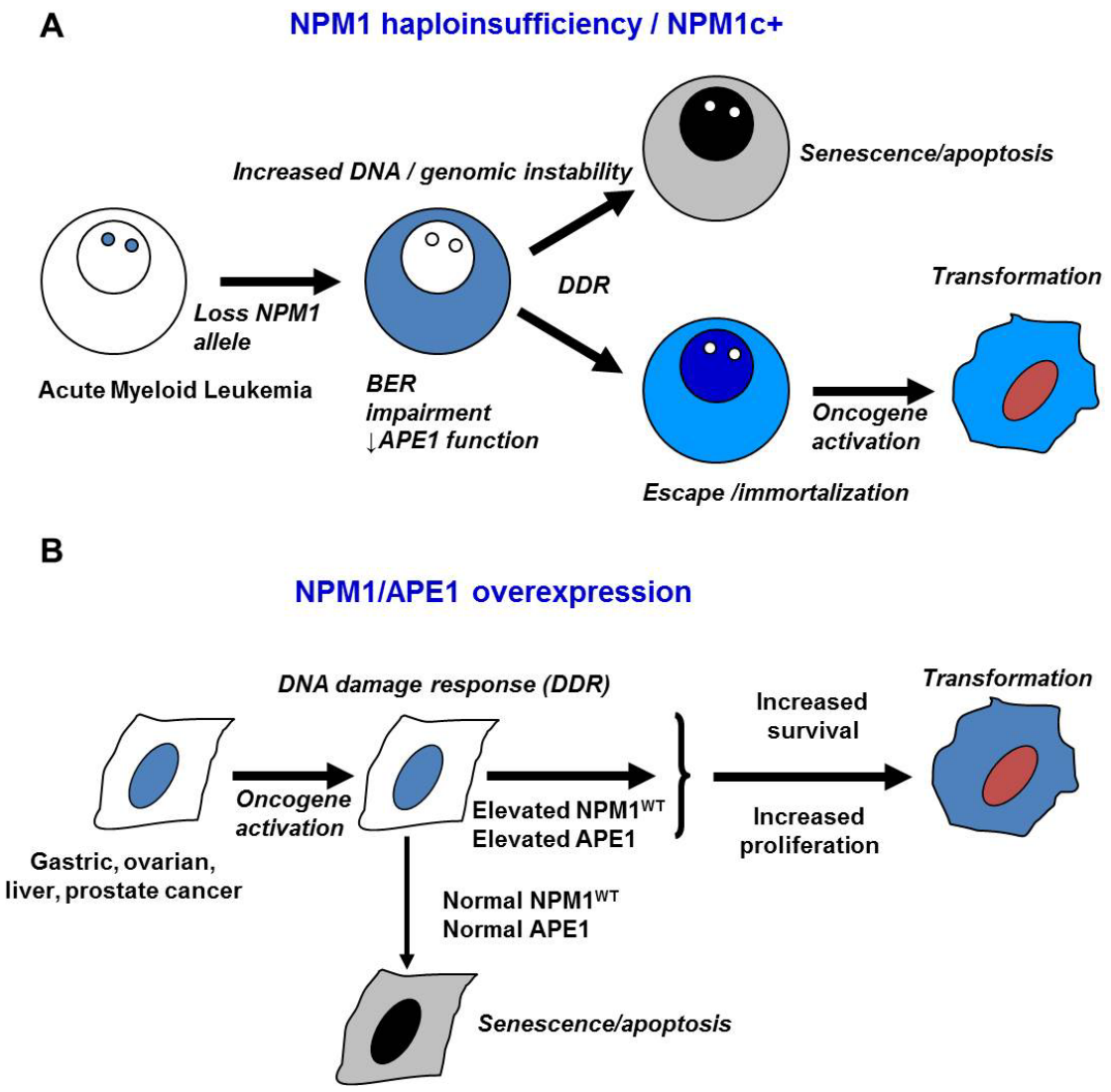

Figure 53: APE/NPM1 role in cellular transformation. A | Reduced nuclear NPM1 levels, caused by the loss of one wt allele, lead to genomic instability thorugh BER impairment and accumulation of DNA damage. As a result, DNA damage response may block cell proliferation, but few cells may escape and an immortalized clone could be transformed by oncogene activation. **B |** In solid tumors, with elevated NPM1 expression levels, DNA damage response may be limited by augmented BER, supporting cell survival and transformation. This model also includes APE1 protein in both the cases; in the first APE1 may have a causative role in transformation whereas in the latter its increased expression level may generate a permissive condition for transformation.

Notably, up to now, deleterious mutations in the core BER components, as APE1, Polβ and XRCC1, have not been clearly associated with human pathologies, even if an increasing number of evidences indicated a possible linkage between APE1 and cancer etiology. The absence of "disease alleles", due to the vital role of APE1 within cells, has prompted different scientist to pursue the hypothesis of "susceptibility alleles". Mild reduction in BER capacity might be associated with enhanced disease risk. As the majority of the polymorphisms involve residues not apparently responsible for neither the AP endonuclease activity nor the redox regulatory function, other mechanisms may account for the possible role of APE1 genetic variants in tumors. A reasonable explanation for the APE1 variants effect observed in tumors may be ascribed to alterations of a complex network of interactions affecting the APE1 functional status. Nowadays, the molecular basis is still unknown. Through the work conducted herein, I explored the functional consequences of a subgroup of APE1 genetic variants for APE1 subcellular localization and in terms of macromolecular associations. Different computational methods used for predicting the genetic variants impact on protein structure/ function provided a negative outcome for most of the mutations, excluding D148E and E126D. Despite the result of the computational approach, none of the previous studies show a parallel significant biochemical or structural defects for most of them. To gain further insights in APE1 polymorphisms effects, the subcellular localization of APE1 genetic variants was analyzed, showing any significant difference with the wild-type protein. Then, the macromolecular associations for three variants (L104R, R237C and D148E) with partners involved both in RNA metabolism and DNA repair were studied. Interestingly, our evidences indicated that the APE1 single point mutations (L104R and R237C) negatively affect APE1 protein-protein interactions. Notably, the endometrial cancer-related R237C variant has recently been shown to have reduced functions. Although the precise mechanism for the impaired function is still unknown, the authors implied a probable disturbance of the local structural integrity, with a consequent reduced overall complex stability with nucleic acids[170]. The data presented here are in accordance with a reduced stability of macromolecule associations for this variant. To check the cellular response to DNA damages elicited by BER and to test the biological impact of these variants in a cellular context, I generated reconstituted cell lines expressing each of the polymorphic variants in place of the endogenous APE1 which was knocked down through RNAi technology. Unexpectledy, all the polymorphisms tested, with some different magnitude, showed an increased resistance to genotoxic damage, somehow in contrast with the previous *in vitro* studies indicating a reduced BER activity for D283G and R237C[170,237]. This behavior might be explained through the different macromolecule network, highlighted for these APE1 genetic variants, as already observed for the K-to-A APE1 mutant, that loses NPM1 interaction[92]. Notably, the mutant shows a higher resistance to genotoxic damages, including MMS and cisplatin (Poletto *et al.*, submitted to MBoC)[92], supporting recent unpublished data from our group regarding an active role for APE1 and, possibly, other BER enzymes, in regulation of ribosome biogenesis. Nowadays, an impact for these polymorphisms on APE1 ribosomal function(s) could not be excluded, yet. Experiments are now ongoing to explore these hypotheses. Further studies for a better comprehension of the molecular

mechanisms and the impact of these genetic variants are needed. Whether the APE1 single point mutations are causative to disease etiology are still matter of debate and it will be absorbed a lot of future energies of the scientists to clarify it.

5 MATERIALS AND METHODS

5.1 CELL LINES CULTURE AND REAGENTS

HeLa, MEF p53$^{-/-}$ NPM1$^{+/+}$ (NPM1$^{+/+}$)[342] and MEF p53$^{-/-}$ NPM1$^{-/-}$ (NPM1$^{-/-}$)[342] cell lines were grown in Dulbecco's modified Eagle's medium (Invitrogen, Carlsbad, CA) supplemented with 10% fetal bovine serum (Euroclone, Milan, Italy), 100 U/ml penicillin and 10 μg/ml streptomycin sulfate (Euroclone). OCI/AML2 and 3 cells were grown in alpha-MEM (Euroclone) supplemented with 20% fetal bovine serum (Euroclone), 100 U/ml penicillin and 10 μg/ml streptomycin sulfate (Euroclone). Leukemic cells were obtained from the bone marrow of patients with acute leukemia during diagnostic procedures. Mononuclear cells were separated on a Ficoll‑Hystopaque 1077 (Sigma-Aldrich, Milan, Italy) density gradient, then were washed twice in phosphate-buffered saline, checked for viability by using the trypan blue exclusion test and suspended in phosphate-buffered saline. Presence of mutations in the NPM1 gene was detected as previously described[385]. Blasts from patients were grown in RPMI (Invitrogen, Monza, Italy) supplemented with 20% fetal bovine serum (Euroclone). All chemical reagents were supplied from Sigma-Aldrich (Sigma-Aldrich) unless otherwise specified. Cisplatin was freshly resuspended in dimethylformamide before each use. Bleomycin Sulfate was purchased from Santa Cruz (Santa Cruz Biotechnology, Santa Cruz, CA, USA).

5.2 APE1 AND NPM1 PLASMID CONSTRUCTS

Human APE1 variant expression constructs (L104R, P112L, E126D, D148E, R237A, R237C and D283G) were created using the QuikChange II Site-Directed Mutagenesis Kit (Stratagene, La Jolla, CA, USA). Forward and reverse primers containing the relevant nucleotide change (Table 6) were generated following the mutagenic primer design guidelines of the manufacturer. To obtain duplex DNAs that harbor the specified nucleotide/amino acid change, the appropriate primer pair (125 ng of each oligonucleotide) was mixed with 20 ng of wild-type pCMV5.1-FLAG- or p3X-FLAG-CMV-APE1 plasmids, dNTPs and Pfu-Ultra HF DNA polymerase, and subjected to the basic thermal cycling protocol outlined by the manufacturer. After digestion with Dpn1, the DNA mix was transformed into XL1-blue Competent cells (Stratagene), and selected clones were sequence confirmed by sequencing (Eurofins MWG Operon, Ebersberg, Germany). To avoid nonspecific mutagenesis, the APE1 variants cDNA were digested with EcoRI and BamHI (Thermo Fisher Scientific, Waltham, MA, USA) and subcloned into the same empty vector of origin (Sigma-Aldrich). Recombinant plasmid sequences were confirmed by endonuclease restriction analysis.

The construct pcDNA3-HA-NPM1c+ was generated by using the Quickchange II XL Mutagenesis kit (Stratagene) and the pcDNA3-HA-NPM1-WT as template following the manufacturer's instructions. Direct sequencing was performed in order to verify the sequence accuracy (Eurofins MWG Operon). NPM1wt and NPM1c+ cDNA were also

subcloned in pCMV5.1-FLAG and p3X-FLAG-CMV vectors for reconstitution experiments on MEF-NPM1$^{-/-}$ cells.

Table 6: List of oligonucleotides used for mutageneis. The mutated bases are underlined.

Primer name	Sequence (5'to 3')
L104R	**For -** AAATGTTCAGAGAACAAACGACCAGCTGAACTTCAGGAG **Rev -** CTCCTGAAGTTCAGCTGGTCGTTTGTTCTCTGAACATTT
P112L	**For -** TGAACTTCAGGAGCTGCTTGGACTCTCTCATCAAT **Rev -** ATTGATGAGAGAGTCCAAGCAGCTCCTGAAGTTCA
E126D	**For -** CAGCTCCTTCGGACAAGGACGGGTACAGTG **Rev -** CACTGTACCCGTCCTTGTCCGAAGGAGCTG
D148E	**For -** CTTACGGCATAGGCGAAGAGGAGCATGATCAGG **Rev -** CCTGATCATGCTCCTCTTCGCCTATGCCGTAAG
R237A	**For -** CACGCCACAAGAGGCCCAAGGCTTCGGG **Rev -** CCCGAAGCCTTGGGCCTCTTGTGGCGTG
R237C	**For -** CACGCCACAAGAGTGCCAAGGCTTCGG **Rev -** CCGAAGCCTTGGCACTCTTGTGGCGTG
D283G	**For -** TGTTGGTTGGCGCCTTGGTTACTTTTTGTTGTCCC **Rev -** GGGACAACAAAAAGTAACCAAGGCGCCAACCAACA

5.3 GENERATION OF STABLE CELL LINES RE-EXPRESSING NPM1WT IN NPM1$^{-/-}$ BACKGROUND

Stable cell lines re-expressing NPM1wt in the MEF NPM1$^{-/-}$ background were obtained as previously described[18]. Briefly, for generation of the reconstituted MEF NPM1$^{-/-}$ cell line, NPM1$^{-/-}$ cells were transfected with the p3X-FLAG-CMV/NPM1wt vector, previously linearized with ScaI (Thermo Fisher Scientific). Positive transfectants underwent selection with Geneticin (Invitrogen) for 14 days and individual clones were isolated by using cell cloning cylinders (Sigma-Aldrich). As control, a mock-reconstituted NPM1$^{-/-}$ cell line was generated by transfection with the p3X-FLAG-CMV-14 empty vector. Stable cell clone were grown in Dulbecco's modified Eagle's medium (Invitrogen) in presence of Geneticin (700μg/ml).

5.4 INDUCIBLE APE1 KNOCK-DOWN AND GENERATION OF APE1 KNOCK-IN CELL LINES

The procedure for the generation of the inducible APE1 knock-down clone has been previously described[18,92]. For generation of APE1 genetic variants knock-in cell lines, the APE1 siRNA clone was transfected with p3X-FLAG-CMV/APE1 genetic variants constructs (L104R, R237C and D283G), previously digested with ScaI (Thermo Fisher

Scientific); 48 hr after transfection, the cells were subjected to selection with Geneticin (Invitrogen) for 14 days and selected for the acquired resistance. Thirty individual clones for each polymorphism were isolated by using cell cloning cylinders (Sigma-Aldrich), transferred, and grown stepwise into 48-well, 24-well, 12-well, and 6-well plates for expansion to 10^7 cells in the presence of selective antibiotics. After 8 days of doxycycline treatment at the final concentration of 1 μg/ml, total cellular extracts were analyzed for APE1 expression by immunoblotting, thus revealing the silencing of the endogenus APE1 and the expression of the ectopic flagged-mutant forms of the protein. The HeLa control cell clone was identified as SCR-1, while the APE1-knocked-down cell clone was identified as CL.3. All biologic data were reproduced in at least two different cell clones for each model.

5.5 TRANSIENT TRANSFECTION EXPERIMENTS

One day before transfection, cells were seeded in 10 cm plates at a density of 3×10^6 cells/plate. Cells were then transiently transfected with plasmids of interest by using Lipofectamine 2000 reagent (Invitrogen), according to the manufacturer's instructions. Cells were harvested 48 hr after transfection.

5.6 PREPARATION OF TOTAL, CYTOPLASMIC AND NUCLEAR CELL EXTRACTS

For preparation of total cell lysates and co-immunoprecipitation, cells were harvested by trypsinization and centrifuged at 250 x g for 5 min at 4°C. Supernatant was removed, and the pellet was washed once with ice-cold phosphate-buffered saline (PBS) and then centrifuged again as described before. Cell pellet was resuspended in Lysis buffer containing 50 mM Tris HCl (pH 7.4), 150 mM NaCl, 1mM EDTA, and 1% [wt/vol] Triton X-100 supplemented with 1x protease inhibitor cocktail (Sigma-Aldrich), 0.5 mM phenylmethylsulfonyl fluoride (PMSF), 1 mM NaF, and 1mM Na_3VO_4, at a cell density of 10^7 cells/ml and rotated for 30 min at 4°C. After centrifugation at 12,000 x g for 10 min at 4°C, the supernatant was collected as total cell lysate.

Cytoplasmic and nuclear cell extracts were prepared as follows. Cells were washed and scraped into cold PBS and then centrifuged at 2,000 x g for 10 min at 4°C. Supernatant was removed, and the pellet was resuspended in buffer A (10 mM Tris-HCl [pH 7.5], 1.5 mM $MgCl_2$, and 10 mM KCl supplemented with 1x protease inhibitor cocktail, 0.5 mM PMSF, 1 mM NaF and 1 mM Na_3VO_4) at a cell density of 3 x 10^7 cells/ml and incubated on ice for 10 min. The nuclei were collected by centrifugation at 2,000 x g for 10 min at 4°C. The resulting supernatant was considered as cytoplasmic fraction. Then, nuclear pellet were resuspended in buffer B (20 mM Tris-HCl [pH 7.5], 0.42 M KCl, 1.5 mM $MgCl_2$, 20% [vol/vol] glycerol supplemented with 1x protease inhibitor cocktail, 0.5 mM PMSF, 1 mM NaF, and 1 mM Na_3VO_4) and rotated for 30 min at 4°C. The suspension was centrifuged at 15,000 x g for 30 min at 4°C. The supernatant was collected as nuclear

protein extract. The protein concentration was determined using Bio-Rad protein assay reagent (Bio-Rad, Hercules, CA, USA).

5.7 CO-IMMUNOPRECIPITATION

Cells transfected with FLAG-tagged APE1wt and genetic variants were lysed in 50 mM Tris-HCl (pH 7.4), 150 mM NaCl, 1 mM EDTA, 1% Triton X-100 supplemented with 1x protease inhibitor cocktail, 0.5 mM PMSF, 1 mM NaF, 1 mM Na_3VO_4 under gentle rocking for 20 minutes at 4°C. The cell extract was clarified by centrifugation and co-immunoprecipitation was carried out for 3 hours using the anti-FLAG M2 affinity gel (Sigma-Aldrich) as per manufacturer's indications. Co-immunoprecipitated material was eventually eluted by incubation with 0.15 mg/ml 1x FLAG peptide in Tris-buffered saline (TBS) and analyzed as indicated.

5.8 ANTIBODIES AND WESTERN BLOTTING ANALYSIS

For Western blotting analyses, the indicated amounts of cell extracts were resolved in 12% SDS-PAGE and transferred to nitrocellulose membranes (Schleicher & Schuell, BioScience, Dassel, Germany). Membranes were blocked with 5% w/v non-fat dry milk in PBS containing 0.1% (vol/vol) Tween-20 and probed with the indicated antibodies; blots were developed by using the ECL enhanced chemiluminescence procedure (GE Healthcare, Piscataway, NJ, USA) or Western Lightning Ultra (Perkin Elmer, Waltham, MA, USA). Polyclonal and monoclonal anti-APE1 were from Novus (NB 100-101 and NB 100-116, respectively) (Novus Biologicals, Littleton, CO, USA), monoclonal or polyclonal anti-NPM1 were from Invitrogen (32-5200) and Abcam (ab15440) (Abcam, Cambridge, England), respectively, monoclonal anti-XRCC1 was from Thermo Fisher Scientific (MS-434-P0), polyclonal anti-Polβ was from Abcam (ab26343), a monoclonal anti-Nucleolin was from Invitrogen (39-6400), polyclonal anti-YB-1 was from Abcam (ab12148), monoclonal anti-PABP-1 was from Abcam (ab6125), polyclonal anti-SFPQ was from Abcam (ab38148), monoclonal anti-PRDX-6 was from Abcam (ab16947), polyclonal anti-PRP-19 was from Abcam (ab27692), monoclonal anti-hnRNP-U was from Abcam (ab89413), polyclonal anti-APE1 acetyl K6K7 and monoclonal anti-NPM1c+ were a kind gift from Dr. Kishor K. Bhakat (University of Nebraska Medical Center) and from Dr. Emanuela Colombo (European Institute of Oncology), respectively. Normalization was performed by using a monoclonal anti-Tubulin antibody (Sigma-Aldrich, T0198), a polyclonal anti-Actin (Sigma-Aldrich, A2066), a polyclonal anti-LSD1 (Abcam, ab129195) or a monoclonal anti-FLAG (Sigma-Aldrich, A8592). Blots were quantified by using a Chemidoc XRS video densitometer (Bio-Rad).

5.9 DETERMINATION OF AP ENDONUCLEASE ACTIVITY AND ABASIC SITE ASSAY

The determination of AP endonuclease activity was performed using an oligonucleotide cleavage assay as described previously[92]. Nuclear cell extracts were incubated with a 5'-

^{32}P-end-labeled 26-mer oligonucleotide containing a single tetrahydrofuranyl (here called dsFDNA) artificial AP site at position 14, which is cleaved to a 14-mer in the presence of AP endonuclease activity. Reactions from reaction mixtures (10 μl) containing the proteins of interest, 2.5 pmol of the 5'-^{32}P end-labeled oligonucleotide dsFDNA, 50 mM HEPES, 50 mM KCl, 10 mM $MgCl_2$,1 μg/μl bovine serum albumin, and 0.05% (wt/vol) Triton X-100 (pH 7.5) were allowed to proceed for the indicated time points in a 37°C water bath. Reactions were halted by adding 10 μl of 96% (vol/vol) formamide and 10 mM EDTA, with xylene cyanol and bromophenol blue as dyes. AP assay products (5 μl) were separated on a 20% polyacrylamide gel containing 7 M urea. Gels were wrapped in Saran wrap and exposed to film for autoradiography. The amount of 14-mer to 26-mer was determined by scanning the exposed film by a Gel Doc scanner (Bio-Rad).

Total abasic damage in chromosomal DNA was measured with an aldehyde-reactive probe as previously described[92]. Genomic DNA was isolated from 2 x 10^6 cells by using DNAzol® Reagent (Invitrogen) and then concentration and purity were determined using a Nanodrop 2000 spectrophotometer (Thermo Fisher Scientific). Samples of 0.1 mg/ml of genomic DNA were analysed by using the DNA Damage Quantification Kit (Dojndo, Gaithersburg, MD, USA), according to the manufacturer's instructions.

5.10 RECOMBINANT APE1 PROTEINS PURIFICATION

pTAC-MAT expression plasmids (Sigma-Aldrich) containing either wild-type APE1 or APE1 R237C variant or pGEX-4T expression vectors (Sigma-Aldrich) containing either wild-type NPM1 or the empty vector were transformed into *E. coli* BL21 (DE3) bacterial cells (Stratagene). Bacterial cells were grown at 37°C to an absorbance of 0.8 at OD_{600}. Isopropyl-b-D-thiogalactopyranoside (IPTG) was then added to a final concentration of 1 mM, and cells were grown for 4 hr for NPM1 and GST and for 5 hr for APE1 proteins at 37°C. Bacteria were harvested and lysed by sonication, and the recombinant proteins were purified from the clarified extracts on an AKTA Prime FPLC system (GE Healthcare) using GSTrap HP and HisTrap HP columns (GE Healthcare) for GST-tagged and MAT-tagged proteins, respectively. The quality of purification was checked by Coomassie-stained SDS–PAGE analysis. Extensive dialysis against PBS was performed to remove any trace of imidazole from the HisTrap-purified proteins. Accurate quantification of all recombinant proteins was performed by colorimetric Bradford assays (Bio-Rad) and confirmed by SDS–PAGE and western blotting analysis using anti-GST peroxidase-conjugated antibody (Sigma-Aldrich, A7340) and anti-MAT tag antibody (Sigma-Aldrich, M6693).

5.11 GST PULL-DOWN ASSAY

For the GST pull-down experiments, 0.15 nmol of either GST or full-length GST-NPM1 protein was incubated, together with 0.45 nmol of either APE1wt-MAT tag or APE1 R237C-MAT tag, in cold PBS supplemented with 1 mM DTT and 0.5 mM PMSF for 2 hr under rotation at 4°C. Then 15μl of glutathione-Sepharose 4B beads (GE Healthcare)

were added to the mixture. Binding with the beads was performed in cold PBS supplemented with 1 mM DTT and 0.5 mM PMSF for 2 hr under rotation at 4°C. The beads were washed five times with washing buffer (PBS supplemented with 0.1% (vol/vol) Igepal CA-630 (Sigma-Aldrich), 1 mM DTT, and 0.5 mM PMSF). Beads were boiled in 1x Laemmli sample buffer containing 100 mM DTT for 5 min, and the supernatant was loaded onto 12% (wt/vol) SDS-PAGE gels followed by Western blotting. The presence of APE1 protein was detected using anti-APE1 monoclonal antibody, while the presence of NPM1 protein was revealed using anti-GST peroxidase-conjugated antibody.

5.12 CELL VIABILITY ASSAYS

Cell viability was measured by using the MTS assay (Celltiter 96 Aqueous One solution cell proliferation assay; Promega, Madison, WI) on HeLa and MEF cells grown in 96-well plates. Briefly, 5 x 10^3 cells were plated and after MMS, $KBrO_3$ or acute H_2O_2 treatment, 20 µl of the MTS solution was added to each well and the plates were incubated for 2 hr at 37°C. Absorbance was measured at 490 nm by using a EnSpire multimode plate reader (Perkin Elmer). The values were standardized to wells containing media alone. Cytotoxicity induced by BLM was evaluated using a trypan blue exclusion assay. A total of 4 x 10^4 cells per well were plated in six-well plates, treated for 60 min with reported amounts of BLM and then grown for 2 additional days in fresh media. Cell viability for OCI/AML cell lines (2.5 x 10^4 cells) was measured by CellTiter-Glo Luminescent Cell Viability Assay (Promega) according to the manufacturer's protocol. Cells were incubated with the indicated doses of MMS for 8 hr at 37°C in agitation. Luminescent signals were measured using the Turner BioSystems Luminometer (Promega). Cell survival upon inhibition of APE1 AP endonuclease activity was measured with the Cell Counting Kit-8 assay (Dojindo). MEF cells were seeded onto 96-well plates (6x10^3 cells) and allowed to adhere for 24 hr. MEFs were then incubated with the indicated amounts of compound 3 (N-(3-(benzo[*d*]thiazol-2-yl)-6-isopropyl-4,5,6,7-tetrahydrothieno[2,3-c]pyridin-2-yl)acetamide)[165], and viability was measured 24 hr later as per the manufacturer's instructions.

5.13 RNA ISOLATION, REVERSE TRANSCRIPTION AND QPCR

Total RNA from MEF cells were extracted with the SV Total RNA isolation System kit (Promega). One microgram of total RNA was reverse transcribed using the iScript cDNA synthesis kit (Bio-Rad), according to the manufacturer's instructions. qRT-PCR was performed with a CFX96 Real-Time System (Bio-Rad. The following primers for mouse APE1 were used: APE1_for: 5'-CGTCACAGCGATGCCAAAGC-3' and APE1_rev: 5'-ATCTGGAGGGTCCTCGTACAGG-3'. DNA was amplified in 96-well plates using primers for APE1_for and APE1_rev using the 2x iQ™ SYBR® Green Supermix (Bio-Rad) (100 mM KCl, 40 mM Tris-HCl [pH 8.4], 0.4 mM of each deoxynucleoside triphosphate [dNTP], 50U/ml iTaq DNA polymerase, 6 mM $MgCl_2$,

SYBR green I, 20 nM fluorescein, and stabilizers) and 10 μM of the specific sense and antisense primers, in a final volume of 15 μl for each well. Each analysis was performed in triplicate. As negative control, a sample without template was used. The cycling parameters were: i) denaturation at 95°C, for 10 s; ii) annealing/extension at 60°C, for 30 s (repeated 40 times). In order to verify the specificity of the amplification, a melting-curve analysis was performed, immediately after the amplification protocol. Gene expression analysis was carried out using the CFX Manager™ Software (Bio-Rad) and *ACTB* as reference gene. The results of the qRT-PCR assay for each sample were reported as fold of activation respect to the APE1 mRNA in MEF NPM1$^{+/+}$.

5.14 IMMUNOFLUORESCENCE AND PLA

For immunofluorescence analysis on HeLa and MEFs, cells were grown on glass coverslips, whereas blasts and OCI/AML2 and 3 cells were centrifuged onto glass slides using a cytospin. Then, cells were fixed with 4% (wt/vol) paraformaldehyde for 20 min at room temperature and permeabilized for 5 min with phosphate-buffered saline-0.25% (vol/vol) Triton X-100. Cells were incubated for 30 min with 10% fetal bovine serum in TBS‑0.1% (vol/vol) Tween-20 (blocking solution) to block unspecific binding of the antibodies. Cells were then incubated with primary antibodies diluted in blocking solutions: monoclonal anti-APE1 (diluted 1:50, 3hr, 37°C), polyclonal or monoclonal anti-NPM1 (diluted 1:200, overnight, 4°C), monoclonal a-FLAG-FITC conjugated (diluted 1:100, 3 hr, 37°C) and polyclonal anti-HA (diluted 1:500, overnight, 4°C). Then cells were washed three times for 5 min each with TBS-0.1% (vol/vol) Tween-20 (Washing Solution) and incubated with secondary antibody: anti-mouse or anti-rabbit Rhodamine Red-conjugated or Alexa Fluor 488-conjugated (diluted 1:200, 2 hr, 25°C) (Jackson Immuno, West Grove, PA). After washing three times, coverslips were mounted on microscope slides with a mounting media containing TO-PRO®-3 Iodide (Invitrogen) or 4', 6-diamidino-2-phenylindole (DAPI) as nuclear counterstains and an anti-fade reagent. For PLA analysis on HeLa cells transiently transfected with construct encoding for NPM1c+ or blasts from patient's, primary antibody anti-APE1 was previously labeled with the Zenon anti-Mouse IgG Labeling Kit (Invitrogen) using the Alexa Fluor 488 according to the manufacturer's instructions. To study the interaction of APE1 with NPM1 *in vivo*, we used the *in situ* PLA technology (Olink Bioscience, Uppsala, Sweden). After incubation with monoclonal anti-APE1 (1:50) or anti-FLAG antibody (1:100) for 3hr at 37°C, cells were incubated with polyclonal anti-NPM1 (1:200) or polyclonal anti-HA antibody (Sigma-Aldrich, H9658) (1:500) overnight at 4°C. PLA was performed following the manufacturer's instructions and as previously reported[92]. Technical controls, represented by the omission of anti-NPM1/anti-HA primary antibody, resulted in the complete loss of PLA signal. Images were captured through a confocal microscope, and quantification of PLA signal was performed using the Blob Finder software (Center for Image Analysis, Uppsala University).

5.15 CONFOCAL LASER SCANNING MICROSCOPY

All images were collected using a confocal laser scanning microscopy LEICA TCS SP (Leica Microsystems, Milan, Italy) supplemented with an Argon laser, a Helium/Neon laser and equipped with 63x oil immersion lenses or a DMB6000B inverted microscope equipped with a DFC300FX digital camera (Leica Microsystems). In double and triple staining, confocal sections of fluorescent signals were taken using the sequential mode (between lines) and merged images of the two signals were obtained using confocal microscope software (Leica Microsystems).

5.16 IDENTIFICATION OF APE1 PROTEIN BINDING PARTNERS

Identification of differential protein interacting partners of APE1-SCR-1, APE1wt and APE1-NΔ33 was performed as already described[18,380]. Protein samples were added with sample buffer containing DTT, boiled and separated by SDS-PAGE. Gel lanes were cut into 6 identical portions in the region 40-350kDa, which were minced and washed with water. Proteins were *in-gel* alkylated and digested with trypsin, as previously reported[386]. Protein digests were analyzed by nanoLC-ESI-LIT-MS/MS using a LTQ XL mass spectrometer (Thermo Fisher Scientific, San Jose, CA, USA) equipped with a Proxeon nanospray source connected to an Easy-nanoLC (Proxeon, Odense, Denmark)[386,387]. Peptide mixtures were separated on an Easy C18 column (10 × 0.075 mm, 3 mm) (Proxeon A/S, Odens C, Denmark) using a gradient of acetonitrile containing 0.1% formic acid in aqueous 0.1% formic acid; acetonitrile ramped from 5% to 40% over 40 min, from 40% to 80% over 10 min, and from 80% to 80% over 5 min, at a flow rate of 300 nL/min. Spectra were acquired in the range m/z 400-2000. Acquisition was controlled by a data-dependent product ion scanning procedure over the three most abundant ions, enabling dynamic exclusion (repeat count 1 and exclusion duration 1 min). The mass isolation window and collision energy in CID experiments were set to m/z 3 and 35%, respectively. Each analysis was performed in duplicate. SEQUEST (Thermo Fisher Scientific) and MASCOT (Matrix Science, UK) within the Proteome Discoverer software package version 1.0 SP1 (Thermo Fisher Scientific) were used to identify proteins present within each gel portion unambiguously from an updated human non-redundant sequence database (UniProtKB). Thus, nanoLC-ESI-LIT-MS/MS data were searched by using a mass tolerance value of 2 Da for precursor ion and 0.8 Da for MS/MS fragments, trypsin as proteolytic enzyme, a missed cleavages maximum value of 2 and Cys carbamidomethylation and Met oxidation as fixed and variable modification, respectively. Candidates with more than 2 assigned tryptic peptides with an individual SEQUEST score versus charge state > 1.5 for charged state (CS) 1, >2.0 for CS 2, >2.5 for CS 3, > 3.0 for CS 4, > 3.2 for CS 5, and/or a MASCOT score >20 (corresponding to $p<0.01$ for a significant identification) were considered confidently identified. They were further evaluated by the comparison with their calculated mass values, using the experimental values obtained from SDS-PAGE. To identify real APE1 binding partners,

protein identification lists from APE1wt, APE1-NΔ33 and APE1-TSA-treated samples were subtracted with data from corresponding control (APE1-SCR-1).

5.17 GENE ANNOTATIONS CO-OCCURRENCE ANALYSIS

Gene IDs corresponding to the list of APE1 interacting proteins identified by mass spectrometry analysis and the list of all the APE1 interacting partners were submitted to GeneCodis (http://genecodis.cnb.csic.es/), a web-based tool for the ontological analysis, selecting Homo sapiens as the source for the annotations and Gene Ontology categories to perform the gene annotation co-occurrence analysis.

5.18 STATISTICAL ANALYSES

Statistical analyses were performed by using the Excel (Microsoft, Redmond, WA, USA) data analysis program for Student's t test analysis. $P < 0.05$ was considered as statistically significant.

6 REFERENCES

1. Watson, J.D. & Crick, F.H.C. Molecular structure of nucleic acids: a structure for deoxyribose nucleic acid. *Nature* **4356**, 737-8 (1953).
2. Garinis, G.A., van der Horst, G.T., Vijg, J. & Hoeijmakers, J.H. DNA damage and ageing: new-age ideas for an age-old problem. *Nat Cell Biol* **10**, 1241-7 (2008).
3. Hoeijmakers, J.H. Genome maintenance mechanisms for preventing cancer. *Nature* **411**, 366-74 (2001).
4. Hoeijmakers, J.H. DNA damage, aging, and cancer. *N Engl J Med* **361**, 1475-85 (2009).
5. De Bont, R. & van Larebeke, N. Endogenous DNA damage in humans: a review of quantitative data. *Mutagenesis* **19**, 169-85 (2004).
6. Lindahl, T. Instability and decay of the primary structure of DNA. *Nature* **362**, 709-15 (1993).
7. Postel-Vinay, S. et al. The potential of exploiting DNA-repair defects for optimizing lung cancer treatment. *Nat Rev Clin Oncol* **9**, 144-55 (2012).
8. Jackson, S.P. & Bartek, J. The DNA-damage response in human biology and disease. *Nature* **461**, 1071-8 (2009).
9. David, S.S., O'Shea, V.L. & Kundu, S. Base-excision repair of oxidative DNA damage. *Nature* **447**, 941-50 (2007).
10. Jiricny, J. The multifaceted mismatch-repair system. *Nat Rev Mol Cell Biol* **7**, 335-46 (2006).
11. Shuck, S.C., Short, E.A. & Turchi, J.J. Eukaryotic nucleotide excision repair, from understanding mechanisms to influencing biology. *Cell Res* **18**, 64-72 (2008).
12. Lieber, M.R. The mechanism of human nonhomologous DNA end joining. *J Biol Chem* **283**, 1-5 (2008).
13. San Filippo, J., Sung, P. & Klein, H. Mechanism of eukaryotic homologous recombination. *Annu Rev Biochem* **77**, 229-57 (2008).
14. Sung, J.S. & Demple, B. Roles of base excision repair subpathways in correcting oxidized abasic sites in DNA. *FEBS J* **273**, 1620-9 (2006).
15. Tell, G., Quadrifoglio, F., Tiribelli, C. & Kelley, M.R. The many functions of APE1/Ref-1: not only a DNA repair enzyme. *Antioxid Redox Signal* **11**, 601-20 (2009).
16. Tell, G., Damante, G., Caldwell, D. & Kelley, M.R. The intracellular localization of APE1/Ref-1: more than a passive phenomenon? *Antioxid Redox Signal* **7**, 367-84 (2005).
17. Robson, C.N. & Hickson, I.D. Isolation of cDNA clones encoding a human apurinic/apyrimidinic endonuclease that corrects DNA repair and mutagenesis defects in E. coli xth (exonuclease III) mutants. *Nucleic Acids Res* **19**, 5519-23 (1991).
18. Vascotto, C. et al. APE1/Ref-1 interacts with NPM1 within nucleoli and plays a role in the rRNA quality control process. *Mol Cell Biol* **29**, 1834-54 (2009).
19. Berquist, B.R., McNeill, D.R. & Wilson, D.M.r. Characterization of abasic endonuclease activity of human Ape1 on alternative substrates, as well as effects of ATP and sequence context on AP site incision. *J Mol Biol* **379**, 17-27 (2008).
20. Barnes, T. et al. Identification of Apurinic/apyrimidinic endonuclease 1 (APE1) as the endoribonuclease that cleaves c-myc mRNA. *Nucleic Acids Res* **37**, 3946-58 (2009).
21. Tell, G., Wilson, D.M., 3rd & Lee, C.H. Intrusion of a DNA repair protein in the RNome world: is this the beginning of a new era? *Mol Cell Biol* **30**, 366-71 (2010).
22. Okazaki, T. et al. A redox factor protein, ref1, is involved in negative gene regulation by extracellular calcium. *J Biol Chem* **269**, 27855-62 (1994).
23. Fantini, D. et al. Critical lysine residues within the overlooked N-terminal domain of human APE1 regulate its biological functions. *Nucleic Acids Res* **38**, 8239-56 (2010).
24. Busso, C.S., Iwakuma, T. & Izumi, T. Ubiquitination of mammalian AP endonuclease (APE1) regulated by the p53-MDM2 signaling pathway. *Oncogene* **28**, 1616-25 (2009).
25. Bhakat, K.K., Izumi, T., Yang, S.H., Hazra, T.K. & Mitra, S. Role of acetylated human AP-endonuclease (APE1/Ref-1) in regulation of the parathyroid hormone gene. *EMBO J* **22**, 6299-309 (2003).
26. Busso, C.S., Wedgeworth, C.M. & Izumi, T. Ubiquitination of human AP-endonuclease 1 (APE1) enhanced by T233E substitution and by CDK5. *Nucleic Acids Res* **39**, 8017-28 (2011).
27. Di Maso, V. et al. Subcellular localization of APE1/Ref-1 in human hepatocellular carcinoma: possible prognostic significance. *Mol Med* **13**, 89-96 (2007).
28. Silber, J.R. et al. The apurinic/apyrimidinic endonuclease activity of Ape1/Ref-1 contributes to human glioma cell resistance to alkylating agents and is elevated by oxidative stress. *Clin Cancer Res* **8**, 3008-18 (2002).

29. Bobola, M.S. et al. Apurinic/apyrimidinic endonuclease is inversely associated with response to radiotherapy in pediatric ependymoma. *Int J Cancer* **129**, 2370-9 (2011).
30. Robson, C.N. et al. Structure of the human DNA repair gene HAP1 and its localisation to chromosome 14q 11.2-12. *Nucleic Acids Res* **20**, 4417-21 (1992).
31. Li, M. & Wilson, D.M., 3rd. Human Apurinic/Apyrimidinic Endonuclease 1. *Antioxid Redox Signal* (2013).
32. Evans, A.R., Limp-Foster, M. & Kelley, M.R. Going APE over ref-1. *Mutat Res* **461**, 83-108 (2000).
33. Dlakic, M. Functionally unrelated signalling proteins contain a fold similar to Mg2+-dependent endonucleases. *Trends Biochem Sci* **25**, 272-3 (2000).
34. Gorman, M.A. et al. The crystal structure of the human DNA repair endonuclease HAP1 suggests the recognition of extra-helical deoxyribose at DNA abasic sites. *EMBO J* **16**, 6548-58 (1997).
35. Jayaraman, L. et al. Identification of redox/repair protein Ref-1 as a potent activator of p53. *Genes Dev* **11**, 558-70 (1997).
36. Beernink, P.T. et al. Two divalent metal ions in the active site of a new crystal form of human apurinic/apyrimidinic endonuclease, Ape1: implications for the catalytic mechanism. *J Mol Biol* **307**, 1023-34 (2001).
37. Hegde, M.L., Izumi, T. & Mitra, S. Oxidized base damage and single-strand break repair in mammalian genomes: role of disordered regions and posttranslational modifications in early enzymes. *Prog Mol Biol Transl Sci* **110**, 123-53 (2012).
38. Yu, E., Gaucher, S.P. & Hadi, M.Z. Probing conformational changes in Ape1 during the progression of base excision repair. *Biochemistry* **49**, 3786-96 (2010).
39. Xanthoudakis, S. & Curran, T. Identification and characterization of Ref-1, a nuclear protein that facilitates AP-1 DNA-binding activity. *EMBO J* **11**, 653–665 (1992).
40. Walker, L.J., Robson, C.N., Black, E., Gillespie, D. & Hickson, I.D. Identification of residues in the human DNA repair enzyme HAP1 (Ref-1) that are essential for redox regulation of Jun DNA binding. *Mol Cell Biol* **13**, 5370-6 (1993).
41. Huang, L.E., Arany, Z., Livingston, D.M. & Bunn, H.F. Activation of hypoxia-inducible transcription factor depends primarily upon redox-sensitive stabilization of its alpha subunit. *J Biol Chem* **271**, 32253-9 (1996).
42. Nishi, T. et al. Spatial redox regulation of a critical cysteine residue of NF-kappa B in vivo. *J Biol Chem* **277**, 44548-56 (2002).
43. Luo, M. et al. Characterization of the redox activity and disulfide bond formation in apurinic/apyrimidinic endonuclease. *Biochemistry* **51**, 695-705 (2012).
44. Georgiadis, M.M. et al. Evolution of the redox function in mammalian apurinic/apyrimidinic endonuclease. *Mutat Res* **643**, 54-63 (2008).
45. Ordway, J.M., Eberhart, D. & Curran, T. Cysteine 64 of Ref-1 is not essential for redox regulation of AP-1 DNA binding. *Mol Cell Biol* **23**, 4257-66 (2003).
46. Rothwell, D.G. & Hickson, I.D. Asparagine 212 is essential for abasic site recognition by the human DNA repair endonuclease HAP1. *Nucleic Acids Res* **24**, 4217-21 (1996).
47. Mol, C.D., Izumi, T., Mitra, S. & Tainer, J.A. DNA-bound structures and mutants reveal abasic DNA binding by APE1 and DNA repair coordination. *Nature* **403**, 451-6 (2000).
48. Manvilla, B.A., Pozharski, E., Toth, E.A. & Drohat, A.C. Structure of human apurinic/apyrimidinic endonuclease 1 with the essential Mg(2+) cofactor. *Acta Crystallogr D Biol Crystallogr* **69**, 2555-62 (2013).
49. Tsutakawa, S.E. et al. Conserved structural chemistry for incision activity in structurally non-homologous apurinic/apyrimidinic endonuclease APE1 and endonuclease IV DNA repair enzymes. *J Biol Chem* **288**, 8445-55 (2013).
50. Mol, C.D., Kuo, C.F., Thayer, M.M., Cunningham, R.P. & Tainer, J.A. Structure and function of the multifunctional DNA-repair enzyme exonuclease III. *Nature* **374**, 381-6 (1995).
51. Suck, D. & Oefner, C. Structure of DNase I at 2.0 A resolution suggests a mechanism for binding to and cutting DNA. *Nature* **321**, 620-5 (1986).
52. Lipton, A.S. et al. Characterization of Mg2+ binding to the DNA repair protein apurinic/apyrimidic endonuclease 1 via solid-state 25Mg NMR spectroscopy. *J Am Chem Soc* **130**, 9332-41 (2008).
53. Fortini, P. & Dogliotti, E. Base damage and single-strand break repair: mechanisms and functional significance of short- and long-patch repair subpathways. *DNA Repair (Amst)* **6**, 398-409 (2007).
54. Hegde, M.L., Hazra, T.K. & Mitra, S. Early steps in the DNA base excision/single-strand interruption repair pathway in mammalian cells. *Cell Res* **18**, 27-47 (2008).

55. Fortini, P. The Type of DNA Glycosylase Determines the Base Excision Repair Pathway in Mammalian Cells. *Journal of Biological Chemistry* **274**, 15230-15236 (1999).
56. Jeppesen, D.K., Bohr, V.A. & Stevnsner, T. DNA repair deficiency in neurodegeneration. *Prog Neurobiol* **94**, 166-200 (2011).
57. Caldecott, K.W., Aoufouchi, S., Johnson, P. & Shall, S. XRCC1 polypeptide interacts with DNA polymerase beta and possibly poly (ADP-ribose) polymerase, and DNA ligase III is a novel molecular 'nick-sensor' in vitro. *Nucleic Acids Res* **24**, 4387-94 (1996).
58. Caldecott, K.W. Protein-protein interactions during mammalian DNA single-strand break repair. *Biochem Soc Trans* **31**, 247-51 (2003).
59. Parsons, J.L. & Dianov, G.L. Co-ordination of base excision repair and genome stability. *DNA Repair (Amst)* **12**, 326-33 (2013).
60. Sidorenko, V.S., Nevinsky, G.A. & Zharkov, D.O. Mechanism of interaction between human 8-oxoguanine-DNA glycosylase and AP endonuclease. *DNA Repair (Amst)* **6**, 317-28 (2007).
61. Vidal, A.E., Boiteux, S., Hickson, I.D. & Radicella, J.P. XRCC1 coordinates the initial and late stages of DNA abasic site repair through protein-protein interactions. *EMBO J* **20**, 6530-9 (2001).
62. Bennett, R.A., Wilson, D.M., 3rd, Wong, D. & Demple, B. Interaction of human apurinic endonuclease and DNA polymerase beta in the base excision repair pathway. *Proc Natl Acad Sci U S A* **94**, 7166-9 (1997).
63. Tell, G., Fantini, D. & Quadrifoglio, F. Understanding different functions of mammalian AP endonuclease (APE1) as a promising tool for cancer treatment. *Cell Mol Life Sci* **67**, 3589-608 (2010).
64. Moran, L.K., Gutteridge, J.M. & Quinlan, G.J. Thiols in cellular redox signalling and control. *Curr Med Chem* **8**, 763-72 (2001).
65. Ray, P.D., Huang, B.W. & Tsuji, Y. Reactive oxygen species (ROS) homeostasis and redox regulation in cellular signaling. *Cell Signal* **24**, 981-90 (2012).
66. Abdelmohsen, K. et al. Ubiquitin-mediated proteolysis of HuR by heat shock. *EMBO J* **28**, 1271-82 (2009).
67. Kelley, M.R., Georgiadis, M.M. & Fishel, M.L. APE1/Ref-1 role in redox signaling: translational applications of targeting the redox function of the DNA repair/redox protein APE1/Ref-1. *Curr Mol Pharmacol.* **5**, 36-53 (2012).
68. Tell, G. et al. Redox effector factor-1 regulates the activity of thyroid transcription factor 1 by controlling the redox state of the N transcriptional activation domain. *J Biol Chem* **277**, 14564-74 (2002).
69. Ando, K. et al. A new APE1/Ref-1-dependent pathway leading to reduction of NF-kappaB and AP-1, and activation of their DNA-binding activity. *Nucleic Acids Res* **36**, 4327-36 (2008).
70. Hirota, K. et al. AP-1 transcriptional activity is regulated by a direct association between thioredoxin and Ref-1. *Proc Natl Acad Sci U S A* **94**, 3633-8 (1997).
71. Barzilay, G., Walker, L.J., Robson, C.N. & Hickson, I.D. Site-directed mutagenesis of the human DNA repair enzyme HAP1: identification of residues important for AP endonuclease and RNase H activity. *Nucleic Acids Res* **23**, 1544-50 (1995).
72. Antoniali, G., Lirussi, L., Poletto, M. & Tell, G. Emerging Roles of the Nucleolus in Regulating the DNA Damage response: the non-canonical DNA repair enzyme APE1/Ref-1 as a paradigmatical example. *Antioxid Redox Signal* (2013).
73. Chattopadhyay, R. et al. Regulatory role of human AP-endonuclease (APE1/Ref-1) in YB-1-mediated activation of the multidrug resistance gene MDR1. *Mol Cell Biol* **28**, 7066-80 (2008).
74. Kuninger, D.T., Izumi, T., Papaconstantinou, J. & Mitra, S. Human AP-endonuclease 1 and hnRNP-L interact with a nCaRE-like repressor element in the AP-endonuclease 1 promoter. *Nucleic Acids Res* **30**, 823-9 (2002).
75. Kim, W.C. et al. Characterization of the endoribonuclease active site of human apurinic/apyrimidinic endonuclease 1. *J Mol Biol* **411**, 960-71 (2011).
76. Izumi, T., Henner, W.D. & Mitra, S. Negative regulation of the major human AP-endonuclease, a multifunctional protein. *Biochemistry* **35**, 14679-83 (1996).
77. Chung, U. et al. The interaction between Ku antigen and REF1 protein mediates negative gene regulation by extracellular calcium. *J Biol Chem* **271**, 8593-8 (1996).
78. Yamamori, T. et al. SIRT1 deacetylates APE1 and regulates cellular base excision repair. *Nucleic Acids Res* **38**, 832-45 (2010).
79. Antoniali, G. et al. SIRT1 gene expression upon genotoxic damage is regulated by APE1 through nCaRE-promoter elements. *Mol Biol Cell* (2013).
80. Gavin, A.C. et al. Proteome survey reveals modularity of the yeast cell machinery. *Nature* **440**, 631-6 (2006).

81. Harrison, L., Ascione, A.G., Wilson, D.M.r. & Demple, B. Characterization of the promoter region of the human apurinic endonuclease gene (APE). *J Biol Chem* **270**, 5556-64 (1995).
82. Rivkees, S.A. & Kelley, M.R. Expression of a multifunctional DNA repair enzyme gene, apurinic/apyrimidinic endonuclease (APE; Ref-1) in the suprachiasmatic, supraoptic and paraventricular nuclei. *Brain Res* **666**, 137-42 (1994).
83. Fung, H., Bennett, R.A. & Demple, B. Key role of a downstream specificity protein 1 site in cell cycle-regulated transcription of the AP endonuclease gene APE1/APEX in NIH3T3 cells. *J Biol Chem* **276**, 42011-7 (2001).
84. Zaky, A. et al. Regulation of the human AP-endonuclease (APE1/Ref-1) expression by the tumor suppressor p53 in response to DNA damage. *Nucleic Acids Res* **36**, 1555-66 (2008).
85. Asai, T., Kambe, F., Kikumori, T. & Seo, H. Increase in Ref-1 mRNA and protein by thyrotropin in rat thyroid FRTL-5 cells. *Biochem Biophys Res Commun* **236**, 71-4 (1997).
86. Ramana, C.V., Boldogh, I., Izumi, T. & Mitra, S. Activation of apurinic/apyrimidinic endonuclease in human cells by reactive oxygen species and its correlation with their adaptive response to genotoxicity of free radicals. *Proc Natl Acad Sci U S A* **95**, 5061-6 (1998).
87. Tell, G. et al. TSH controls Ref-1 nuclear translocation in thyroid cells. *J Mol Endocrinol* **24**, 383-90 (2000).
88. Grosch, S., Fritz, G. & Kaina, B. Apurinic endonuclease (Ref-1) is induced in mammalian cells by oxidative stress and involved in clastogenic adaptation. *Cancer Res* **58**, 4410-6 (1998).
89. Grosch, S. & Kaina, B. Transcriptional activation of apurinic/apyrimidinic endonuclease (Ape, Ref-1) by oxidative stress requires CREB. *Biochem Biophys Res Commun* **261**, 859-63 (1999).
90. Pines, A. et al. Cross-regulation between Egr-1 and APE/Ref-1 during early response to oxidative stress in the human osteoblastic HOBIT cell line: evidence for an autoregulatory loop. *Free Radic Res* **39**, 269-81 (2005).
91. Fantini, D. et al. APE1/Ref-1 regulates PTEN expression mediated by Egr-1. *Free Radic Res* **42**, 20-9 (2008).
92. Lirussi, L. et al. Nucleolar accumulation of APE1 depends on charged lysine residues that undergo acetylation upon genotoxic stress and modulate its BER activity in cells. *Mol Biol Cell* **23**, 4079-96 (2012).
93. Stamler, J.S. Redox signaling: nitrosylation and related target interactions of nitric oxide. *Cell* **78**, 931-6 (1994).
94. Hess, D.T., Matsumoto, A., Kim, S.O., Marshall, H.E. & Stamler, J.S. Protein S-nitrosylation: purview and parameters. *Nat Rev Mol Cell Biol* **6**, 150-66 (2005).
95. Marshall, H.E., Merchant, K. & Stamler, J.S. Nitrosation and oxidation in the regulation of gene expression. *FASEB J* **14**, 1889-900 (2000).
96. Hara, M.R. et al. S-nitrosylated GAPDH initiates apoptotic cell death by nuclear translocation following Siah1 binding. *Nat Cell Biol* **7**, 665-74 (2005).
97. Jaiswal, M., LaRusso, N.F., Burgart, L.J. & Gores, G.J. Inflammatory cytokines induce DNA damage and inhibit DNA repair in cholangiocarcinoma cells by a nitric oxide-dependent mechanism. *Cancer Res* **60**, 184-90 (2000).
98. Qu, J., Liu, G.H., Huang, B. & Chen, C. Nitric oxide controls nuclear export of APE1/Ref-1 through S-nitrosation of cysteines 93 and 310. *Nucleic Acids Res* **35**, 2522-32 (2007).
99. Wu, H.H. et al. Subcellular localization of apurinic endonuclease 1 promotes lung tumor aggressiveness via NF-kappaB activation. *Oncogene* **29**, 4330-40 (2010).
100. Wu, H.H. et al. Cytoplasmic Ape1 Expression Elevated by p53 Aberration May Predict Survival and Relapse in Resected Non-Small Cell Lung Cancer. *Ann Surg Oncol* **20 Suppl 3**, S336-47 (2013).
101. Hsieh, M.M., Hegde, V., Kelley, M.R. & Deutsch, W.A. Activation of APE/Ref-1 redox activity is mediated by reactive oxygen species and PKC phosphorylation. *Nucleic Acids Res* **29**, 3116-22 (2001).
102. Yacoub, A., Kelley, M.R. & Deutsch, W.A. The DNA repair activity of human redox/repair protein APE/Ref-1 is inactivated by phosphorylation. *Cancer Res* **57**, 5457-9 (1997).
103. Fritz, G. & Kaina, B. Phosphorylation of the DNA repair protein APE/REF-1 by CKII affects redox regulation of AP-1. *Oncogene* **18**, 1033-40 (1999).
104. Huang, E. et al. The role of Cdk5-mediated apurinic/apyrimidinic endonuclease 1 phosphorylation in neuronal death. *Nat Cell Biol* **12**, 563-71 (2010).
105. Pickart, C.M. Mechanisms underlying ubiquitination. *Annu Rev Biochem* **70**, 503-33 (2001).
106. Hicke, L. Protein regulation by monoubiquitin. *Nat Rev Mol Cell Biol* **2**, 195-201 (2001).
107. Meisenberg, C. et al. Ubiquitin ligase UBR3 regulates cellular levels of the essential DNA repair protein APE1 and is required for genome stability. *Nucleic Acids Res* **40**, 701-11 (2012).

108. Yoshida, A., Pourquier, P. & Pommier, Y. Purification and characterization of a Mg2+-dependent endonuclease (AN34) from etoposide-treated human leukemia HL-60 cells undergoing apoptosis. *Cancer Res* **58**, 2576-82 (1998).
109. Yoshida, A. et al. Human apurinic/apyrimidinic endonuclease (Ape1) and its N-terminal truncated form (AN34) are involved in DNA fragmentation during apoptosis. *J Biol Chem* **278**, 37768-76 (2003).
110. Pinkoski, M.J. & Green, D.R. Granzyme A: the road less traveled. *Nat Immunol* **4**, 106-8 (2003).
111. Fan, Z. et al. Cleaving the oxidative repair protein Ape1 enhances cell death mediated by granzyme A. *Nat Immunol* **4**, 145-53 (2003).
112. Guo, Y., Chen, J., Zhao, T. & Fan, Z. Granzyme K degrades the redox/DNA repair enzyme Ape1 to trigger oxidative stress of target cells leading to cytotoxicity. *Mol Immunol* **45**, 2225-35 (2008).
113. Chattopadhyay, R. et al. Identification and characterization of mitochondrial abasic (AP)-endonuclease in mammalian cells. *Nucleic Acids Res* **34**, 2067-76 (2006).
114. Li, M. et al. Identification and characterization of mitochondrial targeting sequence of human apurinic/apyrimidinic endonuclease 1. *J Biol Chem* **285**, 14871-81 (2010).
115. Vascotto, C. et al. Knock-in reconstitution studies reveal an unexpected role of Cys-65 in regulating APE1/Ref-1 subcellular trafficking and function. *Mol Biol Cell* **22**, 3887-901 (2011).
116. Gaiddon, C., Moorthy, N.C. & Prives, C. Ref-1 regulates the transactivation and pro-apoptotic functions of p53 in vivo. *EMBO J* **18**, 5609-21 (1999).
117. Wei, S.J. et al. Thioredoxin nuclear translocation and interaction with redox factor-1 activates the activator protein-1 transcription factor in response to ionizing radiation. *Cancer Res* **60**, 6688-95 (2000).
118. Dianova, II, Bohr, V.A. & Dianov, G.L. Interaction of human AP endonuclease 1 with flap endonuclease 1 and proliferating cell nuclear antigen involved in long-patch base excision repair. *Biochemistry* **40**, 12639-44 (2001).
119. Parker, A. et al. Human homolog of the MutY repair protein (hMYH) physically interacts with proteins involved in long patch DNA base excision repair. *J Biol Chem* **276**, 5547-55 (2001).
120. Fritz, G., Grosch, S., Tomicic, M. & Kaina, B. APE/Ref-1 and the mammalian response to genotoxic stress. *Toxicology* **193**, 67-78 (2003).
121. Hegde, V., Wang, M. & Deutsch, W.A. Human ribosomal protein S3 interacts with DNA base excision repair proteins hAPE/Ref-1 and hOGG1. *Biochemistry* **43**, 14211-7 (2004).
122. Gembka, A. et al. The checkpoint clamp, Rad9-Rad1-Hus1 complex, preferentially stimulates the activity of apurinic/apyrimidinic endonuclease 1 and DNA polymerase beta in long patch base excision repair. *Nucleic Acids Res* **35**, 2596-608 (2007).
123. Curtis, C.D. et al. Apurinic/apyrimidinic endonuclease 1 alters estrogen receptor activity and estrogen-responsive gene expression. *Mol Endocrinol* **23**, 1346-59 (2009).
124. Cheng, P.C., Chang, H.K. & Chen, S.H. Quantitative nanoproteomics for protein complexes (QNanoPX) related to estrogen transcriptional action. *Mol Cell Proteomics* **9**, 209-24 (2010).
125. Waters, T.R., Gallinari, P., Jiricny, J. & Swann, P.F. Human thymine DNA glycosylase binds to apurinic sites in DNA but is displaced by human apurinic endonuclease 1. *J Biol Chem* **274**, 67-74 (1999).
126. Ranalli, T.A., Tom, S. & Bambara, R.A. AP endonuclease 1 coordinates flap endonuclease 1 and DNA ligase I activity in long patch base excision repair. *J Biol Chem* **277**, 41715-24 (2002).
127. Kristensen, A.R., Gsponer, J. & Foster, L.J. A high-throughput approach for measuring temporal changes in the interactome. *Nat Methods* **9**, 907-9 (2012).
128. Vuong, B.Q. et al. A DNA break- and phosphorylation-dependent positive feedback loop promotes immunoglobulin class-switch recombination. *Nat Immunol* (2013).
129. Hu, X.V. et al. Identification of RING finger protein 4 (RNF4) as a modulator of DNA demethylation through a functional genomics screen. *Proc Natl Acad Sci U S A* **107**, 15087-92 (2010).
130. Merluzzi, S., D'Orlando, O., Leonardi, A., Vitale, G. & Pucillo, C. TRAF2 and p38 are involved in B cells CD40-mediated APE/Ref-1 nuclear translocation: a novel pathway in B cell activation. *Mol Immunol* **45**, 76-86 (2008).
131. Gray, M.J. et al. HIF-1alpha, STAT3, CBP/p300 and Ref-1/APE are components of a transcriptional complex that regulates Src-dependent hypoxia-induced expression of VEGF in pancreatic and prostate carcinomas. *Oncogene* **24**, 3110-20 (2005).
132. Sengupta, S., Mantha, A.K., Mitra, S. & Bhakat, K.K. Human AP endonuclease (APE1/Ref-1) and its acetylation regulate YB-1-p300 recruitment and RNA polymerase II loading in the drug-induced activation of multidrug resistance gene MDR1. *Oncogene* **30**, 482-93 (2011).

133. Grant, M.M. Identification of SUMOylated proteins in neuroblastoma cells after treatment with hydrogen peroxide or ascorbate. *BMB Rep* **43**, 720-5 (2010).
134. Golebiowski, F. et al. System-wide changes to SUMO modifications in response to heat shock. *Sci Signal* **2**, ra24 (2009).
135. Meierhofer, D., Wang, X., Huang, L. & Kaiser, P. Quantitative analysis of global ubiquitination in HeLa cells by mass spectrometry. *J Proteome Res* **7**, 4566-76 (2008).
136. Carrero, P. et al. Redox-regulated recruitment of the transcriptional coactivators CREB-binding protein and SRC-1 to hypoxia-inducible factor 1alpha. *Mol Cell Biol* **20**, 402-15 (2000).
137. Vinayagam, A. et al. A directed protein interaction network for investigating intracellular signal transduction. *Sci Signal* **4**, rs8 (2011).
138. Yan, M.D. et al. Ubiquitin Conjugating Enzyme Ubc9 is Involved in Protein Degradation of Redox Factor-1 (Ref-1). *Sheng Wu Hua Xue Yu Sheng Wu Wu Li Xue Bao (Shanghai)* **32**, 63-68 (2000).
139. Olah, J. et al. Interactions of pathological hallmark proteins: tubulin polymerization promoting protein/p25, beta-amyloid, and alpha-synuclein. *J Biol Chem* **286**, 34088-100 (2011).
140. Ravasi, T. et al. An atlas of combinatorial transcriptional regulation in mouse and man. *Cell* **140**, 744-52 (2010).
141. Lee, O.H. et al. Genome-wide YFP fluorescence complementation screen identifies new regulators for telomere signaling in human cells. *Mol Cell Proteomics* **10**, M110 001628 (2011).
142. Havugimana, P.C. et al. A census of human soluble protein complexes. *Cell* **150**, 1068-81 (2012).
143. Naji, S. et al. Host cell interactome of HIV-1 Rev includes RNA helicases involved in multiple facets of virus production. *Mol Cell Proteomics* **11**, M111 015313 (2012).
144. Ku, W.C. et al. Complementary quantitative proteomics reveals that transcription factor AP-4 mediates E-box-dependent complex formation for transcriptional repression of HDM2. *Mol Cell Proteomics* **8**, 2034-50 (2009).
145. Shamay, M. et al. A protein array screen for Kaposi's sarcoma-associated herpesvirus LANA interactors links LANA to TIP60, PP2A activity, and telomere shortening. *J Virol* **86**, 5179-91 (2012).
146. Hanson, S., Kim, E. & Deppert, W. Redox factor 1 (Ref-1) enhances specific DNA binding of p53 by promoting p53 tetramerization. *Oncogene* **24**, 1641-7 (2005).
147. Mendez, F. et al. Heat-shock proteins associated with base excision repair enzymes in HeLa cells. *Radiat Res* **153**, 186-95 (2000).
148. Kenny, M.K. et al. Heat shock protein 70 binds to human apurinic/apyrimidinic endonuclease and stimulates endonuclease activity at abasic sites. *J Biol Chem* **276**, 9532-6 (2001).
149. Sgarra, R. et al. Interaction proteomics of the HMGA chromatin architectural factors. *Proteomics* **8**, 4721-32 (2008).
150. Varjosalo, M. et al. The protein interaction landscape of the human CMGC kinase group. *Cell Rep* **3**, 1306-20 (2013).
151. Jackson, E.B., Theriot, C.A., Chattopadhyay, R., Mitra, S. & Izumi, T. Analysis of nuclear transport signals in the human apurinic/apyrimidinic endonuclease (APE1/Ref1). *Nucleic Acids Res* **33**, 3303-12 (2005).
152. Scott, T.L., Rangaswamy, S., Wicker, C.A. & Izumi, T. Repair of Oxidative DNA Damage and Cancer: Recent Progress in DNA Base Excision Repair. *Antioxid Redox Signal* (2013).
153. Leung, A.K. et al. NOPdb: Nucleolar Proteome Database. *Nucleic Acids Res* **34**, D218-20 (2006).
154. Angkeow, P. et al. Redox factor-1: an extra-nuclear role in the regulation of endothelial oxidative stress and apoptosis. *Cell Death Differ* **9**, 717-25 (2002).
155. Pinz, K.G. & Bogenhagen, D.F. Efficient repair of abasic sites in DNA by mitochondrial enzymes. *Mol Cell Biol* **18**, 1257-65 (1998).
156. Szczesny, B., Tann, A.W., Longley, M.J., Copeland, W.C. & Mitra, S. Long patch base excision repair in mammalian mitochondrial genomes. *J Biol Chem* **283**, 26349-56 (2008).
157. Takao, M., Aburatani, H., Kobayashi, K. & Yasui, A. Mitochondrial targeting of human DNA glycosylases for repair of oxidative DNA damage. *Nucleic Acids Res* **26**, 2917-22 (1998).
158. Koehler, C.M., Beverly, K.N. & Leverich, E.P. Redox pathways of the mitochondrion. *Antioxid Redox Signal* **8**, 813-22 (2006).
159. Xanthoudakis, S., Smeyne, R.J., Wallace, J.D. & Curran, T. The redox/DNA repair protein, Ref-1, is essential for early embryonic development in mice. *Proc Natl Acad Sci U S A* **93**, 8919-23 (1996).
160. Izumi, T. et al. Two essential but distinct functions of the mammalian abasic endonuclease. *Proc Natl Acad Sci U S A* **102**, 5739-43 (2005).
161. Kisby, G.E., Milne, J. & Sweatt, C. Evidence of reduced DNA repair in amyotrophic lateral sclerosis brain tissue. *Neuroreport* **8**, 1337-40 (1997).

162. Andersen, J.K. Oxidative stress in neurodegeneration: cause or consequence? *Nat Med* **10 Suppl**, S18-25 (2004).
163. Abbotts, R. & Madhusudan, S. Human AP endonuclease 1 (APE1): from mechanistic insights to druggable target in cancer. *Cancer Treat Rev* **36**, 425-35 (2010).
164. Bobola, M.S. et al. Apurinic/apyrimidinic endonuclease activity is associated with response to radiation and chemotherapy in medulloblastoma and primitive neuroectodermal tumors. *Clin Cancer Res* **11**, 7405-14 (2005).
165. Rai, G. et al. Synthesis, biological evaluation, and structure-activity relationships of a novel class of apurinic/apyrimidinic endonuclease 1 inhibitors. *J Med Chem* **55**, 3101-12 (2012).
166. Wilson, D.M., 3rd, Kim, D., Berquist, B.R. & Sigurdson, A.J. Variation in base excision repair capacity. *Mutat Res* **711**, 100-12 (2011).
167. Karahalil, B., Bohr, V.A. & Wilson, D.M., 3rd. Impact of DNA polymorphisms in key DNA base excision repair proteins on cancer risk. *Hum Exp Toxicol* **31**, 981-1005 (2012).
168. Shen, M.R., Jones, I.M. & Mohrenweiser, H. Nonconservative amino acid substitution variants exist at polymorphic frequency in DNA repair genes in healthy humans. *Cancer Res* **58**, 604-8 (1998).
169. Hakem, R. DNA-damage repair; the good, the bad, and the ugly. *EMBO J* **27**, 589-605 (2008).
170. Illuzzi, J.L. et al. Functional assessment of population and tumor-associated APE1 protein variants. *PLoS One* **8**, e65922 (2013).
171. Olkowski, Z.L. Mutant AP endonuclease in patients with amyotrophic lateral sclerosis. *Neuroreport* **9**, 239-42 (1998).
172. Hu, J.J., Smith, T.R., Miller, M.S., Lohman, K. & Case, L.D. Genetic regulation of ionizing radiation sensitivity and breast cancer risk. *Environ Mol Mutagen* **39**, 208-15 (2002).
173. Zhang, Y. et al. Genetic polymorphisms in base-excision repair pathway genes and risk of breast cancer. *Cancer Epidemiol Biomarkers Prev* **15**, 353-8 (2006).
174. Thomas, G. et al. A multistage genome-wide association study in breast cancer identifies two new risk alleles at 1p11.2 and 14q24.1 (RAD51L1). *Nat Genet* **41**, 579-84 (2009).
175. Easton, D.F. et al. Genome-wide association study identifies novel breast cancer susceptibility loci. *Nature* **447**, 1087-93 (2007).
176. Stacey, S.N. et al. Common variants on chromosome 5p12 confer susceptibility to estrogen receptor-positive breast cancer. *Nat Genet* **40**, 703-6 (2008).
177. Turnbull, C. et al. Genome-wide association study identifies five new breast cancer susceptibility loci. *Nat Genet* **42**, 504-7 (2010).
178. Hayward, C., Colville, S., Swingler, R.J. & Brock, D.J. Molecular genetic analysis of the APEX nuclease gene in amyotrophic lateral sclerosis. *Neurology* **52**, 1899-901 (1999).
179. Coppede, F. et al. Lack of association between the APEX1 Asp148Glu polymorphism and sporadic amyotrophic lateral sclerosis. *Neurobiol Aging* **31**, 353-5 (2010).
180. Gencer, M. et al. DNA repair genes in Parkinson's disease. *Genet Test Mol Biomarkers* **16**, 504-7 (2012).
181. Parildar-Karpuzoglu, H. et al. Single nucleotide polymorphisms in base-excision repair genes hOGG1, APE1 and XRCC1 do not alter risk of Alzheimer's disease. *Neurosci Lett* **442**, 287-91 (2008).
182. Pieretti, M., Khattar, N.H. & Smith, S.A. Common polymorphisms and somatic mutations in human base excision repair genes in ovarian and endometrial cancers. *Mutat Res* **432**, 53-9 (2001).
183. Chen, L. et al. Association between polymorphisms in the DNA repair genes XRCC1 and APE1, and the risk of prostate cancer in white and black Americans. *J Urol* **175**, 108-12; discussion 112 (2006).
184. Ito, H. et al. Gene-environment interactions between the smoking habit and polymorphisms in the DNA repair genes, APE1 Asp148Glu and XRCC1 Arg399Gln, in Japanese lung cancer risk. *Carcinogenesis* **25**, 1395-401 (2004).
185. Li, C. et al. Genetic variants of the ADPRT, XRCC1 and APE1 genes and risk of cutaneous melanoma. *Carcinogenesis* **27**, 1894-901 (2006).
186. Li, C. et al. Genetic polymorphisms in DNA base-excision repair genes ADPRT, XRCC1, and APE1 and the risk of squamous cell carcinoma of the head and neck. *Cancer* **110**, 867-75 (2007).
187. Olshan, A.F., Shaw, G.M., Millikan, R.C., Laurent, C. & Finnell, R.H. Polymorphisms in DNA repair genes as risk factors for spina bifida and orofacial clefts. *Am J Med Genet A* **135**, 268-73 (2005).
188. Zienolddiny, S. et al. Polymorphisms of DNA repair genes and risk of non-small cell lung cancer. *Carcinogenesis* **27**, 560-7 (2006).

189. Terry, P.D., Umbach, D.M. & Taylor, J.A. APE1 genotype and risk of bladder cancer: evidence for effect modification by smoking. *Int J Cancer* **118**, 3170-3 (2006).
190. Wei, C. et al. Genetic variants of the APE1 gene and the risk of vitiligo in a Chinese population: a genotype-phenotype correlation study. *Free Radic Biol Med* **58**, 64-72 (2013).
191. Wei, W. et al. Association between the OGG1 Ser326Cys and APEX1 Asp148Glu polymorphisms and lung cancer risk: a meta-analysis. *Mol Biol Rep* **39**, 11249-62 (2012).
192. Hung, R.J., Hall, J., Brennan, P. & Boffetta, P. Genetic polymorphisms in the base excision repair pathway and cancer risk: a HuGE review. *Am J Epidemiol* **162**, 925-42 (2005).
193. De Ruyck, K. et al. Polymorphisms in base-excision repair and nucleotide-excision repair genes in relation to lung cancer risk. *Mutat Res* **631**, 101-10 (2007).
194. Canbay, E. et al. Association of APE1 and hOGG1 polymorphisms with colorectal cancer risk in a Turkish population. *Curr Med Res Opin* **27**, 1295-302 (2011).
195. Li, Y. et al. Polymorphisms in genes of APE1, PARP1, and XRCC1: risk and prognosis of colorectal cancer in a northeast Chinese population. *Med Oncol* **30**, 505 (2013).
196. Liu, C. et al. APE1 Asp148Glu gene polymorphism and bladder cancer risk: a meta-analysis. *Mol Biol Rep* **40**, 171-6 (2013).
197. Lin, C.H. et al. The APE1 Asp/Asp genotype and the combination of APE1 Asp/Asp and hOGG1-Cys variants are associated with increased p53 mutation in non-small cell lung cancer. *J Epidemiol* **22**, 537-42 (2012).
198. Ji, Y.N., Zhan, P., Wang, J., Qiu, L.X. & Yu, L.K. APE1 Asp148Glu gene polymorphism and lung cancer risk: a meta-analysis. *Mol Biol Rep* **38**, 4537-43 (2011).
199. Gu, D., Wang, M., Wang, S., Zhang, Z. & Chen, J. The DNA repair gene APE1 T1349G polymorphism and risk of gastric cancer in a Chinese population. *PLoS One* **6**, e28971 (2011).
200. Zhou, B. et al. The association of APE1 -656T > G and 1349 T > G polymorphisms and cancer risk: a meta-analysis based on 37 case-control studies. *BMC Cancer* **11**, 521 (2011).
201. Chen, W.C. et al. The contribution of DNA apurinic/apyrimidinic endonuclease genotype and smoking habit to Taiwan lung cancer risk. *Anticancer Res* **33**, 2775-8 (2013).
202. Li, Q. et al. Association of DNA base-excision repair XRCC1, OGG1 and APE1 gene polymorphisms with nasopharyngeal carcinoma susceptibility in a Chinese population. *Asian Pac J Cancer Prev* **14**, 5145-51 (2013).
203. Kim, K.Y., Han, W., Noh, D.Y., Kang, D. & Kwack, K. Impact of genetic polymorphisms in base excision repair genes on the risk of breast cancer in a Korean population. *Gene* **532**, 192-6 (2013).
204. Sapkota, Y. et al. Assessing SNP-SNP interactions among DNA repair, modification and metabolism related pathway genes in breast cancer susceptibility. *PLoS One* **8**, e64896 (2013).
205. Gokkusu, C. et al. Association between genetic variants of DNA repair genes and coronary artery disease. *Genet Test Mol Biomarkers* **17**, 307-13 (2013).
206. Cincin, Z.B., Iyibozkurt, A.C., Kuran, S.B. & Cakmakoglu, B. DNA repair gene variants in endometrial carcinoma. *Med Oncol* **29**, 2949-54 (2012).
207. Figl, A. et al. Single nucleotide polymorphisms in DNA repair genes XRCC1 and APEX1 in progression and survival of primary cutaneous melanoma patients. *Mutat Res* **661**, 78-84 (2009).
208. Kuptsova, N. et al. Polymorphisms in DNA repair genes and therapeutic outcomes of AML patients from SWOG clinical trials. *Blood* **109**, 3936-44 (2007).
209. Su, D. et al. Genetic polymorphisms and treatment response in advanced non-small cell lung cancer. *Lung Cancer* **56**, 281-8 (2007).
210. Krajinovic, M. et al. Polymorphisms in genes encoding drugs and xenobiotic metabolizing enzymes, DNA repair enzymes, and response to treatment of childhood acute lymphoblastic leukemia. *Clin Cancer Res* **8**, 802-10 (2002).
211. Frank, B. et al. DNA repair gene polymorphisms and risk of chronic atrophic gastritis: a case-control study. *BMC Cancer* **11**, 440 (2011).
212. Li, Z. et al. Genetic polymorphism of DNA base-excision repair genes (APE1, OGG1 and XRCC1) and their correlation with risk of lung cancer in a Chinese population. *Arch Med Res* **42**, 226-34 (2011).
213. Ibarrola-Villava, M. et al. Genetic polymorphisms in DNA repair and oxidative stress pathways associated with malignant melanoma susceptibility. *Eur J Cancer* **47**, 2618-25 (2011).
214. Kuasne, H. et al. Base excision repair genes XRCC1 and APEX1 and the risk for prostate cancer. *Mol Biol Rep* **38**, 1585-91 (2011).
215. Palli, D. et al. Polymorphic DNA repair and metabolic genes: a multigenic study on gastric cancer. *Mutagenesis* **25**, 569-75 (2010).
216. Wang, M. et al. Genetic variants of XRCC1, APE1, and ADPRT genes and risk of bladder cancer. *DNA Cell Biol* **29**, 303-11 (2010).

217. Vural, P. et al. Genetic polymorphisms in DNA repair gene APE1, XRCC1 and XPD and the risk of pre-eclampsia. *Eur J Obstet Gynecol Reprod Biol* **146**, 160-4 (2009).
218. Stern, M.C. et al. Polymorphisms in DNA repair genes, smoking, and bladder cancer risk: findings from the international consortium of bladder cancer. *Cancer Res* **69**, 6857-64 (2009).
219. McKean-Cowdin, R. et al. Associations between polymorphisms in DNA repair genes and glioblastoma. *Cancer Epidemiol Biomarkers Prev* **18**, 1118-26 (2009).
220. Zhao, Z. et al. The association between the APE1 Asp148Glu polymorphism and breast cancer susceptibility: a meta-analysis based on case-control studies. *Tumour Biol* (2014).
221. Cuchra, M. et al. The role of the 148 Asp/Glu polymorphism of the APE1 gene in the development and progression of primary open angle glaucoma development in the Polish population. *Pol J Pathol* **64**, 296-302 (2013).
222. Huang, W.Y. et al. Selected base excision repair gene polymorphisms and susceptibility to biliary tract cancer and biliary stones: a population-based case-control study in China. *Carcinogenesis* **29**, 100-5 (2008).
223. Matakidou, A. et al. Genetic variation in the DNA repair genes is predictive of outcome in lung cancer. *Hum Mol Genet* **16**, 2333-40 (2007).
224. Lochan, R., Daly, A.K., Reeves, H.L. & Charnley, R.M. Genetic susceptibility in pancreatic ductal adenocarcinoma. *Br J Surg* **95**, 22-32 (2008).
225. Chiang, F.Y. et al. Association between polymorphisms in DNA base excision repair genes XRCC1, APE1, and ADPRT and differentiated thyroid carcinoma. *Clin Cancer Res* **14**, 5919-24 (2008).
226. Mitra, A.K. et al. Association of polymorphisms in base excision repair genes with the risk of breast cancer: a case-control study in North Indian women. *Oncol Res* **17**, 127-35 (2008).
227. Berndt, S.I. et al. Genetic variation in base excision repair genes and the prevalence of advanced colorectal adenoma. *Cancer Res* **67**, 1395-404 (2007).
228. Li, D. et al. Effects of base excision repair gene polymorphisms on pancreatic cancer survival. *Int J Cancer* **120**, 1748-54 (2007).
229. Huang, M. et al. High-order interactions among genetic variants in DNA base excision repair pathway genes and smoking in bladder cancer susceptibility. *Cancer Epidemiol Biomarkers Prev* **16**, 84-91 (2007).
230. Hall, J. et al. The association of sequence variants in DNA repair and cell cycle genes with cancers of the upper aerodigestive tract. *Carcinogenesis* **28**, 665-71 (2007).
231. Hill, D.A. et al. Risk of non-Hodgkin lymphoma (NHL) in relation to germline variation in DNA repair and related genes. *Blood* **108**, 3161-7 (2006).
232. Jiao, L. et al. Selected polymorphisms of DNA repair genes and risk of pancreatic cancer. *Cancer Detect Prev* **30**, 284-91 (2006).
233. Chang-Claude, J. et al. Association between polymorphisms in the DNA repair genes, XRCC1, APE1, and XPD and acute side effects of radiotherapy in breast cancer patients. *Clin Cancer Res* **11**, 4802-9 (2005).
234. Hao, B. et al. Identification of genetic variants in base excision repair pathway and their associations with risk of esophageal squamous cell carcinoma. *Cancer Res* **64**, 4378-84 (2004).
235. Shen, M. et al. Polymorphisms in the DNA base excision repair genes APEX1 and XRCC1 and lung cancer risk in Xuan Wei, China. *Anticancer Res* **25**, 537-42 (2005).
236. Hu, J.J. et al. Amino acid substitution variants of APE1 and XRCC1 genes associated with ionizing radiation sensitivity. *Carcinogenesis* **22**, 917-22 (2001).
237. Hadi, M.Z., Coleman, M.A., Fidelis, K., Mohrenweiser, H.W. & Wilson, D.M.r. Functional characterization of Ape1 variants identified in the human population. *Nucleic Acids Res* **28**, 3871-9 (2000).
238. Hernandez-Verdun, D., Roussel, P., Thiry, M., Sirri, V. & Lafontaine, D.L. The nucleolus: structure/function relationship in RNA metabolism. *Wiley Interdiscip Rev RNA* **1**, 415-31 (2010).
239. Boisvert, F.M., van Koningsbruggen, S., Navascues, J. & Lamond, A.I. The multifunctional nucleolus. *Nat Rev Mol Cell Biol* **8**, 574-85 (2007).
240. Andersen, J.S. et al. Directed proteomic analysis of the human nucleolus. *Curr Biol* **12**, 1-11 (2002).
241. Lam, Y.W., Trinkle-Mulcahy, L. & Lamond, A.I. The nucleolus. *J Cell Sci* **118**, 1335-7 (2005).
242. Sirri, V., Urcuqui-Inchima, S., Roussel, P. & Hernandez-Verdun, D. Nucleolus: the fascinating nuclear body. *Histochem Cell Biol* **129**, 13-31 (2008).
243. Coute, Y. et al. Deciphering the human nucleolar proteome. *Mass Spectrom Rev* **25**, 215-34 (2006).

244. Stark, L.A. & Taliansky, M. Old and new faces of the nucleolus. Workshop on the Nucleolus and Disease. *EMBO Rep* **10**, 35-40 (2009).
245. Milkereit, P. et al. Maturation and intranuclear transport of pre-ribosomes requires Noc proteins. *Cell* **105**, 499-509 (2001).
246. Trotta, C.R., Lund, E., Kahan, L., Johnson, A.W. & Dahlberg, J.E. Coordinated nuclear export of 60S ribosomal subunits and NMD3 in vertebrates. *EMBO J* **22**, 2841-51 (2003).
247. Milkereit, P. et al. A Noc complex specifically involved in the formation and nuclear export of ribosomal 40 S subunits. *J Biol Chem* **278**, 4072-81 (2003).
248. Hinsby, A.M. et al. A wiring of the human nucleolus. *Mol Cell* **22**, 285-95 (2006).
249. Boulon, S., Westman, B.J., Hutten, S., Boisvert, F.M. & Lamond, A.I. The nucleolus under stress. *Mol Cell* **40**, 216-27 (2010).
250. Suzuki, A. et al. A new PICTure of nucleolar stress. *Cancer Sci* **103**, 632-7 (2012).
251. Scherl, A. et al. Functional proteomic analysis of human nucleolus. *Mol Biol Cell* **13**, 4100-9 (2002).
252. Shcherbik, N. & Pestov, D.G. Ubiquitin and ubiquitin-like proteins in the nucleolus: multitasking tools for a ribosome factory. *Genes Cancer* **1**, 681-689 (2010).
253. Lam, Y.W., Lamond, A.I., Mann, M. & Andersen, J.S. Analysis of nucleolar protein dynamics reveals the nuclear degradation of ribosomal proteins. *Curr Biol* **17**, 749-60 (2007).
254. Pederson, T. & Tsai, R.Y. In search of nonribosomal nucleolar protein function and regulation. *J Cell Biol* **184**, 771-6 (2009).
255. Pederson, T. The nucleolus. *Cold Spring Harb Perspect Biol* **3**, pii: a000638 (2011).
256. Olson, M.O. & Dundr, M. The moving parts of the nucleolus. *Histochem Cell Biol* **123**, 203-16 (2005).
257. Emmott, E. & Hiscox, J.A. Nucleolar targeting: the hub of the matter. *EMBO Rep* **10**, 231-8 (2009).
258. Nishimura, Y., Ohkubo, T., Furuichi, Y. & Umekawa, H. Tryptophans 286 and 288 in the C-terminal region of protein B23.1 are important for its nucleolar localization. *Biosci. Biotechnol. Biochem* **66**, 2239–2242 (2002).
259. Raska, I., Shaw, P.J. & Cmarko, D. Structure and function of the nucleolus in the spotlight. *Curr Opin Cell Biol* **18**, 325-34 (2006).
260. Mekhail, K., Gunaratnam, L., Bonicalzi, M.E. & Lee, S. HIF activation by pH-dependent nucleolar sequestration of VHL. *Nat Cell Biol* **6**, 642-7 (2004).
261. Andersen, J.S. et al. Nucleolar proteome dynamics. *Nature* **433**, 77-83 (2005).
262. Nalabothula, N., Indig, F.E. & Carrier, F. The Nucleolus Takes Control of Protein Trafficking Under Cellular Stress. *Mol Cell Pharmacol.* **2**, 203-12 (2010).
263. Ahmad, Y., Boisvert, F.M., Gregor, P., Cobley, A. & Lamond, A.I. NOPdb: Nucleolar Proteome Database--2008 update. *Nucleic Acids Research* **37**, D181-D184 (2009).
264. Lo, S.J., Lee, C.C. & Lai, H.J. The nucleolus: reviewing oldies to have new understandings. *Cell Res* **16**, 530-8 (2006).
265. Mayer, C. & Grummt, I. Cellular stress and nucleolar function. *Cell Cycle* **4**, 1036-8 (2005).
266. Rubbi, C.P. & Milner, J. Disruption of the nucleolus mediates stabilization of p53 in response to DNA damage and other stresses. *EMBO J* **22**, 6068-77 (2003).
267. Boyd, M.T., Vlatkovic, N. & Rubbi, C.P. The nucleolus directly regulates p53 export and degradation. *J Cell Biol* **194**, 689-703 (2011).
268. Tembe, V. & Henderson, B.R. Protein trafficking in response to DNA damage. *Cell Signal* **19**, 1113-20 (2007).
269. Horn, H.F. & Vousden, K.H. Cancer: guarding the guardian? *Nature* **427**, 110-1 (2004).
270. Essers, J., Vermeulen, W. & Houtsmuller, A.B. DNA damage repair: anytime, anywhere? *Curr Opin Cell Biol* **18**, 240-6 (2006).
271. Jarboui, M.A. et al. Nucleolar protein trafficking in response to HIV-1 Tat: rewiring the nucleolus. *PLoS One* **7**, e48702 (2012).
272. Sengupta, S., Peterson, T.R. & Sabatini, D.M. Regulation of the mTOR complex 1 pathway by nutrients, growth factors, and stress. *Mol Cell* **40**, 310-22 (2010).
273. *Protein of the nucleolus. Regulation, translocation and biomedical functions*, (2013).
274. Boisvert, F.M., Lam, Y.W., Lamont, D. & Lamond, A.I. A quantitative proteomics analysis of subcellular proteome localization and changes induced by DNA damage. *Mol Cell Proteomics* **9**, 457-70 (2010).
275. Emmott, E. et al. Quantitative proteomics using stable isotope labeling with amino acids in cell culture reveals changes in the cytoplasmic, nuclear, and nucleolar proteomes in Vero cells infected with the coronavirus infectious bronchitis virus. *Mol Cell Proteomics.* **9**, 1920-36 (2010).

276. Boisvert, F.M. & Lamond, A.I. p53-Dependent subcellular proteome localization following DNA damage. *Proteomics* **10**, 4087-97 (2010).
277. Bassermann, F. et al. The Cdc14B-Cdh1-Plk1 axis controls the G2 DNA-damage-response checkpoint. *Cell* **134**, 256-67 (2008).
278. Thoms, H.C. et al. Nucleolar targeting of RelA(p65) is regulated by COMMD1-dependent ubiquitination. *Cancer Res* **70**, 139-49 (2010).
279. Lee, J.T. & Gu, W. The multiple levels of regulation by p53 ubiquitination. *Cell Death Differ* **17**, 86-92 (2010).
280. Lim, M.J. & Wang, X.W. Nucleophosmin and human cancer. *Cancer Detect Prev* **30**, 481-90 (2006).
281. Grisendi, S., Mecucci, C., Falini, B. & Pandolfi, P.P. Nucleophosmin and cancer. *Nat Rev Cancer* **6**, 493-505 (2006).
282. Rau, R. & Brown, P. Nucleophosmin (NPM1) mutations in adult and childhood acute myeloid leukaemia: towards definition of a new leukaemia entity. *Hematol Oncol* **27**, 171-81 (2009).
283. Eirin-Lopez, J.M., Frehlick, L.J. & Ausio, J. Long-term evolution and functional diversification in the members of the nucleophosmin/nucleoplasmin family of nuclear chaperones. *Genetics* **173**, 1835-50 (2006).
284. Itahana, K. et al. Tumor suppressor ARF degrades B23, a nucleolar protein involved in ribosome biogenesis and cell proliferation. *Mol Cell* **12**, 1151-64 (2003).
285. Colombo, E., Alcalay, M. & Pelicci, P.G. Nucleophosmin and its complex network: a possible therapeutic target in hematological diseases. *Oncogene* **30**, 2595-609 (2011).
286. Falini, B. et al. Cytoplasmic nucleophosmin in acute myelogenous leukemia with a normal karyotype. *N Engl J Med* **352**, 254-66 (2005).
287. Falini, B., Nicoletti, I., Martelli, M.F. & Mecucci, C. Acute myeloid leukemia carrying cytoplasmic/mutated nucleophosmin (NPMc+ AML): biologic and clinical features. *Blood* **109**, 874-85 (2007).
288. Okuwaki, M. The structure and functions of NPM1/Nucleophsmin/B23, a multifunctional nucleolar acidic protein. *J Biochem* **143**, 441-8 (2008).
289. Swaminathan, V., Kishore, A.H., Febitha, K.K. & Kundu, T.K. Human histone chaperone nucleophosmin enhances acetylation-dependent chromatin transcription. *Mol Cell Biol* **25**, 7534-45 (2005).
290. Grummitt, C.G., Townsley, F.M., Johnson, C.M., Warren, A.J. & Bycroft, M. Structural consequences of nucleophosmin mutations in acute myeloid leukemia. *J Biol Chem* **283**, 23326-32 (2008).
291. Federici, L. & Falini, B. Nucleophosmin mutations in acute myeloid leukemia: A tale of protein unfolding and mislocalization. *Protein Sci* **22**, 545-56 (2013).
292. Falini, B. et al. Both carboxy-terminus NES motif and mutated tryptophan(s) are crucial for aberrant nuclear export of nucleophosmin leukemic mutants in NPMc+ AML. *Blood* **107**, 4514-23 (2006).
293. Cuomo, M.E. et al. p53-Driven apoptosis limits centrosome amplification and genomic instability downstream of NPM1 phosphorylation. *Nat Cell Biol* **10**, 723-30 (2008).
294. Shandilya, J. et al. Acetylated NPM1 localizes in the nucleoplasm and regulates transcriptional activation of genes implicated in oral cancer manifestation. *Mol Cell Biol* **29**, 5115-27 (2009).
295. Tago, K., Chiocca, S. & Sherr, C.J. Sumoylation induced by the Arf tumor suppressor: a p53-independent function. *Proc Natl Acad Sci U S A* **102**, 7689-94 (2005).
296. Kuo, M.L., den Besten, W., Thomas, M.C. & Sherr, C.J. Arf-induced turnover of the nucleolar nucleophosmin-associated SUMO-2/3 protease Senp3. *Cell Cycle* **7**, 3378-87 (2008).
297. Liu, X. et al. Sumoylation of nucleophosmin/B23 regulates its subcellular localization, mediating cell proliferation and survival. *Proc Natl Acad Sci U S A* **104**, 9679-84 (2007).
298. Ramsamooj, P., Notario, V. & Dritschilo, A. Modification of nucleolar protein B23 after exposure to ionizing radiation. *Radiat Res* **143**, 158-64 (1995).
299. Sato, K. et al. Nucleophosmin/B23 is a candidate substrate for the BRCA1-BARD1 ubiquitin ligase. *J Biol Chem* **279**, 30919-22 (2004).
300. Tarapore, P. et al. Thr199 phosphorylation targets nucleophosmin to nuclear speckles and represses pre-mRNA processing. *FEBS Lett* **580**, 399-409 (2006).
301. Tokuyama, Y., Horn, H.F., Kawamura, K., Tarapore, P. & Fukasawa, K. Specific phosphorylation of nucleophosmin on Thr(199) by cyclin-dependent kinase 2-cyclin E and its role in centrosome duplication. *J Biol Chem* **276**, 21529-37 (2001).
302. Krause, A. & Hoffmann, I. Polo-like kinase 2-dependent phosphorylation of NPM/B23 on serine 4 triggers centriole duplication. *PLoS One* **5**, e9849 (2010).

303. Okuwaki, M., Tsujimoto, M. & Nagata, K. The RNA binding activity of a ribosome biogenesis factor, nucleophosmin/B23, is modulated by phosphorylation with a cell cycle-dependent kinase and by association with its subtype. *Mol Biol Cell* **13**, 2016-30 (2002).
304. Hisaoka, M., Ueshima, S., Murano, K., Nagata, K. & Okuwaki, M. Regulation of nucleolar chromatin by B23/nucleophosmin jointly depends upon its RNA binding activity and transcription factor UBF. *Mol Cell Biol* **30**, 4952-64 (2010).
305. Zou, Y. et al. Nucleophosmin/B23 negatively regulates GCN5-dependent histone acetylation and transactivation. *J Biol Chem* **283**, 5728-37 (2008).
306. Zhang, Y. The ARF-B23 connection: implications for growth control and cancer treatment. *Cell Cycle* **3**, 259-62 (2004).
307. Lin, C.Y. et al. Dephosphorylation of nucleophosmin by PP1beta facilitates pRB binding and consequent E2F1-dependent DNA repair. *Mol Biol Cell* **21**, 4409-17 (2010).
308. Velimezi, G. et al. Functional interplay between the DNA-damage-response kinase ATM and ARF tumour suppressor protein in human cancer. *Nat Cell Biol* **15**, 967-77 (2013).
309. Meder, V.S., Boeglin, M., de Murcia, G. & Schreiber, V. PARP-1 and PARP-2 interact with nucleophosmin/B23 and accumulate in transcriptionally active nucleoli. *J Cell Sci* **118**, 211-22 (2005).
310. Szebeni, A., Hingorani, K., Negi, S. & Olson, M.O. Role of protein kinase CK2 phosphorylation in the molecular chaperone activity of nucleolar protein b23. *J Biol Chem* **278**, 9107-15 (2003).
311. Okuwaki, M., Matsumoto, K., Tsujimoto, M. & Nagata, K. Function of nucleophosmin/B23, a nucleolar acidic protein, as a histone chaperone. *FEBS Lett* **506**, 272-6 (2001).
312. Hingorani, K., Szebeni, A. & Olson, M.O. Mapping the functional domains of nucleolar protein B23. *J Biol Chem* **275**, 24451-7 (2000).
313. Yu, Y. et al. Nucleophosmin is essential for ribosomal protein L5 nuclear export. *Mol Cell Biol* **26**, 3798-809 (2006).
314. Lindstrom, M.S. NPM1/B23: A Multifunctional Chaperone in Ribosome Biogenesis and Chromatin Remodeling. *Biochem Res Int* **2011**, 195-209 (2011).
315. Gadad, S.S. et al. HIV-1 infection induces acetylation of NPM1 that facilitates Tat localization and enhances viral transactivation. *J Mol Biol* **410**, 997-1007 (2011).
316. Gadad, S.S. et al. The multifunctional protein nucleophosmin (NPM1) is a human linker histone H1 chaperone. *Biochemistry* **50**, 2780-9 (2011).
317. Okuwaki, M. et al. Function of homo- and hetero-oligomers of human nucleoplasmin/nucleophosmin family proteins NPM1, NPM2 and NPM3 during sperm chromatin remodeling. *Nucleic Acids Res* **40**, 4861-78 (2012).
318. Murano, K., Okuwaki, M., Hisaoka, M. & Nagata, K. Transcription regulation of the rRNA gene by a multifunctional nucleolar protein, B23/nucleophosmin, through its histone chaperone activity. *Mol Cell Biol* **28**, 3114-26 (2008).
319. Yip, S.P., Siu, P.M., Leung, P.H.M., Zhao, Y. & Yung, B.Y.M. The Multifunctional Nucleolar Protein Nucleophosmin/NPM/B23 and the Nucleoplasmin Family of Proteins. in *The nucleolus (Protein reviews)* (ed. Olson, M.O.) 213-252 (Springer, 2011).
320. Savkur, R.S. & Olson, M.O. Preferential cleavage in pre-ribosomal RNA byprotein B23 endoribonuclease. *Nucleic Acids Res* **26**, 4508-15 (1998).
321. Herrera, J.E., Savkur, R. & Olson, M.O. The ribonuclease activity of nucleolar protein B23. *Nucleic Acids Res* **23**, 3974-9 (1995).
322. Grisendi, S. et al. Role of nucleophosmin in embryonic development and tumorigenesis. *Nature* **437**, 147-53 (2005).
323. Colombo, E., Marine, J.C., Danovi, D., Falini, B. & Pelicci, P.G. Nucleophosmin regulates the stability and transcriptional activity of p53. *Nat Cell Biol* **4**, 529-33 (2002).
324. Dhar, S.K., Lynn, B.C., Daosukho, C. & St Clair, D.K. Identification of nucleophosmin as an NF-kappaB co-activator for the induction of the human SOD2 gene. *J Biol Chem* **279**, 28209-19 (2004).
325. Inouye, C.J. & Seto, E. Relief of YY1-induced transcriptional repression by protein-protein interaction with the nucleolar phosphoprotein B23. *J Biol Chem* **269**, 6506-10 (1994).
326. Korgaonkar, C. et al. Nucleophosmin (B23) targets ARF to nucleoli and inhibits its function. *Mol Cell Biol* **25**, 1258-71 (2005).
327. Liu, X. et al. Nucleophosmin (NPM1/B23) interacts with activating transcription factor 5 (ATF5) protein and promotes proteasome- and caspase-dependent ATF5 degradation in hepatocellular carcinoma cells. *J Biol Chem* **287**, 19599-609 (2012).

328. Kondo, T. et al. Identification and characterization of nucleophosmin/B23/numatrin which binds the anti-oncogenic transcription factor IRF-1 and manifests oncogenic activity. *Oncogene* **15**, 1275-81 (1997).
329. Bonetti, P. et al. Nucleophosmin and its AML-associated mutant regulate c-Myc turnover through Fbw7 gamma. *J Cell Biol* **182**, 19-26 (2008).
330. Li, Z., Boone, D. & Hann, S.R. Nucleophosmin interacts directly with c-Myc and controls c-Myc-induced hyperproliferation and transformation. *Proc Natl Acad Sci U S A* **105**, 18794-9 (2008).
331. Li, Z. & Hann, S.R. Nucleophosmin is essential for c-Myc nucleolar localization and c-Myc-mediated rDNA transcription. *Oncogene* **32**, 1988-94 (2013).
332. Gurumurthy, M. et al. Nucleophosmin interacts with HEXIM1 and regulates RNA polymerase II transcription. *J Mol Biol* **378**, 302-17 (2008).
333. Bergstralh, D.T. et al. Global functional analysis of nucleophosmin in Taxol response, cancer, chromatin regulation, and ribosomal DNA transcription. *Exp Cell Res* **313**, 65-76 (2007).
334. Lessard, F. et al. The ARF tumor suppressor controls ribosome biogenesis by regulating the RNA polymerase I transcription factor TTF-I. *Mol Cell* **38**, 539-50 (2010).
335. Ahn, J.Y. et al. Nucleophosmin/B23, a nuclear PI(3,4,5)P(3) receptor, mediates the antiapoptotic actions of NGF by inhibiting CAD. *Mol Cell* **18**, 435-45 (2005).
336. Ye, K. Nucleophosmin/B23, a multifunctional protein that can regulate apoptosis. *Cancer Biol Ther* **4**, 918-23 (2005).
337. Wu, M.H., Chang, J.H. & Yung, B.Y. Resistance to UV-induced cell-killing in nucleophosmin/B23 over-expressed NIH 3T3 fibroblasts: enhancement of DNA repair and up-regulation of PCNA in association with nucleophosmin/B23 over-expression. *Carcinogenesis* **23**, 93-100 (2002).
338. Li, J., Zhang, X., Sejas, D.P., Bagby, G.C. & Pang, Q. Hypoxia-induced nucleophosmin protects cell death through inhibition of p53. *J Biol Chem* **279**, 41275-9 (2004).
339. Li, J., Zhang, X., Sejas, D.P. & Pang, Q. Negative regulation of p53 by nucleophosmin antagonizes stress-induced apoptosis in human normal and malignant hematopoietic cells. *Leuk Res* **29**, 1415-23 (2005).
340. Pang, Q. et al. Nucleophosmin interacts with and inhibits the catalytic function of eukaryotic initiation factor 2 kinase PKR. *J Biol Chem* **278**, 41709-17 (2003).
341. Gao, H. et al. B23 regulates GADD45a nuclear translocation and contributes to GADD45a-induced cell cycle G2-M arrest. *J Biol Chem* **280**, 10988-96 (2005).
342. Colombo, E. et al. Nucleophosmin is required for DNA integrity and p19Arf protein stability. *Mol Cell Biol* **25**, 8874-86 (2005).
343. Brady, S.N., Yu, Y., Maggi, L.B., Jr. & Weber, J.D. ARF impedes NPM/B23 shuttling in an Mdm2-sensitive tumor suppressor pathway. *Mol Cell Biol* **24**, 9327-38 (2004).
344. Sherr, C.J. Divorcing ARF and p53: an unsettled case. *Nature Reviews Cancer* **6**, 663-673 (2006).
345. Levine, A.J. p53, the cellular gatekeeper for growth and division. *Cell* **88**, 323-31 (1997).
346. Kurki, S. et al. Nucleolar protein NPM interacts with HDM2 and protects tumor suppressor protein p53 from HDM2-mediated degradation. *Cancer Cell* **5**, 465-75 (2004).
347. Wanzel, M. et al. A ribosomal protein L23-nucleophosmin circuit coordinates Miz1 function with cell growth. *Nature Cell Biology* **10**, 1051-1061 (2008).
348. Kuo, M.L., den Besten, W., Bertwistle, D., Roussel, M.F. & Sherr, C.J. N-terminal polyubiquitination and degradation of the Arf tumor suppressor. *Genes Dev* **18**, 1862-74 (2004).
349. Bertwistle, D., Sugimoto, M. & Sherr, C.J. Physical and Functional Interactions of the Arf Tumor Suppressor Protein with Nucleophosmin/B23. *Molecular and Cellular Biology* **24**, 985-996 (2004).
350. Sugimoto, M., Kuo, M.L., Roussel, M.F. & Sherr, C.J. Nucleolar Arf tumor suppressor inhibits ribosomal RNA processing. *Mol Cell* **11**, 415-24 (2003).
351. Koike, A. et al. Recruitment of phosphorylated NPM1 to sites of DNA damage through RNF8-dependent ubiquitin conjugates. *Cancer Res* **70**, 6746-56 (2010).
352. Lee, S.Y. et al. A proteomics approach for the identification of nucleophosmin and heterogeneous nuclear ribonucleoprotein C1/C2 as chromatin-binding proteins in response to DNA double-strand breaks. *Biochem J* **388**, 7-15 (2005).
353. Szebeni, A. & Olson, M.O. Nucleolar protein B23 has molecular chaperone activities. *Protein Sci* **8**, 905-12 (1999).
354. Falini, B. et al. Translocations and mutations involving the nucleophosmin (NPM1) gene in lymphomas and leukemias. *Haematologica* **92**, 519-32 (2007).

355. Bolli, N. et al. Born to be exported: COOH-terminal nuclear export signals of different strength ensure cytoplasmic accumulation of nucleophosmin leukemic mutants. *Cancer Res* **67**, 6230-7 (2007).
356. Chiarella, S. et al. Nucleophosmin mutations alter its nucleolar localization by impairing G-quadruplex binding at ribosomal DNA. *Nucleic Acids Res* **41**, 3228-39 (2013).
357. Federici, L. et al. Nucleophosmin C-terminal leukemia-associated domain interacts with G-rich quadruplex forming DNA. *J Biol Chem* **285**, 37138-49 (2010).
358. Bolli, N. et al. A dose-dependent tug of war involving the NPM1 leukaemic mutant, nucleophosmin, and ARF. *Leukemia* **23**, 501-9 (2009).
359. den Besten, W., Kuo, M.L., Williams, R.T. & Sherr, C.J. Myeloid leukemia-associated nucleophosmin mutants perturb p53-dependent and independent activities of the Arf tumor suppressor protein. *Cell Cycle* **4**, 1593-8 (2005).
360. Colombo, E. et al. Delocalization and destabilization of the Arf tumor suppressor by the leukemia-associated NPM mutant. *Cancer Res* **66**, 3044-50 (2006).
361. Leong, S.M. et al. Mutant nucleophosmin deregulates cell death and myeloid differentiation through excessive caspase-6 and -8 inhibition. *Blood* **116**, 3286-96 (2010).
362. Falini, B. et al. Acute myeloid leukemia with mutated nucleophosmin (NPM1): is it a distinct entity? *Blood* **117**, 1109-20 (2011).
363. Wong, H.K. et al. Cockayne syndrome B protein stimulates apurinic endonuclease 1 activity and protects against agents that introduce base excision repair intermediates. *Nucleic Acids Res* **35**, 4103-13 (2007).
364. Poletto, M. et al. Role of the unstructured N-terminal domain of the hAPE1 (human apurinic/apyrimidinic endonuclease 1) in the modulation of its interaction with nucleic acids and NPM1 (nucleophosmin). *Biochem J* **452**, 545-57 (2013).
365. Boal, A.K. et al. Redox signaling between DNA repair proteins for efficient lesion detection. *Proc Natl Acad Sci U S A* **106**, 15237-42 (2009).
366. Adelmant, G. et al. DNA ends alter the molecular composition and localization of Ku multicomponent complexes. *Mol Cell Proteomics* **11**, 411-421 (2012).
367. Jobert, L. et al. The human base excision repair enzyme SMUG1 directly interacts with DKC1 and contributes to RNA quality control. *Mol Cell* **49**, 339-45 (2013).
368. Fung, H. & Demple, B. A vital role for Ape1/Ref1 protein in repairing spontaneous DNA damage in human cells. *Mol Cell* **17**, 463-70 (2005).
369. Svilar, D., Goellner, E.M., Almeida, K.H. & Sobol, R.W. Base excision repair and lesion-dependent subpathways for repair of oxidative DNA damage. *Antioxid Redox Signal* **14**, 2491-507 (2011).
370. Kaina, B. et al. BER, MGMT, and MMR in defense against alkylation-induced genotoxicity and apoptosis. *Prog Nucleic Acid Res Mol Biol* **68**, 41-54 (2001).
371. Ballmaier, D. & Epe, B. DNA damage by bromate: mechanism and consequences. *Toxicology* **221**, 166-71 (2006).
372. Chen, J. & Stubbe, J. Bleomycins: towards better therapeutics. *Nat Rev Cancer* **5**, 102-12 (2005).
373. Jiang, Y. et al. Role of APE1 in differentiated neuroblastoma SH-SY5Y cells in response to oxidative stress: use of APE1 small molecule inhibitors to delineate APE1 functions. *DNA Repair (Amst)* **8**, 1273-82 (2009).
374. Huang, S.H. et al. PJ34, an inhibitor of PARP-1, suppresses cell growth and enhances the suppressive effects of cisplatin in liver cancer cells. *Oncol Rep* **20**, 567-72 (2008).
375. Vascotto, C. et al. Functional regulation of the apurinic/apyrimidinic endonuclease 1 by nucleophosmin: impact on tumor biology. *Oncogene* (2013).
376. Choi, Y., Sims, G.E., Murphy, S., Miller, J.R. & Chan, A.P. Predicting the functional effect of amino acid substitutions and indels. *PLoS One* **7**, e46688 (2012).
377. Kumar, P., Henikoff, S. & Ng, P.C. Predicting the effects of coding non-synonymous variants on protein function using the SIFT algorithm. *Nat Protoc* **4**, 1073-81 (2009).
378. Adzhubei, I.A. et al. A method and server for predicting damaging missense mutations. *Nat Methods* **7**, 248-9 (2010).
379. Parthiban, V., Gromiha, M.M. & Schomburg, D. CUPSAT: prediction of protein stability upon point mutations. *Nucleic Acids Res* **34**, W239-42 (2006).
380. Vascotto, C. et al. Genome-wide analysis and proteomic studies reveal APE1/Ref-1 multifunctional role in mammalian cells. *Proteomics* **9**, 1058-74 (2009).
381. Rezaee, M., Sanche, L. & Hunting, D.J. Cisplatin enhances the formation of DNA single- and double-strand breaks by hydrated electrons and hydroxyl radicals. *Radiat Res* **179**, 323-31 (2013).

382. Kothandapani, A. et al. Novel role of base excision repair in mediating cisplatin cytotoxicity. *J Biol Chem* **286**, 14564-74 (2011).
383. Wilson, D.M., 3rd & Seidman, M.M. A novel link to base excision repair? *Trends Biochem Sci* **35**, 247-52 (2010).
384. Kothandapani, A. & Patrick, S.M. Evidence for base excision repair processing of DNA interstrand crosslinks. *Mutat Res* **743-744**, 44-52 (2013).
385. Pitiot, A.S. et al. A new type of NPM1 gene mutation in AML leading to a C-terminal truncated protein. *Leukemia* **21**, 1564-6 (2007).
386. Arena, S. et al. Modern proteomic methodologies for the characterization of lactosylation protein targets in milk. *Proteomics* **10**, 3414-34 (2010).
387. Scippa, G.S. et al. The proteome of lentil (Lens culinaris Medik.) seeds: discriminating between landraces. *Electrophoresis* **31**, 497-506 (2010).

7 APPENDIX

Supplementary Table 1: Complete data reporting all the significant functional enrichments obtained performing GeneCodis analysis for the APE1 interactors identified in this work of Thesis. 'GO term ID' and 'Annotations' columns represent the Gene Ontology codes of annotations and the textual description of annotations, respectively. MF and BP refer to 'molecular function' and 'biological process' category of Gene Ontology annotation, respectively. Third and fourth columns represent the number of genes in the input list and the reference list for a given annotation, respectively. P-values calculated using hypergeometric distribution and its correction using the stimulation-based approach are reported. The 'Genes' column identifies the set of genes in the input list showing a given annotation.

GO term ID	Annotations	# of annotated genes in the input list (Total # of genes in the input list)	# of annotated genes in the reference list (Total # of genes in the reference list)	Hypergeometric Distribution (Fisher's exact test)	Corrected Hypergeometric Dist. (Fisher's exact test)	Genes
GO:0005515,GO:0006281	protein binding (MF), DNA repair (BP)	3 (26)	195 (34208)	0.000430529	0.000463647	NPM1,PRPF19,SFPQ
GO:0005515,GO:0044419	protein binding (MF), interspecies interaction between organisms (BP)	3 (26)	232 (34208)	0.000713427	0.000730828	NPM1,KRT8,RPLP0
GO:0019901	protein kinase binding (MF)	3 (26)	237 (34208)	0.000758852	0.000758852	NPM1,MSN,KIF11
GO:0005524,GO:0000166, GO:0042803	ATP binding (MF), nucleotide binding (MF), protein homodimerization activity (MF)	3 (26)	76 (34208)	2.64088e-05	2.99775e-05	PRPS1,MYH9,PRPS2
GO:0003677,GO:0005515, GO:0008380,GO:0003723	DNA binding (MF), protein binding (MF), RNA splicing (BP), RNA binding (MF)	3 (26)	16 (34208)	2.1683e-07	3.79453e-07	HNRNPU,YBX1,SFPQ
GO:0003677,GO:0005515, GO:0000398,GO:0008380	DNA binding (MF), protein binding (MF), nuclear mRNA splicing, via spliceosome (BP), RNA splicing	3 (26)	17 (34208)	2.63161e-07	4.42111e-07	HNRNPU,PRPF19,YBX1

GO term ID	Annotations	# of annotated genes in the input list (Total # of genes in the input list)	# of annotated genes in the reference list (Total # of genes in the reference list)	Hypergeometric Distribution (Fisher's exact test)	Corrected Hypergeometric Dist. (Fisher's exact test)	Genes
	(BP)					
GO:0005515,GO:0003723, GO:0010467,GO:0044267, GO:0006412,GO:0016070, GO:0016071	protein binding (MF), RNA binding (MF), gene expression (BP), cellular protein metabolic process (BP), translation (BP), RNA metabolic process (BP), mRNA metabolic process (BP)	3 (26)	19 (34208)	3.74626e-07	5.82752e-07	RPL14,PABPC1,RPLP0
GO:0003779,GO:0005516	actin binding (MF), calmodulin binding (MF)	3 (26)	44 (34208)	5.05613e-06	6.43508e-06	MYO1C,MYH9,SPTBN1
GO:0000166,GO:0008022	nucleotide binding (MF), protein C-terminus binding (MF)	3 (26)	45 (34208)	5.41456e-06	6.49747e-06	PABPC1,MYO1C,NCL
GO:0003677,GO:0005515, GO:0000166,GO:0003723	DNA binding (MF), protein binding (MF), nucleotide binding (MF), RNA binding (MF)	3 (26)	22 (34208)	5.94481e-07	8.91722e-07	HNRNPU,NCL,SFPQ
GO:0005515,GO:0000166, GO:0000398,GO:0008380, GO:0003723,GO:0010467, GO:0003676	protein binding (MF), nucleotide binding (MF), nuclear mRNA splicing, via spliceosome (BP), RNA splicing (BP), RNA binding (MF), gene expression (BP), nucleic acid binding (MF)	3 (26)	23 (34208)	6.83309e-07	9.56633e-07	PABPC1,HNRNPU,HNRNPH1

GO term ID	Annotations	# of annotated genes in the input list (Total # of genes in the input list)	# of annotated genes in the reference list (Total # of genes in the reference list)	Hypergeometric Distribution (Fisher's exact test)	Corrected Hypergeometric Dist. (Fisher's exact test)	Genes
GO:0005515,GO:0010467, GO:0006414,GO:0031018, GO:0044267,GO:0006412, GO:0016070,GO:0016032, GO:0016071,GO:0006415, GO:0019058,GO:0019083, GO:0003735	protein binding (MF), gene expression (BP), translational elongation (BP), endocrine pancreas development (BP), cellular protein metabolic process (BP), translation (BP), RNA metabolic process (BP), viral reproduction (BP), mRNA metabolic process (BP), translational termination (BP), viral infectious cycle (BP), viral transcription (BP), structural constituent of ribosome (MF)	3 (26)	23 (34208)	6.83309e-07	9.56633e-07	RPL14,RPSA,RPLP0
GO:0042803	protein homodimerization activity (MF)	4 (26)	514 (34208)	0.000579314	0.000608279	PRPS1,NPM1,MYH9,PRPS2
GO:0003677,GO:0005515, GO:0003723	DNA binding (MF), protein binding (MF), RNA binding (MF)	4 (26)	50 (34208)	5.89425e-08	1.23779e-07	HNRNPU,NCL,YBX1,SFPQ
GO:0005515,GO:0000166, GO:0008380,GO:0003723	protein binding (MF), nucleotide binding (MF), RNA splicing (BP), RNA binding (MF)	4 (26)	53 (34208)	7.48294e-08	1.36645e-07	PABPC1,HNRNPU,SFPQ,HNRNPH1
GO:0005515,GO:0000398, GO:0008380,GO:0003723, GO:0010467	protein binding (MF), nuclear mRNA splicing, via spliceosome (BP), RNA splicing (BP), RNA binding (MF), gene expression (BP)	4 (26)	53 (34208)	7.48294e-08	1.36645e-07	PABPC1,HNRNPU,YBX1,HNRNPH1

GO term ID	Annotations	# of annotated genes in the input list (Total # of genes in the input list)	# of annotated genes in the reference list (Total # of genes in the reference list)	Hypergeometric Distribution (Fisher's exact test)	Corrected Hypergeometric Dist. (Fisher's exact test)	Genes
GO:0003723,GO:0010467, GO:0006414,GO:0031018, GO:0044267,GO:0006412, GO:0016070,GO:0016032, GO:0016071,GO:0006415, GO:0019058,GO:0019083, GO:0003735	RNA binding (MF), gene expression (BP), translational elongation (BP), endocrine pancreas development (BP), cellular protein metabolic process (BP), translation (BP), RNA metabolic process (BP), viral reproduction (BP), mRNA metabolic process (BP), translational termination (BP), viral infectious cycle (BP), viral transcription (BP), structural constituent of ribosome (MF)	4 (26)	53 (34208)	7.48294e-08	1.36645e-07	RPL3,RPL14,RPLP0,RPL4
GO:0003677,GO:0005515, GO:0008380	DNA binding (MF), protein binding (MF), RNA splicing (BP)	4 (26)	27 (34208)	4.54521e-09	1.46845e-08	HNRNPU,PRPF19,YBX1,SFPQ
GO:0005515,GO:0003779	protein binding (MF), actin binding (MF)	4 (26)	106 (34208)	1.23529e-06	1.67362e-06	MSN,MYH9,SPTBN1,ACTN1
GO:0005515,GO:0010467, GO:0044267,GO:0006412, GO:0016070,GO:0016071	protein binding (MF), gene expression (BP), cellular protein metabolic process (BP), translation (BP), RNA metabolic process (BP), mRNA metabolic process (BP)	4 (26)	31 (34208)	8.13224e-09	2.27703e-08	RPL14,PABPC1,RPSA,RPLP0
GO:0005515,GO:0000166, GO:0003723,GO:0003676	protein binding (MF), nucleotide binding (MF), RNA binding (MF), nucleic acid binding (MF)	4 (26)	74 (34208)	2.90873e-07	4.69872e-07	PABPC1,HNRNPU,NCL,HNRNPH1

GO term ID	Annotations	# of annotated genes in the input list (Total # of genes in the input list)	# of annotated genes in the reference list (Total # of genes in the reference list)	Hypergeometric Distribution (Fisher's exact test)	Corrected Hypergeometric Dist. (Fisher's exact test)	Genes
GO:0010467,GO:0006414, GO:0031018,GO:0044267, GO:0006412,GO:0016070, GO:0016032,GO:0016071, GO:0006415,GO:0019058, GO:0019083,GO:0003735	gene expression (BP), translational elongation (BP), endocrine pancreas development (BP), cellular protein metabolic process (BP), translation (BP), RNA metabolic process (BP), viral reproduction (BP), mRNA metabolic process (BP), translational termination (BP), viral infectious cycle (BP), viral transcription (BP), structural constituent of ribosome (MF)	5 (26)	81 (34208)	4.15404e-09	1.45392e-08	RPL3,RPL14,RPSA,RPLP0,RPL4
GO:0005515,GO:0003723, GO:0003676	protein binding (MF), RNA binding (MF), nucleic acid binding (MF)	5 (26)	85 (34208)	5.30725e-09	1.59217e-08	NPM1,PABPC1,HNRNPU,NCL, HNRNPH1
GO:0005515,GO:0008380, GO:0003723	protein binding (MF), RNA splicing (BP), RNA binding (MF)	5 (26)	96 (34208)	9.83423e-09	2.58149e-08	PABPC1,HNRNPU,YBX1,SFPQ, HNRNPH1
GO:0005515,GO:0000398, GO:0008380	protein binding (MF), nuclear mRNA splicing, via spliceosome (BP), RNA splicing (BP)	5 (26)	100 (34208)	1.20882e-08	2.98649e-08	PABPC1,HNRNPU,PRPF19,YB X1,HNRNPH1
GO:0003779	actin binding (MF)	5 (26)	289 (34208)	2.36456e-06	3.10349e-06	MSN,MYO1C,MYH9,SPTBN1,A CTN1
GO:0003723,GO:0010467, GO:0044267,GO:0006412, GO:0016070,GO:0016071	RNA binding (MF), gene expression (BP), cellular protein metabolic process (BP), translation (BP),RNA metabolic process (BP),	5 (26)	58 (34208)	7.51703e-10	3.50795e-09	RPL3,RPL14,PABPC1,RPLP0,R PL4

GO term ID	Annotations	# of annotated genes in the input list (Total # of genes in the input list)	# of annotated genes in the reference list (Total # of genes in the reference list)	Hypergeometric Distribution (Fisher's exact test)	Corrected Hypergeometric Dist. (Fisher's exact test)	Genes
	mRNA metabolic process (BP)					
GO:0005515,GO:0000166, GO:0003723	protein binding (MF), nucleotide binding (MF), RNA binding (MF)	5 (26)	119 (34208)	2.90402e-08	6.41942e-08	PABPC1,HNRNPU,NCL,SFPQ,HNRNPH1
GO:0003677,GO:0005515	DNA binding (MF), protein binding (MF)	5 (26)	564 (34208)	5.91104e-05	6.53326e-05	HNRNPU,PRPF19,NCL,YBX1,SFPQ
GO:0005515,GO:0000166	protein binding (MF), nucleotide binding (MF)	6 (26)	784 (34208)	2.21198e-05	2.58064e-05	PABPC1,MYH9,HNRNPU,NCL,SFPQ,HNRNPH1
GO:0005515,GO:0003723, GO:0010467	protein binding (MF), RNA binding (MF), gene expression (BP)	6 (26)	81 (34208)	3.23481e-11	2.71724e-10	RPL14,PABPC1,HNRNPU,RPLP0,YBX1,HNRNPH1
GO:0010467,GO:0044267, GO:0006412,GO:0016070, GO:0016071	gene expression (BP), cellular protein metabolic process (BP), translation (BP), RNA metabolic process (BP), mRNA metabolic process (BP)	6 (26)	90 (34208)	6.17785e-11	4.32449e-10	RPL3,RPL14,PABPC1,RPSA,RPLP0,RPL4
GO:0005515,GO:0008380	protein binding (MF), RNA splicing (BP)	6 (26)	157 (34208)	1.81169e-09	6.91735e-09	PABPC1,HNRNPU,PRPF19,YBX1,SFPQ,HNRNPH1
GO:0005515,GO:0010467	protein binding (MF), gene expression (BP)	7 (26)	235 (34208)	3.8862e-10	2.04026e-09	RPL14,PABPC1,RPSA,HNRNPU,RPLP0,YBX1,HNRNPH1
GO:0044267	cellular protein metabolic process	7 (26)	284 (34208)	1.45109e-09	6.09459e-09	RPL3,RPL14,PABPC1,RPSA,TC

GO term ID	Annotations	# of annotated genes in the input list (Total # of genes in the input list)	# of annotated genes in the reference list (Total # of genes in the reference list)	Hypergeometric Distribution (Fisher's exact test)	Corrected Hypergeometric Dist. (Fisher's exact test)	Genes
	(BP)					P1,RPLP0,RPL4
GO:0003723,GO:0010467	RNA binding (MF), gene expression (BP)	8 (26)	139 (34208)	8.90125e-14	3.73852e-12	RPL3,RPL14,PABPC1,HNRNPU,RPLP0,YBX1,HNRNPH1,RPL4
GO:0005524,GO:0000166	ATP binding (MF), nucleotide binding (MF)	8 (26)	1367 (34208)	5.22756e-06	6.45758e-06	PRPS1,KIF11,MYO1C,MYH9,TCP1,HNRNPU,PRPS2,THRAP3
GO:0010467	gene expression (BP)	9 (26)	408 (34208)	1.16833e-11	1.22675e-10	RPL3,RPL14,PABPC1,RPSA,HNRNPU,RPLP0,YBX1,HNRNPH1,RPL4
GO:0005515,GO:0003723	protein binding (MF), RNA binding (MF)	9 (26)	268 (34208)	2.70313e-13	5.67657e-12	NPM1,RPL14,PABPC1,HNRNPU,RPLP0,NCL,YBX1,SFPQ,HNRNPH1
GO:0003723	RNA binding (MF)	11 (26)	623 (34208)	4.04001e-13	5.65601e-12	RPL3,NPM1,RPL14,PABPC1,HNRNPU,RPLP0,NCL,YBX1,SFPQ,HNRNPH1,RPL4
GO:0000166	nucleotide binding (MF)	12 (26)	2120 (34208)	1.32823e-08	3.09921e-08	PRPS1,PABPC1,KIF11,MYO1C,MYH9,TCP1,HNRNPU,PRPS2,NCL,SFPQ,HNRNPH1,THRAP3
GO:0005515	protein binding (MF)	18 (26)	4463 (34208)	6.36433e-11	3.8186e-10	PRDX6,NPM1,MSN,RPL14,PABPC1,RPSA,MYH9,KRT8,HNRNPU,PRPF19,SPTBN1,ACTN1,RPLP0,BASP1,NCL,YBX1,SFPQ,H

GO term ID	Annotations	# of annotated genes in the input list (Total # of genes in the input list)	# of annotated genes in the reference list (Total # of genes in the reference list)	Hypergeometric Distribution (Fisher's exact test)	Corrected Hypergeometric Dist. (Fisher's exact test)	Genes
						NRNPH1

Supplementary Table 2: Complete data reporting all the significant functional enrichments obtained performing GeneCodis analysis for all the APE1 interactors. 'GO term ID' and 'Annotations' columns represent the Gene Ontology codes of annotations and the textual description of annotations, respectively. MF and BP refer to 'molecular function' and 'biological process' category of Gene Ontology annotation, respectively. Third and fourth columns represent the number of genes in the input list and the reference list for a given annotation, respectively. P-values calculated using hypergeometric distribution and its correction using the stimulation-based approach are reported. The 'Genes' column identifies the set of genes in the input list showing a given annotation.

GO term ID	Annotations	# of annotated genes in the input list (Total # of genes in the input list)	# of annotated genes in the reference list (Total # of genes in the reference list)	Hypergeometric Distribution (Fisher's exact test)	Corrected Hypergeometric Dist. (Fisher's exact test)	Genes
GO:0005515	protein binding (MF)	59 (73)	4463 (34208)	2,58E-39	9,98E-37	HOXC13,XRCC6,MCC,SIRT1,PRDX6,GZMA,NPM1,UBE2I,CDKN1A,TRAF6,MDM2,MSN,RPL14,MUTYH,PABPC1,HMGB2,OGG1,SPTA1,TXN,RPSA,HIF1A,SET,TP53,CSNK2A1,MYH9,ESR1,HNRNPL,KRT8,UBC,HDAC1,DCTN1,XRCC1,Cdk5,PCNA,SUMO2,SUMO1,MPG,HNRNPU,FEN1,EIF6,CCNA1,ANP32A,EP300,PAK2,PRPF19,SPTBN1,ACTN1,RPLP0,XRCC5,BASP1,NCL,YBX1,HMGA1,SFPQ,HNRNPH1,NME1,HSPA1A,ARF6,POLB
GO:0000166	nucleotide binding (MF)	23 (73)	2120 (34208)	4,11E-11	6,90E-10	PRPS1,XRCC6,UBE2I,PABPC1,NXF2,KIF11,MYO1C,CSNK2A1,MYH9,HNRNPL,TCP1,Cdk5,HNRNPU,PAK2,PRPS2,XRCC5,NCL,SFPQ,HNRNPH1,NME1,HSPA1A,THRAP3,ARF6
GO:0003677	DNA binding (MF)	19 (73)	1785 (34208)	4,16E-09	3,08E-08	XRCC6,HMGB2,HIF1A,TP53,TCF21,ESR1,PCNA,MPG,HNRNPU,FEN1,POLR3D,EP300,PRPF19,XRCC5,NCL,YBX1,HMGA1,SFPQ,POLB
GO:0003677,GO:0005515	DNA binding (MF), protein binding (MF)	17 (73)	564 (34208)	2,92E-15	1,61E-13	XRCC6,HMGB2,HIF1A,TP53,ESR1,PCNA,MPG,HNRNPU,FEN1,EP300,PRPF19,XRCC5,NCL,YBX1,HMGA1,SFPQ,POLB

GO term ID	Annotations	# of annotated genes in the input list (Total # of genes in the input list)	# of annotated genes in the reference list (Total # of genes in the reference list)	Hypergeometric Distribution (Fisher's exact test)	Corrected Hypergeometric Dist. (Fisher's exact test)	Genes
GO:0005524	ATP binding (MF)	17 (73)	1489 (34208)	1,15E-08	5,43E-08	PRPS1,XRCC6,UBE2I,KIF11,TP53,MYO1C,CSNK2A1,MYH9,TCP1,Cdk5,HNRNPU,PAK2,PRPS2,XRCC5,NME1,HSPA1A,THRAP3
GO:0005515,GO:0000166	protein binding (MF), nucleotide binding (MF)	16 (73	784 (34208)	7,79E-12	1,88E-10	XRCC6,UBE2I,PABPC1,CSNK2A1,MYH9,HNRNPL,Cdk5,HNRNPU,PAK2,XRCC5,NCL,SFPQ,HNRNPH1,NME1,HSPA1A,ARF6
GO:0005524,GO:0000166	ATP binding (MF), nucleotide binding (MF)	16 (73)	1367 (34208)	2,38E-08	1,01E-07	PRPS1,XRCC6,UBE2I,KIF11,MYO1C,CSNK2A1,MYH9,TCP1,Cdk5,HNRNPU,PAK2,PRPS2,XRCC5,NME1,HSPA1A,THRAP3
GO:0005515,GO:0006281	protein binding (MF), DNA repair (BP)	15 (73)	195 (34208)	1,37E-19	2,65E-17	XRCC6,SIRT1,NPM1,MUTYH,OGG1,UBC,XRCC1,PCNA,SUMO1,MPG,FEN1,PRPF19,XRCC5,SFPQ,POLB
GO:0005515,GO:0045892	protein binding (MF), negative regulation of transcription, DNA-dependent (BP)	15 (73)	283 (34208)	3,79E-17	3,66E-15	XRCC6,SIRT1,UBE2I,TRAF6,MDM2,HMGB2,SET,TP53,HDAC1,Cdk5,SUMO1,XRCC5,BASP1,YBX1,HMGA1
GO:0006355	regulation of transcription, DNA-dependent (BP)	14 (73)	1609 (34208)	6,68E-06	1,02E-05	HOXC13,OGG1,TXN,HIF1A,TP53,CSNK2A1,TCF21,ESR1,HDAC1,ANP32A,EP300,YBX1,HMGA1,SFPQ
GO:0006355,GO:0005515	regulation of transcription, DNA-dependent (BP), protein binding (MF)	13 (73)	518 (34208)	7,15E-11	1,15E-09	HOXC13,OGG1,TXN,HIF1A,TP53,CSNK2A1,ESR1,HDAC1,ANP32A,EP300,YBX1,HMGA1,SFPQ
GO:0003723	RNA binding (MF)	13 (73)	623 (34208)	6,80E-10	6,56E-09	RPL3,NPM1,RPL14,PABPC1,NXF2,HNRNPL,HNRNPU,RPLP0,NCL,YBX1,SFPQ,HNRNPH1,RPL4
GO:0044419	interspecies interaction between organisms (BP)	12 (73)	328 (34208)	5,38E-12	1,48E-10	SIRT1,NPM1,UBE2I,MDM2,TP53,KRT8,HDAC1,EP300,PAK2,HLA-B,RPLP0,HMGA1

GO term ID	Annotations	# of annotated genes in the input list (Total # of genes in the input list)	# of annotated genes in the reference list (Total # of genes in the reference list)	Hypergeometric Distribution (Fisher's exact test)	Corrected Hypergeometric Dist. (Fisher's exact test)	Genes
GO:0005515,GO:0044419	protein binding (MF), interspecies interaction between organisms (BP)	11 (73)	232 (34208)	2,71E-12	8,04E-11	SIRT1,NPM1,UBE2I,MDM2,TP53,KRT8,HDAC1,EP300,PAK2,RPLP0,HMGA1
GO:0010467	gene expression (BP)	11 (73)	408 (34208)	1,11E-09	1,05E-08	RPL3,RPL14,PABPC1,RPSA,ESR1,HNRNPL,HNRNPU,RPLP0,YBX1,HNRNPH1,RPL4
GO:0000122	negative regulation of transcription from RNA polymerase II promoter (BP)	11 (73)	416 (34208)	1,37E-09	1,25E-08	SIRT1,UBE2I,TRAF6,MDM2,TXN,TP53,TCF21,HDAC1,PCNA,EP300,YBX1
GO:0005524,GO:0005515	ATP binding (MF), protein binding (MF)	11 (73)	578 (34208)	4,03E-08	1,44E-07	XRCC6,UBE2I,TP53,CSNK2A1,MYH9,Cdk5,HNRNPU,PAK2,XRCC5,NME1,HSPA1A
GO:0045944	positive regulation of transcription from RNA polymerase II promoter (BP)	11 (73)	578 (34208)	4,03E-08	1,44E-07	XRCC6,SIRT1,TRAF6,HMGB2,HIF1A,TP53,TCF21,ESR1,HDAC1,EP300,THRAP3
GO:0016070,GO:0016071	RNA metabolic process (BP), mRNA metabolic process (BP)	10 (73)	218 (34208)	3,93E-11	6,90E-10	RPL3,RPL14,PABPC1,RPSA,SET,UBC,ANP32A,RPLP0,HSPA1A,RPL4
GO:0005515,GO:0000122	protein binding (MF), negative regulation of transcription from RNA polymerase II promoter (BP)	10 (73)	255 (34208)	1,83E-10	2,35E-09	SIRT1,UBE2I,TRAF6,MDM2,TXN,TP53,HDAC1,PCNA,EP300,YBX1
GO:0005515,GO:0003723	protein binding (MF), RNA binding (MF)	10 (73)	268 (34208)	2,97E-10	3,18E-09	NPM1,RPL14,PABPC1,HNRNPL,HNRNPU,RPLP0,NCL,YBX1,SFPQ,HNRNPH1
GO:0016032	viral reproduction (BP)	10 (73)	329 (34208)	2,15E-09	1,84E-08	XRCC6,RPL3,RPL14,RPSA,UBC,PAK2,RPLP0,XRCC5,HMGA1,RPL4
GO:0005524,GO:0005515,GO:0000166	ATP binding (MF), protein binding (MF), nucleotide binding (MF)	10 (73)	547 (34208)	2,54E-07	6,12E-07	XRCC6,UBE2I,CSNK2A1,MYH9,Cdk5,HNRNPU,PAK2,XRCC5,NME1,HSPA1A
GO:0005515,GO:0006284	protein binding (MF), base-excision repair (BP)	9 (73)	26 (34208)	1,67E-18	2,15E-16	MUTYH,OGG1,TP53,XRCC1,PCNA,MPG,FEN1,HMGA1,POLB
GO:0005515,GO:0042981	protein binding (MF), regulation of apoptotic process (BP)	9 (73)	135 (34208)	1,39E-11	3,15E-10	SIRT1,TRAF6,TP53,ESR1,UBC,Cdk5,PAK2,ACTN1,NME1
GO:0003723,GO:0010467	RNA binding (MF),gene expression (BP)	9 (73)	139 (34208)	1,81E-11	3,88E-10	RPL3,RPL14,PABPC1,HNRNPL,HNRNPU,RPLP0,YBX1,HNRNP

GO term ID	Annotations	# of annotated genes in the input list (Total # of genes in the input list)	# of annotated genes in the reference list (Total # of genes in the reference list)	Hypergeometric Distribution (Fisher's exact test)	Corrected Hypergeometric Dist. (Fisher's exact test)	Genes
						H1,RPL4
GO:0005515,GO:0010467	protein binding (MF), gene expression (BP)	9 (73)	235 (34208)	1,94E-09	1,70E-08	RPL14,PABPC1,RPSA,ESR1,HNRNPL,HNRNPU,RPLP0,YBX1,HNRNPH1
GO:0005515,GO:0045944	protein binding (MF), positive regulation of transcription from RNA polymerase II promoter (BP)	9 (73)	330 (34208)	3,66E-08	1,47E-07	XRCC6,SIRT1,TRAF6,HMGB2,HIF1A,TP53,ESR1,HDAC1,EP300
GO:0046872,GO:0005515	metal ion binding (MF), protein binding (MF)	9 (73)	768 (34208)	3,72E-05	4,73E-05	SIRT1,CDKN1A,TRAF6,MDM2,MUTYH,TP53,ESR1,EP300,POLB
GO:0003677,GO:0005515,GO:0006281	DNA binding (MF), protein binding (MF), DNA repair (BP)	8 (73)	80 (34208)	7,42E-12	1,91E-10	XRCC6,PCNA,MPG,FEN1,PRPF19,XRCC5,SFPQ,POLB
GO:0005515,GO:0019899	protein binding (MF), enzyme binding (MF)	8 (73)	124 (34208)	2,62E-10	3,16E-09	SIRT1,UBE2I,MDM2,TP53,ESR1,HDAC1,HMGA1,POLB
GO:0005515,GO:0016070,GO:0016071	protein binding (MF), RNA metabolic process (BP), mRNA metabolic process (BP)	8 (73)	125 (34208)	2,79E-10	3,27E-09	RPL14,PABPC1,RPSA,SET,UBC,ANP32A,RPLP0,HSPA1A
GO:0005515,GO:0016032	protein binding (MF), viral reproduction (BP)	8 (73)	156 (34208)	1,63E-09	1,47E-08	XRCC6,RPL14,RPSA,UBC,PAK2,RPLP0,XRCC5,HMGA1
GO:0005515,GO:0008134	protein binding (MF), transcription factor binding (MF)	8 (73)	175 (34208)	4,05E-09	3,06E-08	UBE2I,HIF1A,TP53,ESR1,HDAC1,PCNA,EP300,HMGA1
GO:0019901	protein kinase binding (MF)	8 (73)	237 (34208)	4,30E-08	1,50E-07	NPM1,TRAF6,MSN,HIF1A,KIF11,TP53,CCNA1,PAK2
GO:0003700,GO:0005515	sequence-specific DNA binding transcription factor activity (MF), protein binding (MF)	8 (73)	336 (34208)	6,15E-07	1,30E-06	HOXC13,HMGB2,HIF1A,TP53,ESR1,HDAC1,YBX1,HMGA1
GO:0006915,GO:0005515	apoptotic process (BP), protein binding (MF)	8 (73)	344 (34208)	7,34E-07	1,54E-06	GZMA,TRAF6,HMGB2,TP53,UBC,EP300,PAK2,ARF6
GO:0007165,GO:0005515	signal transduction (BP), protein binding (MF)	8 (73)	493 (34208)	1,04E-05	1,52E-05	MCC,NPM1,TRAF6,TXN,HIF1A,CSNK2A1,ESR1,PAK2
GO:0006355,GO:0003677	regulation of transcription, DNA-dependent (BP), DNA binding (MF)	8 (73)	977 (34208)	0,00112218	0,00119	HIF1A,TP53,TCF21,ESR1,EP300,YBX1,HMGA1,SFPQ
GO:0005515,GO:0006281,GO:0006284	protein binding (MF), DNA repair (BP), base-excision repair (BP)	7 (73)	19 (34208)	7,40E-15	3,57E-13	MUTYH,OGG1,XRCC1,PCNA,MPG,FEN1,POLB
GO:0005515,GO:0003684	protein binding (MF), damaged	7 (73)	38 (34208)	1,80E-12	5,77E-11	HMGB2,OGG1,TP53,XRCC1,MP

GO term ID	Annotations	# of annotated genes in the input list (Total # of genes in the input list)	# of annotated genes in the reference list (Total # of genes in the reference list)	Hypergeometric Distribution (Fisher's exact test)	Corrected Hypergeometric Dist. (Fisher's exact test)	Genes
	DNA binding (MF)					G,FEN1,POLB
GO:0005515,GO:0003723,GO:0010467	protein binding (MF), RNA binding (MF), gene expression (BP)	7 (73)	81 (34208)	4,60E-10	4,67E-09	RPL14,PABPC1,HNRNPL,HNRNPU,RPLP0,YBX1,HNRNPH1
GO:0005515,GO:0000122,GO:0045892	protein binding (MF), negative regulation of transcription from RNA polymerase II promoter (BP), negative regulation of transcription, DNA-dependent (BP)	7 (73)	102 (34208)	2,36E-09	1,98E-08	SIRT1,UBE2I,TRAF6,MDM2,TP53,HDAC1,YBX1
GO:0005515,GO:0044212	protein binding (MF), transcription regulatory region DNA binding (MF)	7 (73)	124 (34208)	9,26E-09	6,27E-08	XRCC6,HMGB2,HIF1A,TP53,HNRNPL,XRCC5,BASP1
GO:0005515,GO:0008380	protein binding (MF), RNA splicing (BP)	7 (73)	157 (34208)	4,74E-08	1,59E-07	PABPC1,HNRNPL,HNRNPU,PRPF19,YBX1,SFPQ,HNRNPH1
GO:0008022	protein C-terminus binding (MF)	7 (73)	159 (34208)	5,17E-08	1,71E-07	XRCC6,SIRT1,UBE2I,PABPC1,MYO1C,XRCC5,NCL
GO:0005515,GO:0019901	protein binding (MF), protein kinase binding (MF)	7 (73)	164 (34208)	6,39E-08	2,04E-07	NPM1,TRAF6,MSN,HIF1A,TP53,CCNA1,PAK2
GO:0006355,GO:0003700,GO:0005515	regulation of transcription, DNA-dependent (BP), sequence-specific DNA binding transcription factor activity (MF), protein binding (MF)	7 (73)	177 (34208)	1,08E-07	3,10E-07	HOXC13,HIF1A,TP53,ESR1,HDAC1,YBX1,HMGA1
GO:0003677,GO:0045944	DNA binding (MF), positive regulation of transcription from RNA polymerase II promoter (BP)	7 (73)	242 (34208)	8,90E-07	1,80E-06	XRCC6,HMGB2,HIF1A,TP53,TCF21,ESR1,EP300
GO:0006355,GO:0003677,GO:0005515	regulation of transcription, DNA-dependent (BP), DNA binding (MF), protein binding (MF)	7 (73)	247 (34208)	1,02E-06	2,01E-06	HIF1A,TP53,ESR1,EP300,YBX1,HMGA1,SFPQ
GO:0000166,GO:0003723	nucleotide binding (MF), RNA binding (MF)	7 (73)	282 (34208)	2,46E-06	4,31E-06	PABPC1,NXF2,HNRNPL,HNRNPU,NCL,SFPQ,HNRNPH1
GO:0044267	cellular protein metabolic process (BP)	7 (73)	284 (34208)	2,58E-06	4,48E-06	RPL3,RPL14,PABPC1,RPSA,TCP1,RPLP0,RPL4
GO:0007049	cell cycle (BP)	7 (73)	435 (34208)	4,05E-05	5,08E-05	UBE2I,CDKN1A,KIF11,TP53,CSNK2A1,Cdk5,EP300
GO:0045893	positive regulation of transcription, DNA-dependent (BP)	7 (73)	468 (34208)	6,42E-05	7,65E-05	XRCC6,HMGB2,HIF1A,TP53,HDAC1,HMGA1,THRAP3

GO term ID	Annotations	# of annotated genes in the input list (Total # of genes in the input list)	# of annotated genes in the reference list (Total # of genes in the reference list)	Hypergeometric Distribution (Fisher's exact test)	Corrected Hypergeometric Dist. (Fisher's exact test)	Genes
GO:0005515,GO:0044419,GO:0045892,GO:0019899	protein binding (MF), interspecies interaction between organisms (BP), negative regulation of transcription, DNA-dependent (BP), enzyme binding (MF)	6 (73)	8 (34208)	2,14E-15	1,37E-13	SIRT1,UBE2I,MDM2,TP53,HDAC1,HMGA1
GO:0005515,GO:0003684,GO:0006284	protein binding (MF), damaged DNA binding (MF), base-excision repair (BP)	6 (73)	8 (34208)	2,14E-15	1,37E-13	OGG1,TP53,XRCC1,MPG,FEN1,POLB
GO:0003677,GO:0005515,GO:0006284	DNA binding (MF), protein binding (MF), base-excision repair (BP)	6 (73)	18 (34208)	1,39E-12	4,89E-11	TP53,PCNA,MPG,FEN1,HMGA1,POLB
GO:0005515,GO:0044419,GO:0000122	protein binding (MF), interspecies interaction between organisms (BP), negative regulation of transcription from RNA polymerase II promoter (BP)	6 (73)	27 (34208)	2,19E-11	4,02E-10	SIRT1,UBE2I,MDM2,TP53,HDAC1,EP300
GO:0000166,GO:0008022	nucleotide binding (MF), protein C-terminus binding (MF)	6 (73)	45 (34208)	5,84E-10	5,78E-09	XRCC6,UBE2I,PABPC1,MYO1C,XRCC5,NCL
GO:0006355,GO:0005515,GO:0008134	regulation of transcription, DNA-dependent (BP), protein binding (MF), transcription factor binding (MF)	6 (73)	67 (34208)	6,89E-09	4,93E-08	HIF1A,TP53,ESR1,HDAC1,EP300,HMGA1
GO:0005515,GO:0045944,GO:0045892	protein binding (MF), positive regulation of transcription from RNA polymerase II promoter (BP), negative regulation of transcription, DNA-dependent (BP)	6 (73)	82 (34208)	2,36E-08	1,01E-07	XRCC6,SIRT1,TRAF6,HMGB2,TP53,HDAC1
GO:0005515,GO:0003723,GO:0003676	protein binding (MF), RNA binding (MF), nucleic acid binding (MF)	6 (73)	85 (34208)	2,93E-08	1,20E-07	NPM1,PABPC1,HNRNPL,HNRNPU,NCL,HNRNPH1
GO:0003677,GO:0005515,GO:0008134	DNA binding (MF), protein binding (MF), transcription factor binding (MF)	6 (73)	90 (34208)	4,14E-08	1,45E-07	HIF1A,TP53,ESR1,PCNA,EP300,HMGA1
GO:0010467,GO:0044267,GO:0006412,GO:0016070,GO:0016071	gene expression (BP), cellular protein metabolic process (BP), translation (BP), RNA metabolic process (BP), mRNA metabolic process (BP)	6 (73)	90 (34208)	4,14E-08	1,45E-07	RPL3,RPL14,PABPC1,RPSA,RPLP0,RPL4

GO term ID	Annotations	# of annotated genes in the input list (Total # of genes in the input list)	# of annotated genes in the reference list (Total # of genes in the reference list)	Hypergeometric Distribution (Fisher's exact test)	Corrected Hypergeometric Dist. (Fisher's exact test)	Genes
GO:0005515,GO:0008380,GO:0003723	protein binding (MF), RNA splicing (BP), RNA binding (MF)	6 (73)	96 (34208)	6,10E-08	1,98E-07	PABPC1,HNRNPL,HNRNPU,YBX1,SFPQ,HNRNPH1
GO:0005515,GO:0000398,GO:0008380	protein binding (MF), nuclear mRNA splicing, via spliceosome (BP), RNA splicing (BP)	6 (73)	100 (34208)	7,79E-08	2,46E-07	PABPC1,HNRNPL,HNRNPU,PRPF19,YBX1,HNRNPH1
GO:0003677,GO:0005515,GO:0045892	DNA binding (MF), protein binding (MF), negative regulation of transcription, DNA-dependent (BP)	6 (73)	114 (34208)	1,70E-07	4,66E-07	XRCC6,HMGB2,TP53,XRCC5,YBX1,HMGA1
GO:0005515,GO:0008022	protein binding (MF), protein C-terminus binding (MF)	6 (73)	116 (34208)	1,89E-07	4,79E-07	XRCC6,SIRT1,UBE2I,PABPC1,XRCC5,NCL
GO:0005515,GO:0000166,GO:0003723	protein binding (MF), nucleotide binding (MF), RNA binding (MF)	6 (73)	119 (34208)	2,20E-07	5,47E-07	PABPC1,HNRNPL,HNRNPU,NCL,SFPQ,HNRNPH1
GO:0005515,GO:0006916	protein binding (MF), anti-apoptosis (BP)	6 (73)	124 (34208)	2,80E-07	6,68E-07	NPM1,TRAF6,UBC,HDAC1,HSPA1A,POLB
GO:0016070,GO:0016032,GO:0016071	RNA metabolic process (BP), viral reproduction (BP), mRNA metabolic process (BP)	6 (73)	132 (34208)	4,05E-07	9,21E-07	RPL3,RPL14,RPSA,UBC,RPLP0,RPL4
GO:0003677,GO:0005515,GO:0045944	DNA binding (MF), protein binding (MF), positive regulation of transcription from RNA polymerase II promoter (BP)	6 (73)	151 (34208)	8,93E-07	1,79E-06	XRCC6,HMGB2,HIF1A,TP53,ESR1,EP300
GO:0005515,GO:0007411	protein binding (MF), axon guidance (BP)	6 (73)	151 (34208)	8,93E-07	1,79E-06	SPTA1,CSNK2A1,MYH9,Cdk5,PAK2,SPTBN1
GO:0045944,GO:0000122	positive regulation of transcription from RNA polymerase II promoter (BP), negative regulation of transcription from RNA polymerase II promoter (BP)	6 (73)	154 (34208)	1,00E-06	1,98E-06	SIRT1,TRAF6,TP53,TCF21,HDAC1,EP300
GO:0006355,GO:0000122	regulation of transcription, DNA-dependent (BP), negative regulation of transcription from RNA polymerase II promoter (BP)	6 (73)	155 (34208)	1,04E-06	2,04E-06	TXN,TP53,TCF21,HDAC1,EP300,YBX1
GO:0005515,GO:0043066	protein binding (MF), negative regulation of apoptotic process (BP)	6 (73)	179 (34208)	2,40E-06	4,23E-06	SIRT1,CDKN1A,MDM2,TP53,HDAC1,XRCC5
GO:0045944,GO:0045893	positive regulation of transcription from RNA polymerase II promoter	6 (73)	180 (34208)	2,48E-06	4,33E-06	XRCC6,HMGB2,HIF1A,TP53,HDAC1,THRAP3

GO term ID	Annotations	# of annotated genes in the input list (Total # of genes in the input list)	# of annotated genes in the reference list (Total # of genes in the reference list)	Hypergeometric Distribution (Fisher's exact test)	Corrected Hypergeometric Dist. (Fisher's exact test)	Genes
	(BP), positive regulation of transcription, DNA-dependent (BP)					
GO:0005515,GO:0008285	protein binding (MF), negative regulation of cell proliferation (BP)	6 (73)	189 (34208)	3,29E-06	5,57E-06	NPM1,CDKN1A,TP53,HMGA1,NME1,HSPA1A
GO:0005515,GO:0042802	protein binding (MF), identical protein binding (MF)	6 (73)	190 (34208)	3,39E-06	5,71E-06	SIRT1,TP53,PCNA,PAK2,PRPF19,NME1
GO:0006355,GO:0045944	regulation of transcription, DNA-dependent (BP), positive regulation of transcription from RNA polymerase II promoter (BP)	6 (73)	201 (34208)	4,69E-06	7,63E-06	HIF1A,TP53,TCF21,ESR1,HDAC1,EP300
GO:0003677,GO:0003700,GO:0005515	DNA binding (MF), sequence-specific DNA binding transcription factor activity (MF), protein binding (MF)	6 (73)	203 (34208)	4,96E-06	7,98E-06	HMGB2,HIF1A,TP53,ESR1,YBX1,HMGA1
GO:0005515,GO:0000278	protein binding (MF), mitotic cell cycle (BP)	6 (73)	203 (34208)	4,96E-06	7,98E-06	CDKN1A,UBC,DCTN1,PCNA,FEN1,CCNA1
GO:0005515,GO:0007049	protein binding (MF), cell cycle (BP)	6 (73)	259 (34208)	1,98E-05	2,68E-05	UBE2I,CDKN1A,TP53,CSNK2A1,Cdk5,EP300
GO:0005515,GO:0045893	protein binding (MF), positive regulation of transcription, DNA-dependent (BP)	6 (73)	306 (34208)	5,02E-05	6,15E-05	XRCC6,HMGB2,HIF1A,TP53,HDAC1,HMGA1
GO:0046872,GO:0008270,GO:0005515	metal ion binding (MF), zinc ion binding (MF), protein binding (MF)	6 (73)	468 (34208)	0,000498533	0,000540545	SIRT1,TRAF6,MDM2,TP53,ESR1,EP300
GO:0016787	hydrolase activity (MF)	6 (73)	971 (34208)	0,0175277	0,0177577	XRCC6,PRDX6,MUTYH,NUDT3,HDAC1,MPG
GO:0005515,GO:0044419,GO:0000122,GO:0045892,GO:0019899	protein binding (MF), interspecies interaction between organisms (BP), negative regulation of transcription from RNA polymerase II promoter (BP), negative regulation of transcription, DNA-dependent (BP), enzyme binding (MF)	5 (73)	5	3,85E-14	1,65E-12	SIRT1,UBE2I,MDM2,TP53,HDAC1
GO:0005515,GO:0003684,GO:0006281,GO:0006284	protein binding (MF), damaged DNA binding (MF), DNA repair (BP), base-excision repair (BP)	5 (73)	7	8,06E-13	3,11E-11	OGG1,XRCC1,MPG,FEN1,POLB

GO term ID	Annotations	# of annotated genes in the input list (Total # of genes in the input list)	# of annotated genes in the reference list (Total # of genes in the reference list)	Hypergeometric Distribution (Fisher's exact test)	Corrected Hypergeometric Dist. (Fisher's exact test)	Genes
GO:0005515,GO:0008134,GO:0019899	protein binding (MF), transcription factor binding (MF), enzyme binding (MF)	5 (73)	16	1,65E-10	2,20E-09	UBE2I,TP53,ESR1,HDAC1,HMGA1
GO:0005524,GO:0005515,GO:0045892	ATP binding (MF), protein binding (MF), negative regulation of transcription, DNA-dependent (BP)	5 (73)	17	2,33E-10	2,91E-09	XRCC6,UBE2I,TP53,Cdk5,XRCC5
GO:0003677,GO:0005515,GO:0003684	DNA binding (MF), protein binding (MF), damaged DNA binding (MF)	5 (73)	18	3,23E-10	3,37E-09	HMGB2,TP53,MPG,FEN1,POLB
GO:0005515,GO:0044419,GO:0008134	protein binding (MF), interspecies interaction between organisms (BP), transcription factor binding (MF)	5 (73)	28	3,64E-09	2,87E-08	UBE2I,TP53,HDAC1,EP300,HMGA1
GO:0046872,GO:0005515,GO:0019899	metal ion binding (MF), protein binding (MF), enzyme binding (MF)	5 (73)	33	8,72E-09	6,01E-08	SIRT1,MDM2,TP53,ESR1,POLB
GO:0005515,GO:0045892,GO:0043066	protein binding (MF), negative regulation of transcription, DNA-dependent (BP), negative regulation of apoptotic process (BP)	5 (73)	33	8,72E-09	6,01E-08	SIRT1,MDM2,TP53,HDAC1,XRCC5
GO:0006355,GO:0003700,GO:0005515,GO:0008134	regulation of transcription, DNA-dependent (BP), sequence-specific DNA binding transcription factor activity (MF), protein binding (MF), transcription factor binding (MF)	5 (73)	35	1,19E-08	5,53E-08	HIF1A,TP53,ESR1,HDAC1,HMGA1
GO:0006355,GO:0005515,GO:0045944,GO:0008134	regulation of transcription, DNA-dependent (BP), protein binding (MF), positive regulation of transcription from RNA polymerase II promoter (BP), transcription factor binding (MF)	5 (73)	37	1,59E-08	7,06E-08	HIF1A,TP53,ESR1,HDAC1,EP300
GO:0005515,GO:0000166,GO:0008022	protein binding (MF), nucleotide binding (MF), protein C-terminus binding (MF)	5 (73)	37	1,59E-08	7,06E-08	XRCC6,UBE2I,PABPC1,XRCC5,NCL
GO:0006355,GO:0003677,GO:0005515,GO:0008134	regulation of transcription, DNA-dependent (BP), DNA binding (MF), protein binding (MF), transcription factor binding (MF)	5 (73)	46	4,93E-08	1,64E-07	HIF1A,TP53,ESR1,EP300,HMGA1

GO term ID	Annotations	# of annotated genes in the input list (Total # of genes in the input list)	# of annotated genes in the reference list (Total # of genes in the reference list)	Hypergeometric Distribution (Fisher's exact test)	Corrected Hypergeometric Dist. (Fisher's exact test)	Genes
GO:0003677,GO:0005515,GO:0003690	DNA binding (MF), protein binding (MF), double-stranded DNA binding (MF)	5 (73)	48	6,14E-08	1,97E-07	XRCC6,HMGB2,FEN1,XRCC5,YBX1
GO:0005515,GO:0000166,GO:0008380,GO:0003723	protein binding (MF), nucleotide binding (MF), RNA splicing (BP), RNA binding (MF)	5 (73)	53	1,02E-07	2,96E-07	PABPC1,HNRNPL,HNRNPU,SFPQ,HNRNPH1
GO:0005515,GO:0000398,GO:0008380,GO:0003723,GO:0010467	protein binding (MF), nuclear mRNA splicing, via spliceosome (BP), RNA splicing (BP), RNA binding (MF), gene expression (BP)	5 (73)	53	1,02E-07	2,96E-07	PABPC1,HNRNPL,HNRNPU,YBX1,HNRNPH1
GO:0005515,GO:0045892,GO:0044212	protein binding (MF), negative regulation of transcription, DNA-dependent (BP), transcription regulatory region DNA binding (MF)	5 (73)	55	1,23E-07	3,50E-07	XRCC6,HMGB2,TP53,XRCC5,BASP1
GO:0003723,GO:0010467,GO:0044267,GO:0006412,GO:0016070,GO:0016071	RNA binding (MF), gene expression (BP), cellular protein metabolic process (BP), translation (BP), RNA metabolic process (BP), mRNA metabolic process (BP)	5 (73)	58	1,62E-07	4,52E-07	RPL3,RPL14,PABPC1,RPLP0,RPL4
GO:0005515,GO:0008134,GO:0000122	protein binding (MF), transcription factor binding (MF), negative regulation of transcription from RNA polymerase II promoter (BP)	5 (73)	67	3,35E-07	7,80E-07	UBE2I,TP53,HDAC1,PCNA,EP300
GO:0046872,GO:0008270,GO:0005515,GO:0045944	metal ion binding (MF), zinc ion binding (MF), protein binding (MF), positive regulation of transcription from RNA polymerase II promoter (BP)	5 (73)	68	3,61E-07	8,35E-07	SIRT1,TRAF6,TP53,ESR1,EP300
GO:0005515,GO:0000166,GO:0003723,GO:0003676	protein binding (MF), nucleotide binding (MF), RNA binding (MF), nucleic acid binding (MF)	5 (73)	74	5,53E-07	1,19E-06	PABPC1,HNRNPL,HNRNPU,NCL,HNRNPH1
GO:0046872,GO:0008270,GO:0005515,GO:0000122	metal ion binding (MF), zinc ion binding (MF), protein binding (MF), negative regulation of transcription from RNA polymerase II promoter	5 (73)	75	5,92E-07	1,26E-06	SIRT1,TRAF6,MDM2,TP53,EP300

GO term ID	Annotations	# of annotated genes in the input list (Total # of genes in the input list)	# of annotated genes in the reference list (Total # of genes in the reference list)	Hypergeometric Distribution (Fisher's exact test)	Corrected Hypergeometric Dist. (Fisher's exact test)	Genes
	(BP)					
GO:0010467,GO:0006414,GO:0031018,GO:0044267,GO:0006412,GO:0016070,GO:0016032,GO:0016071,GO:0006415,GO:0019058,GO:0019083,GO:0003735	gene expression (BP), translational elongation (BP), endocrine pancreas development (BP), cellular protein metabolic process (BP), translation (BP), RNA metabolic process (BP), viral reproduction (BP), mRNA metabolic process (BP), translational termination (BP), viral infectious cycle (BP), viral transcription (BP), structural constituent of ribosome (MF)	5 (73)	81	8,70E-07	1,77E-06	RPL3,RPL14,RPSA,RPLP0,RPL4
GO:0003677,GO:0005515,GO:0044212	DNA binding (MF), protein binding (MF), transcription regulatory region DNA binding (MF)	5 (73)	85	1,11E-06	2,13E-06	XRCC6,HMGB2,HIF1A,TP53,XRCC5
GO:0003677,GO:0005515,GO:0000166	DNA binding (MF), protein binding (MF), nucleotide binding (MF)	5 (73)	92	1,64E-06	3,00E-06	XRCC6,HNRNPU,XRCC5,NCL,SFPQ
GO:0005515,GO:0006974	protein binding (MF), response to DNA damage stimulus (BP)	5 (73)	92	1,64E-06	3,00E-06	XRCC6,SIRT1,CDKN1A,TP53,POLB
GO:0005524,GO:0007049	ATP binding (MF), cell cycle (BP)	5 (73)	94	1,82E-06	3,32E-06	UBE2I,KIF11,TP53,CSNK2A1,Cdk5
GO:0006355,GO:0005515,GO:0000122	regulation of transcription, DNA-dependent (BP), protein binding (MF), negative regulation of transcription from RNA polymerase II promoter (BP)	5 (73)	97	2,13E-06	3,79E-06	TXN,TP53,HDAC1,EP300,YBX1
GO:0003700,GO:0005515,GO:0045892	sequence-specific DNA binding transcription factor activity (MF), protein binding (MF), negative regulation of transcription, DNA-dependent (BP)	5 (73)	99	2,36E-06	4,17E-06	HMGB2,TP53,HDAC1,YBX1,HMGA1
GO:0005515,GO:0045892,GO:0045893	protein binding (MF), negative regulation of transcription, DNA-dependent (BP), positive regulation	5 (73)	101	2,60E-06	4,50E-06	XRCC6,HMGB2,TP53,HDAC1,HMGA1

GO term ID	Annotations	# of annotated genes in the input list (Total # of genes in the input list)	# of annotated genes in the reference list (Total # of genes in the reference list)	Hypergeometric Distribution (Fisher's exact test)	Corrected Hypergeometric Dist. (Fisher's exact test)	Genes
	of transcription, DNA-dependent (BP)					
GO:0005515,GO:0045944,GO:0000122	protein binding (MF), positive regulation of transcription from RNA polymerase II promoter (BP), negative regulation of transcription from RNA polymerase II promoter (BP)	5 (73)	104	3,00E-06	5,13E-06	SIRT1,TRAF6,TP53,HDAC1,EP300
GO:0006355,GO:0003677,GO:0045944	regulation of transcription, DNA-dependent (BP), DNA binding (MF), positive regulation of transcription from RNA polymerase II promoter (BP)	5 (73)	118	5,59E-06	8,69E-06	HIF1A,TP53,TCF21,ESR1,EP300
GO:0003700,GO:0005515,GO:0045893	sequence-specific DNA binding transcription factor activity (MF), protein binding (MF), positive regulation of transcription, DNA-dependent (BP)	5 (73)	120	6,06E-06	9,40E-06	HMGB2,HIF1A,TP53,HDAC1,HMGA1
GO:0006355,GO:0003677,GO:0003700,GO:0005515	regulation of transcription, DNA-dependent (BP), DNA binding (MF), sequence-specific DNA binding transcription factor activity (MF), protein binding (MF)	5 (73)	121	6,31E-06	9,71E-06	HIF1A,TP53,ESR1,YBX1,HMGA1
GO:0005515,GO:0004842	protein binding (MF), ubiquitin-protein ligase activity (MF)	5 (73)	134	1,04E-05	1,52E-05	UBE2I,TRAF6,MDM2,UBC,PRPF19
GO:0005515,GO:0042493	protein binding (MF), response to drug (BP)	5 (73)	135	1,08E-05	1,57E-05	CDKN1A,TP53,XRCC1,EP300,NME1
GO:0005515,GO:0045944,GO:0045893	protein binding (MF), positive regulation of transcription from RNA polymerase II promoter (BP), positive regulation of transcription, DNA-dependent (BP)	5 (73)	138	1,20E-05	1,72E-05	XRCC6,HMGB2,HIF1A,TP53,HDAC1
GO:0003677,GO:0005515,GO:0045893	DNA binding (MF), protein binding (MF), positive regulation of transcription, DNA-dependent (BP)	5 (73)	140	1,28E-05	1,81E-05	XRCC6,HMGB2,HIF1A,TP53,HMGA1

GO term ID	Annotations	# of annotated genes in the input list (Total # of genes in the input list)	# of annotated genes in the reference list (Total # of genes in the reference list)	Hypergeometric Distribution (Fisher's exact test)	Corrected Hypergeometric Dist. (Fisher's exact test)	Genes
GO:0003700,GO:0005515,GO:0045944	sequence-specific DNA binding transcription factor activity (MF), protein binding (MF), positive regulation of transcription from RNA polymerase II promoter (BP)	5 (73)	156	2,16E-05	2,90E-05	HMGB2,HIF1A,TP53,ESR1,HDAC1
GO:0008283,GO:0005515	cell proliferation (BP), protein binding (MF)	5 (73)	157	2,23E-05	2,98E-05	TXN,TP53,Cdk5,PCNA,XRCC5
GO:0005515,GO:0030154	protein binding (MF), cell differentiation (BP)	5 (73)	173	3,55E-05	4,57E-05	SIRT1,HIF1A,TP53,NME1,ARF6
GO:0000287	magnesium ion binding (MF)	5 (73)	178	4,07E-05	5,06E-05	PRPS1,NUDT3,FEN1,PRPS2,NME1
GO:0003677,GO:0000122	DNA binding (MF), negative regulation of transcription from RNA polymerase II promoter (BP)	5 (73)	193	5,97E-05	7,16E-05	TP53,TCF21,PCNA,EP300,YBX1
GO:0016301	kinase activity (MF)	5 (73)	227	0,000128113	0,000146306	PRPS1,CDKN1A,Cdk5,PRPS2,NME1
GO:0005515,GO:0016787	protein binding (MF), hydrolase activity (MF)	5 (73)	259	0,000236292	0,000264373	XRCC6,PRDX6,MUTYH,HDAC1,MPG
GO:0003779	actin binding (MF)	5 (73)	289	0,000390608	0,000425918	MSN,MYO1C,MYH9,SPTBN1,ACTN1
GO:0007399	nervous system development (BP)	5 (73)	410	0,00185907	0,00193946	PRPS1,DCTN1,EP300,NME1,ARF6
GO:0007596	blood coagulation (BP)	5 (73)	457	0,00296893	0,00306419	KIF11,TP53,HDAC1,Cdk5,ACTN1
GO:0042803	protein homodimerization activity (MF)	5 (73)	514	0,0048797	0,00499619	PRPS1,GZMA,NPM1,MYH9,PRPS2
GO:0005515,GO:0044419,GO:0000122,GO:0045892,GO:0019899,GO:0043066	protein binding (MF), interspecies interaction between organisms (BP), negative regulation of transcription from RNA polymerase II promoter (BP), negative regulation of transcription, DNA-dependent (BP), enzyme binding (MF), negative regulation of apoptotic process (BP)	4 (73)	4 (34208)	1,91E-11	3,68E-10	SIRT1,MDM2,TP53,HDAC1

GO term ID	Annotations	# of annotated genes in the input list (Total # of genes in the input list)	# of annotated genes in the reference list (Total # of genes in the reference list)	Hypergeometric Distribution (Fisher's exact test)	Corrected Hypergeometric Dist. (Fisher's exact test)	Genes
GO:0005515,GO:0033158	protein binding (MF), regulation of protein import into nucleus, translocation (BP)	4 (73)	4 (34208)	1,91E-11	3,68E-10	SIRT1,CDKN1A,OGG1,TXN
GO:0046872,GO:0008270,GO:0005515,GO:0045944,GO:0042981	metal ion binding (MF), zinc ion binding (MF), protein binding (MF), positive regulation of transcription from RNA polymerase II promoter (BP), regulation of apoptotic process (BP)	4 (73)	5 (34208)	9,52E-11	1,31E-09	SIRT1,TRAF6,TP53,ESR1
GO:0003677,GO:0005515,GO:0003684,GO:0006284	DNA binding (MF), protein binding (MF), damaged DNA binding (MF), base-excision repair (BP)	4 (73)	5 (34208)	9,52E-11	1,31E-09	TP53,MPG,FEN1,POLB
GO:0005515,GO:0044419,GO:0008134,GO:0045892,GO:0019899	protein binding (MF), interspecies interaction between organisms (BP), transcription factor binding (MF), negative regulation of transcription, DNA-dependent (BP), enzyme binding (MF)	4 (73)	5 (34208)	9,52E-11	1,31E-09	UBE2I,TP53,HDAC1,HMGA1
GO:0005515,GO:0003824,GO:0006281,GO:0006284	protein binding (MF), catalytic activity (MF), DNA repair (BP), base-excision repair (BP)	4 (73)	5 (34208)	9,52E-11	1,31E-09	MUTYH,OGG1,MPG,POLB
GO:0006355,GO:0003700,GO:0005515,GO:0008134,GO:0019899	regulation of transcription, DNA-dependent (BP), sequence-specific DNA binding transcription factor activity (MF), protein binding (MF), transcription factor binding (MF), enzyme binding (MF)	4 (73)	6 (34208)	2,85E-10	3,15E-09	TP53,ESR1,HDAC1,HMGA1
GO:0005515,GO:0000122,GO:0045892,GO:0016567	protein binding (MF), negative regulation of transcription from RNA polymerase II promoter (BP), negative regulation of transcription, DNA-dependent (BP), protein ubiquitination (BP)	4 (73)	6 (34208)	2,85E-10	3,15E-09	SIRT1,UBE2I,TRAF6,MDM2
GO:0046872,GO:0008270,GO:0005515,GO:0044419,GO:0000122	metal ion binding (MF), zinc ion binding (MF), protein binding (MF), interspecies interaction	4 (73)	9 (34208)	2,38E-09	1,92E-08	SIRT1,MDM2,TP53,EP300

GO term ID	Annotations	# of annotated genes in the input list (Total # of genes in the input list)	# of annotated genes in the reference list (Total # of genes in the reference list)	Hypergeometric Distribution (Fisher's exact test)	Corrected Hypergeometric Dist. (Fisher's exact test)	Genes
	between organisms (BP), negative regulation of transcription from RNA polymerase II promoter (BP)					
GO:0005515,GO:0045892,GO:0006281	protein binding (MF), negative regulation of transcription, DNA-dependent (BP), DNA repair (BP)	4 (73)	9 (34208)	2,38E-09	1,92E-08	XRCC6,SIRT1,SUMO1,XRCC5
GO:0005515,GO:0044419,GO:0045944,GO:0000122	protein binding (MF), interspecies interaction between organisms (BP), positive regulation of transcription from RNA polymerase II promoter (BP), negative regulation of transcription from RNA polymerase II promoter (BP)	4 (73)	10 (34208)	3,97E-09	3,06E-08	SIRT1,TP53,HDAC1,EP300
GO:0005515,GO:0044419,GO:0008134,GO:0000122	protein binding (MF), interspecies interaction between organisms (BP), transcription factor binding (MF), negative regulation of transcription from RNA polymerase II promoter (BP)	4 (73)	11 (34208)	6,23E-09	4,53E-08	UBE2I,TP53,HDAC1,EP300
GO:0003677,GO:0005515,GO:0006281,GO:0006284	DNA binding (MF), protein binding (MF), DNA repair (BP), base-excision repair (BP)	4 (73)	13 (34208)	1,34E-08	6,11E-08	PCNA,MPG,FEN1,POLB
GO:0005515,GO:0045892,GO:0042981	protein binding (MF), negative regulation of transcription, DNA-dependent (BP), regulation of apoptotic process (BP)	4 (73)	13 (34208)	1,34E-08	6,11E-08	SIRT1,TRAF6,TP53,Cdk5
GO:0005524,GO:0005515,GO:0000166,GO:0045892	ATP binding (MF), protein binding (MF), nucleotide binding (MF), negative regulation of transcription, DNA-dependent (BP)	4 (73)	14 (34208)	1,88E-08	8,15E-08	XRCC6,UBE2I,Cdk5,XRCC5
GO:0005515,GO:0045892,GO:0002039	protein binding (MF), negative regulation of transcription, DNA-dependent (BP), p53 binding (MF)	4 (73)	14 (34208)	1,88E-08	8,15E-08	SIRT1,MDM2,TP53,Cdk5
GO:0003677,GO:0005515,GO:0006281,GO:0000723	DNA binding (MF), protein binding (MF), DNA repair (BP), telomere maintenance (BP)	4 (73)	15 (34208)	2,56E-08	1,06E-07	XRCC6,PCNA,FEN1,XRCC5

GO term ID	Annotations	# of annotated genes in the input list (Total # of genes in the input list)	# of annotated genes in the reference list (Total # of genes in the reference list)	Hypergeometric Distribution (Fisher's exact test)	Corrected Hypergeometric Dist. (Fisher's exact test)	Genes
GO:0005515,GO:0045892,GO:0008022	protein binding (MF), negative regulation of transcription, DNA-dependent (BP), protein C-terminus binding (MF)	4 (73)	15 (34208)	2,56E-08	1,06E-07	XRCC6,SIRT1,UBE2I,XRCC5
GO:0006355,GO:0005515,GO:0044419,GO:0008134	regulation of transcription, DNA-dependent (BP), protein binding (MF), interspecies interaction between organisms (BP), transcription factor binding (MF)	4 (73)	16 (34208)	3,41E-08	1,38E-07	TP53,HDAC1,EP300,HMGA1
GO:0005515,GO:0043388	protein binding (MF), positive regulation of DNA binding (BP)	4 (73)	17 (34208)	4,45E-08	1,51E-07	HMGB2,TXN,EP300,NME1
GO:0005515,GO:0042802,GO:0042981	protein binding (MF), identical protein binding (MF), regulation of apoptotic process (BP)	4 (73)	17 (34208)	4,45E-08	1,51E-07	SIRT1,TP53,PAK2,NME1
GO:0005515,GO:0006913	protein binding (MF), nucleocytoplasmic transport (BP)	4 (73)	17 (34208)	4,45E-08	1,51E-07	NPM1,SET,Cdk5,ANP32A
GO:0003677,GO:0005515,GO:0003690,GO:0045892	DNA binding (MF), protein binding (MF), double-stranded DNA binding (MF), negative regulation of transcription, DNA-dependent (BP)	4 (73)	18 (34208)	5,71E-08	1,87E-07	XRCC6,HMGB2,XRCC5,YBX1
GO:0045944,GO:0042826	positive regulation of transcription from RNA polymerase II promoter (BP), histone deacetylase binding (MF)	4 (73)	21 (34208)	1,11E-07	3,18E-07	TRAF6,HIF1A,TCF21,HDAC1
GO:0003677,GO:0005515,GO:0006302	DNA binding (MF), protein binding (MF), double-strand break repair (BP)	4 (73)	22 (34208)	1,36E-07	3,82E-07	XRCC6,TP53,FEN1,XRCC5
GO:0006355,GO:0003700,GO:0005515,GO:0008134,GO:0045893	regulation of transcription, DNA-dependent (BP), sequence-specific DNA binding transcription factor activity (MF), protein binding (MF), transcription factor binding (MF), positive regulation of transcription, DNA-dependent (BP)	4 (73)	23 (34208)	1,64E-07	4,52E-07	HIF1A,TP53,HDAC1,HMGA1

GO term ID	Annotations	# of annotated genes in the input list (Total # of genes in the input list)	# of annotated genes in the reference list (Total # of genes in the reference list)	Hypergeometric Distribution (Fisher's exact test)	Corrected Hypergeometric Dist. (Fisher's exact test)	Genes
GO:0005515,GO:0000166,GO:0000398,GO:0008380,GO:0003723,GO:0010467,GO:0003676	protein binding (MF), nucleotide binding (MF), nuclear mRNA splicing, via spliceosome (BP), RNA splicing (BP), RNA binding (MF), gene expression (BP), nucleic acid binding (MF)	4 (73)	23 (34208)	1,64E-07	4,52E-07	PABPC1,HNRNPL,HNRNPU,HNRNPH1
GO:0003677,GO:0005515,GO:0019899	DNA binding (MF), protein binding (MF), enzyme binding (MF)	4 (73)	24 (34208)	1,96E-07	4,92E-07	TP53,ESR1,HMGA1,POLB
GO:0005515,GO:0071456	protein binding (MF), cellular response to hypoxia (BP)	4 (73)	24 (34208)	1,96E-07	4,92E-07	SIRT1,MDM2,HIF1A,TP53
GO:0006355,GO:0003700,GO:0005515,GO:0045944,GO:0008134	regulation of transcription, DNA-dependent (BP), sequence-specific DNA binding transcription factor activity (MF), protein binding (MF), positive regulation of transcription from RNA polymerase II promoter (BP), transcription factor binding (MF)	4 (73)	25 (34208)	2,33E-07	5,66E-07	HIF1A,TP53,ESR1,HDAC1
GO:0046872,GO:0005515,GO:0006974	metal ion binding (MF), protein binding (MF), response to DNA damage stimulus (BP)	4 (73)	25 (34208)	2,33E-07	5,66E-07	SIRT1,CDKN1A,TP53,POLB
GO:0005524,GO:0005515,GO:0042981	ATP binding (MF), protein binding (MF), regulation of apoptotic process (BP)	4 (73)	25 (34208)	2,33E-07	5,66E-07	TP53,Cdk5,PAK2,NME1
GO:0005515,GO:0045944,GO:0019899	protein binding (MF), positive regulation of transcription from RNA polymerase II promoter (BP), enzyme binding (MF)	4 (73)	25 (34208)	2,33E-07	5,66E-07	SIRT1,TP53,ESR1,HDAC1
GO:0046872,GO:0008270,GO:0005515,GO:0019899	metal ion binding (MF), zinc ion binding (MF), protein binding (MF), enzyme binding (MF)	4 (73)	26 (34208)	2,75E-07	6,60E-07	SIRT1,MDM2,TP53,ESR1
GO:0003677,GO:0005515,GO:0008380	DNA binding (MF), protein binding (MF), RNA splicing (BP)	4 (73)	27 (34208)	3,23E-07	7,64E-07	HNRNPU,PRPF19,YBX1,SFPQ
GO:0006355,GO:0003677,GO:0005515,GO:0045944,GO:0008134	regulation of transcription, DNA-dependent (BP), DNA binding (MF), protein binding	4 (73)	28 (34208)	3,76E-07	8,58E-07	HIF1A,TP53,ESR1,EP300

GO term ID	Annotations	# of annotated genes in the input list (Total # of genes in the input list)	# of annotated genes in the reference list (Total # of genes in the reference list)	Hypergeometric Distribution (Fisher's exact test)	Corrected Hypergeometric Dist. (Fisher's exact test)	Genes
	(MF), positive regulation of transcription from RNA polymerase II promoter (BP), transcription factor binding (MF)					
GO:0046872,GO:0008270,GO:0005515,GO:0000122,GO:0045892	metal ion binding (MF), zinc ion binding (MF), protein binding (MF), negative regulation of transcription from RNA polymerase II promoter (BP), negative regulation of transcription, DNA-dependent (BP)	4 (73)	28 (34208)	3,76E-07	8,58E-07	SIRT1,TRAF6,MDM2,TP53
GO:0046872,GO:0008270,GO:0005515,GO:0045944,GO:0000122	metal ion binding (MF), zinc ion binding (MF), protein binding (MF), positive regulation of transcription from RNA polymerase II promoter (BP), negative regulation of transcription from RNA polymerase II promoter (BP)	4 (73)	29 (34208)	4,35E-07	9,82E-07	SIRT1,TRAF6,TP53,EP300
GO:0005515,GO:0010467,GO:0044267,GO:0006412,GO:0016070,GO:0016071	protein binding (MF), gene expression (BP), cellular protein metabolic process (BP), translation (BP), RNA metabolic process (BP), mRNA metabolic process (BP)	4 (73)	31 (34208)	5,75E-07	1,23E-06	RPL14,PABPC1,RPSA,RPLP0
GO:0006355,GO:0003677,GO:0003700,GO:0005515,GO:0008134	regulation of transcription, DNA-dependent (BP), DNA binding (MF), sequence-specific DNA binding transcription factor activity (MF), protein binding (MF), transcription factor binding (MF)	4 (73)	32 (34208)	6,56E-07	1,38E-06	HIF1A,TP53,ESR1,HMGA1
GO:0003677,GO:0005515,GO:0045892,GO:0044212	DNA binding (MF), protein binding (MF), negative regulation of transcription, DNA-dependent (BP), transcription regulatory region DNA binding (MF)	4 (73)	34 (34208)	8,43E-07	1,72E-06	XRCC6,HMGB2,TP53,XRCC5

GO term ID	Annotations	# of annotated genes in the input list (Total # of genes in the input list)	# of annotated genes in the reference list (Total # of genes in the reference list)	Hypergeometric Distribution (Fisher's exact test)	Corrected Hypergeometric Dist. (Fisher's exact test)	Genes
GO:0005515,GO:0006977,GO:0000075	protein binding (MF), DNA damage response, signal transduction by p53 class mediator resulting in cell cycle arrest (BP), cell cycle checkpoint (BP)	4 (73)	34 (34208)	8,43E-07	1,72E-06	CDKN1A,MDM2,TP53,UBC
GO:0007165,GO:0005515,GO:0019901	signal transduction (BP), protein binding (MF), protein kinase binding (MF)	4 (73)	35 (34208)	9,50E-07	1,89E-06	NPM1,TRAF6,HIF1A,PAK2
GO:0005524,GO:0005515,GO:0000166,GO:0007411	ATP binding (MF), protein binding (MF), nucleotide binding (MF), axon guidance (BP)	4 (73)	36 (34208)	1,07E-06	2,07E-06	CSNK2A1,MYH9,Cdk5,PAK2
GO:0005524,GO:0000166,GO:0008022	ATP binding (MF), nucleotide binding (MF), protein C-terminus binding (MF)	4 (73)	36 (34208)	1,07E-06	2,07E-06	XRCC6,UBE2I,MYO1C,XRCC5
GO:0006915,GO:0005515,GO:0045944	apoptotic process (BP), protein binding (MF), positive regulation of transcription from RNA polymerase II promoter (BP)	4 (73)	37 (34208)	1,19E-06	2,28E-06	TRAF6,HMGB2,TP53,EP300
GO:0006355,GO:0003700,GO:0005515,GO:0045892	regulation of transcription, DNA-dependent (BP), sequence-specific DNA binding transcription factor activity (MF), protein binding (MF), negative regulation of transcription, DNA-dependent (BP)	4 (73)	39 (34208)	1,48E-06	2,82E-06	TP53,HDAC1,YBX1,HMGA1
GO:0046872,GO:0005515,GO:0043066	metal ion binding (MF), protein binding (MF), negative regulation of apoptotic process (BP)	4 (73)	45 (34208)	2,66E-06	4,59E-06	SIRT1,CDKN1A,MDM2,TP53
GO:0005515,GO:0006928	protein binding (MF), cellular component movement (BP)	4 (73)	46 (34208)	2,91E-06	4,99E-06	MSN,TXN,MYH9,ARF6
GO:0003700,GO:0005515,GO:0045892,GO:0045893	sequence-specific DNA binding transcription factor activity (MF), protein binding (MF), negative regulation of transcription, DNA-dependent (BP), positive regulation of transcription, DNA-dependent (BP)	4 (73)	47 (34208)	3,18E-06	5,40E-06	HMGB2,TP53,HDAC1,HMGA1

GO term ID	Annotations	# of annotated genes in the input list (Total # of genes in the input list)	# of annotated genes in the reference list (Total # of genes in the reference list)	Hypergeometric Distribution (Fisher's exact test)	Corrected Hypergeometric Dist. (Fisher's exact test)	Genes
GO:0006355,GO:0007165,GO:0005515	regulation of transcription, DNA-dependent (BP), signal transduction (BP), protein binding (MF)	4 (73)	48 (34208)	3,46E-06	5,80E-06	TXN,HIF1A,CSNK2A1,ESR1
GO:0003677,GO:0005515,GO:0045944,GO:0045893,GO:0044212	DNA binding (MF), protein binding (MF), positive regulation of transcription from RNA polymerase II promoter (BP), positive regulation of transcription, DNA-dependent (BP), transcription regulatory region DNA binding (MF)	4 (73)	49 (34208)	3,76E-06	6,28E-06	XRCC6,HMGB2,HIF1A,TP53
GO:0003677,GO:0005515,GO:0003723	DNA binding (MF), protein binding (MF), RNA binding (MF)	4 (73)	50 (34208)	4,08E-06	6,79E-06	HNRNPU,NCL,YBX1,SFPQ
GO:0005515,GO:0045944,GO:0000122,GO:0045892	protein binding (MF), positive regulation of transcription from RNA polymerase II promoter (BP), negative regulation of transcription from RNA polymerase II promoter (BP), negative regulation of transcription, DNA-dependent (BP)	4 (73)	51 (34208)	4,42E-06	7,23E-06	SIRT1,TRAF6,TP53,HDAC1
GO:0003677,GO:0005515,GO:0045892,GO:0045893	DNA binding (MF), protein binding (MF), negative regulation of transcription, DNA-dependent (BP), positive regulation of transcription, DNA-dependent (BP)	4 (73)	52 (34208)	4,78E-06	7,75E-06	XRCC6,HMGB2,TP53,HMGA1
GO:0006355,GO:0045944,GO:0000122	regulation of transcription, DNA-dependent (BP), positive regulation of transcription from RNA polymerase II promoter (BP), negative regulation of transcription from RNA polymerase II promoter (BP)	4 (73)	53 (34208)	5,16E-06	8,13E-06	TP53,TCF21,HDAC1,EP300

GO term ID	Annotations	# of annotated genes in the input list (Total # of genes in the input list)	# of annotated genes in the reference list (Total # of genes in the reference list)	Hypergeometric Distribution (Fisher's exact test)	Corrected Hypergeometric Dist. (Fisher's exact test)	Genes
GO:0003723,GO:0010467,GO:0006414,GO:0031018,GO:0044267,GO:0006412,GO:0016070,GO:0016032,GO:0016071,GO:0006415,GO:0019058,GO:0019083,GO:0003735	RNA binding (MF), gene expression (BP), translational elongation (BP), endocrine pancreas development (BP), cellular protein metabolic process (BP), translation (BP), RNA metabolic process (BP), viral reproduction (BP), mRNA metabolic process (BP), translational termination (BP), viral infectious cycle (BP), viral transcription (BP), structural constituent of ribosome (MF)	4 (73)	53 (34208)	5,16E-06	8,13E-06	RPL3,RPL14,RPLP0,RPL4
GO:0005515,GO:0048015	protein binding (MF), phosphatidylinositol-mediated signaling (BP)	4 (73)	54 (34208)	5,57E-06	8,70E-06	MDM2,HMGB2,PCNA,FEN1
GO:0005515,GO:0016070,GO:0016032,GO:0016071	protein binding (MF), RNA metabolic process (BP), viral reproduction (BP), mRNA metabolic process (BP)	4 (73)	54 (34208)	5,57E-06	8,70E-06	RPL14,RPSA,UBC,RPLP0
GO:0005515,GO:0045944,GO:0045892,GO:0045893	protein binding (MF), positive regulation of transcription from RNA polymerase II promoter (BP), negative regulation of transcription, DNA-dependent (BP), positive regulation of transcription, DNA-dependent (BP)	4 (73)	56 (34208)	6,44E-06	9,87E-06	XRCC6,HMGB2,TP53,HDAC1
GO:0003677,GO:0003700,GO:0005515,GO:0045892	DNA binding (MF), sequence-specific DNA binding transcription factor activity (MF), protein binding (MF), negative regulation of transcription, DNA-dependent (BP)	4 (73)	58 (34208)	7,42E-06	1,13E-05	HMGB2,TP53,YBX1,HMGA1
GO:0005515,GO:0047485	protein binding (MF), protein N-terminus binding (MF)	4 (73)	60 (34208)	8,50E-06	1,27E-05	TRAF6,TP53,CSNK2A1,HSPA1A
GO:0006915,GO:0005515,GO:0042981	apoptotic process (BP), protein binding (MF), regulation of	4 (73)	65 (34208)	1,17E-05	1,69E-05	TRAF6,TP53,UBC,PAK2

GO term ID	Annotations	# of annotated genes in the input list (Total # of genes in the input list)	# of annotated genes in the reference list (Total # of genes in the reference list)	Hypergeometric Distribution (Fisher's exact test)	Corrected Hypergeometric Dist. (Fisher's exact test)	Genes
	apoptotic process (BP)					
GO:0005515,GO:0030308	protein binding (MF), negative regulation of cell growth (BP)	4 (73)	65 (34208)	1,17E-05	1,69E-05	SIRT1,CDKN1A,TP53,HSPA1A
GO:0005524,GO:0005515,GO:0007049	ATP binding (MF), protein binding (MF), cell cycle (BP)	4 (73)	66 (34208)	1,24E-05	1,77E-05	UBE2I,TP53,CSNK2A1,Cdk5
GO:0005515,GO:0000278,GO:0000082	protein binding (MF), mitotic cell cycle (BP), G1/S transition of mitotic cell cycle (BP)	4 (73)	68 (34208)	1,40E-05	1,95E-05	CDKN1A,UBC,PCNA,CCNA1
GO:0005515,GO:0000278,GO:0000084	protein binding (MF), mitotic cell cycle (BP), S phase of mitotic cell cycle (BP)	4 (73)	69 (34208)	1,49E-05	2,06E-05	CDKN1A,UBC,PCNA,FEN1
GO:0003677,GO:0005524,GO:0005515	DNA binding (MF), ATP binding (MF), protein binding (MF)	4 (73)	79 (34208)	2,54E-05	3,36E-05	XRCC6,TP53,HNRNPU,XRCC5
GO:0005515,GO:0001525	protein binding (MF), angiogenesis (BP)	4 (73)	80 (34208)	2,67E-05	3,50E-05	SIRT1,HIF1A,MYH9,NCL
GO:0003700,GO:0005515,GO:0045944,GO:0045893	sequence-specific DNA binding transcription factor activity (MF), protein binding (MF), positive regulation of transcription from RNA polymerase II promoter (BP), positive regulation of transcription, DNA-dependent (BP)	4 (73)	85 (34208)	3,39E-05	4,39E-05	HMGB2,HIF1A,TP53,HDAC1
GO:0005515,GO:0031625	protein binding (MF), ubiquitin protein ligase binding (MF)	4 (73)	86 (34208)	3,55E-05	4,58E-05	TP53,SUMO2,SUMO1,HSPA1A
GO:0003677,GO:0003700,GO:0005515,GO:0045893	DNA binding (MF), sequence-specific DNA binding transcription factor activity (MF), protein binding (MF), positive regulation of transcription, DNA-dependent (BP)	4 (73)	87 (34208)	3,72E-05	4,73E-05	HMGB2,HIF1A,TP53,HMGA1
GO:0006355,GO:0003677,GO:0000122	regulation of transcription, DNA-dependent (BP), DNA binding (MF), negative regulation of transcription from RNA polymerase II promoter (BP)	4 (73)	88 (34208)	3,89E-05	4,92E-05	TP53,TCF21,EP300,YBX1

GO term ID	Annotations	# of annotated genes in the input list (Total # of genes in the input list)	# of annotated genes in the reference list (Total # of genes in the reference list)	Hypergeometric Distribution (Fisher's exact test)	Corrected Hypergeometric Dist. (Fisher's exact test)	Genes
GO:0005524,GO:0000166,GO:0007049	ATP binding (MF), nucleotide binding (MF), cell cycle (BP)	4 (73)	89 (34208)	4,06E-05	5,07E-05	UBE2I,KIF11,CSNK2A1,Cdk5
GO:0005515,GO:0006260	protein binding (MF), DNA replication (BP)	4 (73)	91 (34208)	4,43E-05	5,45E-05	SIRT1,SET,PCNA,FEN1
GO:0003677,GO:0003700,GO:0005515,GO:0045944	DNA binding (MF), sequence-specific DNA binding transcription factor activity (MF), protein binding (MF), positive regulation of transcription from RNA polymerase II promoter (BP)	4 (73)	103 (34208)	7,19E-05	8,52E-05	HMGB2,HIF1A,TP53,ESR1
GO:0005515,GO:0003779	protein binding (MF), actin binding (MF)	4 (73)	106 (34208)	8,04E-05	9,49E-05	MSN,MYH9,SPTBN1,ACTN1
GO:0005515,GO:0019904	protein binding (MF), protein domain specific binding (MF)	4 (73)	111 (34208)	9,62E-05	0,000111815	SIRT1,HMGB2,ACTN1,BASP1
GO:0003677,GO:0005515,GO:0000122	DNA binding (MF), protein binding (MF), negative regulation of transcription from RNA polymerase II promoter (BP)	4 (73)	118 (34208)	0,00012185	0,0001404	TP53,PCNA,EP300,YBX1
GO:0007399,GO:0005515	nervous system development (BP), protein binding (MF)	4 (73)	134 (34208)	0,000198719	0,000224285	DCTN1,EP300,NME1,ARF6
GO:0005515,GO:0048011	protein binding (MF), nerve growth factor receptor signaling pathway (BP)	4 (73)	137 (34208)	0,000216294	0,000242702	TRAF6,MDM2,UBC,HDAC1
GO:0005515,GO:0045087	protein binding (MF), innate immune response (BP)	4 (73)	151 (34208)	0,000313404	0,000345639	TRAF6,TXN,UBC,EP300
GO:0005524,GO:0000166,GO:0016301	ATP binding (MF), nucleotide binding (MF), kinase activity (MF)	4 (73)	155 (34208)	0,000346089	0,000378443	PRPS1,Cdk5,PRPS2,NME1
GO:0007067	mitosis (BP)	4 (73)	187 (34208)	0,000701244	0,00075609	UBE2I,KIF11,DCTN1,CCNA1
GO:0046872,GO:0003677,GO:0005515	metal ion binding (MF), DNA binding (MF), protein binding (MF)	4 (73)	193 (34208)	0,000788856	0,000843486	TP53,ESR1,EP300,POLB
GO:0005515,GO:0007596	protein binding (MF), blood coagulation (BP)	4 (73)	251 (34208)	0,00207178	0,00214975	TP53,HDAC1,Cdk5,ACTN1
GO:0051301	cell division (BP)	4 (73)	286 (34208)	0,00331245	0,00340962	UBE2I,KIF11,Cdk5,CCNA1
GO:0005515,GO:0004872	protein binding (MF), receptor activity (MF)	4 (73)	362 (34208)	0,00756756	0,00770733	MCC,RPSA,ESR1,HSPA1A

GO term ID	Annotations	# of annotated genes in the input list (Total # of genes in the input list)	# of annotated genes in the reference list (Total # of genes in the reference list)	Hypergeometric Distribution (Fisher's exact test)	Corrected Hypergeometric Dist. (Fisher's exact test)	Genes
GO:0016740	transferase activity (MF)	4 (73)	616 (34208)	0,0428217	0,0430447	PRPS1,PRPS2,NME1,POLB
GO:0006355,GO:0003700,GO:0005515,GO:0044419,GO:0008134,GO:0045892,GO:0045893,GO:0019899	regulation of transcription, DNA-dependent (BP), sequence-specific DNA binding transcription factor activity (MF), protein binding (MF), interspecies interaction between organisms (BP), transcription factor binding (MF), negative regulation of transcription, DNA-dependent (BP), positive regulation of transcription, DNA-dependent (BP), enzyme binding (MF)	3 (73)	3 (34208)	9,32E-09	4,44E-08	TP53,HDAC1,HMGA1
GO:0046872,GO:0008270,GO:0005515,GO:0044419,GO:0045944,GO:0000122,GO:0042771	metal ion binding (MF), zinc ion binding (MF), protein binding (MF), interspecies interaction between organisms (BP), positive regulation of transcription from RNA polymerase II promoter (BP), negative regulation of transcription from RNA polymerase II promoter (BP), DNA damage response, signal transduction by p53 class mediator resulting in induction of apoptosis (BP)	3 (73)	3 (34208)	9,32E-09	4,44E-08	SIRT1,TP53,EP300
GO:0046872,GO:0008270,GO:0005515,GO:0044419,GO:0000122,GO:0045892,GO:0019899,GO:0043066,GO:0002039,GO:0071456	metal ion binding (MF), zinc ion binding (MF), protein binding (MF), interspecies interaction between organisms (BP), negative regulation of transcription from RNA polymerase II promoter (BP), negative regulation of transcription, DNA-dependent (BP), enzyme binding (MF), negative regulation of apoptotic process (BP), p53 binding	3 (73)	3 (34208)	9,32E-09	4,44E-08	SIRT1,MDM2,TP53

GO term ID	Annotations	# of annotated genes in the input list (Total # of genes in the input list)	# of annotated genes in the reference list (Total # of genes in the reference list)	Hypergeometric Distribution (Fisher's exact test)	Corrected Hypergeometric Dist. (Fisher's exact test)	Genes
	(MF), cellular response to hypoxia (BP)					
GO:0046872,GO:0008270,GO:0005515,GO:0045944,GO:0000122,GO:0045892,GO:0042981	metal ion binding (MF), zinc ion binding (MF), protein binding (MF), positive regulation of transcription from RNA polymerase II promoter (BP), negative regulation of transcription from RNA polymerase II promoter (BP), negative regulation of transcription, DNA-dependent (BP), regulation of apoptotic process (BP)	3 (73)	3 (34208)	9,32E-09	4,44E-08	SIRT1,TRAF6,TP53
GO:0046872,GO:0005515,GO:0042493,GO:0007049	metal ion binding (MF), protein binding (MF), response to drug (BP), cell cycle (BP)	3 (73)	3 (34208)	9,32E-09	4,44E-08	CDKN1A,TP53,EP300
GO:0046872,GO:0005515,GO:0030308,GO:0071479,GO:0043066,GO:0006974	metal ion binding (MF), protein binding (MF), negative regulation of cell growth (BP), cellular response to ionizing radiation (BP), negative regulation of apoptotic process (BP), response to DNA damage stimulus (BP)	3 (73)	3 (34208)	9,32E-09	4,44E-08	SIRT1,CDKN1A,TP53
GO:0046872,GO:0005515,GO:0043066,GO:0006977,GO:0000075	metal ion binding (MF), protein binding (MF), negative regulation of apoptotic process (BP), DNA damage response, signal transduction by p53 class mediator resulting in cell cycle arrest (BP), cell cycle checkpoint (BP)	3 (73)	3 (34208)	9,32E-09	4,44E-08	CDKN1A,MDM2,TP53
GO:0003677,GO:0005524,GO:0005515,GO:0045892,GO:0044212,GO:0006302	DNA binding (MF), ATP binding (MF), protein binding (MF), negative regulation of transcription, DNA-dependent	3 (73)	3 (34208)	9,32E-09	4,44E-08	XRCC6,TP53,XRCC5

GO term ID	Annotations	# of annotated genes in the input list (Total # of genes in the input list)	# of annotated genes in the reference list (Total # of genes in the reference list)	Hypergeometric Distribution (Fisher's exact test)	Corrected Hypergeometric Dist. (Fisher's exact test)	Genes
	(BP), transcription regulatory region DNA binding (MF), double-strand break repair (BP)					
GO:0003677,GO:0005515,GO:0003690,GO:0006281,GO:0006302,GO:0000723	DNA binding (MF), protein binding (MF), double-stranded DNA binding (MF), DNA repair (BP), double-strand break repair (BP), telomere maintenance (BP)	3 (73)	3 (34208)	9,32E-09	4,44E-08	XRCC6,FEN1,XRCC5
GO:0003677,GO:0005515,GO:0045892,GO:0016032,GO:0019047,GO:0019059,GO:0051575	DNA binding (MF), protein binding (MF), negative regulation of transcription, DNA-dependent (BP), viral reproduction (BP), provirus integration (BP), initiation of viral infection (BP), 5'-deoxyribose-5-phosphate lyase activity (MF)	3 (73)	3 (34208)	9,32E-09	4,44E-08	XRCC6,XRCC5,HMGA1
GO:0003677,GO:0005515,GO:0019899,GO:0006284	DNA binding (MF), protein binding (MF), enzyme binding (MF), base-excision repair (BP)	3 (73)	3 (34208)	9,32E-09	4,44E-08	TP53,HMGA1,POLB
GO:0008283,GO:0005524,GO:0005515,GO:0045892	cell proliferation (BP), ATP binding (MF), protein binding (MF), negative regulation of transcription, DNA-dependent (BP)	3 (73)	3 (34208)	9,32E-09	4,44E-08	TP53,Cdk5,XRCC5
GO:0005524,GO:0005515,GO:0045892,GO:0007049	ATP binding (MF), protein binding (MF), negative regulation of transcription, DNA-dependent (BP), cell cycle (BP)	3 (73)	3 (34208)	9,32E-09	4,44E-08	UBE2I,TP53,Cdk5
GO:0005515,GO:0044419,GO:0045944,GO:0000122,GO:0045892,GO:0019899,GO:0043066	protein binding (MF), interspecies interaction between organisms (BP), positive regulation of transcription from RNA polymerase II promoter (BP), negative regulation of transcription from RNA polymerase II promoter (BP), negative regulation of transcription, DNA-dependent	3 (73)	3 (34208)	9,32E-09	4,44E-08	SIRT1,TP53,HDAC1

GO term ID	Annotations	# of annotated genes in the input list (Total # of genes in the input list)	# of annotated genes in the reference list (Total # of genes in the reference list)	Hypergeometric Distribution (Fisher's exact test)	Corrected Hypergeometric Dist. (Fisher's exact test)	Genes
	(BP), enzyme binding (MF), negative regulation of apoptotic process (BP)					
GO:0005515,GO:0044419,GO:0008134,GO:0000122,GO:0045892,GO:0019899	protein binding (MF), interspecies interaction between organisms (BP), transcription factor binding (MF), negative regulation of transcription from RNA polymerase II promoter (BP), negative regulation of transcription, DNA-dependent (BP), enzyme binding (MF)	3 (73)	3 (34208)	9,32E-09	4,44E-08	UBE2I,TP53,HDAC1
GO:0005515,GO:0044419,GO:0008134,GO:0000122,GO:0007049	protein binding (MF), interspecies interaction between organisms (BP), transcription factor binding (MF), negative regulation of transcription from RNA polymerase II promoter (BP), cell cycle (BP)	3 (73)	3 (34208)	9,32E-09	4,44E-08	UBE2I,TP53,EP300
GO:0005515,GO:0044419,GO:0000122,GO:0008284,GO:0045892,GO:0019899,GO:0043066	protein binding (MF), interspecies interaction between organisms (BP), negative regulation of transcription from RNA polymerase II promoter (BP), positive regulation of cell proliferation (BP), negative regulation of transcription, DNA-dependent (BP), enzyme binding (MF), negative regulation of apoptotic process (BP)	3 (73)	3 (34208)	9,32E-09	4,44E-08	SIRT1,MDM2,HDAC1
GO:0005515,GO:0044419,GO:0000122,GO:0045892,GO:0016567,GO:0019899	protein binding (MF), interspecies interaction between organisms (BP), negative regulation of transcription from RNA polymerase II promoter (BP), negative regulation of transcription, DNA-dependent (BP), protein ubiquitination (BP), enzyme binding	3 (73)	3 (34208)	9,32E-09	4,44E-08	SIRT1,UBE2I,MDM2

GO term ID	Annotations	# of annotated genes in the input list (Total # of genes in the input list)	# of annotated genes in the reference list (Total # of genes in the reference list)	Hypergeometric Distribution (Fisher's exact test)	Corrected Hypergeometric Dist. (Fisher's exact test)	Genes
	(MF)					
GO:0005515,GO:0044419,GO:0045892,GO:0019899,GO:0006461	protein binding (MF), interspecies interaction between organisms (BP), negative regulation of transcription, DNA-dependent (BP), enzyme binding (MF), protein complex assembly (BP)	3 (73)	3 (34208)	9,32E-09	4,44E-08	MDM2,TP53,HMGA1
GO:0005515,GO:0045944,GO:0030154,GO:0071456	protein binding (MF), positive regulation of transcription from RNA polymerase II promoter (BP), cell differentiation (BP), cellular response to hypoxia (BP)	3 (73)	3 (34208)	9,32E-09	4,44E-08	SIRT1,HIF1A,TP53
GO:0005515,GO:0003684,GO:0003824,GO:0006281,GO:0006284	protein binding (MF), damaged DNA binding (MF), catalytic activity (MF), DNA repair (BP), base-excision repair (BP)	3 (73)	3 (34208)	9,32E-09	4,44E-08	OGG1,MPG,POLB
GO:0005515,GO:0045892,GO:0006281,GO:0008022	protein binding (MF), negative regulation of transcription, DNA-dependent (BP), DNA repair (BP), protein C-terminus binding (MF)	3 (73)	3 (34208)	9,32E-09	4,44E-08	XRCC6,SIRT1,XRCC5
GO:0005515,GO:0003824,GO:0006281,GO:0006284,GO:0006285,GO:0045007	protein binding (MF), catalytic activity (MF), DNA repair (BP), base-excision repair (BP), base-excision repair, AP site formation (BP), depurination (BP)	3 (73)	3 (34208)	9,32E-09	4,44E-08	MUTYH,OGG1,MPG
GO:0005515,GO:0030154,GO:0042802,GO:0042981	protein binding (MF), cell differentiation (BP), identical protein binding (MF), regulation of apoptotic process (BP)	3 (73)	3 (34208)	9,32E-09	4,44E-08	SIRT1,TP53,NME1

GO term ID	Annotations	# of annotated genes in the input list (Total # of genes in the input list)	# of annotated genes in the reference list (Total # of genes in the reference list)	Hypergeometric Distribution (Fisher's exact test)	Corrected Hypergeometric Dist. (Fisher's exact test)	Genes
GO:0046872,GO:0008270,GO:0006915,GO:0005515,GO:0045944,GO:0000122	metal ion binding (MF), zinc ion binding (MF), apoptotic process (BP), protein binding (MF), positive regulation of transcription from RNA polymerase II promoter (BP), negative regulation of transcription from RNA polymerase II promoter (BP)	3 (73)	4 (34208)	3,72E-08	1,36E-07	TRAF6,TP53,EP300
GO:0046872,GO:0008270,GO:0005515,GO:0045944,GO:0019899,GO:0042981	metal ion binding (MF), zinc ion binding (MF), protein binding (MF), positive regulation of transcription from RNA polymerase II promoter (BP), enzyme binding (MF), regulation of apoptotic process (BP)	3 (73)	4 (34208)	3,72E-08	1,36E-07	SIRT1,TP53,ESR1
GO:0046872,GO:0008270,GO:0005515,GO:0000122,GO:0045892,GO:0016567	metal ion binding (MF), zinc ion binding (MF), protein binding (MF), negative regulation of transcription from RNA polymerase II promoter (BP), negative regulation of transcription, DNA-dependent (BP), protein ubiquitination (BP)	3 (73)	4 (34208)	3,72E-08	1,36E-07	SIRT1,TRAF6,MDM2
GO:0046872,GO:0005515,GO:0019899,GO:0006974	metal ion binding (MF), protein binding (MF), enzyme binding (MF), response to DNA damage stimulus (BP)	3 (73)	4 (34208)	3,72E-08	1,36E-07	SIRT1,TP53,POLB
GO:0003677,GO:0005515,GO:0003684,GO:0006281,GO:0006284	DNA binding (MF), protein binding (MF), damaged DNA binding (MF), DNA repair (BP), base-excision repair (BP)	3 (73)	4 (34208)	3,72E-08	1,36E-07	MPG,FEN1,POLB
GO:0006468,GO:0005524,GO:0005515,GO:0000166,GO:0046777,GO:0004674,GO:0007411	protein phosphorylation (BP), ATP binding (MF), protein binding (MF), nucleotide binding (MF), protein autophosphorylation (BP), protein serine/threonine kinase	3 (73)	4 (34208)	3,72E-08	1,36E-07	CSNK2A1,Cdk5,PAK2

GO term ID	Annotations	# of annotated genes in the input list (Total # of genes in the input list)	# of annotated genes in the reference list (Total # of genes in the reference list)	Hypergeometric Distribution (Fisher's exact test)	Corrected Hypergeometric Dist. (Fisher's exact test)	Genes
	activity (MF), axon guidance (BP)					
GO:0005524,GO:0005515,GO:0000166,GO:0045892,GO:0008022	ATP binding (MF), protein binding (MF), nucleotide binding (MF), negative regulation of transcription, DNA-dependent (BP), protein C-terminus binding (MF)	3 (73)	4 (34208)	3,72E-08	1,36E-07	XRCC6,UBE2I,XRCC5
GO:0005515,GO:0044419,GO:0042802,GO:0042981	protein binding (MF), interspecies interaction between organisms (BP), identical protein binding (MF), regulation of apoptotic process (BP)	3 (73)	4 (34208)	3,72E-08	1,36E-07	SIRT1,TP53,PAK2
GO:0005515,GO:0045892,GO:0042981,GO:0002039	protein binding (MF), negative regulation of transcription, DNA-dependent (BP), regulation of apoptotic process (BP), p53 binding (MF)	3 (73)	4 (34208)	3,72E-08	1,36E-07	SIRT1,TP53,Cdk5
GO:0045944,GO:0000122,GO:0060766	positive regulation of transcription from RNA polymerase II promoter (BP), negative regulation of transcription from RNA polymerase II promoter (BP), negative regulation of androgen receptor signaling pathway (BP)	3 (73)	4 (34208)	3,72E-08	1,36E-07	SIRT1,TCF21,HDAC1
GO:0006355,GO:0046872,GO:0003677,GO:0008270,GO:0005515,GO:0045944,GO:0008134,GO:0003682	regulation of transcription, DNA-dependent (BP), metal ion binding (MF), DNA binding (MF), zinc ion binding (MF), protein binding (MF), positive regulation of transcription from RNA polymerase II promoter (BP), transcription factor binding (MF), chromatin binding (MF)	3 (73)	5 (34208)	9,29E-08	2,74E-07	TP53,ESR1,EP300

GO term ID	Annotations	# of annotated genes in the input list (Total # of genes in the input list)	# of annotated genes in the reference list (Total # of genes in the reference list)	Hypergeometric Distribution (Fisher's exact test)	Corrected Hypergeometric Dist. (Fisher's exact test)	Genes
GO:0006355,GO:0003677,GO:0003700,GO:0005515,GO:0008134,GO:0019899	regulation of transcription, DNA-dependent (BP), DNA binding (MF), sequence-specific DNA binding transcription factor activity (MF), protein binding (MF), transcription factor binding (MF), enzyme binding (MF)	3 (73)	5 (34208)	9,29E-08	2,74E-07	TP53,ESR1,HMGA1
GO:0006355,GO:0003700,GO:0005515,GO:0045944,GO:0008134,GO:0019899	regulation of transcription, DNA-dependent (BP), sequence-specific DNA binding transcription factor activity (MF), protein binding (MF), positive regulation of transcription from RNA polymerase II promoter (BP), transcription factor binding (MF), enzyme binding (MF)	3 (73)	5 (34208)	9,29E-08	2,74E-07	TP53,ESR1,HDAC1
GO:0003677,GO:0005515,GO:0008134,GO:0006284	DNA binding (MF), protein binding (MF), transcription factor binding (MF), base-excision repair (BP)	3 (73)	5 (34208)	9,29E-08	2,74E-07	TP53,PCNA,HMGA1
GO:0006915,GO:0005515,GO:0019901,GO:0042981	apoptotic process (BP), protein binding (MF), protein kinase binding (MF), regulation of apoptotic process (BP)	3 (73)	5 (34208)	9,29E-08	2,74E-07	TRAF6,TP53,PAK2
GO:0005515,GO:0044419,GO:0007569	protein binding (MF), interspecies interaction between organisms (BP), cell aging (BP)	3 (73)	5 (34208)	9,29E-08	2,74E-07	SIRT1,NPM1,TP53
GO:0005515,GO:0000122,GO:0045892,GO:0016874,GO:0004842,GO:0016567	protein binding (MF), negative regulation of transcription from RNA polymerase II promoter (BP), negative regulation of transcription, DNA-dependent (BP), ligase activity (MF), ubiquitin-protein ligase activity (MF), protein ubiquitination (BP)	3 (73)	5 (34208)	9,29E-08	2,74E-07	UBE2I,TRAF6,MDM2

GO term ID	Annotations	# of annotated genes in the input list (Total # of genes in the input list)	# of annotated genes in the reference list (Total # of genes in the reference list)	Hypergeometric Distribution (Fisher's exact test)	Corrected Hypergeometric Dist. (Fisher's exact test)	Genes
GO:0005515,GO:0006281,GO:0004519,GO:0006284	protein binding (MF), DNA repair (BP), endonuclease activity (MF), base-excision repair (BP)	3 (73)	5 (34208)	9,29E-08	2,74E-07	MUTYH,OGG1,FEN1
GO:0005515,GO:0006281,GO:0016829	protein binding (MF), DNA repair (BP), lyase activity (MF)	3 (73)	5 (34208)	9,29E-08	2,74E-07	XRCC6,OGG1,POLB
GO:0006355,GO:0005515,GO:0044419,GO:0045944,GO:0008134,GO:0000122	regulation of transcription, DNA-dependent (BP), protein binding (MF), interspecies interaction between organisms (BP), positive regulation of transcription from RNA polymerase II promoter (BP), transcription factor binding (MF), negative regulation of transcription from RNA polymerase II promoter (BP)	3 (73)	6 (34208)	1,86E-07	4,74E-07	TP53,HDAC1,EP300
GO:0006355,GO:0005515,GO:0006284	regulation of transcription, DNA-dependent (BP), protein binding (MF), base-excision repair (BP)	3 (73)	6 (34208)	1,86E-07	4,74E-07	OGG1,TP53,HMGA1
GO:0006355,GO:0005515,GO:0050790	regulation of transcription, DNA-dependent (BP), protein binding (MF), regulation of catalytic activity (BP)	3 (73)	6 (34208)	1,86E-07	4,74E-07	HIF1A,TP53,CSNK2A1
GO:0006915,GO:0005515,GO:0050852,GO:0042981	apoptotic process (BP), protein binding (MF), T cell receptor signaling pathway (BP), regulation of apoptotic process (BP)	3 (73)	6 (34208)	1,86E-07	4,74E-07	TRAF6,UBC,PAK2
GO:0005524,GO:0005515,GO:0042802,GO:0042981	ATP binding (MF), protein binding (MF), identical protein binding (MF), regulation of apoptotic process (BP)	3 (73)	6 (34208)	1,86E-07	4,74E-07	TP53,PAK2,NME1
GO:0005515,GO:0000166,GO:0000398,GO:0008380,GO:0003723,GO:0010467,GO:0003676,GO:0006396	protein binding (MF), nucleotide binding (MF), nuclear mRNA splicing, via spliceosome (BP), RNA splicing (BP), RNA binding (MF), gene expression (BP), nucleic acid binding	3 (73)	6 (34208)	1,86E-07	4,74E-07	HNRNPL,HNRNPU,HNRNPH1

GO term ID	Annotations	# of annotated genes in the input list (Total # of genes in the input list)	# of annotated genes in the reference list (Total # of genes in the reference list)	Hypergeometric Distribution (Fisher's exact test)	Corrected Hypergeometric Dist. (Fisher's exact test)	Genes
	(MF), RNA processing (BP)					
GO:0005515,GO:0045944,GO:0045892,GO:0006974	protein binding (MF), positive regulation of transcription from RNA polymerase II promoter (BP), negative regulation of transcription, DNA-dependent (BP), response to DNA damage stimulus (BP)	3 (73)	6 (34208)	1,86E-07	4,74E-07	XRCC6,SIRT1,TP53
GO:0005515,GO:0000122,GO:0045892,GO:0048011	protein binding (MF), negative regulation of transcription from RNA polymerase II promoter (BP), negative regulation of transcription, DNA-dependent (BP), nerve growth factor receptor signaling pathway (BP)	3 (73)	6 (34208)	1,86E-07	4,74E-07	TRAF6,MDM2,HDAC1
GO:0005515,GO:0006281,GO:0006916	protein binding (MF), DNA repair (BP), anti-apoptosis (BP)	3 (73)	6 (34208)	1,86E-07	4,74E-07	NPM1,UBC,POLB
GO:0005515,GO:0004842,GO:0048011	protein binding (MF), ubiquitin-protein ligase activity (MF), nerve growth factor receptor signaling pathway (BP)	3 (73)	6 (34208)	1,86E-07	4,74E-07	TRAF6,MDM2,UBC
GO:0006355,GO:0005515,GO:0008013	regulation of transcription, DNA-dependent (BP), protein binding (MF), beta-catenin binding (MF)	3 (73)	7 (34208)	3,24E-07	7,59E-07	CSNK2A1,ESR1,EP300
GO:0016740,GO:0005524,GO:0000166,GO:0016301,GO:0000287	transferase activity (MF), ATP binding (MF), nucleotide binding (MF), kinase activity (MF), magnesium ion binding (MF)	3 (73)	7 (34208)	3,24E-07	7,59E-07	PRPS1,PRPS2,NME1
GO:0046872,GO:0005515,GO:0006284	metal ion binding (MF), protein binding (MF), base-excision repair (BP)	3 (73)	8 (34208)	5,18E-07	1,12E-06	MUTYH,TP53,POLB

GO term ID	Annotations	# of annotated genes in the input list (Total # of genes in the input list)	# of annotated genes in the reference list (Total # of genes in the reference list)	Hypergeometric Distribution (Fisher's exact test)	Corrected Hypergeometric Dist. (Fisher's exact test)	Genes
GO:0003677,GO:0005515,GO:0003690,GO:0045892,GO:0044212	DNA binding (MF), protein binding (MF), double-stranded DNA binding (MF), negative regulation of transcription, DNA-dependent (BP), transcription regulatory region DNA binding (MF)	3 (73)	8 (34208)	5,18E-07	1,12E-06	XRCC6,HMGB2,XRCC5
GO:0003677,GO:0005515,GO:0048015	DNA binding (MF), protein binding (MF), phosphatidylinositol-mediated signaling (BP)	3 (73)	8 (34208)	5,18E-07	1,12E-06	HMGB2,PCNA,FEN1
GO:0005524,GO:0007596,GO:0007049	ATP binding (MF), blood coagulation (BP), cell cycle (BP)	3 (73)	8 (34208)	5,18E-07	1,12E-06	KIF11,TP53,Cdk5
GO:0005515,GO:0006281,GO:0042802	protein binding (MF), DNA repair (BP), identical protein binding (MF)	3 (73)	8 (34208)	5,18E-07	1,12E-06	SIRT1,PCNA,PRPF19
GO:0005515,GO:0006289,GO:0006284	protein binding (MF), nucleotide-excision repair (BP), base-excision repair (BP)	3 (73)	8 (34208)	5,18E-07	1,12E-06	OGG1,TP53,PCNA
GO:0000122,GO:0043425	negative regulation of transcription from RNA polymerase II promoter (BP), bHLH transcription factor binding (MF)	3 (73)	8 (34208)	5,18E-07	1,12E-06	SIRT1,UBE2I,TCF21
GO:0005524,GO:0005515,GO:0047485	ATP binding (MF), protein binding (MF), protein N-terminus binding (MF)	3 (73)	9 (34208)	7,76E-07	1,60E-06	TP53,CSNK2A1,HSPA1A
GO:0005515,GO:0000166,GO:0044212	protein binding (MF), nucleotide binding (MF), transcription regulatory region DNA binding (MF)	3 (73)	9 (34208)	7,76E-07	1,60E-06	XRCC6,HNRNPL,XRCC5
GO:0005515,GO:0007596,GO:0042981	protein binding (MF), blood coagulation (BP), regulation of apoptotic process (BP)	3 (73)	9 (34208)	7,76E-07	1,60E-06	TP53,Cdk5,ACTN1
GO:0005515,GO:0046982,GO:0019901	protein binding (MF), protein heterodimerization activity (MF), protein kinase binding (MF)	3 (73)	10 (34208)	1,11E-06	2,13E-06	NPM1,HIF1A,TP53
GO:0006355,GO:0003677,GO:0005515,GO:0044419,GO:0008134	regulation of transcription, DNA-dependent (BP), DNA binding (MF), protein binding	3 (73)	11 (34208)	1,52E-06	2,81E-06	TP53,EP300,HMGA1

GO term ID	Annotations	# of annotated genes in the input list (Total # of genes in the input list)	# of annotated genes in the reference list (Total # of genes in the reference list)	Hypergeometric Distribution (Fisher's exact test)	Corrected Hypergeometric Dist. (Fisher's exact test)	Genes
	(MF), interspecies interaction between organisms (BP), transcription factor binding (MF)					
GO:0006355,GO:0045944,GO:0042826	regulation of transcription, DNA-dependent (BP), positive regulation of transcription from RNA polymerase II promoter (BP), histone deacetylase binding (MF)	3 (73)	11 (34208)	1,52E-06	2,81E-06	HIF1A,TCF21,HDAC1
GO:0003677,GO:0005515,GO:0000166,GO:0008022	DNA binding (MF), protein binding (MF), nucleotide binding (MF), protein C-terminus binding (MF)	3 (73)	11 (34208)	1,52E-06	2,81E-06	XRCC6,XRCC5,NCL
GO:0006915,GO:0005515,GO:0045944,GO:0045892	apoptotic process (BP), protein binding (MF), positive regulation of transcription from RNA polymerase II promoter (BP), negative regulation of transcription, DNA-dependent (BP)	3 (73)	11 (34208)	1,52E-06	2,81E-06	TRAF6,HMGB2,TP53
GO:0005515,GO:0016925	protein binding (MF), protein sumoylation (BP)	3 (73)	11 (34208)	1,52E-06	2,81E-06	UBE2I,SUMO2,SUMO1
GO:0045944,GO:0000122,GO:0042826	positive regulation of transcription from RNA polymerase II promoter (BP), negative regulation of transcription from RNA polymerase II promoter (BP), histone deacetylase binding (MF)	3 (73)	11 (34208)	1,52E-06	2,81E-06	TRAF6,TCF21,HDAC1
GO:0005524,GO:0045944,GO:0045893	ATP binding (MF), positive regulation of transcription from RNA polymerase II promoter (BP), positive regulation of transcription, DNA-dependent (BP)	3 (73)	12 (34208)	2,02E-06	3,62E-06	XRCC6,TP53,THRAP3
GO:0005515,GO:0045087,GO:0000122	protein binding (MF), innate immune response (BP), negative regulation of transcription from	3 (73)	12 (34208)	2,02E-06	3,62E-06	TRAF6,TXN,EP300

GO term ID	Annotations	# of annotated genes in the input list (Total # of genes in the input list)	# of annotated genes in the reference list (Total # of genes in the reference list)	Hypergeometric Distribution (Fisher's exact test)	Corrected Hypergeometric Dist. (Fisher's exact test)	Genes
	RNA polymerase II promoter (BP)					
GO:0005515,GO:0000122,GO:0042802	protein binding (MF), negative regulation of transcription from RNA polymerase II promoter (BP), identical protein binding (MF)	3 (73)	12 (34208)	2,02E-06	3,62E-06	SIRT1,TP53,PCNA
GO:0005515,GO:0000122,GO:0051091	protein binding (MF), negative regulation of transcription from RNA polymerase II promoter (BP), positive regulation of sequence-specific DNA binding transcription factor activity (BP)	3 (73)	12 (34208)	2,02E-06	3,62E-06	UBE2I,TRAF6,EP300
GO:0046872,GO:0003677,GO:0005515,GO:0019899	metal ion binding (MF), DNA binding (MF), protein binding (MF), enzyme binding (MF)	3 (73)	15 (34208)	4,16E-06	6,84E-06	TP53,ESR1,POLB
GO:0003677,GO:0006915,GO:0005515,GO:0045944	DNA binding (MF), apoptotic process (BP), protein binding (MF), positive regulation of transcription from RNA polymerase II promoter (BP)	3 (73)	15 (34208)	4,16E-06	6,84E-06	HMGB2,TP53,EP300
GO:0005515,GO:0045892,GO:0007596	protein binding (MF), negative regulation of transcription, DNA-dependent (BP), blood coagulation (BP)	3 (73)	15 (34208)	4,16E-06	6,84E-06	TP53,HDAC1,Cdk5
GO:0006355,GO:0003700,GO:0005515,GO:0000122,GO:0045892	regulation of transcription, DNA-dependent (BP), sequence-specific DNA binding transcription factor activity (MF), protein binding (MF), negative regulation of transcription from RNA polymerase II promoter (BP), negative regulation of transcription, DNA-dependent (BP)	3 (73)	16 (34208)	5,12E-06	8,13E-06	TP53,HDAC1,YBX1
GO:0003677,GO:0005515,GO:0008380,GO:0003723	DNA binding (MF), protein binding (MF), RNA splicing (BP), RNA binding (MF)	3 (73)	16 (34208)	5,12E-06	8,13E-06	HNRNPU,YBX1,SFPQ

GO term ID	Annotations	# of annotated genes in the input list (Total # of genes in the input list)	# of annotated genes in the reference list (Total # of genes in the reference list)	Hypergeometric Distribution (Fisher's exact test)	Corrected Hypergeometric Dist. (Fisher's exact test)	Genes
GO:0005515,GO:0044419,GO:0019901	protein binding (MF), interspecies interaction between organisms (BP), protein kinase binding (MF)	3 (73)	16 (34208)	5,12E-06	8,13E-06	NPM1,TP53,PAK2
GO:0003677,GO:0005515,GO:0000398,GO:0008380	DNA binding (MF), protein binding (MF), nuclear mRNA splicing, via spliceosome (BP), RNA splicing (BP)	3 (73)	17 (34208)	6,21E-06	9,58E-06	HNRNPU,PRPF19,YBX1
GO:0005515,GO:0044419,GO:0008285	protein binding (MF), interspecies interaction between organisms (BP), negative regulation of cell proliferation (BP)	3 (73)	18 (34208)	7,43E-06	1,12E-05	NPM1,TP53,HMGA1
GO:0005515,GO:0045892,GO:0019904	protein binding (MF), negative regulation of transcription, DNA-dependent (BP), protein domain specific binding (MF)	3 (73)	18 (34208)	7,43E-06	1,12E-05	SIRT1,HMGB2,BASP1
GO:0005515,GO:0051092,GO:0006916	protein binding (MF), positive regulation of NF-kappaB transcription factor activity (BP), anti-apoptosis (BP)	3 (73)	18 (34208)	7,43E-06	1,12E-05	NPM1,TRAF6,UBC
GO:0006355,GO:0003700,GO:0005515,GO:0045944,GO:0008134,GO:0045893	regulation of transcription, DNA-dependent (BP), sequence-specific DNA binding transcription factor activity (MF), protein binding (MF), positive regulation of transcription from RNA polymerase II promoter (BP), transcription factor binding (MF), positive regulation of transcription, DNA-dependent (BP)	3 (73)	19 (34208)	8,82E-06	1,30E-05	HIF1A,TP53,HDAC1
GO:0005515,GO:0045944,GO:0042826	protein binding (MF), positive regulation of transcription from RNA polymerase II promoter (BP), histone deacetylase binding (MF)	3 (73)	19 (34208)	8,82E-06	1,30E-05	TRAF6,HIF1A,HDAC1

GO term ID	Annotations	# of annotated genes in the input list (Total # of genes in the input list)	# of annotated genes in the reference list (Total # of genes in the reference list)	Hypergeometric Distribution (Fisher's exact test)	Corrected Hypergeometric Dist. (Fisher's exact test)	Genes
GO:0005515,GO:0003723,GO:0010467,GO:0044267,GO:0006412,GO:0016070,GO:0016071	protein binding (MF), RNA binding (MF), gene expression (BP), cellular protein metabolic process (BP), translation (BP), RNA metabolic process (BP), mRNA metabolic process (BP)	3 (73)	19 (34208)	8,82E-06	1,30E-05	RPL14,PABPC1,RPLP0
GO:0005524,GO:0005515,GO:0000166,GO:0016032	ATP binding (MF), protein binding (MF), nucleotide binding (MF), viral reproduction (BP)	3 (73)	20 (34208)	1,04E-05	1,53E-05	XRCC6,PAK2,XRCC5
GO:0006355,GO:0003677,GO:0003700,GO:0005515,GO:0008134,GO:0045893	regulation of transcription, DNA-dependent (BP), DNA binding (MF), sequence-specific DNA binding transcription factor activity (MF), protein binding (MF), transcription factor binding (MF), positive regulation of transcription, DNA-dependent (BP)	3 (73)	21 (34208)	1,21E-05	1,72E-05	HIF1A,TP53,HMGA1
GO:0003677,GO:0005515,GO:0045944,GO:0045892,GO:0045893,GO:0044212	DNA binding (MF), protein binding (MF), positive regulation of transcription from RNA polymerase II promoter (BP), negative regulation of transcription, DNA-dependent (BP), positive regulation of transcription, DNA-dependent (BP), transcription regulatory region DNA binding (MF)	3 (73)	21 (34208)	1,21E-05	1,72E-05	XRCC6,HMGB2,TP53
GO:0005515,GO:0006281,GO:0016032	protein binding (MF), DNA repair (BP), viral reproduction (BP)	3 (73)	21 (34208)	1,21E-05	1,72E-05	XRCC6,UBC,XRCC5
GO:0003677,GO:0005515,GO:0000166,GO:0003723	DNA binding (MF), protein binding (MF), nucleotide binding (MF), RNA binding (MF)	3 (73)	22 (34208)	1,39E-05	1,95E-05	HNRNPU,NCL,SFPQ
GO:0008283,GO:0005515,GO:0000122	cell proliferation (BP), protein binding (MF), negative regulation of transcription from RNA polymerase II promoter (BP)	3 (73)	22 (34208)	1,39E-05	1,95E-05	TXN,TP53,PCNA

GO term ID	Annotations	# of annotated genes in the input list (Total # of genes in the input list)	# of annotated genes in the reference list (Total # of genes in the reference list)	Hypergeometric Distribution (Fisher's exact test)	Corrected Hypergeometric Dist. (Fisher's exact test)	Genes
GO:0005515,GO:0042493,GO:0008285	protein binding (MF), response to drug (BP), negative regulation of cell proliferation (BP)	3 (73)	22 (34208)	1,39E-05	1,95E-05	CDKN1A,TP53,NME1
GO:0006355,GO:0003677,GO:0003700,GO:0005515,GO:0045944,GO:0008134	regulation of transcription, DNA-dependent (BP), DNA binding (MF), sequence-specific DNA binding transcription factor activity (MF), protein binding (MF), positive regulation of transcription from RNA polymerase II promoter (BP), transcription factor binding (MF)	3 (73)	23 (34208)	1,60E-05	2,18E-05	HIF1A,TP53,ESR1
GO:0003677,GO:0005515,GO:0042802	DNA binding (MF), protein binding (MF), identical protein binding (MF)	3 (73)	23 (34208)	1,60E-05	2,18E-05	TP53,PCNA,PRPF19
GO:0005515,GO:0010467,GO:0006414,GO:0031018,GO:0044267,GO:0006412,GO:0016070,GO:0016032,GO:0016071,GO:0006415,GO:0019058,GO:0019083,GO:0003735	protein binding (MF), gene expression (BP), translational elongation (BP), endocrine pancreas development (BP), cellular protein metabolic process (BP), translation (BP), RNA metabolic process (BP), viral reproduction (BP), mRNA metabolic process (BP), translational termination (BP), viral infectious cycle (BP), viral transcription (BP), structural constituent of ribosome (MF)	3 (73)	23 (34208)	1,60E-05	2,18E-05	RPL14,RPSA,RPLP0
GO:0005515,GO:0008285,GO:0030308	protein binding (MF), negative regulation of cell proliferation (BP), negative regulation of cell growth (BP)	3 (73)	23 (34208)	1,60E-05	2,18E-05	CDKN1A,TP53,HSPA1A
GO:0005515,GO:0006281,GO:0000278,GO:0000084	protein binding (MF), DNA repair (BP), mitotic cell cycle (BP), S phase of mitotic cell cycle (BP)	3 (73)	23 (34208)	1,60E-05	2,18E-05	UBC,PCNA,FEN1

GO term ID	Annotations	# of annotated genes in the input list (Total # of genes in the input list)	# of annotated genes in the reference list (Total # of genes in the reference list)	Hypergeometric Distribution (Fisher's exact test)	Corrected Hypergeometric Dist. (Fisher's exact test)	Genes
GO:0005524,GO:0005515,GO:0000166,GO:0042981	ATP binding (MF), protein binding (MF), nucleotide binding (MF), regulation of apoptotic process (BP)	3 (73)	24 (34208)	1,83E-05	2,48E-05	Cdk5,PAK2,NME1
GO:0006355,GO:0003677,GO:0003700,GO:0005515,GO:0045892	regulation of transcription, DNA-dependent (BP), DNA binding (MF), sequence-specific DNA binding transcription factor activity (MF), protein binding (MF), negative regulation of transcription, DNA-dependent (BP)	3 (73)	25 (34208)	2,07E-05	2,79E-05	TP53,YBX1,HMGA1
GO:0005515,GO:0048011,GO:0006916	protein binding (MF), nerve growth factor receptor signaling pathway (BP), anti-apoptosis (BP)	3 (73)	25 (34208)	2,07E-05	2,79E-05	TRAF6,UBC,HDAC1
GO:0003677,GO:0005515,GO:0006974	DNA binding (MF), protein binding (MF), response to DNA damage stimulus (BP)	3 (73)	26 (34208)	2,34E-05	3,10E-05	XRCC6,TP53,POLB
GO:0005524,GO:0005515,GO:0008285	ATP binding (MF), protein binding (MF), negative regulation of cell proliferation (BP)	3 (73)	26 (34208)	2,34E-05	3,10E-05	TP53,NME1,HSPA1A
GO:0005515,GO:0032436	protein binding (MF), positive regulation of proteasomal ubiquitin-dependent protein catabolic process (BP)	3 (73)	27 (34208)	2,63E-05	3,46E-05	MDM2,SUMO2,SUMO1
GO:0005515,GO:0006334	protein binding (MF), nucleosome assembly (BP)	3 (73)	28 (34208)	2,94E-05	3,85E-05	NPM1,HMGB2,SET
GO:0003677,GO:0008283,GO:0005515	DNA binding (MF), cell proliferation (BP), protein binding (MF)	3 (73)	29 (34208)	3,27E-05	4,25E-05	TP53,PCNA,XRCC5
GO:0007165,GO:0005515,GO:0042981	signal transduction (BP), protein binding (MF), regulation of apoptotic process (BP)	3 (73)	29 (34208)	3,27E-05	4,25E-05	TRAF6,ESR1,PAK2
GO:0003677,GO:0005515,GO:0000166,GO:0006281	DNA binding (MF), protein binding (MF), nucleotide binding (MF), DNA repair (BP)	3 (73)	30 (34208)	3,63E-05	4,64E-05	XRCC6,XRCC5,SFPQ

GO term ID	Annotations	# of annotated genes in the input list (Total # of genes in the input list)	# of annotated genes in the reference list (Total # of genes in the reference list)	Hypergeometric Distribution (Fisher's exact test)	Corrected Hypergeometric Dist. (Fisher's exact test)	Genes
GO:0005515,GO:0051015	protein binding (MF), actin filament binding (MF)	3 (73)	30 (34208)	3,63E-05	4,64E-05	SPTA1,MYH9,ACTN1
GO:0003677,GO:0003700,GO:0005515,GO:0045892,GO:0045893	DNA binding (MF), sequence-specific DNA binding transcription factor activity (MF), protein binding (MF), negative regulation of transcription, DNA-dependent (BP), positive regulation of transcription, DNA-dependent (BP)	3 (73)	31 (34208)	4,01E-05	5,05E-05	HMGB2,TP53,HMGA1
GO:0005515,GO:0006281,GO:0006974	protein binding (MF), DNA repair (BP), response to DNA damage stimulus (BP)	3 (73)	31 (34208)	4,01E-05	5,05E-05	XRCC6,SIRT1,POLB
GO:0006355,GO:0005515,GO:0007049	regulation of transcription, DNA-dependent (BP), protein binding (MF), cell cycle (BP)	3 (73)	32 (34208)	4,42E-05	5,45E-05	TP53,CSNK2A1,EP300
GO:0006915,GO:0005515,GO:0045087	apoptotic process (BP), protein binding (MF), innate immune response (BP)	3 (73)	32 (34208)	4,42E-05	5,45E-05	TRAF6,UBC,EP300
GO:0005515,GO:0045944,GO:0019901	protein binding (MF), positive regulation of transcription from RNA polymerase II promoter (BP), protein kinase binding (MF)	3 (73)	32 (34208)	4,42E-05	5,45E-05	TRAF6,HIF1A,TP53
GO:0006355,GO:0003677,GO:0045944,GO:0000122	regulation of transcription, DNA-dependent (BP), DNA binding (MF), positive regulation of transcription from RNA polymerase II promoter (BP), negative regulation of transcription from RNA polymerase II promoter (BP)	3 (73)	34 (34208)	5,32E-05	6,48E-05	TP53,TCF21,EP300
GO:0005515,GO:0006281,GO:0016787	protein binding (MF), DNA repair (BP), hydrolase activity (MF)	3 (73)	34 (34208)	5,32E-05	6,48E-05	XRCC6,MUTYH,MPG
GO:0006915,GO:0005515,GO:0044419	apoptotic process (BP), protein binding (MF), interspecies interaction between organisms (BP)	3 (73)	35 (34208)	5,81E-05	6,99E-05	TP53,EP300,PAK2

GO term ID	Annotations	# of annotated genes in the input list (Total # of genes in the input list)	# of annotated genes in the reference list (Total # of genes in the reference list)	Hypergeometric Distribution (Fisher's exact test)	Corrected Hypergeometric Dist. (Fisher's exact test)	Genes
GO:0003700,GO:0005515,GO:0045944,GO:0045892,GO:0045893	sequence-specific DNA binding transcription factor activity (MF), protein binding (MF), positive regulation of transcription from RNA polymerase II promoter (BP), negative regulation of transcription, DNA-dependent (BP), positive regulation of transcription, DNA-dependent (BP)	3 (73)	35 (34208)	5,81E-05	6,99E-05	HMGB2,TP53,HDAC1
GO:0005524,GO:0005515,GO:0044419	ATP binding (MF), protein binding (MF), interspecies interaction between organisms (BP)	3 (73)	35 (34208)	5,81E-05	6,99E-05	UBE2I,TP53,PAK2
GO:0005524,GO:0000166,GO:0007049,GO:0051301	ATP binding (MF), nucleotide binding (MF), cell cycle (BP), cell division (BP)	3 (73)	35 (34208)	5,81E-05	6,99E-05	UBE2I,KIF11,Cdk5
GO:0005515,GO:0045087,GO:0002218	protein binding (MF), innate immune response (BP), activation of innate immune response (BP)	3 (73)	36 (34208)	6,33E-05	7,56E-05	TRAF6,TXN,UBC
GO:0003677,GO:0005515,GO:0008134,GO:0000122	DNA binding (MF), protein binding (MF), transcription factor binding (MF), negative regulation of transcription from RNA polymerase II promoter (BP)	3 (73)	37 (34208)	6,88E-05	8,17E-05	TP53,PCNA,EP300
GO:0003677,GO:0003700,GO:0005515,GO:0045944,GO:0045893,GO:0044212	DNA binding (MF), sequence-specific DNA binding transcription factor activity (MF), protein binding (MF), positive regulation of transcription from RNA polymerase II promoter (BP), positive regulation of transcription, DNA-dependent (BP), transcription regulatory region DNA binding (MF)	3 (73)	39 (34208)	8,06E-05	9,49E-05	HMGB2,HIF1A,TP53
GO:0005515,GO:0000209,GO:0004842	protein binding (MF), protein polyubiquitination (BP), ubiquitin-protein ligase activity (MF)	3 (73)	40 (34208)	8,70E-05	0,000101801	TRAF6,UBC,PRPF19

GO term ID	Annotations	# of annotated genes in the input list (Total # of genes in the input list)	# of annotated genes in the reference list (Total # of genes in the reference list)	Hypergeometric Distribution (Fisher's exact test)	Corrected Hypergeometric Dist. (Fisher's exact test)	Genes
GO:0005515,GO:0006979	protein binding (MF), response to oxidative stress (BP)	3 (73)	40 (34208)	8,70E-05	0,000101801	SIRT1,PRDX6,OGG1
GO:0005515,GO:0042393	protein binding (MF), histone binding (MF)	3 (73)	41 (34208)	9,38E-05	0,000109338	SIRT1,NPM1,SET
GO:0046872,GO:0005515,GO:0006281	metal ion binding (MF), protein binding (MF), DNA repair (BP)	3 (73)	43 (34208)	0,000108212	0,000125435	SIRT1,MUTYH,POLB
GO:0003779,GO:0005516	actin binding (MF), calmodulin binding (MF)	3 (73)	44 (34208)	0,000115953	0,000134005	MYO1C,MYH9,SPTBN1
GO:0005515,GO:0006281,GO:0006260	protein binding (MF), DNA repair (BP), DNA replication (BP)	3 (73)	45 (34208)	0,000124045	0,000142081	SIRT1,PCNA,FEN1
GO:0005515,GO:0005200	protein binding (MF), structural constituent of cytoskeleton (MF)	3 (73)	45 (34208)	0,000124045	0,000142081	MSN,SPTA1,SPTBN1
GO:0005515,GO:0044419,GO:0016032	protein binding (MF), interspecies interaction between organisms (BP), viral reproduction (BP)	3 (73)	48 (34208)	0,000150504	0,00017137	PAK2,RPLP0,HMGA1
GO:0007165,GO:0005515,GO:0045944	signal transduction (BP), protein binding (MF), positive regulation of transcription from RNA polymerase II promoter (BP)	3 (73)	49 (34208)	0,000160074	0,000181731	TRAF6,HIF1A,ESR1
GO:0007399,GO:0000166	nervous system development (BP), nucleotide binding (MF)	3 (73)	51 (34208)	0,000180382	0,000204186	PRPS1,NME1,ARF6
GO:0005524,GO:0019901	ATP binding (MF), protein kinase binding (MF)	3 (73)	53 (34208)	0,000202291	0,000227652	KIF11,TP53,PAK2
GO:0006355,GO:0003677,GO:0005515,GO:0000122	regulation of transcription, DNA-dependent (BP), DNA binding (MF), protein binding (MF), negative regulation of transcription from RNA polymerase II promoter (BP)	3 (73)	57 (34208)	0,000251129	0,000279353	TP53,EP300,YBX1
GO:0005515,GO:0000278,GO:0000082,GO:0000084	protein binding (MF), mitotic cell cycle (BP), G1/S transition of mitotic cell cycle (BP), S phase of mitotic cell cycle (BP)	3 (73)	57 (34208)	0,000251129	0,000279353	CDKN1A,UBC,PCNA
GO:0003774	motor activity (MF)	3 (73)	60 (34208)	0,000292354	0,000324278	MYO1C,MYH9,DCTN1
GO:0005515,GO:0000278,G	protein binding (MF), mitotic cell	3 (73)	61 (34208)	0,000307006	0,000339554	CDKN1A,DCTN1,CCNA1

GO term ID	Annotations	# of annotated genes in the input list (Total # of genes in the input list)	# of annotated genes in the reference list (Total # of genes in the reference list)	Hypergeometric Distribution (Fisher's exact test)	Corrected Hypergeometric Dist. (Fisher's exact test)	Genes
O:0000086	cycle (BP), G2/M transition of mitotic cell cycle (BP)					
GO:0003677,GO:0005515,GO:0010467	DNA binding (MF), protein binding (MF), gene expression (BP)	3 (73)	62 (34208)	0,000322124	0,000353238	ESR1,HNRNPU,YBX1
GO:0005524,GO:0005515,GO:0000166,GO:0007049	ATP binding (MF), protein binding (MF), nucleotide binding (MF), cell cycle (BP)	3 (73)	62 (34208)	0,000322124	0,000353238	UBE2I,CSNK2A1,Cdk5
GO:0003677,GO:0005524,GO:0005515,GO:0000166	DNA binding (MF), ATP binding (MF), protein binding (MF), nucleotide binding (MF)	3 (73)	71 (34208)	0,000480156	0,000522085	XRCC6,HNRNPU,XRCC5
GO:0005524,GO:0000166,GO:0042803	ATP binding (MF), nucleotide binding (MF), protein homodimerization activity (MF)	3 (73)	76 (34208)	0,000586093	0,000633703	PRPS1,MYH9,PRPS2
GO:0005515,GO:0008219	protein binding (MF), cell death (BP)	3 (73)	83 (34208)	0,000757873	0,000814872	DCTN1,Cdk5,POLB
GO:0006355,GO:0003700,GO:0005515,GO:0043565	regulation of transcription, DNA-dependent (BP), sequence-specific DNA binding transcription factor activity (MF), protein binding (MF), sequence-specific DNA binding (MF)	3 (73)	84 (34208)	0,000784744	0,00084142	HOXC13,HIF1A,ESR1
GO:0005515,GO:0016301	protein binding (MF), kinase activity (MF)	3 (73)	85 (34208)	0,000812213	0,000866062	CDKN1A,Cdk5,NME1
GO:0000166,GO:0015031	nucleotide binding (MF), protein transport (BP)	3 (73)	94 (34208)	0,00108725	0,00115614	MYO1C,MYH9,ARF6
GO:0005515,GO:0007283	protein binding (MF), spermatogenesis (BP)	3 (73)	96 (34208)	0,00115539	0,00122187	SIRT1,HMGB2,CCNA1
GO:0005515,GO:0007067	protein binding (MF), mitosis (BP)	3 (73)	100 (34208)	0,00129963	0,00137065	UBE2I,DCTN1,CCNA1
GO:0005515,GO:0006886	protein binding (MF), intracellular protein transport (BP)	3 (73)	102 (34208)	0,00137581	0,00144703	NPM1,Cdk5,PCNA
GO:0005515,GO:0001701	protein binding (MF), in utero embryonic development (BP)	3 (73)	106 (34208)	0,00153645	0,00160723	TP53,MYH9,YBX1
GO:0005515,GO:0001666	protein binding (MF), response to hypoxia (BP)	3 (73)	106 (34208)	0,00153645	0,00160723	HIF1A,XRCC1,EP300
GO:0005515,GO:0043065	protein binding (MF), positive	3 (73)	116 (34208)	0,0019881	0,00206848	SIRT1,GZMA,TP53

GO term ID	Annotations	# of annotated genes in the input list (Total # of genes in the input list)	# of annotated genes in the reference list (Total # of genes in the reference list)	Hypergeometric Distribution (Fisher's exact test)	Corrected Hypergeometric Dist. (Fisher's exact test)	Genes
	regulation of apoptotic process (BP)					
GO:0051082	unfolded protein binding (MF)	3 (73)	120 (34208)	0,0021895	0,0022658	NPM1,TCP1,HSPA1A
GO:0051301,GO:0007067	cell division (BP), mitosis (BP)	3 (73)	148 (34208)	0,00395537	0,00406057	UBE2I,KIF11,CCNA1
GO:0005515,GO:0051301	protein binding (MF), cell division (BP)	3 (73)	173 (34208)	0,0061005	0,00622961	UBE2I,Cdk5,CCNA1
GO:0003713	transcription coactivator activity (MF)	3 (73)	220 (34208)	0,0117293	0,0119145	NPM1,EP300,THRAP3
GO:0005515,GO:0042803	protein binding (MF), protein homodimerization activity (MF)	3 (73)	259 (34208)	0,0180844	0,0182737	GZMA,NPM1,MYH9
GO:0005515,GO:0007275	protein binding (MF), multicellular organismal development (BP)	3 (73)	263 (34208)	0,0188251	0,0189726	HOXC13,SIRT1,TP53

8 LIST OF PAPERS PUBLISHED

The work described in this thesis is included in:

Vascotto C, **Lirussi L**, Poletto M, Tiribelli M, Damiani D, Fabbro D, Damante G, Demple B, Colombo E, Tell G. Functional regulation of the apurinic/apyrimidinic endonuclease 1 by nucleophosmin: impact on tumor biology. Oncogene. 2013 Jul 8. doi: 10.1038/onc.2013.251.

Lirussi L, Antoniali G, Vascotto C, D'Ambrosio C, Poletto M, Romanello M,Marasco D, Leone M, Quadrifoglio F, Bhakat KK, Scaloni A, Tell G. Nucleolar accumulation of APE1 depends on charged lysine residues that undergo acetylation upon genotoxic stress and modulate its BER activity in cells. Mol Biol Cell. 2012 Oct;23(20):4079-96. doi: 10.1091/mbc.E12-04-0299.

During my PhD I have been involved in additional projects that are not presented in this thesis but are part of the following manuscript:

Poletto M, **Lirussi L**, Wilson DM 3rd and Tell G. Nucleophosmin modulates stability, activity and nucleolar accumulation of base excision repair proteins. Sent to MBoC.

Antoniali G, **Lirussi L**, D'Ambrosio C, Dal Piaz F, Vascotto C, Casarano E, Marasco D, Scaloni A, Fogolari F and Gianluca Tell. SIRT1 gene expression upon genotoxic damage is regulated by APE1 through nCaRE-promoter elements. Accepted in MBoC.

Antoniali G, **Lirussi L**, Poletto M, Tell G. Emerging Roles of the Nucleolus in Regulating the DNA Damage Response: The Noncanonical DNA Repair Enzyme APE1/Ref-1 as a Paradigmatical Example. Antioxid Redox Signal.

Poletto M, Vascotto C, Scognamiglio PL, **Lirussi L**, Marasco D, Tell G. Role of the unstructured N-terminal domain of the hAPE1 (human apurinic/apyrimidinic endonuclease 1) in the modulation of its interaction with nucleic acids and NPM1 (nucleophosmin). Biochem J. 2013 Jun 15;452(3):545- 57. doi: 10.1042/BJ20121277.

Oncogene (2013), 1–12

www.nature.com/onc

ORIGINAL ARTICLE

Functional regulation of the apurinic/apyrimidinic endonuclease 1 by nucleophosmin: impact on tumor biology

C Vascotto[1], L Lirussi[1], M Poletto[1], M Tiribelli[2], D Damiani[2], D Fabbro[1], G Damante[1], B Demple[3], E Colombo[4] and G Tell[1]

Nucleophosmin 1 (NPM1) is a nucleolar protein involved in ribosome biogenesis, stress responses and maintaining genome stability. One-third of acute myeloid leukemias (AMLs) are associated with aberrant localization of NPM1 to the cytoplasm (NPM1c+). This mutation is critical during leukemogenesis and constitutes a good prognostic factor for chemotherapy. At present, there is no clear molecular basis for the role of NPM1 in DNA repair and the tumorigenic process. We found that the nuclear apurinic/apyrimidinic endonuclease 1 (APE1), a core enzyme in base excision DNA repair (BER) of DNA lesions, specifically interacts with NPM1 within nucleoli and the nucleoplasm. Cytoplasmic accumulation of APE1 is associated with cancers including, as we show, NPM1c+ AML. Here we show that NPM1 stimulates APE1 BER activity in cells. We provide evidence that expression of the NPM1c+ variant causes cytoplasmic accumulation of APE1 in: (i) a heterologous cell system (HeLa cells); (ii) the myeloid cell line OCI/AML3 stably expressing NPM1c+; and (iii) primary lymphoblasts of NPM1c+ AML patients. Consistent with impaired APE1 localization, OCI/AML3 cells and blasts of AML patients have impaired BER activity. Cytoplasmic APE1 in NPM1c+ myeloid cells is truncated due to proteolysis. Thus, the good prognostic response of NPM1c+ AML to chemotherapy may result from the cytoplasmic relocalization of APE1 and the consequent BER deficiency. NPM1 thus has an indirect but significant role in BER *in vivo* that may also be important for NPM1c+ tumorigenesis.

Oncogene (2013) **0,** 000–000. doi:10.1038/onc.2013.251

Keywords: APE1/Ref-1; NPM1; acute myeloid leukemia; base excision repair

INTRODUCTION

The nucleolar protein nucleophosmin 1 (NPM1) is implicated in a variety of cellular processes including ribosome biogenesis and centrosome duplication, and NPM1 is frequently altered in some cancers.[1] NPM1 physically interacts with p53 and is believed to regulate this tumor-suppressor protein, thus contributing to maintenance of genome integrity.[2,3] However, a direct involvement of NPM1 in DNA repair has not been demonstrated.

NPM1 mutations are the most frequently known gene alterations in cytogenetically normal acute myeloid leukemia (AML) patients and are considered as positive prognostic factors.[4] The NPM1 mutations identified so far in cytogenetically normal AML patients generate a new nuclear export signal while also disrupting the nucleolar localization signal (Supplementary Figure S1), which relocalizes mutated NPM1 to the cytoplasm (NPM1c+).[5,6] A formal *in vivo* demonstration that mutant NPM1c+ is endowed with oncogenic potential has been recently presented.[7] A plausible hypothesis is that NPM1c+ causes abnormal cytoplasmic localization of important NPM1-interacting proteins that impairs their functions.[1,8–15] All NPM1c+ AMLs are characterized by haploinsufficient expression, with only one NPM1 allele affected by the mutation. NPM1c+ is dominant by forming mixed oligomers with wild-type (WT) NPM1 and moving it to the cytoplasm. The presence of the NPM1c+ mutation is a favorable marker for relapse-free and overall survival in AML with a normal karyotype, and for complete remission after chemotherapy using DNA-damaging compounds (that is, daunorubicin, cytarabine and so on).

Interestingly, overexpression of WT NPM1 has been described in a number of solid malignancies such as hepatic, gastric, ovarian and prostate cancers.[1,16] In those cases, it has been suggested that increased amounts of NPM1 could limit the DNA-damage response to help effect cellular transformation. However, molecular support for this hypothesis is still lacking.

We recently demonstrated that NPM1 physically interacts with apurinic/apyrimidinic endonuclease 1/redox effector factor 1 (APE1/Ref-1) within nucleoli and in the nucleoplasm of tumor cells.[17] APE1 has a crucial role in the maintenance of genome stability, in redox signaling and other processes,[18] and it is a promising target for augmenting chemotherapy.[18,19] APE1 is the main apurinic/apyrimidinic (AP) endonuclease in mammalian cells and a multifunctional protein. APE1 is an essential enzyme in the base excision DNA repair (BER) pathway for DNA damage caused by both endogenous and exogenous oxidizing or alkylating agents, including chemotherapeutic drugs.[20–23] APE1 can also act as a redox-regulatory protein, maintaining cancer-related transcription factors (Egr-1, NF-κB, p53, HIF-1α, AP-1 and Pax proteins) in an active reduced state,[18,24–28] and it may act as a transcriptional repressor.[29] APE1 binds and cleaves abasic sites in RNA[17,30,31] and can control *c-Myc* expression by nicking its mRNA.[32] In this context, we have shown that the first 35 amino acids of APE1 are required for a stable interaction with NPM1 and other proteins involved in ribosome biogenesis/RNA processing,[17] and for APE1 stable binding to RNA.[30,33] The direct interaction with NPM1 stimulates the enzymatic activity of APE1 on abasic

[1]Department of Medical and Biological Sciences, University of Udine, Udine, Italy; [2]Department of Experimental and Clinical Medical Sciences, University of Udine, Udine, Italy; [3]Department of Pharmacological Sciences, Stony Brook University School of Medicine, Stony Brook, NY, USA and [4]Department of Medicine, Surgery and Dentistry, University of Milan, Milan, Italy. Correspondence: Professor G Tell, Department of Medical and Biological Sciences, University of Udine, Piazzale Kolbe 4, 33100 Udine, Italy
E-mail: gianluca.tell@uniud.it
Received 27 June 2012; revised 24 April 2013; accepted 19 May 2013

DNA *in vitro*,[17,30] although the *in vivo* effects were not known. This work presented here is aimed at filling this gap.

RESULTS

NPM1$^{-/-}$ cells are more sensitive than control cells to DNA damages repaired through the BER pathway

We earlier demonstrated that NPM1 stimulates the APE1 endonuclease activity *in vitro* by means of protein–protein interaction.[17,30] Our data clearly showed that, although the K_m of APE1 for the abasic substrate is not significantly affected by the presence of NPM1, its catalytic activity is increased almost 10-fold in the presence of a two-fold excess of NPM1 recombinant protein. As product release by APE1 appears to be rate-limiting,[34,35] these observations suggest that interaction with NPM1 increases the speed of this reaction step. To evaluate the role of the APE1/NPM1 interaction *in vivo*, we tested the effect of NPM1 absence on the BER capacity exploiting a NPM1$^{-/-}$ cell model developed on the p53$^{-/-}$ background for immortalization.[36]

First, we checked whether NPM1 expression affected the amount of APE1 protein and its subcellular localization. APE1 and NPM1 protein levels were evaluated by immunoblot analysis of nuclear and cytoplasmic fractions of p53$^{-/-}$ mouse embryonic fibroblasts (MEFs) with NPM1$^{+/+}$ or NPM1$^{-/-}$ alleles[36] (Figure 1a left and Supplementary Figure S2). Quantification of the immunoblots (Figure 1a right and Supplementary Figure S3) showed that NPM1$^{-/-}$ cells had about 40% more nuclear APE1

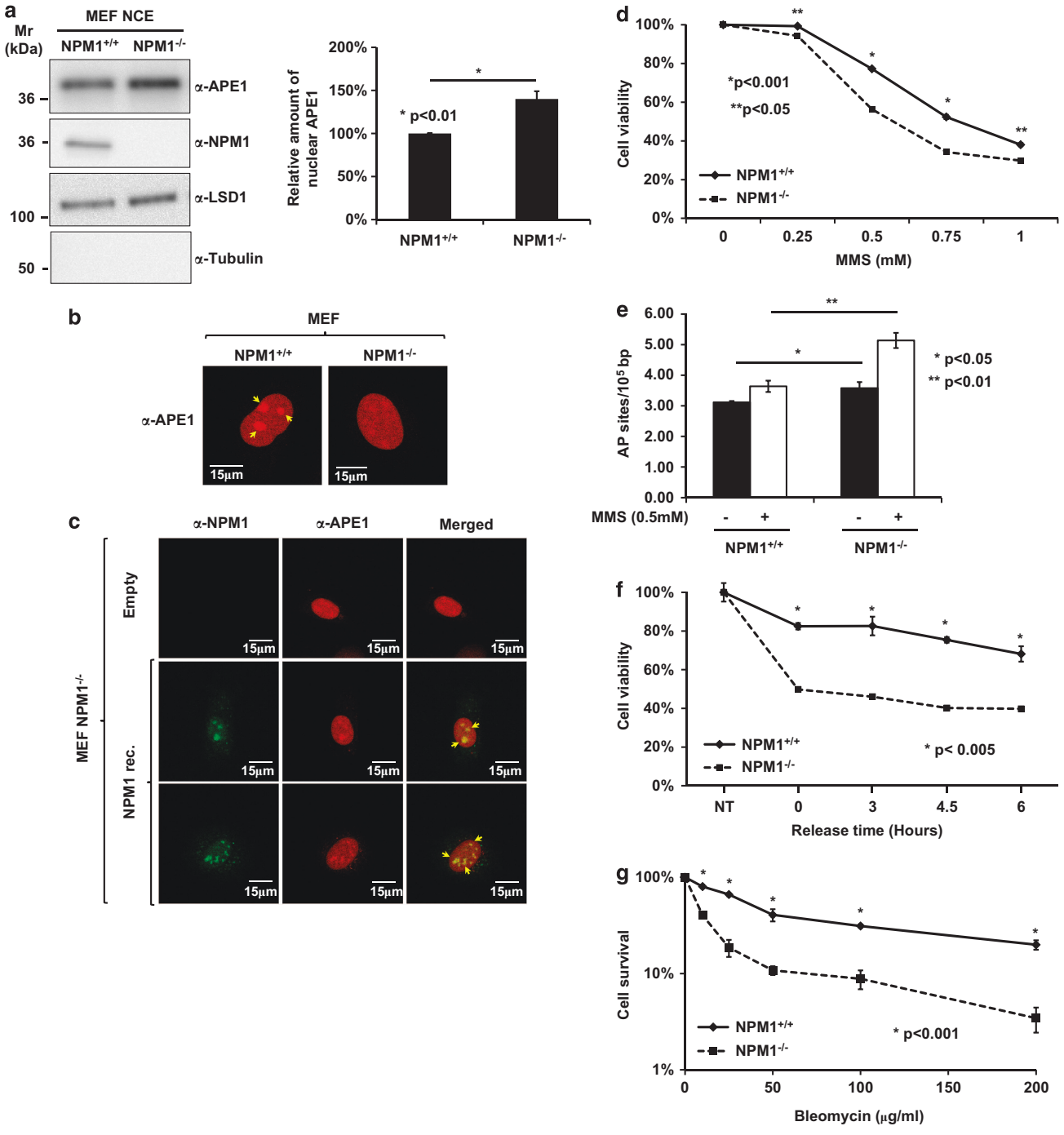

than cells expressing WT NPM1 protein. This increased content was associated with a slightly increased APE1 transcription, as measured by quantitative PCR analysis (not shown). Immunofluorescence (IF) analysis (Figure 1b) showed that, in NPM1$^{+/+}$ cells, APE1 localization was nuclear with a strong accumulation in nucleolar structures, as previously shown for some tumor cell lines.[17] In contrast, in NPM1$^{-/-}$ cells, APE1 did not accumulate within nucleoli, although nucleolar structures are still intact in these cells (data not shown).[36] Reexpression of NPM1 in MEF-NPM1$^{-/-}$ cells promoted APE1 nucleolar accumulation (Figure 1c and Supplementary Figure S4), demonstrating that interaction with NPM1 is essential for APE1 nucleolar distribution. Moreover, recent data from our laboratory also showed that expression of an APE1 mutant not able to interact with NPM1 was unable to accumulate within nucleoli, demonstrating that a functional interaction with NPM1 is required for physical accumulation of APE1 within nucleoli.[37]

To test the functional relevance of NPM1 in BER, we next assayed the sensitivity of the NPM1$^{-/-}$ cells to different genotoxic treatments known to cause DNA lesions that are repaired through the BER pathway.[38] First, we used methyl methanesulfonate (MMS), which is a monofunctional methylating agent causing lesions repaired predominantly by BER pathway.[39] Cell viability experiments showed that NPM1$^{-/-}$ cells were significantly more sensitive than NPM1$^{+/+}$ cells to MMS (Figure 1d). We then evaluated the ability of the MEFs to efficiently remove AP sites from the DNA of MMS-treated cells. As shown in Figure 1e, NPM1$^{-/-}$ cells retained a significantly higher level of AP sites following MMS treatment than did NPM1$^{+/+}$ cells. Notably, this difference was also apparent under basal conditions, further pointing to an impairment in the AP-site incision step within the BER pathway in NPM1$^{-/-}$ cells.

BER removes also damages caused by reactive oxygen species, such as oxidized bases (for example, 8-oxoG). Thus, we performed cell viability experiments with acute doses of H_2O_2 as genotoxic agent, combined with treatment of the cells with methoxyamine, an inhibitor of APE1-dependent repair.[40] Data reported in Supplementary Figure S5A clearly showed that NPM1$^{-/-}$ cells were significantly more sensitive to this treatment than NPM1$^{+/+}$ cells. To confirm this result with an alternative oxidizing agent, we used $KBrO_3$, a carcinogenic agent known to induce predominantly 8-oxoG lesions on DNA after reduction of the bromate by cellular thiols, such as glutathione, or reduced cysteines.[41] As displayed in Figure 1f, treatment with $KBrO_3$, NPM1$^{-/-}$ cells were significantly less viable than control cells at all the release time points.

We also determined the sensitivity of NPM1$^{-/-}$ cells to the radiomimetic bleomycin (BLM), as still another DNA-damaging agent that requires BER intervention.[42] BLM, which targets both single-stranded DNA and double-stranded DNA, as well as RNA molecules, causes formation of 4-oxidized AP sites or 3′-phosphoglycolate products that account for the majority of the BLM-induced DNA lesions.[42,43] Cell viability was measured on MEFs after a 1-h treatment with increasing doses of BLM, followed by 48 h of recovery. Data reported in Figure 1g and Supplementary Figure S5B clearly confirmed the protective function exerted by NPM1 against BLM treatment. Notably, the differential sensitivity of the two isogenic cell lines was not apparent when using the poly (ADP-ribose) polymerase-inhibitor PJ34 (Supplementary Figure S6A) or upon ultraviolet-C irradiation, which promotes DNA damages repaired through NER (Supplementary Figure S6B). Comet assay analysis performed under basal condition (data not shown) did not reveal any significant difference between the steady-state level of DNA damage of the two isogenic cell lines. The latter observations suggest that, if any, only a marginal involvement of the other pathways, besides BER, may account for the observed effects on cell viability exerted by the genotoxicants used in this study, which, besides AP sites, may cause DNA-strand breaks.

Collectively, these data indicate that NPM1 is essential for cell protection from different genotoxic treatments that elicit a BER response.

The lower APE1 BER activity of NPM1$^{-/-}$ cells is rescued by NPM1 reconstitution

To define the BER defect accompanying NPM1 deficiency, we measured the APE1 enzymatic activity in nuclear extracts from the two MEF cell lines. Endonuclease assays showed that despite the higher expression levels of APE1 protein in NPM1$^{-/-}$ cells, their AP endonuclease activity did not significantly differ from that of the control cells (Figure 2a). Treatment of the two cell lines with two different APE1 inhibitors (that is, methoxyamine[39] and compound 3[44]) alone demonstrated that NPM1$^{-/-}$ cells were significantly more sensitive to AP endonuclease activity inhibition, confirming the hypothesis that APE1 functional activity, under genotoxic conditions, strictly depends on NPM1 expression

Figure 1. Absence of NPM1 is associated to a higher sensitivity of cells to genotoxic treatments causing DNA lesions repaired through BER. (**a**) Left: representative western blotting analysis of MEF-NPM1$^{+/+}$ and NPM1$^{-/-}$ nuclear extracts of three independent subfractionation experiments. Nuclear cell extracts of 5 μg of the two cell lines were analyzed through western blotting for the expression of APE1 and NPM1 content. Lysine demethylase (LSD1) was used as nuclear marker and loading control, whereas tubulin was used to evaluate cytoplasmic contaminations. Right: relative percentages of chemiluminescence intensity of APE1 signals are reported in the histogram showing a significant increase of APE1 nuclear expression in NPM1$^{-/-}$ clone (40 ± 9%) with respect to NPM1$^{+/+}$ cells. Histograms, showing the amount of APE1 nuclear protein, represent the mean ± s.d. values of three independent experiments. (**b**) APE1 subcellular localization was detected through confocal analysis on MEF-NPM1$^{+/+}$ and NPM1$^{-/-}$ cells using a specific monoclonal α-APE1 antibody and a secondary antibody α-mouse conjugated with Rhodamine-Red. Yellow arrows indicate APE1 accumulation within nucleoli. A diffused nuclear staining without nucleolar accumulation could be observed in the NPM1$^{-/-}$ cells. (**c**) Confocal analysis of APE1/NPM1 colocalization in MEF-NPM1$^{-/-}$ after reexpression of NPM1. NPM1$^{-/-}$ cells transfected with the empty vector (Empty) showed a uniform nuclear staining for APE1 (red). On the contrary, NPM1$^{-/-}$ cells transfected with pCMV5.1 vector expressing NPM1 in fusion with a C-term FLAG (NPM1 rec.) show APE1 accumulation within nucleolar structure and colocalization with NPM1 (yellow arrows). (**d**) MTS assay was used to evaluate cell viability of MEF-NPM1$^{+/+}$ and NPM1$^{-/-}$ cells after treatment with increasing amounts of MMS for 8 h. Absence of NPM1 negatively affects cell viability making NPM1$^{-/-}$ cells more sensitive to genotoxic damages. Mean ± s.d. values are the result of three independent experiments. (**e**) The amount of abasic (AP) sites was measured in MEF-NPM1$^{+/+}$ and NPM1$^{-/-}$ cells under basal conditions and after treatment with 0.5 mM of MMS for 4 h. NPM1$^{-/-}$ cells display a significantly higher amount of AP sites if compared with NPM1$^{+/+}$ cells. Treatment with an alkylating agent leads to the accumulation of AP sites in NPM1$^{-/-}$ cells (5.14 ± 0.25/10^5 bp) if compared with NPM1$^{+/+}$ cells (3.58 ± 0.20/10^5 bp). Mean ± s.d. values are the result of three independent experiments. (**f**) MTS assay was used to evaluate cell viability of MEF-NPM1$^{+/+}$ and NPM1$^{-/-}$ cells. After Potassium bromate (40 mM for 30 min) treatment, cells were allowed to recover for the indicated periods of time. Absence of NPM1 negatively affects cell viability, making NPM1$^{-/-}$ cells more sensitive to genotoxic damages. Mean ± s.d. values are the result of three independent experiments. (**g**) Trypan blue cell counting was used to measure cytotoxicity of BLM in MEF cells. Mean ± s.d. values are the result of three independent experiments.

(Figures 2b and c). We circumstantiated these findings by measuring the endonuclease activity of APE1, using nuclear extracts of MEF cells after normalization for APE1 content. Consistent with our previous *in vitro* findings,[17] APE1 endonuclease activity in NPM1$^{-/-}$ extracts was significantly lower than that from NPM1$^{+/+}$ cells (Figure 2d). Thus, the

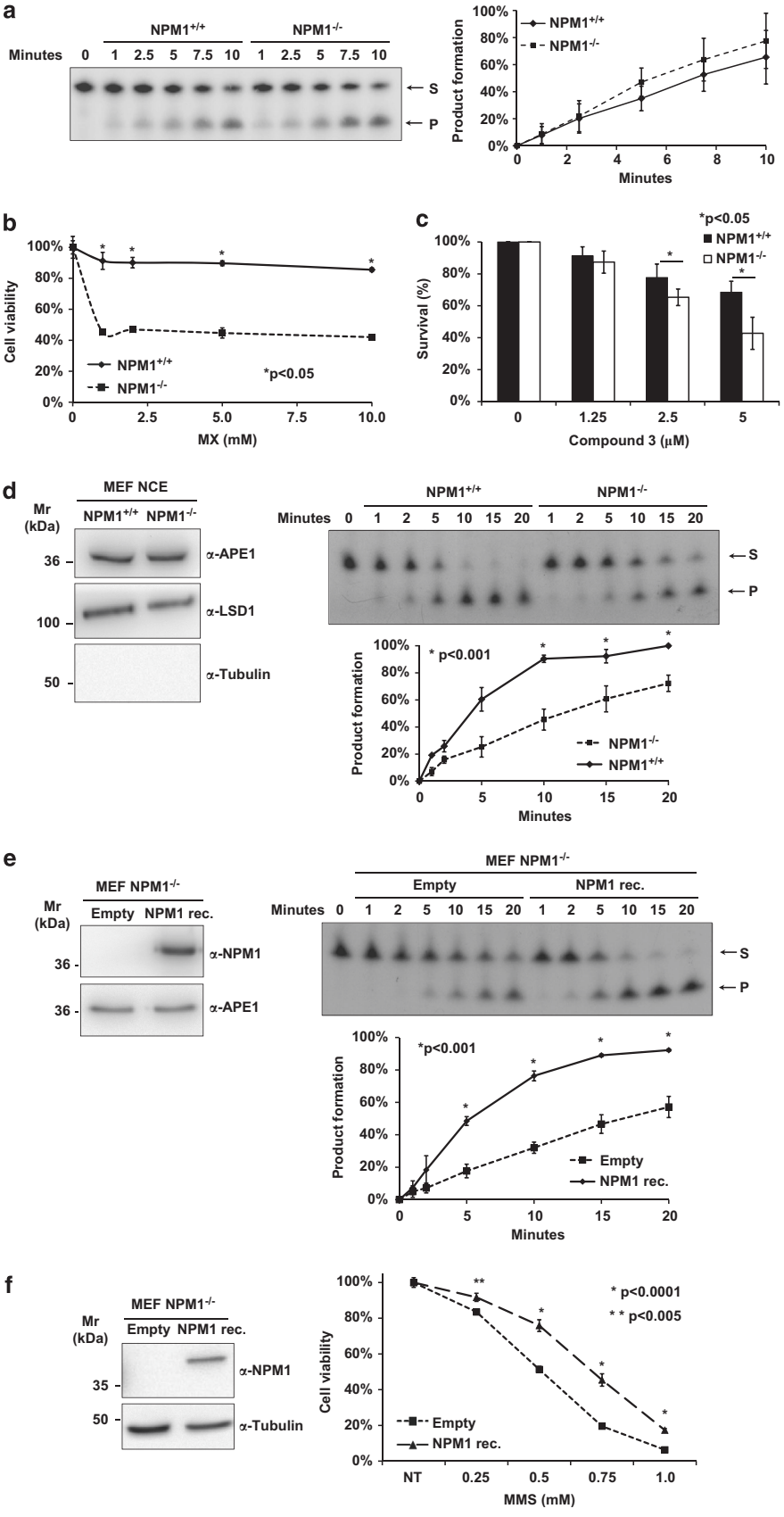

increased APE1 nuclear content observed in NPM1$^{-/-}$ cells could reflect a compensatory mechanism to maintain overall BER activity that still remains insufficient to efficiently correct genotoxic damage. To confirm that the APE1 defect observed in NPM1$^{-/-}$ cells was due to NPM1 loss, rather than some other effect of the knockout gene, we restored NPM1 in the NPM1$^{-/-}$ cell lines by ectopic expression of the WT protein from a plasmid vector and measured the AP endonuclease activity in these cells (Figure 2e). The results showed that NPM1 reexpression in NPM1$^{-/-}$ cells increased their AP endonuclease activity when compared with control cells transfected with the empty expression vector. We biologically circumstantiated these biochemical data, by performing cell viability experiments in stable cell lines reexpressing the WT NPM1 protein in the NPM1$^{-/-}$ background. Data reported in Figure 2f confirmed the hypothesis made, clearly showing that reexpression of NPM1 significantly reduced the sensitivity of NPM1$^{-/-}$ cells to genotoxic treatment.

Collectively, our data demonstrate that NPM1 is a novel indirect effector of BER by regulating APE1 localization and activity *in vivo*.

Ectopic expression of the NPM1c+ AML protein causes increased cytoplasmic APE1 localization in HeLa cells

We examined the oncological relevance of our findings by testing the effect of the NPM1c+ mutation on BER, and by studying the effect of NPM1c+ on the APE1–NPM1 interaction. To address the latter, we assessed the extent of APE1–NPM1 interaction using the proximity ligation assay (PLA).[45] HeLa cells expressing the NPM1c+ mutant protein showed relocalization of NPM1 to the cytoplasmic compartment of the protein. As expected, the control WT protein presented its typical nucleolar staining (Figure 3a). The specificity of the PLA analysis was tested by comparing the ability of NPM1 to interact with APE1^{WT}, or with an APE1$^{N\Delta 33}$-deletion mutant that has lower affinity for NPM1.[17] Specificity was clearly demonstrated (Supplementary Figure S7 and Supplementary Movies) by the presence of nuclear and nucleolar PLA spots only when APE1^{WT} was expressed. When the APE1$^{N\Delta 33}$ protein was instead expressed, the PLA signals were reduced in number and relocalized to the cytoplasmic compartment in accordance with APE1$^{N\Delta 33}$ pancellular localization. We then tested the ability of the NPM1c+[46] mutant protein to interact with Flag-tagged APE1 protein. In control cells (NPM1^{WT}), the APE1–NPM1 interaction occurred primarily in the nucleolar and nucleoplasmic compartments, whereas the interaction with NPM1c+ protein was mostly apparent in the cytoplasmic compartment (Figure 3b). Quantification of these results, through scoring of the PLA signals, showed that the NPM1c+ mutation significantly reduced the APE1–NPM1 association within the nuclei of transfected cells, leading to a significant increase of the APE1–NPM1 interaction within the cytoplasmic compartment. Accordingly, only in the case of cells expressing the NPM1c+ mutant protein, the APE1 staining was extranuclear, consistent with the PLA signal distribution (Figures 3b and c). These observations indicate the existence of a direct correlation between expression of the NPM1c+ protein and the presence of APE1 in the cytoplasm.

NPM1c+ expression is associated with altered APE1 protein stability in both AML cell lines and blasts from AML patients

We assessed the biochemical relevance of the APE1 cytoplasmic relocalization due to NPM1c+ expression in the myeloid cell line OCI/AML3, which stably expresses a NPM1c+ mutant protein.[47] We analyzed the distribution of APE1 using IF and by quantification of the nuclear and cytoplasmic levels of APE1 in subcellular fractions of OCI/AML3 and control OCI/AML2 cell lines through western blot analysis. The mRNA expression levels of APE1 were similar between the two cell lines, as demonstrated by quantitative PCR analyses (data not shown). IF analysis showed that NPM1c+ expression was associated with APE1 accumulation in the cytoplasmic compartment of OCI/AML3 cells (Figure 4a). Immunoblot analysis indicated that a significant amount of truncated APE1 protein could be detected in the whole and in the cytoplasmic extracts of OCI/AML3 cell line (Figure 4b). Strikingly, accumulation of this truncated protein form was also apparent in blasts from AML patients (Figure 4c), confirming the biological relevance of this observation. Several groups have demonstrated that APE1 is targeted by granzymes A and K, to generate truncation products (APE1$^{N\Delta 31\text{-}35}$) that functionally inactivate APE1 in DNA repair and to take part in apoptosis.[48–50] We have also recently shown that expression of non-cleavable proficient form of APE1 protein protects cells from genotoxic stresses,[51] thus confirming that the N-terminal deletion of the protein causes its functional impairment *in vivo*. This truncated protein corresponded to the APE1$^{N\Delta 33}$ truncation derivative already described,[48–50] but was due to a specific proteolytic activity, independent of granzyme A protein, which is not expressed in these cell lines (Lirussi *et al.*, in preparation).

Figure 2. Absence of NPM1 negatively affects APE1 endonuclease activity. (**a**) The same amount of whole-cell extracts (600 ng) from MEF-NPM1$^{+/+}$ and NPM1$^{-/-}$ was used to evaluate APE1's endonuclease activity in the two cell lines. A representative image shows the conversion of the substrate (S) to product (P) operated by APE1. In the diagram on the right, the mean ± s.d. values of the densitometric analyses of three independent experiments are reported. (**b**) MTS assay was used to evaluate cell viability of MEF-NPM1$^{+/+}$ and NPM1$^{-/-}$ cells after treatment with increasing amount of methoxyamine (MX) for 24 h. Absence of NPM1 negatively affects cell viability, making NPM1$^{-/-}$ cells more sensitive to the damage. Mean ± s.d. values are the result of three independent experiments. (**c**) WST-8 assay was used to evaluate the sensitization of MEF-NPM1$^{+/+}$ and NPM1$^{-/-}$ cells to the inhibition of the APE1 endonuclease activity. Cells were incubated with the indicated amounts of the APE1-inhibitor compound 3, and viability was measured 24 h later. Mean ± s.d. values are the result of three independent experiments. (**d**) Left: on the basis of western blotting analysis of MEF-NPM1$^{+/+}$ and NPM1$^{-/-}$ cells reported in Figure 1a, normalized amount of nuclear cell extract (NCE) was loaded onto SDS–PAGE to obtain equal amounts of APE1. Immunoblot analysis confirmed the presence of the same amount of APE1 protein in the nuclear extracts of the two cell lines. LSD1 was used as nuclear marker, whereas tubulin was used to evaluate cytoplasmic contaminations. Right: normalized amount of NCE from both cell lines was used to evaluate APE1 endonuclease activity. A representative image shows the conversion of the substrate (S) to product (P) operated by APE1. In the diagram below are reported the mean ± s.d. values of the densitometric analysis of three independent experiments. (**e**) Left: MEF-NPM1$^{-/-}$ cells were transiently transfected with pCMV5.1 vector expressing NPM1 in fusion with a C-term FLAG (NPM1 rec.) or the empty vector (Empty) as control. Total cell extracts of 7.5 μg from Empty and NPM1-transfected cells were separated onto SDS–PAGE, and western blotting analysis was performed using α-NPM1 and α-APE1 antibodies. Right: cell extracts of 50 ng from Empty and NPM1-reconstituted MEF-NPM1$^{-/-}$ cells were used to evaluate APE1 endonuclease activity. The representative image reported shows the conversion of the substrate (S) to product (P) by the endonuclease activity of APE1. In the diagram below are reported the mean ± s.d. values of the densitometric analyses of three independent experiments. (**f**) Left: MEF-NPM1$^{-/-}$ cells were stably transfected with p3X-FLAG-CMV vector expressing NPM1 in fusion with a C-term FLAG (NPM1) or the empty vector (Empty) as control. Total cell extracts of 7.5 μg of each clone were separated onto SDS–PAGE, and western blotting analysis was performed using α-NPM1 and α-tubulin antibodies. Right: MTS assay was used to evaluate cell viability of MEF-NPM1$^{-/-}$ cells reconstituted with NPM1 after treatment with increasing amounts of MMS for 8 h. Reexpression of NPM1 rescues cell viability, making NPM1$^{-/-}$ reconstituted cells less sensitive to genotoxic damages. Mean ± s.d. values are the result of three independent experiments.

Though total APE1 protein levels were comparable between OCI/AML3 and OCI/AML2 control cells, NPM1c+ expressing cells, having almost 50% less WT NPM1 protein, have lower APE1 nuclear content (Figure 4b). AP endonuclease assays performed with nuclear extracts of the two cell lines confirmed that OCI/AML3 cells have a significantly reduced APE1 DNA incision

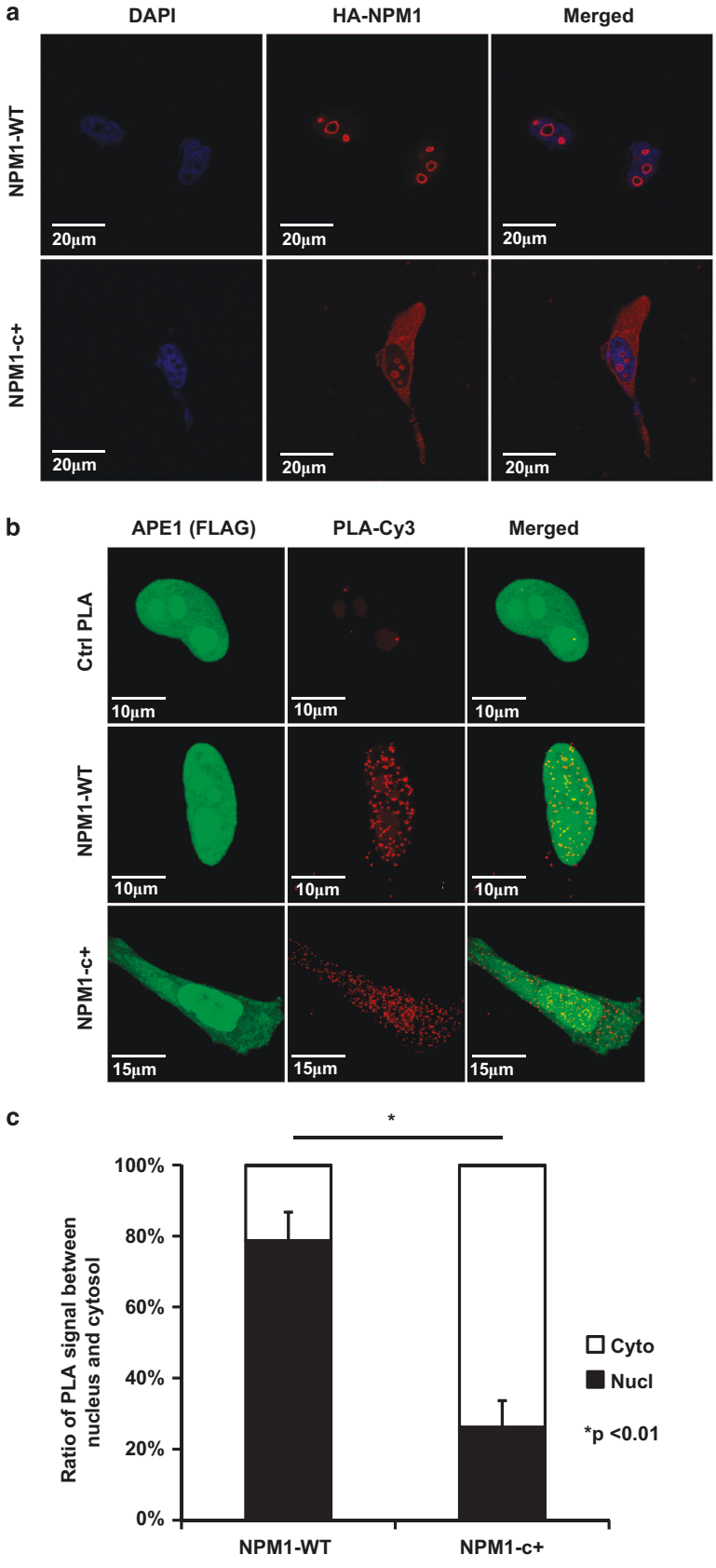

activity (Figure 4d). We then evaluated the ability of the AML cells to efficiently remove AP sites from the DNA of MMS-treated cells. As shown in Figure 4e, OCI/AML3 cells retained a significantly higher level of AP sites both under basal conditions and following MMS treatment than did OCI/AML2 cells. Cell-viability experiments were in agreement with these observations showing that OCI/AML3 cells were significantly more sensitive to MMS treatment than OCI/AML2 cells (Figure 4f).

To provide additional mechanistic insights into the role of APE1 delocalization in NPM1c+ cells and to prove which of the APE1 known functions (that is, DNA repair or redox) are affected by NPM1c+ expression accounting for the higher sensitivity of OCI/AML3 cells to genotoxicants, we performed sensitization experiments to MMS treatment with specific APE1 inhibitors. Methoxyamine, as an APE1 DNA-repair inhibitor, and the well-known E3330 redox inhibitor[52] were used for this purpose. Data obtained (Supplementary Fig S8) show that treatment with the DNA-repair inhibitor, but not with the E3330 redox inhibitor, sensitizes OCI/AML2 cells to MMS treatment and phenocopies the response of the NMP1c+ expressing cells. Moreover, this experiment demonstrates that the functional impairment of the APE1 DNA repair in NPM1c+ cells does not further increase the sensitivity of NPM1c+ cells to genotoxic damage.

Altogether, these data allow to conclude that APE1 functional suppression by NPM1c+ induced relocalization is important for regulating cellular sensitivity to DNA damage in NPM1c+ cells.

Blasts from AML patients, expressing the NPM1c+ mutant protein, have increased cytoplasmic APE1–NPM1 interaction and show impaired BER activity

We tested whether the altered interaction between APE1 and NPM1c+ observed upon ectopic expression of the mutant protein in cell lines also occurs in blasts from AML patients constitutively expressing the NPM1c+ protein. IF and PLA analyses (Figures 5a and b) clearly showed that the NPM1c+ mutations leads to a reduction of the APE1/NPM1 interaction in nuclei, coupled to a strong increase of the APE1/NPM1 association in the cytoplasms of AML blasts. This phenotype is associated with the relocalization of APE1 protein to the cytoplasm, as previously observed in a heterologous cell system (Figure 3b).

To evaluate the physiological relevance of the altered interaction between APE1 and NPM1c+, we compared the sensitivity of blasts from AML patients expressing either the WT or the c+ form of NPM1 with that of healthy donors to DNA-alkylation damage induced by MMS. Cell-viability experiments demonstrated that blasts from AML patients expressing the NPM1c+ form were significantly more sensitive to MMS than healthy control cells and AML-WT NPM1 blasts (Figure 5c). These data support the conclusion that alteration of APE1 distribution due to the NPM1c+ mutation has a significant impact on the BER activity *in vivo* and has a functional relevance in AML pathogenesis.

DISCUSSION

Here we demonstrated that NPM1 has an indirect but significant role in BER through functional regulation of the APE1 endonuclease activity. This observation is the first evidence highlighting a clear function of NPM1 in DNA repair, and these new results provide a possible alternative explanation for a role of NPM1 in the maintenance of genomic stability in addition to its known effect on p53 stability.[2,3] It has been recently shown that homologous recombination-impaired BRCA-deficient cells are hypersensitive to poly (ADP-ribose) polymerase inhibitors that block repair of single-strand breaks, a subpathway of BER. Interestingly, NPM1 functionally interacts with BRCA2 having a role in centrosome duplication.[53] Therefore, it could be speculated that the differential sensitivity of NPM1$^{-/-}$ cells to genotoxicants used in this study could be ascribed to an impaired ability of these cells to repair DNA-strand breaks. However, our data showing no differential sensitivity to poly (ADP-ribose) polymerase inhibitors, together with a similar efficiency of repair of strand breaks (as measured through comet assays) by the two isogenic cell lines, would exclude this hypothesis, leaving BER impairment as the main process affected by the loss of NPM1 expression. Moreover, our findings may illuminate the prompt response to chemotherapy of AML expressing the NPM1c+ mutation. Our data support the hypothesis that some biological effects of NPM1c+ may be exerted through impaired functions of important NPM1-interacting proteins caused by their abnormal cytoplasmic localization.[1,8–13]

APE1 subcellular distribution within different cell types is mainly nuclear and critically controls the cellular proliferation rate,[54–56] however, in some tumors APE1 can be cytoplasmic or nuclear/cytoplasmic.[18,28] Increased expression of APE1 is associated with different tumorigenic processes.[28] In particular, a higher expression of APE1, with consequently increased BER activity, has been described in several cancer types,[28] where it correlates with a higher tumor aggressiveness and is associated with chemoresistance.[18] Extranuclear APE1 has a role within mitochondria in repairing mitochondrial DNA damage[57–59] and in controlling the intracellular reactive oxygen species production through inhibition of Rac1.[60,61] However, a possible causal role of an increased APE1 expression in tumorigenesis, as well as the mechanisms responsible for the unusual APE1 accumulation in the cytoplasmic compartment, has never been investigated in detail.

The observations reported herein provide a molecular explanation for the delocalization of APE1 to the cytoplasm observed in AML tumors associated with NPM1c+. Because APE1 interacts with many different partners involved in RNA metabolism,[17,31,37] the occurrence of extranuclear APE1 localization may be explained on the basis of altered expression levels of its protein partners that may undergo delocalization, as is the case of NPM1c+ itself. Alternatively, increased expression of APE1 cytoplasmic partners, rather than mutations occurring in APE1 itself, may directly affect the distribution of the protein. Notably, no polymorphisms

Figure 3. NPM1 mutation alters APE1 localization in HeLa cells. (**a**) Representative confocal microscopy images of HeLa cells transiently transfected with pcDNA-HA vectors expressing WT NPM1 or the NPM1c+ mutant. Twenty-four hours after transfection cells were fixed and stained with a primary antibody α-HA-Tag and a secondary antibody α-rabbit conjugated with Rhodamine Red. In cells expressing WT NPM1, the ectopic HA-tagged protein localizes, as expected, only within the granular component of nucleoli. On the contrary, cells expressing NPM1c+ mutant show also strong cytoplasm positivity. (**b**) PLA technology was used on HeLa cells to quantify the occurrence of *in vivo* interaction between APE1 and NPM1. Cells were transiently transfected with APE1-FLAG and NPM1-HA-WT or the NPM1c+ mutant. Confocal microscopy analysis highlights the presence of distinct fluorescent red dots (PLA signals), indicating the occurrence of *in vivo* interaction between APE1-FLAG and NPM1-HA, whereas green fluorescence shows APE1-FLAG-tagged protein localization. PLA control is represented by cells incubated only with α-FLAG antibody. In cells transfected with WT NPM1, APE1 accumulates within the nucleus where also PLA signals are mostly present. In NPM1c+ expressing cells, a diffused cytoplasmic APE1 staining could be observed along with the relocalization of PLA signal. (**c**) *Blob Finder* software was used to quantify the relative distribution of PLA signals between nucleus and cytoplasm of cells transfected with WT NPM1 or NPM1c+ mutant. In NPM1c+ expressing cells, most of the interaction between APE1 and NPM1 occurs within the cytoplasm (nuclear: 26 ± 7%), whereas in WT NPM1 cells, PLA signal is predominantly nuclear (nuclear: 79 ± 8%). Reported results are the mean of 30 cells for each condition.

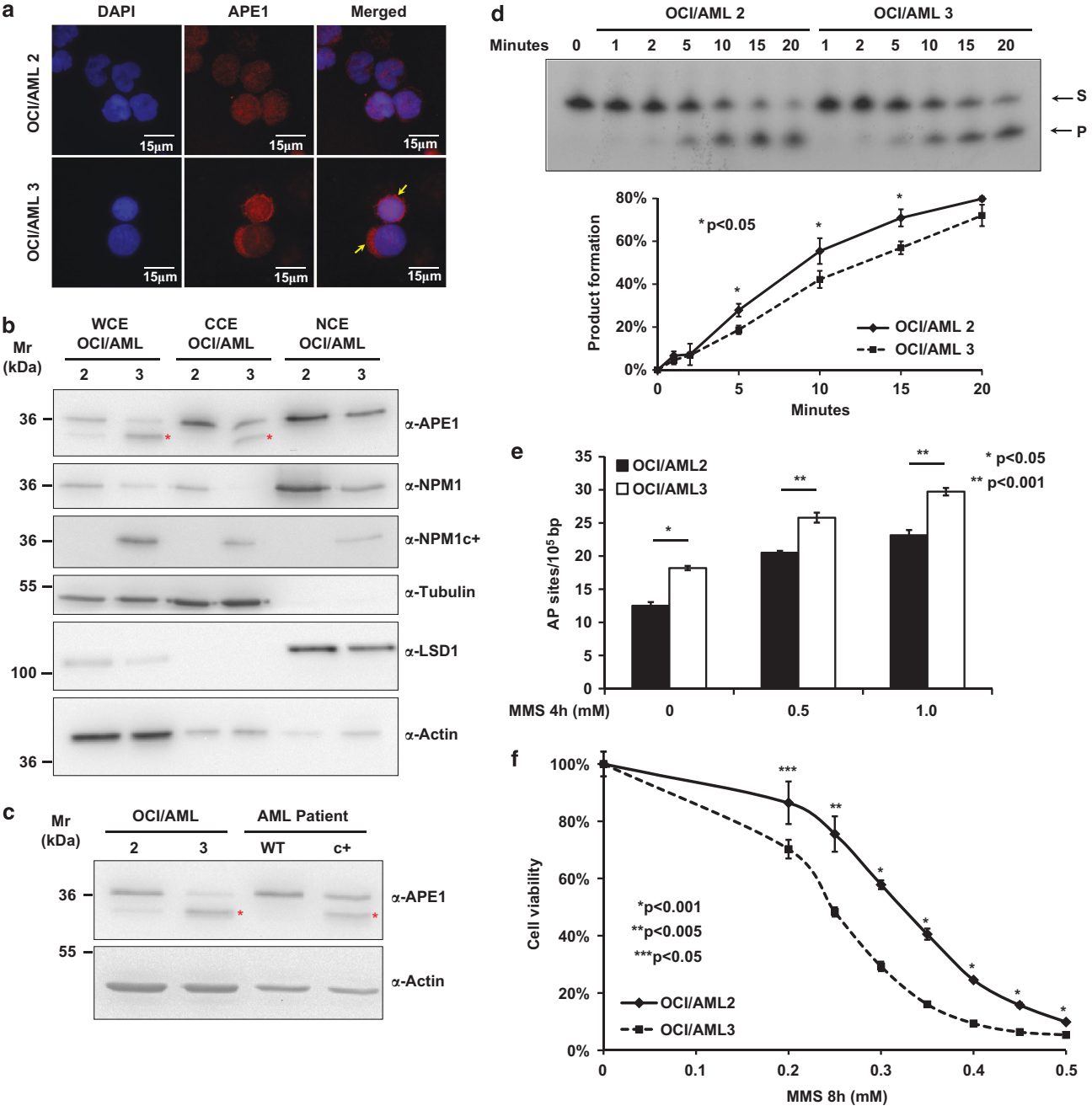

Figure 4. NPM1c+ mutation alters APE1 subcellular localization and affects its endonuclease activity in OCI/AML3 cell line. (**a**) Representative images of fluorescence microscopy analysis of APE1 on OCI/AML2 (WT NPM1) and OCI/AML3 (NPM1c+) cell lines. A total of 2×10^4 cells were centrifuged onto glass slides using a cytospin, and IF was performed as reported in Materials and Methods section. A secondary α-mouse Rhodamine Red-conjugated antibody was used to visualize APE1. Nuclei are stained with 4′,6-diamidino-2-phenylindole. A predominant cytoplasmic positivity of APE1 could be observed in OCI/AML3 cells only, linking NPM1c+ mutation with APE1 cytoplasmic relocalization. (**b**) In all, 10 μg of total cell extract (WCE), 10 μg of cytoplasmic cell extract (CCE) and 5 μg of nuclear cell extract (NCE) of OCI/AML2 and 3 were separated onto SDS–PAGE, immunoblotted and analyzed for their content of APE1 and NPM1 (WT and c+). NPM1c+ protein was detected with a specific antibody recognizing only the NPM1c+ mutant form.[47] Western blotting analysis showed the presence of truncated APE1 protein (*) only in the whole and cytoplasmic extracts from OCI/AML3 cell line. Actin was used as loading control, whereas tubulin and LSD1 were used as markers of cytoplasmic and nuclear fraction enrichment, respectively. (**c**) Total cell extracts of 10 μg from OCI/AML2 and 3 and of blast from AML patients expressing WT NPM and NPM1c+ mutant were separated onto SDS–PAGE, immunoblotted and analyzed for their APE1 content. The expression of NPM1c+ mutant form is associated with the presence of truncated APE1 protein (*) in extracts from both the OCI/AML3 cell line and blasts from a patient carrying this mutation. Actin was used as loading control. (**d**) OCI/AML2 and OCI/AML3 nuclear cell extracts of 50 ng were used to evaluate the APE1 endonuclease activity. A representative image shows the conversion of the substrate (S) to product (P) operated by APE1. OCI/AML3 cells show lower AP-incision activity, in accordance with the decreased nuclear APE1 content. The diagram below reports the mean ± s.d. values obtained from the densitometric analysis of three independent experiments. (**e**) The amount of abasic (AP) sites was measured in OCI/AML2 and OCI/AML3 cells under basal conditions and after treatment with 0.5 and 1 mM MMS for 4 h. OCI/AML3 cells display a significantly higher amount of AP sites if compared with OCI/AML2 cells. Mean ± s.d. values are the result of three independent experiments. (**f**) CellTiter-Glo Luminescent Cell Viability assay was used to evaluate the sensitization of OCI/AML2 and OCI/AML3 cells to MMS. Cells were incubated with the indicated amounts of MMS for 8 h. Expression of NPM1c+ negatively affects cell viability. Mean ± s.d. values are the result of three independent experiments.

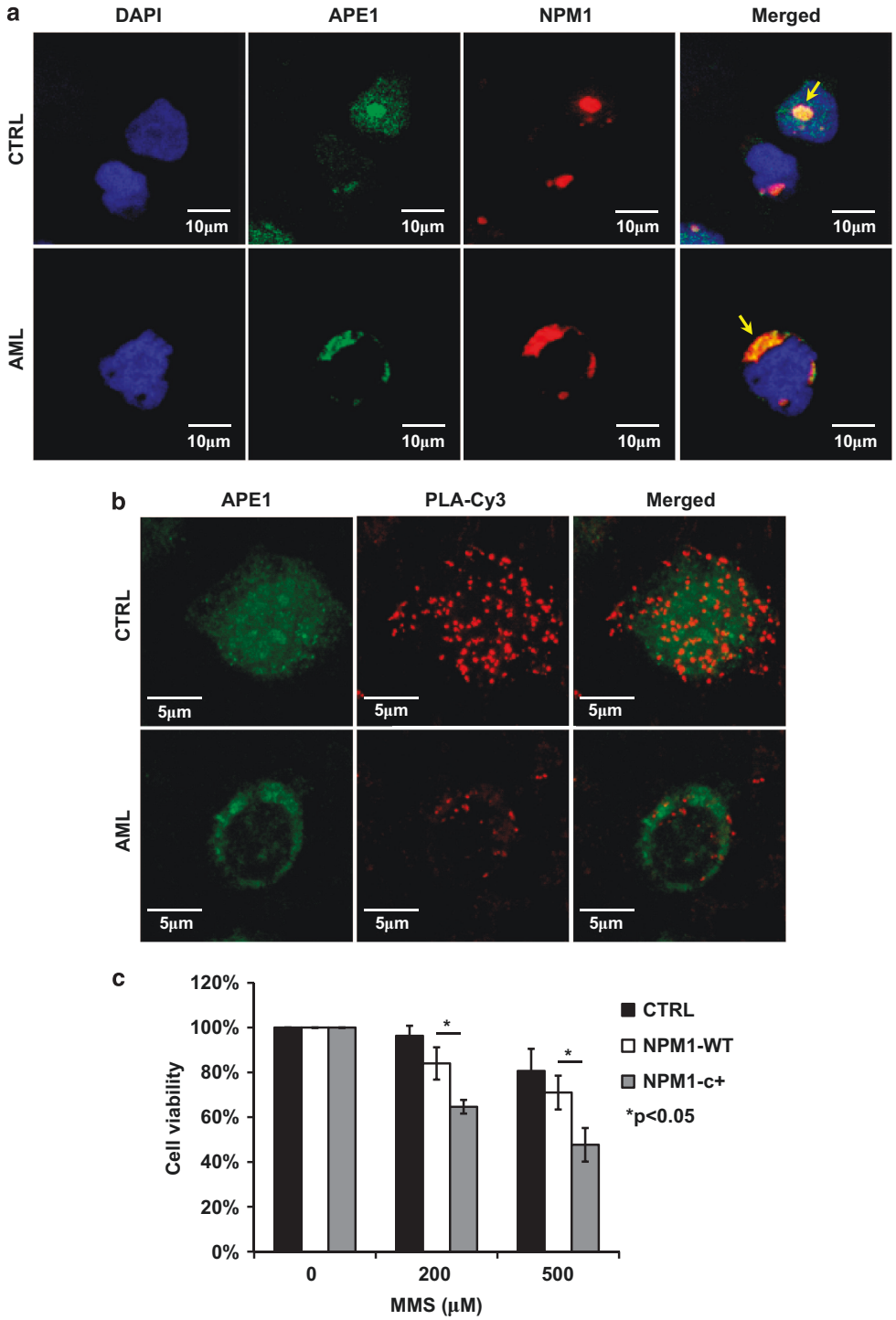

Figure 5. NPM1 mutation alters APE1 localization, reducing cell resistance to genotoxic damage in blasts from AML patients. (**a**) Representative images of fluorescence microscopy analysis of APE1 and NPM1 on blasts from AML patients (AML) carrying NPM1c+ mutation and healthy donors (CTRL). A total of 2×10^4 cells were centrifuged onto glass slides using a cytospin, and IF analyses were performed as reported in Materials and Methods section. A secondary α-mouse-Alexa Fluor 488-conjugated antibody was used to visualize APE1 (green), and a secondary α-rabbit-Rhodamine-conjugated antibody was used to visualize NPM1 (red). Nuclei are stained with 4′,6-diamidino-2-phenylindole. In merged images, yellow arrows indicate the occurrence of colocalization between APE1 and NPM1. In control cells, NPM1 accumulates within nucleoli while being mainly excluded from this subcellular compartment in blasts from AML patients, which show a predominant cytoplasmic positivity. Accordingly, APE1 delocalizes from nucleus to cytoplasm in blasts from AML patients. (**b**) Representative images of PLA analysis to evaluate the interaction between APE1 and NPM1 on blasts from AML patients (AML) carrying NPM1c+ mutation and healthy donors (CTRL). A total of 2.5×10^4 cells were centrifuged onto glass slides using a cytospin, and PLA was performed as reported in Materials and Methods section. APE1 (green) accumulates within the nucleus in control cells while being mainly excluded from this subcellular compartment in blasts from AML patients. In accordance, also PLA signal delocalizes from nucleus to cytoplasm in blasts from AML patients. (**c**) Cell viability of blasts from healthy donors (CTRL, $n = 3$), AML patients expressing WT NPM1 (NPM1-WT, $n = 3$) or the NPM1c+ mutant form (NPM1c+, $n = 4$) after 4 h of treatment with the indicated doses of MMS was measured through the MTS assay. AML cells expressing the NPM1-c+ are more sensitive to the alkylating agent than blasts from healthy donors and AML patients expressing the NPM1-WT form. Mean ± s.d. values are the result of three independent experiments.

occurring on the known bipartite NLS of APE1 have been described so far, nor alternative splicing forms have been found that could explain the cytoplasmic accumulation of APE1 in tumors. As the majority of the polymorphisms described in literature involve residues not responsible for either the DNA repair or the redox functions of the protein, but rather changes that often fall within the N domain involved in protein–protein interactions and protein stability,[33,62] a reasonable explanation for the delocalization of the protein observed in tumors may be ascribed to alterations of a complex network of interactions affecting, in turn, APE1 functional status. Here, we showed that in OCI/AML3 cells expressing the NPM1c+ allele, as well as in blasts from AML patients, APE1 protein is destabilized (Figures 4b and c). It can be inferred that, similarly to the case of $p19^{Arf}$, the physiological function of NPM1 is to ensure the proper localization of APE1 and to protect it from degradation, being possible that NPM1 protein may function as a chaperone for APE1, allowing its correct folding.

Our model (Figure 6a) is in accordance and further extends a previous one[1] trying to explain the relative contribution (direct or indirect) of NPM1 expression to cellular transformation. Our model takes into account the evidence that tumors of hematopoietic origin, such as AML, are associated with WT NPM1 deficiency, whereas a number of solid tumors (that is, gastric, hepatic and ovarian) show increased expression of WT NPM1. In the first case, the contribution of a NPM1 mutation is causally linked to the transformation process. Indeed, reduced nuclear NPM1 levels, as a consequence of the mutation of one WT allele, may lead to genomic instability due to BER impairment, and thus to an increased cellular burden of DNA damage. Therefore, the impaired DNA-damage response may block cell proliferation inefficiently, such that some cells would escape the checkpoint and establish an immortalized clone prone to further oncogenic transformation. Alternatively (Figure 6b), elevated WT NPM1 expression levels would contribute to the generation of permissive condition for oncogenic transformation. In that case, the presence of high NPM1 levels may limit DNA damage and promote the DNA-damage response (due to increased BER), associated with oncogenic stress signals in a normal cell, and therefore may support cell survival and eventually transformation. This model could also involve the APE1 protein in two ways: through an impaired BER response and the resulting genetic instability; and through the establishment of conditions permissive for transformation. Our evidence suggests that defects in the APE1–NPM1 interaction can be associated with the genomic instability observed in tumors, which supports the concept that interfering with this interaction may sensitize cancer cells to chemotherapy and radiotherapy.

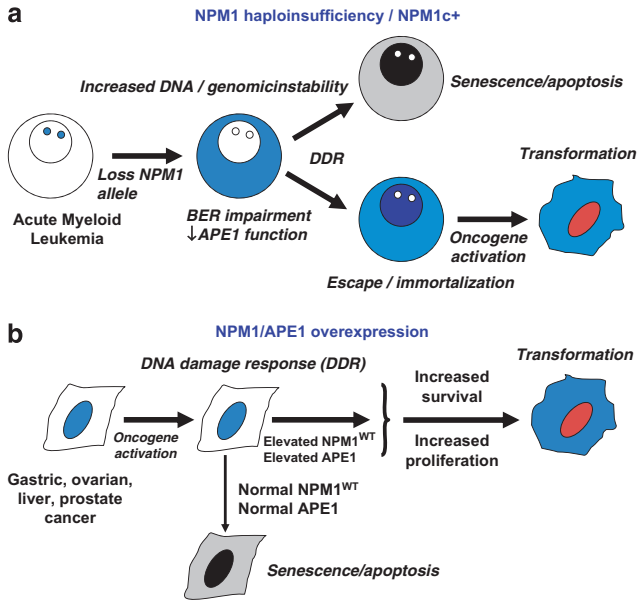

Figure 6. Relative contribution of NPM1/APE1 expression to cellular transformation: a model for APE1 role in tumorigenesis? (**a**) Reduced NPM1 levels due to loss of one WT allele leads to genomic instability through impairment of BER and increased DNA damage. As a consequence, the DNA-damage response blocks cellular proliferation. Few cells may escape the block and establish an immortalized clone prone to be transformed by oncogene activation. (**b**) Oncogene activation in a normal cell leads to unscheduled DNA replication and DNA damage. Cellular checkpoints are activated favoring apoptosis or senescence as response to uncontrolled proliferative signals. The presence of high NPM1/APE1 levels may limit DNA damage and DNA-damage response, and therefore support cell survival and eventually transformation. This model also includes APE1 protein both in the first case as having a causative role in the transformation process itself and in the second case, in which NPM1 and APE1 expression levels are simultaneously elevated, generating a permissive condition for transformation.

MATERIALS AND METHODS

Cell lines and materials

HeLa, MEF $p53^{-/-}$/$NPM1^{+/+}$ ($NPM1^{+/+}$)[36] and MEF $p53^{-/-}$/$NPM1^{-/-}$ ($NPM1^{-/-}$)[36] cell lines were grown in Dulbecco's modified Eagle's medium (Euroclone, Milan, Italy) supplemented with 10% fetal bovine serum (Euroclone), 100 U/ml penicillin and 10 μg/ml streptomycin sulfate. OCI/AML2 and 3 cells were grown in alpha-MEM (Euroclone) supplemented with 20% fetal bovine serum, 100 U/ml penicillin and 10 μg/ml streptomycin sulfate. Leukemic cells were obtained from the bone marrow of patients with acute leukemia during diagnostic procedures. Mononuclear cells were separated on a Ficoll–Hystopaque 1077 (Sigma Aldrich, Milan, Italy) density gradient, then were washed twice in phosphate-buffered saline, checked for viability by using the trypan blue exclusion test and suspended in phosphate-buffered saline. Presence of mutations in the *NPM1* gene was detected as previously described.[63] Blast from patients were grown in RPMI (Invitrogen, Monza, Italy) supplemented with 20% fetal bovine serum. Stable cell lines reexpressing WT NPM1 in the $NPM1^{-/-}$ background were obtained as previously described.[17] All chemical reagents were supplied from Sigma Aldrich unless otherwise specified.

Cell-viability analyses

Cell viability was measured by using the MTS assay (Promega, Milan, Italy) on MEF cells (5×10^3 cells) and blasts from patients (60×10^3 cells) grown in 96-well plates. Cells were plated, and after MMS, $KBrO_3$ or acute H_2O_2 treatment, 20 μl of MTS solution was added to each well and plates were incubated for 2 h at 37 °C. Absorbance (at 490 nm) was measured by using a multiwell plate reader. The values were standardized to wells containing media alone. Cytotoxicity induced by BLM was evaluated using a trypan blue exclusion assay. A total of 4×10^4 cells per well were plated in six-well plates, treated for 60 min with reported amounts of BLM and then grown for 2 additional days in fresh media. Cell viability for OCI/AML cell lines (2.5×10^4 cells) was measured by CellTiter-Glo Luminescent Cell Viability Assay (Promega) according to the manufacturer's protocol. Cells were incubated with the indicated doses of MMS for 8 h at 37 °C in agitation. Luminescent signals were measured using the Turner BioSystems Luminometer (Promega). Cell survival upon inhibition of APE1 AP endonuclease activity was measured with the WST-8 assay. MEF cells were seeded onto 96-well plates (6×10^3 cells) and allowed to adhere for 24 h. MEFs were then incubated with the indicated amounts of compound 3 (*N*-(3-(benzo[*d*]thiazol-2-yl)-6-isopropyl-4,5,6,7-tetrahydrothieno[2,3-*c*]pyridin-2-yl)acetamide),[44] and viability was measured 24 h later using the CCK-8 Kit (Dojindo, Munich, Germany) as per the manufacturer's instructions.

Plasmid preparation

The construct pcDNA3-HA-NPM1c+ was generated by using the Quickchange II XL Mutagenesis kit (Stratagene, Milan, Italy) and the pcDNA3-HA-NPM1-WT as template following the manufacturer's instructions. Direct sequencing was performed in order to verify the sequence accuracy. WT NPM1 and NPM1c+ cDNA were also subcloned in pCMV5.1-FLAG and p3X-FLAG-CMV vectors for reconstitution experiments on MEF-$NPM1^{-/-}$ cells.

AP-sites measurements

Genomic DNA was isolated from 2×10^6 cells by using the DNAzol Reagent (Invitrogen), and then concentration and purity were determined spectrophotometrically. Samples of 0.1 mg/ml of genomic DNA were analyzed to quantify abasic damage in chromosomal DNA using the DNA Damage Quantification Kit (Dojindo) according to the manufacturer's instructions.

IF and PLA analysis

For IF analysis on HeLa and MEFs, cells were grown on glass coverslips, whereas blasts and OCI/AML 2 and 3 cells were centrifuged onto glass slides using a cytospin. Then, cells were fixed with 4% (wt/vol) paraformaldehyde for 20 min at room temperature and permeabilized for 5 min with phosphate-buffered saline–0.25% (vol/vol) Triton X-100. Cells were incubated for 30 min with 10% fetal bovine serum in TBS–0.1% (vol/vol) Tween 20 (blocking solution) to block unspecific binding of the antibodies. Cells were then incubated with primary antibodies diluted in blocking solutions: monoclonal-α-APE1 (diluted 1:50, 3 h, 37 °C), polyclonal α-NPM1 (diluted 1:200, overnight, 4 °C), monoclonal α-FLAG-FITC-conjugated (diluted 1:100, 3 h, 37 °C) and polyclonal α-HA (diluted 1:500, overnight, 4 °C). Then cells were washed three times for 5 min each with TBS–0.1% (vol/vol) Tween 20 (Washing Solution) and incubated with secondary antibody: α-mouse or α-rabbit Rhodamine Red-conjugated or Alexa Fluor 488-conjugated (diluted 1:200, 2 h, 25 °C) (Jackson Immuno, West Grove, PA, USA). After washing three times, coverslips were mounted on microscope slides with a mounting media containing 4′,6-diamidino-2-phenylindole and an anti-fade reagent. For PLA analysis on blasts from patient's primary antibody α-APE1 was previously labeled with the Zenon α-Mouse IgG Labeling Kit (Invitrogen) using the Alexa Fluor 488 according to the manufacturer's instructions.

To study the interaction of APE1 with NPM1 *in vivo*, we used the *in situ* PLA technology (Olink Bioscience, Uppsala, Sweden). After incubation with monoclonal α-APE1 (1:50) or α-FLAG antibody (1:100) for 3 h at 37 °C, cells were incubated with polyclonal α-NPM1 (1:200) or polyclonal α-HA antibody (Sigma-Aldrich) (1:500) overnight at 4 °C. PLA was performed following the manufacturer's instructions and as previously reported.[36] Technical controls, represented by the omission of α-NPM1/α-HA primary antibody, resulted in the complete loss of PLA signal. Images were captured through a confocal microscope, and quantification of PLA signal was performed using the *Blob Finder* software (Center for Image Analysis, Uppsala University).

Cells were visualized through a Leica TCS SP laser-scanning confocal microscope (Leica Microsystems, Milan, Italy) or a DMB6000B inverted microscope equipped with a DFC300FX digital camera (Leica Microsystems).

Preparation of cell extracts and protein quantification

Cell extracts were prepared as already described in Vascotto *et al.*[17] and as reported in Supplementary Information.

Cell transfection and western blotting analyses

Plasmids were prepared and used for transfection and western blotting analysis, as already described in Fantini *et al.*[30] and as reported in Supplementary Information.

Incision assays on abasic double-stranded DNA

APE1 endonuclease activity was evaluated as already described[17] and as reported in Supplementary Information.

Statistical analysis

Statistical analysis on biological data was performed using the Microsoft Excel data analysis program for Student's *t*-test analysis.

ABBREVIATIONS

AML, acute myeloid leukemia; APE1/Ref-1, apurinic/apyrimidinic endonuclease 1/redox effector factor 1; BER, base excision DNA repair; NPM1, nucleophosmin 1.

CONFLICT OF INTEREST

The authors declare no conflict of interest.

ACKNOWLEDGEMENTS

We greatly thank the National Center for Advancing Translational Sciences (NCATS) and Dr David M Wilson III for providing the APE1 specific inhibitor (compound 3). We also thank Dr Malgorzata M Kamocka from the Indiana University School of Medicine, Department of Medicine, Division of Nephrology, Indiana Center for Biological Microscopy, Indianapolis, IN, USA. for her helpful suggestions during IF analyses, Dr Laura Cesaratto for cell-viability assays and Sofia Tell for kind support. This work was supported by grants from: AIRC (IG10269) and MIUR (FIRB_RBRN07BMCT and PRIN2008_CCPKRP_003) to GT. This work has been also supported by a UICC Yamagiwa-Yoshida Memorial International Cancer Study Grant to GT.

REFERENCES

1 Colombo E, Alcalay M, Pelicci PG. Nucleophosmin and its complex network: a possible therapeutic target in hematological diseases. *Oncogene* 2011; **30**: 2595–2609.
2 Colombo E, Marine JC, Danovi D, Falini B, Pelicci PG. Nucleophosmin regulates the stability and transcriptional activity of p53. *Nat Cell Biol* 2002; **4**: 529–533.
3 Lee C, Smith BA, Bandyopadhyay K, Gjerset RA. DNA damage disrupts the p14ARF-B23 (nucleophosmin) interaction and triggers a transient subnuclear redistribution of p14ARF. *Cancer Res* 2005; **65**: 9834–9842.
4 Mrózek K, Marcucci G, Paschka P, Whitman SP, Bloomfield CD. Clinical relevance of mutations and gene-expression changes in adult acute myeloid leukemia with normal cytogenetics: are we ready for a prognostically prioritized molecular classification? *Blood* 2007; **109**: 431–448.
5 Falini B, Bolli N, Shan J, Martelli MP, Liso A, Pucciarini A *et al.* Both carboxy-terminus NES motif and mutated tryptophan(s) are crucial for aberrant nuclear export of nucleophosmin leukemic mutants in NPMc+ AML. *Blood* 2006; **107**: 4514–4523.
6 Pianta A, Fabbro D, Damiani D, Tiribelli M, Fanin R, Franzoni A *et al.* Two novel NPM1 mutations in a therapy-responder AML patient. *Hematol Oncol* 2010; **28**: 151–155.
7 Vassiliou GS, Cooper JL, Rad R, Li J, Rice S, Uren A *et al.* Mutant nucleophosmin and cooperating pathways drive leukemia initiation and progression in mice. *Nat Genet* 2011; **43**: 470–475.
8 den Besten W, Kuo ML, Williams RT, Sherr CJ. Myeloid leukemia-associated nucleophosmin mutants perturb p53-dependent and independent activities of the Arf tumor suppressor protein. *Cell Cycle* 2005; **4**: 1593–1598.
9 Colombo E, Martinelli P, Zamponi R, Shing DC, Bonetti P, Luzi L *et al.* Delocalization and destabilization of the Arf tumor suppressor by the leukemia-associated NPM mutant. *Cancer Res* 2006; **66**: 3044–3050.
10 Bonetti P, Davoli T, Sironi C, Amati B, Pelicci PG, Colombo E. Nucleophosmin and its AML-associated mutant regulate c-Myc turnover through Fbw7 gamma. *J Cell Biol* 2008; **182**: 19–26.
11 Cilloni D, Messa F, Rosso V, Arruga F, Defilippi I, Carturan S *et al.* Increase sensitivity to chemotherapeutical agents and cytoplasmatic interaction between NPM leukemic mutant and NF-kappaB in AML carrying NPM1 mutations. *Leukemia* 2008; **22**: 1234–1240.
12 Gurumurthy M, Tan CH, Ng R, Zeiger L, Lau J, Lee J *et al.* Nucleophosmin interacts with HEXIM1 and regulates RNA polymerase II transcription. *J Mol Biol* 2008; **378**: 302–317.
13 Wanzel M, Russ AC, Kleine-Kohlbrecher D, Colombo E, Pelicci PG, Eilers M. A ribosomal protein L23-nucleophosmin circuit coordinates Mizl function with cell growth. *Nat Cell Biol* 2008; **10**: 1051–1061.
14 Falini B, Nicoletti I, Martelli MF, Mecucci C. Acute myeloid leukemia carrying cytoplasmic/mutated nucleophosmin (NPMc+ AML): biologic and clinical features. *Blood* 2007; **109**: 874–885.
15 Falini B, Martelli MP, Bolli N, Sportoletti P, Liso A, Tiacci E *et al.* Acute myeloid leukemia with mutated nucleophosmin (NPM1): is it a distinct entity? *Blood* 2011; **117**: 1109–1120.
16 Londero AP, Orsaria M, Tell G, Marzinotto S, Capodicasa V, Poletto M *et al.* Expression and prognostic significance of APE1/Ref1 and NPM1 proteins in ovarian serous cancer; submitted.
17 Vascotto C, Fantini D, Romanello M, Cesaratto L, Deganuto M, Leonardi A *et al.* APE1/Ref-1 interacts with NPM1 within nucleoli and plays a role in the rRNA quality control process. *Mol Cell Biol* 2009; **29**: 1834–1854.
18 Tell G, Fantini D, Quadrifoglio F. Understanding different functions of mammalian AP endonuclease (APE1) as a promising tool for cancer treatment. *Cell Mol Life Sci* 2010; **67**: 3589–3608.
19 Wilson 3rd DM, Simeonov A. Small molecule inhibitors of DNA repair nuclease activities of APE1. *Cell Mol Life Sci* 2010; **67**: 3621–3631.
20 Xanthoudakis S, Curran T. Identification and characterization of Ref-1, a nuclear protein that facilitates AP-1 DNA-binding activity. *EMBO J* 1992; **11**: 653–665.

21 Xanthoudakis S, Miao GG, Curran T. The redox and DNA-repair activities of Ref-1 are encoded by nonoverlapping domains. *Proc Natl Acad Sci USA* 1994; **91**: 23–27.
22 Ueno M, Masutani H, Arai RJ, Yamauchi A, Hirota K, Sakai T *et al.* Thioredoxin-dependent redox regulation of p53-mediated p21 activation. *J Biol Chem* 1999; **274**: 35809–35815.
23 Seemann S, Hainaut P. Roles of thioredoxin reductase 1 and APE/Ref-1 in the control of basal p53 stability and activity. *Oncogene* 2005; **24**: 3853–3863.
24 Hirota K, Matsui M, Iwata Z, Nishiyama A, Mori K, Yodoi J. AP-1 transcriptional activity is regulated by a direct association between thioredoxin and Ref-1. *Proc Natl Acad Sci USA* 1997; **94**: 3633–3638.
25 Wei SJ, Botero A, Hirota K, Bradbury CM, Markovina S, Laszlo A *et al.* Thioredoxin nuclear translocation and interaction with redox factor-1 activates the activator protein-1 transcription factor in response to ionizing radiation. *Cancer Res* 2000; **60**: 6688–6695.
26 Ziel KA, Campbell CC, Wilson GL, Gillespie MN. Ref-1/Ape is critical for formation of the hypoxia-inducible transcriptional complex on the hypoxic response element of the rat pulmonary artery endothelial cell VEGF gene. *FASEB J* 2004; **18**: 986–988.
27 Gray MJ, Zhang J, Ellis LM, Semenza GL, Evans DB, Watowich SS *et al.* HIF-1alpha, STAT3, CBP/p300 and Ref-1/APE are components of a transcriptional complex that regulates Src-dependent hypoxia-induced expression of VEGF in pancreatic and prostate carcinomas. *Oncogene* 2005; **24**: 3110–3120.
28 Tell G, Damante G, Caldwell D, Kelley MR. The intracellular localization of APE1/Ref-1: more than a passive phenomenon? *Antioxid Redox Signal* 2005; **7**: 367–384.
29 Bhakat KK, Izumi T, Yang SH, Hazra TK, Mitra S. Role of acetylated human AP-endonuclease (APE1/Ref-1). in regulation of the parathyroid hormone gene. *EMBO J* 2003; **22**: 6299–6309.
30 Fantini D, Vascotto C, Marasco D, D'Ambrosio C, Romanello M, Vitagliano L *et al.* Critical lysine residues within the overlooked N-terminal domain of human APE1 regulate its biological functions. *Nucleic Acids Res* 2010; **38**: 8239–8256.
31 Tell G, Wilson 3rd DM, Lee CH. Intrusion of a DNA repair protein in the RNome world: is this the beginning of a new era? *Mol Cell Biol* 2010; **30**: 366–371.
32 Barnes T, Kim WC, Mantha AK, Kim SE, Izumi T, Mitra S *et al.* Identification of apurinic/apyrimidinic endonuclease 1 (APE1) as the endoribonuclease that cleaves c-myc mRNA. *Nucleic Acids Res* 2009; **37**: 3946–3958.
33 Poletto M, Vascotto C, Scognamiglio PL, Lirussi L, Marasco D, Tell G. Role of the unstructured N-terminal domain of the human apurinic/apyrimidinic endonuclease 1 (hAPE1) in the modulation of its interaction with nucleic acids and nucleophosmin (NPM1). *Biochem J* 2013; **452**: 545–557.
34 Mol CD, Izumi T, Mitra S, Tainer JA. DNA-bound structures and mutants reveal abasic DNA binding by APE1 and DNA repair coordination (corrected). *Nature* 2000; **403**: 451–456.
35 Masuda Y, Bennett RA, Demple B. Dynamics of the interaction of human apurinic endonuclease (Ape1) with its substrate and product. *J Biol Chem* 1998; **273**: 30352–30359.
36 Colombo E, Bonetti P, Lazzerini Denchi E, Martinelli P, Zamponi R, Marine JC *et al.* Nucleophosmin is required for DNA integrity and p19Arf protein stability. *Mol Cell Biol* 2005; **25**: 8874–8886.
37 Lirussi L, Antoniali G, Vascotto C, D'Ambrosio C, Poletto M, Romanello M *et al.* Nucleolar accumulation of APE1 depends on charged lysine residues that undergo acetylation upon genotoxic stress and modulate its BER activity in cells. *Mol Biol Cell* 2012; **23**: 4079–4096.
38 Svilar D, Goellner EM, Almeida KH, Sobol RW. Base excision repair and lesion-dependent subpathways for repair of oxidative DNA damage. *Antioxid Redox Signal* 2011; **14**: 2491–2507.
39 Kaina B, Ochs K, Grosch S, Fritz G, Lips J, Tomicic M *et al.* BER, MGMT, and MMR in defense against alkylation-induced genotoxicity and apoptosis. *Prog Nucleic Acid Res Mol Biol* 2001; **68**: 41–54.
40 Jiang Y, Guo C, Fishel ML, Wang ZY, Vasko MR, Kelley MR. Role of APE1 in differentiated neuroblastoma SH-SY5Y cells in response to oxidative stress: use of APE1 small molecule inhibitors to delineate APE1 functions. *DNA Repair (Amst)* 2009; **8**: 1273–1282.
41 Ballmair D, Epe B. DNA damage by bromate: mechanism and consequences. *Toxicology* 2006; **221**: 166–171.
42 Chen J, Stubbe J. Bleomycins: towards better therapeutics. *Nat Rev Cancer* 2005; **5**: 102–112.
43 Fung H, Demple B. Distinct roles of Ape1 protein in the repair of DNA damage induced by ionizing radiation or bleomycin. *J Biol Chem* 2011; **286**: 4968–4977.
44 Rai G, Vyjayanti VN, Dorjsuren D, Simeonov A, Jadhav A, Wilson 3rd DM *et al.* Synthesis, biological evaluation, and structure-activity relationships of a novel class of apurinic/apyrimidinic endonuclease 1 inhibitors. *J Med Chem* 2012; **55**: 3101–3112.
45 Weibrecht I, Leuchowius KJ, Clausson CM, Conze T, Jarvius M, Howell WM *et al.* Proximity ligation assays: a recent addition to the proteomics toolbox. *Expert Rev Proteomics* 2010; **7**: 401–409.
46 Falini B, Mecucci C, Tiacci E, Alcalay M, Rosati R, Pasqualucci L *et al.* GIMEMA Acute Leukemia Working Party. Cytoplasmic nucleophosmin in acute myelogenous leukemia with a normal karyotype. *N Engl J Med* 2005; **352**: 254–266Erratum in: *N Engl J Med* 2005; **352**: 740.
47 Quentmeier H, Martelli MP, Dirks WG, Bolli N, Liso A, Macleod RA *et al.* Cell line OCI/AML3 bears exon-12 NPM gene mutation-A and cytoplasmic expression of nucleophosmin. *Leukemia* 2005; **19**: 1760–1767.
48 Yoshida A, Urasaki Y, Waltham M, Bergman AC, Pourquier P, Rothwell DG *et al.* Human apurinic/apyrimidinic endonuclease (Ape1) and its N-terminal truncated form (AN34) are involved in DNA fragmentation during apoptosis. *J Biol Chem* 2003; **278**: 37768–37776.
49 Fan Z, Beresford PJ, Zhang D, Xu Z, Novina CD, Yoshida A *et al.* Cleaving the oxidative repair protein Ape1 enhances cell death mediated by granzyme A. *Nat Immunol* 2003; **4**: 145–153.
50 Guo Y, Chen J, Zhao T, Fan Z. Granzyme K degrades the redox/DNA repair enzyme Ape1 to trigger oxidative stress of target cells leading to cytotoxicity. *Mol Immunol* 2008; **45**: 2225–2235.
51 Vascotto C, Bisetto E, Li M, Zeef LA, D'Ambrosio C, Domenis R *et al.* Knock-in reconstitution studies reveal an unexpected role of Cys-65 in regulating APE1/Ref-1 subcellular trafficking and function. *Mol Biol Cell* 2011; **22**: 3887–3901.
52 Kelley MR, Luo M, Reed A, Su D, Delaplane S, Borch RF *et al.* Functional analysis of novel analogues of E3330 that block the redox signaling activity of the multifunctional AP endonuclease/redox signaling enzyme APE1/Ref-1. *Antioxid Redox Signal* 2011; **14**: 1387–1401.
53 Wang HF, Takenaka K, Nakanishi A, Miki Y. BRCA2 and nucleophosmin coregulate centrosome amplification and form a complex with the Rho effector kinase ROCK2. *Cancer Res* 2011; **71**: 68–77.
54 Fung H, Demple B. A vital role for APE1/Ref1 protein in repairing spontaneous DNA damage in human cells. *Mol. Cell* 2005; **17**: 463–470.
55 He T, Weintraub NL, Goswami PC, Chatterjee P, Flaherty DM, Domann FE *et al.* Redox factor-1 contributes to the regulation of progression from G0/G1 to S by PDGF in vascular smooth muscle cells. *Am J Physiol Heart Circ Physiol* 2003; **285**: H804–H812.
56 Izumi T, Brown DB, Naidu CV, Bhakat KK, Macinnes MA, Saito H *et al.* Two essential but distinct functions of the mammalian abasic endonuclease. *Proc Natl Acad Sci USA* 2005; **102**: 5739–5743.
57 Szczesny B, Tann AW, Longley MJ, Copeland WC, Mitra S. Long patch base excision repair in mammalian mitochondrial genomes. *J Biol Chem* 2008; **283**: 26349–26356.
58 Szczesny B, Tann AW, Mitra S. Age- and tissue-specific changes in mitochondrial and nuclear DNA base excision repair activity in mice: Susceptibility of skeletal muscles to oxidative injury. *Mech Ageing Dev* 2010; **131**: 330–337.
59 Tell G, Crivellato E, Pines A, Paron I, Pucillo C, Manzini G *et al.* Mitochondrial localization of APE/Ref-1 in thyroid cells. *Mutat Res* 2001; **485**: 143–152.
60 Angkeow P, Deshpande SS, Qi B, Liu YX, Park YC, Jeon BH *et al.* Redox factor-1: an extra-nuclear role in the regulation of endothelial oxidative stress and apoptosis. *Cell Death Differ* 2002; **9**: 717–725.
61 Ozaki M, Suzuki S, Irani K. Redox factor-1/APE suppresses oxidative stress by inhibiting the rac1 GTPase. *FASEB J* 2002; **16**: 889–890.
62 Yu ET, Hadi MZ. Bioinformatic processing to identify single nucleotide polymorphism that potentially affect Ape1 function. *Mutat Res* 2011; **722**: 140–146.
63 Pitiot AS, Santamaría I, García-Suárez O, Centeno I, Astudillo A, Rayón C *et al.* A new type of NPM1 gene mutation in AML leading to a C-terminal truncated protein. *Leukemia* 2007; **21**: 1564–1566.

Supplementary Information accompanies this paper on the Oncogene website (http://www.nature.com/onc)

Nucleolar accumulation of APE1 depends on charged lysine residues that undergo acetylation upon genotoxic stress and modulate its BER activity in cells

Lisa Lirussi[a,*], Giulia Antoniali[a,*], Carlo Vascotto[a], Chiara D'Ambrosio[b], Mattia Poletto[a], Milena Romanello[a], Daniela Marasco[c,d], Marilisa Leone[d], Franco Quadrifoglio[a], Kishor K. Bhakat[e], Andrea Scaloni[b], and Gianluca Tell[a]

[a]Department of Medical and Biological Sciences, University of Udine, 33100 Udine, Italy; [b]Proteomics and Mass Spectrometry Laboratory, Istituto di Ricerche per il Sistema Produzione Animale in Ambiente Mediterraneo, National Research Council, 80147 Naples, Italy; [c]Department of Biological Sciences, University of Naples "Federico II," 80134 Naples, Italy; [d]Institute of Biostructures and Bioimaging, National Research Council, 80134 Naples, Italy; [e]Department of Biochemistry and Molecular Biology, University of Texas Medical Branch, Galveston, TX 77555

ABSTRACT **Apurinic/apyrimidinic endonuclease 1 (APE1) is the main abasic endonuclease in the base excision repair (BER) pathway of DNA lesions caused by oxidation/alkylation in mammalian cells; within nucleoli it interacts with nucleophosmin and rRNA through N-terminal Lys residues, some of which ($K^{27}/K^{31}/K^{32}/K^{35}$) may undergo acetylation in vivo. Here we study the functional role of these modifications during genotoxic damage and their in vivo relevance. We demonstrate that cells expressing a specific K-to-A multiple mutant are APE1 nucleolar deficient and are more resistant to genotoxic treatment than those expressing the wild type, although they show impaired proliferation. Of interest, we find that genotoxic treatment induces acetylation at these K residues. We also find that the charged status of $K^{27}/K^{31}/K^{32}/K^{35}$ modulates acetylation at K^{6}/K^{7} residues that are known to be involved in the coordination of BER activity through a mechanism regulated by the sirtuin 1 deacetylase. Of note, structural studies show that acetylation at $K^{27}/K^{31}/K^{32}/K^{35}$ may account for local conformational changes on APE1 protein structure. These results highlight the emerging role of acetylation of critical Lys residues in regulating APE1 functions. They also suggest the existence of cross-talk between different Lys residues of APE1 occurring upon genotoxic damage, which may modulate APE1 subnuclear distribution and enzymatic activity in vivo.**

Monitoring Editor
Karsten Weis
University of California, Berkeley

Received: Apr 17, 2012
Revised: Jul 25, 2012
Accepted: Aug 16, 2012

This article was published online ahead of print in MBoC in Press (http://www.molbiolcell.org/cgi/doi/10.1091/mbc.E12-04-0299) on August 23, 2012.

*These authors contributed equally to this work

The authors declare that they have no conflict of interests.

Address correspondence to: Gianluca Tell (gianluca.tell@uniud.it).

Abbreviations used: APE1/Ref-1, apurinic/apyrimidinic endonuclease/redox effector factor 1; BER, base excision repair; MMS, methyl methanesulfonate; MTS, 3-(4-5-dimethylthiazol-2-yl)-5-(3-carboxymethoxyphenyl)-2-(4-sulfophenyl)-2H-tetrazolium salt; NPM1, nucleophosmin 1; SIRT1, sirtuin 1; TBHP, *tert*-butyl hydroperoxide.

INTRODUCTION

Apurinic/apyrimidinic endonuclease 1/redox effector factor-1 (APE1) plays a central role in the maintenance of genome stability and redox signaling (Bapat *et al.*, 2009, 2010; Tell *et al.*, 2010a; Wilson and Simeonov, 2010). Through its C-terminal domain (residues 61–318), it acts as an essential enzyme in the base excision repair (BER) pathway of DNA damages caused by both endogenous and exogenous oxidizing/alkylating agents, including many chemotherapeutic drugs. In combination with thioredoxin (Ueno *et al.*, 1999; Seemann and Hainaut, 2005) and through its N-terminal domain (residues 1–127), it also functions as a regulatory redox agent to maintain cancer-related transcription factors (Egr-1, NF-κB, p53, HIF-1α, AP-1, and Pax proteins) in an active reduced state (Hirota *et al.*, 1997;

Supplemental Material can be found at:
http://www.molbiolcell.org/content/suppl/2012/08/20/mbc.E12-04-0299.DC1.html

Wei *et al.*, 2000; Ziel *et al.*, 2004; Gray *et al.*, 2005; Pines *et al.*, 2005; Tell *et al.*, 2005, 2010a). APE1 can also act as a transcriptional repressor through indirect binding to negative Ca^{2+}-response elements (nCaRE), which are regulated by K^6/K^7 acetylation (Bhakat *et al.*, 2003). Recently APE1 was demonstrated to bind/cleave abasic RNA (Vascotto *et al.*, 2009b; Fantini *et al.*, 2010; Tell *et al.*, 2010b) and to control *c-Myc* expression by cleaving its mRNA (Barnes *et al.*, 2009). These discoveries pointed to a new function of APE1 in regulating gene expression through posttranscriptional mechanisms and brought to light the fact that this protein is a possible target for anticancer therapy.

In this context, we showed that the first 35 amino acids in the nonstructured N-terminal domain of APE1 are required for a stable interaction with rRNA, nucleophosmin 1 (NPM1), and other proteins involved in ribosome biogenesis/RNA processing (Vascotto *et al.*, 2009b; Tell *et al.*, 2010b). In particular, K residues within the protein region spanning amino acids 24–35 are involved in the interaction of APE1 with both rRNA and NPM1 and also regulate its in vitro enzymatic activity (Fantini *et al.*, 2010). Of interest, some of these critical K residues, namely $K^{27}/K^{31}/K^{32}/K^{35}$, undergo in vivo acetylation. These results suggest that protein–protein interactions and/or posttranslational modifications (PTMs) involving the APE1 N-terminal domain may play important roles in vivo in coordinating and fine-tuning the protein's BER activity and functions on rRNA metabolism. Recently it was also demonstrated that APE1 K^6/K^7 may undergo acetylation during cell response to genotoxic treatment (Fantini *et al.*, 2008) and that the acetylation status of these K residues, controlled by the sirtuin 1 (SIRT1) deacetylase activity, should be important in modulating protein DNA-repair function by regulating the kinetics of its interaction with other enzymes involved in BER, for example, XRCC1 (Yamamori *et al.*, 2010).

APE1 is mainly a nuclear protein and is critical for controlling cellular proliferative rates (Fung and Demple, 2005; Izumi *et al.*, 2005; Vascotto *et al.*, 2009b). We also showed that a considerable amount of APE1 is accumulated within the nucleoli of different cell lines (Vascotto *et al.*, 2009b; Fantini *et al.*, 2010), but its role within this compartment is unknown. Cytoplasmic, mitochondrial, and endoplasmic reticulum localizations have also been ascertained (Tell *et al.*, 2001; Szczesny and Mitra, 2005; Chattopadhyay *et al.*, 2006; Grillo *et al.*, 2006; Mitra *et al.*, 2007). APE1 is an abundant and relatively stable protein in mammalian cells (Tell *et al.*, 2009, 2010a). Fine-tuning of the multiple APE1 functions may therefore depend on the modulation of its PTMs and, eventually, on its interactome. Although a functional role has been determined for some PTMs (K^6/K^7 acetylation and $K^{24}/K^{25}/K^{27}$ ubiquitination; Bhakat *et al.*, 2003; Fantini *et al.*, 2008; Busso *et al.*, 2009), the identity and importance of various interacting partners in modulating APE1 biological functions are still under investigation (Parlanti *et al.*, 2007; Busso *et al.*, 2009; Vascotto *et al.*, 2009b). APE1 may affect cell growth by directly acting on rRNA quality control mechanisms; in particular, APE1 interaction with NPM1 may affect its activity over rRNA molecules. However, many aspects of this new function are undefined (Vascotto *et al.*, 2009b; Tell *et al.*, 2010b).

In this study, we address the biological role of APE1 acetylation at $K^{27}/K^{31}/K^{32}/K^{35}$ and, in light of recent evidence showing the emerging function of the nucleolus as a central sensor of protein trafficking during DNA repair after genotoxic treatment (Nalabothula *et al.*, 2010), the role of the nucleolus itself on the APE1 protective function toward genotoxic damage. We used a reconstitution strategy with APE1 mutants in which the charged Lys residues were replaced by either Ala or Arg to mimic constitutive acetylated ($APE1^{K4pleA}$) and nonacetylatable ($APE1^{K4pleR}$) protein forms, respectively. These mutants are reintroduced into APE1-silenced cell clones to determine the role of these crucial amino acids during cell response to genotoxic treatment.

RESULTS

Positively charged $K^{27}/K^{31}/K^{32}/K^{35}$ residues are essential for APE1 nucleolar accumulation through stabilization of protein interaction with NPM1 and rRNA

We previously demonstrated that charged K residues, located within the unstructured APE1 N-terminal domain (i.e., $K^{24}/K^{25}/K^{27}/K^{31}/K^{32}$), are crucial for APE1 interaction with rRNA and NPM1 and for modulating its catalytic activity on abasic DNA through regulation of product binding. Of interest, some of these critical amino acids (i.e., $K^{27}/K^{31}/K^{32}$ in addition to K^{35}) may undergo in vivo acetylation under basal conditions (Fantini *et al.*, 2010). We hypothesized that the degree of positive charges, modified by acetylation at these residues, may modulate APE1's different functions through its redirection to different substrates and/or stimulation of its DNA-repair enzymatic activity (Fantini *et al.*, 2010). To address this issue, we inspected the role of the positively charged residues within the region 27–35 in modulating the interaction between APE1 and NPM1. Colocalization experiments in HeLa cells transiently transfected with either FLAG-tagged, wild-type APE1 ($APE1^{WT}$), a K-to-A mutant ($APE1^{K4pleA}$) in which the positive charges have been removed as in the case of constitutive acetylation, or a nonacetylatable K-to-R APE1 mutant ($APE1^{K4pleR}$) showed that $APE1^{K4pleA}$ mutant has a marked exclusion from the nucleoli apparent in all expressing cells (Figure 1A). Silencing of the endogenous APE1 protein did not alter either the ability of the $APE1^{WT}$ and $APE1^{K4pleR}$ proteins to accumulate within the nucleolar compartment or the inability of the $APE1^{K4pleA}$ to accumulate within the nucleolus (unpublished data). These data thus demonstrate that $APE1^{WT}$ and $APE1^{K4pleR}$ nucleolar accumulation is not the consequence of their overexpression.

To complement these observations and also to exclude a possible contribution of the FLAG tag used to generate recombinant ectopic proteins, we exploited a live-cell imaging system as suggested by Schnell *et al.* (2012). APE1 cDNA was cloned into a pDendra2 vector to express APE1 in fusion with the green photoconvertible fluorophore Dendra (Chudakov *et al.*, 2007). As reported in Figure 1B, the fluorophore alone is present in both the cytoplasm and the nuclear compartment, but it is completely excluded from the nucleoli, as demonstrated by quantitative fluorescence signal analyses. In contrast, whereas the expression of Dendra in fusion with $APE1^{WT}$ and $APE1^{K4pleR}$ results in an efficient accumulation of the protein within the nucleolar compartment, the Dendra-$APE1^{K4pleA}$ mutant displays a homogeneous nuclear distribution. This approach confirms immunofluorescence-based data on the reduced accumulation of FLAG-tagged $APE1^{K4pleA}$ within the nucleoli and supports the evidence that the nucleolar accumulation of APE1 protein does not depend on the protein abundance nor does it depend on the specific tag used to generate the ectopic recombinant proteins (see also Supplemental Figure S1).

We supported our immunofluorescence data with biochemical interaction experiments. Coimmunoprecipitation analysis showed that the $APE1^{K4pleA}$ mutant has a significantly reduced interaction with NPM1 (Figure 2A), in accordance with its impaired nucleolar accumulation. The altered electrophoretic mobility observed for the $APE1^{K4pleA}$ mutant (Figure 2A) was further confirmed by SDS–PAGE analysis of recombinant proteins expressed in *Escherichia coli* and purified by chromatography. The effect is likely due to alteration of its overall charge, since electrospray ionization mass spectrometry analysis confirmed the correctness of protein mass values, and the

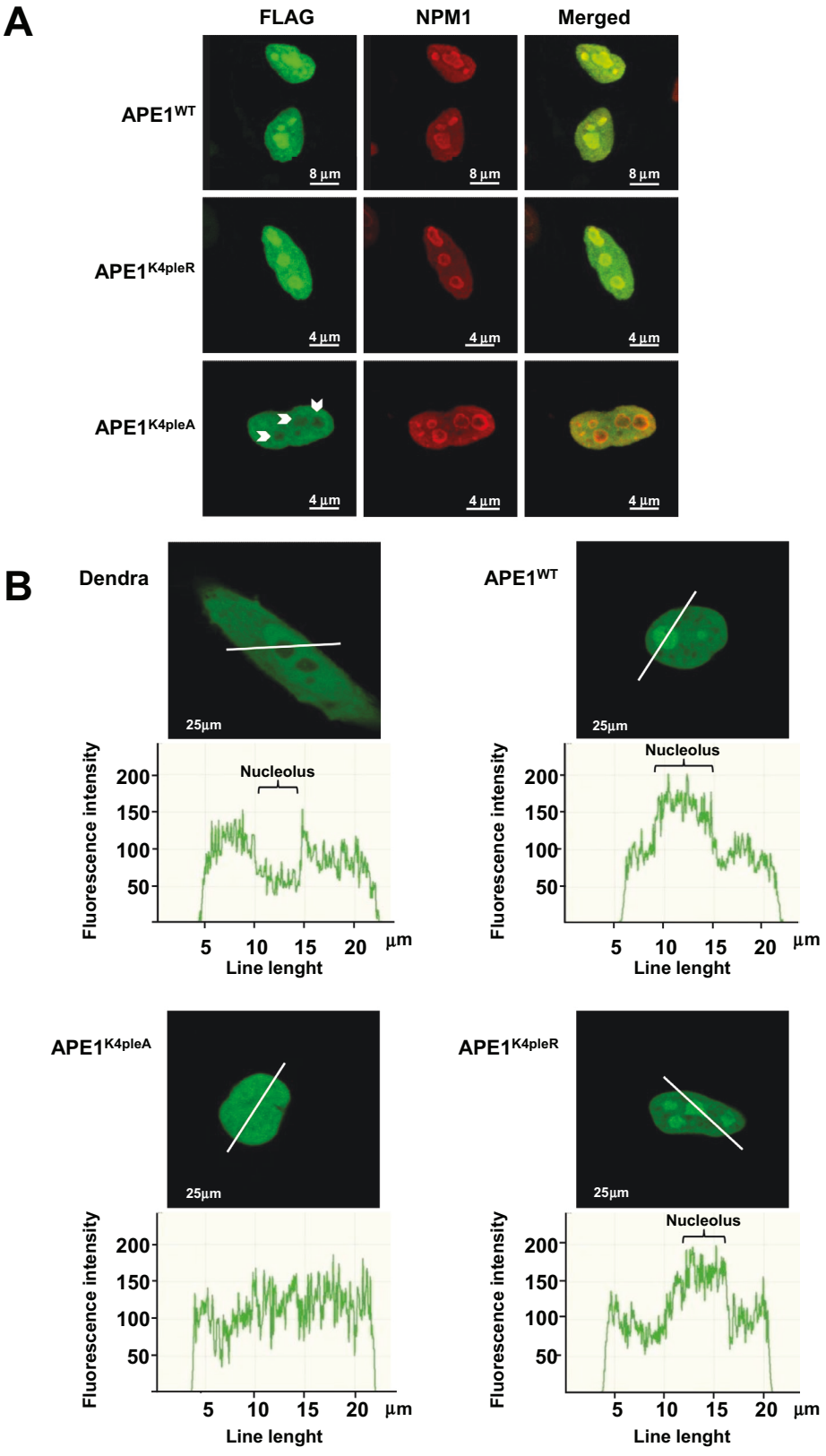

FIGURE 1: Positively charged $K^{27}/K^{31}/K^{32}/K^{35}$ residues are required for APE1 nucleolar accumulation. (A) Confocal microscopy of HeLa cells transfected with $APE1^{WT}$, $APE1^{K4pleA}$, or $APE1^{K4pleR}$ FLAG-tagged proteins and stained with antibodies against NPM1 (red) and ectopic FLAG-APE1 (green). Overlap of staining (yellow) demonstrated colocalization of the two proteins. Of note, the $APE1^{K4pleA}$ mutant was completely excluded from nucleoli (white arrowheads), whereas both $APE1^{WT}$ and the $APE1^{K4pleR}$ were accumulated within. Images are representative of 100% of transfected cells. (B) HeLa cells transfected with pDendra2-N empty vector or encoding APE1 (wild-type and mutants) in fusion with Dendra fluorophore were analyzed with a live confocal microscopy workstation. Cells transfected with empty vector (Dendra) showed diffuse green fluorescence within cytoplasm and nucleus, with exclusion of the nucleolar compartment. $APE1^{WT}$ and $APE1^{K4pleR}$ mutant mainly localized within the nuclear compartment and accumulated within nucleoli. In contrast, $APE1^{K4pleA}$ did not show any nucleolar accumulation. Images were captured by using the same settings (488-nm laser at 10% of intensity and PMT at 760 V). Fluorescence intensity analysis was carried out on a 25-µm-long line (white). Graphs represent the fluorescence intensity measured through a cross section of the nucleus and demonstrate an incremental fluorescence in corresponding nucleoli only in the case of $APE1^{WT}$ and $APE1^{K4pleR}$-Dendra fusion protein–expressing cells.

difference in their apparent mobility observed in SDS–PAGE was abolished when separating various mutants in urea-containing denaturing gels (Supplemental Figure S2 and unpublished data). It was also observed for other K-to-A mutants of APE1 (Fantini *et al.*, 2010). We then evaluated the contribution of the single K residues to the extent of APE1 nucleolar localization (Supplemental Figure S3) and the ability to interact with NPM1 (Figure 2B). Double mutants $APE1^{K27/35A}$, $APE1^{K31/32A}$, $APE1^{K27/35R}$, and $APE1^{K31/32R}$ and a deletion mutant lacking 33 amino acids at the protein N-terminus ($APE1^{N\Delta33}$) were compared with $APE1^{WT}$. Whereas $APE1^{WT}$, $APE1^{K27/35R}$, and $APE1^{K31/32R}$ displayed a nucleolar and nucleoplasmic staining, $APE1^{K27/35A}$ and $APE1^{K31/32A}$ showed two alternative stainings, exhibiting nucleolar/nucleoplasmic or only nucleoplasmic positivity, respectively (Supplemental Figure S3). Coimmunoprecipitation experiments (Figure 2B) were in accordance with immunofluorescence analyses and showed a substantial reduction of the interaction in the case of $APE1^{K4pleA}$ and $APE1^{N\Delta33}$ mutants and a moderate impairment for $APE1^{K27/35A}$ and $APE1^{K31/32A}$ mutants. Glutathione *S*-transferase (GST) pull-down assays with recombinant purified proteins confirmed that these results were due to effects on direct interaction between APE1 and NPM1 (Figure 2C). This confirmed previous hypotheses (Fantini *et al.*, 2010). We also checked the effect of the K-to-A mutation on the ability of APE1 to bind nucleolar rRNA (Vascotto *et al.*, 2009b). As expected, rRNA–chromatin immunoprecipitation (ChIP) analyses showed that K-to-A mutations significantly alter APE1 binding to

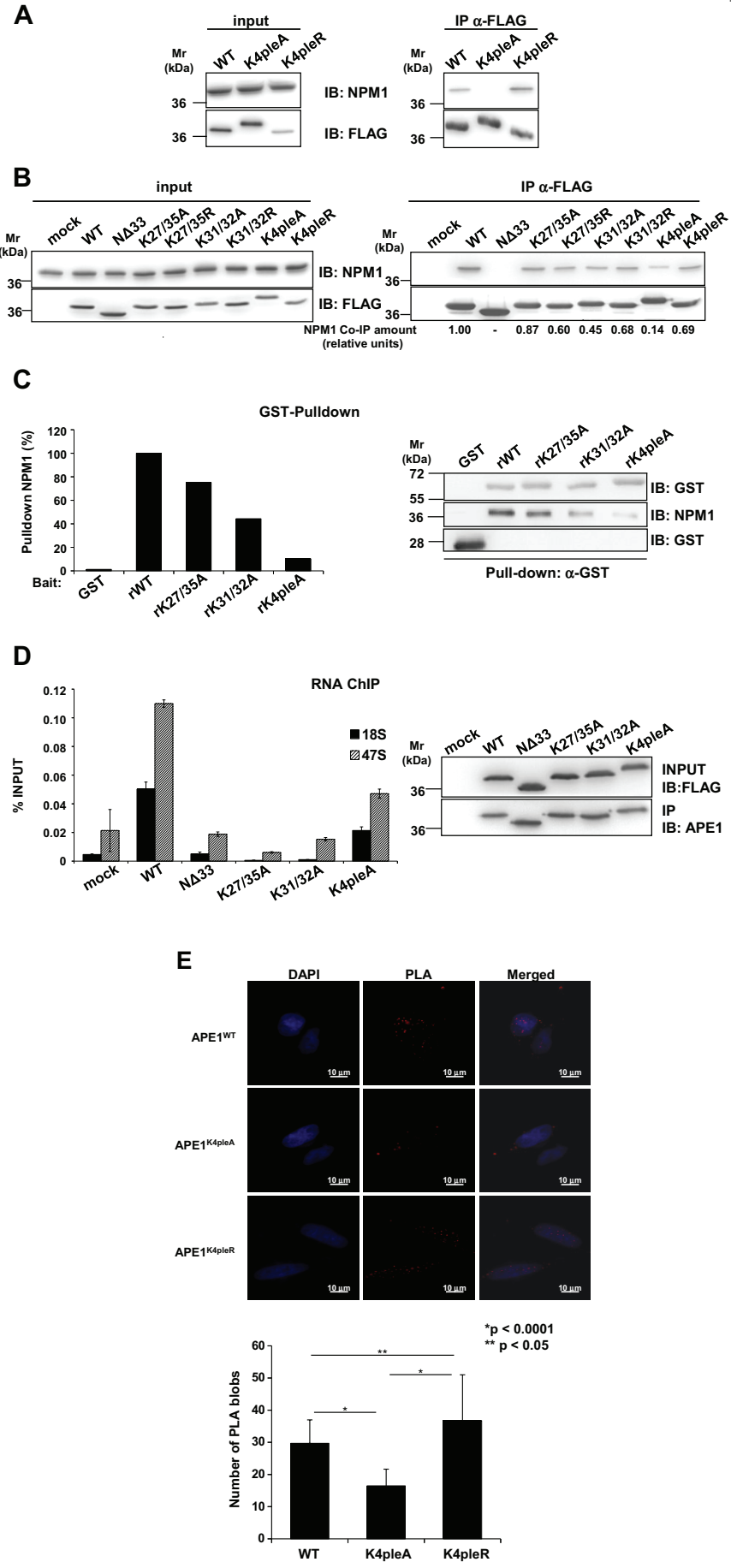

FIGURE 2: Positively charged $K^{27}/K^{31}/K^{32}/K^{35}$ residues are required for NPM1 interaction. (A) The $APE1^{K4pleA}$ mutant shows impaired interaction with NPM1. Coimmunoprecipitation (CoIP) analysis on HeLa cells transfected with $APE1^{WT}$, $APE1^{K4pleA}$, or $APE1^{K4pleR}$ FLAG-tagged proteins with endogenous NPM1. Western blot analysis was used to quantify the interaction among the different APE1 forms and NPM1 by using specific antibodies. IB, immunoblot. (B) $K^{27}/K^{31}/K^{32}/K^{35}$ residues are responsible for proper interaction of APE1 with NPM1. CoIP analysis on HeLa cells transfected with FLAG-tagged $APE1^{WT}$, $APE1^{N\Delta33}$, or the APE1 double ($APE1^{K27/35A}$, $APE1^{K31/32A}$, $APE1^{K27/35R}$, and $APE1^{K31/32R}$) or quadruple ($APE1^{K4pleA}$ and $APE1^{K4pleR}$) K-to-A or K-to-R mutants. Western blot analysis was performed on total cell extracts (left) and on immunoprecipitated material (right) with specific antibody for endogenous NPM1. Normalized coimmunoprecipitated amounts of NPM1 are indicated under each relative bar. Anti-FLAG staining was used as loading control. (C) Interaction of K-to-A APE1 mutants with NPM1 and rRNA. A 150-pmol amount of each bait GST-APE1 recombinant purified protein (rAPE1) was incubated with an equimolar amount of recombinant NPM1, as described in *Materials and Methods*. After GST pull-down, samples underwent Western blot analysis by using the indicated antibodies (right). NPM1 band intensities were normalized vs. those of GST-APE1 proteins, and the resulting values, expressed as percentage of bound with respect to $APE1^{WT}$, were plotted in the histogram (left). Each bar represents the mean of two independent experiments whose variation was <10%. (D) Interaction of K-to-A APE1 mutants with NPM1 and rRNA. After transfection of HeLa cells, total cell lysates were prepared as described in *Materials and Methods*, and an RNA-ChIP assay was performed to measure the rRNA-binding activity of the different APE1 mutants. Immunoprecipitated samples underwent either Western blot analysis (right) or RNA extraction and quantification by reverse transcription and quantitative PCR analysis, using 18S and 47S rRNA–specific primers. Data are presented as a fold percentage of the amount of total 18S or 47S rRNA with respect to the amount of immunoprecipitated FLAG-tagged APE1 protein, respectively. The resulting values are plotted in the histograms (left), showing the average values with SD of three independent experiments. (E) Nucleoplasmic interaction between APE1 and NPM1 is affected by K-to-A mutation on APE1. PLA technology was used to evaluate in vivo the effect of positively charged $K^{27}/K^{31}/K^{32}/K^{35}$ residues on APE1 interaction with NPM1 in the nuclear compartment. Stable HeLa clones expressing $APE1^{WT}$, $APE1^{K4pleA}$, or $APE1^{K4pleR}$ FLAG-tagged proteins were seeded on a glass coverslip, and PLA reaction was carried out using anti-FLAG and anti-NPM1 antibodies. 4′,6-Diamidino-2-phenylindole staining is used as a reference for the nuclei. The histogram represents the average number of PLA blobs scored for at least 30 cells per slide. Asterisks represent a significant difference between $APE1^{WT}$ and mutants.

rRNA molecules (Figure 2D) and that a partial removal of positive charges in the region 27–35 strongly affects the protein binding to rRNA molecules.

Interaction between APE1 and NPM1 may also occur in the nucleoplasmic compartment of cells. We measured the effect of the K-to-A mutation on the nucleoplasmic interaction of APE1 with NPM1 through proximity ligation assay (PLA) analysis, which allows in situ detection of two proteins that are at interacting distance of <40 nm (Weibrecht *et al.*, 2010). Data displayed in Figure 2E show that nucleoplasmic interaction between APE1 and NPM1 was significantly affected by the K-to-A mutation. Taken together, these data demonstrate that charged lysines within the 27–35 region are essential for APE1 maintenance within the nucleoli and for a proper/stable interaction of this protein with NPM1 or rRNA molecules. Moreover, our data suggest that APE1 must lose the positive charge at more than two K residues (among $K^{27}/K^{31}/K^{32}/K^{35}$) to get a significant reduction of the APE1/NPM1 interaction in the nucleus and loss of APE1 nucleolar accumulation.

Loss of APE1 nucleolar accumulation causes impairment of cell proliferation

APE1 protects cells against genotoxic damaging agents (Tell and Wilson, 2010). To clarify the biological relevance of the APE1 nucleolar accumulation, we estimated the effect of the expression of the nucleolar-deficient form of APE1 (i.e., $APE1^{K4pleA}$) on cell viability with respect to $APE1^{WT}$ and $APE1^{K4pleR}$ mutant. To test the effects of the mutant proteins and exclude the contribution of the endogenous one, we used inducible APE1-silenced (through small interfering RNA [siRNA] technology) HeLa cells, which were reconstituted with siRNA-resistant APE1 ectopic proteins in place of the endogenous one (Figure 3A; Vascotto *et al.*, 2009a). The levels of the ectopic proteins expressed by the different cell clones used for the following experiments were comparable to that of the wild-type endogenous one before silencing, as demonstrated by quantitative Western blot analysis (Supplemental Figure S4); the extent of the residual endogenous protein was <10%. Quantification of the nuclear amount of ectopic proteins after doxycycline treatment, demonstrated by Western blot analysis with a calibration curve, gave the following results (expressed as nanograms of APE1 per microgram of nuclear extract): 23.22 ± 6.04 for $APE1^{WT}$, 18.63 ± 4.84 for $APE1^{K4pleA}$, and 17.69 ±4.60 for $APE1^{K4pleR}$ (Supplemental Figure S4B). Therefore these cell lines represent a reliable system for testing our hypothesis. On the basis of previous data showing that nucleolar APE1 may act as a cleansing factor in rRNA quality control, possibly affecting cellular proliferation through an impairment of the overall protein synthesis machinery (Vascotto *et al.*, 2009b; Tell *et al.*, 2010b), we investigated the effect of the nucleolar-deficient form $APE1^{K4pleA}$ on cell proliferation rate under basal conditions. Of interest, by cell counting assays performed on reconstituted cell clones, we obtained proof that $APE1^{K4pleA}$ acts as a loss-of-function mutation in terms of cell proliferation, whereas $APE1^{K4pleR}$ behaves similarly to $APE1^{WT}$ (Figure 3B). These data, confirmed by using at least two different clones for each mutant cell line, suggest that nucleolar APE1 is required for appropriate control of cell proliferation, perhaps through its role in rRNA metabolism (Tell *et al.*, 2010b). Colony formation assays confirmed cell proliferation data (Figure 3C). However, although the cell number in each colony of $APE1^{K4pleR}$-expressing cells was always similar to that expressing $APE1^{WT}$, these cells grew in a more widespread manner, possibly due to an altered migrating phenotype and/or an intercellular adhesion pattern. These data were indicative that abolition of the acetylatable residues of APE1 at $K^{27}/K^{31}/K^{32}/K^{35}$ may significantly affect cell biology, even though it is also possible that the lower expression level of the $APE1^{K4pleR}$ (~76%) with respect to $APE1^{WT}$ may also have an effect on this phenotype.

Increased APE1 acetylation at $K^{27}/K^{31}/K^{32}/K^{35}$ residues upon genotoxic damage

APE1 acetylation at K^6/K^7 is known to be enhanced after genotoxic insult by methyl methanesulfonate (MMS) and it has been shown to play a role in modulating APE1 interaction with XRCC1, possibly coordinating different enzymatic steps in the BER pathway (Yamamori *et al.*, 2010). We therefore tested whether MMS treatment, which promotes generation of DNA damage specifically repaired through BER, may also induce APE1 acetylation at $K^{27}/K^{31}/K^{32}/K^{35}$ residues. Immunopurified APE1 samples from control and MMS-treated cells were separated by SDS–PAGE and excised bands and then analyzed by peptide mapping experiments. Semiquantitative nano–electrospray linear ion trap tandem mass spectrometry (nanoLC-ESI-LIT-MS/MS) analysis was performed on identical quantities of immunopurified $APE1^{WT}$-FLAG protein samples obtained from HeLa cells before and after MMS treatment (Supplemental Figure S5). In particular, we evaluated the amount of the peptides (15–33)Ac_3 and (15–35)Ac_4 in each APE1 endoprotease AspN digest and compared them to that of the nonmodified counterparts. Analysis was performed by extracting and integrating the corresponding nanoLC-ESI-LIT-MS peak areas equivalent to the assigned *m/z* values for the acetylated and nonacetylated peptides in the same total ion chromatogram. After MMS treatment, the amount of the peptide (15–33)Ac_3 was significantly increased, and the peptide (15–35)Ac_4 was almost doubled as compared with that of the nonmodified counterparts (Figure 4A). The MMS-induced acetylation on the aforementioned residues was further demonstrated by Western blotting using a commercial anti–Ac-Lys antibody on immunopurified proteins from HeLa cells transiently transfected with the FLAG-tagged $APE1^{WT}$ and the nonacetylatable $APE1^{K4pleR}$ forms. It is striking that a significant increase of APE1 acetylation was observed after MMS treatment but mainly for $APE1^{WT}$ rather than for $APE1^{K4pleR}$ (Supplemental Figure S6). These data show that, besides increasing the acetylation status of K^6/K^7 (see later discussion and Yamamori *et al.*, 2010), MMS treatment also promotes acetylation at $K^{27}/K^{31}/K^{32}/K^{35}$ residues. The mild increase of Lys acetylation level in the mutant $APE1^{K4pleR}$ may possibly be ascribed to K^6/K^7 acetylation (see later discussion).

We then investigated the cellular distribution pattern of acetylated APE1 at $K^{27}/K^{31}/K^{32}/K^{35}$ residues by using an ad hoc–developed antibody that specifically recognized the peptide 25–38 fully acetylated at $K^{27}/K^{31}/K^{32}/K^{35}$, hereafter referred to as anti-$APE1^{K27\text{-}35Ac}$ (Poletto *et al.*, 2012). This antibody was particularly efficient in recognizing acetylation at K^{35} with a measured affinity in the nanomolar range (196 nM for the tetra-acetylated stretch vs. 26,800 nM for the nonacetylated one, as assessed by surface plasmon resonance (SPR; Poletto *et al.*, 2012). Preincubation of the antibody with the acetylated and nonacetylated peptides confirmed the specificity of the antibody (Poletto *et al.*, 2012). The distribution pattern of $APE1^{WT}$, $APE1^{K4pleA}$, and $APE1^{K4pleR}$ was compared by using anti-FLAG and anti-$APE1^{K27\text{-}35Ac}$ antibodies. Of interest, staining with the anti-$APE1^{K27\text{-}35Ac}$ antibody gave a pattern quite similar (i.e., nucleolar exclusion) to that of the anti-FLAG antibody but only in the case of the $APE1^{K4pleA}$ mutant (Figure 4B). PLA was also carried out to demonstrate the in vivo occurrence of acetylation on endogenous APE1 by using either the anti-$APE1^{K27\text{-}35Ac}$ antibody alone (as a control) or together with an anti-APE1 antibody (Figure 4C). This assay clearly highlighted the proximity between the target of both

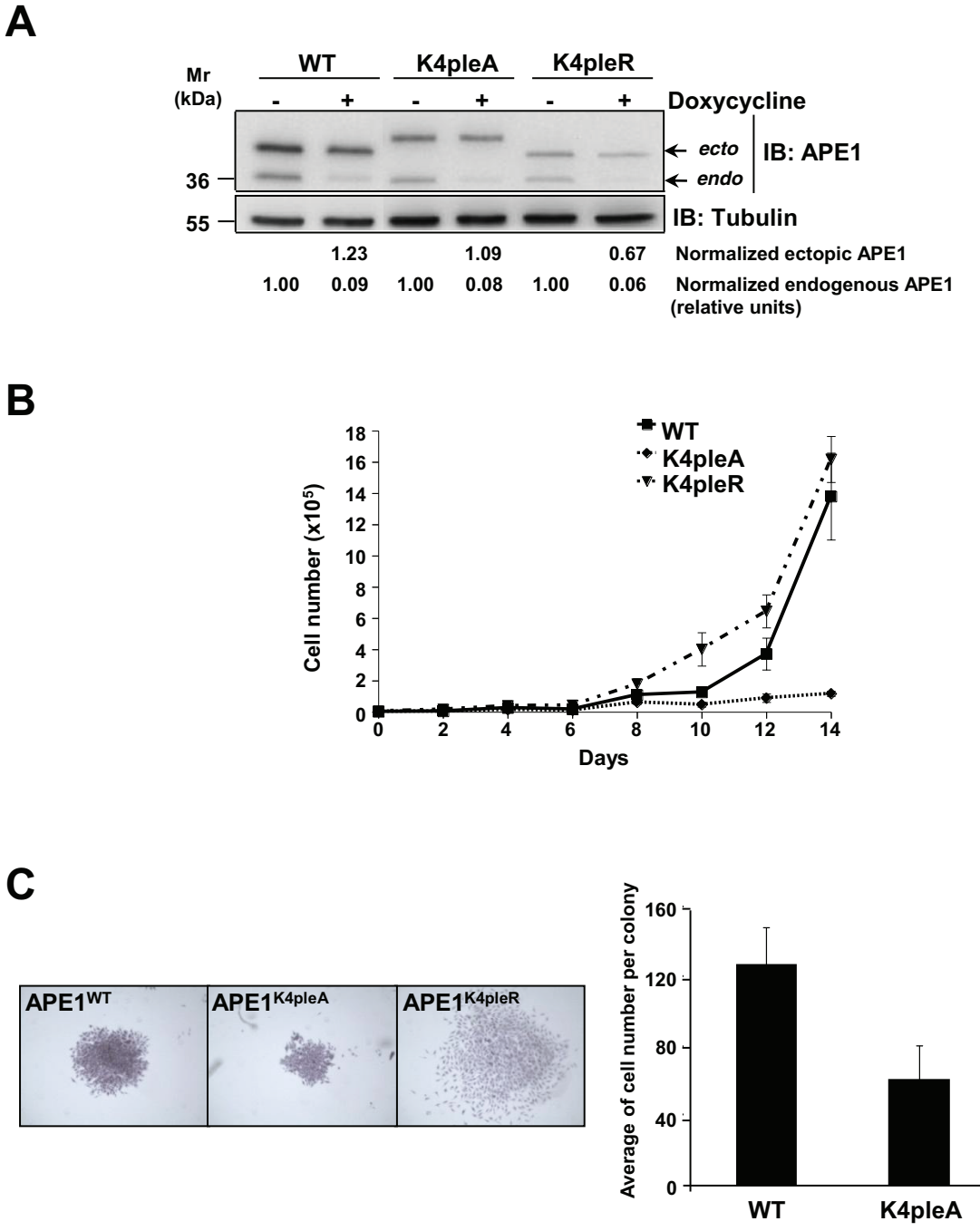

FIGURE 3: Expression of the nucleolus-deficient APE1 mutant causes impaired cell proliferation. (A) Generation of reconstituted cell lines expressing APE1^{K4pleA} and APE1^{K4pleR} mutants. HeLa cells were stably transfected with the inducible siRNA vectors and siRNA resistant APE1^{WT}, APE1^{K4pleA}, and APE1^{K4pleR}–expressing vectors, as previously described (Vascotto *et al.*, 2009a; Fantini *et al.*, 2010). Expression of ectopic APE1 forms without silencing and after the suppression of endogenous APE1 expression after 10 d of treatment with doxycycline (Doxy) was assayed by Western blotting on total cellular extracts with an anti-APE1 antibody. Normalized expression levels for each clone of ectopic and endogenous APE1 protein after the silencing are indicated under each relative band. β-Tubulin was used as loading control. (B) Cell proliferation assays for APE1-reconstituted cell lines. APE1-expressing cell clones were seeded in 60-mm Petri dishes. Growth was followed by measuring cell numbers at various times upon doxycycline treatment, as indicated. Cells were harvested at the indicated times, stained with trypan blue, and counted in triplicate. Data, expressed as cell number, are the mean ± SD of three independent experiments. (C) Colony formation assays for APE1-reconstituted cell lines. After 8 d of doxycycline treatment, 200 cells of APE1^{WT} and the indicated APE1 mutants were seeded in 60-mm Petri dishes and grown for 8 d in medium supplemented with doxycycline to promote endogenous APE1 silencing. Then cells were stained with crystal violet and images captured by using a Leica S8 microscope with 80× magnification. Data, expressed as number of cells per colony, are the mean ± SD of 10 colonies for each clone.

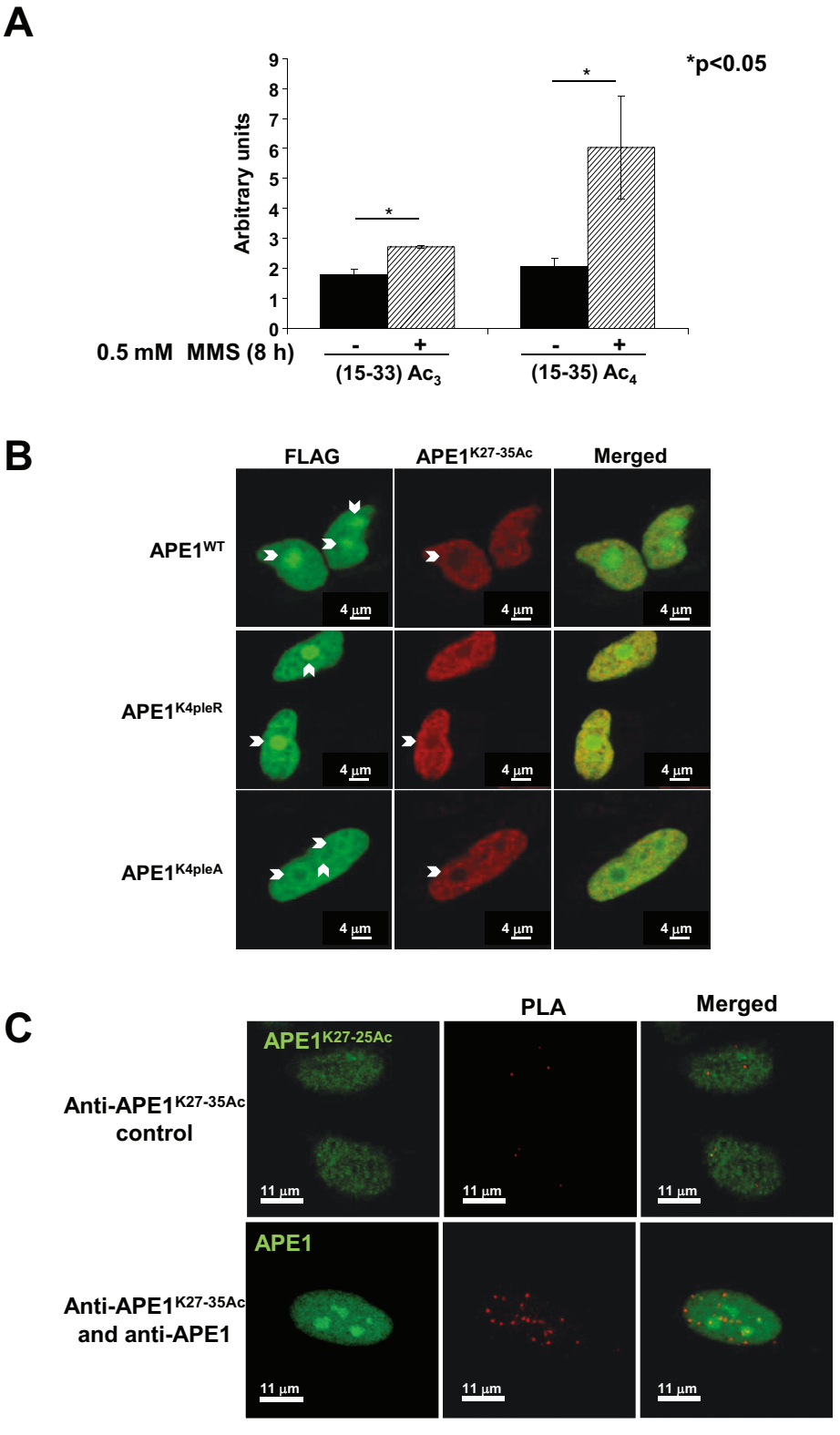

FIGURE 4: Genotoxic treatment promotes APE1 acetylation at $K^{27}/K^{31}/K^{32}/K^{35}$ residues. (A) Relative quantitative changes of APE1 acetylation at $K^{27}/K^{31}/K^{32}/K^{35}$ after MMS treatment. Mass spectrometry analysis of acetylated peptides present in the endoprotease AspN digest of FLAG-tagged $APE1^{WT}$ purified from HeLa cells (see *Materials and Methods* for details). Histograms indicate the relative amounts of the peptides (15–33)Ac_3 and (15–35)Ac_4 with respect to their nonmodified counterparts before and after MMS treatment. Identical ionization tendencies were assumed for each peptide pair. Each bar represents the mean of three independent experiments. (B) Acetylated APE1 at $K^{27}/K^{31}/K^{32}/K^{35}$ residues is present within cell nucleoplasm but is excluded from nucleoli. Confocal microscopy of HeLa cells transfected with $APE1^{WT}$, $APE1^{K4pleA}$, or $APE1^{K4pleR}$ FLAG-tagged proteins and stained with antibodies against endogenous $APE1^{K27–35Ac}$ (anti-$APE1^{K27–35Ac}$, red) and ectopic APE1 FLAG-tagged (green). Overlap of staining (yellow) demonstrated the codetection of the two protein forms. Images are representative of 100% of transfected cells. (C) APE1 acetylation at $K^{27}/K^{31}/K^{32}/K^{35}$ occurs in vivo. PLA signal obtained using the anti-$APE1^{K27–35Ac}$ antibody together with the anti-APE1 antibody on fixed HeLa cells. A technical control, using the anti-$APE1^{K27–35Ac}$ antibody alone, was introduced (top). Nuclei were counterstained using an Alexa Fluor 488–conjugated secondary anti-rabbit (recognizing the endogenous $APE1^{K27–35Ac}$, in the control reaction) or anti-mouse antibody (recognizing the endogenous APE1 protein in the PLA reaction; green).

antibodies, further suggesting that, in vivo, APE1 is acetylated at $K^{27}/K^{31}/K^{32}/K^{35}$ residues and that these acetylated forms are excluded from the nucleoli. Taken together, these data suggest that acetylation at these charged amino acids may control the nucleolar/nucleoplasmic distribution of APE1 within cells.

Removal of positively charged $K^{27}/K^{31}/K^{32}/K^{35}$ residues increases APE1 DNA-repair activity in vivo

We tested whether abolition of positive charges on acetylatable residues may affect the APE1 DNA repair function in cells, as previously demonstrated in vitro by using recombinant purified proteins bearing two different clusters of K-to-A mutation (i.e., on residues 24/25/27 and on residues 24/25/27/31/32; Fantini *et al.*, 2010). For this purpose we used nuclear extracts from reconstituted cell clones after precise normalization for the APE1 ectopic nuclear content with a titration curve (as shown in Supplemental Figure S4). This normalization for APE1 ectopic protein expression allowed comparison of the enzymatic activities of the different protein mutants in the nuclear fractions from each clone. Figure 5A shows that the AP-endonuclease activity of the $APE1^{K4pleA}$ mutant, measured through cleavage assays performed with nuclear extracts, was significantly increased with respect to $APE1^{WT}$-and $APE1^{K4pleR}$-expressing cells. Moreover, Figure 5B shows a lower amount of abasic DNA lesions accumulated after MMS treatment by the $APE1^{K4pleA}$- as compared with the $APE1^{WT}$-expressing cells. These results suggest that removal of positive charges at Lys 27–35, as exerted by acetylation, may result in a more enzymatically active protein.

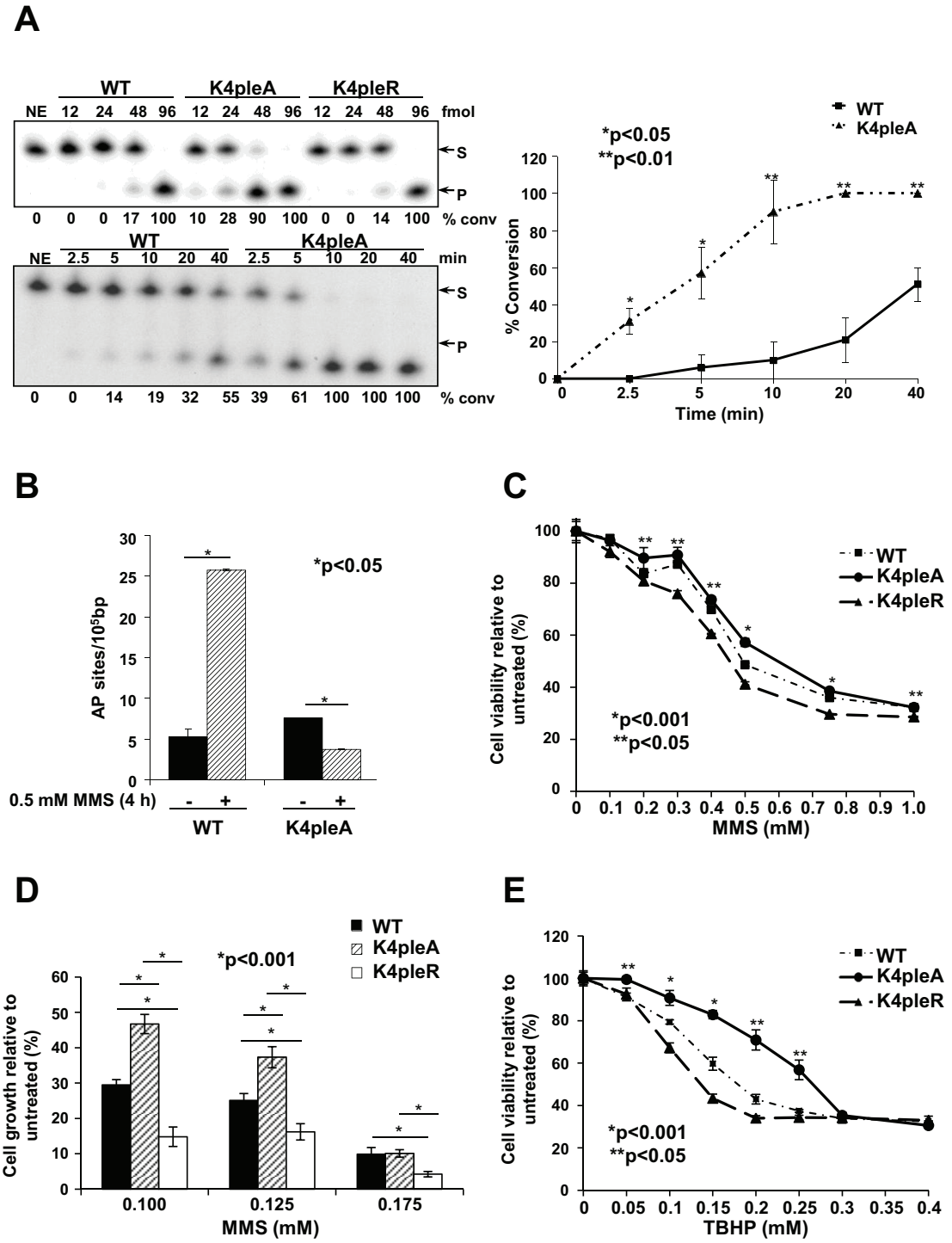

FIGURE 5: Abolition of positively charges $K^{27}/K^{31}/K^{32}/K^{35}$ residues increases APE1 DNA-repair activity. (A) Nuclear extracts from $APE1^{K4pleA}$ mutant present an increased AP endonuclease activity on abasic DNA. AP-site incision activity of the nuclear extracts from HeLa-reconstituted cell clones was tested using an AP endonuclease activity assay as described in *Material and Methods*. The nuclear APE1 content in each clone was precisely quantified through a titration curve obtained using purified recombinant APE1 (Supplemental Figure S4). Nuclear ectopic APE1 protein levels were then normalized between the different cell clones in order to compare their relative enzymatic activities. Top left, concentration-dependent conversion of an AP site–containing DNA substrate (S) to the incised product (P). A representative image of the denaturing polyacrylamide gel of the enzymatic reactions is shown. The amounts (femtomoles) of APE1 used in the reaction and the percentage of substrate converted into product, as determined by standard phosphorimager analysis, are indicated. NE, no cell extract control. Bottom left, time-dependent kinetics of APE1 (2.15 ng) endonuclease activity from nuclear extracts of the different reconstituted cell clones. The image of a representative gel analysis is shown (bottom). Right, graph depicting the time-course kinetics of APE1 from incision results shown on the left. Average values are plotted ± SD of three independent experiments. Asterisks represent a

Cell viability experiments, after MMS treatment, were carried out to verify the enzymatic data. Thus, the effect of $K^{27}/K^{31}/K^{32}/K^{35}$ mutation on cell viability after MMS treatment was measured by 3-(4-5-dimethylthiazol-2-yl)-5-(3-carboxymethoxyphenyl)-2-(4-sulfophenyl)-2H-tetrazolium salt (MTS) and clonogenic assays using the reconstituted cell clones. The MTS data (Figure 5C) showed that the $APE1^{K4pleA}$-mutant–expressing cells were significantly more resistant to MMS treatment than those expressing the nonacetylatable $APE1^{K4pleR}$ mutant. Of note, clonogenic assay experiments (Figure 5D) confirmed these results and highlighted the relevant acetylation occurring at the K residues, as demonstrated by the higher sensitivity of $APE1^{K4pleR}$-expressing cells after MMS treatment. We extended our observations on the protective function of the $APE1^{K4pleA}$ mutant by using *tert*-butyl-hydroperoxide (TBHP) as a reactive oxygen species (ROS) generator (Lazzé *et al.*, 2003). We recently demonstrated that APE1 knockdown sensitizes HeLa cells to TBHP treatment (Li *et al.*, 2012). Therefore we now measured the sensitivity of the different reconstituted cell clones to TBHP in a dose–response experiment (Figure 5E). As in the case of MMS treatment, expression of the $APE1^{K4pleA}$ mutant exerted a protective function with regard to TBHP treatment with respect to $APE1^{WT}$-expressing cells. Similarly to MMS treatment, the $APE1^{K4pleR}$-mutant–expressing clone evidenced even more sensitivity than the $APE1^{WT}$-expressing one. Taken together, these data show that acetylation at residues $K^{27}/K^{31}/K^{32}/K^{35}$ is associated with cell response to DNA damage and confers protection to genotoxic treatment. The increased activity of the $APE1^{K4pleA}$ mutant may explain its proficient protective effect in vivo against genotoxic treatment, even though further explanatory mechanisms, such as its altered protein association in the cell or its possible higher stability (Vascotto *et al.*, 2011), could also be invoked.

K^6/K^7 deacetylation by SIRT1 is modulated by the charged status of $K^{27}/K^{31}/K^{32}/K^{35}$residues

It was recently demonstrated that APE1 K^6/K^7 may undergo acetylation during cell response to genotoxic treatment (Fantini *et al.*, 2008; Yamamori *et al.*, 2010) and that modulation of the acetylation status of these residues through SIRT1 deacetylase activity is important for the regulation of APE1 DNA-repair function after MMS treatment (Yamamori *et al.*, 2010). However, the molecular mechanism regulating the SIRT1-mediated modification at these amino acids during MMS treatment is unknown. We thus checked whether the charged status of $K^{27}/K^{31}/K^{32}/K^{35}$ residues might play a role in modulating the acetylation status of K^6/K^7 through the contribution of SIRT1. First, we evaluated the effect of the modification at $K^{27}/K^{31}/K^{32}/K^{35}$ on the ability of SIRT1 to deacetylate K^6/K^7 in APE1. We found that recombinant purified APE1 protein is nonenzymatically acetylated after incubation with acetyl-CoA, as demonstrated for other proteins (Garbutt and Abraham, 1981). Thus, to obtain a significant amount of acetylated recombinant APE1 protein on K^6/K^7 residues, we treated purified recombinant rAPE1 obtained from *E. coli* with acetyl-CoA, as described in the Supplemental Information. Then we treated in vitro–acetylated $rAPE1^{WT}$, $rAPE1^{K4pleA}$, $rAPE1^{K27/35A,}$ or $rAPE1^{K31/32A}$ with purified recombinant SIRT1 protein and measured the acetylation level on K^6/K^7 through a specific antibody that recognizes only acetylation at these residues (Fantini *et al.*, 2008; Sengupta *et al.*, 2011). Of interest, although $APE1^{WT}$ was efficiently deacetylated by SIRT1 at K^6/K^7 (Figure 6A), the $APE1^{K4pleA}$ mutant did not show any deacetylation in this region; concomitant K-to-A substitutions at positions 27 and 35 ($APE1^{K27/35A}$ mutant) or at positions 31 and 32 ($APE1^{K31/32A}$ mutant) caused an intermediate effect.

We then verified the ability of SIRT1 to directly deacetylate APE1 at $K^{27}/K^{31}/K^{32}/K^{35}$ residues through in vitro deacetylation assays carried out on acetylated purified recombinant $rAPE1^{WT}$ or mutant proteins as substrates (Supplemental Figure S7). Protein acetylation level was monitored by using the anti-$APE1^{K27\text{-}35Ac}$ (Figure 6B). Incubation with recombinant-purified SIRT1 protein revealed a marked decrease in acetyl-APE1 signal but only when $APE1^{WT}$ was used. These data were corroborated by qualitative peptide mapping experiments on in vitro–acetylated $rAPE1^{WT}$ before and after incubation with SIRT1. This analysis demonstrated that SIRT1 was indeed able to deacetylate in vitro–acetylated $rAPE1^{WT}$ at least at $K^{25}/K^{27}/K^{32}$ residues (Supplemental Table S1).

The ability of SIRT1 to deacetylate in vitro APE1 at $K^{27}/K^{31}/K^{32}/K^{35}$ was also analyzed on APE1 (25–38) peptides (Figure 6C), which were chemically synthesized either in their nonacetylated or tetra-acetylated form at these K residues. These peptides were used in a competitive fluorescence-based assay in which a fluorogenic p53 acetylated peptide was used as SIRT1 substrate (Marcotte *et al.*, 2004). As expected, we observed a dose-dependent decrease in the

significant difference between $APE1^{WT}$ and $APE1^{K4pleA}$. (B) Accumulation of genomic abasic (AP) lesions after MMS treatment (0.5 mM, 4 h) of reconstituted cell clones with $APE1^{WT}$ and $APE1^{K4pleA}$ mutant as measured by an aldehyde-reactive probe. $APE1^{WT}$ and $APE1^{K4pleA}$-expressing HeLa cells were grown in medium supplemented with Doxy (10 d) to silence endogenous APE1 expression and were treated with 0.5 mM MMS for 4 h. Counting at the AP sites was performed by using the AP-site quantification kit, as described in *Materials and Methods*. In the histogram, data are expressed as number of AP sites per 10^5 base pairs and represent the mean ± SD of four independent experiments. Asterisks represent a significant difference between the two conditions (untreated and MMS-treated cells). (C) Effects of APE1 acetylation mutants on cell viability after MMS treatment in reconstituted cells. $APE1^{WT}$, $APE1^{K4pleA}$-, and $APE1^{K4pleR}$-expressing cells were grown in medium supplemented with Doxy to silence APE1 endogenous protein and treated with increasing concentrations of MMS for 8 h; the cytotoxic effect of this compound was determined by the MTS assay (see *Materials and Methods* for details). Each point, shown as percentage viability with respect to untreated clones, represents the mean ± SD of four observations, repeated in at least two independent assays. Asterisks represent a significant difference between $APE1^{K4pleA}$ and $APE1^{K4pleR}$ mutants. (D) Cell growth as measured by colony survival assay. One thousand cells of $APE1^{WT}$-, $APE1^{K4pleA}$-, and $APE1^{K4pleR}$-expressing clones treated with increasing concentrations of MMS for 8 h were seeded in Petri dishes and then treated with Doxy for 10 d to silence endogenous APE1. Data, expressed as the percentage of change with respect to untreated clones, are the mean ± SD of three independent experiments. (E) Effects of APE1 acetylation mutants on cell viability after TBHP treatment in $APE1^{WT}$-, $APE1^{K4pleA}$-, and $APE1^{K4pleR}$-expressing cells grown in medium supplemented with Doxy to silence APE1 endogenous protein. Cells were treated with increasing concentrations of TBHP for 6 h, and the cytotoxic effects were determined by the MTS assay. Each point, shown as percentage viability with respect to untreated clones, represents the mean ± SD of four observations, repeated in at least two independent assays. Asterisks represent a significant difference between $APE1^{K4pleA}$ and $APE1^{K4pleR}$ mutants.

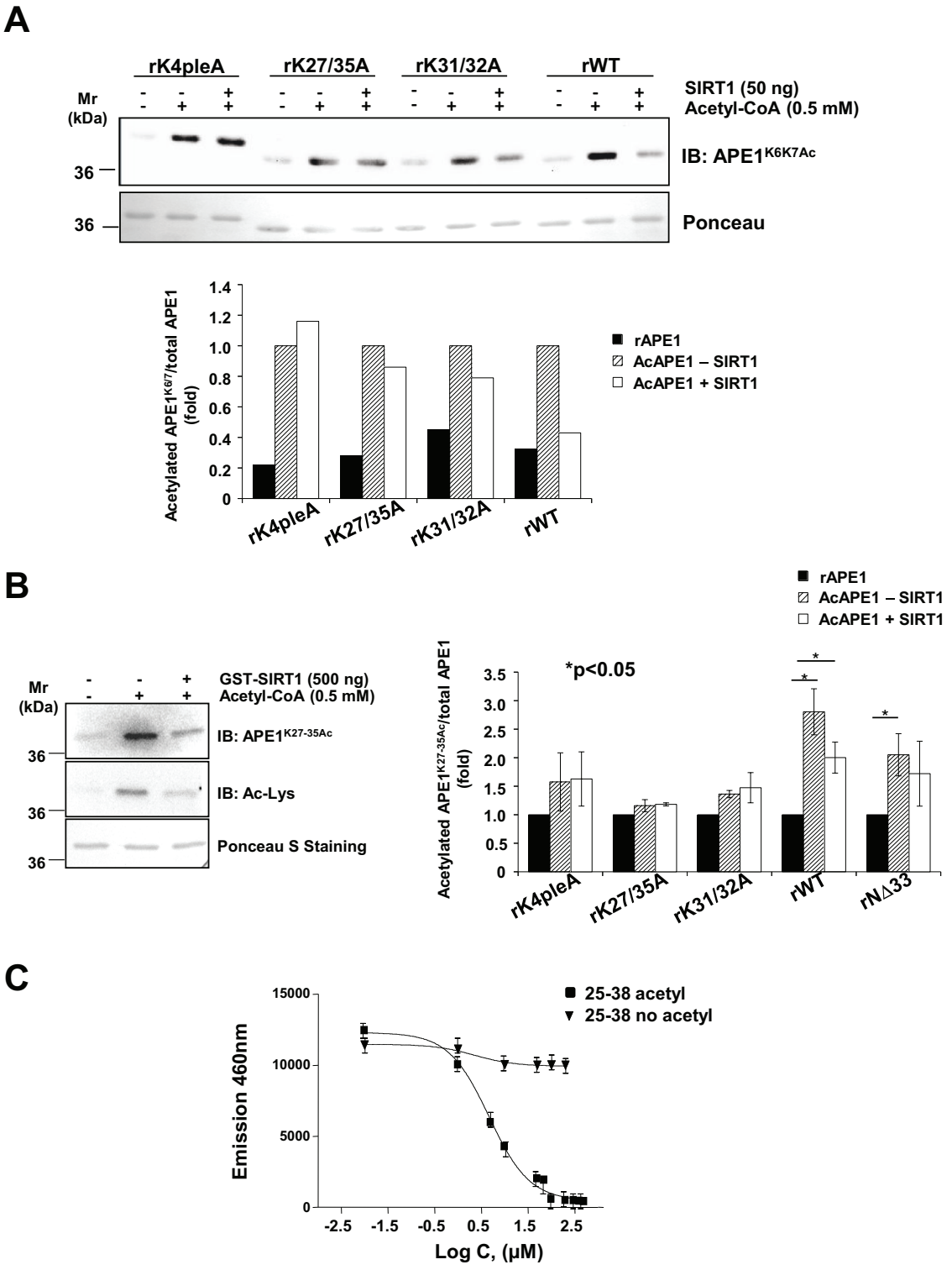

FIGURE 6: SIRT1 deacetylase activity on K^6/K^7 depends on the charged status of $K^{27}/K^{31}/K^{32}/K^{35}$ residues. (A) K^6/K^7 acetylation, modulated by SIRT1, depends on the charged status of $K^{27}/K^{31}/K^{32}/K^{35}$ residues. Western blot analysis on purified recombinant APE1 proteins in vitro acetylated with acetyl-CoA and then incubated in the presence/absence of recombinant GST-SIRT1, as indicated. The analysis was carried out using an antibody specific for acetylated K^6/K^7 APE1 (top). The histogram reports data obtained from densitometric quantification of the bands for each APE1 protein after normalization on Ponceau S staining (bottom). Data shown are the mean of two independent experimental sets whose variation was <10%. (B) SIRT1 deacetylates rAPE1 at $K^{27}/K^{31}/K^{32}/K^{35}$. Left, Western blot analysis on the in vitro–acetylated and deacetylated purified recombinant APE1, further subjected to MS analysis (Supplemental Table S1). $rAPE1^{WT}$ was incubated with 0.5 mM acetyl-CoA and then with recombinant SIRT1 protein, as shown. Samples were separated onto 10% SDS–PAGE, and Western blot analysis was performed by using the anti-$APE1^{K27-35Ac}$ antibody. Ponceau S staining was used as loading control. Right, the histogram shows the densitometric quantification of the

fluorescence signal by using different amounts of the tetra-acetylated peptide (25–38); the nonacetylated counterpart was used as a negative control substrate. Best data fitting was observed with a one-site competition equation, which provided an IC_{50} value of 4.6 ± 0.3 μM. These data support the conclusion that the acetylated APE1 region spanning amino acids 27–35 is a substrate for SIRT1 deacetylase activity. Taken together, these results demonstrate that SIRT1's ability to efficiently deacetylate APE1 at K^6/K^7 residues relies on the presence of positive charges at $K^{27}/K^{31}/K^{32}/K^{35}$. Moreover, SIRT1 is also able to bind and possibly deacetylate in vitro–acetylated APE1 $K^{27}/K^{31}/K^{32}/K^{35}$ residues.

Cross-talk between the charged state of $K^{27}/K^{31}/K^{32}/K^{35}$ and the acetylation status of K^6/K^7 residues through SIRT1

To understand whether SIRT1 activity on acetylated K^6/K^7 residues might be modulated in vivo by MMS as a function of the charged status of $K^{27}/K^{31}/K^{32}/K^{35}$, we performed coimmunoprecipitation experiments on transiently transfected HeLa cells. As shown in Figure 7A, an intact N-terminal domain is required for stable APE1 binding to SIRT1. The APE1/SIRT1 association was induced after MMS treatment and was abolished in the case of both $APE1^{N\Delta33}$ and $APE1^{K4pleA}$ mutants. Substitution of $K^{27}/K^{31}/K^{32}/K^{35}$ residues with nonacetylatable R residues was ineffective, suggesting that SIRT1 binding depends on the presence of positively charged amino acids spanning the APE1 region 27–35. Measurements of K^6/K^7 acetylation status with the specific antibody (performed on the same samples) clearly showed that, in agreement with the binding data, K^6/K^7 residues resulted in more acetylation both under basal and after MMS treatment but only in the case of the $APE1^{K4pleA}$ mutant. In addition, the acetylation status of $APE1^{WT}$ and $APE1^{K4pleR}$, both under basal conditions and after MMS treatment, was comparable (Figure 7B), supporting the existence of cross-talk between the charged status of $K^{27}/K^{31}/K^{32}/K^{35}$ and the acetylation level of K^6/K^7.

We then investigated the cross-talk between K^6/K^7 and $K^{27}/K^{31}/K^{32}/K^{35}$ acetylation status through siRNA experiments. HeLa cell lines stably expressing both endogenous APE1 and $APE1^{WT}$, $APE1^{K4pleA}$, and $APE1^{K4pleR}$ ectopic forms were silenced for SIRT1 expression as described in *Materials and Methods*. The acetylation level of K^6/K^7 was then measured through Western blotting. Data shown in Figure 7C demonstrate that the K^6/K^7 acetylation level of the ectopic APE1 forms was increased ~30–40% upon SIRT1 silencing but only in the case of $APE1^{WT}$- and $APE1^{K4pleR}$-expressing cells, whereas acetylation of K^6/K^7 of $APE1^{K4pleA}$ was <10%. As a control, the acetylation level of endogenous APE1 always increased (~60–70%) upon SIRT1 silencing in all the cell lines tested (unpublished data). Taken together, these data demonstrate that the acetylation/charged status of $K^{27}/K^{31}/K^{32}/K^{35}$ residues controls the stability of the SIRT1/APE1 complex, thus playing a role in the acetylation level of K^6/K^7.

Possible relevance of acetylation for APE1 subnuclear distribution and protein local conformation

The data suggest that a coordinated acetylation/deacetylation dynamic modulated by SIRT1 may occur within the cell nucleus and could be responsible for APE1 subnuclear trafficking. Thus, we examined the subnuclear distribution of SIRT1 on c-myc-SIRT1–transfected cells through immunofluorescence analysis. We found that transiently transfected c-myc-SIRT1 mainly localized in the nucleoplasmic compartment and was not found in the nucleoli (Figure 8A, left); quantification of the endogenous SIRT1 protein in biochemically purified nucleoli confirmed its absence from this subnuclear compartment (Figure 8A, right). Evaluation of the acetylation status of APE1 present in nucleolar or nucleoplasmic fractions under basal conditions showed that APE1 acetylated at K^6/K^7 is mainly present within the nucleoplasm but almost absent in the nucleolus (Figure 8B). Of note, these findings may have important implications for SIRT1-mediated deacetylation at K^6/K^7 and demonstrate the possibility that APE1 acetylation modulates the protein's subnuclear distribution and enzymatic functions, corroborating our previous work (Fantini *et al.*, 2010).

It is known that Lys acetylation may control local conformational stability of proteins, thus affecting their activity, subcellular distribution, and protein–protein interaction network. To examine the effect of acetylation on the local structure of the N-terminal APE1 region, we analyzed the conformational behavior of the protein portion of residues 14–38, which contain $K^{27}/K^{31}/K^{32}/K^{35}$ residues acetylatable in vivo. To this end, we chemically synthesized and purified four peptides bearing differential acetylation at positions 27, 31, 32, and 35 (Supplemental Table S2). To evaluate the effect of acetylation on peptide conformation, we undertook structural analysis of these peptides in solution by far-ultraviolet (UV) circular dichroism (CD) and nuclear magnetic resonance (NMR) spectroscopy. Figure 8C shows the overlay of CD spectra of APE1(14–38) and $APE1(14–38)^{K27/31/32/35Ac}$ in aqueous buffer, indicating a minimum at ~200 nm and a shoulder at ~220 nm. These features suggest the presence of mixed conformational states in which an unfolded state coexists with a certain helical content. The propensity of this domain to adopt helical conformation was also confirmed by trifluoroethanol (TFE) titration experiments (Supplemental Figure S8A). In particular, the CD spectrum of the tetra-acetylated peptide showed a minimum at 220 nm that was deeper than that of the nonacetylated counterpart, suggesting a role for the acetyl groups in determining structural changes in this protein region. An intermediate behavior was observed for the monoacetylated and triacetylated peptides, confirming the role of this K modification in modulating the conformation of the N-terminal APE1 region (unpublished data).

To further address this point, we carried out additional NMR experiments. In aqueous buffer, the one-dimensional (1D) spectra presented poor signal dispersion (Figure 8D, left), confirming a rather disordered state for both the tetra-acetylated and nonacetylated peptides. This observation was further strengthened by the analysis of two-dimensional (2D) [^{1}H, ^{1}H] total correlation spectroscopy (TOCSY) spectra (Griesinger *et al.*, 1988; Figure 8D, middle), and 2D [^{1}H, ^{1}H] rotating frame nuclear Overhauser effect spectroscopy (ROESY) spectra (Bax and Davis, 1985; Figure 8D, right). In the latter case, the presence of a restricted set of cross-peaks in the $_N$H-aliphatic side-chain proton correlation region made unfeasible the process of sequential resonance assignments, as often occurs for small, flexible

band intensities, after normalization to the nonacetylated APE1 form, of the in vitro–acetylated and deacetylated purified APE1 mutants. Data are the mean ± SD of three independent replicates. Asterisks represent a significant difference. (C) The acetylated APE1 25–38 peptide is a substrate of SIRT1 activity. Purified APE1 peptides (25–38) either in fully acetylated form at $K^{27}/K^{31}/K^{32}/K^{35}$ residues or not acetylated were analyzed as competitors in an in vitro deacetylase SIRT1 assay based on a fluorogenic acetylated peptide derived from p53 (region 379–382). Dose–response signals allowed an estimated IC_{50} value of 4.6 ± 0.3 μM of the acetylated APE1 25–38 region with respect to the p53 peptide.

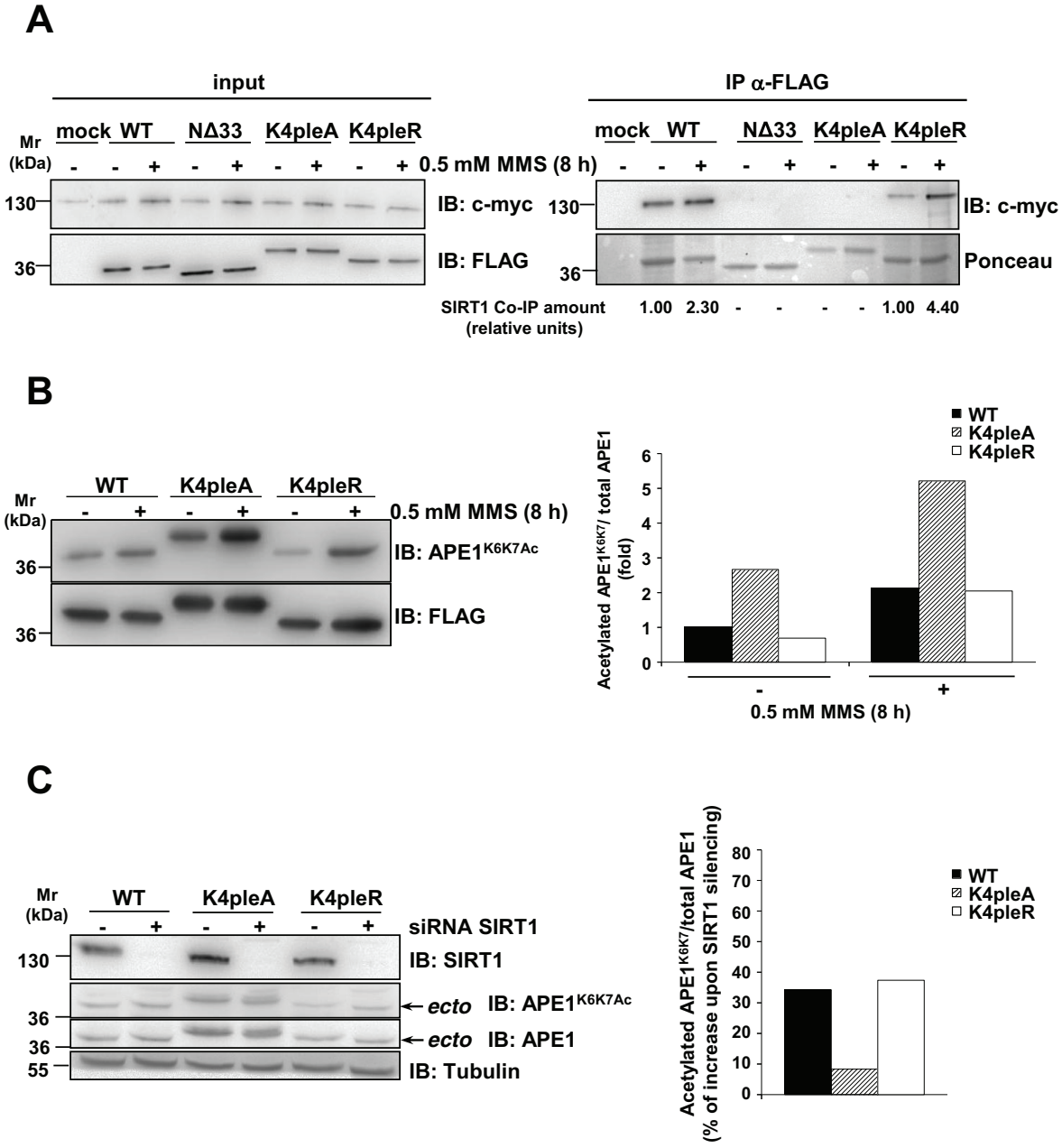

FIGURE 7: Cross-talk between the acetylation status of $K^{27}/K^{31}/K^{32}/K^{35}$ and K^6/K^7 residues through SIRT1. (A) Positive charges at $K^{27}/K^{31}/K^{32}/K^{35}$ residues strongly influence the stability of SIRT1 binding to APE1. Western blot analysis performed on total cell extracts (left) and on immunoprecipitated material (right) from HeLa cells cotransfected with c-myc–tagged SIRT1 and $APE1^{WT}$, $APE1^{N\Delta33}$, $APE1^{K4pleA}$, or $APE1^{K4pleR}$ FLAG-tagged proteins and treated with 0.5 mM MMS for 8 h. Coimmunoprecipitated amounts of SIRT1 normalized with respect to $APE1^{WT}$ or $APE1^{K4pleR}$, respectively, are indicated under each relative bar. Ponceau S staining was used as loading control. (B) Acetylation level of K^6/K^7 in $APE1^{K4pleA}$ mutant is higher than that of $APE1^{WT}$ both under basal conditions and after MMS treatment. Western blot analysis on CoIP material after MMS treatment from HeLa cells transfected with $APE1^{WT}$ and FLAG-tagged mutants is shown. The histogram indicates the relative amount of acetylated $APE1^{K6/K7}$ in the different clones obtained from the densitometric quantification of acetylated APE1 bands, normalized with respect to the amount of APE1 FLAG-tagged immunopurified protein. Data shown are the mean of two independent experimental sets whose variation was <10%. (C) SIRT1 siRNA knockdown increases APE1 K^6/K^7 acetylation. HeLa stable clones expressing $APE1^{WT}$, $APE1^{K4pleA}$, and $APE1^{K4pleR}$ were transfected with siRNA against SIRT1 protein or control siRNA. Western blot analysis was performed to detect differential amount of the acetylated K^6/K^7 APE1 after SIRT1 silencing. Arrows highlight bands of ectopic APE1 protein form; β-tubulin was used as a loading control. The histogram shows densitometric quantification of acetylated K^6/K^7 APE1 form. Data are expressed as percentage of induction of the acetylated K^6/K^7 APE1 after SIRT1 silencing after normalization for the total APE1 protein levels. Data shown are the mean of two independent experimental sets whose variation was <10%.

peptides that tumble very rapidly in solution. On the other hand, a detailed comparison of the 1D NMR data for the nonacetylated and tetra-acetylated APE1 peptides (Figure 8D, left) indicated that acetylation causes a small but clear improvement of spectral dispersion, which can be particularly appreciated in the $_N$H region (Figure 8D, top left). Moreover, the intensity of ROE cross-peaks is increased in the spectra of APE1(14-38)$^{K27/31/32/35Ac}$ peptide as compared with the nonmodified counterpart (Figure 8D, right). This evidence, together with small chemical shift changes, point toward the presence of more organized conformations for the tetra-acetylated peptide in aqueous solution, in agreement with CD data. Similar conclusions are drawn from the analysis of NMR data for APE1(14–38) and APE1(14–38)$^{K27/31/32/35Ac}$ peptides in phosphate:TFE solution (Supplemental Figure S8B), which suggested again the higher propensity of this domain in its acetylated form to adopt a more ordered conformation in contrast to the nonmodified counterpart. Also in this case, monoacetylated and triacetylated peptides showed an intermediate behavior (unpublished data). These data suggest that acetylation may account for local conformational changes on APE1 structure that may modulate its binding ability to different substrates.

DISCUSSION

APE1 is an unusually abundant DNA-repair protein in mammalian cells, with a wide nuclear distribution and an essential role in the BER pathway of DNA lesions (Tell and Wilson, 2010). We calculated that HeLa cells express ~4 × 10^7 molecules per cell (Supplemental Figure S4A), whereas other enzymes of the BER pathway, such as Pol β or XRCC1, are present at an extent of <1/10 (Demple and DeMott, 2002; Parsons *et al.*, 2008). Therefore APE1 involvement in preformed DNA-repair complexes may only partially explain the energy cost used to maintain such high protein concentration within the cells. Recently we found that APE1 may interact with rRNA and with proteins involved in RNA metabolism and is associated with nucleolar structures through its interaction with NPM1 (Vascotto *et al.*, 2009b; Tell *et al.*, 2010b). Interaction with rRNA and NPM1 strictly depends on the positive charge of K residues within the APE1 region 24–35 placed within the unstructured protein N-terminal domain, as demonstrated by the inability of the corresponding K-to-A mutants (resembling constitutive acetylation at these residues) to stably bind both rRNA and NPM1 (Fantini *et al.*, 2010). Of interest, some of these amino acids (i.e., $K^{27}/K^{31}/K^{32}/K^{35}$), which have been acquired during evolution, may undergo in vivo acetylation (Fantini *et al.*, 2010). We conjectured that, under physiological conditions, nonacetylated APE1 may be stored in the nucleolar compartment through its binding to NPM1 and rRNA, but the in vivo relevance of APE1 nucleolar accumulation was still unclear. This study was aimed at addressing this issue.

We also found that APE1^{K4pleA} binds poorly to NPM1 and rRNA in vivo and as a result is unable to accumulate within the nucleoli, whereas it is present in the nucleoplasm. Moreover, reconstitution of HeLa cells with this mutant gave improved protection from genotoxic damage induced by alkylating agents, such as MMS, and oxidative stress-generating compounds, such as TBHP, through increased DNA-repair activity. As expected for a regulated phenomenon such as the response to a genome insult, an in vivo–augmented acetylation at $K^{27}/K^{31}/K^{32}/K^{35}$ residues was observed during cell response to genotoxic damage. Furthermore, cross-talk involving the SIRT1 deacetylase occurred within cells between acetylation at $K^{27}/K^{31}/K^{32}/K^{35}$ and at K^6/K^7 residues. Therefore we hypothesized that genotoxic stress may shift the equilibrium between the nonacetylated and acetylated APE1 forms toward the latter, which would result in the most enzymatically active one on abasic DNA. This also corresponds to our previous data obtained in vitro with recombinant purified proteins (Fantini *et al.*, 2010). In many cases, the presence of the unstructured N-terminal domain of APE1 seemed essential for interaction of APE1 with different substrates (i.e., nucleic acids or proteins). Interaction also increased after histone deacetylase (HDAC) inhibition, which promotes APE1 acetylation at K^6/K^7 residues (Bhakat *et al.*, 2003; Yamamori *et al.*, 2010). This evidence strongly support the notion that this unstructured domain is responsible for the modulation of APE1's different functions through the recruitment of APE1 in different protein complexes by means of various amino acid side-chain modification events. From an evolutionary perspective, it can be hypothesized that mammalian APE1 activity was made adjustable (through PTMs and/or interaction with other proteins), or expanded toward other substrates, with the acquisition of a protein N-terminus containing positively charged residues, without major modifications on the enzyme catalytic site, which retained the "canonical" function toward abasic DNA. The existence of such an N-terminal extension in only mammals may suggest its evolutionary significance in the face of increased functional complexity. For the noncomplexed protein in solution, the intrinsic lack of a secondary structure associated with this domain can confer functional advantages to mammalian APE1, including the ability to bind to different protein targets (e.g., NPM1, XRCC1, CSB, RNA, etc.; Vidal *et al.*, 2001; Wong *et al.*, 2007; Vascotto *et al.*, 2009a; Tell *et al.*, 2010a), thus allowing efficient control over the thermodynamics in the binding process to different substrates. Because the protein's N-terminus is required for the stabilization of APE1 interaction with NPM1 or rRNA and for the control of the overall endonuclease activity (possibly decreasing the rate of product release once in the positively charged state; Fantini *et al.*, 2010; Figure 5), this region-specific multitasking function can provide a "trigger" for molecular regulation with important biological significance. This should be regarded, however, in light of BER coordination to prevent formation of harmful, unprotected DNA strand breaks. Therefore subcellular distribution of APE1 and its enzymatic activity seem to be finely tuned to demand and in a time-dependent manner through multiple interactions with various protein partners and the coordinated occurrence of different PTMs, such as acetylation and ubiquitination (Busso *et al.*, 2009, 2011). The observation that acetylation at $K^{27}/K^{31}/K^{32}/K^{35}$ residues may favor a transition toward a more organized conformation (Supplemental Figure S8) would support the notion that this modification may significantly modulate the interaction with several protein partners on a structural basis. In addition, acetylation at the mentioned K residues may profoundly affect APE1 protein stability, based on a recent report showing that the same K residues can be also polyubiquitinated by UBR3, targeting the protein for degradation by the proteasome (Meisenberg *et al.*, 2011). Given that acetylation competes with ubiquitination for the same K residues, it may represent the switch for controlling protein turnover rate. In this context, the acetylation at these residues that we observed during cell response to genotoxicants may stabilize protein half-life, thus preventing its degradation.

Few studies have reported on the effect of acetylation on the structure of small, ordered (Hughes and Waters, 2006; Liu and Duan, 2008) and disordered (Smet-Nocca *et al.*, 2010) peptides. Molecular dynamic simulations carried out on a peptide from the histone H3 N-terminal tail in the nonacetylated and doubly acetylated forms revealed that acetylation, although not appreciably disturbing the overall structure of the most-populated states, influenced peptide stability (Liu and Duan, 2008). The effect of acetylation at K residues on the conformational properties of small random-coil peptides from the histone H4 N-terminal tail and from nonhistone thymine DNA glycosylase indicated that acetylation had little effect on the

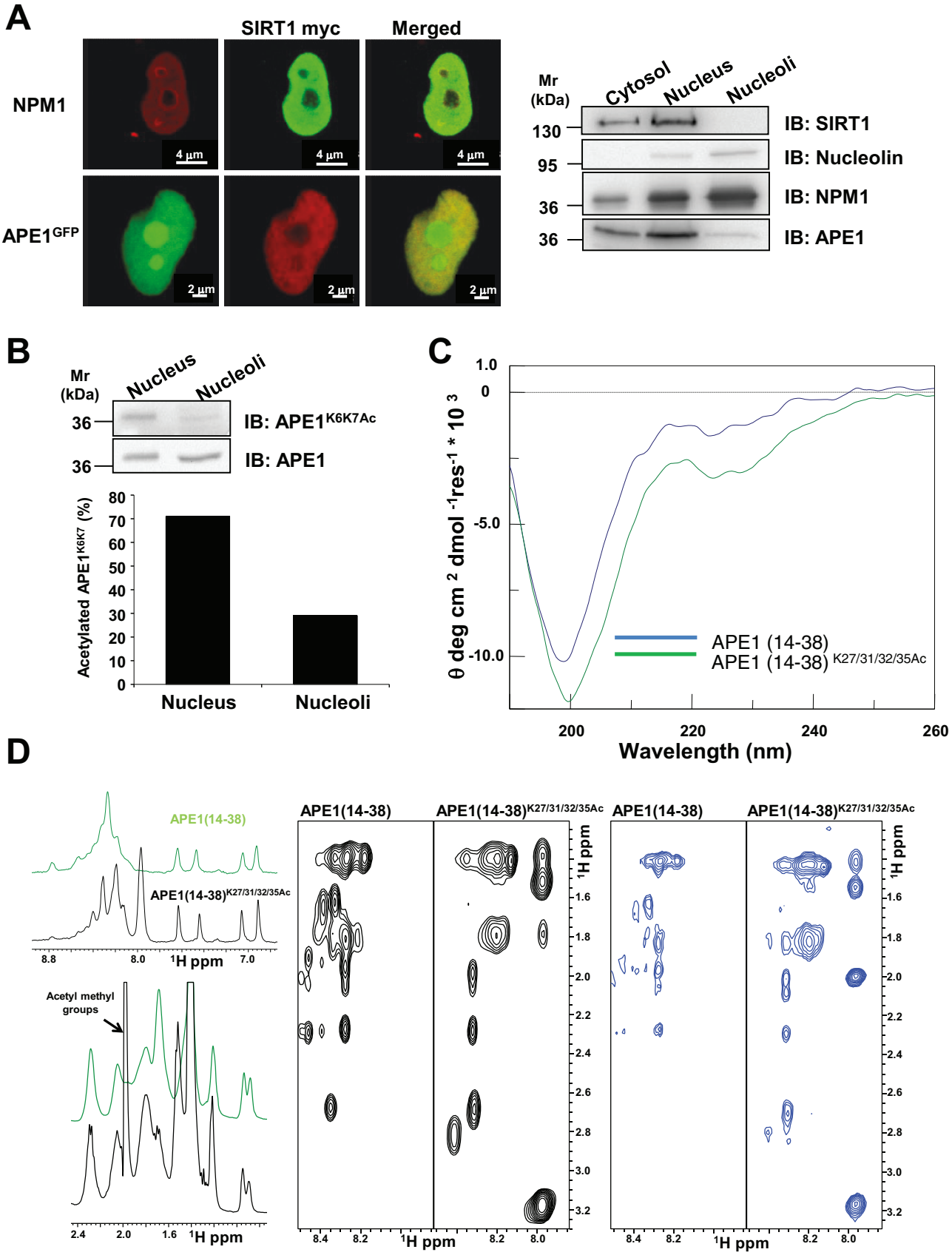

FIGURE 8: Nucleolar APE1 hypoacetylated on K^6/K^7 and conformational impact of acetylation at $K^{27}/K^{31}/K^{32}/K^{35}$ on APE1 local structure. (A) SIRT1 resides within the nucleoplasm of HeLa cells. Left, confocal microscopy of HeLa cells cotransfected with green fluorescent protein–fused APE1 ($APE1^{GFP}$) and c-myc-SIRT1 after fixing and staining with antibodies against NPM1 (red) and c-myc-SIRT1 (top, green; bottom, red). SIRT1, clearly excluded from nucleoli,

overall polypeptide structure, while inducing local conformational changes (Smet-Nocca *et al.*, 2010). In agreement with these studies, APE1(14–38) and APE1(14–38)$^{K27/31/32/35Ac}$ became disordered, as shown by the lack of ROE (Bax and Davis, 1985) cross-peak patterns, which are characteristic of ordered secondary structure elements. However, small differences in the NMR spectra (Figure 8 and Supplemental Figure S8), concerning both chemical shift values and signal intensities, seem to indicate that at least local conformational changes may occur following acetylation. We cannot ignore that these changes may be important for the interaction of APE1 with SIRT1 deacetylase and with NPM1; they highlight the role that the charged status of K residues within this region may play at the protein structural level. Based on our data, it can be speculated that full acetylation of $K^{27–35}$ may reduce SIRT1 binding to APE1, thus delaying its enzymatic activity on K^6/K^7. This mechanism could represent a way to coordinate the kinetics of the overall acetylation status of the protein. According to this hypothesis, SIRT1 should first deacetylate $K^{27–35Ac}$ before deacetylating K^{6}/K^{7Ac}. Our ability to identify APE1 peptides with varying amounts of acetylation on $K^{27–35}$ supports the existence of a dynamic equilibrium between multiple acetylated forms of the protein within cells and thus its functional regulatory role. Moreover, the presence of SIRT1, found exclusively in the nucleoplasm but not in the nucleoli (similar to the APE1 acetylated on $K^{27–35}$ and the reduced nucleolar presence of APE1 acetylated on K^6/K^7; Figure 8, A and B), suggests that acetylation of APE1 may force its exit from nucleoli to nucleoplasm, where it can be deacetylated by SIRT1. This model is further supported by the significantly reduced interaction of AcAPE1K^{27-35} with NPM1 (Figure 2). Further studies to identify the acetyltransferase able to acetylate APE1 within the nucleoli are in progress. Furthermore, this work supports findings by Yu *et al.* (2010), who demonstrated that these K residue conformational adjustments were concomitant with DNA binding and catalysis or with interaction with Pol β.

The nucleolar role of APE1 storage and regulation, as described here, may have profound biological consequences during cell response to stressor signals, especially in light of recent evidence pointing to the nucleolus as a central hub in DNA damage (Nalabothula *et al.*, 2010). Accordingly, the nucleolus seems responsible for actively transmitting signals to the molecular complex regulating p53 activity mediated by ARF–NPM1 interaction (Colombo *et al.*, 2002; Lee *et al.*, 2005; Nalabothula *et al.*, 2010), and thus it is involved in the maintenance of genome stability. A careful elucidation of the NPM1-ARF-p53 signaling networks and their involvement in the DNA-repair pathway coordinated by APE1 is an important subject for molecular carcinogenesis and deserves further study. This is also underway in our laboratory. Of note, data obtained in this work not only show that nucleoli may act as a storage site so that an appropriate amount of APE1 is readily available for maintenance of genome stability, but also emphasize that nucleolar accumulation of APE1 controls cell proliferation, possibly through its rRNA cleansing function. Compatible with this, APE1^{K4pleA}-expressing cells, under basal conditions, showed impairment in proliferation rate with respect to APE^{WT}-expressing ones (Figure 3). Therefore it can be speculated that nucleolar APE1 is responsible for functional activity of the nucleolus in ribosome biogenesis. APE1 release from the nucleoli after genotoxic treatment may constitute a signal to block active protein synthesis and allow activation of the proper DNA-repair mechanisms. Experiments are in progress along these lines to address this in light of the possibility that acetylation may control the APE1 trafficking from nucleoli to nucleoplasm.

In conclusion, our data shed light on novel molecular aspects highlighting the multifunctional nature of APE1 in regulating different biological outcomes and point to acetylation as an important mechanism for the fine-tuning of protein functions, subcellular distribution, and stability. They also emphasize the need for additional investigation of the APE1 N-terminal domain in order to understand the structural details of the regulatory mechanisms for this multifunctional protein. In addition, recent evidence on APE1 acetylation pattern in triple-negative breast cancer reveals that, concomitantly with total APE1 overexpression, a profound deregulation of APE1 acetylation status occurs under pathological conditions (Poletto *et al.*, 2012). This underscores the biological relevance of our findings and the need for future investigation.

MATERIALS AND METHODS

Inducible APE1 knockdown and generation of APE1 knock-in cell lines

Inducible silencing of endogenous APE1 and reconstitution with mutant proteins in HeLa cell clones was performed as described (Vascotto *et al.*, 2009a,b) and as reported in the Supplemental Information. For inducible shRNA experiments, doxycycline (1 μg/ml; Sigma-Aldrich, St. Louis, MO) was added to the cell culture medium, and cells were grown for 10 d. All biological data were reproduced in at least two different cell clones for each model.

Cell culture and transient transfection with plasmids or siRNA knockdown

HeLa cells were grown in DMEM (Invitrogen, Carlsbad, CA) supplemented with 10% fetal bovine serum (EuroClone, Milan, Italy), 100 U/ml penicillin, and 100 μg/ml streptomycin sulfate. One day

colocalizes with APE1 in the nucleoplasm. The inner part of nucleoli, marked in the granular zone by NPM1, is negative for SIRT1. Right, biochemical isolation of nucleoli confirms that SIRT1 localizes in the nucleoplasmic fraction and it is excluded from nucleoli, where nucleolin, NPM1, and APE1 reside (see *Materials and Methods* for details). Nucleolin was used as a positive control for nuclear and nucleolar compartment. (B) Acetylated K^6/K^7-containing APE1 is enriched within the nucleoplasmic compartment with respect to nucleoli. After normalization for total APE1 protein amount, the levels of acetylated APE1 in nucleolar and nucleoplasmic fractions were analyzed through Western blotting. APE1 acetylated at K^6/K^7 residues is predominately present within the nucleoplasmic fraction, whereas it is reduced in the nucleolar fraction. The histogram indicates the relative percentage amount of acetylated APE1 obtained from the densitometric quantification of acetylated APE1 bands normalized with respect to the amount of total APE1 in each fraction. Each bar represents the mean of two independent experiments whose variation was <10%. (C) CD spectra of the APE1(14–38) and APE1(14–38)$^{K27/31/32/35Ac}$ peptides in 10 mM phosphate buffer, pH 7. (D) Comparison of 1D (left), 2D [^{1}H, ^{1}H] TOCSY (middle), and 2D [^{1}H, ^{1}H] ROESY (right) spectra of APE1(14–38) and APE1(14–38)$^{K27/31/32/35Ac}$ peptides in 10 mM phosphate buffer, pH 7.0. Two different expansions of the proton 1D spectrum are shown; the region between 0.8 and 2.4 ppm, in the lower inset, contains signals from side-chain protons. Acetyl methyl groups originate a peak around 2 ppm, which can be clearly seen in the spectrum of the acetylated peptide; peaks of backbone and side-chain $_N$H atoms appear between 7.0 and 8.8 ppm in the upper inset. For 2D [^{1}H, ^{1}H] TOCSY and 2D [^{1}H, ^{1}H] ROESY experiments the H_N-aliphatic protons correlation region of the spectra are reported.

before transfection, cells were seeded in 10-cm plates at a density of 3.0×10^6 cells/plate. Cells were then transiently transfected with the indicated plasmids using the Lipofectamine 2000 reagent (Invitrogen), according to the manufacturer's instructions. Cells were harvested either 24 or 48 h after transfection, as indicated.

For SIRT1-knockdown experiments, HeLa clones were transfected with 150 nM siRNA siGENOME SMART pool or negative control siRNA 5′-CCAUGAGGUCAUGGUCUGdTdT-3′ (Dharmacon, Lafayette, CO), using Oligofectamine (Invitrogen). After 72 h the cells were harvested.

Preparation of total cell extracts and anti-FLAG coimmunoprecipitation

Preparation of total cell lysates and coimmunoprecipitation analyses were performed as described (Vascotto *et al.*, 2009a,b).

Determination of AP endonuclease activity and abasic site assay

Determination of APE1 AP endonuclease activity was performed using an oligonucleotide cleavage assay, as described previously (Vascotto *et al.*, 2009b) and detailed in the Supplemental Information.

Mass spectrometric analysis of APE1 acetylation

Characterization of APE1 acetylation was performed on the immunopurified protein obtained from APE1-FLAG–expressing HeLa cells (Vascotto *et al.*, 2009b). APE1 was resolved by SDS–PAGE; corresponding protein bands were excised, S-alkylated, and digested with endoprotease AspN (Fantini *et al.*, 2010). Digest aliquots were directly analyzed by nanoLC-ESI-LIT-MS/MS using an LTQ XL mass spectrometer (ThermoFisher Scientific, Waltham, MA) equipped with a Proxeon nanospray source connected to an Easy-nanoLC (ThermoFisher Scientific; Arena *et al.*, 2010; Scippa *et al.*, 2010), and analysis of APE1 acetylation was performed as described (D'Ambrosio *et al.*, 2006) and detailed in the Supplemental Information. A semiquantitative measurement of the amino acid modification was obtained by extracting and integrating nanoLC-ESI-LIT-MS peak areas corresponding to *m/z* values of the modified and nonmodified peptides in the same total ion chromatogram (Salzano *et al.*, 2011). Modification extent was then assayed by evaluating the peak area of the modified peptide with respect to that of the modified peptide plus that of the nonmodified peptide, assuming identical ionization properties for modified and nonmodified species. All these analyses were performed in triplicate.

Antibodies for immunofluorescence and immunoblotting

Antibodies used were anti-NPM1 monoclonal, anti-nucleolin monoclonal (Zymed, Invitrogen), anti-FLAG peroxidase-conjugated, anti-GST peroxidase-conjugated, anti-SIRT1 polyclonal (Abcam, Cambridge, MA), anti–c-myc (Santa Cruz Biotechnology, Santa Cruz, CA), and anti–β-tubulin monoclonal (Sigma-Aldrich). Anti-APE1 monoclonal (Vascotto *et al.*, 2009a) and anti-APE1^{K6K7Ac} (Bhakat *et al.*, 2003) were described previously. Anti-APE1$^{K27\text{-}35Ac}$ polyclonal antibody was generated by PRIMM (Milan, Italy; Poletto *et al.*, 2012).

Western blot analyses

For Western blot analyses, the indicated amounts of cell extracts were resolved in 12% SDS–PAGE and transferred to nitrocellulose membranes (Schleicher & Schuell BioScience, Dassel, Germany). Membranes were blocked with 5% (wt/vol) nonfat dry milk in phosphate-buffered saline (PBS) containing 0.1% (vol/vol) Tween 20 and probed with the indicated antibodies; blots were developed by using the ECL enhanced chemiluminescence procedure (GE Healthcare Piscataway, NJ) or Western Lightning Ultra (PerkinElmer, Waltham, MA). Normalization was performed by using a monoclonal anti-tubulin antibody (Sigma-Aldrich). Blots were quantified by using a Chemidoc XRS video densitometer (Bio-Rad, Hercules, CA).

Plasmids and expression of recombinant proteins

Expression and purification of recombinant proteins from *E. coli* were performed as previously described (Vascotto *et al.*, 2009b; Fantini *et al.*, 2010). Where recombinant proteins were used for in vitro assays, the acronym rAPE1 is used.

GST pull-down assay

A 150-pmol amount of either GST-tagged rAPE1^{WT} or mutant proteins was added to 15 μl of glutathione–Sepharose 4B beads (GE Healthcare), together with equimolar amounts of recombinant NPM1. Binding was performed in PBS, supplemented with 1 mM dithiothreitol (DTT) and 0.5 mM phenylmethylsulfonyl fluoride (PMSF) for 2 h, under rotation, at 4°C. Beads were washed three times with PBS, supplemented with 0.1% (vol/vol) Igepal CA-630 (Sigma-Aldrich), 1 mM DTT, and 0.5 mM PMSF and resuspended in Laemmli sample buffer for Western blot analysis.

DNA–RNA ChIP assays

DNA–RNA ChIP assays were carried out by using a modified version of a protocol described earlier (Gilbert *et al.*, 2000) and as detailed in the Supplemental Information.

Enzymatic fluorescence assays

To examine in vitro deacetylase activity on the acetylated APE1 region 25–38, we used the SIRT Fluorescent Activity Assay Kit (Biomol, Plymouth, PA). Optimizing manufacturer's instructions, we used white plates (OPTI PLATE; PerkinElmer) with 384 wells at reduced volume (total reaction volume, 20 μl). Purified peptides were incubated in 25 mM Tris-HCl, pH 8.0, 2.7 mM KCl, 137 mM NaCl, 1 mM $MgCl_2$, and 1 mg/ml bovine serum albumin containing the enzyme (0.04 U/μl) and 25 μM Fluor de Lys-p53 peptide substrate (Arg-His-Lys-Lys [Ac], from region 379–382 of human p53) in the presence/absence of 250 μM NAD^+ for 30 min at 37°C. Deacetylase activity was measured in arbitrary fluorescence units at 460 nm. Dose–response experiments were carried out by using a 0–500 μM range of peptide concentration. Data fitting was performed using the GraphPad Prism 4 software, version 4.02 (GraphPad, La Jolla, CA). Data were in triplicate/duplicate from three independent assays.

Immunofluorescence confocal and proximity ligation analyses

Immunofluorescence procedures and PLA were carried out as described earlier (Vascotto *et al.*, 2009b, 2011). To study the interaction between APE1 and NPM1 in vivo, we used the in situ Proximity Ligation Assay technology (Olink Bioscience, Uppsala, Sweden). After incubation with monoclonal anti-APE1 (1:50) or anti-FLAG antibody (1:200) for 3 h at 37°C, cells were incubated with polyclonal anti-NPM1 (1:200) overnight at 4°C. PLA was performed following manufacturer's instructions. Technical controls, represented by the omission of anti-NPM1 primary antibody, resulted in the complete loss of PLA signal. Cells were visualized through a Leica TCS SP laser-scanning confocal microscope (Leica Microsystems, Wetzlar, Germany). Determination of PLA signals was performed using BlobFinder software (Center for Image Analysis, Uppsala University, Uppsala, Sweden). PLA technology was also used to detect acetylated APE1 at $K^{27}/K^{31}/K^{32}/K^{35}$ residues. Cells were incubated with the

anti-APE1$^{K27–35Ac}$ rabbit-polyclonal antibody diluted 1:1500 and then with a mouse-monoclonal anti-APE1 antibody (1:27). PLA was subsequently carried out following manufacturer's instructions.

Confocal analyses of APE1-Dendra fusion protein through in vivo live imaging

For in vivo APE1-Dendra trafficking studies, HeLa cells were seated on glass-bottom Petri dishes (thickness #1.5; WillCo Wells, Amsterdam, Netherlands), transfected with APE1-Dendra constructs, and grown in the presence of DMEM without phenol red. A Leica TCS SP laser-scanning confocal microscope was equipped with a heating system (Incubator S) and a CO_2 controller (CTI Controller 3700 digital) to maintain cells in optimal growing conditions. Images were captured 24 h after transfection using a 63× oil fluorescence objective. For Dendra green fluorescence acquisition a 488-nm argon laser was regulated at 10% of power with PTM 750 V.

Cell viability, cell growth, and clonogenic assays

Cell viability was measured by using the MTS assay (Celltiter 96 Aqueous One solution cell proliferation assay; Promega, Madison, WI) on HeLa cells stably expressing APE1^{WT}, APE1^{K4pleA}, and APE1^{K4pleR} proteins grown in 96-well plates. After MMS (Sigma-Aldrich) treatment or TBHP (Sigma-Aldrich), the MTS solution was added to each well and the plates were incubated for 2 h. Absorbance was measured at 490 nm by using a multiwell plate reader. The values were standardized to wells containing media alone.

Cell growth assays were performed as described (Vascotto *et al.*, 2009a,b) and detailed in the Supplemental Information, and clonogenic assays were performed according to Plumb (1999) and essentially as described previously (Vascotto *et al.*, 2009a,b).

Circular dichroism spectroscopy

CD spectra were recorded on a Jasco J-810 spectropolarimeter (Jasco, Tokyo, Japan) at 25°C in the far-UV region from 190 to 260 nm. Each spectrum was obtained by averaging three scans, subtracting contributions from the corresponding blanks, and converting the signal to mean residue ellipticity in units of deg-cm^2 dmol^{-1} res^{-1}. Other experimental settings were 20 nm/min scan speed, 2.0 nm bandwidth, 0.2 nm resolution, 50 mdeg sensitivity, and 4 s response. Peptide concentration was kept at 100 μM, and a 0.1 cm path-length quartz cuvette was used. Spectra were acquired in 10 mM phosphate buffer, pH 7.0, containing various percentages of TFE.

NMR spectroscopy

NMR samples were prepared by dissolving APE1 peptides (1.5–2 mg) either in 600 μl of a 10 mM phosphate buffer, pH 7, containing 10% (vol/vol) D_2O or in a mixture of 10 mM phosphate buffer:2-2-2 trifluorethanol-d3 (98% deuterium; Armar Chemicals, Döttingen, Switzerland) 70:30 (vol/vol). The 2D [^{1}H, ^{1}H] TOCSY spectra (1024 × 256 total data points, 32 scans per t1 increment, 70 ms mixing time; Griesinger *et al.*, 1988) were recorded at 298 K on a Varian ^{UNITY}INOVA 600 spectrometer (Palo Alto, CA) equipped with a cold-probe. The 1D proton (128 scans and a relaxation delay of 1.5 s) and 2D [^{1}H, ^{1}H] ROESY (2048 × 256 total data points, 64 scans per t1 increment, 200 ms mixing time) spectra were acquired at 298 K on a Varian ^{UNITY}INOVA 400 spectrometer provided with *z*-axis pulsed-field gradients and a triple-resonance probe. Water signal was suppressed by means of either double pulsed field gradient selective echo techniques (Dalvit, 1998) or continuous wave irradiation. Varian software VNMRJ 1.1D was implemented for spectral processing. The programs MestRe-C2.3a (Universidade de Santiago de Compostela, Santiago de Compostela, Spain) and NEASY (Bartels *et al.*, 1995; www.nmr.ch) were used for analysis of 1D and 2D NMR data, respectively.

Statistical analyses

Statistical analyses were performed by using the Excel (Microsoft, Redmond, WA) data analysis program for Student's *t* test. $p < 0.05$ was considered as statistically significant.

ACKNOWLEDGMENTS

We thank Paolo Peruzzo for generation of mutant recombinant proteins, K. Irani for providing SIRT1-encoding plasmids, and Pablo Radicella for helpful comments on the manuscript. We also thank Julie Driscol for excellent help in editing the manuscript. This work was supported by the Associazione Italiana per la Ricerca sul Cancro (IG10269) and the Ministero dell'Istruzione, dell'Università e della Ricerca (FIRB_RBRN07BMCT and PRIN2008_CCPKRP_003 to G.T.; PRIN2008_CCPKRP_002 and FIRB2008_RBNE08YFN3_003 to A.S.). This work was also supported by a UICC Yamagiwa-Yoshida Memorial International Cancer Study Grant to G.T. and by the Regione Friulia Venezia Giulia for the Project MINA under the Programma per la Cooperazione Transfrontaliera Italia-Slovenia 2007–2013.

REFERENCES

Arena S, Renzone G, Novi G, Paffetti A, Bernardini G, Santucci A, Scaloni A (2010). Modern proteomic methodologies for the characterization of lactosylation protein targets in milk. Proteomics 10, 3414–3434.

Bapat A, Fishel ML, Kelley MR (2009). Going Ape as an approach to cancer therapeutics. Antioxid Redox Signal 11, 651–668.

Bapat A, Glass LS, Luo M, Fishel ML, Long EC, Georgiadis MM, Kelley MR (2010). Novel small-molecule inhibitor of apurinic/apyrimidinic endonuclease 1 blocks proliferation and reduces viability of glioblastoma cells. J Pharmacol Exp Ther 334, 988–998.

Barnes T, Kim WC, Mantha AK, Kim SE, Izumi T, Mitra S, Lee CH (2009). Identification of apurinic/apyrimidinic endonuclease 1 (APE1) as the endoribonuclease that cleaves c-myc mRNA. Nucleic Acids Res 37, 3946–3958.

Bartels C, Xia T, Billeter M, Gunthert P, Wüthrich K (1995). The program XEASY for computer-supported NMR spectral analysis of biological macromolecules. J Biomol NMR 6, 1–10.

Bax A, Davis DG (1985). Practical aspects of two-dimensional transverse NOE spectroscopy. J Magn Reson 63, 207–213.

Bhakat KK, Izumi T, Yang SH, Hazra TK, Mitra S (2003). Role of acetylated human AP-endonuclease (APE1/Ref-1) in regulation of the parathyroid hormone gene. EMBO J 1, 6299–6309.

Busso CS, Iwakuma T, Izumi T (2009). Ubiquitination of mammalian AP endonuclease (APE1) regulated by the p53-MDM2 signaling pathway. Oncogene 28, 1616–1625.

Busso CS, Wedgeworth CM, Izumi T (2011). Ubiquitination of human AP-endonuclease 1 (APE1) enhanced by T233E substitution and by CDK5. Nucleic Acids Res 39, 8017–8028.

Chattopadhyay R, Wiederhold L, Szczesny B, Boldogh I, Hazra TK, Izumi T, Mitra S (2006). Identification and characterization of mitochondrial abasic (AP)-endonuclease in mammalian cells. Nucleic Acids Res 34, 2067–2076.

Chudakov DM, Lukyanov S, Lukyanov KA (2007). Tracking intracellular protein movements using photoswitchable fluorescent protein PS-CFP2 and Dendra2. Nat Protoc 2, 2024–2032.

Colombo E, Marine JC, Danovi D, Falini B, Pelicci PG (2002). Nucleophosmin regulates the stability and transcriptional activity of p53. Nat Cell Biol 4, 529–533.

Dalvit C (1998). Efficient multiple-solvent suppression for the study of the interaction of organic solvents with biomolecules. J Biomol NMR 11, 437–444.

D'Ambrosio C, Arena S, Fulcoli G, Scheinfeld MH, Zhou D, D'Adamio L, Scaloni A (2006). Hyperphosphorylation of JNK-interacting protein 1, a protein associated with Alzheimer disease. Mol Cell Proteomics 5, 97–113.

Demple B, DeMott MS (2002). Dynamics and diversions in base excision DNA repair of oxidized abasic lesions. Oncogene 21, 8926–8934.

Fantini D *et al.* (2008). APE1/Ref-1 regulates PTEN expression mediated by Egr1. Free Radic Res 42, 20–29.

Fantini D *et al*. (2010). Critical lysine residues within the overlooked N-terminal domain of human APE1 regulate its biological functions. Nucleic Acids Res 38, 8239–8256.
Fung H, Demple B (2005). A vital role for APE1/Ref1 protein in repairing spontaneous DNA damage in human cells. Mol Cell 17, 463–470.
Garbutt GJ, Abraham EC (1981). Non-enzymatic acetylation of human hemoglobins. Biochim Biophys Acta 670, 190–194.
Gilbert SL, Pehrson JR, Sharp PA (2000). XIST RNA associates with specific regions of the inactive X chromatin. J Biol Chem 275, 36491–36494.
Gray MJ, Zhang J, Ellis LM, Semenza GL, Evans DB, Watowich SS, Gallick GE (2005). HIF-1alpha, STAT3, CBP/p300 and Ref-1/APE are components of a transcriptional complex that regulates Src-dependent hypoxia-induced expression of VEGF in pancreatic and prostate carcinomas. Oncogene 24, 3110–3120.
Griesinger C, Otting G, Wüthrich K, Ernst RR (1988). Clean TOCSY for 1H spin system identification in macromolecules. J Am Chem Soc 110, 7870–7872.
Grillo C, D'Ambrosio C, Scaloni A, Maceroni M, Merluzzi S, Turano C, Altieri F (2006). Cooperative activity of Ref-1/APE and ERp57 in reductive activation of transcription factors. Free Radic Biol Med 41, 1113–1123.
Hirota K, Matsui M, Iwata Z, Nishiyama A, Mori K, Yodoi J (1997). AP-1 transcriptional activity is regulated by a direct association between thioredoxin and Ref-1. Proc Natl Acad Sci USA 94, 3633–3638.
Hughes RM, (2006). Effects of lysine acetylation in a beta-hairpin peptide: comparison of an amide-pi and a cation-pi interaction. J Am Chem Soc 128, 13586–13591.
Izumi T, Brown DB, Naidu CV, Bhakat KK, Macinnes V, Saito H, Chen DJ, Mitra S (2005). Two essential but distinct functions of the mammalian abasic endonuclease. Proc Natl Acad Sci USA 102, 5739–5743.
Lazzé MC, Pizzala R, Savio M, Stivala LA, Prosperi E, Bianchi L (2003). Anthocyanins protect against DNA damage induced by tert-butyl-hydroperoxide in rat smooth muscle and hepatoma cells. Mutat Res 535, 103–115.
Lee C, Smith BA, Bandyopadhway K, Gjerset RA (2005). DNA damage disrupts the p14ARF-B23(nucleophosmin) interaction and triggers a transient subnuclear redistribution of p14ARF. Cancer Res 65, 9834–9842.
Li M, Vascotto C, Xu S, Dai N, Qing Y, Zhong Z, Tell G, Wang D (2012). Human AP endonuclease/redox factor APE1/ref-1modulates mitochondrial function after oxidative stress by regulating the transcriptional activity of NRF1. Free Radic Biol Med 53, 237–248.
Liu H, Duan Y (2008). Effects of posttranslational modifications on the structure and dynamics of histone H3 N-terminal Peptide. Biophys J 94, 4579–4585.
Marcotte PA, Richardson PL, Guo J, Barrett LW, Xu N, Gunasekera A, Glaser KB (2004). Fluorescence assay of SIRT protein deacetylases using an acetylated peptide substrate and a secondary trypsin reaction. Anal Biochem 332, 90–99.
Meisenberg C *et al*. (2011). Ubiquitin ligase UBR3 regulates cellular levels of the essential DNA repair protein APE1 and is required for genome stability. Nucleic Acids Res 40, 701–711.
Mitra S, Izumi T, Boldogh I, Bhakat KK, Chattopadhyay R, Szczesny B (2007). Intracellular trafficking and regulation of mammalian AP-endonuclease 1 (APE1), an essential DNA repair protein. DNA Repair 6, 461–469.
Nalabothula N, Indig FE, Carrier F (2010). The nucleolus takes control of protein trafficking under cellular stress. Mol Cell Pharmacol 2, 203–212.
Parlanti E, Locatelli G, Maga G, Dogliotti E (2007). Human base excision repair complex is physically associated to DNA replication and cell cycle regulatory proteins. Nucleic Acids Res 35, 1569–1577.
Parsons JL, Tait PS, Finch D, Dianova II, Allinson SL, Dianov GL (2008). CHIP-mediated degradation and DNA damage-dependent stabilization regulate base excision repair proteins. Mol Cell 29, 477–487.
Pines A, Bivi N, Romanello M, Damante G, Kelley MR, Adamson ED, D'Andrea P, Quadrifoglio F, Moro L, Tell G (2005). Cross-regulation between Egr-1 and APE/Ref-1 during early response to oxidative stress in the human osteoblastic HOBIT cell line: evidence for an autoregulatory loop. Free Radic Res 39, 269–281.
Poletto M, Loreto CD, Marasco D, Poletto E, Puglisi F, Damante G, Tell G (2012). Acetylation on critical lysine residues of apurinic/apyrimidinic endonuclease 1 (APE1) in triple negative breast cancers. Biochem Biophys Res Commun 424, 34–39.
Plumb JA (1999). Cell sensitivity assays: clonogenic assay. Methods Mol 28, 17–23.
Salzano AM, Renzone G, Scaloni A, Torreggiani A, Ferreri C, Chatgilialoglu C (2011). Human serum albumin modifications associated with reductive radical stress. Mol Biosyst 7, 889–898.
Schnell U, Dijk F, Sjollema KA, Giepmans BN (2012). Immunolabeling artifacts and the need for live-cell imaging. Nat Methods 9, 152–158.
Scippa GS, Rocco M, Ialicicco M, Trupiano D, Viscosi V, Di Michele M, Arena S, Chiatante D, Scaloni A (2010). The proteome of lentil (*Lens culinaris* Medik.) seeds: discriminating between landraces. Electrophoresis 31, 497–506.
Seemann S, Hainaut P (2005). Roles of thioredoxin reductase 1 and APE/Ref-1 in the control of basal p53 stability and activity. Oncogene 24, 3853–3863.
Sengupta S, Mantha AK, Mitra S, Bhakat KK (2011). Human AP endonuclease (APE1/Ref-1) and its acetylation regulate YB-1-p300 recruitment and RNA polymerase II loading in the drug-induced activation of multidrug resistance gene MDR1. Oncogene 30, 482–493.
Smet-Nocca C, Wieruszeski JM, Melnyk O, Benecke A (2010). NMR-based detection of acetylation sites in peptides. J Pept Sci 16, 414–423.
Szczesny B, Mitra S (2005). Effect of aging on intracellular distribution of abasic (AP) endonuclease 1 in the mouse liver. Mech Ageing Dev 126, 1071–1078.
Tell G, Crivellato E, Pines A, Paron I, Pucillo C, Manzini G, Bandiera A, Kelley MR, Di Loreto C, Damante G (2001). Mitochondrial localization of APE/Ref-1 in thyroid cells. Mutat Res 485, 143–152.
Tell G, Damante G, Caldwell D, Kelley MR (2005). The intracellular localization of APE1/Ref-1: more than a passive phenomenon. Antioxid Redox Signal 7, 367–384.
Tell G, Fantini D, Quadrifoglio F (2010a). Understanding different functions of mammalian AP endonuclease (APE1) as a promising tool for cancer treatment. Cell Mol Life Sci 67, 3589–3608.
Tell G, Quadrifoglio F, Tiribelli C, Kelley MR (2009). The many functions of APE1/Ref-1: not only a DNA-repair enzyme. Antioxid Redox Signal 11, 601–620.
Tell G, Wilson DM 3rd (2010). Targeting DNA repair proteins for cancer treatment. Cell Mol Life Sci 67, 3569–3572.
Tell G, Wilson DM 3rd, Lee CH (2010b). Intrusion of a DNA repair protein in the RNome world: is this the beginning of a new era. Mol Cell Biol 30, 366–371.
Ueno M, Masutani H, Arai RJ, Yamauchi A, Hirota K, Sakai T, Inamoto T, Yamaoka Y, Yodoi J, Nikaido T (1999). Thioredoxin-dependent redox regulation of p53-mediated p21 activation. J Biol Chem 274, 35809–35815.
Vascotto C *et al*. (2011). Knock-in reconstitution studies reveal an unexpected role of Cys-65 in regulating APE1/Ref-1 subcellular trafficking and function. Mol Biol Cell 22, 3887–3901.
Vascotto C *et al*. (2009a). Genome-wide analysis and proteomic studies reveal APE1/Ref-1 multifunctional role in mammalian cells. Proteomics 9, 1058–1074.
Vascotto C *et al*. (2009b). APE1/Ref-1 interacts with NPM1 within nucleoli and plays a role in the rRNA quality control process. Mol Cell Biol 29, 1834–1854.
Vidal AE, Boiteux S, Hickson ID, Radicella JP (2001). XRCC1 coordinates the initial and late stages of DNA abasic site repair through protein-protein interactions. EMBO J 20, 6530–6539.
Wei SJ, Botero A, Hirota K, Bradbury CM, Markovina S, Laszlo A, Spitz DR, Goswami PC, Yodoi J, Gius D (2000). Thioredoxin nuclear translocation and interaction with redox factor-1 activates the activator protein-1 transcription factor in response to ionizing radiation. Cancer Res 60, 6688–6695.
Weibrecht I, Leuchowius KJ, Clausson CM, Conze T, Jarvius M, Howell WM, Kamali-Moghaddam M, Söderberg O (2010). Proximity ligation assays: a recent addition to the proteomics toolbox. Expert Rev Proteomics 7, 401–409.
Wilson DM 3rd, (2010). Small molecule inhibitors of DNA repair nuclease activities of APE1. Cell Mol Life Sci 67, 3621–3631.
Wong HK, Muftuoglu M, Beck G, Imam SZ, Bohr VA, Wilson DM 3rd (2007). Cockayne syndrome B protein stimulates apurinic endonuclease 1 activity and protects against agents that introduce base excision repair intermediates. Nucleic Acids Res 35, 4103–4113.
Yacoub A, Kelley MR, Deutsch WA (1997). The DNA repair activity of human redox/repair protein APE/Ref-1 is inactivated by phosphorylation. Cancer Res 57, 5457–5459.
Yamamori T, DeRicco J, Naqvi A, Hoffman TA, Mattagajasingh I, Kasuno K, Jung SB, Kim CS, Irani K (2010). SIRT1 deacetylates APE1 and regulates cellular base excision repair. Nucleic Acids Res 38, 832–845.
Yu E, Gaucher SP, Hadi MZ (2010). Probing conformational changes in Ape1 during the progression of base excision repair. Biochemistry 49, 3786–3796.
Ziel KA, Campbell CC, Wilson GL, Gillespie MN (2004). Ref-1/Ape is critical for formation of the hypoxia-inducible transcriptional complex on the hypoxic response element of the rat pulmonary artery endothelial cell VEGF gene. FASEB J 18, 986–988.

SIRT1 gene expression upon genotoxic damage is regulated by APE1 through nCaRE-promoter elements

Giulia Antoniali[a], Lisa Lirussi[a], Chiara D'Ambrosio[b], Fabrizio Dal Piaz[c], Carlo Vascotto[a], Elena Casarano[a], Daniela Marasco[d,e], Andrea Scaloni[b], Federico Fogolari[a], and Gianluca Tell[a]

[a]Department of Biomedical Sciences and Technologies, University of Udine, 33100 Udine, Italy; [b]Proteomics and Mass Spectrometry Laboratory, ISPAAM, National Research Council, 80147 Naples, Italy; [c]Department of Biomedical and Pharmaceutical Sciences, University of Salerno, 84084 Fisciano (Salerno), Italy; [d]Department of Pharmacy, University of Naples "Federico II," 80134 Naples, Italy; [e]Institute of Biostructures and Bioimaging, National Research Council, 80134 Naples, Italy

ABSTRACT **Apurinic/apyrimidinic endonuclease 1 (APE1) is a multifunctional protein contributing to genome stability via repair of DNA lesions via the base excision repair pathway. It also plays a role in gene expression regulation and RNA metabolism. Another, poorly characterized function is its ability to bind to negative calcium responsive elements (nCaRE) of some gene promoters. The presence of many functional nCaRE sequences regulating gene transcription can be envisioned, given their conservation within ALU repeats. To look for functional nCaRE sequences within the human genome, we performed bioinformatic analyses and identified 57 genes potentially regulated by APE1. We focused on sirtuin-1 (SIRT1) deacetylase due to its involvement in cell stress, including senescence, apoptosis, and tumorigenesis, and its role in the deacetylation of APE1 after genotoxic stress. The human SIRT1 promoter presents two nCaRE elements stably bound by APE1 through its N-terminus. We demonstrate that APE1 is part of a multiprotein complex including hOGG1, Ku70, and RNA Pol II, which is recruited on SIRT1 promoter to regulate SIRT1 gene functions during early response to oxidative stress. These findings provide new insights into the role of nCaRE sequences in the transcriptional regulation of mammalian genes.**

Monitoring Editor
A. Gregory Matera
University of North Carolina

Received: May 28, 2013
Revised: Dec 3, 2013
Accepted: Dec 9, 2013

INTRODUCTION

Apurinic/apyrimidinic endonuclease 1 (APE1), also known as redox effector factor-1 (Ref-1), is a multifunctional and essential protein in mammals. It plays a vital role during cellular response to oxidative stress (Fung and Demple, 2005) and contributes to the maintenance of genome integrity (Tell *et al.*, 2005, 2009, 2010a). As an AP endonuclease, APE1 is involved in the base excision repair (BER) pathway, which deals with DNA damage induced by oxidative and alkylating agents, including chemotherapeutic agents (Chen and Stubbe, 2005). APE1 also has transcriptional regulatory activity, modulating gene expression through a redox-based coactivating function on several transcription factors involved in cancer promotion and progression (Huang and Adamson, 1993; Tell *et al.*, 1998; Gaiddon *et al.*, 1999). These two major APE1 activities are independent and located in distinct protein domains. The N-terminal portion of the protein is devoted to the transcriptional coactivating function, and the C-terminal domain exerts the endonuclease activity on DNA abasic sites (Xanthoudakis *et al.*, 1996; Tell *et al.*, 2005). The latter domain is highly conserved, whereas the N-terminal region presents wider variability among different organisms, being more conserved in mammals, thus suggesting recent acquisition during evolution (Georgiadis *et al.*, 2008; Fantini *et al.*, 2010; Poletto *et al.*, 2013). Through its N-terminal portion, APE1 also interacts with different proteins involved in ribosome biogenesis, pre-mRNA maturation/splicing, and ribonucleotide catabolism. These observations highlight an unexpected role of APE1 in RNA metabolism (Vascotto

This article was published online ahead of print in MBoC in Press (http://www.molbiolcell.org/cgi/doi/10.1091/mbc.E13-05-0286) on December 19, 2013.

Address correspondence to: Gianluca Tell (gianluca.tell@uniud.it).

Abbreviations used: 8-oxodG, 8-oxodeoxyguanine; APE1, apurinic apyrimidinic endonuclease 1; BER, base excision repair; GO, Gene Ontology; LC-ESI-MS, liquid chromatography–electrospray ionization–mass spectrometry; nCaRE, negative calcium responsive element; PTH, parathyroid hormone; SIRT1, sirtuin-1; SPR, surface plasmon resonance; THF, tetrahydrofuran; zAPE1, zebrafish APE1.

et al., 2009b; Tell *et al.*, 2010b), as also shown by two independent studies that demonstrated the ability of APE1 to cleave abasic RNA in vitro and in vivo (Berquist *et al.*, 2008; Barnes *et al.*, 2009). Accordingly, APE1 has been proposed to be a main factor in the abasic RNA cleansing process, suggesting that some of the activities of APE1 in gene expression may involve posttranscriptional mechanisms (Tell *et al.*, 2010b).

Another interesting, yet poorly characterized aspect of APE1 transcriptional activity is its role as a component of a *trans*-acting complex that acts as a Ca^{2+}-dependent repressor of the parathyroid hormone (PTH) gene by binding the negative calcium responsive elements (nCaRE) in its promoter region (Okazaki *et al.*, 1991). In particular, an increase in extracellular Ca^{2+} concentration inhibits PTH expression through a mechanism involving APE1 binding to two nCaRE elements, nCaRE-A and nCaRE-B (Yamamoto *et al.*, 1989). This observation was further extended to the promoter region of renin (Fuchs *et al.*, 2003), Bax (Bhattacharyya *et al.*, 2009), and APE1 itself (Izumi *et al.*, 1996). This last case represents the first example of such a negative regulatory mechanism for a DNA repair enzyme. Other experiments demonstrated that APE1 requires additional factors, such as heterogeneous ribonucleoprotein L (Kuninger *et al.*, 2002), Ku antigen (Chung *et al.*, 1996), and PARP-1 (Bhattacharyya *et al.*, 2009), to stably bind to nCaRE elements.

nCaRE-B sequences are located within ALU repeats (McHaffie and Ralston, 1995; Shankar *et al.*, 2004). Therefore, given that ALU elements are transposable elements that occupy at least 1/10 of the expressed human genome, many other functional nCaRE-B sequences could exist and play a role in the transcriptional regulation of genes. However, information is lacking on 1) an accurate numbering, 2) the identity of genes containing these sequences within their promoter, and 3) the active biological function of these elements. Thus the quest is for functional nCaRE-B sequences in the human genome to identify new potential genes whose expression may be regulated by APE1 through nCaRE binding.

The present work is devoted to this issue and focuses on the characterization of the molecular mechanisms responsible for APE1 binding to nCaRE-B sequences on sirtuin-1 (SIRT1) promoter. Bioinformatic analyses of human gene expression data obtained upon APE1 knockdown in cells (Vascotto *et al.*, 2009a) show the presence of multiple nCaRE-B sequences in genes deregulated upon APE1 silencing and conserved in the mouse genome. Among these, we focus on the two nCaRE sequences present within the promoter region of the human deacetylase SIRT1 gene and their role in regulating the corresponding gene transcription. SIRT1 is a deacetylase participating in cell growth, adaptation to caloric restriction, apoptosis, and tumorigenesis (Gorospe and de Cabo, 2008; Kim and Um, 2008), as well as in cell response to genotoxic agents through the deacetylation of APE1 (Yamamori *et al.*, 2010). Together the data show the importance of APE1 during transcriptional initiation in positively promoting transcription of genes under genotoxic conditions.

RESULTS

Bioinformatic search for nCaRE sequence–containing genes reveals the SIRT1 gene as a novel candidate target of APE1 regulation

Bioinformatic analysis of the systematic retrieval of functional nCaRE-B sequences in the human genome was carried out by filtering biological data obtained from the gene expression profile of HeLa cells knocked down for APE1 (Vascotto *et al.*, 2009a). Here we develop a method that integrates different approaches to the problem on a whole-genome scale while minimizing the number of false positives. To this purpose, classic DNA pattern-matching studies are integrated with independent information on gene regulation. We use three main sources for data filtering: 1) functional annotation data collected via the Gene Ontology (GO) project; 2) gene expression data derived from the microarray profile of APE1-knockdown HeLa cells (Vascotto *et al.*, 2009a); and 3) human–mouse gene sequence comparisons. In fact, both expression data and functional annotation database provide a wealth of information about coregulation. This is of particular interest, since coregulated genes likely share similar transcriptional regulatory mechanisms. Comparison with orthologous gene promoters highlights sequences retained during evolution, whose conservation suggests their potential functionality. As a final result, we obtain a set of genes that pass the mentioned filters and are considered bona fide candidates coregulated through nCaRE-B sequences (Supplemental Figure S1).

We collected the 6000–base pair upstream regions of all human and mouse protein-coding genes, which we then analyzed for the presence of nCaRE-B elements using Glsearch for local alignment (Pearson, 2000). We found 8724 human genes to contain one or more nCaRE-B matches within their promoters; 2173 matches were retrieved in the mouse genome. We then cross-checked candidate genes with gene expression data obtained from APE1-knockdown cells (Vascotto *et al.*, 2009a), verifying coexpression between genes carrying nCaRE-B elements. Through this analysis, we identified 384 common genes in the two data sets (Figure 1A). Then we considered the GO annotations of these 384 genes, searching for statistically significant common annotations. We observed strong overrepresentation of terms related to RNA processing and metabolism, in accordance with our previous studies (Vascotto *et al.*, 2009a). All the significant associations between genes and GO terms are reported in Supplemental Table S1. Finally, we applied the phylogenetic footprinting filter, which evaluates whether a significant fraction of the selected genes, as obtained through the GO filter, share homologous genes containing nCaRE-B-related sequences in the upstream region with respect to the mouse gene data set. As a final result, we extracted 57 genes that may be considered bona fide candidates bearing the putative nCaRE-B sequences within their regulatory elements (Supplemental Table S2). We performed a functional enrichment analysis to determine whether the 57 genes found are involved in common biological processes. This showed that candidate genes were associated with processes related to gene expression, activation, or increment of the extent of transcription from an RNA polymerase II–driven promoter (Figure 1B and Supplemental Table S3). Among these 57 genes, several are involved with DNA repair process and cellular response to external stimuli and DNA damage: for example, SWI/SNF-related, matrix-associated, actin-dependent regulator of chromatin, subfamily a member 4 (SMARCA4), sirtuin 1 (SIRT1), valosin-containing protein (VCP), multiple endocrine neoplasia I (MEN1), structural maintenance of chromosomes protein 6 (SMC6), early growth response 1 (EGR-1), and APE1 itself. We paid particular attention to SIRT1, a NAD-dependent histone deacetylase belonging to class III of the sirtuin family, based on the recent demonstration of a functional involvement of this enzyme in the deacetylation of some K residues in the N-terminal region of APE1 (Yamamori *et al.*, 2010; Lirussi *et al.*, 2012). The latter information and the data derived from our bioinformatic analysis led us to hypothesize the existence of an autoregulatory loop between APE1 and SIRT1.

APE1 binds the nCaRE-B sequences present in the human SIRT1 promoter

To prove the functional relevance of the nCaRE-B sequences identified in the human SIRT1 promoter, we first tested the ability of APE1

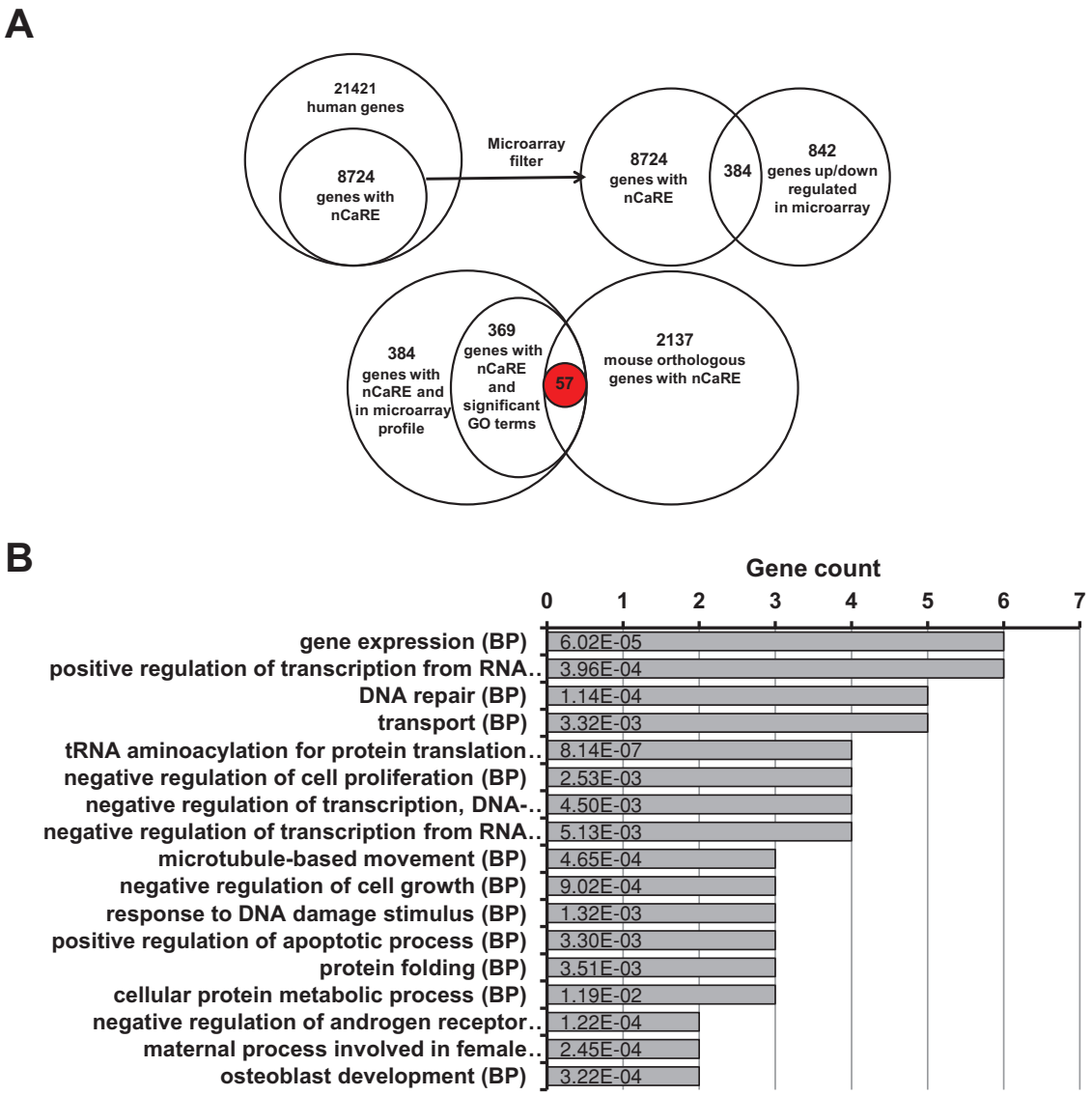

FIGURE 1: Bioinformatic research on nCaRE sequences. (A) Results obtained from the application of the different filters. Top, data derived from alignment research on nCaRE sequences on human gene promoters and subsequent cross-checking with microarray data. Bottom, final results from combined GO and phylogenetic footprinting analyses. (B) Functional enrichment analysis of the 57 putative genes regulated by APE1 performed according to their biological process annotations. For simplicity, only the most representative functional categories are reported. The number of genes for each category is provided on the horizontal axis, together with the list of the first 17 co-occurrence terms. Statistical significance for each category is shown within each bar.

to specifically bind these elements in vitro. Thus we performed electrophoretic mobility shift assay (EMSA) analyses using different APE1 recombinant protein forms and two double-stranded (ds) oligonucleotides containing the SIRT1 nCaRE-B elements corresponding to the sequences present at −2701 (SIRT1-A) and −1754 base pairs (SIRT1-B) from the transcription start site (TSS), respectively (Figure 2A). Full-length human wild-type (WT) APE1 ($APE1^{WT}$), the N-terminal APE1-deletion mutant ($APE1^{N\Delta 33}$), and the orthologous zebrafish APE1 (zAPE1) expressed in *Escherichia coli* were used for this purpose. As clearly demonstrated by EMSA analyses, only the $APE1^{WT}$ protein was able to stably bind to both the SIRT1 nCaRE-B sequences (Figure 2B, lanes 2 and 6), whereas a complete absence of retarded complex was observed in the case of the truncated $APE1^{N\Delta 33}$ form (Figure 2B, lanes 3 and 7). These findings show the importance of the first 33 amino acids at the APE1 N-terminus for proper binding of the protein to nCaRE-B sequences. Similar poor DNA-binding activity was apparent in the case of zAPE1 (Figure 2B, lanes 4 and 8), which bears a nonrelated N-terminal domain (Fantini *et al.*, 2010). Together these results suggest that the phylogenetically evolved N-terminal domain of the protein is essential for stable interaction between APE1 and the nCaRE-B sequences. It is conceivable that K residues present within this region and acquired during evolution in mammals (Georgiadis *et al.*, 2008; Fantini *et al.*, 2010; Poletto *et al.*, 2013) play a major role in protein binding to these DNA elements.

We then estimated the affinity of APE1 for SIRT1 nCaRE-B sequences through surface plasmon resonance (SPR) analysis (Figure 2C). Biotinylated versions of the nCaRE-B (SIRT1-B) or polyT

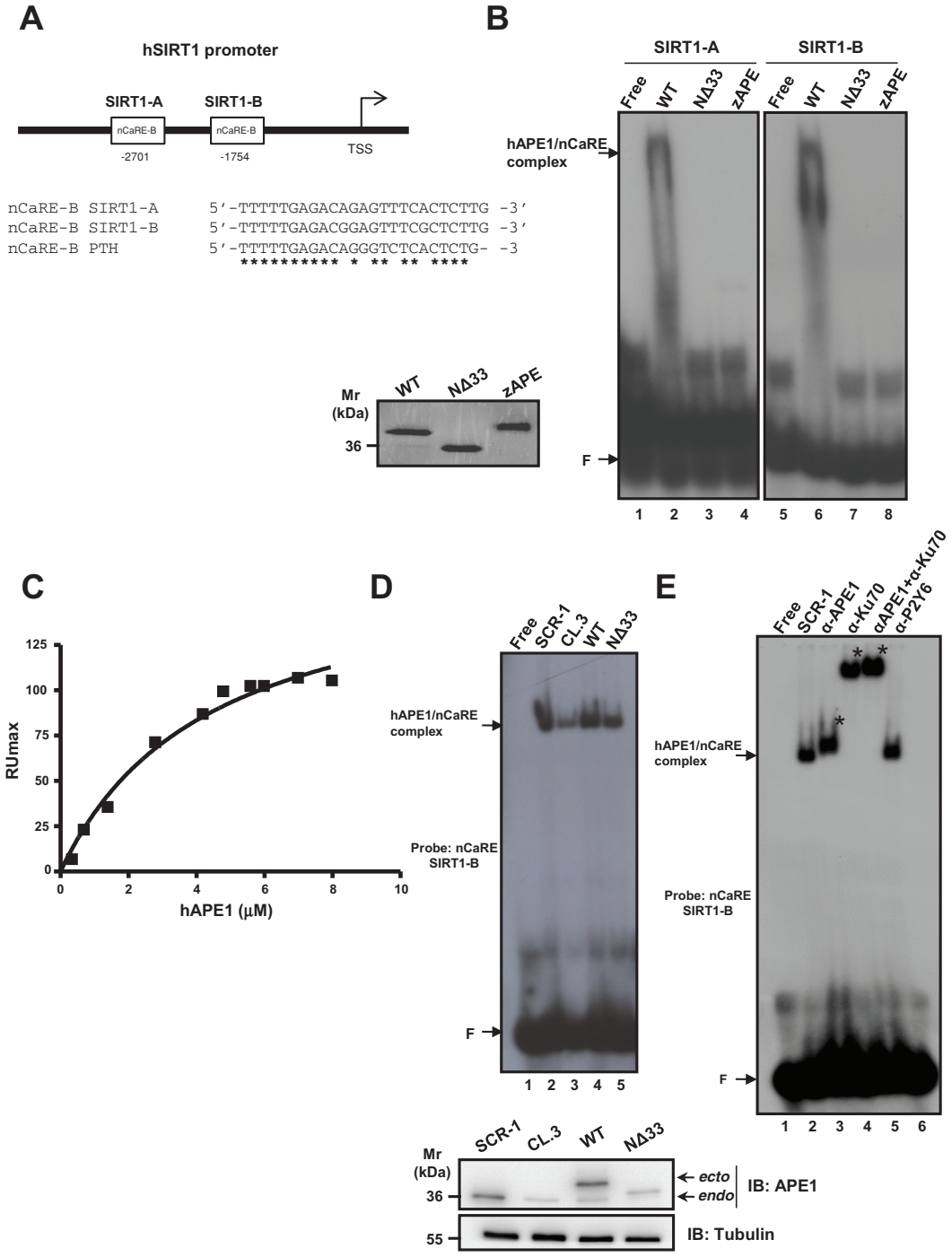

FIGURE 2: APE1 is part of a nuclear protein complex that binds to the SIRT1 nCaRE sequence through its N-terminal domain. (A) Schematic representation (top) and multiple sequence alignment (bottom) of two nCaRE-B sequences found on the human SIRT1 gene promoter (SIRT1-A and SIRT1-B) with the nCaRE sequence found on the human PTH promoter (Okazaki *et al*., 1991). (B) EMSA analysis of nCaRE SIRT1-A and SIRT1-B sequence challenged with 10 pmol of purified $APE1^{WT}$, $APE1^{N\Delta33}$, and zAPE1 proteins. Left, Coomassie staining of the purified recombinant proteins. (C) SPR analysis of the human APE1 (hAPE1)–nCaRE interaction. Recombinant hAPE1 and biotinylated nCaRE SIRT1-B (Table 1) were used as analyte and ligand, respectively. Plot of RUmax from each binding vs. hAPE1 concentrations (0.5–8 μM); data were fitted by nonlinear regression analysis. (D) Top, EMSA analysis of nCaRE SIRT1-B incubated with HeLa nuclear extract of different clones: control clone, $APE1^{SCR\text{-}1}$ (lane 2), clone silenced for APE1, $APE1^{CL.3}$ (lane 3), and clones reconstituted with $APE1^{WT}$ (lane 4) or $APE1^{N\Delta33}$ (lane 5). Bottom, Western blot analysis of APE1 protein in HeLa nuclear cell extracts. (E) EMSA analysis of nCaRE SIRT1-B with HeLa nuclear extract from $APE1^{SCR\text{-}1}$ clone alone (lane 2) or preincubated with monoclonal antibody against APE1 (lane 3) or/and with an antibody against Ku-70 (lanes 4 and 5). Lane 6 corresponds to $APE1^{SCR\text{-}1}$ nuclear extract incubated with a nonspecific antibody (α-P2Y6). Free indicates probe alone; F shows the position of the free oligonucleotide probe. Specific APE1/nCaRE interaction is indicated by the arrow. Asterisk indicates supershift.

Ligand	K_a (ms × 10^5)	K_d (1/s)	K_D (μM)
SIRT1-B nCaRE	0.270	0.105	3.90 ± 0.08
SIRT1-B mutated	0.0198	0.236	119 ± 8
polyT	0.004	0.112	308 ± 3

TABLE 1: Dissociation constant and kinetic parameter values as determined for APE1 by SPR analysis.

sequences were immobilized onto a streptavidin chip for use as ligands in SPR experiments. $APE1^{WT}$ and $APE1^{N\Delta33}$ were then analyzed for their DNA-binding properties. When testing $APE1^{WT}$ as analyte, K_D = 3.90 ± 0.08 μM was measured (Poletto *et al.*, 2013); corresponding kinetic parameters are shown in Table 1. Conversely, when using $APE1^{N\Delta33}$, we did not observe any SPR signal variation (unpublished data), in accordance with EMSA experiments (Figure 2B). This result confirmed that the protein region 1–33 is essential for stable interaction of APE1 with these DNA elements. As a DNA-repair enzyme, APE1 has intrinsic ability to bind to DNA in a sequence-independent manner. Moreover, independent observations clearly point to a role of the nucleic acid secondary structure in positively modulating this activity (Poletto *et al.*, 2013). Here we evaluated the protein capacity to bind to a single-stranded 24-mer oligo-dT (here called polyT). A K_D = 308 ± 3 μM was measured in the case of $APE1^{WT}$, whereas no binding was observed for $APE1^{N\Delta33}$ (Table 1 and Supplemental Figure S2), in agreement with EMSA analysis. These results indicate that APE1 poorly recognizes a nonstructured oligonucleotide formed by a stretch of thymidines, confirming that this protein may bind to DNA with different affinities and the oligo-dT sequence may be used in EMSA analysis as a nonspecific competitor.

Our EMSA and SPR analyses on APE1 binding activity to the SIRT1 nCaRE-B sequences showed low affinity for recombinant APE1 alone. Therefore we tested whether additional factors present in nuclear extracts of the cells may increase protein-binding affinity to its oligonucleotide target. To this aim, further EMSA analyses, performed using HeLa cell nuclear fractions, confirmed that nuclear activity able to specifically bind nCaRE-B sequences was indeed present (Figure 2D). The high-affinity complex measured, even using much lower amounts of APE1 (0.63 pmol, as estimated from Lirussi *et al.*, 2012) with respect to that obtained with the recombinant purified protein alone (10 pmol; Figure 2B), suggested that additional factors are required for efficient APE1 binding to SIRT1 nCaRE-B sequences. To demonstrate the presence of APE1 in the retarded complex observed in Figure 2D, we used nuclear extracts obtained from a HeLa line (CL.3) for which endogenous APE1 protein expression was previously knocked down through stable short hairpin RNA (shRNA) transfection (Vascotto *et al.*, 2009a). As is apparent from lane 3 in Figure 2D, an overall reduction of the intensity (almost 70% with respect to lane 2) of the retarded nCaRE-bound complex was observed, similar to what occurred for the clone expressing $APE1^{N\Delta33}$ (lane 5; almost 50% with respect to lane 2). Nuclear extracts obtained from HeLa cells reconstituted with ectopic $APE1^{WT}$ (lane 4) showed the same amount of bound complex as the control cell clone expressing a scrambled shRNA vector (indicated as SCR-1; recovery of almost 80% with respect to lane 2). Preincubation of the nuclear extract from the SCR-1 clone with an anti-APE1 antibody resulted in the formation of a supershifted complex (Figure 2E, lane 3). This complex was absent when a nonrelated antibody was used (lane 6), clearly demonstrating that APE1, present in the nuclear cell extract, is involved in the recognition of the nCaRE-B elements of the SIRT1 promoter. The reduced intensity of the retarded complex band upon APE1 silencing or in the reconstituted cells expressing $APE1^{N\Delta33}$ protein (Figure 2D), as well as the lower apparent electrophoretic mobility of the protein–DNA retarded complex when using nuclear extracts in place of the recombinant purified protein (Figure 2B), suggests that APE1 may be part of a multiprotein complex. Because Ku70 antigen protein was already demonstrated to bind nCaRE-A sequences in complex with APE1 (Chung *et al.*, 1996), we incubated the HeLa nuclear extract with an antibody recognizing the Ku70 antigen. We then subjected the reaction to EMSA analysis, showing the formation of a supershifted complex (Figure 2E, lane 4). The concurrent presence of APE1 and Ku70 in the same retarded complex was confirmed by performing simultaneous preincubation with antibodies specific for these proteins (Figure 2E, lane 5). The presence of Ku70 in the complex with APE1 was also corroborated by additional EMSA analysis performed with the purified recombinant protein attesting that, when present alone, Ku70 is not able to stably bind to the SIRT1 nCaRE-B sequence per se. On the contrary, when concomitantly incubated with APE1, Ku70 significantly enhances APE1 DNA-binding activity to SIRT1 nCaRE-B element (Supplemental Figure S3, compare lanes 2–5 and 8–10). Unpublished data demonstrated that this stimulatory activity on APE1 binding required interaction through the APE1 33N-terminal domain. Overall these data demonstrate that APE1 must be part of a multiprotein complex containing Ku70 to elicit its high-affinity binding potential with regard to the nCaRE-B sequences present on the SIRT1 promoter.

Topology of the APE1-nCaRE complex

nCaRE-B element consists of a palindromic sequence that can fold into self-complementary hairpins (Figure 3A, left). In silico analyses with the mfold program suggested that these elements could fold into cruciform-like structures. To evaluate whether SIRT1 nCaRE-B sequences can fold into cruciform duplexes and specifically assess whether APE1 binding to this element may depend on such secondary structures, we performed footprinting analyses by using the T7 endonuclease I (Figure 3A, right). This protein is a structure-sensitive enzyme that specifically recognizes conformationally branched DNA and Holliday structures or junctions (Parkinson and Lilley, 1997; Déclais *et al.*, 2003; Fan *et al.*, 2006). Footprinting data support the hypothesis of the existence of a secondary structure for the nCaRE-B sequences (Figure 3A and Supplemental Figure S4). In particular, our experiments show the predominant formation of two bands (respectively 10 and 19 nucleotides in length) in the digested samples, which correspond to a cutting site close to the predicted loop or immediately adjacent to the predicted stem (Figure 3A, arrows). Of interest, preincubation of the SIRT1 nCaRE-B oligonucleotide with APE1 impairs T7 endonuclease digestion (Figure 3A, lane 4). Consistent with these observations, EMSA analysis demonstrated that digestion of the SIRT1 nCaRE-B oligonucleotide with T7 endonuclease affects APE1 binding to this element, but, conversely, when APE1 was first incubated with the nCaRE-B probe and then digested with T7 endonuclease, the binding was not affected. These data suggest a protective role of APE1 with regard to T7 endonuclease action, strongly supporting the hypothesis that these proteins may compete for the same binding site on the nCaRE-B sequences (Figure 3B).

The first 33 N-terminal amino acids of APE1 are required for protein binding to the nCaRE sequences (Figure 2, A and D). To further investigate the role of this protein portion on APE1's ability to bind to DNA elements, we performed combined limited proteolysis-mass spectrometry experiments on recombinant APE1 protein in either

the absence or the presence of its target nCaRE oligonucleotide (Figure 3C, left). In particular, parallel experiments with a specific proteolytic enzyme (used at a defined APE1/protease weight/weight ratio) were carried out on a time-course basis on 1) isolated APE1, 2) APE1 complexed with SIRT1 nCaRE-B oligonucleotide, and 3) APE1 complexed with PTH nCaRE-B oligonucleotide (Okazaki *et al.*, 1992; Supplemental Figure S5 and Supplemental Table S4). This last was used as control. Resulting differential peptide maps provided information on amino acid(s) eventually protected from proteolytic attack as result of their presence at the protein–DNA complex interface (Figure 3C, left). The data were interpreted according to the concept of "molecular shielding" of amino acids from proteolytic attack (Scaloni *et al.*, 1998, 1999; Renzone *et al.*, 2007) and were rationalized on the basis of x-ray crystallographic APE1 structures (Gorman *et al.*, 1997; Beernink *et al.*, 2001). To maximize information resulting from limited proteolysis experiments, we used different proteolytic enzymes in separate assays.

Figure 3C (right) summarizes the results of the limited proteolysis experiments, as obtained by using different proteases on recombinant APE1 alone (Figure 3C, top) or after its complex formation with the SIRT1 nCaRE substrate (Figure 3C, bottom; see Supplemental Figure S5 and Supplemental Table S4 for experimental details). General considerations concerning the native protein are as follows. Preferential hydrolyzed peptide bonds on isolated APE1 gathered into a specific region of the protein, namely the most exposed segment, the unstructured N-terminal domain, which contained six proteolytic sites (K6, K7, A9, A11, D15, and L17). An additional site was within the globular APE1 domain (L111). Of interest, no other cleavage sites were detected in other protein regions, although exposed on the molecular surface (Gorman *et al.*, 1997; Beernink *et al.*, 2001). After complex formation with nCaRE-B oligonucleotides, a marked protective effect was observed, as demonstrated by the large decrease in the number of proteolytic sites present in the N-terminal region (from six to one), thus confirming the involvement of this APE1 portion in binding to these DNA elements.

Transcriptional regulation of SIRT1 expression by APE1 protein

To determine whether the observations obtained in vitro regarding APE1 binding to SIRT1 nCaRE-B sequences have any relevance in vivo, we examined the APE1 occupancy of the nCaRE-B sequence in the SIRT1 promoter through chromatin immunoprecipitation (ChIP) analyses. To this purpose, we used HeLa cells cotransfected with a human SIRT1 promoter–containing plasmid (Yamamori *et al.*, 2010) and FLAG-tagged $APE1^{WT}$- or $APE1^{N\Delta33}$-expressing plasmids. The amount of immunoprecipitated SIRT1 promoter was significantly enriched in $APE1^{WT}$-transfected cells compared with that obtained from control cells transfected with the empty vector alone (Figure 4A). As expected, $APE1^{N\Delta33}$-transfected cells had a remarkable reduction, although not completely so, in the amount of immunoprecipitated SIRT1 promoter. A similar degree of reduction was observed when ChIP analysis was performed by using a SIRT1 promoter bearing a mutated sequence within the nCaRE-B motif (Figure 4B), whose reduced specificity was previously assessed through SPR analysis (Table 1 and Supplemental Figure S2). These experiments revealed that the mutation introduced in the nCaRE-B sequence significantly reduced the APE1 binding to DNA, lowering the affinity of the complex by 30-fold ($K_D = 119 \pm 3$ μM). Competitive EMSA analyses were in agreement with these findings. In fact, addition of the unlabeled nCaRE ds oligonucleotide resulted in almost complete elimination of bound complex formation. On the other hand, competition with the unlabeled mutant nCaRE oligo (nCaRE-mut) caused only a slight reduction of the nCaRE-binding complex, in agreement with ChIP and SPR data, supporting the notion of sequence-dependent binding specificity (unpublished data). These data were also confirmed with the endogenous APE1 promoter via ChIP followed by high-throughput sequencing (ChIP-Seq) analyses (unpublished data), further demonstrating the physiological relevance of these findings. Together these results confirm our in vitro observations (Figure 2) and support the hypothesis that, under basal conditions, APE1 is associated with the nCaRE-B sequence within the SIRT1 promoter also in vivo, possibly as part of a multiprotein complex.

We then evaluated whether APE1 binding to SIRT1 promoter plays a role in SIRT1 transcriptional regulation by performing promoter-reporter assays. HeLa cells were cotransfected with a luciferase reporter vector bearing the SIRT1 promoter and $APE1^{WT}$ FLAG-tagged vector (Figure 4C). SIRT1 promoter-reporter assays showed that there was a significant increase in the luciferase signal detected in the presence of APE1 compared with that of the promoter alone. We evaluated the effect of APE1 silencing on endogenous SIRT1 mRNA expression levels through an inducible shRNA knockdown strategy (Vascotto *et al.*, 2009a,b). Endogenous APE1 knockdown (CL.3) caused a significant reduction in the SIRT1 endogenous expression levels (Figure 4D), which was rescued in cells reconstituted with a siRNA-resistant APE1 cDNA expression plasmid (WT). These data demonstrated a positive effect of APE1 on SIRT1 transcriptional activation. Although unexpected, since previous data reported a transcriptional repressive role for APE1 through nCaRE sequence binding (Okazaki *et al.*, 1991; Fuchs *et al.*, 2003), these data agree with our previous observations from gene expression profiling analysis (Vascotto *et al.*, 2009a), in which reduced expression of SIRT1 in APE1-knockdown HeLa cells was apparent.

Oxidative stress induces SIRT1 transcription via recruitment of BER enzymes

To better understand, at the molecular level, the transcriptional function exerted by APE1 through binding to nCaRE-B sequences, we investigated whether APE1's positive role in SIRT1 transcription relied on its enzymatic activity on DNA. First, we observed that under basal conditions APE1 has no endonuclease activity on the SIRT1 nCaRE-B sequence, as assessed through an oligonucleotide cleavage assay (Figure 5A). APE1 cleavage, occurring at any site on the cruciform nCaRE-B sequence, should lead to a site-specific, single-stranded break that can be detected by the appearance of an extra fragment in the cleavage assay. Even using an increasing amount of purified recombinant APE1 protein, we did not detect any nuclease activity that, on the contrary, was readily visible when using a radiolabeled 26-mer ds oligonucleotide containing a tetrahydrofuran mimicking an AP site (here referred to as THF; Berquist *et al.*, 2008). Substitution of the guanine residue at position 12, within the predicted loop of the nCaRE-B sequence, with a THF residue resulted instead in efficient APE1 cleavage activity on the nCaRE-B sequence. This activity depends on APE1 catalytic function, since the catalytically inactive $APE1^{E96A}$ mutant (Izumi *et al.*, 1999) was unable to efficiently cleave the same substrate (Figure 5B).

Prompted by these findings, we hypothesized that the APE1-positive function that we observed on the SIRT1 promoter may be ascribed to the APE1 catalytic activity on nCaRE-B sequences. This can occur after specific stimuli, such as oxidative stress, which can lead to abasic site formation on nCaRE-B sequences (Amente *et al.*, 2010; Francia *et al.*, 2012). It is well known that SIRT1 expression and function are regulated by external stressors, including exposure to genotoxic agents (Cohen *et al.*, 2004; Kim and Um, 2008;

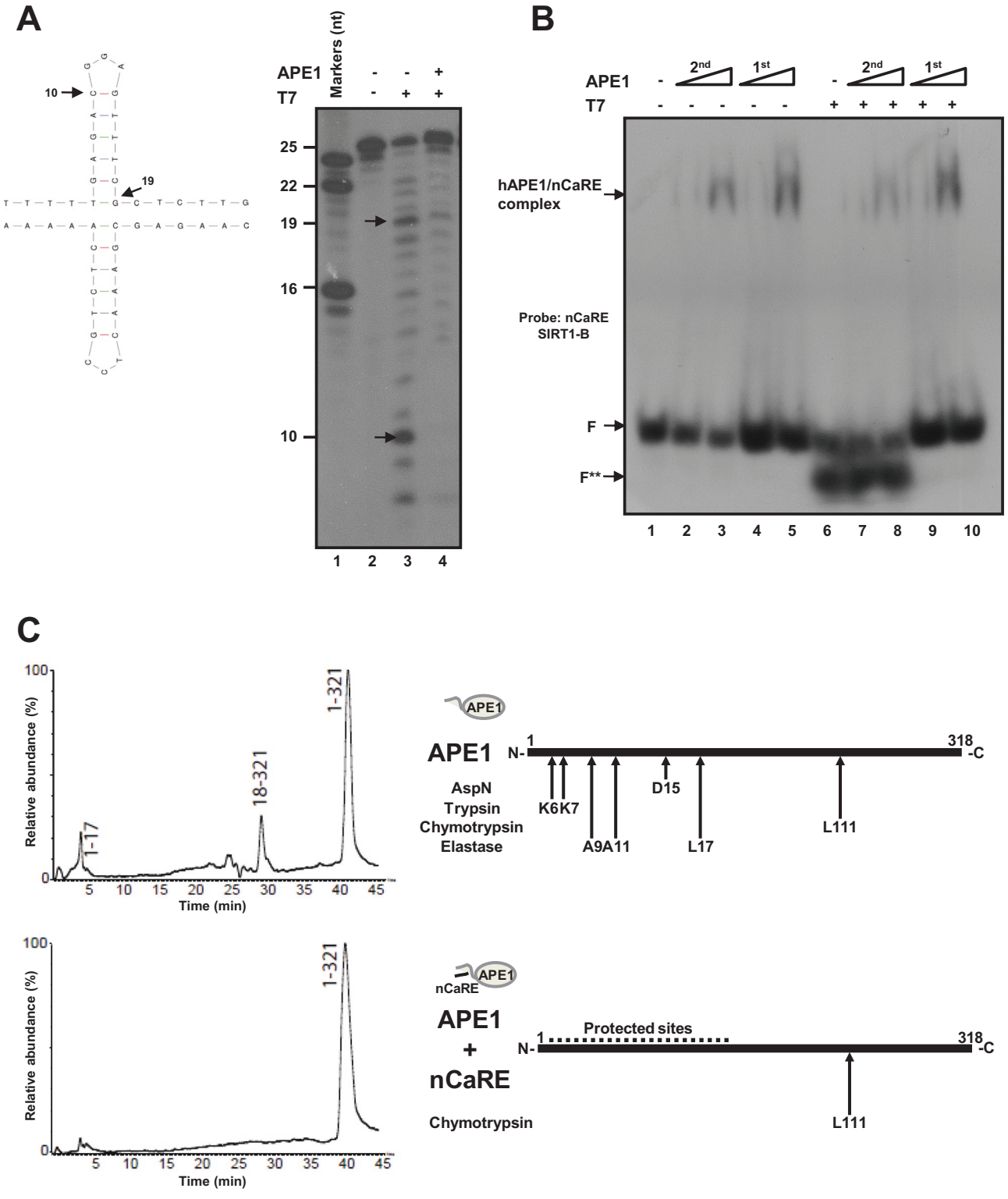

FIGURE 3: APE1 recognizes structured nCaRE sequences through its N-terminal domain. (A) Left, predicted cruciform structure of nCaRE SIRT1-B ds oligonucleotide. Arrows indicate the cleavage site of T7 endonuclease I and the length of the products. Right, 5′-^{32}P-end-labeled nCaRE was preincubated (lane 4) or not (lane 3) with APE1 recombinant protein and then subject to T7 endonuclease digestion. (B) EMSA analysis of APE1 binding to nCaRE sequence after digestion with T7 endonuclease (lanes 7 and 8) or upon preincubation with APE1 and subsequent digestion with T7 endonuclease (lanes 9 and 10). Lane 1 is the probe alone; APE1 incubation with the probe was performed temporally before (1st) or after (2nd) T7 digestion; F shows the position of the free oligonucleotide probe. F** indicates the T7 endonuclease–digested probe. Specific APE1/nCaRE interaction is indicated by the arrow. (C) Schematic representation of the amino acids within the N-terminal domain of APE1 and involved in nCaRE oligonucleotide binding. Left, proteolytic maps obtained after incubation of recombinant APE1 alone (top) or recombinant APE1 complexed with SIRT1 nCaRE-B

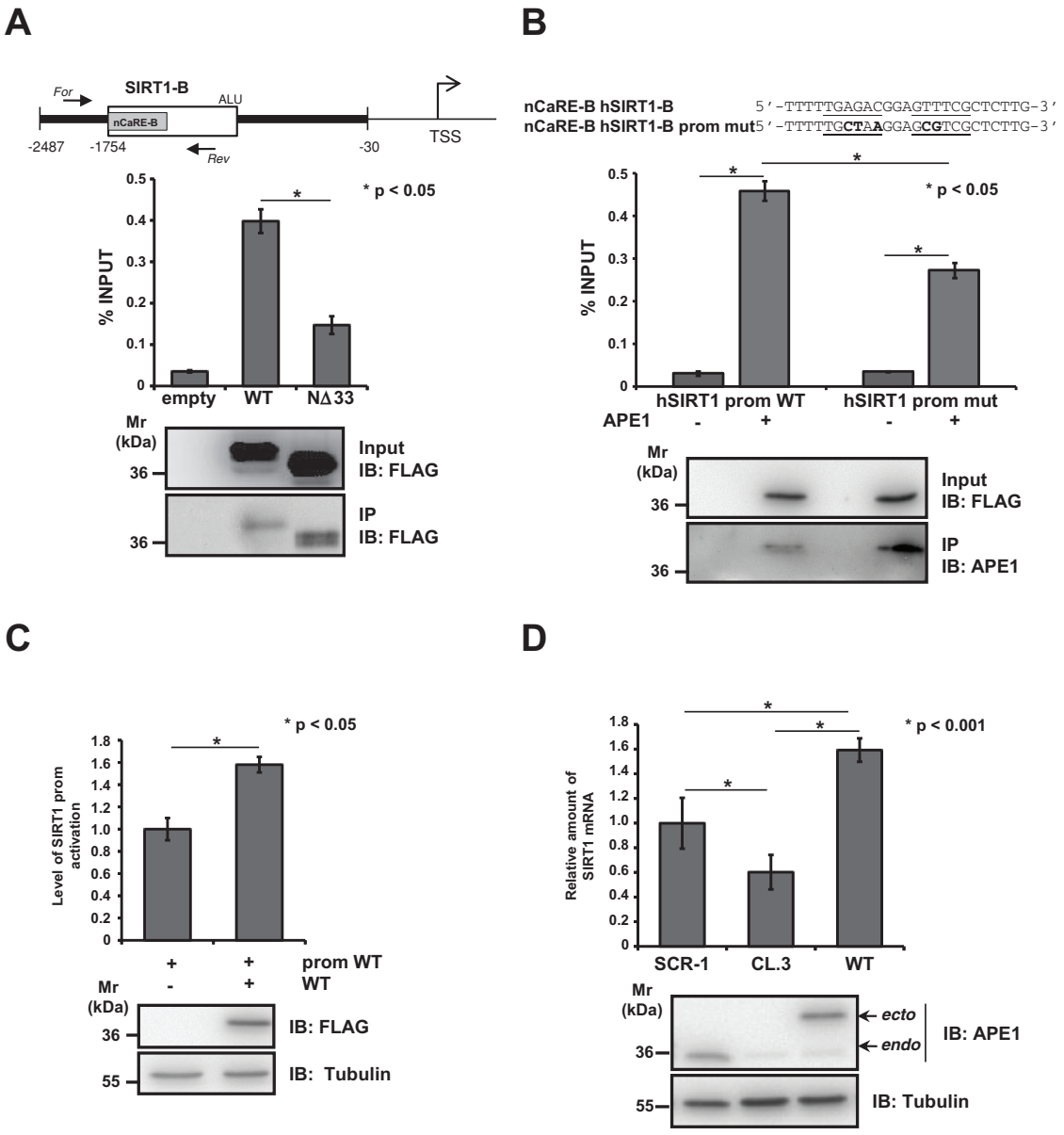

FIGURE 4: APE1 positively regulates SIRT1 expression at the promoter level. (A). Top, schematic representation of the human SIRT1 promoter used for HeLa transfection. For and Rev arrows indicated the reverse transcription-PCR primer designed for the quantification of the human SIRT1 nCaRE sequence bound to APE1. Bottom, ChIP assay for APE1-nCaRE sequence association. Percentage of immunoprecipitated nCaRE DNA relative to that present in total input chromatin. Data were further normalized to the amount of immunoprecipitated protein. Western blot analysis was performed on total cell extracts (input) and immunoprecipitated material (IP) with specific antibody for FLAG and APE1. IB, immunoblot. (B) ChIP analysis on mutated human SIRT1 promoter. Top, base composition of the nCaRE SIRT1-B mutated sequence used for site-directed mutagenesis of SIRT1 promoter. Divergent sequences in the mutant nCaRE are bold. Bottom, HeLa cells were cotransfected with vector expressing $APE1^{WT}$ and, alternatively, wild-type or mutated hSIRT1 promoter. The histogram represents the amount of hSIRT1 promoter sequence that was immunoprecipitated. Data are percentage of input and are normalized to the amount of APE1 immunoprecipitated, as evaluated by Western blot analysis. (C) hSIRT1 promoter is activated in presence of APE1, as shown in the reporter assay. Western blot analysis showing the normalization of protein levels. (D) Analysis of SIRT1 mRNA level with qPCR in clones expressing $APE1^{WT}$ or APE1 silenced (CL.3) cells. Western blot analysis on protein extract of clones showing the suppression of endogenous APE1 expression upon 10 d of treatment with doxycycline.

oligonucleotide (bottom) with endoprotease AspN. Experiments were performed on a recombinant APE1 form bearing three additional amino acids at the protein N-terminus with respect to the native counterpart. Peptides identified by mass spectrometry analysis are indicated at the top of the corresponding chromatographic peaks. Right, proteolytic sites identified in native APE1 alone (top) and in APE1 complexed with SIRT1 nCaRE-B oligonucleotide (bottom); summary of results from independent experiments performed by using different proteases. See the Supplemental Information for experimental details and Supplemental Figure S4 and Supplemental Table S4 for complete data.

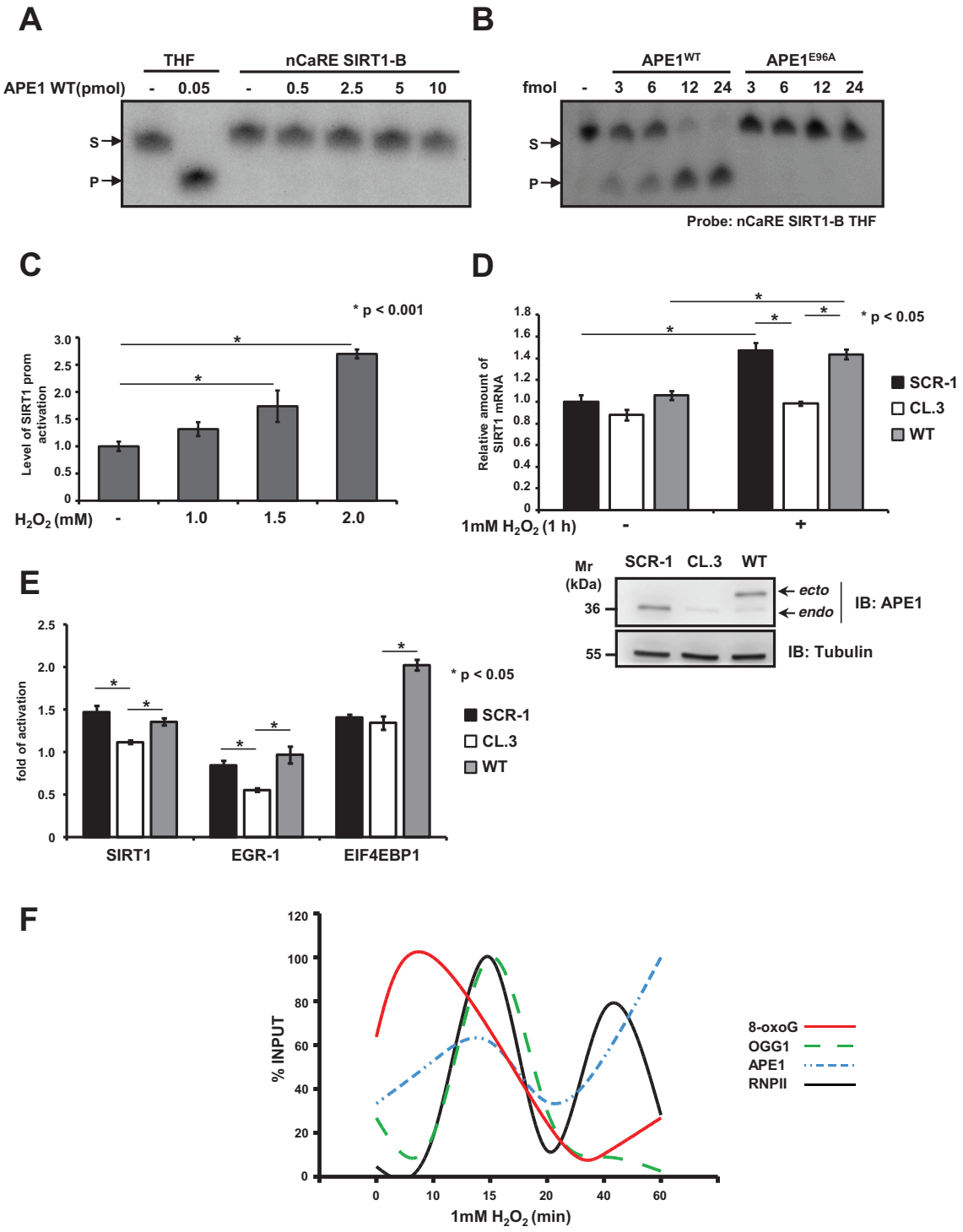

FIGURE 5: Recruitment of BER enzymes on the SIRT1 promoter. (A) APE1 endonuclease activity on ds, nCaRE SIRT1-B radiolabeled oligonucleotide. A radiolabeled ds, THF-containing deoxyoligonucleotide (THF) was used as control. Reactions were performed with increasing amounts (picomoles) of recombinant $APE1^{WT}$ protein. (B) APE1 AP endonuclease activity on nCaRE SIRT1-B THF-containing probe incubated with increasing amounts of recombinant $APE1^{WT}$ protein or a catalytic inactive APE1 mutant ($APE1^{E96A}$). (C) Reporter assay with HeLa cells transfected with hSIRT1 firefly reporter vector and challenged with increasing doses of H_2O_2 for 1 h as indicated. (D) qPCR analysis of SIRT1 mRNA levels in clones expressing $APE1^{WT}$ or APE1-silenced cells $APE1^{CL.3}$ after 1 mM H_2O_2 treatment for 1 h. Western blot analysis on the protein extracts. (E) qPCR analysis of SIRT1, EGR-1, and EIF4EBP mRNA levels in $APE1^{CL.3}$ or $APE1^{WT}$ clones after 1 mM H_2O_2 treatment for 1 h. Data shown are reported as fold of activation after H_2O_2 treatment. (F) Results of four independent ChIP analyses relative to accumulation of 8-oxodeoxyguanine, OGG1, APE1, and RNA polymerase II protein on the SIRT1 promoter after 1 mM H_2O_2 treatment for different times (as reported). Data are percentage of input and normalized to quantity of DNA immunoprecipitated by α-tubulin (α-tub). See Supplemental Figure S4 for detailed information.

Yamamori *et al.*, 2010). We therefore measured SIRT1 transcription after oxidative stress, such as that generated by H_2O_2 exposure. First, we demonstrated that SIRT1 promoter activation was increased by H_2O_2 treatment in a concentration-dependent manner (Figure 5C). Next we examined the effect of APE1 silencing or re-expression on SIRT1 transcriptional activation in HeLa cell clones upon H_2O_2 treatment (Figure 5D and Supplemental Figure S6). We treated control (SCR-1), APE1-silenced (CL.3), and $APE1^{WT}$ cell clones with 1 mM H_2O_2 for 1 h. SIRT1 mRNA levels were then evaluated by quantitative PCR (qPCR) and compared with those for untreated clones. On oxidative treatment, SIRT1 mRNA significantly increased, and, of note, this response was higher in the presence of $APE1^{WT}$ protein, whereas it was lower in the case of APE1-knockdown–expressing cells. The residual activation of SIRT1 mRNA expression, which was apparent also in APE1-knockdown cells, might be ascribable to the presence of residual endogenous APE1 protein and/or of further limiting factors, as already speculated (Chung *et al.*, 1996; Kuninger *et al.*, 2002; Bhattacharyya *et al.*, 2009). The observed induction of SIRT1 mRNA transcription in HeLa cells upon oxidative stress correlates with a parallel increase in its protein levels. Confirmation of the biological relevance of our findings comes from the observation of concomitant increased deacetylation activity of SIRT1 protein toward its substrate, that is, K382 of p53 (Vaziri *et al.*, 2001; Supplemental Figure S6).

We also confirmed the general relevance of our model by testing other hypothetical APE1 target genes containing an nCaRE-B element in their promoters and resulting dysregulation in the APE1-kd cell model (Figure 1 and Supplemental Table S2; Vascotto *et al.*, 2009a). To this aim, we evaluated by qPCR the expression levels, upon H_2O_2 treatment, of EGR-1 and eukaryotic translation initiation factor 4E–binding protein 1 (EIF4EBP1) in the HeLa cell inducible-kd (CL.3) clone and the reconstituted cell clone (WT) used here (Figure 5E). Similar results were obtained using another genotoxic agent, methyl methanesulfonate (Supplemental Figure S9). These data, showing inducible expression of these genes dependent on APE1 expression to a similar extent of that observed in the case of SIRT1, were suggestive of a general mechanism of gene activation upon DNA damage that involves APE1 binding to nCaRE-B elements.

To find a relationship between SIRT1 transcription induced by oxidative stress and the APE1 regulatory activity on the nCaRE-B sequences located within the promoter, we studied the dynamics of oxidative repair enzyme recruitment on the SIRT1 nCaRE-B sequence at early time upon H_2O_2 treatment. DNA base oxidation determines the formation of 8-oxodeoxyguanine (8-oxodG), which is recognized by the DNA glycosylase OGG1. This enzyme initiates the BER pathway by removing the 8-oxodG lesion, which is further processed by APE1, which cleaves the apurinic site. To assess the dynamics of occupation of the nCaRE-B sequence on the SIRT1 promoter by these enzymes upon oxidative stress, we performed a time-course ChIP analysis on the SIRT1 nCaRE-B sequence after 1 mM H_2O_2 treatment (Figure 5F and Supplemental Figure S7). We immunoprecipitated SIRT1 nCaRE-B sequence with antibodies against 8-oxodG, OGG1, and APE1. We observed that the signal of 8-oxodG promptly reached its plateau 10 min after H_2O_2 treatment and subsequently decreased, concomitant with accumulation of OGG1, which is recruited immediately after (15 min), in accordance with the BER processes. Occupancy by APE1 follows OGG1 recruitment. To demonstrate a direct link between DNA repair and SIRT1 transcriptional initiation, we examined the assembly of RNA polymerase II (RNPII) on the SIRT1 nCaRE-B sequence. Under basal condition, RNPII was found with relatively low abundance on the SIRT1 nCaRE-B sequence; conversely, the polymerase was progressively recruited as soon as the oxidative stress began (15 min after H_2O_2 treatment). Afterward (40 min after H_2O_2 addition), RNAPII was again recruited on the SIRT1 promoter, showing a wave-like behavior. In concert with this observation, we also noticed augmented interaction between APE1 and RNPII in accordance with the kinetics observed during ChIP analysis (Supplemental Figure S8). This oxidatively induced recruitment of RNPII to the SIRT1 promoter may suggest that oxidative stress can trigger SIRT1 transcriptional activation. One could envision a mechanism in which H_2O_2, causing oxidation of the guanine at the SIRT1 nCaRE-B sequence, promotes recruitment of components of the base excision repair system—OGG1 and APE1, together with proteins involved in nCaRE-B binding such as Ku70. When recruited to the SIRT1 promoter, APE1 (through its endonuclease activity) produces nicks on the SIRT1 nCaRE-B sequence, possibly favoring the DNA relaxation necessary for the formation of chromatin loops that bring RNAPII at the transcription start site (Figure 6); this last enzyme in turn can initiate transcription.

DISCUSSION

After its cloning by independent groups, first as a DNA-repair enzyme (Demple *et al.*, 1991; Robson and Hickson, 1991) and then as a redox coactivator protein (Xanthoudakis and Curran, 1992), a number of articles described different APE1 functions, elucidating its involvement in several biological contexts. As the main apurinic/apyrimidinic endonuclease in mammalian cells, APE1 is classically known for its essential function as a DNA-repair enzyme in the BER pathway. Besides this crucial role in the maintenance of genome stability, APE1 was demonstrated to be involved in redox signaling and the regulation of gene expression (Tell *et al.*, 2010a; Wilson and Simeonov, 2010), supporting the notion that it is a multifunctional protein, with features that go beyond the classic activities of a DNA-repair enzyme. Of note, its multifunctional nature suggests APE1 as an ideal candidate protein linking DNA-damage sensing/repair and transcriptional regulation of genes during cell response to genotoxic damage. Among these non-canonical activities, another interesting APE1 function is its ability to bind the nCaRE sequence of some gene promoters, thus acting as a transcriptional regulator. Okazaki's group was the first to identify two nCaRE sequences within the PTH gene promoter (nCaRE-A and nCaRE-B; Okazaki *et al.*, 1991). The presence of these elements was also described in the regulatory region of a few other genes, such as human APE1 (Izumi *et al.*, 1996), rat atrial natriuretic polypeptide (Okazaki *et al.*, 1992), human renin (Fuchs *et al.*, 2003), and Bax (Bhattacharyya *et al.*, 2009). Besides these few genes, no further evidence has been provided. However, since nCaRE-B elements are present within ALU repeats, which are widely distributed throughout the expressed genome, it is expected that APE1 could regulate the expression of a large number of genes. Here we performed an unbiased investigation of the whole human genome, searching for putative genes whose transcription may be mediated through APE1's ability to bind nCaRE-B elements. In particular, although nCaRE elements seem to be active also at downstream regions (Izumi *et al.*, 1996), here we specifically focused on nCaRE-B elements present only on the upstream sequence of human genes. In the near future, we plan to extend this approach to downstream and intron regions. Bioinformatic analyses revealed a number of genes potentially regulated by APE1, which are involved in several pathways related to gene expression (Figure 1). Among the 57 candidate genes retrieved

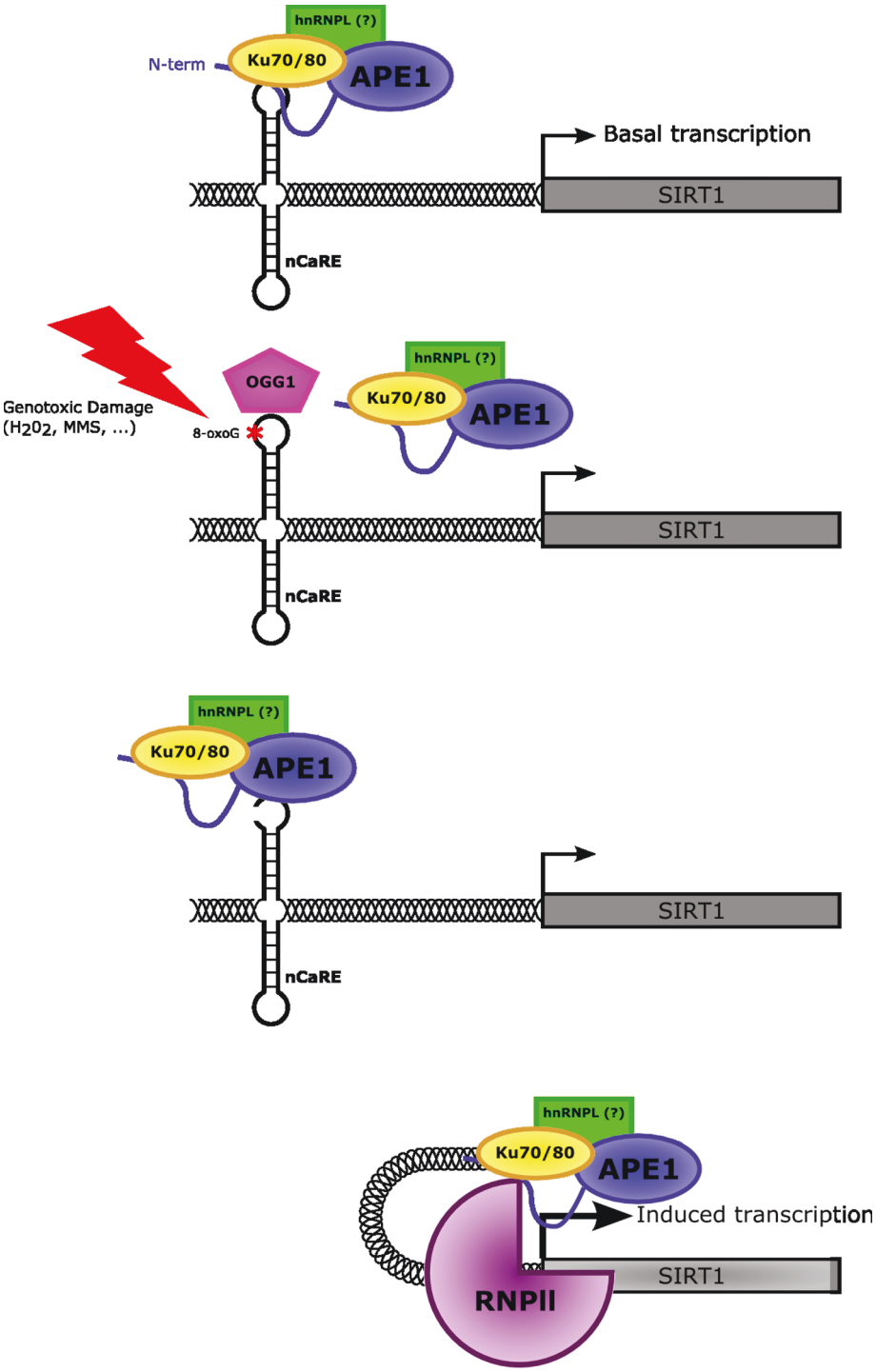

FIGURE 6: Mechanistic model for the role of APE1 in oxidatively mediated SIRT1 transcription. Under normal conditions, APE1, together with other protein factors, is bound to the nCaRE element present within the SIRT1 promoter involved in the basal activation of SIRT1 transcription. Conversely, upon oxidative stress conditions, DNA oxidation determines the formation of 8-oxodeoxyguanine (8-oxoG) lesions at the nCaRE sequence present in the SIRT1 promoter, which are recognized and processed by BER enzymes, including APE1. The nicks introduced at the chromatin level by APE1 during 8-oxoG removal might promote the formation of chromatin loops moving the active form of RNA polymerase II closer to the TSS of the gene, turning on the transcription.

from our bioinformatic analysis, we chose to study the human deacetylase SIRT1, which bears two nCaRE-B elements in its promoter. Increased interest in SIRT1 was due to recent articles showing that this deacetylase controls the acetylation status of APE1 lysine residues K6-7 (Yamamori *et al.*, 2010) and K27-35, thus modulating the subnuclear distribution of this protein and coordinating its enzymatic functions in the BER pathway (Lirussi *et al.*, 2012). Therefore we hypothesized the existence of a possible autoregulatory loop between the two proteins: APE1 modulates SIRT1 expression, which, in turn, regulates APE1 function through deacetylation.

To investigate APE1's transcriptional regulatory function on SIRT1 expression, we first examined APE1's ability to bind the nCaRE-B sequences found in the SIRT1 promoter. Through different in vitro approaches, we showed that APE1 is able to bind SIRT1 nCaRE-B sequences (Figures 2 and 3). In particular, by a combination of EMSA and SPR analyses with limited proteolysis experiments, we demonstrated that the APE1 N-terminal domain is essential for the proper binding of these elements. The essential role of this protein domain in DNA binding is remarkable, particularly if one considers the phylogenesis of the nCaRE-B elements and that of the APE1 N-terminal region. nCaRE-B sequences are present within ALU repeats, which belong to the short interspersed nucleotide element family of repetitive sequences that originally derived from the reverse transposition of 7SL RNA. This event took place in the genome of an ancestor of Supraprimates (Kriegs *et al.*, 2007): these repetitive elements have been found exclusively in primates (Deininger *et al.*, 1981), scandentians (Nishihara *et al.*, 2002), and rodents (Krayev *et al.*, 1980), all members of the placental mammalian clade Supraprimates (Euarchontoglires; Murphy *et al.*, 2001). Similarly, information on the sequence homology of the APE1 N-terminal domain across species points to the recent phylogenetic acquisition of this region. Sequence conservation of this domain is very high in mammals but almost absent in other organisms, with the exception of *Danio rerio*, *Dictyostelium*, and *Drosophila*. Accordingly, it could be envisioned that once ALU elements appeared in primates and were stabilized in their genomes, progressively losing their transcriptional potential, these organisms needed to evolve novel mechanisms to cope with the acquired RNA Pol II regulatory sites present within the ALU region. The concomitant acquisition of the APE1 N-terminal domain in mammals could explain new modulatory functions toward these DNA elements. The observation that specific K residues (K24-27) within this reduced APE1 portion seem to be required for the correct binding of nCaRE-B (unpublished data) nicely fits with

this hypothesis. The zebrafish homologue of APE1, which shares <40% of the N-terminal amino acid sequence with the human protein and lacks two of five K residues in this region, is indeed no longer able to stably bind these nCaRE-B sequences (Figure 2B; Poletto *et al.*, 2013). Similar results were obtained using a human recombinant APE1 mutant protein bearing specific K-to-A multiple substitution at K27/31/32/35, in which the positive charges at the amino acid side chain were removed to mimic a condition similar to that exerted by K acetylation (unpublished data).

The APE1 N-terminal domain seems required for stable binding to the SIRT1 nCaRE-B elements, even though it is not sufficient (Poletto *et al.*, 2013). EMSA analysis, performed with nuclear extracts of HeLa cells expressing the deletion form of APE1, demonstrated that APE1 is part of a multiprotein complex, not the limiting factor in the binding reaction. As speculated by Okazaki and also in later work, the binding affinity observed for the multiprotein complex is higher than that detected when using purified APE1 protein alone (Figure 2). This suggested that other factors are necessary and cooperate with APE1 to fully exert this function, confirming previous observations (Chung *et al.*, 1996; Kuninger *et al.*, 2002). The two subunits of Ku antigen (Ku70 and Ku80) were among the protein factors already described by Chung *et al.* (1996) to be involved in the specific binding of nCaRE-A sequences. Here we demonstrated that Ku70 binding is not exclusively limited to the nCaRE-A elements, since we identified this protein in the complex that binds to the nCaRE-B sequence of SIRT1. The Ku heterodimer is a main component of the nonhomologous end-joining pathway that repairs DNA double-strand breaks (DSBs), which are generally produced upon extensive oxidative and infrared damage to DNA (Lieber, 2010). The peculiar structure of Ku allows recognition and tight binding to DSBs, together with the recruitment of DNA-PKcs and other factors to form the active protein kinase complex DNA-PK that facilitates processing and ligation of broken ends (Walker *et al.*, 2001; Postow, 2011). Its involvement in nCaRE binding is not clear, but emerging evidence suggests a biological role in its noncanonical functions (Adelmant *et al.*, 2012). We envisage that Ku70 association with nCaRE elements could further facilitate APE1 binding, especially after DNA damage, since we observed increased interaction between the two proteins upon oxidative stress (Supplemental Figure S8).

We also better characterized the topology of the APE1-nCaRE complex. The palindromic nature of nCaRE-B sequences was described by Okazaki *et al.* (1991), who suggested the possible involvement of a dimeric nuclear protein in this process. Here we suggest that the SIRT1 nCaRE-B, due to its palindromic sequence, can potentially fold into a cruciform-like structure, and APE1 binding activity toward these elements strongly relies on the secondary conformation adopted by the oligonucleotide, as established for other DNA and RNA substrates (Figure 3B and Supplemental Figure S4; Poletto *et al.*, 2013). Formation of similar cruciform-like structures by palindromic sequences has been described in eukaryotic cells, and their biological consequences have been related to different processes, including regulation of transcriptional events when present in close proximity to gene promoters (Pearson *et al.*, 1994; Shlyakhtenko *et al.*, 2000; Alvarez *et al.*, 2002; Cunningham *et al.*, 2003; Kurahashi *et al.*, 2004). We therefore hypothesize a similar mechanism for SIRT1 transcriptional regulation. However, the requirement of a specific recognition motif cannot be excluded since mutations in the SIRT1 nCaRE-B sequence, determining only a partial disruption of the oligonucleotide secondary structure, did not completely affect APE1-binding activity in vivo (Figure 4B).

We further studied APE1's transcriptional function on the SIRT1 promoter. We found that APE1 is able to bind the nCaRE-B sequence of SIRT1 promoter in vivo and confirmed this through ChIP-Seq analysis (unpublished data). In particular we observed that APE1 positively affects SIRT1 gene transcription. Although APE1 was implicated in the repression of PTH gene transcription in a Ca^{2+}-dependent manner, APE1 overexpression activated the SIRT1 promoter (Figure 4C) apparently through a Ca^{2+}-independent mechanism. This unexpected positive function on the transcription of an nCaRE-containing promoter was also reported in other work, in which the authors suggested that the role of the nCaRE sequences in the context of different promoters and cells conditions could affect nCaRE activity (Bhakat *et al.*, 2003; Fuchs *et al.*, 2003). Of interest, we noticed that the positive effect of APE1 was particularly pronounced during oxidative stress, through its binding to SIRT1 nCaRE-B sequences (Figure 5D). Treatment with H_2O_2 leads to activation of the SIRT1 promoter, which determines an increase of the corresponding transcriptional expression in an APE1-dependent manner. This positive transcriptional effect was also observed when we looked at the expression of other genes that have nCaRE-B elements in their promoters (Figure 5E), thus corroborating the hypothesis of a general mechanism of *SIRT1* gene activation upon DNA damage that involves functional activation of APE1. These findings are in line with data from Yamamori *et al.* (2010) showing that genotoxic insult stimulates SIRT1 expression and therefore its deacetylase activity on APE1 K6/7, favoring APE1 binding to XRCC1. Of interest, these authors sowed that a decrease of APE1 acetylation at later times after oxidative treatment is usually accompanied by SIRT1 up-regulation. Together these findings are in accordance with a model of a positive autoregulatory loop between the two proteins. Thus SIRT1 seems to be involved in a feedback mechanism that shuts off the cellular response mediated by APE1 acetylation (Yamamori *et al.*, 2010). Further proof of APE1 and SIRT1 collaboration comes from the recent demonstration that APE1 stimulates SIRT1 activity in endothelial cells by reducing thiol moieties of cysteine residues in SIRT1, thus protecting endothelium from oxidative stress (Jung *et al.*, 2013).

It has been suggested that DNA oxidation could trigger positive transcription in the context of Myc-mediated transcription through the involvement of BER enzymes, including APE1 (Perillo *et al.*, 2008; Gillespie *et al.*, 2010). Similarly, we speculated that APE1's positive effect on SIRT1 transcription might depend on APE1 endonuclease activity over the nCaRE-B elements present within the SIRT1 promoter. We propose a model in which oxidative-mediated DNA repair and gene transcription are linked (Figure 6). During oxidative stress, DNA oxidation determines the formation of 8-oxodG lesions, which are recognized and processed by enzymes of the BER pathway, including APE1. In our model, the oxidative burst is an early event, essential for formation of a productive transcription initiation complex, which relies on initial recruitment of BER enzymes. The nicks introduced at the chromatin level by APE1 during 8-oxodG removal might promote the local relaxation required for formation of chromatin loops moving the active form of RNA polymerase II closer to the TSS of the gene, as previously recruited by APE1 on the nCaRE-B sequence, turning on the transcription. Our data therefore can be generalized to a regulatory model for all genes that contain nCaRE-B elements. Accordingly, a new hypothesis can be proposed for the molecular activation of specific genes during early response to DNA damage. This model links DNA-repair enzymes and transcriptional regulation effectors and may constitute a general model for explaining the adaptive cell response to oxidative stress involving gene regulation and DNA damage in which APE1 plays a central role.

MATERIALS AND METHODS

Bioinformatic analysis

All human and mouse DNA sequences were retrieved from the Ensembl database, release 56 (www.ensembl.org/), by using a dedicated program written in Perl that collects entries from this archive. A sequence window was selected that contains 5′ genomic DNA of every gene coding for a protein. This region extends from 6000 base pairs upstream and 1000 base pairs downstream of each transcriptional start site. Gene Ontology (GO) annotations were obtained from the Ensembl database by using the data-mining tool BioMart (www.ensembl.org/; Spudich *et al.*, 2007). Human and mouse promoter regions were scanned for significant similarities to nCaRE-B by using Glsearch as program for local alignment (available in the Fasta3 program package; Pearson, 2000). Glsearch was chosen because it calculates an alignment that is global in the query and local in the library. The following nCaRE-B sequences were used as query (Izumi *et al.*, 1996):

Name	Sequence (5′ to 3′)
nCaRE-B (PTH)	TTTTTGAGACAGGGTCTCACTCTG
nCaRE-B1 (APE1)	TTTTGAGACAGTCTCAGCTCTG
nCaRE-B2 (APE1)	TTTTGAGACAGAGTTTCACTCTTG

Alignments were computed with Altschul and Gish's statistical estimates, which are more suitable for searching short query sequences (–z 3 option; Altschul, 1991). We selected only those promoter genes that showed one or more matches for nCaRE-B sequences, allowing up to two mismatches in the case of the human genome and up to three mismatches in the case of the mouse genome; in fact, in the latter case, most alignments were found with three mismatches. From mouse promoter genes that contained nCaRE-B elements, we retrieved only orthologous human/mouse genes, as obtained from the BioMart Ensembl database. For the microarray filter, we cross-checked human genes selected from alignment search with microarray data obtained from the gene expression profile of HeLa cells silenced for APE1 by RNA interference (Vascotto *et al.*, 2009a). The GO filter identified co-regulated human genes, as determined by microarray analysis, studying the prevalence of their GO annotation terms. This analysis was obtained by using a Perl program kindly provided by Corà *et al.* (2004), which performs an exact Fisher's test based on hypergeometric distribution to determine whether the term appears in the set significantly more often than what is expected by chance. This program uses four different entries: 1) a file containing the whole GO database structure (OBO version 1.2; www.geneontology.org/); 2) the list of genes from the whole human genome, 4) a list of all genes with all the GO terms associated with them (as obtained from Ensembl), and 4) the set of genes to be tested. In general, a GO annotation term was considered to be significantly overexpressed when the corresponding *p* value (not corrected for multiple testing) was <1E-4. Phylogenetic footprinting analysis consisted of the last selection from significant data obtained from the GO filter of that gene also present in the mouse orthologous data set.

Gene annotation co-occurrence analysis

Gene identifiers corresponding to the list of 57 putative genes regulated by APE1 were submitted to GeneCodis (http://genecodis.cnb.csic.es/), a Web-based tool for ontological analysis (Carmona-Saez *et al.*, 2007; Nogales-Cadenas *et al.*, 2009; Tabas-Madrid *et al.*, 2012), selecting *Homo sapiens* as the source for annotations and Biological Process as the GO category to perform the gene annotation cooccurrence analysis.

Cell culture and transient transfection experiments

HeLa cells were grown in DMEM (Invitrogen, Carlsbad, CA) supplemented with 10% fetal bovine serum (Euroclone, Milan, Italy), 100 U/ml penicillin, and 10 μg/ml streptomycin sulfate. One day before transfection, cells were seeded in 10-cm plates at a density of 3×10^6 cells/plate. Cells were then transiently transfected with plasmids of interest by using Lipofectamine 2000 reagent (Invitrogen), according to the manufacturer's instructions. Cells were harvested 48 h after transfection.

Inducible APE1 knockdown and generation of APE1 knock-in cell lines

Inducible silencing of endogenous APE1 and reconstitution with mutant proteins in HeLa cell clones was performed as described (Vascotto *et al.*, 2009a,b). For inducible shRNA experiments, doxycycline (1 μg/ml) (Sigma-Aldrich, St. Louis, MO) was added to the cell culture medium, and cells were grown for 10 d.

Plasmids and expression of recombinant proteins

Plasmid containing the human SIRT1 promoter was kindly provided by K. Irani, University of Pittsburgh (Pittsburgh, PA). This plasmid consists of a fragment of the human SIRT1 promoter (–1266 to +137 relative to transcription start site) cloned into the pGL4.1 firefly luciferase reporter vector (Promega, Madison, WI; Yamamori *et al.*, 2010). The human SIRT1 promoter carrying the mutation at nCaRE-B sequences was generated with a Site-Directed Mutagenesis Kit (Stratagene, Santa Clara, CA), using the primers SIRT1-B mut, forward, 5′-TCATCTAGGTTTTATTTATATATTTTTTTGCTAAGGAGCGTCGCTCTTGCTGCCCAGGCTGGTGTG-3′, and SIRT1-B mut, reverse, 5′-CACACCAGCCTGGGCAGCAAGAGCGACGCTCCTTAGCAAAAAAATATATAAATAAAACCTAGATGA-3′.

Expression and purification of recombinant proteins from *E. coli* were performed as previously described (Vascotto *et al.*, 2009b; Fantini *et al.*, 2010).

Antibodies and Western blot analysis

For Western blot analyses, the indicated amounts of cell extracts were resolved in 10% SDS–PAGE and transferred to nitrocellulose membranes (Schleicher & Schuell, BioScience, Dassel, Germany). Membranes were blocked with 5% (wt/vol) nonfat dry milk in phosphate-buffered saline containing 0.1% (vol/vol) Tween 20 and probed with monoclonal anti-FLAG antibody (Sigma), monoclonal anti-APE1 antibody (Vascotto *et al.*, 2009a), monoclonal anti-Ku70 (sc-12729; Santa Cruz Biotechnology, Santa Cruz, CA), monoclonal anti–RNA polymerase II (Abcam, Cambridge, MA), monoclonal anti-SIRT1 (Abcam), monoclonal anti-p32 (Santa Cruz Biotechnology), and polyclonal anti-p53(acetyl K382) (Abcam). Blots were developed by using the enhanced chemiluminescence procedure (GE Healthcare, Piscataway, NJ) or Western Lightning Ultra (Perkin Elmer, Waltham, MA). Data normalization was performed by using a monoclonal anti-tubulin antibody (Sigma). Blots were quantified by using a Chemidoc XRS video densitometer (Bio-Rad, Hercules, CA).

Alignments and secondary structure predictions

Multiple alignments were performed using CLUSTALW2 (www.ebi.ac.uk/Tools/msa/clustalw2/).

Potential secondary structures for SIRT1-B nCaRE-B oligonucleotide were determined by using the mfold Web Server program (http://mfold.rna.albany.edu/?q=mfold). Structure predictions were run by setting the program parameters as close as possible to the conditions used in binding assays (37°C and 50 mM monovalent cation).

Chromatin immunoprecipitation analysis

ChIP assay was performed by using a protocol described previously (Lirussi *et al.*, 2012) on HeLa cells cotransfected with hSIRT1 promoter and APE1-FLAG–tagged expressing vectors.

Preparation of nuclear cell extracts

Nuclear protein extracts were prepared as described earlier (Ziel *et al.*, 2005).

Electrophoretic mobility shift assay analysis

APE1 binding to nucleic acids was assessed as already described (Fantini *et al.*, 2010), with some modifications. Briefly, the indicated amount of recombinant proteins or 5 µg of the reported nuclear extract was incubated at 37°C for 15 min with 250 pmol of unlabeled poly(dT) or 250 ng of sonicated salmon sperm DNA (Sigma). A 2.5-pmol amount of ^{32}P-labeled, ds oligonucleotides was then added, incubated for additional 15 min, and further separated onto a native 6% wt/vol polyacrylamide gel at 150 V for 4 h. When performing supershift assays, 5 µl of monoclonal anti-APE1 (Vascotto *et al.*, 2009a), anti-Ku-70 (sc-12729; Santa Cruz Biotechnology) or anti-P2Y6 (Alomone Labs, Jerusalem, Israel) was preincubated with HeLa nuclear extract from APE1^{SCR-1} clone at 4°C for 3 h.

Oligonucleotides used for EMSA were the following:

Name	Sequence (5′ to 3′)
nCaRE-B SIRT1-A	Forward TTTTTGAGACAGAGTTTCACTCTTG
	Reverse CAAGAGTGAAACTCTGTCTCAAAAA
nCaRE-B SIRT1-B	Forward TTTTTGAGACGGAGTTTCGCTCTTG
	Reverse CAAGAGCGAAACTCCGTCTCAAAAA
Poly(dT)	Forward TTTTTTTTTTTTTTTTTTTTTTTT

T7 endonuclease I footprinting

Footprinting analysis on the SIRT1 nCaRE-B sequence was conducted using T7 endonuclease I. Briefly, 5′-^{32}P-end-labeled nCaRE-B SIRT1-B was digested with 5 U of T7 endonuclease I at 37°C for 1 h and then incubated with 35 pmol of APE1 recombinant protein for 15 min at 37°C. The reaction mixtures were then loaded and separated for 2 h onto a denaturing 8 M urea sequencing gel. After separation, the gel was incubated for 30 min in a 10% methanol and 10% acetic acid solution and then wrapped in Saran wrap and exposed to film for autoradiography.

Determination of AP endonuclease activity

Determination of APE1 AP endonuclease activity was performed using an oligonucleotide cleavage assay, as described previously (Vascotto *et al.*, 2009b). The indicated amount of recombinant APE1 protein was incubated with a 5′-^{32}P-end-labeled 26-mer ds oligonucleotide containing a single THF artificial AP site at position 14, which is cleaved to a 14-mer in the presence of AP endonuclease activity. Alternatively, a 5′-^{32}P-end-labeled ds SIRT1-B nCaRE-B oligonucleotide or a 5′-^{32}P-end-labeled ds nCaRE SIRT1-B oligonucleotide, bearing a single THF residue at position 12 (bold) 5′-TTTTTGAGACG**G**AGTTTCGCTCTTG-3′ (Integrated DNA Technologies, Munich, Germany), was used. The conversion of the radiolabeled THF-containing oligonucleotide substrate (S) to the shorter product (P) was evaluated on a denaturing 20% polyacrylamide gel.

Reporter assays

For reporter assay experiments, we used a human SIRT1 promoter plasmid allowing for promoter activity measurements upon luciferase assay, as already described (Yamamori *et al.*, 2010). To this purpose, 2.5×10^4 HeLa cells were seeded in a 96-well plate and cotransfected with 15 ng of human SIRT1 promoter, 0.3 ng of a constitutive *Renilla* reporter plasmid, and 75 ng of a vector expressing FLAG-tagged APE1 protein. When performing luciferase assays upon H_2O_2, cells were challenged with increasing amounts of H_2O_2 in serum-free medium for 1 h at 37°C, and then firefly and *Renilla* luciferase activities were measured 24 h after the treatment by using the Dual-Glo Luciferase assay system (Promega), according to manufacturer's recommendations. Firefly activity was normalized to *Renilla* activity to correct for differences in transfection efficiency. Results are from triplicate experiments.

Quantitative PCR

Total RNA from cell lines was extracted with the SV Total RNA isolation System kit (Promega). One microgram of total RNA was reverse transcribed using the iScript cDNA synthesis kit (Bio-Rad), according to the manufacturer's instructions. Quantitative reverse-transcription PCR was performed with a CFX96 Real-Time System (Bio-Rad) using iQ SYBR Green Supermix (Bio-Rad). Primer sequences for human SIRT1 were those reported in Yamamori *et al.* (2010). Human glyceraldehyde-3-phosphate dehydrogenase was used as internal control; sense, 5′-CCCTTCATTGACCTCAACTACATG-3′; antisense, 5′-TGGGATTTCCATTGATGACAAGC-3′.

Surface plasmon resonance analysis

Real-time binding assays were performed on a Biacore 3000 SPR instrument (GE Healthcare). Biotinylated ds oligonucleotides were immobilized on an SA-chip at the desired level, as a result of their injection at a concentration of 500 nM in HBS (20 mM 4-(2-hydroxyethyl)-1-piperazineethanesulfonic acid, 150 mM NaCl, 3.4 mM EDTA, and 0.005% [vol/vol] P20 surfactant, 0.1 mM Tris(2-carboxyethyl)phosphine) at 10 µl/min as flow rate. Flow cell 2 contained 100 RU of poly(dT); flow cells 3 and 4 contained 77 and 60 RU of SIRT1-B nCaRE-B and SIRT1-B nCaRE-B mutated, respectively; and flow cell 1 (with streptavidin) was left blank to be used as a reference surface. APE1 and its deletion mutant APE1$^{N\Delta 33}$ were serially diluted in running buffer to the indicated concentrations and injected at a flow rate of 20 µl/min for 4.5 min at 20°C. Disruption of any complex that remained bound after a 3-min dissociation was achieved by using an injection of 1 M NaCl at 20 µl/min for 1 min. The BIAevaluation analysis package, version 4.1 (GE Healthcare), was used to subtract blank signal and evaluate kinetic and dissociation constants. Kinetic parameters were estimated assuming a 1:1 binding model and using Evaluation, version 7 4.1 (GE Healthcare). An affinity steady-state model was applied to fit the RUmax data versus protein concentrations, and fitting was performed with Prism, version 4.00 (GraphPad, San Diego, CA; Fantini *et al.*, 2010).

Limited proteolysis

Suitable experimental conditions were chosen by testing proteolysis with different enzyme/substrate values; no preventive removal of DNA was performed. Thus limited proteolysis experiments on recombinant APE1 were conducted in 50 mM NH_4HCO_3, pH 7.5 (reaction buffer), at 37°C by using an enzyme-to-substrate ratio ranging from 1:500 to 1:5000 (wt/wt). Three identical aliquots of APE1 (500 pmol) were combined with reaction buffer or DNA nCaRE-B ds oligonucleotides (PTH or nCaRE SIRT1-B; 5:1 mol DNA/protein) dissolved in reaction buffer to generate samples (100-µl final volume each), which were incubated for 15 min at 37°C before protease addition. After digestion started, the extent of proteolysis was monitored on a time-course basis by sampling 10 µl of the mixture at time intervals ranging from 5 to 120 min. Reaction samples were immediately quenched with 5% formic acid and then frozen in dry ice before liquid chromatography–electrospray ionization–mass spectrometry (LC-ESI-MS) analysis.

LC-ESI-MS analysis

APE1 digests were analyzed with a Q-TOF Premier mass spectrometer (Waters, Milford, MA) equipped with a nanospray source. Peptide mixtures were separated on an Atlantis C_{18} column (100 µm × 100 mm, 3 µm), using a linear gradient ranging from 30 to 60% acetonitrile in 1% formic acid, over a period of 50 min at a flow rate of 800 nl/min. Spectra were acquired in the m/z = 650–2500 range. Data were processed by using MassLynx software (Waters). Mass calibration was performed using multiply charged ions from horse heart myoglobin (Sigma). Depending on polypeptide size, mass values are reported as monoisotopic or average values. Observed mass values are assigned to specific polypeptides by using Paws software (Proteometrics, New York, NY), based on APE1 sequence and selectivity of the protease used for protein digestion.

Statistical analysis

Statistical analyses were performed by using the Excel (Microsoft, Redmond, WA) data analysis program for Student's t test analysis. $p < 0.05$ was considered as statistically significant.

ACKNOWLEDGMENTS

We thank Mattia Poletto for helpful suggestions during recombinant protein purification and critical comments on the manuscript. This work was supported by grants from the Italian Association for Cancer Research (IG10269 and IG14038) and the Ministry of Education, Universities and Research, Italy (FIRB_RBRN07BMCT and PRIN2008_CCPKRP_003 to G.T.; FIRB_ RBNE08YFN3_003 and PRIN2008_CCPKRP_002 to A.S.). This project was funded under the Cross-Border Cooperation Program Italy-Slovenia 2007–2013 by the European Regional Development Fund and national funds.

REFERENCES

Adelmant G *et al.* (2012). DNA ends alter the molecular composition and localization of Ku multicomponent complexes. Mol Cell Proteomics 11, 411–421.

Altschul SF (1991). Amino acid substitution matrices from an information theoretic perspective. J Mol Biol 219, 555–565.

Alvarez D, Novac O, Callejo M, Ruiz MT, Price GB, Zannis-Hadjopoulos M (2002). 14-3-3sigma is a cruciform DNA binding protein and associates in vivo with origins of DNA replication. J Cell Biochem 87, 194–207.

Amente S, Bertoni A, Morano A, Lania L, Avvedimento EV, Majello B (2010). LSD1-mediated demethylation of histone H3 lysine 4 triggers Myc-induced transcription. Oncogene 29, 3691–3702.

Barnes T, Kim W, Mantha AK, Kim S, Izumi T, Mitra S, Lee CH (2009). Identification of Apurinic/apyrimidinic endonuclease 1 (APE1) as the endoribonuclease that cleaves c-myc mRNA. Nucleic Acids Res 37, 3946–3958.

Beernink PT, Segelke BW, Hadi MZ, Erzberger JP, Wilson DM 3rd, Rupp B (2001). Two divalent metal ions in the active site of a new crystal form of human apurinic/apyrimidinic endonuclease, Ape1: implications for the catalytic mechanism. J Mol Biol 307, 1023–1034.

Berquist BR, McNeill DR, Wilson DM (2008). Characterization of abasic endonuclease activity of human Ape1 on alternative substrates, as well as effects of ATP and sequence context on AP site incision. J Mol Biol 379, 17–27.

Bhakat KK, Izumi T, Yang S, Hazra TK, Mitra S (2003). Role of acetylated human AP-endonuclease (APE1/Ref-1) in regulation of the parathyroid hormone gene. EMBO J 22, 6299–6309.

Bhattacharyya A, Chattopadhyay R, Burnette BR, Cross JV, Mitra S, Ernst PB, Bhakat KK, Crowe SE (2009). Acetylation of apurinic/apyrimidinic endonuclease-1 regulates *Helicobacter pylori*-mediated gastric epithelial cell apoptosis. Gastroenterology 136, 2258–2269.

Carmona-Saez P, Chagoyen M, Tirado F, Carazo JM, Pascual-Montano A (2007). GENECODIS: a Web-based tool for finding significant concurrent annotations in gene lists. Genome Biol 8, R3.

Chen J, Stubbe J (2005). Bleomycins: towards better therapeutics. Nat Rev Cancer 5, 102–112.

Chung U *et al.* (1996). The interaction between Ku antigen and REF1 protein mediates negative gene regulation by extracellular calcium. J Biol Chem 271, 8593–8598.

Cohen HY, Miller C, Bitterman KJ, Wall NR, Hekking B, Kessler B, Howitz KT, Gorospe M, de Cabo R, Sinclair DA (2004). Calorie restriction promotes mammalian cell survival by inducing the SIRT1 deacetylase. Science 305, 390–392.

Corà D, Cunto FD, Provero P, Silengo L, Caselle M (2004). Computational identification of transcription factor binding sites by functional analysis of sets of genes sharing overrepresented upstream motifs. BMC Bioinformatics 5, 57.

Cunningham LA, Coté AG, Cam-Ozdemir C, Lewis SM (2003). Rapid, stabilizing palindrome rearrangements in somatic cells by the center-break mechanism. Mol Cell Biol 23, 8740–8750.

Déclais A, Fogg JM, Freeman ADJ, Coste F, Hadden JM, Phillips SEV, Lilley DMJ (2003). The complex between a four-way DNA junction and T7 endonuclease I. EMBO J 22, 1398–1409.

Deininger PL, Jolly DJ, Rubin CM, Friedmann T, Schmid CW (1981). Base sequence studies of 300 nucleotide renatured repeated human DNA clones. J Mol Biol 151, 17–33.

Demple B, Herman T, Chen DS (1991). Cloning and expression of APE, the cDNA encoding the major human apurinic endonuclease: definition of a family of DNA repair enzymes. Proc Natl Acad Sci USA 88, 11450–11454.

Fan J, Matsumoto Y, Wilson DM 3rd (2006). Nucleotide sequence and DNA secondary structure, as well as replication protein A, modulate the single-stranded abasic endonuclease activity of APE1. J Biol Chem 281, 3889–3898.

Fantini D *et al.* (2010). Critical lysine residues within the overlooked N-terminal domain of human APE1 regulate its biological functions. Nucleic Acids Res 38, 8239–8256.

Francia S, Michelini F, Saxena A, Tang D, de Hoon M, Anelli V, Mione M, Carninci P, d'Adda di Fagagna F (2012). Site-specific DICER and DROSHA RNA products control the DNA-damage response. Nature 488, 231–235.

Fuchs S, Philippe J, Corvol P, Pinet F (2003). Implication of Ref-1 in the repression of renin gene transcription by intracellular calcium. J Hypertens 21, 327–335.

Fung H, Demple B (2005). A vital role for Ape1/Ref1 protein in repairing spontaneous DNA damage in human cells. Mol Cell 17, 463–470.

Gaiddon C, Moorthy NC, Prives C (1999). Ref-1 regulates the transactivation and pro-apoptotic functions of p53 in vivo. EMBO J 18, 5609–5621.

Georgiadis MM, Luo M, Gaur RK, Delaplane S, Li X, Kelley MR (2008). Evolution of the redox function in mammalian apurinic/apyrimidinic endonuclease. Mutat Res 643, 54–63.

Gillespie MN, Pastukh VM, Ruchko MV (2010). Controlled DNA "damage" and repair in hypoxic signaling. Respir Physiol Neurobiol 174, 244–251.

Gorman MA, Morera S, Rothwell DG, Fortelle EDL, Mol CD, Tainer JA, Hickson ID, Freemont PS (1997). The crystal structure of the human DNA repair endonuclease HAP1 suggests the recognition of extra-helical deoxyribose at DNA abasic sites. EMBO J 16, 6548–6558.

Gorospe M, de Cabo R (2008). AsSIRTing the DNA damage response. Trends Cell Biol 18, 77–83.

Huang RP, Adamson ED (1993). Characterization of the DNA-binding properties of the early growth response-1 (Egr-1) transcription factor: evidence for modulation by a redox mechanism. DNA Cell Biol 12, 265–273.
Izumi T, Henner WD, Mitra S (1996). Negative regulation of the major human AP-endonuclease, a multifunctional protein. Biochemistry 35, 14679–14683.
Izumi T, Malecki J, Chaudhry MA, Weinfeld M, Hill JH, Lee JC, Mitra S (1999). Intragenic suppression of an active site mutation in the human apurinic/apyrimidinic endonuclease. J Mol Biol 287, 47–57.
Jung S, Kim C, Kim Y, Naqvi A, Yamamori T, Kumar S, Kumar A, Irani K (2013). Redox factor-1 activates endothelial SIRTUIN1 through reduction of conserved cysteine sulfhydryls in its deacetylase domain. PLoS One 8, e65415.
Kim E, Um S (2008). SIRT1: roles in aging and cancer. BMB Rep 41, 751–756.
Krayev AS, Kramerov DA, Skryabin KG, Ryskov AP, Bayev AA, Georgiev GP (1980). The nucleotide sequence of the ubiquitous repetitive DNA sequence B1 complementary to the most abundant class of mouse fold-back RNA. Nucleic Acids Res 8, 1201–1215.
Kriegs JO, Churakov G, Jurka J, Brosius J, Schmitz J (2007). Evolutionary history of 7SL RNA-derived SINEs in Supraprimates. Trends Genet 23, 158–161.
Kuninger DT, Izumi T, Papaconstantinou J, Mitra S (2002). Human AP-endonuclease 1 and hnRNP-L interact with a nCaRE-like repressor element in the AP-endonuclease 1 promoter. Nucleic Acids Res 30, 823–829.
Kurahashi H, Inagaki H, Yamada K, Ohye T, Taniguchi M, Emanuel BS, Toda T (2004). Cruciform DNA structure underlies the etiology for palindrome-mediated human chromosomal translocations. J Biol Chem 279, 35377–35383.
Lieber MR (2010). The mechanism of double-strand DNA break repair by the nonhomologous DNA end-joining pathway. Annu Rev Biochem 79, 181–211.
Lirussi L *et al.* (2012). Nucleolar accumulation of APE1 depends on charged lysine residues that undergo acetylation upon genotoxic stress and modulate its BER activity in cells. Mol Biol Cell 23, 4079–4096.
McHaffie GS, Ralston SH (1995). Origin of a negative calcium response element in an ALU-repeat: implications for regulation of gene expression by extracellular calcium. Bone 17, 11–14.
Murphy WJ *et al.* (2001). Resolution of the early placental mammal radiation using Bayesian phylogenetics. Science 294, 2348–2351.
Nishihara H, Terai Y, Okada N (2002). Characterization of novel Alu- and tRNA-related SINEs from the tree shrew and evolutionary implications of their origins. Mol Biol Evol 19, 1964–1972.
Nogales-Cadenas R, Carmona-Saez P, Vazquez M, Vicente C, Yang X, Tirado F, Carazo JM, Pascual-Montano A (2009). GeneCodis: interpreting gene lists through enrichment analysis and integration of diverse biological information. Nucleic Acids Res 37, W317–322.
Okazaki T, Ando K, Igarashi T, Ogata E, Fujita T (1992). Conserved mechanism of negative gene regulation by extracellular calcium. Parathyroid hormone gene versus atrial natriuretic polypeptide gene. J Clin Invest 89, 1268–1273.
Okazaki T, Zajac JD, Igarashi T, Ogata E, Kronenberg HM (1991). Negative regulatory elements in the human parathyroid hormone gene. J Biol Chem 266, 21903–21910.
Parkinson MJ, Lilley DM (1997). The junction-resolving enzyme T7 endonuclease I: quaternary structure and interaction with DNA. J Mol Biol 270, 169–178.
Pearson CE, Ruiz MT, Price GB, Zannis-Hadjopoulos M (1994). Cruciform DNA binding protein in HeLa cell extracts. Biochemistry 33, 14185–14196.
Pearson WR (2000). Flexible sequence similarity searching with the FASTA3 program package. Methods Mol Biol 132, 185–219.
Perillo B, Ombra MN, Bertoni A, Cuozzo C, Sacchetti S, Sasso A, Chiariotti L, Malorni A, Abbondanza C, Avvedimento EV (2008). DNA oxidation as triggered by H3K9me2 demethylation drives estrogen-induced gene expression. Science 319, 202–206.
Poletto M, Vascotto C, Scognamiglio PL, Lirussi L, Marasco D, Tell G (2013). Role of the unstructured N-terminal domain of the human apurinic/apyrimidinic endonuclease 1 (hAPE1) in the modulation of its interaction with nucleic acids and nucleophosmin (NPM1). Biochem J 452, 545–557.
Postow L (2011). Destroying the ring: freeing DNA from Ku with ubiquitin. FEBS Lett 585, 2876–2882.
Renzone G, Vitale RM, Scaloni A, Rossi M, Amodeo P, Guagliardi A (2007). Structural characterization of the functional regions in the archaeal protein Sso7d. Proteins 67, 189–197.
Robson CN, Hickson ID (1991). Isolation of cDNA clones encoding a human apurinic/apyrimidinic endonuclease that corrects DNA repair and mutagenesis defects in E. coli xth (exonuclease III) mutants. Nucleic Acids Res 19, 5519–5523.
Scaloni A, Miraglia N, Orrù S, Amodeo P, Motta A, Marino G, Pucci P (1998). Topology of the calmodulin-melittin complex. J Mol Biol 277, 945–958.
Scaloni A, Monti M, Acquaviva R, Tell G, Damante G, Formisano S, Pucci P (1999). Topology of the thyroid transcription factor 1 homeodomain-DNA complex. Biochemistry 38, 64–72.
Shankar R, Grover D, Brahmachari SK, Mukerji M (2004). Evolution and distribution of RNA polymerase II regulatory sites from RNA polymerase III dependant mobile Alu elements. BMC Evol Biol 4, 4–37.
Shlyakhtenko LS, Hsieh P, Grigoriev M, Potaman VN, Sinden RR, Lyubchenko YL (2000). A cruciform structural transition provides a molecular switch for chromosome structure and dynamics. J Mol Biol 296, 1169–1173.
Spudich G, Fernández-Suárez XM, Birney E (2007). Genome browsing with Ensembl: a practical overview. Brief Funct Genomic Proteomic 6, 202–219.
Tabas-Madrid D, Nogales-Cadenas R, Pascual-Montano A (2012). GeneCodis3: a non-redundant and modular enrichment analysis tool for functional genomics. Nucleic Acids Res 40, W478–483.
Tell G, Damante G, Caldwell D, Kelley MR (2005). The intracellular localization of APE1/Ref-1: more than a passive phenomenon? Antioxid Redox Signal 7, 367–384.
Tell G, Fantini D, Quadrifoglio F (2010a). Understanding different functions of mammalian AP endonuclease (APE1) as a promising tool for cancer treatment. Cell Mol Life Sci 67, 3589–3608.
Tell G, Pellizzari L, Cimarosti D, Pucillo C, Damante G (1998). Ref-1 controls pax-8 DNA-binding activity. Biochem Biophys Res Commun 252, 178–183.
Tell G, Quadrifoglio F, Tiribelli C, Kelley MR (2009). The many functions of APE1/Ref-1: not only a DNA repair enzyme. Antioxid Redox Signal 11, 601–620.
Tell G, Wilson DM3rd, Lee CH (2010b). Intrusion of a DNA repair protein in the RNome world: is this the beginning of a new era? Mol Cell Biol 30, 366–371.
Vascotto C *et al.* (2009a). Genome-wide analysis and proteomic studies reveal APE1/Ref-1 multifunctional role in mammalian cells. Proteomics 9, 1058–1074.
Vascotto C *et al.* (2009b). APE1/Ref-1 interacts with NPM1 within nucleoli and plays a role in the rRNA quality control process. Mol Cell Biol 29, 1834–1854.
Vaziri H, Dessain SK, Ng Eaton E, Imai SI, Frye RA, Pandita TK, Guarente L, Weinberg RA (2001). hSIR2(SIRT1) functions as an NAD-dependent p53 deacetylase. Cell 107, 149–159.
Walker JR, Corpina RA, Goldberg J (2001). Structure of the Ku heterodimer bound to DNA and its implications for double-strand break repair. Nature 412, 607–614.
Wilson DM 3rd, Simeonov A (2010). Small molecule inhibitors of DNA repair nuclease activities of APE1. Cell Mol Life Sci 67, 3621–3631.
Xanthoudakis S, Curran T (1992). Identification and characterization of Ref-1, a nuclear protein that facilitates AP-1 DNA-binding activity. EMBO J 11, 653–665.
Xanthoudakis S, Smeyne RJ, Wallace JD, Curran T (1996). The redox/DNA repair protein, Ref-1, is essential for early embryonic development in mice. Proc Natl Acad Sci USA 93, 8919–8923.
Yamamori T, DeRicco J, Naqvi A, Hoffman TA, Mattagajasingh I, Kasuno K, Jung S, Kim C, Irani K (2010). SIRT1 deacetylates APE1 and regulates cellular base excision repair. Nucleic Acids Res 38, 832–845.
Yamamoto M, Igarashi T, Muramatsu M, Fukagawa M, Motokura T, Ogata E (1989). Hypocalcemia increases and hypercalcemia decreases the steady-state level of parathyroid hormone messenger RNA in the rat. J Clin Invest 83, 1053–1056.
Ziel KA, Grishko V, Campbell CC, Breit JF, Wilson GL, Gillespie MN (2005). Oxidants in signal transduction: impact on DNA integrity and gene expression. FASEB J 19, 387–394.

ANTIOXIDANTS & REDOX SIGNALING
Volume 20, Number 4, 2014

DOI: 10.1089/ars.2013.5491

Discoveries

FORUM REVIEW ARTICLE

Emerging Roles of the Nucleolus in Regulating the DNA Damage Response: The Noncanonical DNA Repair Enzyme APE1/Ref-1 as a Paradigmatical Example

Giulia Antoniali,* Lisa Lirussi,* Mattia Poletto,* and Gianluca Tell

Abstract

Significance: An emerging concept in DNA repair mechanisms is the evidence that some key enzymes, besides their role in the maintenance of genome stability, display also unexpected noncanonical functions associated with RNA metabolism in specific subcellular districts (*e.g.,* nucleoli). During the evolution of these key enzymes, the acquisition of unfolded domains significantly amplified the possibility to interact with different partners and substrates, possibly explaining their phylogenetic gain of functions. ***Recent Advances:*** After nucleolar stress or DNA damage, many DNA repair proteins can freely relocalize from nucleoli to the nucleoplasm. This process may represent a surveillance mechanism to monitor the synthesis and correct assembly of ribosomal units affecting cell cycle progression or inducing p53-mediated apoptosis or senescence. ***Critical Issues:*** A paradigm for this kind of regulation is represented by some enzymes of the DNA base excision repair (BER) pathway, such as apurinic/apyrimidinic endonuclease 1 (APE1). In this review, the role of the nucleolus and the noncanonical functions of the APE1 protein are discussed in light of their possible implications in human pathologies. ***Future Directions:*** A productive cross-talk between DNA repair enzymes and proteins involved in RNA metabolism seems reasonable as the nucleolus is emerging as a dynamic functional hub that coordinates cell growth arrest and DNA repair mechanisms. These findings will drive further analyses on other BER proteins and might imply that nucleic acid processing enzymes are more versatile than originally thought having evolved DNA-targeted functions after a previous life in the early RNA world. *Antioxid. Redox Signal.* 20, 621–639.

Overview on RNA Oxidative Damages, a Glimpse on Human Pathologies

An emerging body of evidence links DNA repair proteins to specific aspects of RNA metabolism associated with quality control processes toward damaged RNA molecules (*e.g.,* oxidized or abasic RNA) (Fig. 1). Due to its intrinsic nature (*i.e.,* mostly single-stranded and with bases not protected by hydrogen bonding or binding to specific proteins) and to its relatively higher amount, RNA may be more susceptible to oxidative insults than DNA (107). Not only 8-hydroxyguanosine (8-OHG) but also 5-hydroxycytidine, 5-hydroxyuridine, and 8-hydroxyadenosine have been identified in oxidized RNA (160). While oxidative damage to DNA is essentially repaired through the base excision repair (BER) pathway, no evidences of similar repair processes have been described for RNA molecules, even though some BER proteins recently entered the arena of the RNome world (138). If not repaired, damage to RNA molecules may lead to ribosomal dysfunctions and erroneous translation; thus, significantly affecting the overall protein synthesis mechanism (38, 135). Moreover, RNA damage has been shown to cause cell cycle arrest and cell death with or without the contribution of p53 and inhibition of protein synthesis (11). Oxidative RNA modifications can occur not only in protein-coding RNAs, but also in noncoding RNAs that recently have been revealed to

Department of Medical and Biological Sciences, University of Udine, Udine, Italy.
*These authors equally contributed to this work.

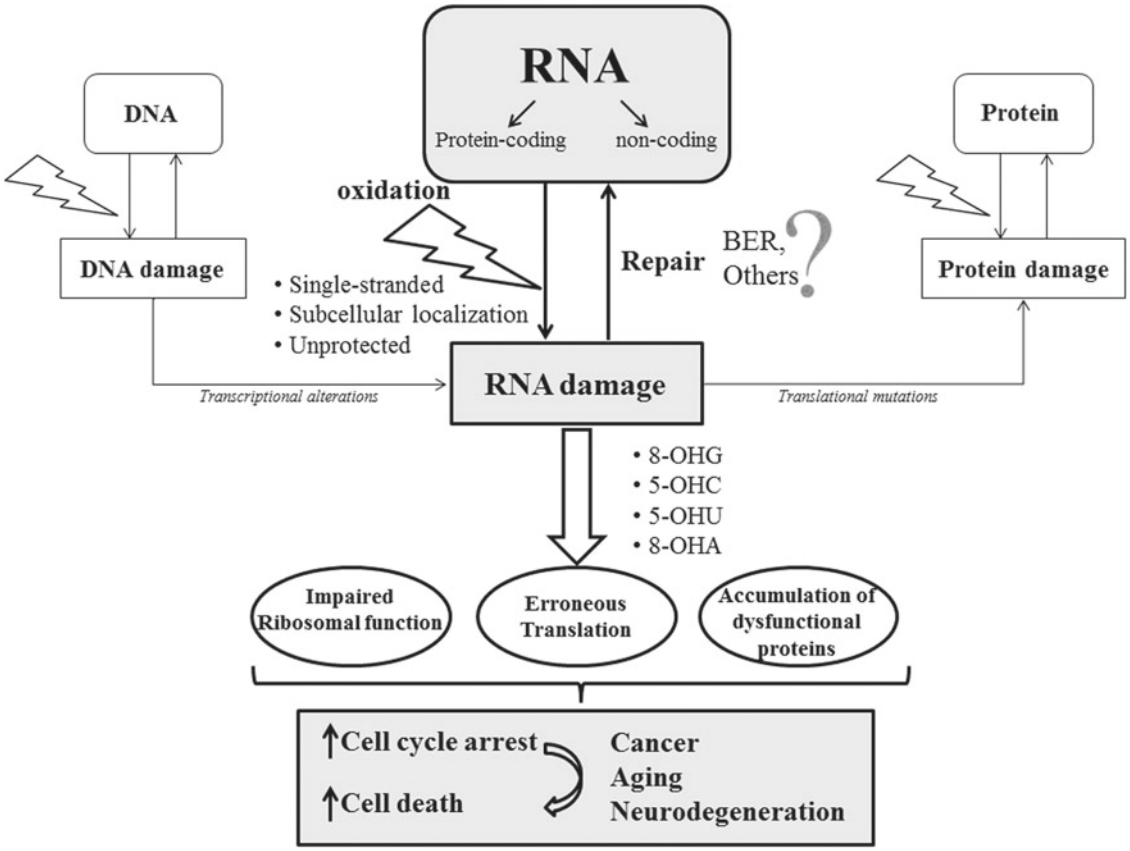

FIG. 1. Potential consequences of unrepaired RNA damage. RNA intrinsic nature renders it more susceptible to damage, such as oxidation. The molecular and surveillance mechanisms that cope with RNA damage are still poorly understood. If unrepaired, aberrant RNA may give rise to translation of defective and toxic protein aggregates that eventually leads to cell cycle arrest and consequently to cell death. These molecular processes have been associated with cancer onset, aging, and neurodegeneration.

contribute to the complexity of the mammalian brain (109). It has been hypothesized that RNA oxidation, causing aberrant expression of microRNAs and proteins, may initiate inappropriate cell fate pathways. Such sublethal damage to cells, while less toxic than genomic mutations and not inheritable, might be associated with underlying mechanisms of degeneration, such as age-associated neurodegeneration.

Currently, little is known about how cells may cope with damaged RNA, either modified or oxidized, but it is clear that such RNA can impair protein synthesis; thus, affecting cell function and viability. Therefore, specific surveillance mechanisms are needed to remove damaged molecules from the RNA pool to guarantee the biological integrity of cells. The idea that quality control mechanisms might exist to repair RNA was put forward after the identification of the biochemical activities of the mammalian AlkB homologs. In particular, it was discovered that AlkB (from *Escherichia coli*) and the human homolog hABH3, besides being able to directly reverse alkylation damage on DNA bases, were able to demethylate damaged bases on RNA; thus, playing a key role in the repair of specific RNA lesions (1, 111). While repair mechanisms have been demonstrated for alkylated RNA, the existence of such cleansing activities has not yet been identified for oxidatively damaged RNA. However, their existence appears unlikely, in the absence of direct reversal strategies, due to the lack of a template for accurate repair, as happens in the case of double-stranded DNA. The observation that under oxidative stress RNA modifications can occur up to a 10–20-fold higher extent than DNA (88), raises the question of how oxidized RNA may be specifically removed or repaired. The recent findings by Berquist *et al.* (12), Barnes *et al.* (7), and Vascotto *et al.* (149) highlight a novel "moonlighting" role for the repair apurinic/apyrimidinic (AP) endonuclease 1 (APE1) in RNA metabolism, both as a possible "cleansing" factor for damaged abasic RNA and as a regulator of *c-myc* gene expression through mRNA decay. In agreement with this hypothesis, a significant reduction in the protein synthesis rate occurs upon silencing of APE1 expression (149). Enzymatic (*e.g.*, by specific N-ribohydrolases, including the toxin ricin) (126), besides spontaneous (91), generation of abasic sites occurs upon ribosomal RNA (rRNA) oxidation. A role for the Y box binding protein 1 (YB-1) in recognizing 8-OHG sites has also been hypothesized (56), but no specific enzymatic mechanisms that can remove the oxidized base have been described yet. The accumulation of the 8-OHG substrates, which occurs upon silencing of APE1 expression (149), may thus, be explained under the assumption that enzymatic removal of oxidized RNA bases represents the limiting step in the process. According to this model, as already hypothesized for DNA substrates, APE1 could act through stimulation of a yet unknown glycosylase activity, by allowing a faster turnover (152). The APE1 interaction with RNA and with proteins

involved in ribosome assembly (*i.e.,* RSSA, RLA0) and RNA maturation (*i.e.,* PRP19) within the cytoplasm (149), could also represent a molecular proof of concept for the "extranuclear" functions of this noncanonical DNA repair enzyme. The RNA-mediated association with some of the APE1 protein partners would reinforce the view of APE1 as an essential factor in the RNA quality control process and may also explain the cytoplasmic accumulation of APE1 observed in a number of tumoral cell types (136, 137). An age-associated increase in oxidative nucleic acids damage, predominantly to RNA, has been recently highlighted in neurons from human and rodent brains; this phenomenon may play a fundamental role in the development of age-associated neurodegeneration (109). Oxidative damage to RNA molecules, both coding for proteins (mRNA) or performing translation (rRNA and tRNA), has been recently associated with the occurrence of neurodegenerative diseases, such as Alzheimer's disease (AD), Parkinson disease (PD), dementia with Lewy bodies, and amyotrophic lateral sclerosis (107) and its impact in cancer development cannot be excluded, at present (11). Remarkably, studies performed on either human samples or experimental models, show that RNA oxidation is a characteristic of aging neurons. Its prominent occurrence in vulnerable neurons at early stage of age-associated neurodegenerative disorders indicates that RNA oxidation actively contributes to the development of the degeneration. Therefore, all the hypotheses concerning the involvement of APE1 in the development of such pathologies should be re-interpreted in light of these findings. The role played by APE1 in RNA-related processes needs further investigations, since its ability to recognize and cleave the RNA abasic sites (12, 42, 89, 138, 149) is compatible with a leading role in the early stages of the RNA quality control process. Additional studies aiming at the understanding the mechanisms related to oxidative RNA damage processing and their consequences may provide significant insights into the pathogenesis of neurodegenerative disorders, leading to improvements in the current therapeutic strategies.

The vast majority of cellular RNA is transcribed, assembled, and processed within nucleoli. These subcellular compartments appear to be perfect sensors for cellular stress, as they integrate RNA damage and growth control with signals to the DNA repair machineries. The following paragraphs will describe the emerging dynamics roles of this organelle in regulating the trafficking of DNA repair proteins during genotoxic damage.

Structure, Composition, and Classical Functions of the Nucleolus

The nucleolus is considered the ribosome factory of eukaryotic cells (18, 62) in which synthesis, maturation, and processing of rRNA, as well as assembly of rRNA with ribosomal proteins (RPs) take place (62) (Fig. 2). This membraneless organelle is considered a dynamic structure (4, 84), where protein complexes are continuously exchanged with the nucleoplasm. Its classical tripartite organization has been dissected using electron microscopy and reflects the different steps of ribosomal biogenesis (130): (i) the fibrillar center, where the RNA polymerase I (Pol I) transcription starts; (ii) the dense fibrillar component, where the initial stages of pre-rRNA processing occur and (iii) the granular component involved in the late processing steps (62). Transcription of the ribosomal DNA (rDNA) repeats generates a 47S pre-rRNA precursor that is further cleaved and processed into 28S, 18S, and 5.8S rRNAs and concomitantly assembled into large and small ribosomal subunits together with the 5S rRNA molecules (18, 32a). These complex series of events is controlled, in yeast, by roughly 150 small nucleolar RNAs (snoRNAs) and two large ribonucleoprotein complexes, named small subunit processosome (for the 40S ribosomal subunit) and large subunit processosome (for the 60S ribosomal subunit) (130). Two types of nucleotide modifications (2′-*O*-methylation and pseudouridylation) are introduced during the maturation process by snoRNAs belonging to the box C/D or box H/ACA families and mediate endonucleolytic cleavages of pre-RNAs (130, 32a). In addition, ribosomal gene transcription is regulated through the modulation of the transcriptional apparatus and epigenetic silencing (131). Large and small mature ribosome particles are independently exported to the cytoplasm through an exportin 1 (CRM1) and Ran-GTP-dependent mechanism: export of 60S subunit requires the exchange of complexes Noc1-Noc2 by Noc3-Noc2 (102) and the association with the adaptor shuttling protein NMD3 (142), whereas the 40S needs the heterodimer Noc4p/Nop14p (103). The work by Hinsby *et al.* exploited a machine learning-based predictor of nuclear export signals to analyze the late stage pre-40S complex, suggesting a role also for the human homolog of yeast DIM2p in the targeting and translocation of the late 40S to the cytoplasm (63).

The organization, the number, and the size of nucleoli in each cell is directly linked to the nucleolar activity (*i.e.,* Pol I transcription rate), which, in turn, depends on cell growth and metabolism (20). Generally, highly proliferating cells present many small nucleoli (62, 130). Ribosomal biosynthesis is a highly energy- and resources-consuming process (134); this explains why this process is tightly regulated by changes in cell proliferation, growth rates, and metabolic activities. Nucleoli constantly integrate different signaling events, maintaining the ribosomal subunit pool required to properly support protein synthesis during cell growth and division (18).

Biosynthesis of ribosomes is a very efficient process, since it has been estimated that 14,000 new ribosomal subunits can be synthesized every minute in an exponentially growing cell (125). The process has to be fine-tuned and several evidences indicate that ubiquitin and ubiquitin-like proteins-based regulatory circuits may control different stages of ribosome formation (129). Lam *et al.* (83) demonstrated that the levels of unassembled RPs within nucleoli exceed the required RP:rRNA ratio and identified an ubiquitin-proteasome-mediated mechanism, that monitors and degrades this excess (115). Ribosomal structural proteins are imported from the cytoplasm in supra-stoichiometric complexes and exported in the form of assembled ribosomal subunits; this ensures that RPs are never rate-limiting for the ribosomal assembly (83). The excess of protein undergoes ubiquitylation and degradation in the nucleoplasm through the proteasome system (114, 129), indicating that mammalian cells produce large amount of these proteins and degrade those that are not assembled with rRNA.

"Dynamic Trafficking:" Keywords of the Nucleolar Physiology

The nucleolus appears as a very dynamic organelle and different types of rearrangements involve this subnuclear

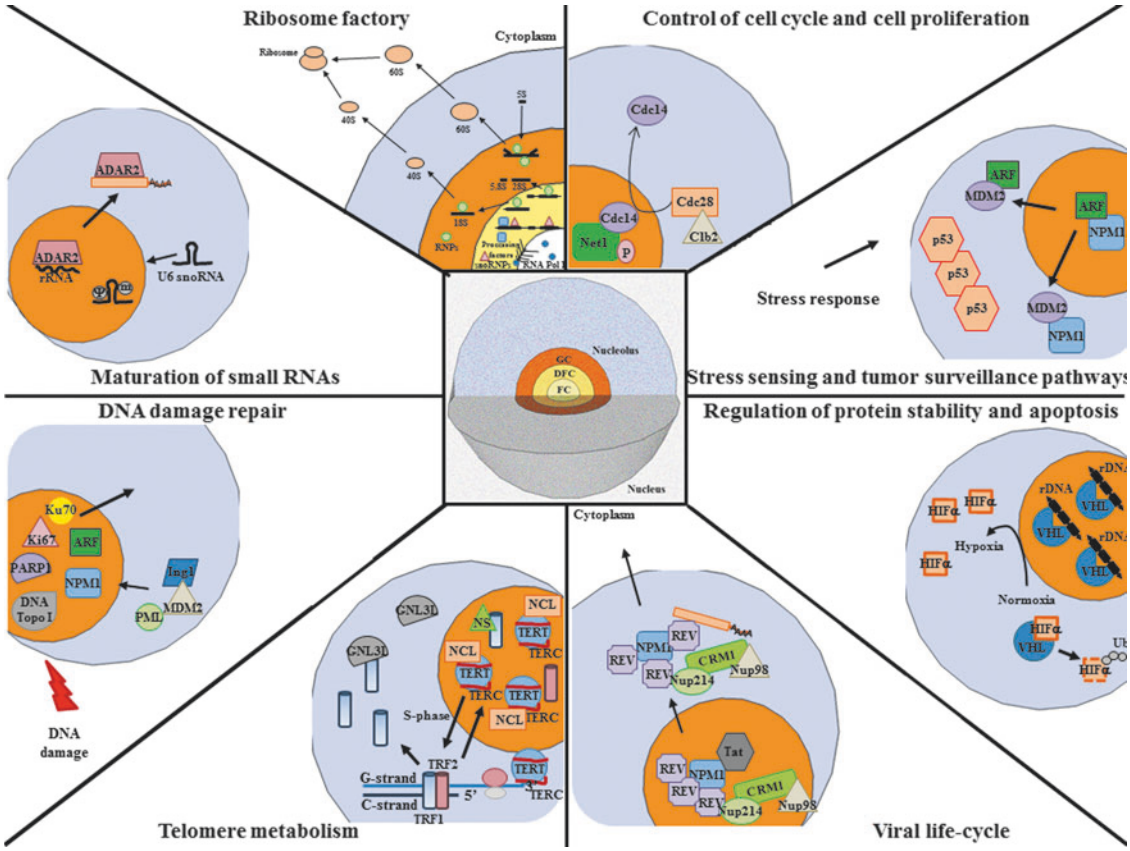

FIG. 2. The nucleolus, a multifunctional domain. The unveiling of the "nucleolome" allowed the understanding of the complexity of the nucleolus, firstly described only as a ribosome factory. The multifunctionality of the nucleolus includes different noncanonical functions as the control of cell proliferation and cell growth, regulation of protein stability, stress and DDR, telomere metabolism, maturation of small RNAs, and control of viral life-cycle. An illustrative mechanism for each function is summarized. MDM2, mouse double minute 2 homolog; ARF, p14 alternative reading frame; ADAR2, double-stranded RNA-specific adenosine deaminase 2; NS, nucleostemin; VHL, von Hippel-Lindau protein; HIF, hypoxia-inducible factor; ING1, inhibitor of growth family protein, member 1; PML, promyelocytic leukemia protein; DNA Topo I, DNA topoisomerase I; TERC, telomerase RNA component; TERT, telomerase reverse transcriptase; GNL3L, guanine nucleotide binding protein-like 3 (nucleolar)-like; TRF, telomeric repeat-binding factor 2; REV, regulator of expression of virion protein; Tat, trans-activator of transcription; Ub, ubiquitin; DDR, DNA damage response. To see this illustration in color, the reader is referred to the web version of this article at www.liebertpub.com/ars

district. First, the ribosome assembly is a vectorial process, in which the ribosomal particles move away from their biogenesis sites. The second dynamic aspect is represented by the constant flux of proteins from the nucleoli to the nucleoplasm. Lastly, nucleolar components present scheduled reorganization every cell cycle, with assembly and disassembly steps required for the redistribution of nucleolar components between the two daughter cells (110).

The cyclic reorganization observed during cell cycle involves the nucleolus as a whole, as this organelle assembles at the end of each mitosis to remain functionally active until the beginning of the next one (4, 62). The nucleolar disassembly observed during mitosis is linked to rDNA transcriptional repression induced by CDK1-cyclin B-directed phosphorylation of components of the rDNA transcription machinery (130). Conversely, the formation of functional nucleoli at the exit of mitosis is not uniquely controlled by the resumption of rDNA transcription, but by a two-steps process regulated by cyclin-dependent kinases that connects the resumption of rDNA transcription and the restoration of rRNA processing (130). During late telophase, nucleoli form around the nucleolar organization regions, which are chromosomal domains where rDNAs, clustered in head-to-tail arrays (62, 84), are transcribed. This sub-nuclear compartmentalization allows the cells to locally concentrate all the factors required for the ribosomal biogenesis (18, 20).

The Way to Move: Visitors *Versus* Resident Nucleolar Proteins

Differently from nuclear localization signals (NLSs), nucleolar localization sequences (NoLSs) are not well characterized and no clear consensus sequences have been described yet (115, 130). NoLSs identified so far are rich in basic residues (*e.g.*, Arg and Lys) (40), but also Trp residues were described to play a functional role for the nucleolar localization of nucleophosmin 1 (NPM1) (108a). Since the mass per unit nucleolar volume is only twofold higher compared with the nucleoplasm, all diffusing macromolecules should theoretically be able to enter nucleoli: it is now clear that the residence time of nucleolar proteins depends on their relative affinity for preanchored complexes present within the nucleolus itself

(114, 115). The ability of different proteins to localize within the nucleolus has been linked to the stable interaction with anchored resident proteins, such as NPM1 or nucleolin (NCL), that may act as carriers, or as a retention scaffolds, supporting the idea that the residence time of proteins within the nucleolar compartment is strongly related to their specific interactions in a process known as "nucleolar sequestration" (40, 115, 130). Though all the molecules resident in the nucleoplasm may, in principle, enter into nucleoli, only those with an affinity for nucleolar resident proteins, are retained for longer times (110). For this reason some authors suggested the concept of "retention signal" in place of "targeting signal" for the nucleoli (121). Since the residence time is quite short and most of the nucleolar proteins shuttle from nucleoli to nucleoplasm and vice versa, the interaction of visitor proteins with anchored nucleolar residents has to be reversible (110, 115). Current models show that proteins and RNAs continuously flow and freely diffuse through the nuclear space (131): the average residence time for most nucleolar proteins within nucleoli is estimated to be only a few tens of seconds. Thus, nucleolus appears as a steady state structure with its component in a dynamic equilibrium with the surrounding nucleoplasm (121). However, in spite of this continual exchange of molecules between these two compartments, nucleolar domains are maintained because the number of retained proteins is higher than the amount of molecules that are released from the same domain (32a). Resident factors, able to connect and bind multiple protein partners, are considered as "hub proteins" and might be responsible for the nucleolar localization of the vast majority of visitor proteins in the absence of RNA–protein interactions. Each hub protein may have different recognition requirements; thus, possibly explaining the occurrence of different NoLSs. Two typical examples of hub proteins are NCL and NPM1, which contain disordered regions involved in protein–RNA interactions (40).

Recently, an additional protein retention mechanism based on GTP-driven cycles has been identified for nucleostemin (121). The GTP-GDP exchange mechanism is not the only intracellular signal able to move nucleolar proteins: stimuli as the hydrogen ion were already described by Mekhail *et al.* (98), who demonstrated how the nucleolar sequestration of the von Hippel-Lindau protein after a pH change promotes the stabilization of the hypoxia-inducible factor, triggering a general cell response to hypoxic conditions (115).

New Concepts in the Nucleolus Physiology: Beyond the Ribosome Factory

In the 60s, after the identification of the localization of ribosomal genes, the main function of the nucleolus was nicely summarized as "an organelle formed by the act of building a ribosome" (63). In the last decades, thanks to the development of technologies, such as protocols for the isolation of large amounts of nucleoli and the improvement of high-throughput mass-spectrometry-based proteomic approaches, several proteomic analyses were undertaken, unveiling the "nucleolome" (4, 5, 18, 32a, 125). Over 4500 proteins were described to localize within nucleoli and both bibliographic and bioinformatics analyses allowed to classify eight major functional groups (RPs, ribosome biogenesis, chromatin structure, mRNA metabolism, translation, chaperones, fibrous proteins, and others [see Fig. 3 for further details]) (3, 18, 32a, 108). Characterization of the nucleolar proteome under different stress conditions (*e.g.*, actinomycin D) further underlined the complexity of the nucleolome dynamics (5).

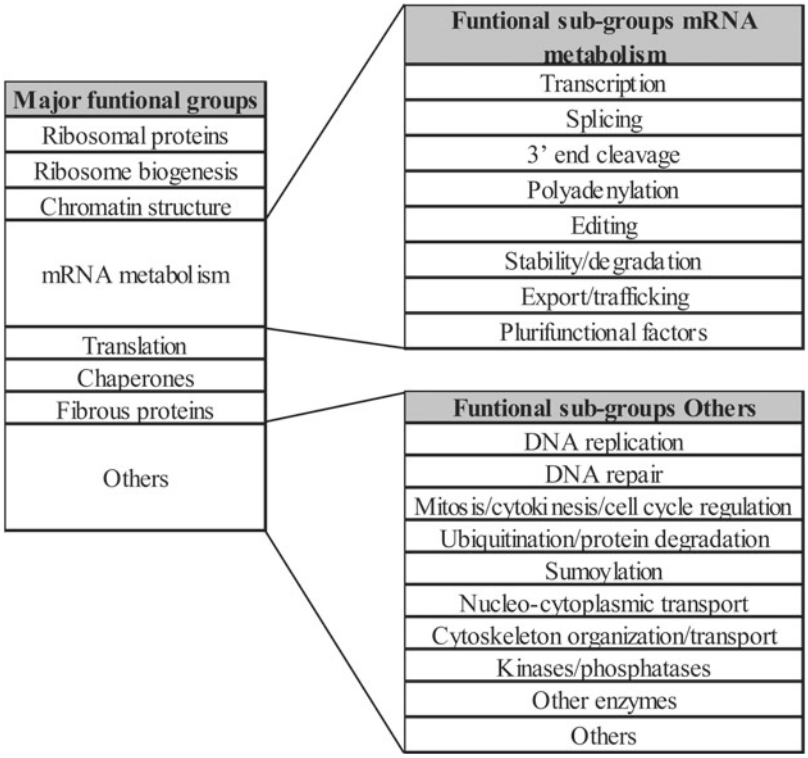

FIG. 3. Classification of functional groups and subgroups for the "nucleolome."

The nucleolome includes proteins related to cell cycle regulation, DNA damage and pre-mRNA processing (84), suggesting that this organelle may act as a multitasking district, being more than a simple ribosome factory (18, 62, 63, 84, 125). These particular multifunctional features are possibly related to the presence of many different nucleolar proteins endowed with multiple roles (*e.g.,* NCL and Nopp140) (90a). Nucleolar proteins unrelated to ribosome assembly mostly contain an RNA-binding motif or have a chaperone function and are able to shuttle between the nucleolus and the nucleoplasm (90a). It is currently known that nucleoli carry out many nonribosomal activities, such as: control of cell cycle and proliferation (62, 63, 130), stress sensing (18, 21, 64, 96, 108, 124, 139), tumor surveillance, DNA damage repair (18, 41, 84), regulation of protein stability and apoptosis, telomere metabolism (18), maturation of small RNAs, including tRNAs and small nuclear RNAs, maturation of the spliceosome and of the signal recognition particle (63, 115, 121), and also control of viral lifecycle (62, 71), acting in several ways as a sequestration core facility (Fig. 2) (21, 40, 63).

The assumption that a protein acts and executes its functions where it is more abundant is invalid for some nucleolar components: a high protein concentration in a given cellular compartment might not correspond to a quantitative signal for its activity (114). A clear example is represented by the many DNA repair proteins that reside within nucleoli (see Table 1 for more details), which in this instance, appear to act as storage sites (see below). After nucleolar stress or DNA damage, these proteins can relocalize to the nucleoplasm. The nucleolar stress response may therefore, act as a mechanism of surveillance monitoring the synthesis and the correct assembly of ribosomal units: it may halt the cell cycle progression until enough functional ribosomes are built or it may induce p53-mediated apoptosis or senescence (134). This represents an elegant and efficient way to coordinate arrest of cell growth and induction of DNA repair by controlling only the subcellular distribution of proteins.

Linking Nucleolar Physiology to Human Diseases

Several reports highlighted the presence of a layer of heterochromatin, called perinucleolar compartment (PNC), at the nucleolar periphery. The PNC is associated with specific DNA loci and it is enriched in RNA-binding proteins and RNA polymerase III transcripts (62, 114). These discoid-shaped caps are usually found in mammalian transformed cells, tumor-derived cell lines, and tumor biopsies, accounting for a possible connection between PNC and tumor initiation and progression (114). Despite the apparent link between cancer and PNC, the exact role of these nucleolar subdomains has not been identified yet.

Nucleoli are closely linked to cellular homeostasis and human health (62): rapidly proliferating cells, such as cancer cells, usually present a strong upregulation of genes involved in the ribosomal biogenesis. This phenomenon accounts for the presence of several prominent nucleoli that are a typical cytological feature of neoplastic cells (129). Morphological and functional changes associated with cancer usually correlate with quantitative and qualitative differences in the ribosome biosynthesis rate (62) and are a consequence of the increased metabolic needs of the cell (105). This could indicate that the nucleolus undergoes an adaptive response upon cellular transformation; on the other hand, the increased rate of ribosome biogenesis might be actively involved in, and contribute to, tumorigenesis (105). More recently, the accumulation of chemically modified ribosomes upon oxidative stress (*e.g.,* bearing 8-OHG modifications, or cross-linked rRNA-RPs complexes) is emerging as a contributing factor in the progression of neurodegenerative diseases, such as AD and PD (62). In addition, a novel link between nucleolar damage and neurodegeneration has recently been established through the association of PD with nucleolar integrity. These interesting findings also establish the existence of a direct signaling axis connecting the ribosomal synthesis rate and oxidative stress (122). Under this perspective, the deep understanding of changes related to tumor progression and the composition and dynamics of the nucleolome might be important to clarify the mechanisms of tumorigenesis and for designing new therapeutic strategies.

Dynamics of DNA Repair Proteins During Genotoxic Damage: Nucleolus and RNA Binding

Cellular life is continuously threatened by stressful conditions, such as viral infections, oncogenic activations, temperature shocks, and genotoxic damage, which must be immediately dealt with by the cell to maintain its homeostasis. DNA damage typically involves the storage sites of the genetic material, such as nucleus and mitochondria. Depending on the origin of the genotoxin (exogenous *vs.* endogenous), its nature (physical *vs.* chemical) or its uptake mechanisms, differential burden of damage can be accumulated both in nuclear and in mitochondrial DNA. Upon genotoxic insults a dynamic redistribution of DNA repair proteins to the site of damage is frequently observed; this phenomenon leads to the accumulation of DNA repair factors, often into spatially restricted foci. Relocalization events usually occur through cytoplasmic-mitochondrial, cytoplasmic-nucleoplasmic, and nucleolar-nucleoplasmic shuttling regulated by post-translational modifications (PTMs) and triggered by the damage itself (51).

Why nature selected such a time-consuming process involving reorganization of cell proteome upon DNA damage, instead of constitutively accumulating each DNA repair factor within the proper target compartment? Is there any functional relationship between RNA metabolism and the DNA damage response (DDR), which may involve an active site of RNA production, such as the nucleolus? These legitimate questions are still a matter of debate; however, based on existing data at least four possible explanations, not mutually exclusive, appear reliable: (i) the concentration, under physiological levels of DNA damage, of high amounts of DNA repair proteins in specific subcellular regions might be deleterious for nucleic acids integrity. Many repair proteins, in fact, are endowed with DNA trimming or modifying activities. Examples include APE1 or the DNA polymerase β (Polβ); overexpression of these proteins has already been shown to promote genomic instability, possibly due to the lack of coordination of their enzymatic activities (26); (ii) repair factors may exert more than one specific function that cannot be directly linked to their DNA repair activity. This situation is nicely exemplified by the APE1 protein, which nucleolar localization is necessary for cellular proliferation (see below), or by proteins, such as the Werner syndrome helicase (WRN), or the flap

Table 1. DNA Repair Protein Composition in the Nucleolus

Protein name	Putative role inside the nucleolus	Role(s) outside the nucleolus	Genotoxic stress leading to protein relocalization		References
			Imported	Exported	
APE1	RNA processing	AP endonuclease		Actinomycin D	(5, 149)
ATM		DNA damage signaling			(106)
ATR		DNA damage signaling			(106)
BLM	rDNA transcription	DNA helicase		Camptothecin	(5, 120, 163)
BRCA1/BARD1		E3 Ligase involved in HR		IR	(53)
CSB		Core NER factor			(99)
DNA-PK catalytic subunit		Kinase involved in NHEJ		UV, cisplatin	(36, 106)
FEN1	Resolution of stalled replication forks	Structure-specific nuclease		UV	(54)
ILF2 and ILF3		dsRNA binding proteins interacting with Ku70/80 and DNA-PK		UV	(106)
Ku70/80		DSB recognition in the NHEJ pathway		UV, cisplatin, IR, Actinomycin D, mitomycin C, hydroxyurea, doxorubicin	(2, 36, 106)
LigIII		DNA ligase involved in the BER pathway and in the SSB repair		UV, IR	(106)
MRE11		Nuclease involved in DSB repair			(5, 108)
MSH6		MMR factor		MNNG	(95)
Mus81	rDNA repair	Structure-specific endonuclease			(48)
OGG1		DNA glycosylase	Ro19-8022 + light (405 nm), $KBrO_3$		(25, 99)
p53		Multifunctional tumor suppressor, auxiliary roles in NER and BER		UV	(123, 139)
PARP1 and PARP2		DNA damage signaling and transcriptional modulation		Actinomycin D, H_2O_2, MMS, camptothecin, UV	(5, 97, 106)
PCNA		Sliding clamp involved in DNA repair and replication			(161)
PNK		DNA end trimming kinase/phosphatase			(5, 63)
Polβ		DNA polymerase involved in the BER pathway			(63)
Rad9B	rDNA repair	Poorly understood	UV, Actinomycin D		(117)
Rad17		DNA repair and replication modulator		UV, IR, MMS, adriamycin	(28)
Rad50		Part of the MRN complex			(5)
Rad52	rDNA repair	DSB responsive protein			(32)
RECQL4		DNA helicase	H_2O_2, streptonigrin		(156)
RNF8	Modulation of ribosome biogenesis	E3 ligase involved in HR		IR	(53)
RPA		Single-strand DNA binding protein involved in DNA repair and replication			(108)
Slx1-Slx4 complex	rDNA repair	Structure-specific endonuclease			(32)
SMUG1	rRNA quality control	DNA glycosylase			(73)
SSRP1		Structure-specific protein binding to cisplatin-DNA adducts		Cisplatin	(36)
TDP1		Tyrosyl DNA phosphodiesterase		Camptothecin	(8)
TOPBP1		DNA repair and replication modulator			(106)
Topo I		DNA topoisomerase		UV, camptothecin	(22, 93, 104)
Top2a and Top2b		DNA topoisomerases			(5)
WRN	rDNA transcription	DNA helicase implicated in BER and recombination		UV, IR, MMC, MMS, bleomycin, camptothecin, etoposide, cisplatin	(5, 16, 36, 75, 94)
XPC		Core NER factor	Ro19-8022 + light (405 nm)		(99)
XPG	rDNA transcription	NER endonuclease		UV	(112)
XRCC1		Scaffold protein in the BER pathway		Camptothecin	(5, 63, 120)

APE1, apurinic/apyrimidinic endonuclease 1; ATM, ataxia telangiectasia mutated; ATR, ataxia telangiectasia and Rad3-related; BER, base excision repair; DSB, double-strand break; FEN1, flap endonuclease 1; HR, homologous recombination; IR, ionizing radiation; NER, nucleotide excision repair; NHEJ, nonhomologous end joining; OGG1, 8-OHG DNA glycosylase; PARP, poly [ADP-ribose] polymerase; PCNA, proliferating cell nuclear antigen; Polβ, DNA polymerase β; rDNA, ribosomal DNA; rRNA, ribosomal RNA; RPA, replication protein A; SSB, single-strand break; WRN, Werner syndrome helicase; XRCC1, X-ray repair cross-complementing protein 1.

endonuclease 1 (FEN1) (54), that are required for the active transcription of ribosomal genes in the nucleolus. All these factors promptly relocalize to the nucleoplasm to exert their DNA repair function upon UV irradiation; (iii) while a lower steady-state amount of DNA repair enzymes is sufficient to grant a basal level of genome stability maintenance, it is likely that genotoxin-induced protein accumulation mechanisms have evolved, to cope with sustained DNA damage. Thus, increasing the local concentration of DNA repair factors may be a simple and fast way to amplify the local DNA repair capacity; (iv) disruption of the nucleolar structure, often observed occurring upon DNA damage, may halt rRNA production; thus, leading to a block of the protein synthesis machinery and allowing proper DNA repair. This may represent an efficient coupling mechanism involving nucleolus dynamics, RNA-binding, and DNA repair, which allows synchronization of DDR and arrest of cellular growth.

While many examples of proteome dynamics have been reported to occur during DDR, this review will focus on the relocalization of nucleolar proteins; for detailed information concerning general subcellular reorganization, please refer to Tembe and Henderson (139) and references therein.

The Nucleolus as DNA Damage Sensor and Storage Facility for DNA Repair Proteins

As already mentioned, recent proteomic analyses have pointed at the nucleolus as a mediator of the cell cycle regulation, tumor suppressing or protumorigenic activities, and DDR (5, 17, 63, 108). The presence of rRNA and hub proteins, such as NCL and NPM1 is likely the critical factor for the nucleolar accumulation of many proteins not uniquely related to ribosome biogenesis (27, 40). Among these, many DNA repair factors have been shown to localize within the nucleolus (Table 1), which acts as a stress response organelle and responds, in a unique damage-specific manner, to different cellular stresses (5, 17, 30, 106). During a stress response a broad reorganization of the nucleolar proteome occurs; interestingly, the vast majority of nucleolar proteins migrate toward the nucleoplasm and not vice versa, indicating that the nucleolus may act as a reservoir able to release critical factors upon DNA damage (108, 139). Very few proteins have been reported to migrate to the nucleolus during the stress response. Among these ING1 and PML, which are thought to participate in triggering of apoptosis and in cell cycle arrest, respectively (139). Intriguingly, chaperones, such as Hsc70 are targeted to the nucleolus after the stress response, possibly to restore the nucleolar function during the cellular recovery from stress. Typically, during the response to DNA damage or transcriptional inhibition, one of the first events is represented by the interruption of the ribosomal synthesis (108). This mechanism likely represents a cellular strategy to maintain homeostasis, indeed, as already pointed out, the ribosomal biogenesis is a rather expensive energy-consuming process (20). The impairment of rRNA transcription and processing is often, but not always, associated with nucleolar disintegration and condensation phenomena that lead to the formation of caps and necklace-like structures (20, 106). An extensive analysis of the effects of chemotherapeutic drugs on ribosome biogenesis and nucleolar integrity has recently been carried out by Burger *et al.* (23). For a broader list of responses to different stress stimuli, please refer to Boulon *et al.* (20). Along with the inhibition of ribosomal biogenesis, massive reorganization occurs, with a rapid outflow of "nucleolar effectors", such as $p14^{Arf}$, NCL, and NPM1, which slow down or arrest the cell-cycle in both p53-dependent and independent manners (20, 31, 34, 49, 86). Concurrently, also DNA repair factors stored within nucleoli and frequently bound to NCL and NPM1 are released into the nucleoplasm; the transient arrest of the cell-cycle progression possibly facilitates the DNA repair process. Only after resolution of DNA damage, rRNA synthesis is restored, as suggested by the inverse correlation existing between the rDNA transcription rate and γ-H2AX foci number (80). Notably, many nucleolar effectors also play a role within the nucleoplasm: beside the contribution to the modulation of the cell-cycle, several reports have pointed out that NCL or NPM1 may directly participate in the DDR. For instance, NCL has been shown to tune proliferating cell nuclear antigen (PCNA) activity in the nucleotide excision repair (NER) pathway (161), while NPM1 has been involved in the BER modulation (see below). Interestingly, both these proteins display strand annealing activity *in vitro* (19, 55) and have been identified as stress-responsive RNA-binding proteins, suggesting that upon genotoxic damage these factors may modulate DNA, as well as RNA repair or cleansing (162). More importantly, emerging evidences further highlight the importance of nucleolar hub proteins in human pathology. The link between NPM1 and oncogenesis, for example, is a well-established paradigm (31, 52, 151) and we recently demonstrated that in acute myeloid leukemia bearing NPM1 mutations, the cytoplasmic de-localization of the mutant NPM1c+ leads to extensive BER impairment due to APE1 nuclear deprivation (150). This evidence denotes how the deregulation of an important nucleolar factor might impact on the overall cellular dynamics and not only on the ribosome biogenesis, supporting the view of the nucleolus as a multifunctional and versatile organelle. Recent evidences from Lewinska *et al.* showed that, in yeast, the nucleolus acts as stress sensor also for oxidative stress. Their work linked the nucleolar exit of the Pol I-specific transcription factor Rrn3p, to the response to oxidation, suggesting that oxidative damage is indeed a cellular stress that is sensed from the nucleolus leading to arrest of the ribosome transcription (87). Interestingly, diethyl maleate-induced oxidative stress has been demonstrated to modulate also the whole nuclear export system through impairment of the CRM1-mediated nuclear export, coupled to relocalization of the nuclear pore component Nup98 to the nucleolus (33). Altogether, these observations underline the role of the nucleolus as stress sensor, further confirming the validity of the aforementioned model involving arrest of ribosome biogenesis, followed by nucleoplasmic and nucleolar proteome rewiring.

The damage-specificity of the nucleolar response is clearly depicted by the differential response to diverse DNA damaging stimuli: DNA repair factors undergo selective mobilization upon specific genotoxic conditions (Table 1). UV and ionizing radiation (IR), for instance, elicit markedly differential responses in terms of nucleolar proteome reorganization. Whereas UV stress is characterized by fast and persistent (hours), fluctuations of nucleolar nonhomologous end joining (NHEJ) proteins, IR lead to quicker (minutes), but less persistent responses, which are more limited, in terms of magnitude (106). The dynamic reorganization of nucleolar proteins upon DNA damage has been nicely described by

Adelmant *et al.*, who showed that microinjection of sheared DNA, to mimic the presence of strand breaks, leads to the rearrangement of Ku complexes. Intriguingly, in the absence of DNA damage, Ku associates with rRNA- and RP-containing complexes; a DDR onset elicits the exit of Ku from nucleoli and the modification of its interactome (2). This process likely represents a general response mechanism, where the nucleolus acts as a sensitive "antenna" for stress and DNA damage and as central hub for the coordination of the cellular response to stress conditions. The ability to undergo highly dynamic and selective reorganization allow for prompt release of DNA repair factors that are stored within this organelle. An essential question still remains to be answered: which is the triggering event that begins the signaling cascade linking DNA damage to the early nucleolar response? PTMs are usually a quick way to rewire the cellular proteome. APE1 and WRN translocation from the nucleolus is for instance triggered by acetylation (16, 89); on the contrary, FEN1 has been shown to migrate to the nucleoplasm upon UV irradiation in a phosphorylation-dependent manner. Remarkably, mutations that mimic or impair the UV-induced FEN1 phosphorylation, cause UV sensitivity (54), suggesting that DNA damage-induced protein translocation is essential for a correct DDR. Griffiths *et al.* pointed to SUMOylation as the major PTM targeting DNA glycosylases in yeast (51); this PTM has also been implicated in the modulation of rDNA repair through export of the rDNA double-strand breaks (DSBs) to the nucleoplasm by the homologous recombination (HR) machinery (39). In addition, the nucleolus has been reported to contain several DNA damage sensors (*e.g.*, the ataxia telangiectasia mutated [ATM], the ataxia telangiectasia and Rad3-related [ATR], and p53) (5, 123) and it has been demonstrated that, upon DNA damage induction, Pol I-mediated transcription is blocked in an ATM-dependent manner, and not by the DNA damage itself. Interestingly, through microirradiation studies, Kruhlak *et al.* showed that transcription of rDNA is transiently arrested only in damaged nucleoli, whereas the neighboring ones maintain normal transcriptional activity (80). Moreover, Rubbi and Milner, have elegantly shown that nucleolar disruption, rather than DNA damage, may lead to p53 stabilization, suggesting that the nucleolus may constitutively promote p53 degradation, unless DNA damage occurs (124). It would be interesting to understand if and how the extra-nucleolar DNA damage is ultimately signaled to the nucleolus and which is the event that triggers the nucleolar segregation.

The Paradigmatic Example of the APE1/NPM1 Interaction

APE1 is a typical example of DNA repair protein activated during the nucleolar stress response. APE1 is a multifunctional and essential factor in mammals that was identified about 20 years ago as the major AP-endonuclease in the BER pathway, as well as a redox coactivator of transcription factors (37, 157). The recent observation that APE1 is able to bind and cleave RNA highlighted previously unsuspected roles for the protein (77, 138). We found indeed that this protein associates with NPM1 in the nucleolus, where it may have a functional role as RNA cleansing factor. This hypothesis is corroborated by studies performed with inducible HeLa APE1 knock down cell lines, which showed how APE1 depletion leads to a widespread accumulation of unrepaired oxidized RNA species (*i.e.*, 8-OHG) upon oxidative stress. Notably, under unstressed conditions, APE1 knock down cells display impaired translation ability, lower protein content and overall cell growth impairment (149). These evidences point to a major contribution for APE1 as cellular scavenger of damaged RNA species. The nucleolar storage of APE1 is mediated by the interaction of the flexible and evolutionarily acquired N-terminal extension of the protein with both rRNA and NPM1 (42, 89, 116). However, the protein does not constitutively accumulate in the nucleoli; in fact, upon Pol I inhibition with actinomycin D, APE1 shuttles to the nucleoplasm (149). The evidence that treatment with the E3330 redox inhibitor (45) causes APE1 nucleolar exit and its accumulation to the nucleoplasm (147) suggests that the redox status of APE1 may play a significant role in controlling its subcellular trafficking. Interestingly, the APE1/NPM1 association is also impaired during oxidative stress (149), suggesting that the protein may be released from the nucleolus during stress conditions, possibly to operate within the BER pathway. In accordance with this observation, we delineated a complex regulatory pattern of NPM1 on APE1 endonuclease activities: NPM1 acts as an inhibitor of the APE1 ribonuclease function, but as an activator of the AP-endonuclease function on DNA (149, 150). This model suggests that when APE1 resides within the nucleolus, its activity is mainly focused on the rRNA quality control machinery, possibly modulated by NPM1. Whereas, during the DDR, the simultaneous outflow of APE1 and NPM1 to the nucleoplasm, leads to the activation of the APE1 AP-endonuclease function (Fig. 4). In agreement with this view, many reports point to the involvement of NPM1 in different aspects of the DDR, yet, the exact contribution(s) of this protein to the stress response is currently elusive (31, 79, 127). It is worth pointing out that the lack of NPM1 has been proved to sensitize cells to genotoxins that elicit a BER response and that APE1 catalytic activity is impaired in NPM1 knock out cells (150). These elements suggest that NPM1 plays a direct role in the BER modulation, which is still poorly understood. As discussed in the previous section of this review, the key event that triggers the APE1 release from nucleoli upon genotoxic stress is still a matter of debate. It is known that the APE1/NPM1 interaction is modulated by acetylation on the N-terminal domain of APE1 (42, 89). Acetylation of this protein region is induced upon genotoxic stress (89, 128); it is therefore, likely that, once again, stress-induced PTMs drive APE1 shuttling to the nucleoplasm in response to DNA damage. In an effort to characterize the response of APE1 to genotoxic stress, we generated a quadruple lysine to alanine substitution that mimics constitutive APE1 acetylation. As anticipated, the inability of this mutant to interact with NPM1 leads to nucleolar exclusion of the APE1 mutant. Interestingly, the lack of APE1 nucleolar accumulation causes a severe impairment of cellular proliferation, indicating that the presence of APE1 within nucleoli is required to ensure a proper cellular growth rate (89). These aspects of the APE1 biology still deserve thorough investigation and fascinatingly open novel perspectives for antitumor therapy, as targeting the APE1/NPM1 interaction may prove effective in counteracting cellular proliferation.

The APE1 protein is commonly renowned as DNA repair protein and only recently it has been identified as an enzyme active on abasic RNA molecules, unveiling its noncanonical function. Perhaps earlier examples of this versatility of function in dealing with genotoxic damage were described for the RP S3, both in *Drosophila* and humans. Specifically, S3 has

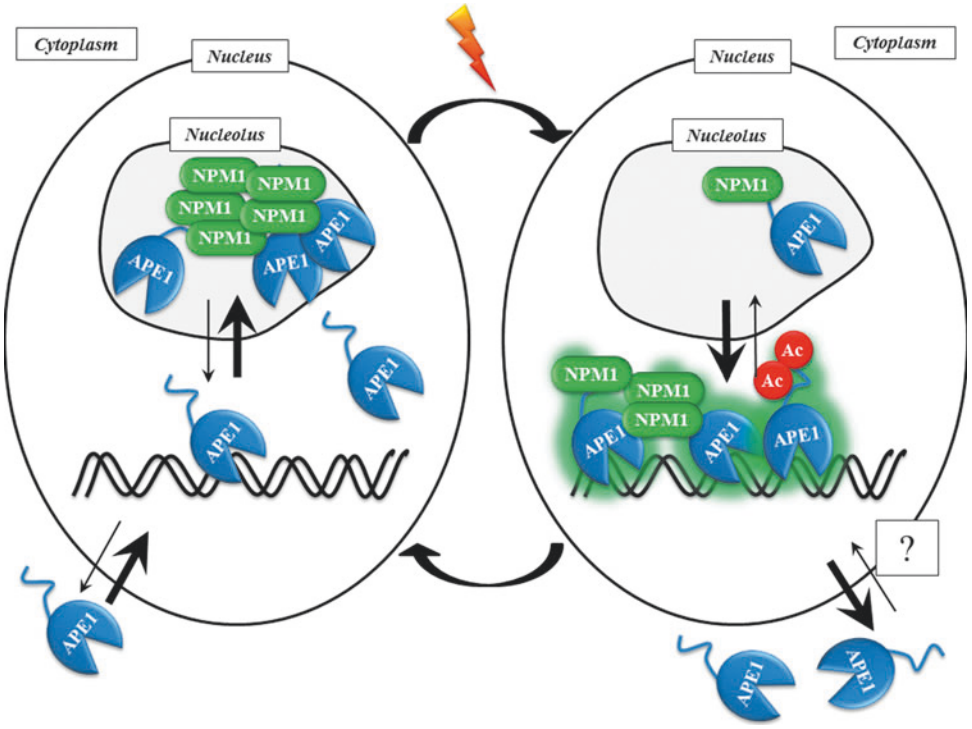

FIG. 4. Dynamic turnover of the APE1/NPM1 complex in response to cellular stress. Under basal conditions (left) the cellular APE1 pool is dynamically distributed throughout the cell, with prevalent accumulation in the nucleus and nucleoli. This accounts for the maintenance of a basal DNA repair capacity (both nuclear and mitochondrial), redox-mediated transcriptional modulation, cell proliferation, and RNA cleansing activity. Upon genotoxic stress and/or arrest of Pol I transcription (right) the dynamic equilibrium of APE1 localization is tipped towards a nucleoplasmic accumulation of the protein (149). The APE1 relocalization is likely mediated by simultaneous migration of NPM1 outside the nucleolus and hyperacetylation of the N-terminal region of APE1 itself (90). This situation ensures a potentiated DNA repair response, as both the nucleoplasmic APE1/NPM1 association and its acetylation have been linked to increased catalytic activity of the protein. The absence of APE1 from nucleoli, moreover, might favor a temporary arrest of cellular proliferation, useful to allow for more efficient DNA repair. If the DNA damage is sustained, it is likely a redistribution of a pool of APE1 to the cytoplasm. This phenomenon should boost the mitochondrial BER and possibly contribute to the cellular RNA cleansing capacity. APE1, apurinic/apyrimidinic endonuclease 1; BER, base excision repair; NPM1, nucleophosmin 1; Pol I, RNA polymerase I. To see this illustration in color, the reader is referred to the web version of this article at www.liebertpub.com/ars

been found to protect cells from genotoxic stress through: (i) its DNase activity on abasic sites in *Drosophila* (155); (ii) its ability to stimulate, the activity of the uracil-DNA glycosylase hUNG in human cells (78); (iii) its ability to bind with high affinity the oxidative lesion 8-OHG in humans (60) and (iv) its functional interaction, always in human cells, with other well-known DNA repair proteins, such as the 8-OHG DNA glycosylase (OGG1) and APE1 (61). Recent findings are increasingly pointing to the involvement of noncanonical proteins (57) and even of noncoding RNA molecules (46) in the DDR, adding more layers of complexity to this mechanism. An intriguing emerging evidence is that the association of DNA repair proteins to noncanonical binding partners (*i.e.*, RNA and RNA-binding proteins) is mainly driven by the presence of unfolded protein domains acquired during phylogenesis, which may be responsible for novel gain of function activities.

Relevance of the Unfolded Domains in BER Proteins: The Missing Link for a Phylogenetic Gain of Function?

Until recently, BER was considered the simplest among the DNA repair pathways since an *in vitro* reconstituted nuclear BER required only four or five core enzymes. However, recent studies have revealed that BER is much more complex, involving a network of distinct and integrated cell cycle- and genome-specific sub-pathways in which numerous noncanonical proteins take part (58, 59). Notably, many of these proteins are involved in RNA-metabolism processes. Actually, several noncanonical factors have been demonstrated to participate BER, even though their *in vivo* functions are yet to be fully unraveled. The list of non-BER proteins includes for instance: YB-1 [which has been shown to interact with the endonuclease VIII-like 2 (NEIL2) glycosylase (35), the endonuclease III-like glycosylase (NTH1) and APE1 (29)], NEIL2 [which was also found to interact with the RNA-binding protein hnRNP-U (6)], HMGB1 [which has been implicated in single-strand break (SSB) repair involving Polβ (90)] and the tumor suppressor p53, which was also shown to play a role in DNA damage repair through direct binding to APE1 and Polβ (168). The list of these non-BER proteins is still growing, supporting the notion that BER *in vivo* is far more complex than the simple model that we can reconstitute *in vitro*. In particular, the characterization of the BER interactome identified multiprotein complexes; thus, suggesting that complete

repair occurs through the action of BER complexes formed by core proteins and noncanonical factors (BERosomes) (59). The previous and simplistic view of the BER mechanism, based on the analysis of cocrystal structures of substrate-bound proteins, proposed a pathway consisting of sequential steps in which individual repair enzymes carry out reactions independently. In contrast with this original concept, recent discoveries showed that early BER enzymes stably interact with most of the downstream repair components. The initial view of BER as a "hand-off" or "passing the baton" process has been revisited by Hegde *et al.* who introduced, rather, a new paradigm in which the dynamic interplay of highly coordinated interactions between different BER proteins would increase the efficiency and the versatility of the process.

It has been observed that frequently those machines whose operations must be tuned rapidly in response to specific and diverse cellular needs, present components that are not fully structured. Such "malleable machines" (47), conversely to rigid entities, might presumably better respond to different conditions, for instance by promoting conformational rearrangements and facilitating multiple targets recognition. Structural analyses exploiting both experimental and modeling approaches have indeed evidenced the presence of disordered segments preferentially localized at the N- or C-terminus of different mammalian DNA repair proteins, a peculiar feature which is absent in their bacterial prototypes. These observations thus, suggest that, during evolution, higher organisms have acquired these binding domains to regulate multiprotein interactions and to improve pathways (*e.g.,* BER) efficiency, in an increasingly oxidizing environment. Long disordered segments are a common feature observed in a large percentage of proteins; being prevalent especially among proteins involved in vital processes, such as transcription, translation, signal transduction, and protein phosphorylation (47, 145). Such unstructured regions may provide versatility in recognizing multiple targets, promoting communication with many proteins in response to environmental changes; thus, expanding the capacities of ordered complexes and representing a powerful strategy selected by nature to quickly explore a vast interaction space with unique thermodynamic advantages (132). Disordered regions were shown to be prevalent in DNA binding proteins, particularly in those involved in targeted sequence binding (*e.g.,* repair proteins and transcription factors) (143, 153). Disordered prediction tools (PONDR and PrDOS) have been used to compare the secondary structure of human and bacterial early BER proteins (59). These analyses showed that mammalian DNA glycosylases are endowed with unique nonconserved extensions at their N- or C-termini, which are absent in their homologs in lower organisms (58). The human NEIL1 glycosylase, for instance, contains an extended disordered region spanning about 100 residues at the C-terminus, absent in the *E. coli* Nei-like protein. Similar comparisons between the human DNA glycosylases hNTH1, the MutY homolog (hMYH), and their *E. coli* prototypes (*i.e.,* endonuclease III and MutY, respectively), indicate that both hNTH1 and hMYH have extended disordered tails at the N-terminus that are absent in the *E. coli* enzymes (66, 140). Likewise, the N-terminal disordered region present in the human APE1 is absent in exonuclease III (Xth), its *E. coli* ortholog. The size range of the unstructured extensions is about 50–100 residues. In the case of human APE1 it consists of ~65 residues, being mostly disordered (59).

These disordered regions, due to their structural flexibility and plasticity have been shown to provide BER proteins with functional advantages and appear to be essential for their biological functions, including damage sensing (153), protein–protein interactions, repair regulation *via* PTMs and containing NLSs (118). Furthermore, the presence of disordered segments only in eukaryotic proteins, with the highest degree of disorder in mammals, suggests their evolutionary acquisition and well correlates with the increase in regulatory complexity observed in higher organisms.

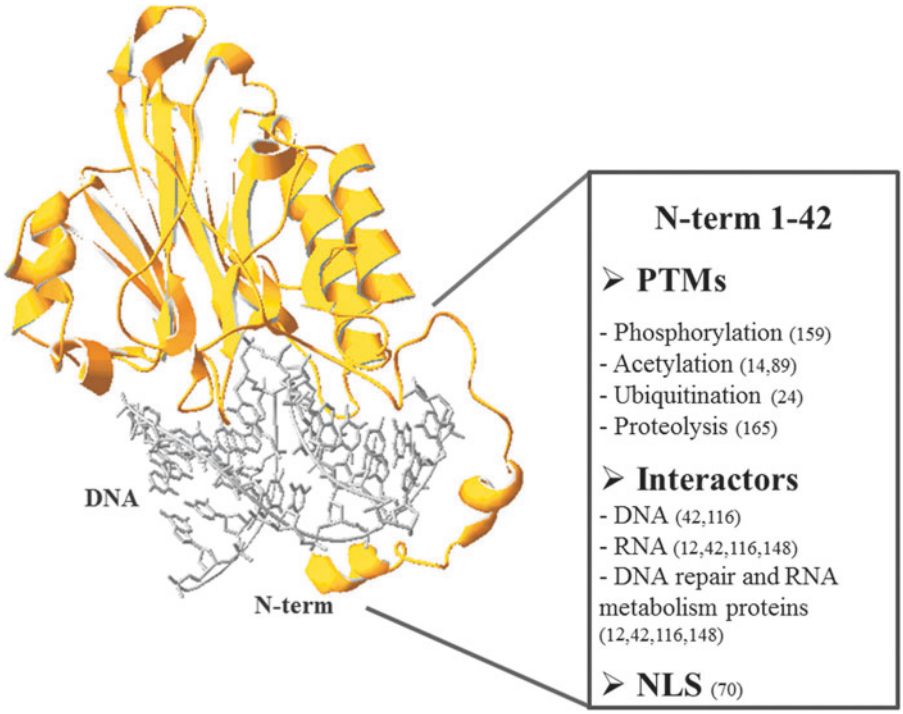

FIG. 5. Schematic representation of multiple regulatory functions of the APE1 disordered N-terminal region. APE1 crystal structure (yellow) bound to abasic DNA (grey) is from the pdb (1DEW) and displayed using the PDBV software. The deposited APE1 crystal structure was obtained using a truncated APE1 form (residues 40–318); missing residues have been manually added. The unstructured N-terminal portion of APE1 (residues 1–42) is essential for APE1 biological functions being site of PTMs, target of many interactions and, including the NLS. NLS, nuclear localization signal; PTMs, post-translational modifications. To see this illustration in color, the reader is referred to the web version of this article at www.liebertpub.com/ars

Among the BER enzymes, APE1 offers a paradigmatic example of how a disordered tail can endow a protein with unique activities. The first crystallographic structure of the human APE1 in complex with DNA was obtained using a truncated protein lacking the first 35 amino acids and reveled that this protein consists of two symmetric alpha/beta fold with a significant structural similarity to both bovine DNase I and its *E. coli* homologue Xth (50). A crystal structure of the full-length protein has also been reported, but again, the N-terminal region was unresolved (10). Three functionally independent domains can be distinguished within the APE1 protein (Fig. 5): (i) the first 33–35 amino acid region consists of a structurally disordered segment (133) essential for the interaction with other proteins (148, 149) and harboring sites for PTMs (14, 24, 70, 89, 159, 165, 166) and RNA interaction (89); (ii) the redox domain is located in a region between amino acids 35 and 127; and (iii) the DNA repair domain, which spans the C-terminal domain of the protein from about residue 61 onwards (42, 68). Whereas the APE1 C-terminal domain involved in AP endonuclease activity is conserved from bacteria to humans, the N-terminal region is unique to mammals suggesting a recent acquisition during evolution.

Remarkably, this peculiar region also accounts for noncanonical activities that have been ascribed to APE1, including its role in RNA metabolism (42, 89, 116, 138, 148, 149). Over the past two decades, knowledge of the biological functions, mechanisms of action, interactions, and regulation of the APE1 protein has increased exponentially. In particular, it has become apparent that APE1 participates in multiple cellular processes not only confined to the maintenance of genome stability, in accordance with the current general view that many DNA repair enzymes may exert miscellaneous activities, being implicated, for example, in different steps of gene regulation (74, 113). As already mentioned, RNA decay and processing events require a wide spectrum of proteins, including RNA helicases, polymerases and, above all, exoribonucleases and endoribonucleases. For many years, it has been assumed that eukaryotes RNA cleavage relies mostly on the action of exoribonucleases, in contrast with prokaryotes, where RNA decay is mainly mediated by endoribonucleolytic processes (82, 101). In recent years, the unexpected implication of numerous endoribonucleases in the RNA turnover in eukaryotes significantly contributed to a change of perspective on the eukaryotic RNA metabolism (141). APE1 is among the several examples of recently identified enzymes whose endoribonucleolytic activity has been found to associate with the regulation of RNA stability. Evidence of its RNase H-like activity was first suggested by Barzilay *et al.* who demonstrated that APE1 is able to bind with relatively low affinity undamaged single- and double-stranded RNA molecules, albeit not exhibiting unspecific nuclease activity (9). Later on, it has been discovered that APE1 possesses the ability to cleave AP sites within single-stranded RNA molecules and that the nucleic acid secondary structure significantly influences the APE1 incision activity (12). Despite these first *in vitro* suggestions of APE1 biological relevance in the removal of AP-site-containing RNA, the unequivocal demonstration of APE1 involvement in RNA processing was brought only few years later. Very recently, in fact, Barnes *et al.* identified APE1 as the major endonuclease associated with polysomes and capable of cleaving the coding region determinant of the *c-myc* mRNA; thus, influencing *c-myc* half-life in cells (7). Surprisingly, recent biochemical studies performed using recombinant APE1 demonstrated that the APE1 endoribonuclease function is not limited to *c-myc* mRNA, but it may potentially influence the biogenesis and hence, the stability of other transcripts, including also miRNAs (77). These works demonstrated that APE1-mediated RNA cleavage occurred, *in vitro*, at single-stranded or weakly paired regions, preferentially 3′ of pyrimidines at UA, UG, and CA sites. This latter finding, in particular, led to hypothesize the possible involvement of APE1 in mRNA splicing events, since CA repeats are renowned as potent splicing modulators (15). Furthermore, the *in vivo* involvement of APE1 in RNA metabolic pathways was further corroborated by the observation of the APE1 association, through its N-terminal domain, with rRNA and the ribosome processing protein NPM1 within nucleoli (149). Furthermore, APE1 has been shown to interact with factors involved in the splicing process, such as the heterogeneous nuclear ribonucleoprotein L (81) [which is a key regulator of splicing that binds CA repeats with high affinity (65)], YB-1 (29, 119), as well as with proteins involved in the ribosome assembly and RNA maturation within cytoplasm (149).

So far, many studies have characterized the involvement of the APE1 C-terminal domain in RNA metabolism, demonstrating that the APE1 endoribonuclease activity and its nuclease function on DNA share the same active site (76). However, few groups have investigated the role of the unstructured N-terminal extension, possibly as a consequence of its disordered nature. A recent work published form our group systematically characterized the binding properties of the APE1 N-terminal disordered region towards nucleic acids and NPM1. We demonstrated that the N-terminus, in particular acquired Lys residues therein located, appear to be essential for the stabilization of both protein–protein and nucleic acids–protein interactions, as well as influencing the thermal stability of the protein. These evidences clearly support the notion that this unstructured domain might represent an evolutionary gain function necessary for mammals to cope with a progressively complex cellular environment (116).

In light of these recent findings and taking into account also previous reports on the pivotal role of APE1 disordered N-terminal region, we speculate that the targeting of this unfolded protein domain could be a valuable tool to interfere with the different APE1 functions *in vivo*.

Relevance of the Unstructured Domain of BER Proteins for Designing Novel Anticancer Strategies

BER proteins have been broadly explored as targets for cancer therapy (67); in particular, current approaches to cancer treatment report more effective results when specific DNA repair inhibitors are used in combination with DNA damaging drugs. The foremost rationale of the combined therapy is that impairment of BER enzymes is likely to sensitize cancer cells to chemotherapeutic agents. Druggable BER targets for cancer treatment include: FEN1, Polβ, APE1, and the poly [ADP-ribose] polymerase 1 (PARP1); while targeting of DNA glycosylases results inefficacious because of the functional redundancy of this class of enzymes (58).

In the last decade, remarkable attention has been posed on the development of PARP1 and APE1 inhibitors. The APE1 relevance for cell survival is demonstrated by the fact that

knocking out the APE1 gene induces either apoptosis in differentiated cells (69) or developmental failure during embryogenesis (158). Accumulating evidences have indicated that deregulation of APE1 in both expression and subcellular localization is indeed associated with different tumorigenic processes: APE1 upregulation or dysregulated expression has been described in a variety of cancers, including prostate, pancreatic, ovarian, cervical, germ cell, rhabdomyosarcoma, and colon (43, 92). Furthermore, it has been reported that elevated APE1 levels and anomalous intracellular localization are also typically correlated with aggressive proliferation and increased resistance to chemotherapeutic drugs and IR, implying that APE1 enhances repair and survival of tumor cells (92). Therefore, considering that APE1 expression appears to be linked to chemoresistance and taking into account that several studies have shown that decreasing APE1 levels may lead to cell growth arrest and to an increased cellular sensitivity to DNA damaging agents (44, 45, 85, 154), APE1 represents a promising target for pharmacological treatment. A description of all the APE1-targeting molecules currently under investigation is beyond the focus of this review, for an exhaustive review on APE1 inhibitors, the reader is redirected to (146). All the APE1 small-molecule inhibitors developed so far were designed to target specific APE1 functions, namely the DNA repair or the redox activity of the protein. It is however, still a matter of debate whether the enhanced sensitivity to cytotoxic agents observed upon APE1 inhibition is solely related to the loss of DNA repair activity, or is also linked to the loss of its transcriptional regulatory function, or both. Despite the efforts aimed at determining the relative importance of the attenuation of the APE1's repair or transcriptional functions, all currently available APE1 inhibitors display limited specificity for cancer cells. Therefore, exploration of novel opportunities for APE1 targeting is obviously a path that deserves further consideration. Based on several observations attesting the critical role of disordered segments in many BER enzyme functions, we propose that the N-terminal unstructured portion of the APE1 protein could be considered as a new potential target for cancer therapy. Classical pharmacological strategies usually target structured regions of proteins; however, considering the biological relevance of intrinsically disordered proteins, the ability to interfere with their interactions opens enormous potentials for drug discovery. Actually, there is a continuous progress in the development of small molecules directed against disordered protein regions; several low molecular weight compounds are effective in the specific inhibition of molecular interactions based on intrinsically disordered domains. For example, small molecules binding the disordered regions of *c-myc*, Aβ, EWS-Fli1 have recently been discovered (100, 144). Although the binding of a small molecule to a disordered region/protein may appear counterintuitive due to the intrinsic poor selectivity, this may also be considered a major advantage because it would facilitate the screening of initial compounds, which affinity and specificity could be successively improved through standard molecular optimization procedures.

In conclusion, we suggest that it would be interesting to investigate novel pharmacological approaches aimed at interfering with the APE1 N-terminal region in light of its important role in the coordination of many different functions of the protein, both in DNA repair and RNA metabolism.

Conclusions and Speculations

Different independent studies provided *in vitro* and *in vivo* evidence that many DNA repair proteins, particularly in the BER pathway (*e.g.,* APE1), are involved in RNA metabolism. Interestingly, many of these proteins are also part of the nucleolar proteome where they bind specific carrier proteins (*e.g.,* NPM1, NCL) and rRNA. Upon genotoxic stress, many DNA repair proteins exit from nucleoli and switch their interactome network from proteins involved in RNA metabolism to DNA repair complexes. Although still in the early phases, these findings have raised many questions and speculations concerning the role of these proteins, including APE1 as a paradigmatic example, in RNA metabolism. For instance:

1. Why should a protein involved in DNA repair play a role in RNA metabolism? One possible explanation is that this duality would preserve genetic stability not only through the DNA repair activity, but also through the ability to cleanse damaged RNA that may otherwise be inaccurately translated, or degrade unwanted foreign RNA (*e.g.,* viral RNA).
2. Do the redox function of APE1 and its role in RNA metabolism represent two sides of the same coin devoted to modulate gene expression through transcriptional and post-transcriptional mechanisms? Modulation of APE1 subcellular distribution through its redox status may represent an elegant, specific, and energetically economic mechanism to tune gene expression upon genotoxic stress conditions.
3. Is APE1 an ancient protein with a newly identified and yet unappreciated role? The current information regarding the primary amino acid sequence of APE1 across species seems to suggest a phylogenetic "gain-of-function" and hence, support this hypothesis. However, further experimental and bioinformatics studies of APE1 orthologs may reveal additional insights into this question.
4. Suppressing the amount of APE1 has proven effective in sensitizing cancer cells to chemotherapeutic agents. This finding has led to the proposal that selective inhibition of the APE1 DNA repair activity is an attractive avenue for the development of novel anticancer therapies. Similarly, one can envision targeting the non-DNA repair functions of APE1, namely its RNA-repair and/or RNA-cleavage activities, as novel approaches for the treatment of cancer or neurological disorders. Nonetheless, such therapeutic aims still need further studies to increase our understanding of the role of APE1 in its noncanonical functions.

In closing, a productive cross-talk between DNA repair enzymes and proteins involved in RNA metabolism seems reasonable and nucleolus is emerging as a dynamic functional hub that coordinates cell growth arrest and DNA repair mechanisms. These findings will drive further analysis of other BER proteins, such as FEN1, and might imply that nucleic acid processing enzymes are more versatile than originally thought and may have evolved DNA-targeted functions after a prior life in the early RNA world. The observation of cytoplasmic localization for canonical DNA repair proteins, such as APE1, simply beyond their mitochondrial targeting, may therefore, suggest much more than just an "abnormal" distribution pattern.

Acknowledgments

We regret the omission of many important references due to space limitations. This work was supported by grants from: AIRC (IG10269) and MIUR (FIRB_RBRN07BMCT) to G.T.

References

1. Aas PA, Otterlei M, Falnes PO, Vågbø CB, Skorpen F, Akbari M, Sundheim O, Bjørås M, Slupphaug G, Seeberg E, and Krokan HE. Human and bacterial oxidative demethylases repair alkylation damage in both RNA and DNA. *Nature* 421: 859–863, 2003.
2. Adelmant G, Calkins AS, Garg BK, Card JD, Askenazi M, Miron A, Sobhian B, Zhang Y, Nakatani Y, Silver PA, Iglehart JD, Marto JA, and Lazaro J. DNA ends alter the molecular composition and localization of Ku multicomponent complexes. *Mol Cell Proteomics* 11: 411–421, 2012.
3. Ahmad Y, Boisvert FM, Gregor P, Cobley A, and Lamond AI. NOPdb: Nucleolar Proteome Database—2008 update. *Nucleic Acids Res* 37: D181–D184, 2009.
4. Andersen JS, Lyon CE, Fox AH, Leung AK, Lam YW, Steen H, Mann M, and Lamond AI. Directed proteomic analysis of the human nucleolus. *Curr Biol* 12: 1–11, 2002.
5. Andersen JS, Lam YW, Leung AKL, Ong S, Lyon CE, Lamond AI, and Mann M. Nucleolar proteome dynamics. *Nature* 433: 77–83, 2005.
6. Banerjee D, Mandal SM, Das A, Hegde ML, Das S, Bhakat KK, Boldogh I, Sarkar PS, Mitra S, and Hazra TK. Preferential repair of oxidized base damage in the transcribed genes of mammalian cells. *J Biol Chem* 286: 6006–6016, 2011.
7. Barnes T, Kim W, Mantha AK, Kim S, Izumi T, Mitra S, and Lee CH. Identification of Apurinic/apyrimidinic endonuclease 1 (APE1) as the endoribonuclease that cleaves c-myc mRNA. *Nucleic Acids Res* 37: 3946–3958, 2009.
8. Barthelmes HU, Habermeyer M, Christensen MO, Mielke C, Interthal H, Pouliot JJ, Boege F, and Marko D. TDP1 overexpression in human cells counteracts DNA damage mediated by topoisomerases I and II. *J Biol Chem* 279: 55618–55625, 2004.
9. Barzilay G, Walker LJ, Robson CN, and Hickson ID. Site-directed mutagenesis of the human DNA repair enzyme HAP1: identification of residues important for AP endonuclease and RNase H activity. *Nucleic Acids Res* 23: 1544–1550, 1995.
10. Beernink PT, Segelke BW, Hadi MZ, Erzberger JP, Wilson DM, and Rupp B. Two divalent metal ions in the active site of a new crystal form of human apurinic/apyrimidinic endonuclease, Ape1: implications for the catalytic mechanism. *J Mol Biol* 307: 1023–1034, 2001.
11. Bellacosa A and Moss EG. RNA repair: damage control. *Curr Biol* 13: R482–R484, 2003.
12. Berquist BR, McNeill DR, and Wilson DM. Characterization of abasic endonuclease activity of human Ape1 on alternative substrates, as well as effects of ATP and sequence context on AP site incision. *J Mol Biol* 379: 17–27, 2008.
13. This reference has been deleted.
14. Bhakat KK, Izumi T, Yang S, Hazra TK, and Mitra S. Role of acetylated human AP-endonuclease (APE1/Ref-1) in regulation of the parathyroid hormone gene. *EMBO J* 22: 6299–6309, 2003.
15. Black DL. Mechanisms of alternative pre-messenger RNA splicing. *Annu Rev Biochem* 72: 291–336, 2003.
16. Blander G, Zalle N, Daniely Y, Taplick J, Gray MD, and Oren M. DNA damage-induced translocation of the Werner helicase is regulated by acetylation. *J Biol Chem* 277: 50934–50940, 2002.
17. Boisvert F, Lam YW, Lamont D, and Lamond AI. A quantitative proteomics analysis of subcellular proteome localization and changes induced by DNA damage. *Mol Cell Proteomics* 9: 457–470, 2010.
18. Boisvert F, van Koningsbruggen S, Navascues J, and Lamond AI. The multifunctional Nucleolus. *Nat Rev Mol Cell Biol* 8: 574–585, 2007.
19. Borggrefe T, Wabl M, Akhmedov AT, and Jessberger R. A B-cell-specific DNA recombination complex. *J Biol Chem* 273: 17025–17035, 1998.
20. Boulon S, Westman BJ, Hutten S, Boisvert F, and Lamond AI. The nucleolus under stress. *Mol Cell* 40: 216–227, 2010.
21. Boyd MT, Vlatkovic N, and Rubbi CP. The nucleolus directly regulates p53 export and degradation. *J Cell Biol* 194: 689–703, 2011.
22. Buckwalter CA, Lin AH, Tanizawa A, Pommier YG, Cheng YC, and Kaufmann SH. RNA synthesis inhibitors alter the subnuclear distribution of DNA topoisomerase I. *Cancer Res* 56: 1674–1681, 1996.
23. Burger K, Mühl B, Harasim T, Rohrmoser M, Malamoussi A, Orban M, Kellner M, Gruber-Eber A, Kremmer E, Hölzel M, and Eick D. Chemotherapeutic drugs inhibit ribosome biogenesis at various levels. *J Biol Chem* 285: 12416–12425, 2010.
24. Busso CS, Iwakuma T, and Izumi T. Ubiquitination of mammalian AP endonuclease (APE1) regulated by the p53-MDM2 signaling pathway. *Oncogene* 28: 1616–1625, 2009.
25. Campalans A, Amouroux R, Bravard A, Epe B, and Radicella JP. UVA irradiation induces relocalisation of the DNA repair protein hOGG1 to nuclear speckles. *J Cell Sci* 120: 23–32, 2007.
26. Canitrot Y, Cazaux C, Fréchet M, Bouayadi K, Lesca C, Salles B, and Hoffmann JS. Overexpression of DNA polymerase beta in cell results in a mutator phenotype and a decreased sensitivity to anticancer drugs. *Proc Natl Acad Sci USA* 95: 12586–12590, 1998.
27. Carmo-Fonseca M, Mendes-Soares L, and Campos I. To be or not to be in the nucleolus. *Nat Cell Biol* 2: E107–E112, 2000.
28. Chang MS, Sasaki H, Campbell MS, Kraeft SK, Sutherland R, Yang CY, Liu Y, Auclair D, Hao L, Sonoda H, Ferland LH, and Chen LB. HRad17 colocalizes with NHP2L1 in the nucleolus and redistributes after UV irradiation. *J Biol Chem* 274: 36544–36549, 1999.
29. Chattopadhyay R, Das S, Maiti AK, Boldogh I, Xie J, Hazra TK, Kohno K, Mitra S, and Bhakat KK. Regulatory role of human AP-endonuclease (APE1/Ref-1) in YB-1-mediated activation of the multidrug resistance gene MDR1. *Mol Cell Biol* 28: 7066–7080, 2008.
30. Cohen AA, Geva-Zatorsky N, Eden E, Frenkel-Morgenstern M, Issaeva I, Sigal A, Milo R, Cohen-Saidon C, Liron Y, Kam Z, Cohen L, Danon T, Perzov N, and Alon U. Dynamic proteomics of individual cancer cells in response to a drug. *Science* 322: 1511–1516, 2008.
31. Colombo E, Alcalay M, and Pelicci PG. Nucleophosmin and its complex network: a possible therapeutic target in hematological diseases. *Oncogene* 30: 2595–2609, 2011.
32. Coulon S, Noguchi E, Noguchi C, Du L, Nakamura TM, and Russell P. Rad22Rad52-dependent repair of ribosomal DNA repeats cleaved by Slx1-Slx4 endonuclease. *Mol Biol Cell* 17: 2081–2090, 2006.

32a. Couté Y, Burgess JA, Diaz JJ, Chichester C, Lisacek F, Greco A, and Sanchez JC. Deciphering the human nucleolar proteome. *Mass Spectrom Rev* 25: 215–234, 2006.

33. Crampton N, Kodiha M, Shrivastava S, Umar R, and Stochaj U. Oxidative stress inhibits nuclear protein export by multiple mechanisms that target FG nucleoporins and Crm1. *Mol Biol Cell* 20: 5106–5116, 2009.
34. Daniely Y, Dimitrova DD, and Borowiec JA. Stress-dependent nucleolin mobilization mediated by p53-nucleolin complex formation. *Mol Cell Biol* 22: 6014–6022, 2002.
35. Das S, Chattopadhyay R, Bhakat KK, Boldogh I, Kohno K, Prasad R, Wilson SH, and Hazra TK. Stimulation of NEIL2-mediated oxidized base excision repair via YB-1 interaction during oxidative stress. *J Biol Chem* 282: 28474–28484, 2007.
36. Dejmek J, Iglehart JD, and Lazaro J. DNA-dependent protein kinase (DNA-PK)-dependent cisplatin-induced loss of nucleolar facilitator of chromatin transcription (FACT) and regulation of cisplatin sensitivity by DNA-PK and FACT. *Mol Cancer Res* 7: 581–591, 2009.
37. Demple B, Herman T, and Chen DS. Cloning and expression of APE, the cDNA encoding the major human apurinic endonuclease: definition of a family of DNA repair enzymes. *Proc Natl Acad Sci USA* 88: 11450–11454, 1991.
38. Ding Q, Markesbery WR, Chen Q, Li F, and Keller JN. Ribosome dysfunction is an early event in Alzheimer's disease. *J Neurosci* 25: 9171–9175, 2005.
39. Eckert-Boulet N and Lisby M. Regulation of rDNA stability by sumoylation. *DNA Repair (Amst)* 8: 507–516, 2009.
40. Emmott E and Hiscox JA. Nucleolar targeting: the hub of the matter. *EMBO Rep* 10: 231–238, 2009.
41. Essers J, Vermeulen W, and Houtsmuller AB. DNA damage repair: anytime, anywhere?. *Curr Opin Cell Biol* 18: 240–246, 2006.
42. Fantini D, Vascotto C, Marasco D, D'Ambrosio C, Romanello M, Vitagliano L, Pedone C, Poletto M, Cesaratto L, Quadrifoglio F, Scaloni A, Radicella JP, and Tell G. Critical lysine residues within the overlooked N-terminal domain of human APE1 regulate its biological functions. *Nucleic Acids Res* 38: 8239–8256, 2010.
43. Fishel ML and Kelley MR. The DNA base excision repair protein Ape1/Ref-1 as a therapeutic and chemopreventive target. *Mol Aspects Med* 28: 375–395, 2007.
44. Fishel ML, He Y, Reed AM, Chin-Sinex H, Hutchins GD, Mendonca MS, and Kelley MR. Knockdown of the DNA repair and redox signaling protein Ape1/Ref-1 blocks ovarian cancer cell and tumor growth. *DNA Repair (Amst)* 7: 177–186, 2008.
45. Fishel ML, He Y, Smith ML, and Kelley MR. Manipulation of base excision repair to sensitize ovarian cancer cells to alkylating agent temozolomide. *Clin Cancer Res* 13: 260–267, 2007.
46. Francia S, Michelini F, Saxena A, Tang D, de Hoon M, Anelli V, Mione M, Carninci P, and d'Adda di Fagagna F. Site-specific DICER and DROSHA RNA products control the DNA-damage response. *Nature* 488: 231–235, 2012.
47. Fuxreiter M, Tompa P, Simon I, Uversky VN, Hansen JC, and Asturias FJ. Malleable machines take shape in eukaryotic transcriptional regulation. *Nat Chem Biol* 4: 728–737, 2008.
48. Gao H, Chen X, and McGowan CH. Mus81 endonuclease localizes to nucleoli and to regions of DNA damage in human S-phase cells. *Mol Biol Cell* 14: 4826–4834, 2003.
49. Gjerset RA and Bandyopadhyay K. Regulation of p14ARF through subnuclear compartmentalization. *Cell Cycle* 5: 686–690, 2006.
50. Gorman MA, Morera S, Rothwell DG, de La Fortelle E, Mol CD, Tainer JA, Hickson ID, and Freemont PS. The crystal structure of the human DNA repair endonuclease HAP1 suggests the recognition of extra-helical deoxyribose at DNA abasic sites. *EMBO J* 16: 6548–6558, 1997.
51. Griffiths LM, Swartzlander D, Meadows KL, Wilkinson KD, Corbett AH, and Doetsch PW. Dynamic compartmentalization of base excision repair proteins in response to nuclear and mitochondrial oxidative stress. *Mol Cell Biol* 29: 794–807, 2009.
52. Grisendi S, Mecucci C, Falini B, and Pandolfi PP. Nucleophosmin and cancer. *Nat Rev Cancer* 6: 493–505, 2006.
53. Guerra-Rebollo M, Mateo F, Franke K, Huen MSY, Lopitz-Otsoa F, Rodríguez MS, Plans V, and Thomson TM. Nucleolar exit of RNF8 and BRCA1 in response to DNA damage. *Exp Cell Res* 318: 2365–2376, 2012.
54. Guo Z, Qian L, Liu R, Dai H, Zhou M, Zheng L, and Shen B. Nucleolar localization and dynamic roles of flap endonuclease 1 in ribosomal DNA replication and damage repair. *Mol Cell Biol* 28: 4310–4319, 2008.
55. Hanakahi LA, Bu Z, and Maizels N. The C-terminal domain of nucleolin accelerates nucleic acid annealing. *Biochemistry* 39: 15493–15499, 2000.
56. Hayakawa H, Uchiumi T, Fukuda T, Ashizuka M, Kohno K, Kuwano M, and Sekiguchi M. Binding capacity of human YB-1 protein for RNA containing 8-oxoguanine. *Biochemistry* 41: 12739–12744, 2002.
57. Hegde ML, Banerjee S, Hegde PM, Bellot LJ, Hazra TK, Boldogh I, and Mitra S. Enhancement of NEIL1 protein-initiated oxidized DNA base excision repair by heterogeneous nuclear ribonucleoprotein U (hnRNP-U) via direct interaction. *J Biol Chem* 287: 34202–34211, 2012.
58. Hegde ML, Hazra TK, and Mitra S. Early steps in the DNA base excision/single-strand interruption repair pathway in mammalian cells. *Cell Res* 18: 27–47, 2008.
59. Hegde ML, Hazra TK, and Mitra S. Functions of disordered regions in mammalian early base excision repair proteins. *Cell Mol Life Sci* 67: 3573–3587, 2010.
60. Hegde V, Wang M, and Deutsch WA. Characterization of human ribosomal protein S3 binding to 7,8-dihydro-8-oxoguanine and abasic sites by surface plasmon resonance. *DNA Repair (Amst)* 3: 121–126, 2004.
61. Hegde V, Wang M, and Deutsch WA. Human ribosomal protein S3 interacts with DNA base excision repair proteins hAPE/Ref-1 and hOGG1. *Biochemistry* 43: 14211–14217, 2004.
62. Herandez-Verdun D, Roussel P, Thiry M, Sirri V, and Lafontaine DLJ. The nucleolus: structure/function relationship in RNA metabolism. *Wiley Interdiscip Rev RNA* 1: 415–431, 2010.
63. Hinsby AM, Kiemer L, Karlberg EO, Lage K, Fausbøll A, Juncker AS, Andersen JS, Mann M, and Brunak S. A wiring of the human nucleolus. *Mol Cell* 22: 285–295, 2006.
64. Horn HF and Vousden KH. Cancer: Guarding the guardian? *Nature* 427: 110–111, 2004.
65. Hung L, Heiner M, Hui J, Schreiner S, Benes V, and Bindereif A. Diverse roles of hnRNP L in mammalian mRNA processing: a combined microarray and RNAi analysis. *RNA* 14: 284–296, 2008.
66. Ikeda S, Biswas T, Roy R, Izumi T, Boldogh I, Kurosky A, Sarker AH, Seki S, and Mitra S. Purification and characterization of human NTH1, a homolog of *Escherichia coli* endonuclease III. Direct identification of Lys-212 as the active nucleophilic residue. *J Biol Chem* 273: 21585–21593, 1998.
67. Illuzzi JL and Wilson DM. Base excision repair: contribution to tumorigenesis and target in anticancer treatment paradigms. *Curr Med Chem* 19: 3922–3936, 2012.

68. Izumi T and Mitra S. Deletion analysis of human AP-endonuclease: minimum sequence required for the endonuclease activity. *Carcinogenesis* 19: 525–527, 1998.
69. Izumi T, Brown DB, Naidu CV, Bhakat KK, Macinnes MA, Saito H, Chen DJ, and Mitra S. Two essential but distinct functions of the mammalian abasic endonuclease. *Proc Natl Acad Sci USA* 102: 5739–5743, 2005.
70. Jackson EB, Theriot CA, Chattopadhyay R, Mitra S, and Izumi T. Analysis of nuclear transport signals in the human apurinic/apyrimidinic endonuclease (APE1/Ref1). *Nucleic Acids Res* 33: 3303–3312, 2005.
71. Jarboui MA, Bidoia C, Woods E, Roe B, Wynne K, Elia G, Hall WW, and Guatier VW. Nucleolar protein trafficking in response to HIV-1 Tat: rewiring the nucleolus. *PLoS One* 7: e48702, 2012.
72. This reference has been deleted.
73. Jobert L, Skjeldam HK, Dalhus B, Galashevskaya A, Vagbo CB, Bjoras M, and Nilsen H. The human base excision repair enzyme SMUG1 directly interacts with DKC1 and contributes to RNA quality control. *Mol Cell* 49: 339–345, 2013.
74. Ju B, Solum D, Song EJ, Lee K, Rose DW, Glass CK, and Rosenfeld MG. Activating the PARP-1 sensor component of the groucho/TLE1 corepressor complex mediates a CaM-Kinase IIdelta-dependent neurogenic gene activation pathway. *Cell* 119: 815–829, 2004.
75. Karmakar P and Bohr VA. Cellular dynamics and modulation of WRN protein is DNA damage specific. *Mech Ageing Dev* 126: 1146–1158, 2005.
76. Kim W, Berquist BR, Chohan M, Uy C, Wilson DM3, and Lee CH. Characterization of the endoribonuclease active site of human apurinic/apyrimidinic endonuclease 1. *J Mol Biol* 411: 960–971, 2011.
77. Kim W, King D, and Lee CH. RNA-cleaving properties of human apurinic/apyrimidinic endonuclease 1 (APE1). *Int J Biochem Mol Biol* 1: 12–25, 2010.
78. Ko SI, Park J, Park MJ, Kim J, Kang L, and Han YS. Human ribosomal protein S3 (hRpS3) interacts with uracil-DNA glycosylase (hUNG) and stimulates its glycosylase activity. *Mutat Res* 648: 54–64, 2008.
79. Koike A, Nishikawa H, Wu W, Okada Y, Venkitaraman AR, and Ohta T. Recruitment of phosphorylated NPM1 to sites of DNA damage through RNF8-dependent ubiquitin conjugates. *Cancer Res* 70: 6746–6756, 2010.
80. Kruhlak M, Crouch EE, Orlov M, Montaño C, Gorski SA, Nussenzweig A, Misteli T, Phair RD, and Casellas R. The ATM repair pathway inhibits RNA polymerase I transcription in response to chromosome breaks. *Nature* 447: 730–734, 2007.
81. Kuninger DT, Izumi T, Papaconstantinou J, and Mitra S. Human AP-endonuclease 1 and hnRNP-L interact with a nCaRE-like repressor element in the AP-endonuclease 1 promoter. *Nucleic Acids Res* 30: 823–829, 2002.
82. Kushner SR. mRNA decay in prokaryotes and eukaryotes: different approaches to a similar problem. *IUBMB Life* 56: 585–594, 2004.
83. Lam YW, Lamond AI, Mann M, and Andersen JS. Analysis of nucleolar protein dynamics reveals the nuclear degradation of ribosomal proteins. *Curr Biol* 17: 749–760, 2007.
84. Lam YW, Trinkle-Mulcahy L, and Lamond AI. The nucleolus. *J Cell Sci* 118: 1335–1337, 2005.
85. Lau JP, Weatherdon KL, Skalski V, and Hedley DW. Effects of gemcitabine on APE/ref-1 endonuclease activity in pancreatic cancer cells, and the therapeutic potential of antisense oligonucleotides. *Br J Cancer* 91: 1166–1173, 2004.
86. Lee C, Smith BA, Bandyopadhyay K, and Gjerset RA. DNA damage disrupts the p14ARF-B23(nucleophosmin) interaction and triggers a transient subnuclear redistribution of p14ARF. *Cancer Res* 65: 9834–9842, 2005.
87. Lewinska A, Wnuk M, Grzelak A, and Bartosz G. Nucleolus as an oxidative stress sensor in the yeast *Saccharomyces cerevisiae*. *Redox Rep* 15: 87–96, 2010.
88. Li Z, Wu J, and Deleo CJ. RNA damage and surveillance under oxidative stress. *IUBMB Life* 58: 581–588, 2006.
89. Lirussi L, Antoniali G, Vascotto C, D'Ambrosio C, Poletto M, Romanello M, Marasco D, Leone M, Quadrifoglio F, Bhakat KK, Scaloni A, and Tell G. Nucleolar accumulation of APE1 depends on charged lysine residues that undergo acetylation upon genotoxic stress and modulate its BER activity in cells. *Mol Biol Cell* 23: 4079–4096, 2012.
90. Liu Y, Prasad R, and Wilson SH. HMGB1: roles in base excision repair and related function. *Biochim Biophys Acta* 1799: 119–130, 2010.
90a. Lo SJ, Lee CC, and Lai HJ. The nucleolus: reviewing oldies to have new understandings. *Cell Res* 16: 530–538, 2006.
91. Loeb LA and Preston BD. Mutagenesis by apurinic/apyrimidinic sites. *Annu Rev Genet* 20: 201–230, 1986.
92. Luo M, He H, Kelley MR, and Georgiadis MM. Redox regulation of DNA repair: implications for human health and cancer therapeutic development. *Antioxid Redox Signal* 12: 1247–1269, 2010.
93. Mao Y, Mehl IR, and Muller MT. Subnuclear distribution of topoisomerase I is linked to ongoing transcription and p53 status. *Proc Natl Acad Sci USA* 99: 1235–1240, 2002.
94. Marciniak RA, Lombard DB, Johnson FB, and Guarente L. Nucleolar localization of the Werner syndrome protein in human cells. *Proc Natl Acad Sci USA* 95: 6887–6892, 1998.
95. Mastrocola AS and Heinen CD. Nuclear reorganization of DNA mismatch repair proteins in response to DNA damage. *DNA Repair (Amst)* 9: 120–133, 2010.
96. Mayer C and Grummt I. Cellular stress and nucleolar function. *Cell Cycle* 4: 1036–1038, 2005.
97. Meder VS, Boeglin M, de Murcia G, and Schreiber V. PARP-1 and PARP-2 interact with nucleophosmin/B23 and accumulate in transcriptionally active nucleoli. *J Cell Sci* 118: 211–222, 2005.
98. Mekhail K, Gunaratnam L, Bonicalz M, and Lee S. HIF activation by pH-dependent nucleolar sequestration of VHL. *Nat Cell Biol* 6: 642–647, 2004.
99. Menoni KH, Hoeijmakers JH, and Vermeulen W. Nucleotide excision repair-initiating proteins bind to oxidative DNA lesions *in vivo*. *J Cell Biol* 199: 1037–1046, 2012.
100. Metallo SJ. Intrinsically disordered proteins are potential drug targets. *Curr Opin Chem Biol* 14: 481–488, 2010.
101. Meyer S, Temme C, and Wahle E. Messenger RNA turnover in eukaryotes: pathways and enzymes. *Crit Rev Biochem Mol Biol* 39: 197–216, 2004.
102. Milkereit P, Gadal O, Podtelejnikov A, Trumtel S, Gas N, Petfalski E, Tollervey D, Mann M, Hurt E, and Tschochner H. Maturation and intranuclear transport of pre-ribosomes requires Noc proteins. *Cell* 105: 499–509, 2001.
103. Milkereit P, Strauss D, Bassler J, Gadal O, Kuhn H, Schutz S, Gas N, Lechner J, Hurt E, and Tschochner H. A Noc complex specifically involved in the formation and nuclear export of ribosomal 40 S subunits. *J Biol Chem* 278: 4072–4081, 2003.
104. Mo X and Dynan WS. Subnuclear localization of Ku protein: functional association with RNA polymerase II elongation sites. *Mol Cell Biol* 22: 8088–8099, 2002.

105. Montanaro L, Trerè D, and Derenzini M. Nucleolus, ribosomes, and cancer. *Am J Pathol* 173: 301–310, 2008.
106. Moore HM, Bai B, Boisvert F, Latonen L, Rantanen V, Simpson JC, Pepperkok R, Lamond AI, and Laiho M. Quantitative proteomics and dynamic imaging of the nucleolus reveal distinct responses to UV and ionizing radiation. *Mol Cell Proteomics* 10: M111.009241, 2011.
107. Moreira PI, Nunomura A, Nakamura M, Takeda A, Shenk JC, Aliev G, Smith MA, and Perry G. Nucleic acid oxidation in Alzheimer disease. *Free Radic Biol Med* 44: 1493–1505, 2008.
108. Nalabothula N, Indig FE, and Carrier F. The nucleolus takes control of protein trafficking under cellular stress. *Mol Cell Pharmacol* 2: 203–212, 2010.
108a. Nishimura Y, Ohkubo T, Furuichi Y, and Umekawa H. Tryptophans 286 and 288 in the C-terminal region of protein B23.1 are important for its nucleolar localization. *Biosci Biotechnol Biochem* 66: 2239–2242, 2002.
109. Nunomura A, Moreira PI, Castellani RJ, Lee H, Zhu X, Smith MA, and Perry G. Oxidative damage to RNA in aging and neurodegenerative disorders. *Neurotox Res* 22: 231–248, 2012.
110. Olson MO and Dundr M. The moving parts of the nucleolus. *Histochem Cell Biol* 123: 203–216, 2005.
111. Ougland R, Zhang C, Liiv A, Johansen RF, Seeberg E, Hou Y, Remme J, and Falnes PØ. AlkB restores the biological function of mRNA and tRNA inactivated by chemical methylation. *Mol Cell* 16: 107–116, 2004.
112. Park MS, Knauf JA, Pendergrass SH, Coulon CH, Strniste GF, Marrone BL, and MacInnes MA. Ultraviolet-induced movement of the human DNA repair protein, Xeroderma pigmentosum type G, in the nucleus. *Proc Natl Acad Sci USA* 93: 8368–8373, 1996.
113. Pavri R, Lewis B, Kim T, Dilworth FJ, Erdjument-Bromage H, Tempst P, de Murcia G, Evans R, Chambon P, and Reinberg D. PARP-1 determines specificity in a retinoid signaling pathway via direct modulation of mediator. *Mol Cell* 18: 83–96, 2005.
114. Pederson T. The nucleolus. *Cold Spring Harbor Perspect Biol* 3: 1–15, 2011.
115. Pederson T and Tsai RY. In search of nonribosomal nucleolar protein function and regulation. *J Cell Biol* 184: 771–776, 2009.
116. Poletto M, Vascotto C, Scognamiglio PL, Lirussi L, Marasco D, and Tell G. Role of the unstructured N-terminal domain of the human apurinic/apyrimidinic endonuclease 1 (hAPE1) in the modulation of its interaction with nucleic acids and nucleophosmin (NPM1). *Biochem J* 452: 545–557, 2013.
117. Pérez-Castro AJ and Freire R. Rad9B responds to nucleolar stress through ATR and JNK signalling, and delays the G1-S transition. *J Cell Sci* 125: 1152–1164, 2012.
118. Radivojac P, Iakoucheva LM, Oldfield CJ, Obradovic Z, Uversky VN, and Dunker AK. Intrinsic disorder and functional proteomics. *Biophys J* 92: 1439–1456, 2007.
119. Raffetseder U, Frye B, Rauen T, Jürchott K, Royer H, Jansen PL, and Mertens PR. Splicing factor SRp30c interaction with Y-box protein-1 confers nuclear YB-1 shuttling and alternative splice site selection. *J Biol Chem* 278: 18241–18248, 2003.
120. Rancourt A and Satoh MS. Delocalization of nucleolar poly(ADP-ribose) polymerase-1 to the nucleoplasm and its novel link to cellular sensitivity to DNA damage. *DNA Repair (Amst)* 8: 286–297, 2009.
121. Raska I, Shaw PJ, and Cmarko D. Structure and function of the nucleolus in the spotlight. *Curr Opin Cell Biol* 18: 325–334, 2006.
122. Rieker C, Engblom D, Kreiner G, Domanskyi A, Schober A, Stotz S, Neumann M, Yuan X, Grummt I, Schütz G, and Parlato R. Nucleolar disruption in dopaminergic neurons leads to oxidative damage and parkinsonism through repression of mammalian target of rapamycin signaling. *J Neurosci* 31: 453–460, 2011.
123. Rubbi CP and Milner J. Non-activated p53 co-localizes with sites of transcription within both the nucleoplasm and the nucleolus. *Oncogene* 19: 85–96, 2000.
124. Rubbi CP and Milner J. Disruption of the nucleolus mediates stabilization of p53 in response to DNA damage and other stresses. *EMBO J* 22: 6068–6077, 2003.
125. Scherl A, Couté Y, Déon C, Callé A, Kindbeiter K, Sanchez J, Greco A, Hochstrasser D, and Diaz J. Functional proteomic analysis of human nucleolus. *Mol Biol Cell* 13: 4100–4109, 2002.
126. Schramm VL. Enzymatic N-riboside scission in RNA and RNA precursors. *Curr Opin Chem Biol* 1: 323–331, 1997.
127. Sekhar KR, Reddy YT, Reddy PN, Crooks PA, Venkateswaran A, McDonald WH, Geng L, Sasi S, Van Der Waal RP, Roti JLR, Salleng KJ, Rachakonda G, and Freeman ML. The novel chemical entity YTR107 inhibits recruitment of nucleophosmin to sites of DNA damage, suppressing repair of DNA double-strand breaks and enhancing radiosensitization. *Clin Cancer Res* 17: 6490–6499, 2011.
128. Sengupta S, Mantha AK, Mitra S, and Bhakat KK. Human AP endonuclease (APE1/Ref-1) and its acetylation regulate YB-1-p300 recruitment and RNA polymerase II loading in the drug-induced activation of multidrug resistance gene MDR1. *Oncogene* 30: 482–493, 2011.
129. Shcherbik N and Pestov DG. Ubiquitin and ubiquitin-like proteins in the nucleolus: multitasking tools for a ribosome factory. *Genes Cancer* 1: 681–689, 2010.
130. Sirri V, Urcuqui-Inchima S, Roussel P, and Hernandez-Verdun D. Nucleolus: the fascinating nuclear body. *Histochem Cell Biol* 129: 13–31, 2008.
131. Stark LA and Taliansky M. Old and new faces of the nucleolus. Workshop on the Nucleolus and Disease. *EMBO Rep* 10: 35–40, 2009.
132. Stein A, Pache RA, Bernadó P, Pons M, and Aloy P. Dynamic interactions of proteins in complex networks: a more structured view. *FEBS J* 276: 5390–5405, 2009.
133. Strauss PR and Holt CM. Domain mapping of human apurinic/apyrimidinic endonuclease. Structural and functional evidence for a disordered amino terminus and a tight globular carboxyl domain. *J Biol Chem* 273: 14435–14441, 1998.
134. Suzuki A, Kogo R, Kawahara K, Sasaki M, Nishio M, Maehama T, Sasaki T, Mimori K, and Mori M. A new PICTure of nucleolar stress. *Cancer Sci* 103: 632–637, 2012.
135. Tanaka M, Chock PB, and Stadtman ER. Oxidized messenger RNA induces translation errors. *Proc Natl Acad Sci USA* 104: 66–71, 2007.
136. Tell G, Damante G, Caldwell D, and Kelley MR. The intracellular localization of APE1/Ref-1: more than a passive phenomenon? *Antioxid Redox Signal* 7: 367–384, 2005.
137. Tell G, Quadrifoglio F, Tiribelli C, and Kelley MR. The many functions of APE1/Ref-1: not only a DNA repair enzyme. *Antioxid Redox Signal* 11: 601–620, 2009.
138. Tell G, Wilson DM, and Lee CH. Intrusion of a DNA repair protein in the RNome world: is this the beginning of a new era? *Mol Cell Biol* 30: 366–371, 2010.

139. Tembe V and Henderson BR. Protein trafficking in response to DNA damage. *Cell Signal* 19: 1113–1120, 2007.
140. Thayer MM, Ahern H, Xing D, Cunningham RP, and Tainer JA. Novel DNA binding motifs in the DNA repair enzyme endonuclease III crystal structure. *EMBO J* 14: 4108–4120, 1995.
141. Tomecki R and Dziembowski A. Novel endoribonucleases as central players in various pathways of eukaryotic RNA metabolism. *RNA* 16: 1692–1724, 2010.
142. Trotta C, Lund E, Kahan L, Johnson A, and Dahlberg J. Coordinated nuclear export of 60S ribosomal subunits and NMD3 in vertebrates. *EMBO J* 22: 2841–2851, 2003.
143. Tóth-Petróczy A, Simon I, Fuxreiter M, and Levy Y. Disordered tails of homeodomains facilitate DNA recognition by providing a trade-off between folding and specific binding. *J Am Chem Soc* 131: 15084–15085, 2009.
144. Uversky VN. Intrinsically disordered proteins and novel strategies for drug discovery. *Expert Opin Drug Discov* 7: 475–488, 2012.
145. Uversky VN, Oldfield CJ, and Dunker AK. Showing your ID: intrinsic disorder as an ID for recognition, regulation and cell signaling. *J Mol Recognit* 18: 343–384, 2005.
146. Vascotto C and Fishel ML. Blockade of base excision repair: inhibition of small lesions results in big consequences to cancer cells. In: *DNA Repair in Cancer Therapy*, edited by Kelley MR. San Diego, CA: Academic Press, 2012, pp. 29–53.
147. Vascotto C, Bisetto E, Li M, Zeef LAH, D'Ambrosio C, Domenis R, Comelli M, Delneri D, Scaloni A, Altieri F, Mavelli I, Quadrifoglio F, Kelley MR, and Tell G. Knock-in reconstitution studies reveal an unexpected role of Cys-65 in regulating APE1/Ref-1 subcellular trafficking and function. *Mol Biol Cell* 22: 3887–3901, 2011.
148. Vascotto C, Cesaratto L, Zeef LAH, Deganuto M, D'Ambrosio C, Scaloni A, Romanello M, Damante G, Taglialatela G, Delneri D, Kelley MR, Mitra S, Quadrifoglio F, and Tell G. Genome-wide analysis and proteomic studies reveal APE1/Ref-1 multifunctional role in mammalian cells. *Proteomics* 9: 1058–1074, 2009.
149. Vascotto C, Fantini D, Romanello M, Cesaratto L, Deganuto M, Leonardi A, Radicella P, Kelley M, D'Ambrosio C, Scaloni A, Quadrifoglio F, and Tell G. APE1/Ref-1 interacts with NPM1 within Nucleoli and plays a role in the rRNA quality control process. *Mol Cell Biol* 29: 1834–1854, 2009.
150. Vascotto C, Lirussi L, Poletto M, Tiribelli M, Damiani D, Fabbro D, Damante G, Demple B, Colombo E, and Tell G. Functional regulation of the apurinic/apyrimidinic endonuclease APE1 by nucleophosmin (NPM1): impact on tumor biology. *Oncogene* (in press); doi:10.1038/onc.2013.251
151. Vassiliou GS, Cooper JL, Rad R, Li J, Rice S, Uren A, Rad L, Ellis P, Andrews R, Banerjee R, Grove C, Wang W, Liu P, Wright P, Arends M, and Bradley A. Mutant nucleophosmin and cooperating pathways drive leukemia initiation and progression in mice. *Nat Genet* 43: 470–475, 2011.
152. Vidal AE, Hickson ID, Boiteux S, and Radicella JP. Mechanism of stimulation of the DNA glycosylase activity of hOGG1 by the major human AP endonuclease: bypass of the AP lyase activity step. *Nucleic Acids Res* 29: 1285–1292, 2001.
153. Vuzman D, Azia A, and Levy Y. Searching DNA via a "Monkey Bar" mechanism: the significance of disordered tails. *J Mol Biol* 396: 674–684, 2010.
154. Wang D, Luo M, and Kelley MR. Human apurinic endonuclease 1 (APE1) expression and prognostic significance in osteosarcoma: enhanced sensitivity of osteosarcoma to DNA damaging agents using silencing RNA APE1 expression inhibition. *Mol Cancer Ther* 3: 679–686, 2004.
155. Wilson DM3, Deutsch WA, and Kelley MR. Drosophila ribosomal protein S3 contains an activity that cleaves DNA at apurinic/apyrimidinic sites. *J Biol Chem* 269: 25359–25364, 1994.
156. Woo LL, Futami K, Shimamoto A, Furuichi Y, and Frank KM. The Rothmund-Thomson gene product RECQL4 localizes to the nucleolus in response to oxidative stress. *Exp Cell Res* 312: 3443–3457, 2006.
157. Xanthoudakis S and Curran T. Identification and characterization of Ref-1, a nuclear protein that facilitates AP-1 DNA-binding activity. *EMBO J* 11: 653–665, 1992.
158. Xanthoudakis S, Smeyne RJ, Wallace JD, and Curran T. The redox/DNA repair protein, Ref-1, is essential for early embryonic development in mice. *Proc Natl Acad Sci USA* 93: 8919–8923, 1996.
159. Yacoub A, Kelley MR, and Deutsch WA. The DNA repair activity of human redox/repair protein APE/Ref-1 is inactivated by phosphorylation. *Cancer Res* 57: 5457–5459, 1997.
160. Yanagawa H, Ogawa Y, and Ueno M. Redox ribonucleosides. Isolation and characterization of 5-hydroxyuridine, 8-hydroxyguanosine, and 8-hydroxyadenosine from Torula yeast RNA. *J Biol Chem* 267: 13320–13326, 1992.
161. Yang C, Kim MS, Chakravarty D, Indig FE, and Carrier F. Nucleolin binds to the proliferating cell nuclear antigen and inhibits nucleotide excision repair. *Mol Cell Pharmacol* 1: 130–137, 2009.
162. Yang C, Maiguel DA, and Carrier F. Identification of nucleolin and nucleophosmin as genotoxic stress-responsive RNA-binding proteins. *Nucleic Acids Res* 30: 2251–2260, 2002.
163. Yankiwski V, Marciniak RA, Guarente L, and Neff NF. Nuclear structure in normal and Bloom syndrome cells. *Proc Natl Acad Sci USA* 97: 5214–5219, 2000.
164. This reference has been deleted.
165. Yoshida A, Pourquier P, and Pommier Y. Purification and characterization of a Mg2+-dependent endonuclease (AN34) from etoposide-treated human leukemia HL-60 cells undergoing apoptosis. *Cancer Res* 58: 2576–2582, 1998.
166. Yoshida A, Urasaki Y, Waltham M, Bergman A, Pourquier P, Rothwell DG, Inuzuka M, Weinstein JN, Ueda T, Appella E, Hickson ID, and Pommier Y. Human apurinic/apyrimidinic endonuclease (Ape1) and its N-terminal truncated form (AN34) are involved in DNA fragmentation during apoptosis. *J Biol Chem* 278: 37768–37776, 2003.
167. This reference has been deleted.
168. Zhou J, Ahn J, Wilson SH, and Prives C. A role for p53 in base excision repair. *EMBO J* 20: 914–923, 2001.

Address correspondence to:
Prof. Gianluca Tell
Department of Medical and Biological Sciences
University of Udine
P.Le M. Kolbe 4
Udine 33100
Italy

E-mail: gianluca.tell@uniud.it

Date of first submission to ARS Central, July 8, 2013; date of acceptance, July 22, 2013.

Abbreviations Used

8-OHG = 8-hydroxyguanosine
AD = Alzheimer's disease
AP = apurinic/apyrimidinic
APE1 = apurinic/apyrimidinic endonuclease 1
ATM = ataxia telangiectasia mutated
ATR = ataxia telangiectasia and Rad3-related
BER = base excision repair
CRM1 = exportin 1
DDR = DNA damage response
DSB = double-strand break
FEN1 = flap endonuclease 1
hMYH = human MutY glycosylase homolog
HR = homologous recombination
IR = ionizing radiation
NCL = nucleolin
NEIL2 = endonuclease VIII-like 2
NER = nucleotide excision repair
NHEJ = nonhomologous end joining
NLS = nuclear localization signal
NPM1 = nucleophosmin 1
NoLS = nucleolar localization sequence
NTH1 = endonuclease III-like glycosylase
OGG1 = 8-OHG DNA glycosylase
PARP1 = poly [ADP-ribose] polymerase 1
PCNA = proliferating cell nuclear antigen
PD = Parkinson disease
PNC = perinucleolar compartment
Polβ = DNA polymerase β
Pol I = RNA polymerase I
PTMs = post-translational modifications
rDNA = ribosomal DNA
rRNA = ribosomal RNA
RP = ribosomal protein
RPA = replication protein A
snoRNA = small nucleolar RNA
SSB = single-strand break
WRN = Werner syndrome helicase
XRCC1 = X-ray repair cross-complementing protein 1
Xth = exonuclease III
YB-1 = Y box binding protein 1

Biochem. J. (2013) **452**, 545–557 (Printed in Great Britain) doi:10.1042/BJ20121277

online data

Role of the unstructured N-terminal domain of the hAPE1 (human apurinic/apyrimidinic endonuclease 1) in the modulation of its interaction with nucleic acids and NPM1 (nucleophosmin)

Mattia POLETTO*, Carlo VASCOTTO*, Pasqualina L. SCOGNAMIGLIO†‡, Lisa LIRUSSI*, Daniela MARASCO†‡ and Gianluca TELL*[1]

*Department of Medical and Biological Sciences, University of Udine, 33100 Udine, Italy, †Department of Pharmacy, CIRPEB (Centro Interuniversitario di Ricerca sui Peptidi Bioattivi), University of Naples 'Federico II', 80134 Naples, Italy, and ‡Institute of Biostructures and Bioimaging CNR, 80134 Naples, Italy

The hAPE1 (human apurinic/apyrimidinic endonuclease 1) is an essential enzyme, being the main abasic endonuclease in higher eukaryotes. However, there is strong evidence to show that hAPE1 can directly bind specifi gene promoters, thus modulating their transcriptional activity, even in the absence of specifi DNA damage. Recent f ndings, moreover, suggest a role for hAPE1 in RNA processing, which is modulated by the interaction with NPM1 (nucleophosmin). Independent domains account for many activities of hAPE1; however, whereas the endonuclease and the redox-active portions of the protein are well characterized, a better understanding of the role of the unstructured N-terminal region is needed. In the present study, we characterized the requirements for the interaction of hAPE1 with NPM1 and undamaged nucleic acids. We show that DNA/RNA secondary structure has an impact on hAPE1 binding in the absence of damage. Biochemical studies, using the isolated N-terminal region of the protein, reveal that the hAPE1 N-terminal domain represents an evolutionary gain of function, since its composition affects the protein's stability and ability to interact with both nucleic acids and NPM1. Although required, however, this region is not suff cient itself to stably interact with DNA or NPM1.

Key words: apurinic/apyrimidinic endonuclease 1 (APE1), nucleophosmin (NPM1), protein–DNA interaction, protein–protein interaction, phylogenesis.

INTRODUCTION

The hAPE1 [human APE1 (apurinic/apyrimidinic endonuclease 1)] is an essential and multifaceted protein involved in the DNA BER (base excision repair) pathway and in the regulation of gene expression, acting both as a redox co-activator for several transcription factors and as a transcriptional repressor on nCaRE (negative calcium response elements)-containing promoters [1–3]. These biological activities are located in two distinct, but partially overlapping, regions. The conserved C-terminal portion (residues 61–318) is responsible for the enzymatic activity on abasic DNA, whereas the N-terminal domain (residues 1–127) is mainly devoted to the redox co-activating function towards different transcription factors such as Egr1 (early growth response 1), NF-κB (nuclear factor κB) and p53 [4,5]. The mechanisms of hAPE1 binding and recognition of its canonical substrate, the abasic site containing DNA, have been thoroughly investigated by several laboratories [6–8]. However, the notion that hAPE1 is constitutively bound to undamaged nucleic acids is getting stronger. Examples include the interaction of the protein with genomic regions, such as the nCaRE sequences [2] or the *MDR1* (multidrug resistance protein 1) gene promoter [9], and the reported association of hAPE1 with undamaged RNA [10]. Acquisition of particular secondary structures (i.e. bulges, hairpins, cruciforms, quadruplex etc.) by nucleic acids and their regulatory roles *in vivo* are a well-known paradigm in molecular biology. A previous study has carefully explored the interaction between hAPE1 and undamaged nucleic acids [11]; nonetheless, potential impacts of the secondary structure of the nucleic acid on the binding affinit of hAPE1 have never been investigated.

In the last few years, an unexpected involvement of hAPE1 in RNA metabolism has been unveiled: the protein is accumulated within nucleoli through interaction with NPM1 (nucleophosmin; also known as nucleolar phosphoprotein B23) and rRNA and affects cell growth by directly acting on the RNA quality control mechanisms [10,12,13]. Notably, the N-terminal domain of hAPE1 (the f rst 43 residues) plays a pivotal role in this non-canonical function of the protein, serving as an adaptable device for protein–protein interactions and modulating its enzymatic activity on abasic DNA, as well as its binding to RNA molecules. Although many studies have thoroughly characterized the structure of the hAPE1 C-terminal globular domain, only a few have addressed the role of its N-terminal extension, perhaps as a consequence of its intrinsic disordered folding [14–16]. A basic cluster of lysine residues located within this region (Lys^{25}–Lys^{35}) controls the binding affinit of hAPE1 for both NPM1 and nucleic acids. Furthermore, several strands of evidence suggest that the different functions of hAPE1 might be rapidly modulated *in vivo* by post-translational modification on its N-terminal domain, such as ubiquitination, acetylation and proteolysis [2,17–21]. Interestingly, whereas the C-terminal portion of the protein shares extensive similarity with most of its orthologue counterparts, from *Escherichia coli* to mammals, its N-terminal extension is considerably less conserved. The importance of this protein region in modulating the many activities of hAPE1 suggests that the N-terminal domain may be a recent acquisition during evolution

Abbreviations used: APE1, apurinic/apyrimidinic endonuclease 1; BER, base excision repair; DSP, dithiobis(succinimidyl propionate); DTT, dithiothreitol; FBS, fetal bovine serum; GST, glutathione transferase; hAPE1, human APE1; MAT, metal-affinity tag; nCaRE: negative calcium response elements; NPM1, nucleophosmin; PLA, proximity ligation assay; RU, response unit; SPR, surface plasmon resonance; zAPE1, zebrafish APE1.

[1] To whom correspondence should be addressed (email gianluca.tell@uniud.it).

[17], as already suggested for other BER proteins [22]. Aberrant hAPE1 expression and localization patterns have been linked to neurodegeneration and cancer; therefore, many groups are currently directing their efforts to develop specifi small-molecule modulators of the different activities of the protein [23].

In the present study, we systematically characterized the functional properties of the hAPE1 N-terminal domain, exploring its nucleic acid-binding properties and its role in hAPE1–NPM1 interaction. In an effort to better characterize the features guiding the binding of hAPE1 to undamaged nucleic acids, we used a combined approach based on SPR (surface plasmon resonance), EMSA analyses and GST (glutathione transferase) pull-down experiments. The results of the present study show that the aff nity of hAPE1 for nucleic acids is enhanced by certain structural elements and that the nucleic acid-binding activity of hAPE1 is promoted by the N-terminal extension of the protein. This region, although necessary for both the stabilization of the hAPE1–nucleic acids and hAPE1–NPM1 interactions, shows only a weak affinit for DNA or NPM1 when isolated from the hAPE1 globular domain. Finally, exploiting a 'domain swapping' approach, we demonstrate that lysine residues located within the N-terminal domain of hAPE1 represent a phylogenetic gain of function for the protein, since the composition of this domain influence the stability of the protein and its ability to interact with both nucleic acids and NPM1. Altogether, these data highlight the role for the hAPE1 N-terminal region in modulating the many functions of this pleiotropic protein. Further structural analyses on this overlooked extension of the protein would be therefore worthwhile in order to fully understand the substrate specificit of hAPE1 and to design new anti-cancer drugs targeting this protein.

EXPERIMENTAL

Cell culture and transient transfection experiments

HeLa cells were grown in DMEM (Dulbecco's modifie Eagle's medium) supplemented with 10 % FBS (fetal bovine serum), 100 units/ml penicillin and 10 mg/ml streptomycin sulfate. At 1 day before transfection, cells were seeded in 10-cm plates at a density of 3×10^6 cells/plate. Cells were then transiently transfected with 6 μg of either pcDNA5.1 (empty vector) or pcDNA5.1-hAPE1 (full-length or amino acids 1–49) plasmids per dish using the Lipofectamine™ 2000 Reagent (Invitrogen) according to the manufacturer's instructions. Cells were harvested at 24 h after transfection.

Multiple sequence alignments

For the multiple sequence alignments full-length hAPE1 orthologous metazoan sequences (human, *Pan troglodytes*, *Macaca mulatta*, *Equus caballus*, *Mus musculus*, *Rattus norvegicus*, *Canis lupus familiaris*, *Sus scrofa*, *Bos taurus*, *Ornithorhyncus anatinus*, *Salmo salar*, *Gasterosteus aculeatus*, *Danio rerio*, *Xenopus tropicalis and Xenopus laevis*) were retrieved from the RefSeq protein database using the BLAST algorithm (http://blast.ncbi.nlm.nih.gov/Blast.cgi) and aligned using the ClustalW2 program with default parameters (http://www.ebi.ac.uk/Tools/msa/clustalw2/).

Western blotting analyses

The protein samples were electrophoresed by SDS/PAGE (10–18 % gels) or discontinuous Tris/Tricine SDS/PAGE [24]. Proteins were then transferred on to nitrocellulose membranes (PerkinElmer), developed as described previously [12] using an ECL (enhanced chemiluminescence) procedure (GE Healthcare) and then quantifie by using a ChemiDoc XRS video-densitometer (Bio-Rad Laboratories).

Plasmids and expression of recombinant proteins

The constructs pGEX-3X-hAPE1 and pGEX-3X-zAPE1, encoding for the GST-fused hAPE1 and zAPE1 (zebrafis APE1) full-length proteins respectively, were provided by Dr Mark R. Kelley (Indiana University, Indianapolis, IN, U.S.A.). The plasmid encoding for full-length GST–NPM1 was provided by Dr P.G. Pelicci (European Institute of Oncology, Milan, Italy). The pTAC-MAT/hAPE1 and the pETM-20/zAPE1 constructs, encoding for C-terminal-tagged MAT (metal-aff nity tag)–hAPE1 and His_6–zAPE1 respectively, were generated by subcloning. All proteins were expressed in *E. coli* BL21(DE3) cells, induced with 1 mM IPTG (isopropyl β-D-thiogalactopyranoside) and then purifie on an ÄKTA Purifie FPLC system (GE Healthcare) by using a GSTrap HP column (GE Healthcare) for the GST-tagged proteins, or a HisTrap HP column (GE Healthcare) for the His_6- and MAT-tagged proteins. The quality of purificatio was checked by SDS/PAGE analysis. Extensive dialysis against PBS was performed to remove any trace of imidazole from the HisTrap-purifie proteins. Accurate quantificatio of all recombinant proteins was performed by colorimetric Bradford assays (Bio-Rad Laboratories) and confirme by SDS/PAGE and Western blotting analysis. To remove the GST tag, GST–hAPE1 was further hydrolysed with Factor X_a as described previously [17]. The zAPE1 K27 'swapping mutant' and the hAPE1 NΔ43 and zAPE1 NΔ36 deletion mutants, as well as the hAPE1 1–48 and 1–49 constructs, were generated using the QuikChange Mutagenesis kit (Stratagene) and the respective full-length constructs as templates, following the manufacturer's instructions and using standard subcloning procedures.

GST pull-down assays with RNA or NPM1 and co-immunoprecipitation

The indicated amount of GST-tagged protein was mixed, together with the prey protein or 10 μg of total RNA, with 10 μl of glutathione–Sepharose 4B beads (GE Healthcare). RNA was extracted using the TRIzol® Reagent (Invitrogen). Binding was performed in PBS supplemented with 5 mM DTT (dithiothreitol) and 0.5 mM PMSF for 2 h under rotation at 4 °C. The beads were washed three times with washing buffer [PBS supplemented with 0.1 % Igepal CA-630 (Sigma), 5 mM DTT and 0.5 mM PMSF]. Beads were then resuspended in Laemmli sample buffer for Western blotting analyses or in TRIzol® Reagent for RNA extraction and rRNA quantification The levels of 28S and 18S rRNA transcripts were determined as described previously [17] by using the iScript cDNA synthesis kit (Bio-Rad Laboratories) according to the manufacturer's instructions. Quantitative PCR was then performed in an iQ5 multicolour real-time PCR detection system (Bio-Rad Laboratories) according to the manufacturer's protocol. GST-tagged proteins were detected with an HRP (horseradish peroxidase)-conjugated anti-GST antibody (Sigma), whereas the prey proteins were detected using the indicated antibodies. Co-immunoprecipitation analyses were performed as described previously [12].

DSP [dithiobis(succinimidyl propionate)] cross-linking

The indicated amounts of recombinant NPM1 and hAPE1 (either full-length or the amino acids 1–48 peptide), were allowed to

interact at 37 °C for 15 min in a total volume of 10 μl; DSP (2 μg in DMSO) was added and cross-linking was carried out for 30 min at room temperature (22 °C). The reactions were quenched by adding 0.5 volumes of ice-cold 0.4 M ammonium acetate and incubating on ice for 10 min. Non-reducing Laemmli sample buffer was immediately added and the samples were separated by SDS/PAGE (8 % gel).

Immunofluorescence confocal analyses and PLA (proximity ligation assay)

Immunofluorescenc was carried out as described previously [12]. FLAG-tagged 1–49 hAPE1 was labelled using an anti-FLAG antibody and stained with a secondary anti-mouse Alexa Fluor™ 488-conjugated antibody (Jackson ImmunoResearch). Nuclei were counterstained with DAPI (4′,6-diamidino-2-phenylindole). For the PLA analyses we used the Duolink II® reagent kit (Olink Bioscience); cells were fi ed in 4 % (w/v) paraformaldehyde, permeabilized with 0.25 % PBS-Triton (PBS with Triton X-100) and saturated with 10 % (v/v) FBS. Slides were incubated with primary antibodies (mouse anti-FLAG, 1:100 dilution and rabbit anti-NPM1, 1:200 dilution) and then reactions were carried out following the manufacturer's instructions. Microscope slides were mounted and visualized through a Leica TCS SP laser-scanning confocal microscope.

hAPE1–nucleic acid binding through EMSA

hAPE1 binding to nucleic acids was assessed as described previously [1] with some modifications Briefl , in order to reduce unspecifi binding and to obtain more define bound complexes, recombinant proteins or peptides were incubated at 37 °C with 250 pmol of unlabelled poly(dT) for 15 min and then 2.5 pmol of ^{32}P-labelled probe was added. The reactions were then incubated for further 15 min and separated by native PAGE (6–10 % gel) at 150 V for 4 h.

Southwestern assays

Bait proteins were separated using a pre-cast SDS/PAGE (Bio-Rad Laboratories), electrotransferred on to a nitrocellulose membrane and subsequently denatured and renatured by washing six times in 1:1 serial dilutions of 6 M guanidinium/HCl in EMSA buffer [40 mM Hepes (pH 8.0), 50 mM KCl, 2 mM EDTA, 10 % (v/v) glycerol and 1 mM DTT]. The membrane was then saturated in 5 % (w/v) BSA in EMSA buffer and incubated with 50 pmol of the indicated ^{32}P-labelled DNA probe at 37 °C, washed in EMSA buffer to remove unspecifi bound probe and f nally subjected to autoradiography.

SPR

Real-time binding assays were performed on a Biacore T-100 SPR instrument (GE Healthcare). Streptavidin was immobilized on to a research-grade CM5 sensor chip using amine-coupling chemistry. The immobilization steps were carried out at a f ow rate of 10 μl/min in Hepes buffer {20 mM Hepes, 150 mM NaCl, 3.4 mM EDTA, 0.005 % P20 surfactant and 0.1 mM TCEP [tris-(2-carboxyethyl)phosphine]}. All surfaces were simultaneously activated for 30 s with a mixture of NHS (*N*-hydroxysuccinimide; 0.05 M) and EDC [*N*-ethyl-*N*′-(3-dimethylaminopropyl)carbodiimide; 0.2 M]. Streptavidin was injected at a concentration of 20 μg/ml in 10 mM sodium acetate (pH 4.5) for 1 min. Ethanolamine (1 M, pH 8.5) was injected for 7 min to saturate the remaining activated groups. An average of 5000 RU (response units) of streptavidin was immobilized on each fl w cell. Biotinylated oligonucleotides were injected at a concentration of 500 nM until the desired level of immobilization was achieved (average value of 300 RU). Proteins were serially diluted in running buffer (80 nM–2.0 μM) and injected at 20 °C at a f ow rate of 60 μl/min for 1 min. Disruption of any complex that remained bound after a 5-min dissociation was achieved using a 30 s injection of 1 M NaCl at 100 μl/min. When the experimental data met the quality criteria, the kinetic parameters were estimated assuming a 1:1 binding model and using version 4.1 Evaluation Software (GE Healthcare). Conversely, an affinit steady-state model was applied to fi the RU_{max} data compared with the protein concentrations and fittin was performed with GraphPad Prism v4.00 [17].

CD

Far-UV CD spectra were recorded on a Jasco J-810 spectropolarimeter (JASCO) in a 195–260 nm interval. Experiments were performed employing a protein concentration of 5 μM in 10 mM phosphate buffer (pH 7.0), supplemented with 1 mM DTT and using a 0.1 cm path-length cuvette. Thermal denaturation profile were obtained by measuring the temperature dependence of the signal at 225 nm in the 20–100 °C range with a resolution of 0.5 °C and 1.0-nm bandwidth. A Peltier temperature controller was used to set up the temperature of the sample with the heating rate set to 1 °C/min. Data were collected at a 0.2-nm resolution, 20 nm/min scan speed and a 4 s response and were reported as the unfolded fraction against the temperature.

Statistical analyses

Statistical analyses were performed by using the Microsoft Excel data analysis software for Student's *t* test analysis. $P < 0.05$ was considered statistically significant

RESULTS AND DISCUSSION

The binding affinity of hAPE1 for undamaged nucleic acids is dependent on their secondary structure

Several studies have thoroughly characterized hAPE1 structure and its enzymatic activities on abasic DNA, examining its substrate specificit and recognition mechanisms [7,11,25–28]. However, when considering undamaged structured nucleic acids, the knowledge of hAPE1 substrate selectivity is still scarce. In the present study we sought to determine whether some particular structural features were favoured by hAPE1 when binding to nucleic acids. Hence, we used a biophysical approach exploiting the SPR technique to quantitatively measure the binding affinit of hAPE1 for intact oligonucleotides [29,30]. We compared the binding affinit of recombinant purifie full-length hAPE1 toward different single-stranded DNA probes, either intrinsically lacking secondary structure (i.e. 34dT), or having a stem and loop-like folding (e.g. Stem10 and Stem20) as predicted by bioinformatics analyses (Figure 1A and Table 1). The results of the SPR experiments (representative sensorgrams in Figure 1B and Supplementary Figure S1C at http://www.biochemj.org/bj/452/bj4520545add.htm) are summarized in Table 2. As already observed by Beloglazova et al. [11], an increased length in the stem region of the oligonucleotides augmented the affinit of hAPE1 for undamaged DNA (compare the Stem10 and the Stem20 sequences). This observation was confirme by direct EMSA experiments (Figure 1C) and by competition EMSA

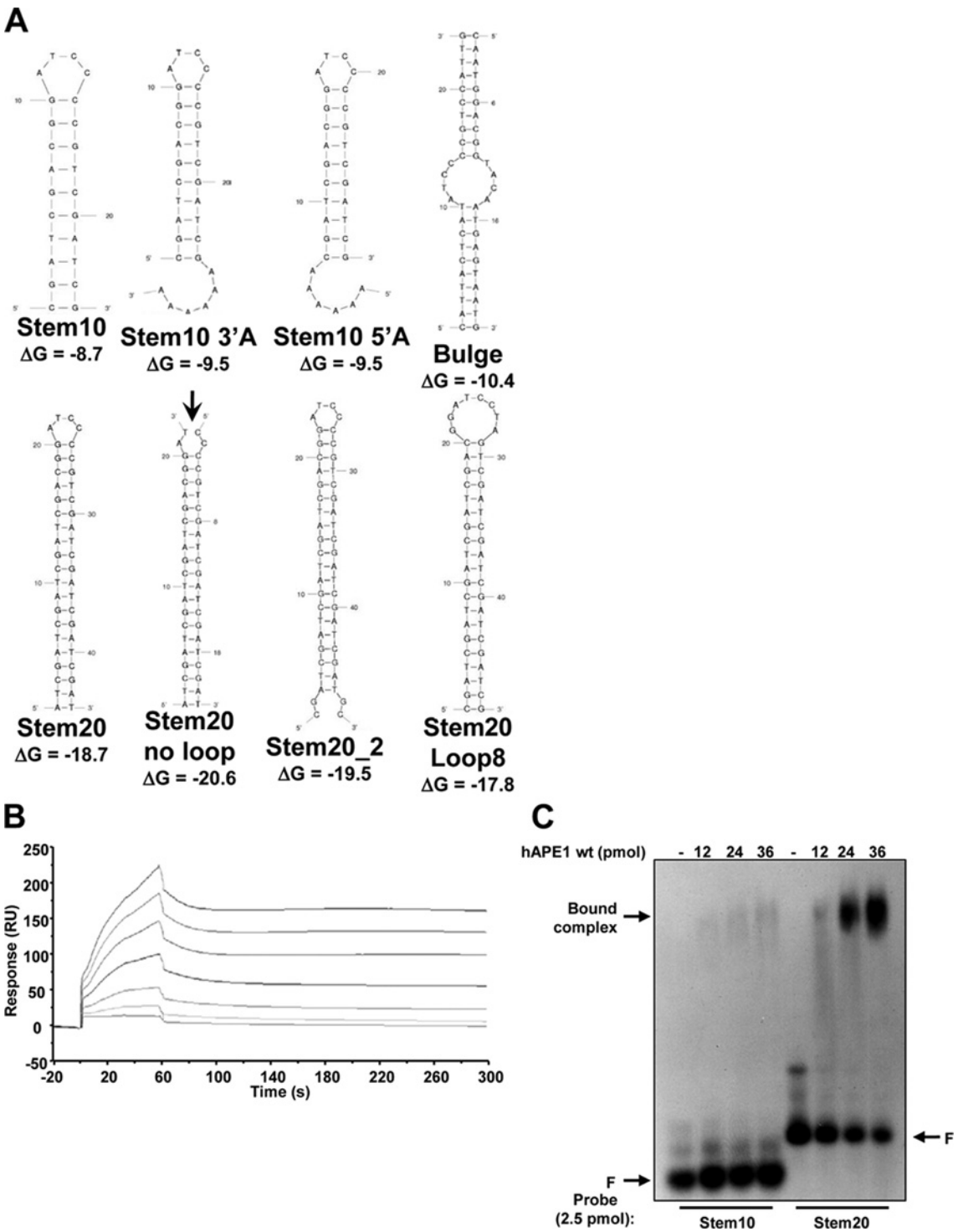

Figure 1 The secondary structure of the substrate determines the binding selectivity of hAPE1

(**A**) The predicted structures for the oligonucleotides used in the present study. Calculations were performed using either the Mfold web server (http://mfold.rna.albany.edu/?q=mfold) or the DINAMelt web server (http://mfold.rna.albany.edu/?q=DINAMelt). The calculated minimum free energy for folding (ΔG) at 37 °C and 50 mM Na^+ is also reported. The arrow indicates the absence of loop in the Stem20 no loop probe. (**B**) Representative overlay sensorgrams relative to a typical SPR experiment for the binding of hAPE1 to immobilized Biot-Stem20. The kinetic parameters were measured injecting purified recombinant hAPE1 solutions at increasing concentrations (i.e. 87.5, 175, 350, 700, 1050, 1400 and 1750 nM). The K_d values were estimated for each concentration using the BIAevaluation v.4.1 software. (**C**) Positive effect of the stem length on ability of hAPE1 to bind undamaged DNA as evaluated through EMSA using the Stem10 and Stem20 oligonucleotides (Table 1). For each reaction the indicated amount of purified recombinant hAPE1 was used. The results confirm a different binding capacity of hAPE1 towards double-stranded oligonucleotides of different lengths. The arrow indicates the hAPE1–DNA complexes, whereas F denotes the position of the free oligonucleotide probe. wt, wild-type.

Table 1 Oligonucleotide sequences used in the present study

The underlined nucleotides denote the position of the predicted loops.

Name	Sequence
34dT	5′-TTTTTTTTTTTTTTTTTTTTTTTTTTTTTTTTTT-3′
Stem10	5′-CGATCGACGGATCCCCGTCGATCG-3′
Stem10 3′ A	5′-CGATCGACGGATCCCCGTCGATCGAAAAAA-3′
Stem10 5′ A	5′-AAAAAACGATCGACGGATCCCCGTCGATCG-3′
Stem20	5′-ATCGATCGATCGATCGACGGATCCCCGTCGATCGATCGATCGATCGAT-3′
Stem20 no loop	Forward, 5′-ATCGATCGATCGATCGACGGAT-3′ and reverse, 5′-CCCCGTCGATCGATCGATCGAT-3′
Stem20_2	5′-CGATCGATCGATCGATCGACGGATCCCCGTCGATCGATCGATCGATGC-3′
Stem20 Loop8	5′-CGATCGATCGATCGATCGACGGATCCTAGTCGATCGATCGATCGATCG-3′
Bulge	Forward, 5′-CATTACTCATATCCCCGTCCATTG-3′ and reverse, 5′-CAATGGACGGTACAATGAGTAATG-3′
nCaRE_B2	Forward, 5′-TTTTTGAGACGGAGTTTCGCTCTTG-3′ and reverse, 5′-CAAGAGCGAAACTCCGTCTCAAAAA-3′

Table 2 Dissociation constants and kinetic parameters for the interaction of full-length hAPE1 with different undamaged oligonucleotides

Data reported were obtained through SPR analyses using hAPE1 as analyte on the indicated biotinylated oligonucleotide ligands. The kinetic parameters highlight the importance of secondary structure for the recognition of undamaged nucleic acids by hAPE1.

Ligand	k_{on} ($M^{-1} \cdot s^{-1} \times 10^5$)	k_{off} (s^{-1})	K_d (μM)
34dT	0.004	0.112	308 ± 3.00
Stem10	0.270	0.020	1.03 ± 0.02
Stem20	0.292	0.007	0.25 ± 0.01
Stem20 no loop	0.068	0.024	4.06 ± 0.01
Stem10 3′A	0.060	0.240	6.20 ± 0.01
Stem10 5′A	0.059	0.059	2.11 ± 0.03
Stem20_2	0.284	0.007	0.25 ± 0.01
Stem20 Loop8	0.061	0.004	0.74 ± 0.02
Bulge	0.834	0.019	0.23 ± 0.02
nCaRE_B2	0.270	0.105	3.90 ± 0.80

experiments demonstrating the poor competitive ability of the Stem10 toward the Stem20 oligonucleotide (results not shown). The effect of the presence of an intact loop structure on the stability of the protein–DNA complex then was investigated by comparing the affinities of the Stem20 and the Stem20 no loop sequences. Notably, hAPE1 showed a reduced affinity toward the ligand without a loop (approximately 16-fold, Table 2). Accordingly, EMSA experiments confirmed these findings, showing a more stable hAPE1–DNA complex in the presence of an intact loop (Supplementary Figures S1A and S1B). Furthermore, competitive EMSA assays demonstrated that the Stem20 probe was a more efficient competitor if compared with the Stem20 no loop (results not shown). Binding affinities were also negatively affected by the presence of an unstructured nucleotide stretch either 3′ or 5′ to the double-stranded stem region (compare Stem10 3′A and Stem10 5′A with the Stem10 sequence). Experimental data allowed us to speculate that the steric hindrance of a free poly(A) tail on the double-stranded region bound by hAPE1 might accelerate the dissociation rate, if protruding from the 3′-side. When using the same stem length the size of the loop region affected the binding: the expansion from 4 to 8 nucleotides reduced the affinity of hAPE1 approximately 3-fold (compare the Stem20_2 and the Stem20 Loop8 sequence). The difference in K_d value can be accounted for by a reduction in the association rate, suggesting that hAPE1 preferentially approaches the DNA molecules from the loop side as the stem side remains invariant between the two oligonucleotides. A lower stability of the stem region in the Stem20 Loop8 sequence could also reflect the decreased binding affinity bioinformatic predictions, however, do not suggest any major difference in the unfolding free energy of the two molecules (Figure 1A). We finally investigated whether the position of the unstructured region might affect the binding capacity of hAPE1 (compare Bulge, Stem20 and Stem20_2). Despite the differences in both the dissociation and the association rates, the overall affinity of hAPE1 for the oligonucleotides remained unchanged, suggesting that a local denaturation of the double helix, rather than its location within the double-stranded region, is a feature that enhances binding of hAPE1 to undamaged DNA. To compare our measurements on synthetic oligonucleotides with a physiologically relevant undamaged DNA substrate, we investigated the binding properties of hAPE1 towards an nCaRE duplex sequence, namely nCaRE_B2 (G. Antoniali, L. Lirussi, C. D'Ambrosio, F. Dal Piaz, C. Vascotto, D. Marasco, A. Scaloni, F. Fogolari and G. Tell, unpublished work). This sequence displayed a K_d value akin to that of the unstructured Stem20 no loop sequence (Table 2). It is worth pointing out that our *in vitro* assays, performed with the isolated purified recombinant protein, might underestimate the real affinity of hAPE1 for this sequence, since interactions with other protein partners [e.g. Ku70/80 and hnRNPL (heterogeneous nuclear ribonucleoprotein L)] significantly increase the protein–DNA complex stability, as already demonstrated previously (G. Antoniali, L. Lirussi, C. D'Ambrosio, F. Dal Piaz, C. Vascotto, D. Marasco, A. Scaloni, F. Fogolari and G. Tell, unpublished work) [31].

EMSA analyses were also performed on RNA substrates to test whether the nature of the sugar backbone might affect the binding activity of hAPE1 toward structured nucleic acids. The results obtained confirmed that the structural requirements for hAPE1 binding to undamaged substrates are not influenced by the composition of the sugar backbone (results not shown). These observations suggest that hAPE1 shows no apparent preference for DNA or RNA substrates, as long as the nucleic acid is undamaged and is endowed with a secondary structure. The results of the present study are in agreement with experimental data from other laboratories that have estimated K_d values for the interaction of hAPE1 with structured RNA that is similar to our values for DNA (~0.9 μM) [32]. It must be noted, however, that these experiments do not allow the exclusion of the existence of a differential affinity of hAPE1 for abasic site-containing DNA or RNA molecules, as has been suggested by others [12,26].

In summary, hAPE1 binding to undamaged nucleic acids appears to be strongly affected by the presence of secondary structural elements. In particular, the presence of a double-stranded region is a primary element required for hAPE1 binding. The occurrence of a single-stranded local distortion, moreover, greatly enhances the interaction with nucleic acids. These factors are corroborated by studies reporting a significant reduction in the APE activity of the protein on single-stranded unstructured (or poorly structured) substrates (e.g. [7]). The requirement of a double-stranded DNA region is conceivable, on the basis of the observation that hAPE1 contacts both of the DNA strands [27,28]. The presence of a loop or a bulge within a double-stranded stem could mimic a local denaturation region that resembles a baseless spot, hence explaining the increased affinity for loop-containing structures displayed *in vitro* by hAPE1.

The N-terminal domain contributes to nucleic acid-binding by hAPE1

We have shown previously that the N-terminal 33 amino acids of hAPE1 is able itself to bind RNA oligonucleotides in solution [17]. Sequence alignment analyses, performed on different metazoan

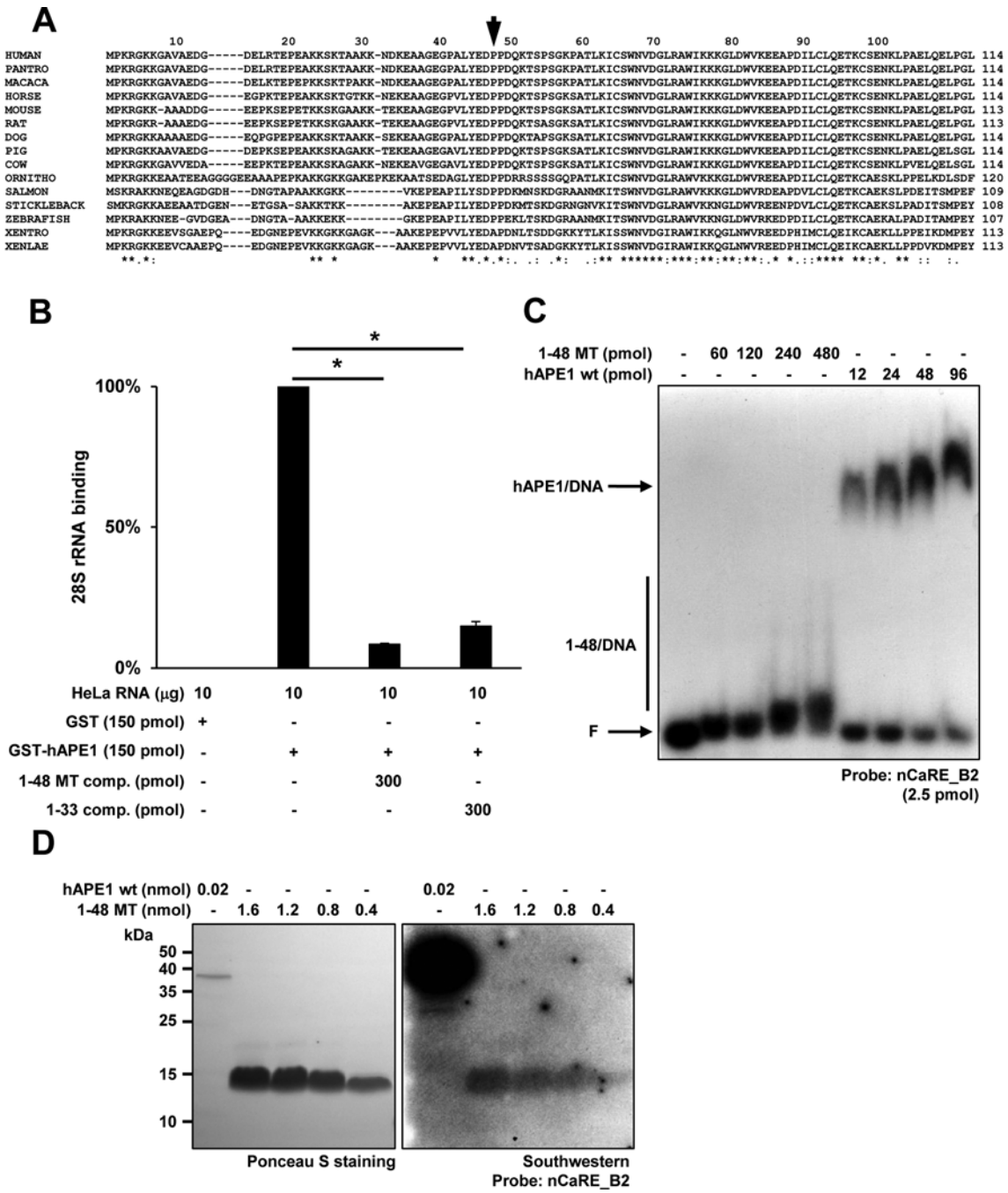

Figure 2 The isolated N-terminal region of hAPE1 interacts weakly with nucleic acids

(**A**) Multiple sequence alignment between full-length APE1 protein sequences from 15 different metazoan species. Only the N-terminal region of the alignment is reported. The arrow indicates the beginning of the high-similarity region within the C-terminal globular domain; whereas the N-terminal part of the sequences is significantly less conserved. (**B**) The isolated recombinant 1–48 hAPE1 N-terminal peptide is able to compete (comp.) with the full-length protein for RNA binding. The binding ability of the peptide was evaluated through competition RNA pull down using GST-tagged full-length hAPE1 as the bait and whole HeLa RNA as the prey in the presence of the indicated competitor. To quantify the amount of residual hAPE1-bound rRNA the pulled-down RNA was then retrotranscribed and 28S or 18S rRNAs were amplified by real-time PCR. The affinity for the 18S rRNA was similar to that shown for the 28S (results not shown). The competition activity of the 1–48 hAPE1 peptide was also confirmed using an untagged synthetic 1–33 hAPE1 peptide. The histogram shows the relative affinity to rRNA with respect to the GST–hAPE1 sample. The error bars represent the S.D. ($n = 3$). *$P < 0.05$. (**C**) EMSA dose–response analysis showing that the 1–48 peptide binds undamaged DNA with a low affinity when compared with the full-length hAPE1 protein. For each reaction the indicated amount of purified recombinant protein was used. F denotes the position of the free oligonucleotide probe. (**D**) Southwestern blot assay showing a dose–response binding of the nCaRE_B2 duplex to the 1–48 peptide. The indicated amounts of protein or peptide were separated by SDS/PAGE, electrotransferred on to nitrocellulose membranes (left-hand panel) and probed with ^{32}P-labelled nCaRE_B2 (right-hand panel). Note the difference in binding affinity between the full-length hAPE1 protein and the isolated peptide. MT, Mat; wt, wild-type.

species, highlight that the phylogenetic conservation of the amino acid sequence among APE1 proteins from different organisms starts at position 48 in the human protein, and is significantl lower in the region spanning amino acids 1–48 (Figure 2A). In order to better clarify the relevance of the non-conserved N-terminal domain in modulating the binding ability of hAPE1 to nucleic

acids, we cloned and expressed in *E. coli* cells the 1–48 amino acid region of hAPE1 in fusion with a C-terminal MAT (Supplementary Figures S2A and S2B at http://www.biochemj.org/bj/452/bj4520545add.htm) and evaluated the binding properties of the recombinant purifie peptide toward different substrates, including DNA and RNA. We indirectly estimated the rRNA-binding activity of the peptide exploiting a GST pull-down competition strategy. In these experiments, the full-length GST–hAPE1 was used as the bait and total HeLa RNA as the prey, while either the recombinant purifie 1–48 peptide or its synthetic untagged 1–33 counterpart were used as soluble competitors. The data obtained revealed that both soluble peptides were able to compete with full-length hAPE1 for rRNA binding, independently of the presence of a tag (Figure 2B).

In order to compare the nucleic acid-binding activity of the 1–48 peptide and that of the full-length hAPE1 protein, we used EMSA analyses. Under our experimental conditions we observed a low-aff nity binding activity for the hAPE1 N-terminal peptide towards the nCaREB_2 duplex sequence (Figure 2C and Supplementary Figure S2C). Although at a reduced affinit , however, the interaction with DNA was specific as demonstrated by both Southwestern assays (Figure 2D and Supplementary Figure S2D) and Western blotting performed after the EMSA analysis (Supplementary Figure S2E). These results, along with the notion that the N-terminal 1–33 amino acid portion of hAPE1 is absolutely required for the stable interaction of the protein with nucleic acids [12,17], suggest that this lysine-rich region might act by stabilizing the association of hAPE1 with nucleic acids through electrostatic interactions, whereas the remaining C-terminal domain accounts for the specifi binding to DNA/RNA. Our data support a two-step model to describe the mechanism through which hAPE1 contacts nucleic acids. The unstructured N-terminal domain would be required for the preliminary low-affinit binding process in search of the proper lesion to be repaired, as suggested for other DNA-binding proteins [33]. Recognition of a local distortion (or an abasic site) involves and is stabilized by a higher-affinit binding event. The whole hAPE1 molecule would, at this point, become necessary for the recognition of the structured nucleic acid region. Intriguingly, this model nicely f ts previous hypothesis proposed by Masuda et al. [34] more than a decade ago.

The N-terminal domain of hAPE1 is necessary, but not sufficient, for a stable binding to NPM1

In our previous work, we demonstrated that the N-terminal 1–33 amino acid domain of hAPE1, besides being essential for stabilizing its binding to nucleic acids, is also required for a stable interaction with NPM1 [12] and that lysine residues spanning the region 27–35 of hAPE1 are directly involved in stabilizing this interaction [17]. However, we did not check whether the N-terminal domain of hAPE1 was able to directly bind to NPM1 itself. In an effort to better characterize the protein–protein interaction features of the hAPE1 N-terminal domain and its relative contribution to the overall binding, we analysed the ability of the 1–48 peptide to directly interact with NPM1. We expressed both the full-length hAPE1 and the 1–48 peptide in fusion with a MAT. The recombinant proteins were aff nity purifie and tested for their binding ability toward GST-tagged NPM1 through GST pull-down assays (Figure 3A). Although the full-length hAPE1 protein was able to directly interact with NPM1 (Figure 3A, left-hand panel), we failed to detect any stable peptide–NPM1 association *in vitro* (Figure 3A, right-hand panel), even under less stringent binding conditions (results not shown). This negative result prompted us to hypothesize that, if present, any peptide–NPM1 association could be too weak to be detected through a direct pull-down assay. We confirme this hypothesis through a competition GST pull-down assay, in which the 1–48 peptide was used to squelch the binding occurring between the full-length hAPE1 and GST–NPM1 (Figure 3B). The peptide, as well as an untagged full-length hAPE1, was able to displace the association between the MAT-tagged hAPE1 and GST–NPM1. However, whereas the competitor untagged hAPE1 was also efficientl recovered in the pulled-down fraction, the competitor 1–48 peptide was not. This indicates that the peptide was able to mask the hAPE1-binding site on NPM1, thus competing with the hAPE1–NPM1 association, although its interaction with the protein was too weak to be maintained during the washing steps. The observed competition effect could also be interpreted by assuming a masking effect of the peptide on the full-length hAPE1 N-terminal region, however, to the best of our knowledge, no oligomerization ability has ever been described for hAPE1.

To definitel prove the ability of the N-terminal peptide to directly associate with NPM1, we performed an *in vitro* stabilization of the complex exploiting the bifunctional cross-linker DSP (Figure 3C). As expected, treatment of NPM1 alone with DSP resulted in the stabilization of slow migrating oligomers, as documented previously [35]. Moreover, the full-length hAPE1 protein and its N-terminal peptide were detected as slow migrating signals only in the presence of both NPM1 and DSP, indicating a direct association for both with NPM1. The lower aff nity of the 1–48 peptide toward NPM1, in comparison with that of the full-length protein, indicates that the C-terminal domain of hAPE1 contributes to the stabilization of the protein–protein interaction.

To evaluate whether the interaction between the hAPE1 N-terminal extension and NPM1 also occurs *in vivo*, we created a HeLa cell line expressing a FLAG-tagged 1–49 hAPE1 peptide upon treatment with doxycycline, as already described previously [36]. As assessed using Western blotting, the peptide expression increased after the addition of doxycycline to the culture medium (Figure 4A, upper panel). Interestingly, the ectopically expressed peptide showed a peculiar localization pattern, being cytoplasmic and nuclear, but excluded from nucleoli (Figure 4A, lower panel), in contrast with the nuclear/nucleolar accumulation observed for the wild-type protein both under basal conditions [12,21] and when ectopically expressed (Figure 4A, lower panel). This result confirm that the C-terminal domain of hAPE1 contributes to the nucleolar accumulation of the protein within cells, despite the fact that the N-terminal domain retains the nuclear localization signal of the protein [37]. This phenomenon may be explained by the relevance that the C-terminal domain has in stabilizing both rRNA and NPM1 binding. By exploiting this cell model, we performed co-immunoprecipitation experiments and demonstrated the occurrence of a molecular interaction between NPM1 and the isolated hAPE1 N-terminal peptide. However, the FLAG-tagged 1–49 peptide was only able to co-precipitate NPM1 poorly when compared with the full-length protein (Figure 4B). This result parallels our *in vitro* results with recombinant purifie proteins and confirm that the unstructured N-terminal region of hAPE1 does indeed interact with NPM1, albeit with a lower affinit in the absence of the remaining C-terminal domain. We further confirme the presence of an interaction occurring between the FLAG-tagged 1–49 hAPE1 peptide and endogenous NPM1 using a PLA [21], which allows the quantificatio of physical proximity between molecules at a distance lower than 40 nm (Supplementary Figure S3A at http://www.biochemj.org/bj/452/bj4520545add.htm) [38]. The PLA signal was present in the nucleoplasmic compartment only in the presence of both the anti-FLAG and the anti-NPM1 antibodies,

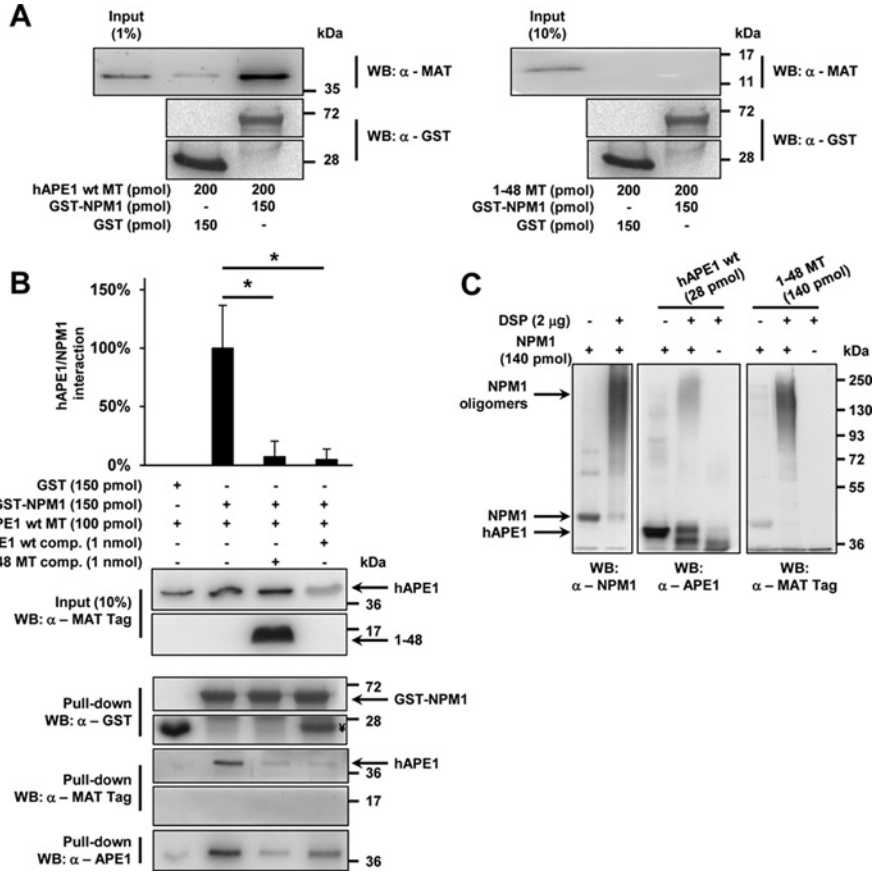

Figure 3 The unstructured N-terminal domain of hAPE1 is required, but not sufficient, for stable binding to NPM1 *in vitro*

(**A**) A representative GST pull-down experiment showing the absence of a stable interaction, *in vitro*, between recombinant GST-tagged NPM1 (bait) and the MAT-tagged 1–48 hAPE1 N-terminal peptide (prey) (right-hand panel). The same assay using full-length MAT-tagged hAPE1 is reported as a positive control (left-hand panel). The assay was performed as described in the Experimental section using the indicated amounts of recombinant proteins. (**B**) The recombinant 1–48 hAPE1 peptide is able to compete, *in vitro*, with the full-length hAPE1 protein for the binding to NPM1. Competition GST pull down using GST–NPM1 as the bait and MAT-tagged full-length hAPE1 as the prey. The hAPE1–NPM1 interaction was evaluated in the presence of a 10-fold excess competitor (comp.; i.e. untagged full-length hAPE1 as a positive control or MAT-tagged 1–48 peptide). The extent of interaction was assessed using an anti-MAT antibody to recognize the pulled down hAPE1 prey. The competing untagged hAPE1 was visualized using an anti-APE1 antibody. The histogram shows the average of three independent experiments with the error bars representing the S.D. $^*P < 0.05$. ¥, Residual GST contaminant in the untagged hAPE1 preparation. (**C**) The low-affinity binding between the N-terminal recombinant hAPE1 peptide and NPM1 is stabilized by *in vitro* cross-linking. Recombinant purified NPM1 was incubated alone or together with either the 1–48 peptide or full-length hAPE1 as indicated. The bifunctional cross-linker DSP was also added where indicated. The presence of high-molecular-mass complexes was assessed by Western blotting using an anti-NPM1, an anti-APE1 or an anti-MAT antibody. The formation of high-molecular-mass complexes in the presence of DSP denotes the ability of the 1–48 peptide to interact weakly with NPM1. MT, Mat; WB, Western blot; wt, wild-type.

being absent when using either the anti-FLAG or the anti-NPM1 alone. This demonstrates the existence of an interaction between the isolated hAPE1 N-terminal domain and endogenous NPM1 only in the nucleoplasmic compartment. We also measured, using PLA, the extent of endogenous hAPE1–NPM1 interaction in the presence or absence of expression of the 1–49 peptide. In this case, the expression of the N-terminal region resulted in a poor, but statistically significant competing effect (about 10 % loss in interaction, Figure 4C). Altogether, these results confir that the unstructured hAPE1 N-terminal domain alone is required, but not suff cient, for a stable binding of hAPE1 to NPM1 both *in vitro* and *in vivo*. Notably, several studies have demonstrated that hAPE1, targeted by granzymes A and K, undergoes proteolysis in living cells and its truncation products (hAPE1 NΔ31 or 35) have been proposed to take part in the apoptotic process [18,39,40]. In light of the results of the present paper, it may be tempting to speculate that the N-terminal proteolytic products (the 1–31 or 1–35 peptides) might also exert an active regulatory function within cell, for example by competing with the full-length protein for binding to nucleic acids or protein partners, such as NPM1, XRCC1 (X-ray repair complementing defective repair in Chinese hamster cells) [41], DNA polymerase β [42] or CSB (Cockayne syndrome B) [43] and thus possibly acting as decoy peptide.

The evolutionarily acquired N-terminal domain of hAPE1 influences the stability and the binding properties of the protein

Given the importance of the unstructured N-terminal region of hAPE1 in tuning many of the protein's functions, the poor evolutionary conservation of this domain appears remarkable. hAPE1 belongs to the exonuclease III family of endonucleases, being 27 % identical with the archetype *E. coli* ExoIII (*xth*) [14]. Although the C-terminal domain of the human protein is conserved from prokaryotes to mammals, the N-terminal portion of hAPE1, comprising the redox domain, is not [17,44]. Metazoan hAPE1 orthologues, in fact, share a unique basic N-terminal extension that heavily affects the isoelectric point of the whole protein. Interestingly, the overall positive charges number within this basic region increased during evolution (from nine in f shes

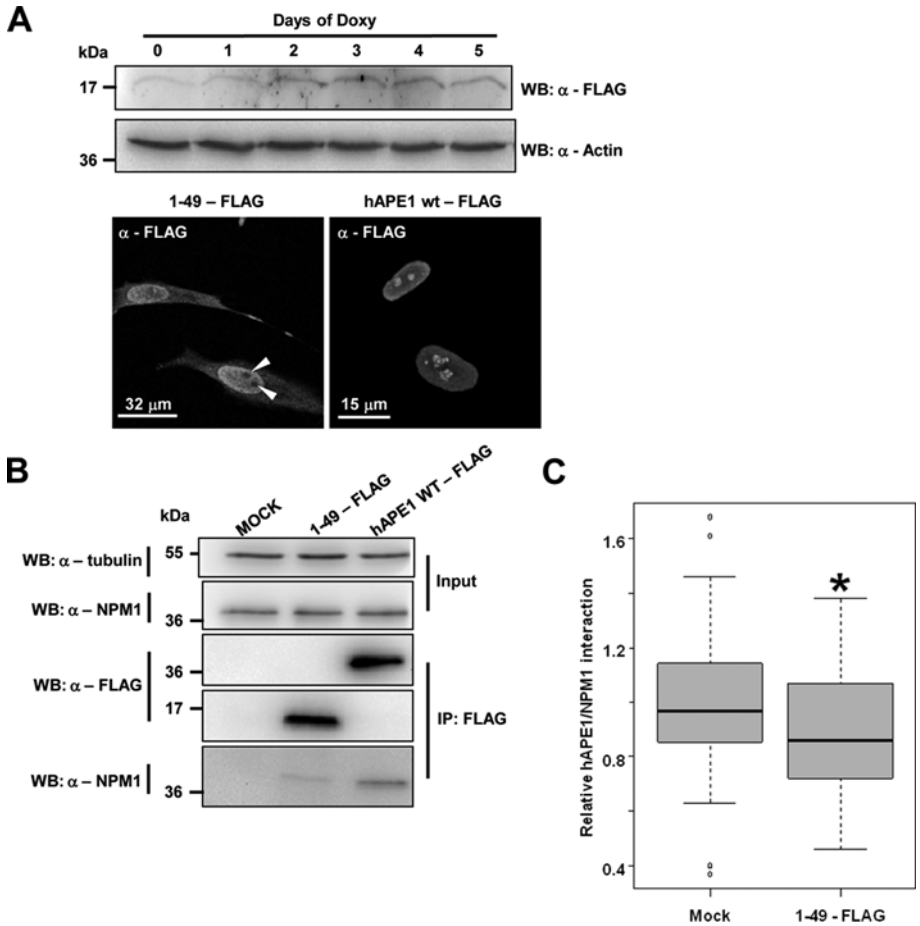

Figure 4 The hAPE1 N-terminal peptide interacts weakly with endogenous NPM1 in HeLa cells

(**A**) Upper panels, Western blotting analysis of the expression kinetics of the FLAG-tagged 1–49 hAPE1 peptide following the doxycycline treatment of HeLa. The peptide expression is induced after 2 days of treatment. Lower panel, immunofluorescence confocal analysis on HeLa cells after 5 days of doxycycline treatment shows the lack of nucleolar accumulation of the 1–49 peptide (white arrowheads), in contrast with the nucleolar positivity shown by the full-length hAPE1. (**B**) The recombinant 1–49 peptide binds poorly to endogenous NPM1 *in vivo*. NPM1 co-immunoprecipitation carried out using HeLa cells transfected either with an empty vector (mock) or a FLAG–full-length hAPE1- or a FLAG–1–49-expressing vector as shown. The amount of immunoprecipitated NPM1 was evaluated using Western blotting with an anti-NPM1 antibody. (**C**) The competition effect of the 1–49 hAPE1 peptide on endogenous hAPE1–NPM1 interaction. The extent of endogenous hAPE1–NPM1 interaction was measured by PLA of HeLa cells either expressing the 1–49 hAPE1 peptide or mock transfected. The hAPE1–NPM1 association was estimated by scoring the interaction signals in transfected cells. Peptide expression resulted in a significant competing effect, leading to a 10% reduction in hAPE1–NPM1 interaction. The boxplot shows the relative amount of hAPE1–NPM1 interaction in 1–49-expressing cells with respect to the mock-transfected cells $\pm$ S.D. ($n = 70$). *$P < 0.05$. IP, immuoprecipitation; WB, Western blot; wt, wild-type.

to 11 in mammals; Figure 2A; [17]), this event has possibly been paralleled by an improved ability of APE1 to cope with a progressively complex cellular environment.

Our recent work showed that the DNA-binding activity of hAPE1 is substantially higher than that of the orthologous protein from a phylogenetically distant organism, such as zebrafis (zAPE1) [17]. In the present study, we hypothesized that evolutionarily acquired amino acids within the N-terminal domain of the protein could account for the increased binding properties of hAPE1 towards both nucleic acids and NPM1. As a proof of concept, we performed interaction experiments with recombinant purifie hAPE1 and zAPE1 enzymes. Initially, through GST pull-down experiments, we confirme that zAPE1 has a lower binding activity towards both NPM1 (Figure 5A) and rRNA (Figure 5B). We then used insertional mutagenesis to generate a mutant recombinant zAPE1 protein (namely, zAPE1 K27) bearing, after Glu^{26}, a lysine residue followed by a TAA (threonine–alanine–alanine) spacer spanning amino acids 28–30, in order to mimic the local charge density and distribution present within the wild-type hAPE1 N-terminal 24–35 region (Figure 5C). Interestingly, the theoretical isoelectric point, calculated for the whole unstructured N-terminal domain, is identical in both the wild-type human protein and the zAPE1 K27 mutant (Table 3).

The NPM1-binding activity of the purifie recombinant proteins was then analysed using GST pull down with equimolar amounts of each protein (Figure 5D and Supplementary Figure S4A at http://www.biochemj.org/bj/452/bj4520545add.htm). The data obtained indicate that, whereas the wild-type zAPE1 is less able to interact with NPM1 than hAPE1, the full NPM1-binding activity of the 'swapping mutant' is clearly restored. Notably, both the hAPE1 NΔ43 and the zAPE1 NΔ36 deletion mutants, lacking the entire N-terminal extension, showed neglectable interaction ability. Although recognizing the limitations of this approach when evaluating the binding of zAPE1 to a human NPM1 protein (even though both human and zebrafis NPM1 share extensive similarity and have a nearly identical pI value), our 'domain swapping' approach supports the notion that the reduction in binding affinit might be a consequence of a decreased

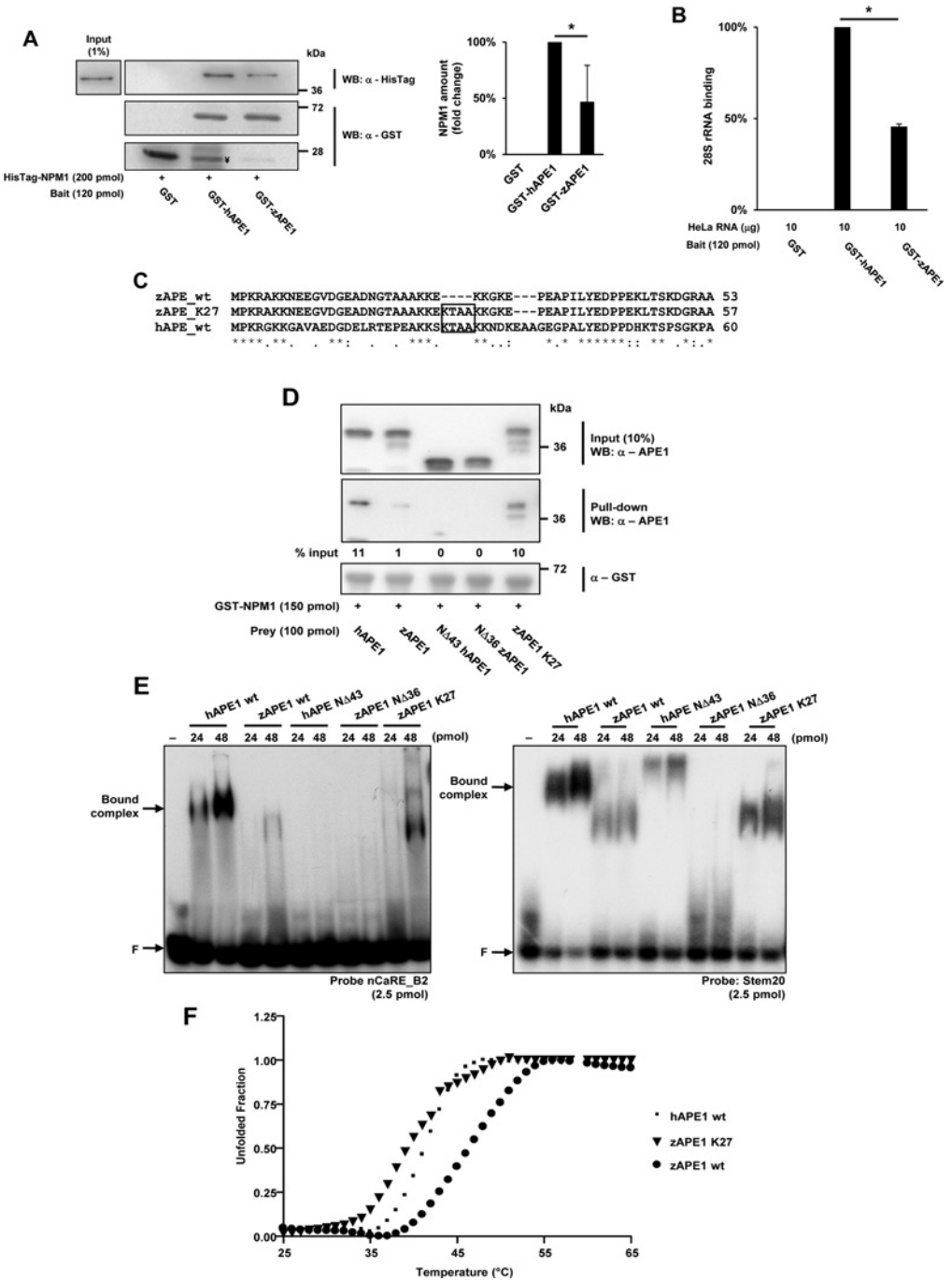

Figure 5 The amino acidic composition of the N-terminal region enhances the affinity of the human APE1 protein for nucleic acids and NPM1

(**A**) zAPE1 has a lower affinity than hAPE1 for NPM1. GST pull-down assay using equimolar amounts of recombinant GST-tagged hAPE1 or zAPE1 as baits and His-tagged NPM1 as the prey. The amount of pulled-down NPM1 was quantified through densitometric analysis (right-hand panel). The histogram show the results from three independent experiments with the error bars representing the S.D. ($n = 3$), $^*P < 0.05$. ¥, Residual GST contaminant in the GST–hAPE1 preparation. (**B**) zAPE1 has lower affinity than hAPE1 for rRNA. The APE1–RNA-binding capacity was evaluated through RNA pull down using GST-tagged full-length hAPE1 or zAPE1 as the bait and whole HeLa RNA as the prey. To quantify the amount of residual hAPE1-bound rRNA the pulled-down RNA was then retrotranscribed and 28S or 18S rRNAs were amplified by real-time PCR. The affinity for the 18S rRNA was similar to what shown for the 28S (results not shown). The histogram reports the relative affinity to rRNA with respect to the GST–hAPE1 sample. Error bars represent the S.D. ($n = 3$). $^*P < 0.001$. (**C**) Multiple sequence alignment of the N-terminal region of wild-type hAPE1, zAPE1 and the mutant zAPE1 K27. The four-amino-acid insertion mutation in zAPE1 K27 is boxed. (**D**) The NPM1-binding affinity of the 'domain swapping' mutant measured using GST pull down. GST-tagged NPM1 was used as the bait, whereas wild-type or mutant APE1 proteins were used as preys. The amount of pulled-down preys was assessed by Western blotting using an anti-APE1 antibody and is shown as the percentage of input prey. Whereas wild-type zAPE1 and the deletion mutants NΔ43 hAPE1 and NΔ36 zAPE1 show a loss of function phenotype, the NPM1-binding capacity of the zAPE1 K27 mutant is restored. (**E**) Binding affinity of the 'domain swapping' mutant for the nCaRE_B2 (left-hand panel) or the Stem20 (right-hand panel) oligonucleotides as measured using EMSA. The nucleic acid-binding activity of the proteins reflects what was observed using SPR (Table 4): the wild-type zAPE1 protein and the deletion mutants NΔ43 hAPE1 and NΔ36 zAPE1 show a reduced binding ability, whereas the zAPE1 K27 mutant displays a gain of function. F, the position of the free oligonucleotide probe. Arrows indicate the bound complex. (**F**) Overlay of thermal melting profiles for recombinant hAPE1, zAPE1 and zAPE1 K27 in the 25–65 °C range shown as the unfolded fraction against temperature, measured by CD at 222 nm. The difference in thermal stability observed between the wild-type hAPE1 and zAPE1 is clearly restored by the N-terminal insertions in the zAPE1 K27 mutant. WB, Western blot; wt, wild-type.

Table 3 Predicted biophysical characteristics of the recombinant proteins used in the present study

The table reports the theoretical molecular masses and isoelectric points calculated using the Expasy pI/Mw tool (http://web.expasy.org/compute_pi/). The pI value of the N-terminal region was calculated restricting the analysis to the human Ala[43] or the homologue Ile[36] in fish. Note the identical pI values between the wild-type (wt) hAPE1 and the zAPE1 K27 N-terminal extensions. N/A, not available.

Protein	Molecular mass	Isoelectric point (whole protein)	Isoelectric point (N-terminal)
hAPE1 wt	35564	8.33	9.10
zAPE1 wt	34881	5.77	8.04
hAPE1 NΔ43	31217	7.59	N/A
zAPE1 NΔ36	31207	5.54	N/A
zAPE1 K27	35252	5.96	9.10

Table 4 Dissociation constants and kinetic parameters for the interaction of the mutated APE1 proteins with the Stem20 and nCaRE_B2 oligonucleotides

Results were obtained using SPR analyses using different APE1 mutants as analytes on the indicated biotinylated oligonucleotide ligands. The affinity values for the nCaRE_B2 sequence were determined through Langmuir isotherm fitting (see the text for details). wt, wild-type.

	Stem20			nCaRE_B2
Protein	k_{on} ($M^{-1} \cdot s^{-1} \times 10^5$)	k_{off} (s^{-1})	K_d (μM)	K_d (μM)
zAPE1 wt	0.174	0.053	3.28 ± 0.07	5.7 ± 0.2
zAPE1 NΔ36	0.232	0.530	23.0 ± 0.5	No binding
hAPE1 NΔ43	0.841	0.733	10.3 ± 0.3	No binding
zAPE1 K27	0.419	0.067	1.60 ± 0.02	2.4 ± 0.9

number of positive charges within the N-terminal region of zAPE1.

A similar functional rescue for the zAPE1 K27 mutant was also observed when analysing the DNA-binding activity of the proteins (Figure 5E). EMSA experiments carried out with either a nCaRE_B2 duplex (Figure 5E, left-hand panel) or the Stem20 sequence (Figure 5E, right-hand panel) revealed a reduced binding activity for wild-type zAPE1 and both the hAPE1 NΔ43 and the zAPE1 NΔ36 deletion mutants, with a restored functionality in the case of the zAPE1 K27 protein. EMSA analyses showed clear differences in the electrophoretic mobility of the hAPE1 and zAPE1 in complex with the nucleic acid substrates, suggesting the existence of possible conformational differences between the two recombinant proteins when bound to the cognate DNA. The formation of a DNA–protein complex between the hAPE1 NΔ43 mutant and the Stem20 substrate (Figure 5E, right-hand panel), but not with the nCaRE_B2 DNA, is probably owing to the presence of a highly stable stem-loop structure within the Stem20 sequence, absent in the case of the nCaRE_B2 duplex (also see the SPR data below). This observation again supports the concept that the C-terminal domain of hAPE1 may account for the high-affinit binding to structured nucleic acid substrates. Moreover, the complete lack of nucleic acid-binding activity observed for the hAPE1 NΔ33 mutant [12,17] suggests that the acidic residues in the 33–42 region might have a negative effect on the overall nucleic acid-binding capacity of the protein.

In order to corroborate these findings we carried out SPR experiments on zAPE1 and its mutants (Table 4) using both the Stem20 and nCaRE_B2 sequences, which showed different affinitie for hAPE1 (Table 2). Interestingly, both the association and dissociation rate constants could be determined when the Stem20 was used as ligand; whereas, they were too high to be determined with the nCaRE_B2 (in this case aff nities were determined through Langmuir isotherm f tting; Supplementary Figure S4B). These results further point to the relevance of the presence of a stable stem-loop secondary structure within the oligonucleotide for a robust APE1–nucleic acid interaction. This result is corroborated by the presence of a detectable binding activity of the N-terminal truncated proteins (hAPE1 NΔ43 and zAPE1 NΔ36) only for the stem-loop substrate (i.e. Stem20). Similarly to what was observed in the EMSA experiments (Figure 5E) with both DNA substrates, the measured K_d values were higher for zAPE1 than for hAPE1 (for the kinetic parameters with the human protein see Table 2). The zAPE1 K27 mutant, in turn, displayed an intermediate behaviour, confirmin the restored binding activity of the 'swapping mutant' (Table 4).

In order to correlate the solution stability with binding ability, we performed CD analyses on wild-type, mutant and truncated APE1 proteins. The crystal structures of two vertebrate redox-inactive enzymes C65A hAPE1 and zAPE1, in their N-terminally truncated variants (C65A 40–318 hAPE1 and 33–310 zAPE1), revealed no substantial differences in the structural organization of the globular region of APE1 [44]. This was confirme by our analyses as the CD spectra of all our proteins exhibited minima at 225 and 208 nm, typical of α-helices and β-strands (results not shown). This indicates that, as expected, the C-terminal globular region of the protein predominantly accounts for the folded portion of the APE1 proteins. Thermal denaturation experiments were carried out to investigate protein stability: the sigmoidal profil of folded fraction against temperature (Figure 5F) shows that the unfolding process was fully co-operative for all of the proteins tested. By comparing the T_m values, however, an influenc of the N-terminal extension on protein stability could be highlighted. Indeed, whereas hAPE1 has a T_m value of 41.5 °C, the T_m value measured for zAPE1 was 46.5 °C. Interestingly, the mutations and insertions in the zAPE1 K27 mutant effectively reduced the stability of the protein, since the measured T_m value (39.5 °C) was closer to that of hAPE1 (Figure 5F). These results suggest a direct correlation between the ability to recognize different oligonucleotides or protein substrates and the fl xibility of the N-terminal region of APE1. Moreover, these data also support the hypothesis that the altered mobility observed in the EMSA experiments between hAPE1 and zAPE1 bound to the cognate DNA sequences (Figure 5E) might be ascribed to substantial conformational differences in the two protein–DNA complexes. Similar CD analyses carried out on both the hAPE1 NΔ43 and the zAPE1 NΔ36 deletion mutants indicated that the differences in thermal stability between human and zebrafis proteins are already present in their globular portions (the T_m values were 44 °C and 50.5 °C respectively), despite the similar structural organization (Supplementary Figure S4C).

Taken together, these results indicate that the amino acid composition and the local charge distribution within the N-terminal domain of hAPE1 are responsible for its evolutionarily acquired binding properties towards both nucleic acids and NPM1 and have an impact on the f exibility of the N-terminal region of APE1. Therefore the results of the present study point to the insertion of human Lys[27], as well as the proper charge distribution, as central steps in the phylogenesis of this protein. From a phylogenic perspective, the acquisition of additional lysine residues could have provided the human protein with novel ways to fine-tun its different activities by the means of new 'hot spots'

that can undergo acetylation or ubiquitination [17,19–21] and regulate substrate accessibility, on the basis of protein plasticity in solution. In conclusion, in light of the results of the present study and others [17,21,42,45], we suggest that the hAPE1 unstructured N-terminal domain might represent a fl xible device that has been selected during evolution to specificall modulate the nucleic acid- and NPM1-binding functions of the protein. It would be interesting to explore novel pharmacological strategies aiming at the functional modulation of the protein using small molecules and/or peptides that target its N-terminal region.

AUTHOR CONTRIBUTION

Mattia Poletto, Daniela Marasco and Gianluca Tell provided substantial contributions to conception and design of the study, substantial contributions to acquisition of data or to analysis and interpretation of data, drafting the article or revising it critically for important intellectual content, and approved the final version. Carlo Vascotto and Lisa Lirussi provided substantial contributions to acquisition of data or to analysis and interpretation of data. Pasqualina Scognamiglio provided substantial contributions to conception and design, and substantial contributions to acquisition of data or to analysis and interpretation of data.

ACKNOWLEDGEMENTS

We thank Dr Mengxia Li and Professor Franco Quadrifoglio for critically reading the paper prior to submission and for their helpful comments and input and Professor A. Zagari and Dr V. Granata of CEINGE-NAPOLI (Naples, Italy) for their helpful discussion on the SPR experiments.

FUNDING

This work was supported the Associazione Italiana per la Ricerca sul Cancro (AIRC) [grant number IG10269] and the Ministero dell'Istruzione, dell'Università e della Ricerca (MIUR) [grant numbers FIRB_RBRN07BMCT and PRIN2008_CCPKRP_003 (to G.T.)]

REFERENCES

1 Fung, H. and Demple, B. (2005) A vital role for Ape1/Ref1 protein in repairing spontaneous DNA damage in human cells. Mol. Cell **17**, 463–470
2 Bhakat, K. K., Izumi, T., Yang, S. H., Hazra, T. K. and Mitra, S. (2003) Role of acetylated human AP-endonuclease (APE1/Ref-1) in regulation of the parathyroid hormone gene. EMBO J. **1**, 6299–6309
3 Vascotto, C., Cesaratto, L., Zeef, L. A., Deganuto, M., D'Ambrosio, C., Scaloni, A., Romanello, M., Damante, G., Taglialatela, G., Delneri, D. et al. (2009) Genome-wide analysis and proteomic studies reveal APE1/Ref-1 multifunctional role in mammalian cells. Proteomics **9**, 1058–1074
4 Tell, G., Damante, G., Caldwell, D. and Kelley, M. R. (2005) The intracellular localization of APE1/Ref-1: more than a passive phenomenon? Antioxid. Redox Signaling **7**, 367–384
5 Xanthoudakis, S., Miao, G. G. and Curran, T. (1994) The redox and DNA-repair activities of Ref-1 are encoded by nonoverlapping domains. Proc. Natl. Acad. Sci. U.S.A. **91**, 23–27
6 Erzberger, J. P., Barsky, D., Schärer, O. D., Colvin, M. E. and Wilson, III, D. M. (1998) Elements in abasic site recognition by the major human and *Escherichia coli* apurinic/apyrimidinic endonucleases. Nucleic Acids Res. **26**, 2771–2778
7 Fan, J., Matsumoto, Y. and Wilson, III, D. M. (2006) Nucleotide sequence and DNA secondary structure, as well as replication protein A, modulate the single-stranded abasic endonuclease activity of APE1. J. Biol. Chem. **281**, 3889–3898
8 Marenstein, D. R., Wilson, III, D. M. and Teebor, G. W. (2004) Human AP endonuclease (APE1) demonstrates endonucleolytic activity against AP sites in single-stranded DNA. DNA Repair **3**, 527–533
9 Sengupta, S., Mantha, A. K., Mitra, S. and Bhakat, K. K. (2011) Human AP endonuclease (APE1/Ref-1) and its acetylation regulate YB-1-p300 recruitment and RNA polymerase II loading in the drug-induced activation of multidrug resistance gene *MDR1*. Oncogene **30**, 482–493
10 Tell, G., Wilson, III, D. M. and Lee, C. H. (2010) Intrusion of a DNA repair protein in the RNome world: is this the beginning of a new era? Mol. Cell. Biol., **30**, 366–371
11 Beloglazova, N. G., Kirpota, O. O., Starostin, K. V., Ishchenko, A. A., Yamkovoy, V. I., Zharkov, D. O., Douglas, K. T. and Nevinsky, G. A. (2004) Thermodynamic, kinetic and structural basis for recognition and repair of abasic sites in DNA by apurinic/apyrimidinic endonuclease from human placenta. Nucleic Acids Res. **32**, 5134–5146
12 Vascotto, C., Fantini, D., Romanello, M., Cesaratto, L., Deganuto, M., Leonardi, A., Radicella, J. P., Kelley, M. R., D'Ambrosio, C., Scaloni, A. et al. (2009) APE1/Ref-1 interacts with NPM1 within nucleoli and plays a role in the rRNA quality control process. Mol. Cell. Biol. **29**, 1834–1854
13 Barnes, T., Kim, W. C., Mantha, A. K., Kim, S. E., Izumi, T., Mitra, S. and Lee, C. H. (2009) Identification of apurinic/apyrimidinic endonuclease 1 (APE1) as the endoribonuclease that cleaves c-myc mRNA. Nucleic Acids Res. **37**, 3946–3958
14 Gorman, M. A., Morera, S., Rothwell, D. G., de La Fortelle, E., Mol, C. D., Tainer, J. A., Hickson, I. D. and Freemont, P. S. (1997) The crystal structure of the human DNA repair endonuclease HAP1 suggests the recognition of extra-helical deoxyribose at DNA abasic sites. EMBO J. **16**, 6548–6558
15 Beernink, P. T., Segelke, B. W., Hadi, M. Z., Erzberger, J. P., Wilson, III, D. M. and Rupp, B. (2001) Two divalent metal ions in the active site of a new crystal form of human apurinic/apyrimidinic endonuclease, Ape1: implications for the catalytic mechanism. J. Mol. Biol. **307**, 1023–1034
16 Strauss, P. R. and Holt, C. M. (1998) Domain mapping of human apurinic/apyrimidinic endonuclease. Structural and functional evidence for a disordered amino terminus and a tight globular carboxyl domain. J. Biol. Chem. **273**, 14435–14441
17 Fantini, D., Vascotto, C., Marasco, D., D'Ambrosio, C., Romanello, M., Vitagliano, L., Pedone, C., Poletto, M., Cesaratto, L., Quadrifoglio, F. et al. (2010) Critical lysine residues within the overlooked N-terminal domain of human APE1 regulate its biological functions. Nucleic Acids Res. **38**, 8239–8256
18 Fan, Z., Beresford, P. J., Zhang, D., Xu, Z., Novina, C. D., Yoshida, A., Pommier, Y. and Lieberman, J. (2003) Cleaving the oxidative repair protein Ape1 enhances cell death mediated by granzyme A. Nat. Immunol. **4**, 145–153
19 Busso, C. S., Iwakuma, T. and Izumi, T. (2009) Ubiquitination of mammalian AP endonuclease (APE1) regulated by the p53–MDM2 signaling pathway. Oncogene **28**, 1616–1625
20 Meisenberg, C., Tait, P. S., Dianova, I. I., Wright, K., Edelmann, M. J., Ternette, N., Tasaki, T., Kessler, B. M., Parsons, J. L., Tae Kwon, Y. and Dianov, G. L. (2011) Ubiquitin ligase UBR3 regulates cellular levels of the essential DNA repair protein APE1 and is required for genome stability. Nucleic Acids Res. **40**, 701–711
21 Lirussi, L., Antoniali, G., Vascotto, C., D'Ambrosio, C., Poletto, M., Romanello, M., Marasco, D., Leone, M., Quadrifoglio, F., Bhakat, K. K. et al. (2012) Nucleolar accumulation of APE1 depends on charged lysine residues that undergo acetylation upon genotoxic stress and modulate its BER activity in cells. Mol. Biol. Cell **23**, 4079–4096
22 Hedge, M. L., Izumi, T. and Mitra, S. (2012) Oxidized base damage and single-strand break repairin mammalian genomes: role of disordered regions and posttranslational modifications in early enzymes. Prog. Mol. Biol. Transl. Sci. **110**, 123–153
23 Tell, G., Fantini, D. and Quadrifoglio, F. (2010) Understanding different functions of mammalian AP endonuclease (APE1) as a promising tool for cancer treatment. Cell. Mol. Life Sci. **67**, 3589–3608
24 Schägger, H. (2006) Tricine-SDS-PAGE. Nat. Protoc. **1**, 16–22
25 Nguyen, L. H., Barsky, D., Erzberger, J. P. and Wilson, III, D. M. (2000) Mapping the protein–DNA interface and the metal-binding site of the major human apurinic/apyrimidinic endonuclease. J. Mol. Biol. **298**, 447–459
26 Berquist, B. R., McNeill, D. R. and Wilson, III, D. M. (2008) Characterization of abasic endonuclease activity of human Ape1 on alternative substrates, as well as effects of ATP and sequence context on AP site incision. J. Mol. Biol. **379**, 17–27
27 Mol, C. D., Izumi, T., Mitra, S. and Tainer, J. A. (2000) DNA-bound structures and mutants reveal abasic DNA binding by APE1 and DNA repair coordination. Nature **403**, 451–456
28 Wilson, III, D. M., Takeshita, M. and Demple, B. (1997) Abasic site binding by the human apurinic endonuclease, Ape, and determination of the DNA contact sites. Nucleic Acids Res. **25**, 933–939
29 Katsamba, P. S., Park, S. and Laird-Offringa, I. A. (2002) Kinetic studies of RNA–protein interactions using surface plasmon resonance. Methods **26**, 95–104
30 Law, M. J., Rice, A. J., Lin, P. and Laird-Offringa, I. A. (2006) The role of RNA structure in the interaction of U1A protein with U1 hairpin II RNA. RNA **12**, 1168–1178
31 Izumi, T., Henner, W. D. and Mitra, S. (1996) Negative regulation of the major human AP-endonuclease, a multifunctional protein. Biochemistry **35**, 14679–14683
32 Kim, W. C., Berquist, B. R., Chohan, M., Uy, C., Wilson, III, D. M. and Lee, C. H. (2011) Characterization of the endoribonuclease active site of human apurinic/apyrimidinic endonuclease 1. J. Mol. Biol. **411**, 960–971
33 Vuzman, D. and Levy, Y. (2012) Intrinsically disordered regions as affinity tuners in protein–DNA interactions. Mol. Biosyst. **8**, 47–57

34 Masuda, Y., Bennett, R. A. O. and Demple, B. (1998) Dynamics of the interaction of human apurinic endonuclease (Ape1) with its substrate and product. J. Biol. Chem. **273**, 30352–30359
35 Yung, B. Y. and Chan, P. K. (1987) Identification and characterization of a hexameric form of nucleolar phosphoprotein B23. Biochim. Biophys. Acta **925**, 74–82
36 Vascotto, C., Bisetto, E., Li, M., Zeef, L. A., D'Ambrosio, C., Domenis, R., Comelli, M., Delneri, D., Scaloni, A., Altieri, F. et al. (2011) Knock-in reconstitution studies reveal an unexpected role of Cys^{65} in regulating APE1/Ref-1 subcellular trafficking and function. Mol. Biol. Cell **22**, 3887–3901
37 Jackson, E. B., Theriot, C. A., Chattopadhyay, R., Mitra, S. and Izumi, T. (2005) Analysis of nuclear transport signals in the human apurinic/apyrimidinic endonuclease (APE1/Ref1). Nucleic Acids Res. **33**, 3303–3312
38 Weibrecht, I., Leuchowius, K. J., Clausson, C. M., Conze, T., Jarvius, M., Howell, W. M., Kamali-Moghaddam, M. and Söderberg, O. (2010) Proximity ligation assays: a recent addition to the proteomics toolbox. Expert Rev. Proteomics **7**, 401–409
39 Yoshida, A., Urasaki, Y., Waltham, M., Bergman, A. C., Pourquier, P., Rothwell, D. G., Inuzuka, M., Weinstein, J. N., Ueda, T., Appella, E. et al. (2003) Human apurinic/apyrimidinic endonuclease (Ape1) and its N-terminal truncated form (AN34) are involved in DNA fragmentation during apoptosis. J. Biol. Chem. **278**, 37768–37776
40 Guo, Y., Chen, J., Zhao, T. and Fan, Z. (2008) Granzyme K degrades the redox/DNA repair enzyme Ape1 to trigger oxidative stress of target cells leading to cytotoxicity. Mol. Immunol. **45**, 2225–2235
41 Vidal, A. E., Boiteux, S., Hickson, I. D. and Radicella, J. P. (2001) XRCC1 coordinates the initial and late stages of DNA abasic site repair through protein–protein interactions. EMBO J. **20**, 6530–6539
42 Yu, E., Gaucher, S. P. and Hadi, M. Z. (2010) Probing conformational changes in Ape1 during the progression of base excision repair. Biochemistry **49**, 3786–3796
43 Wong, H. K., Muftuoglu, M., Beck, G., Imam, S. Z., Bohr, V. A. and Wilson, III, D. M. (2007) Cockayne syndrome B protein stimulates apurinic endonuclease 1 activity and protects against agents that introduce base excision repair intermediates. Nucleic Acids Res. **35**, 4103–4113
44 Georgiadis, M. M., Luo, M., Gaur, R. K., Delaplane, S., Li, X. and Kelley, M. R. (2008) Evolution of the redox function in mammalian apurinic/apyrimidinic endonuclease. Mutat. Res. **643**, 54–63
45 Yamamori, T., DeRicco, J., Naqvi, A., Hoffman, T. A., Mattagajasingh, I., Kasuno, K., Jung, S. B., Kim, C. S. and Irani, K. (2010) SIRT1 deacetylates APE1 and regulates cellular base excision repair. Nucleic Acids Res. **38**, 832–845

Received 14 August 2012/28 March 2013; accepted 2 April 2013
Published as BJ Immediate Publication 2 April 2013, doi:10.1042/BJ20121277

Biochem. J. (2013) **452**, 545–557 (Printed in Great Britain) doi:10.1042/BJ20121277

online data

SUPPLEMENTARY ONLINE DATA

Role of the unstructured N-terminal domain of the hAPE1 (human apurinic/apyrimidinic endonuclease 1) in the modulation of its interaction with nucleic acids and NPM1 (nucleophosmin)

Mattia POLETTO*, Carlo VASCOTTO*, Pasqualina L. SCOGNAMIGLIO†‡, Lisa LIRUSSI*, Daniela MARASCO†‡ and Gianluca TELL*[1]

*Department of Medical and Biological Sciences, University of Udine, 33100 Udine, Italy, †Department of Pharmacy, CIRPEB (Centro Interuniversitario di Ricerca sui Peptidi Bioattivi), University of Naples 'Federico II', 80134 Naples, Italy, and ‡Institute of Biostructures and Bioimaging CNR, 80134 Naples, Italy

RESULTS

Purification of the recombinant hAPE1 1–48 peptide

The recombinant MAT-tagged hAPE1 1–48 peptide (Figure S2A) was purifie to homogeneity by metal-affinit followed by cation-exchange chromatography. The purity of the peptide was verifie by SDS/PAGE separation and silver staining (Figure S2B). The predicted molecular mass for the tagged peptide is 6.3 kDa; however, its migration pattern on SDS/PAGE is quite peculiar as its apparent molecular mass is between 11 and 17 kDa. We hypothesize that this phenomenon could be ascribed to the high content of positive charges of the molecule (predicted isoelectric point = 8.04) that are not efficientl neutralized by SDS treatment. The exact molecular mass of the peptide was confirme through LC/MS (liquid chromatography MS) analysis (results not shown).

Affinity of the recombinant hAPE1 1–48 peptide for nucleic acids

We investigated the nucleic acid-binding activity of the recombinant MAT-tagged 1–48 peptide in order to confir the presence of the hAPE1 N-terminal domain in the low aff nity complexes seen in our EMSA experiments. To this aim, in addition to the Southwestern assays (Figure 2D of the main text and Figure S2D), we performed an EMSA experiment coupled to a Western blotting using an antibody directed against the hAPE1 N-terminal domain (amino acids 1–14; Novus; Figure S2E, right-hand panel). A signal showing the same migration pattern observed in the silver-stained EMSA (Figure S2E, right-hand panel) confirme the presence of the 1–48 hAPE1 peptide in the shifted complex.

[1] To whom correspondence should be addressed (email gianluca.tell@uniud.it).

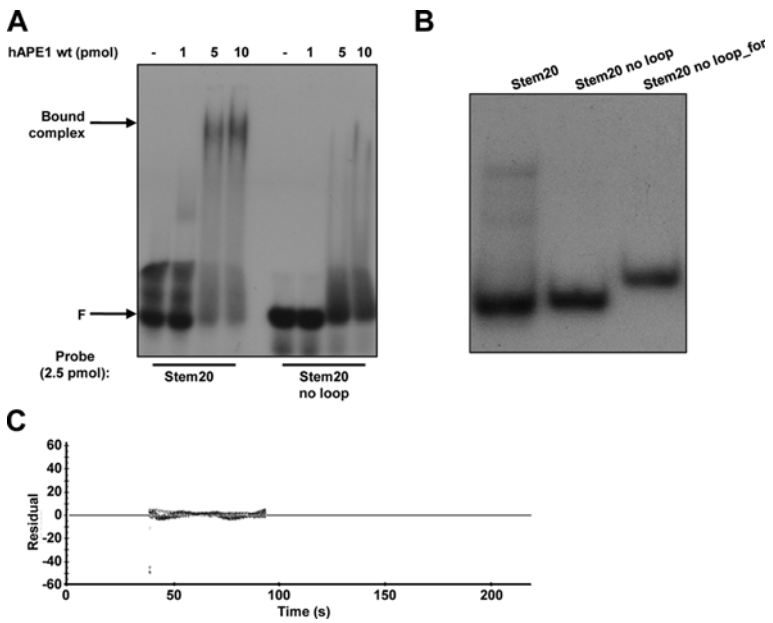

Figure S1 The presence of a single-stranded loop enhances hAPE1-binding capacity

(**A**) The positive effect of the presence of a loop on the ability of hAPE1 to bind undamaged DNA as evaluated by EMSA using the Stem20 and Stem20 no loop oligonucleotides (Table 1 of the main text). For each reaction the indicated amount of purified recombinant hAPE1 was used. The results highlight the lower binding capacity of hAPE1 in the absence of a stem and loop structure. The arrow indicates the hAPE1–DNA complexes, whereas F shows the position of the free oligonucleotide probe. wt, wild-type. (**B**) Annealing control for the Stem20 no loop duplex used in the EMSA in (**A**). Equimolar amounts of the indicated individually ^{32}P-labelled probes were separated by native PAGE (15 % gel). As expected, the Stem20 no loop duplex migrates similarly to the Stem20 probe, but differently from its own forward strand (Stem20 no loop_for, which is the labelled in the duplex probe). (**C**) A representative plot of residuals of the SPR data fitting (related to the experiment reported in Figure 1B of the main text). The adopted 1:1 Langmuir binding model provides low residuals levels both in the association and dissociation phases.

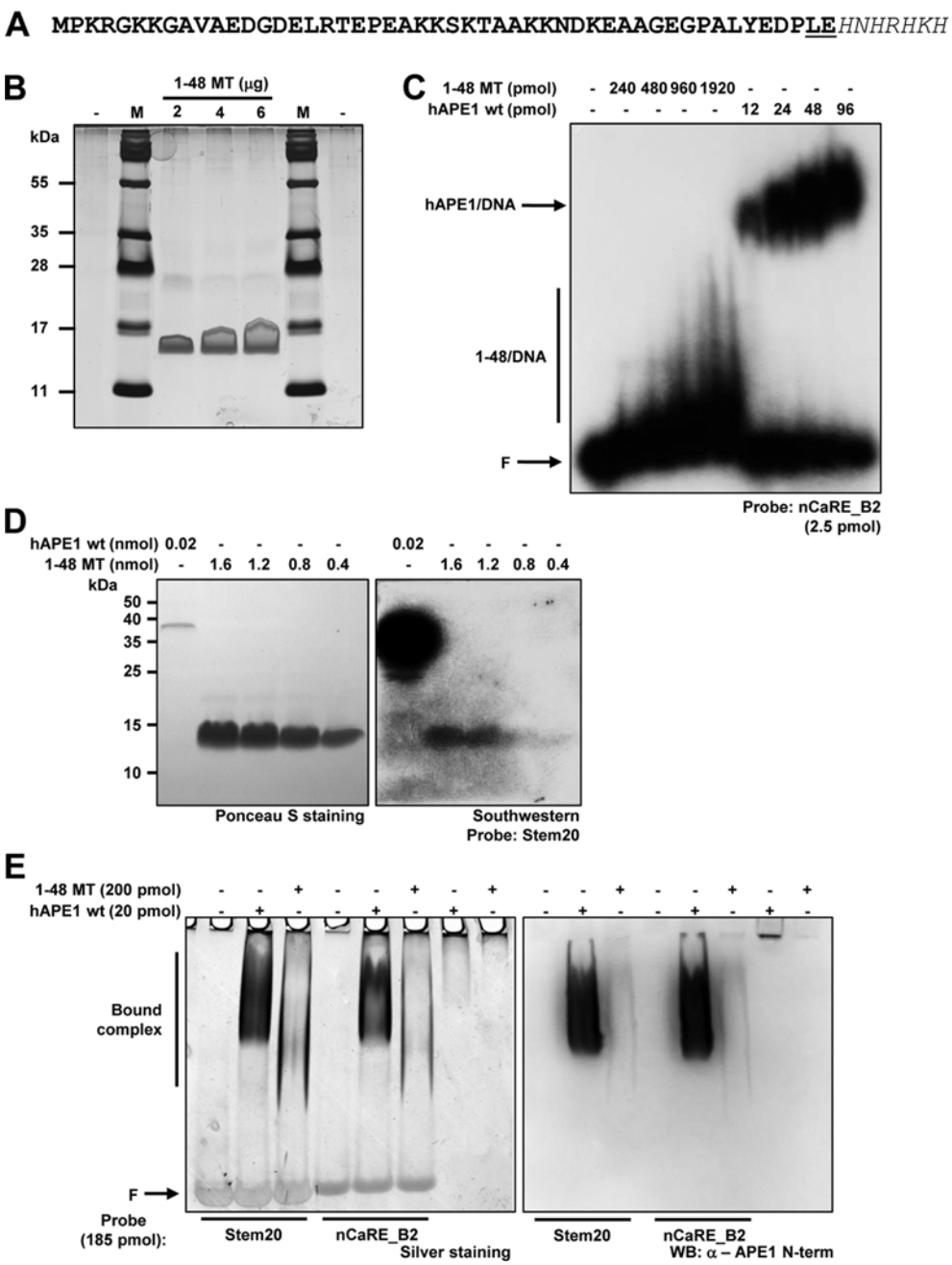

Figure S2 Characterization of the 1–48 hAPE1 recombinant peptide

(**A**) Amino acid sequence of the MAT-tagged hAPE1 1–48 peptide. The two extra residues from the cloning procedures are underlined, whereas the C-terminal MAT is shown in italic font. (**B**) Silver-stained Tris/Tricine SDS/PAGE showing the purified MAT-tagged hAPE1 1–48 peptide. M, molecular mass markers. The molecular mass of the markers is shown on the left-hand side in kDa. (**C**) EMSA dose–response analysis showing that the 1–48 peptide binds undamaged DNA with a low affinity when compared with the full-length hAPE1 protein. For each reaction the indicated amount of purified recombinant protein was used. F, the position of the free oligonucleotide probe. (**D**) Southwestern assay showing a dose–response binding of the Stem20 oligonucleotide to the 1–48 peptide. The indicated amounts of protein or peptide were separated by SDS/PAGE, electrotransferred on to nitrocellulose membranes (left-hand panel) and probed with ^{32}P-labelled Stem20 (right-hand panel). Note the difference in binding affinity between the full-length hAPE1 protein and the isolated peptide. Molecular mass is shown on the left-hand side in kDa. (**E**) EMSA coupled to Western blotting to confirm the presence of the N-terminal hAPE1 peptide in the bound complex. The indicated amounts of hAPE1 protein or peptide were incubated with different unlabelled DNA probes and separated on two parallel native gels. The first one was silver-stained, to reveal the presence of shifted DNA–protein complexes (left-hand), whereas the second one was subjected to Western blotting followed by immunorecognition with an anti-hAPE1 N-terminal antibody (right-hand panel). MT, MAT; wt, wild-type.

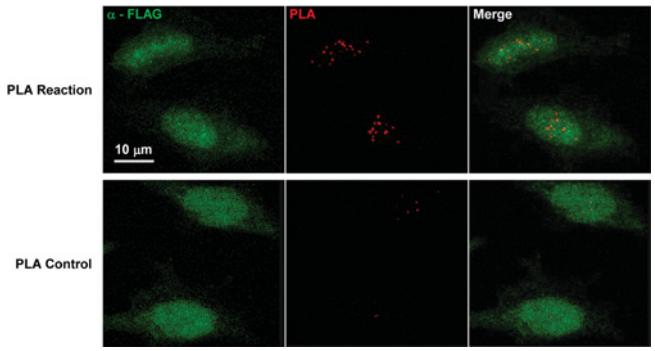

Figure S3 ***In vivo*** **interaction of the 1–49 hAPE1 peptide with endogenous NPM1**

(**A**) PLA analysis of 1–49 hAPE1-expressing HeLa cells using an anti-FLAG and an anti-NPM1 antibody reveals the interaction occurring *in vivo* between the hAPE1 N-terminal peptide and endogenous NPM1 (red dots in the upper middle panel). The lower panels represent the technical control where the immunoreaction was carried out while omitting the anti-NPM1 antibody.

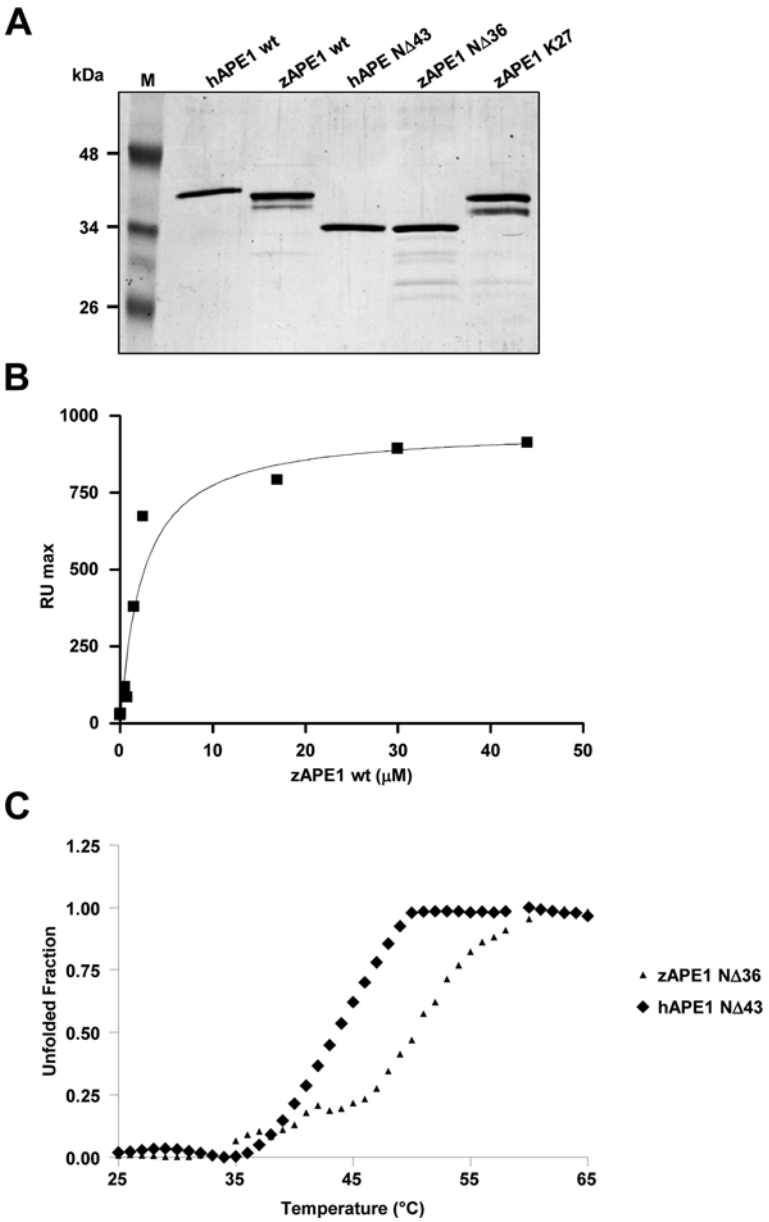

Figure S4 Evolutionary characterization of the hAPE1 N-terminal region

(**A**) A Coomassie Blue-stained gel showing the recombinant purified APE1 proteins used in the present study. M, molecular mass marker. The molecular mass of the markers is shown on the left-hand side in kDa. (**B**) Representative SPR analysis on the wild-type zAPE1–nCaRE_B2 interaction. Recombinant zAPE1 was used as the analyte and biotinylated nCaRE_B2 was used as the ligand. Plot of RU_{max} from each binding against concentration of wild-type zAPE1 is shown. The data were fitted by non-linear regression analysis. (**C**) Overlay of thermal melting profiles of recombinant hAPE1 NΔ43 and zAPE1 NΔ36 in the 25–65 °C range, reported as unfolded fraction against temperature measured using a CD signal at 222 nm. wt, wild-type.

Received 14 August 2012/28 March 2013; accepted 2 April 2013
Published as BJ Immediate Publication 2 April 2013, doi:10.1042/BJ20121277

ACKNOWLEDGMENTS

First, I want to thank my supervisor, Gianluca Tell, who gave me the possibility to join his amazing group during the last seven years, for supporting me and my research project. I am heartily grateful to him for always pushing me into doing better.

I'm grateful to Prof. Bruce Demple who shared with me his knowledge and for his thought-provoking discussions, help and mentoring.

Then, I would like to thank for their help and sharing moments all the people, former and present lab mates, who worked side by side with me during all these years, making my lab days and coffees enjoyable: Milly, Laurina, Erika, Dami, Paolino, Stefi, Roberto and Carlo and all the Demplabites.

A special thank to my colleagues and friends (Giulia, Elena and Mattia) that share with me this PhD course during good and bad days.

I also would like to thank all my friends, going back to a long or short way (Manuela, Andrea, Stefano, Dami, Laura, Stefi, Giorgina, Robi, Vala and Caterina) for encouraging and for spending time listening to me.

And then, a huge thank to all my family for helping, inspiring and guiding me every day.